EIGHT-MEMBERED CYCLIC AMINES AS NOVEL SCAFFOLDS FOR DRUG DISCOVERY

by

SAM CEUSTERS

A thesis submitted to The University of Birmingham for the
degree of
DOCTOR OF PHILOSOPHY

School of Chemistry
College of Engineering and Physical Sciences
The University of Birmingham
July 2022

UNIVERSITY OF BIRMINGHAM

University of Birmingham Research Archive

e-theses repository

ABSTRACT

The research conducted in this PhD thesis is one of the six projects of iDESIGN, an EU-funded European Industrial Doctorate Innovative Training Network (EU-EID-ITN). iDESIGN's principal research objective was to design and synthesise novel compound libraries of structurally and functionally diverse, three-dimensional molecules with attractive physicochemical properties for early-stage drug discovery. Due to their conformational flexibility and presence in various bioactive natural products, eight-membered cyclic amine derivatives were considered valuable starting points for drug discovery as they represent an underexplored – and therefore under-exploited – region of chemical space. Literature compound *N*-Boc-(*Z*)-5-oxo-3,4,5,8-tetrahydroazocine was synthesed in five steps, including an optimised ring-closing metathesis reaction as the key step, which was scaled up to gramme scale. By selectively manipulating the embedded enone functionality in this *N*-Boc-azacyclooctenone parent scaffold, three structurally distinct core scaffolds, comprising an azacyclooctylamine, a family of 8-5/8-6 fused aromatic heterocycles and an 8-5 fused pyrrolidine, were synthesised, each with multiple appendable handles. From these scaffolds, three diverse compound libraries were designed *in silico* and then prepared *via* parallel synthesis. Using KNIME and DataWarrior, the compound libraries were designed to display maximum diversity in drug-like physicochemical, structural and molecular shape space, which was validated using principal component analysis and Tanimoto similarity calculations. From the 200 synthesised library compounds, a representative selection was screened for hERG activity, whilst a broad range of measured ElogD values reflected the effort in maximising calculated physicochemical values (*e.g.*, clogP) during *in silico* library design. All of the library compounds have been submitted to the Haworth Chemically Enabled Compound Collection (HC^3), a collaborative screening collection which is maintained by the Birmingham Drug Discovery Hub. Biological screening of these compounds against *Mycobacteria* and representative ESKAPE pathogens is planned for the near future.

Dedicated to everyone who has supported me in the past four years:

intellectually, practically,

and emotionally.

ACKNOWLEDGEMENTS

First of all, I'd like to thank Dr Liam Cox and Dr Kimberley Roper. As my academic supervisors, you have consistently challenged me to think critically about my results, my progress and my next steps. By asking the difficult questions, you have not only helped me to write a well-grounded thesis, but also shaped me into a way better researcher than I was four years ago.

Second, I'd like to thank Dr Jorg Benningshof for facilitating the cooperation between The University of Birmingham and Symeres in The Netherlands. I have enjoyed my work at Symeres as a PhD student, and I'm very glad to continue my journey there as a Senior Scientist in the Medicinal Chemistry group!

Many thanks to all the people who have helped to generate the data for this thesis, either by running the assays, purifications, experiments or analyses, or by enabling me to do so myself. So thank you Dr Louise Male, Dr Michael Morton, Dr Christopher Williams, Dr Cécile Le Duff, Dr Chimed Jansen and everyone of the Symeres Analytical Facility; without you, my experimental section and appendices would have been way shorter.

The Symeres' Parallel Chemistry Group deserve credit for helping me with my first steps in compound library synthesis, purification and data management, and by providing the well-appreciated ambience in the lab through bad jokes and maybe even worse Dutch music. In particular, I'd like to thank my mentor Wouter Nieuwstraten: your input has been invaluable for my work at Symeres and your passion for chemistry contagiously re-ignited mine. Sharing the joy of confirmed hypotheses and drawing out countless possible mechanisms or next steps on our fume hood sashes was not only useful, but also fun and motivating. As I'm a firm believer of sharing knowledge and excitement, our collaboration was a very pleasant alternative to the more introverted lab environment at Birmingham.

Before diving into the praise of my personal support network, I'd like to thank my current group leader Ruben Leenders, for giving me the space and flexibility to write up a part of my thesis at Symeres. It was nice to be able to share the stress of the PhD with someone has gone through it already, and your understanding of the burden of writing up prevented my combination of PhD and industrial work in the last few months to be even more stressful than it already was.

I'd also like to thank Ana Noble for providing me with an affordable room in Nijmegen (which turned out to be very rare,) pleasant conversations while curfews killed our social lives and the occasional delicious dish when I was too tired to cook for myself.

The Dutch/Flemish word for 'resilience' roughly translates to 'tensile strength' or 'elasticity'. The metaphor is easily made, and over the past four years I can say in all honesty that my spring has been stretched often, sometimes far out for a prolonged time. Throughout those times, I have been blessed with the people around me, who helped me carry the weight that was attached to my spring, preventing my string from breaking. As much as one's resilience may depend on inner motivation and mindset, I think we must not underestimate the vital role of a good support network. For me, Belgian psychiatrist Dirk De Wachter hammered the nail:

"Resilience does not come from within. It is the spring between people.
We get our resilience from the network that carries us."

Therefore, this thesis belongs not only the people who's efforts translated into the data reported in this thesis. Many people have allowed me to perform at my peak capacity, or to keep my head up when things got tough. In this way, these people have contributed significantly my work too. Hence, I don't want to spare any effort in thanking them, making sure that their contributions also transpire in this work, in the form of the following well-deserved lines in the acknowledgement section.

Many thanks to my fellow iDESIGN PhD colleagues, for helping me out both professionally and personally: Órla and Alessandro, it's been great to have you with me in The Netherlands. I have greatly enjoyed our evenings on the boat bar on the river Waal, the years-long Whatsapp group chat exchanging rants, Dutch culture shocks, questions and fine humour; sharing our experiences as isolated PhD students in a foreign country during a pandemic most definitely made the solitude more bearable. Daniel (Dani), starting off together with the same academic supervisors and a shared fume cupboard, we were bound to bond, and boy, did we! I am so glad to have spent my best moments in the UK with you: the music festivals, nights out in Moseley, weekly bouldering sessions and our legendary ascent of mount Snowden via Crib Goch, these are moments that I cherish. You are one of the people that have seen me at my highest (literally) but also at my lowest. I owe you a lot of gratitude for listening, motivating or simply distracting me when I needed it. Gaining you as a friend has been one of the major perks of my PhD! Very much looking forward to meeting in Berlin again.

Daniel (Dan), originator of the 'happy Friday' text message as a way to keep in touch, my spirit guide. Throughout my PhD you have given me precious relationship/work/life advice, and I will never forget our jam sessions with Ale on bass and Dani on the ukelele, sharing our passion for music has been one of the things that kept me going in Brum!

Marjolaine, Nick and Mat, together with Dan and Dani you helped to keep me sane in Birmingham, pulling me out of the often-stressful work environment to enjoy a good plate of Chinese food or falafel for lunch. Marjolaine's drama-exchange lunch talks, Nick's Halloween parties and Mat's slow-cooked minted lamb after a long night out with the gang have become core memories of my time in Birmingham. Thanks for those!

Without a doubt, I'd like to thank my original support crew aka my family. Mama, Papa & Sara, Jonathan & Melissa, Moe and Va, thank you so much for standing by me. It must have been difficult to hear me stressed out/overworked/isolated for weeks on the phone, knowing you couldn't come over. However, your help in moving abroad, administration and logistics, cooking recipes or simply the warm welcome when I came back to Belgium for the holidays or weekends (or for a few months when the world was in lockdown) always enabled me to jump back into my work with renewed energy, knowing you would be there when I needed you.

René and Margriet, Petra and Bert: when home in Belgium was too far away or impossible to access due to COVID-19, you too managed to provide a warm nest where I could escape to with Sofia, and I am very glad that I got to share this journey with you.

Dear Homies; Kobe, Els, Florian, Arno, Jasmien, Joren, Nelis, Nona, Klaas, Rory, Sebastiaan and Eva; Marijn, Lin and Sanne; all my friends from Scouts Averbode; it's been a shame that we didn't get to see each other often, but I am incredibly happy that we're all staying in touch. Thanks to all who paid me a visit in Birmingham or Nijmegen, thanks to everyone who gave me a random call or text to check how I was doing and thanks to everyone who sent me a motivational video for the surprise 'project Sam Support'! I'm looking forward to seeing you all again more often, we will most certainly celebrate together after graduation!

My dear Sofia, you have been incredible. I still can't imagine how lucky I am to have met you in the middle of a pandemic, having made almost no other contacts in Nijmegen in the last two years (except your friends of course). The patience with which you tolerated me working late, working evenings and weekends for months, whilst making sure dinner was served every evening and the laundry was done… Words fall short to express my gratitude for that. Living together with you has been an absolute dream and I am 100% convinced that without you, I would have submitted way later, possibly in a much poorer mental state. With you by my side, I feel like I can conquer the world, and I can't wait to share my future adventures with you, whatever those may be!

Thank you all, sincerely.

TABLE OF CONTENTS

LIST OF ABBREVIATIONS

3D	3-dimensional
Ac	acetyl
aq	aqueous solution
BAST	deoxofluor
BB	building block
BBB	blood-brain barrier
Bn	benzyl
Boc	*tert*-butoxycarbonyl
BP	byproduct
BR	Bredereck's reagent
bRo5	beyond Lipinski's Rule of Five
Bu	butyl
cat	catalytic amounts
cpds	compounds
CuAAC	copper(I)-catalysed azide-alkyne cycloaddition
DAST	diethylaminosulfur trifluoride
DBU	1,8-diazabicyclo[5.4.0]undec-7-ene
DCE	1,2-dichloroethane
DMAP	*N,N*-dimethylaminopyridine
DMF	*N,N*-dimethylformamide
DMF-DMA	*N,N*-dimethylformamide dimethyl acetal
DMSO	dimethyl sulfoxide
DPPA	diphenylphosphoryl azide
DW	DataWarrior
ECFP6	extended-connectivity fingerprint (diameter of 6 bonds)
EDC	*N*-ethyl-*N'*-(3-dimethylaminopropyl)carbodiimide
ELSD	evaporative light scattering detector
eq	equivalent
ESI	electrospray ionisation
Et	ethyl
EU	European Union
EU-EID-ITN	European Industrial Doctorate Innovative Training Network
FCFP6	functional class fingerprint (diameter of 6 bonds)
FDA	Food and Drug Administration
Fmoc	Fluorenylmethyloxycarbonyl
FTIR	Fourier transform infrared spectroscopy
GABA	γ-aminobutyric acid
G-II	Grubbs II catalyst
HC^3	Haworth Chemically Enabled Compound Collection
hERG	human ether-à-go-go-related gene
HG-II	Hoveyda-Grubbs II catalyst
HPLC	high-performance liquid chromatography
HRMS	high-resolution mass spectrometry

IC$_{50}$	half maximal inhibitory concentration
i-Pr	isopropyl
LCMS	liquid chromatography mass spectrometry
LRMS	low resolution mass spectrometry
m/z	mass-to-charge ratio
Me	methyl
mPTP	mitochondrial permeability transition pore
n.a.	not applicable
NBS	*N*-bromosuccinimide
NMR	nuclear magnetic resonance
PCA	principal component analysis
PDA	photodiode-array detection
PhD	philosophiae doctor, Doctor of Philosophy
PMI	principal moment of inertia
p-PTS	pyridinium *p*-toluenesulfonate
Q-NMR	quantitative nuclear magnetic resonance (spectroscopy)
quant.	quantitative yield
R	substituent/moiety/amino acid residue
RCM	ring-closing metathesis
R$_f$	retention factor
RM	reaction mixture
Ro5	Lipinski's Rule of Five
RORγt	retinoic acid receptor-related orphan receptor γt
rt	room temperature
rxn	reaction
SFC	supercritical fluid chromatography
SM	starting material
t-Bu	*tert*-butyl
Tc$_{max}$	maximum Tanimoto similarity
TdP	Torsades des Pointes
TFA	trifluoroacetic acid
THF	tetrahydrofuran
TLC	thin-layer chromatography
TPSA	topological polar surface area
tR	retention time
UPLC	ultra high performance liquid chromatography
UV	ultraviolet (electromagnetic radiation, approximately 10–400 nm wavelength)
UVA	ultraviolet radiation with wavelength 315–400 nm
XRD	X-ray diffraction

DECLARATIONS

All work reported in this thesis was performed by the author, with the following exceptions: X-ray crystallography and crystal structure determination was performed by Dr Louise Male at The University of Birmingham. Compound purification *via* preparative reverse-phase chromatography and supercritical fluid chromatography (SFC), ElogD measurements, determination of chloride ion content, high-temperature and ^{19}F-NMR spectroscopy were performed by the Symeres Analytical Facility. High-resolution mass spectrometry was performed by Dr Christopher Williams at The University of Birmingham, and by the Symeres Analytical Facility in Nijmegen. hERG screening was performed by Dr Michael Morton at ApconiX. The KNIME workflows reported in this thesis were constructed by the author but benefited from review by Symeres' former Principal Computational Scientist, Dr Chimed Janssen.

CHAPTER I: GENERAL INTRODUCTION

1. Introduction

1.1. Past trends in drug discovery

The research described in this dissertation focuses on the synthesis of novel compounds with desirable properties as potential starting points for drug discovery. Throughout the past decades, the field of drug discovery has seen both innovation and the emergence of biases. An analysis of trends unveiled key drivers for our research, enabling the planned synthetic project to be relevant for drug discovery by addressing known challenges and taking advantage of innovations that have resulted in increased output of new drugs.

1.1.1. 1950 – 2012: Decreased R&D efficiency

In 2012, Scannell *et al.* proposed that the overall productivity of drug discovery had declined over the past six decades.[1] Although the average number of new approved drugs each year remained constant over the period, the requirements for demonstrating efficacy and safety increased.[2,3] This led to high attrition rates for experimental drugs in the drug discovery pipeline, demanding greater investment for the same return: between 1950 and 2012, the amount in US dollars spent on research and development (R&D) for an approved drug doubled almost every nine years, leading to an 80-fold decrease in R&D efficiency after taking into account inflation (Figure 1).[1,4]
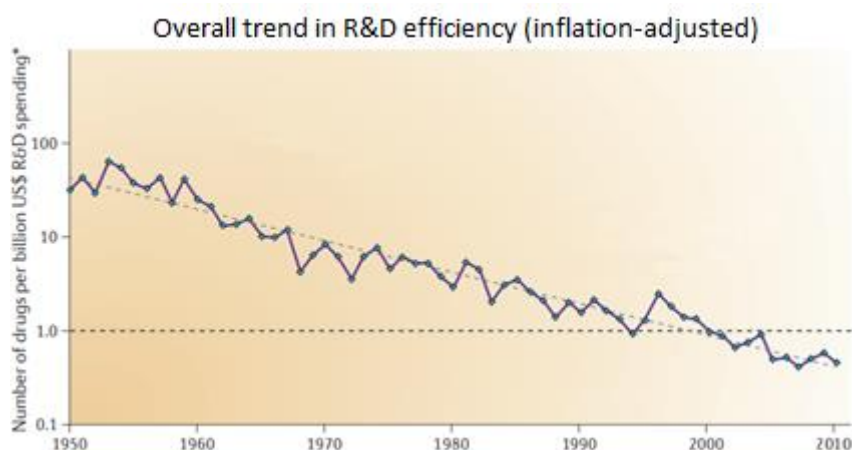
Figure 1: Overall trend in R&D efficiency between 1950 and 2012.[a]

---

[a] Graph adapted from Scannell *et al.*[1]

To stay attractive to investors and to continue delivering new, high-value medicines, it is of great importance for the pharmaceutical sector to critically evaluate their strategies in order to identify current flaws and biases and hence opportunities for improvement. For example, Lipinski's Rule of Five has been a dominant strategy for informing the design of orally bioavailable small-molecule drugs, but an over-reliance on these guidelines may have limited the opportunities for difficult targets.[5]

1.1.2.   Lipinski's Rule of Five

In 2001, Lipinski *et al.* published a review, comparing the physicochemical properties of 2245 phase II orally bioavailable drug molecules.[6] Since phase II drugs have passed the first round of clinical trials and all pre-clinical trials,[7] Lipinski hypothesised that these compounds would exhibit optimal physicochemical properties for good absorption and cellular permeability, necessary for oral bioavailability. Their analysis resulted in the 'Rule of Five', a set of guidance values to predict poor absorption or cellular permeability for small-molecule drugs (Figure 2).[6]

Small-molecule drugs are more likely to show poor absorption or cellular permeability when:

MW > 500

LogP > 5

Number of H-bond acceptors (N or O) > 10

Number of H-bond donors (NH or OH) > 5

Figure 2: Lipinski's Rule of Five.[6]

Compounds with properties that exceed more than one of these set ranges are thus expected to exhibit poor oral bioavailability. Although the Rule of Five provides a good rule of thumb for assessing the oral bioavailability and cell permeability of a small-molecule drug, many exceptions to this rule have been found, including successful, approved drug molecules and substrates for active transport.[6] Taking Lipinski's Rule of Five as a hard criterion for drug development also significantly limits the opportunities for drug discovery, potentially missing out on promising targets such as protein-protein interactions,[5] while molecules can also be formulated for alternative administration routes. As a result, more interest has emerged towards developing molecules beyond the Rule of Five (*e.g.*, macrocycles),[8] as these may

provide new opportunities to discover drugs acting upon novel targets which may have been considered previously as non-druggable or hard-to-drug.[2]

1.1.3.   Avoiding risk by recycling knowledge

With so much time, money and resources at stake, the pharmaceutical industry has tended to stick with known targets and drug molecules, minimising risks of the unknown. This tendency was illustrated by Rask-Andersen and co-workers in 2011, who showed that almost half of all marketed drugs share a similar target-interaction profile, exploiting only a limited part of the proteome.[3] By matching 989 drugs with their 435 targets, the established drug–target network showed higher connectivity between older drugs and targets, in contrast to more isolated, smaller networks for novel targets and drugs. This analysis showed that the sector is prone to building further on thoroughly studied targets and interactions. In this way, the pharmaceutical sector not only neglects opportunities to explore new biological targets, but also to potentially develop novel mechanisms of action.[3]

This bias for de-risking research by building on prior knowledge rather than broadening and exploring new drug targets and interactions also translates to the molecule: in 1996, Bemis and Murcko compared 5120 drug molecules and showed that half of these could be described by just 32 frameworks.[9] In a similar study, Siegel and Vieth found that 30% of all drugs in their dataset (1386 marketed drugs) contained other drugs within their building blocks.[10] In 2009, Wang and Hou compared two other databases of 1240 and 6932 drug molecules, and found that 53% and 59% of all drugs in these databases, respectively, consisted of the same 50 fragments.[11] An analysis of the FDA Orange Book[a] by Taylor in 2014 showed that all marketed drugs before 2013 contained only 351 unique ring systems, covering only 2% of all possible combinations of known monocyclic and bicyclic ring systems (Figure 3).[13,14] Analysis also found that 83 of the 100 most frequently used ring systems in drugs were originally found in drugs developed before 1983[14] and although every year, on average six new ring systems are published, less than a third of new drugs contain new ring systems each year.[14] Although there is always a delay in novel chemistry filtering through to any application, these findings show that medicinal chemistry has tended to focus on only a small fraction of chemical space, using well established molecular frameworks.

---

[a]"Approved Drug Products With Therapeutic Equivalence Evaluations", also known as the Orange Book, contains a list of all drugs which are currently approved by the United States' Food and Drug Administration (FDA).[12]
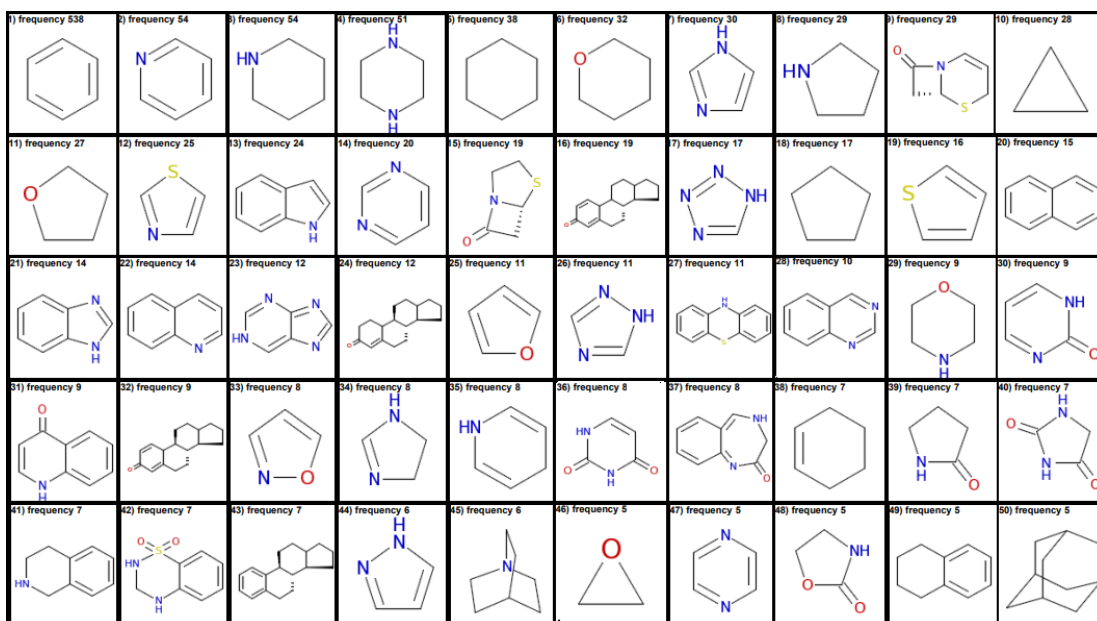
Figure 3: The top 50 most frequently used ring systems in marketed drugs, according to Taylor's analysis of the FDA orange book.[a]

Taylor *et al.* stated that it is likely that 70% of all future drugs will consist of previously established structures,[14] illustrating that drug discovery scientists typically favour a pragmatic approach over exploratory studies, prioritising the exploitation of known chemically validated space.[13] Reflective of this tendency, only 1.4% of all theoretical chemically feasible ring systems have been synthesised so far,[15] and every year only 5–10 novel ring systems are being published in literature.[16] Therefore, there are plenty of novel molecular frameworks for medicinal chemists to explore, which may not only provide excellent opportunities for developing novel compounds, but also for the identification of new targets and ultimately new drugs. One way of accessing novel frameworks is by introducing more sp[3] carbons.

1.1.4. Opportunities through increased saturation

In 2009, Lovering showed that as a compound advances through the various phases of drug discovery and development, the average fraction of sp[3] carbons (Fsp^3) in a molecule increases, illustrated by a 33% enrichment in the number of stereocentres from the initial discovery phase to the marketed drug.[17] The correlation between saturation and the likelihood of a molecule becoming a drug can be rationalised. As the average fraction of sp[3] carbons increases, so does

---

[a] Figure adapted from Taylor *et al.*[14]

the complexity of the molecule,[a] giving access to an increased number of different shapes and conformations, possible isomers and out-of-plane substituents. In this way, increased saturation allows a molecule to cover a more diverse chemical space, potentially increasing the complementarity between the receptor and ligand. Increasing the F_{sp^3} of a molecule also increases aqueous solubility, which is an important physicochemical property in drug discovery.[17] Increased saturation may therefore improve the potency and selectivity for a given target.[b]

Important to note is that increasing saturation provides significantly more possible isomers of a molecule while minimally changing its molecular mass (Figure 4). Given that 40% of the current drugs in 2014 did not contain a single sp^3 carbon in their ring systems,[14] introducing more saturation in ring systems of future drugs will explore and exploit underexplored chemical space and hopefully result in greater success for drug discovery.
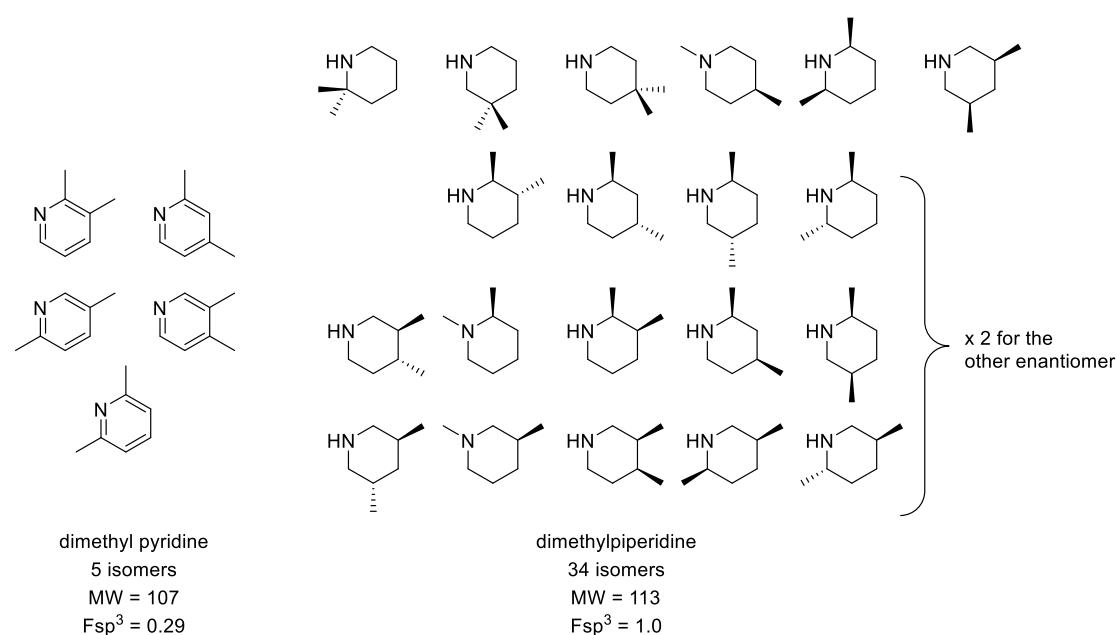
Figure 4: Saturating the pyridine ring turns a flat scaffold into a three-dimensional piperidine ring, significantly increasing the number of possible isomers. MW: molecular weight. Fsp^3: fraction of sp^3 centres in the molecule.[c]

---

[a] Whilst this is true for analogues of an investigated molecule, Fsp^3 cannot be used to compare the complexity of structurally unrelated products: A large, complex molecule may have the same Fsp^3 value as a small, simpler molecule which happens to have the same average fraction of sp^3 carbons.[18]

[b] Access to more and different shapes can allow a molecule to bind to more substrates and hence increase the chance of off-target interactions. However, increased saturation also provides more opportunities to differentiate a hit molecule, which can result in increased potency and selectivity.

[c] Figure adapted from Lovering *et al*.[17]

1.1.5.   Over-representation of rod- and disc-like shapes

Having shown the molecular bias on current drug scaffolds and highlighted the advantages of increased three-dimensionality, it is interesting to explore the extent to which this bias has an influence on the chemical shape space occupied by today's drug compounds. One way to assess this space is by using a normalised principal moment of inertia plot where based on its principal moment of inertia (PMI), a molecule's shape can be described as rod-, disc- or sphere-like.[19] In 2016, Brown and Boström analysed a selection of bioactive molecules with drug-like properties from the ChEMBL database. They showed that the chemical shape space covered was biased, with the rod-like and disc-like corners of the PMI plot densely populated, and sphere-like compounds heavily under-represented (Figure 5).[20, a]
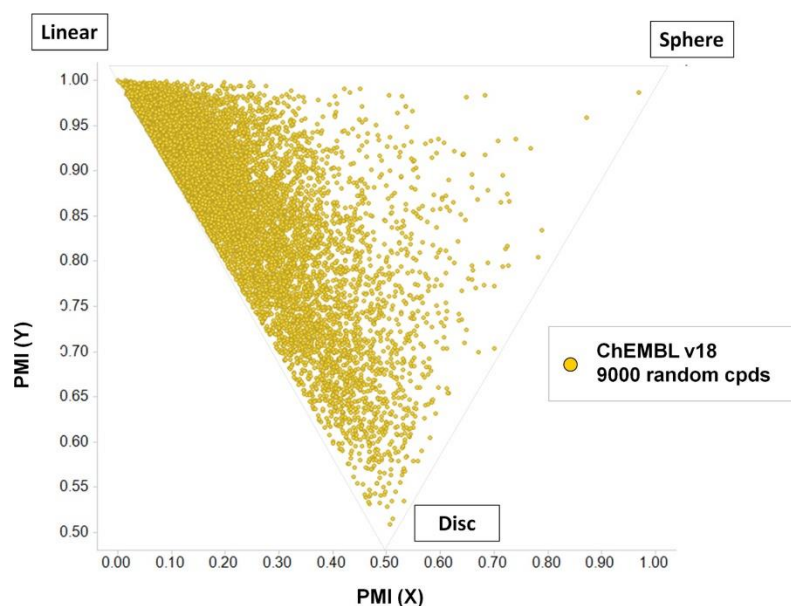
Figure 5: PMI plot for a random selection of 9000 compounds from the ChEMBL database, showing the bias towards rod- and disc-like shapes.[20] Cpds: compounds.

This bias may be expected for any dataset, since there are many more ways to synthesise rod-like and disc-like molecules than sphere-like molecules.[20] However, this does not mean that this bias cannot be mitigated. Brown and Boström reported in 2018 that more than 80% of all reactions used in medicinal chemistry[b] could be attributed to just five reaction types, of which

---

[a] The ChEMBL database contains bioactive molecules with drug-like properties, but these are by no means all marketed drugs. Hence, Brown and Boström suggested that venturing out of the rod-disc space could be an advantage for medicinal chemistry, but made no claims about the relationship between 'flatter' molecules and the chance of attrition or low bioactivity.
[b] The authors compared reactions from a manual extraction of the literature, for a representative set of papers from the Journal of Medicinal Chemistry, Journal of the American Chemical Society and Angewandte, sourcing authors from both academia and industry.

three (covering 64% of all reactions) use aromatic systems or generate sp^2 centres (Figure 6). Increasing the use of complexity-generating reactions and new reaction technologies, such as enantioselective biocatalysis and photochemistry, may therefore increase the amount of sphere-like molecules, thereby reducing the over-representation of rod-like and disc-like molecules.[21]
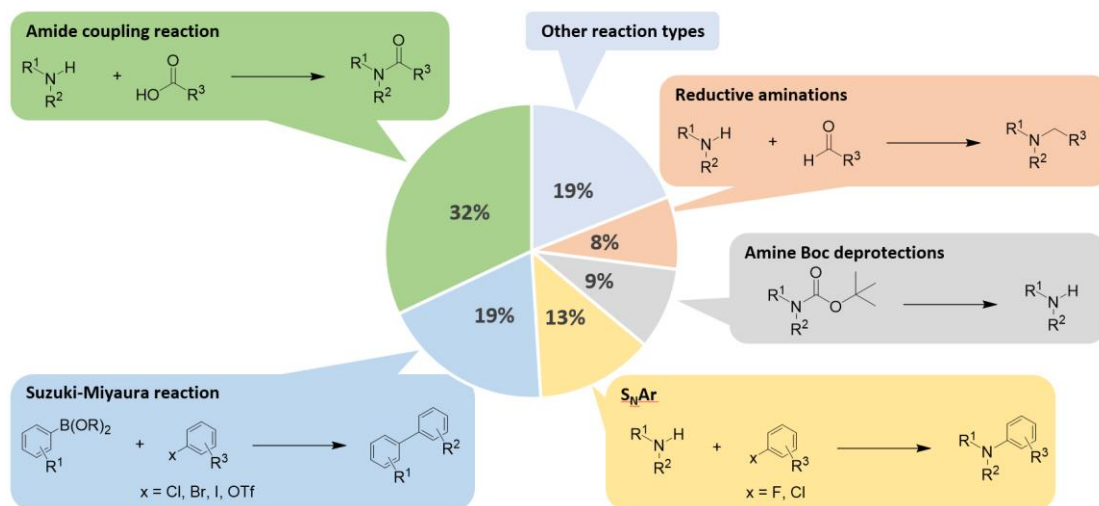
Figure 6: 81% of all used reactions in medicinal chemistry can be attributed by five reaction types.[21]

There is a large body of evidence for the current bias in medicinal chemistry. As illustrated above, pharmaceutical research tends to stick with known targets and drugs, elaborating on what is known and low risk, rather than exploring and expanding new druggable biological and chemical space. As a result, the systematic preference for a low number of robust reactions and frameworks has led to a lack of structural diversity in today's drug libraries, with an over-representation of sp^2-centres and well-established scaffolds, covering only a small fraction of the available chemical space.

Although some of the key principles of medicinal chemistry may have contributed to the current bias, the sector has nevertheless still discovered effective targets and delivered many potent drugs, improving the lives of countless people. Therefore, it wouldn't necessarily be wrong to keep some of the current standards and approaches, namely to target small molecules with high potency, which are easy and efficient to synthesise, and can be obtained from abundant starting materials. What could be beneficial though, is to broaden the approach and seek inspiration out of the (known chemical) box.

1.2.   Diversity-Oriented Synthesis

1.2.1.   Mimicking and transcending Nature's diversity

Venturing outside of the known (well established) chemical space in drug discovery, one may question whether this underexplored space is actually biologically relevant.[22] The answer can be found in the known plethora of biomolecules; billions of years of selection pressure have optimised the interactions between receptors, ligands, enzymes, substrates and inhibitors, with high potency and specificity in every interaction for both binding partners. Since the earliest days of medicine, natural products have been widely used and studied to treat various diseases.[23] Natural products typically contain many sp^3-centres, stereogenic elements and diverse frameworks, highlighting that there is plenty of biologically relevant chemical space for medicinal chemistry to expand into.[24]

In 2000, Schreiber presented the concept of Diversity-Oriented Synthesis (DOS).[25] The aim of DOS is to create in a high-throughput manner libraries of small-molecule compounds, with the features and overall appearance of natural products, without necessarily synthesising only natural-product analogues.[26] In this way, DOS purposefully breaks the link between natural selection and the generation of natural product-like compounds, as structurally diverse molecules can be obtained without a natural analogue,[24] thus exploring currently under-represented regions of chemical space.[27] DOS aims to provide libraries with maximum stereochemical and skeletal diversity *via* efficient synthetic pathways (ideally three to five steps).[24,27,28] Some existing preferences in medicinal chemistry can thus still be maintained: using short reaction pathways, small-molecule libraries can be generated, which are easy to access from readily available reagents and amenable to further post-screening optimisation. In the last two decades, DOS libraries have yielded many novel inhibitors in fields such as oncology, antimalarials and antidiabetics, highlighting DOS as an attractive synthetic strategy for drug discovery.[29–32]

1.2.2.   Diverse library generation and synthesis

Library synthesis using DOS not only provides a way out of the biased medicinal chemistry chemical space, but also facilitates screening for new targets, drug scaffolds and mechanisms of action. Hence, DOS can be used to generate prospecting libraries, with maximum novelty and structural diversity; this approach is in contrast to the classical, focused, target-oriented libraries, which contain analogues of a known bioactive compound, and which are useful for

obtaining structure-activity relationships. Since nothing is known *a priori* about the possible target or mechanism of action, an ideal prospecting library should allow functionalisation or structural change at every position in the library compound. In this way, any aspect of the compound, be it ring size, substitution or stereochemistry, can be systematically changed and optimised to achieve maximum potency and selectivity (Figure 7).[24] In order to facilitate this, DOS steers away from target-oriented synthesis, using a different synthetic approach.
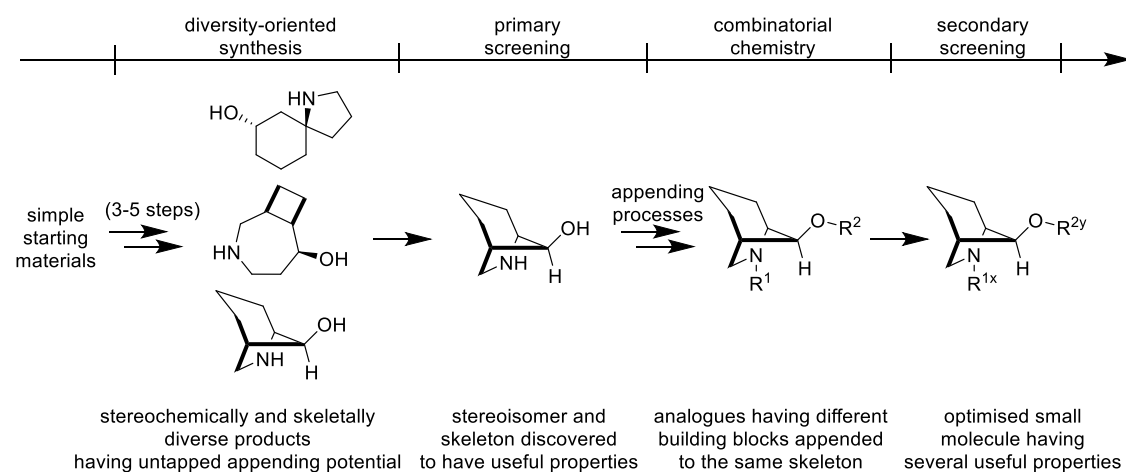
Figure 7: DOS can be used to develop stereochemically and skeletally diverse libraries of small-molecule compounds, amenable to post-screening optimisation.[a]

Target-oriented synthesis (TOS) typically uses the retrosynthetic approach, working backwards from a target compound towards readily available building blocks and creating convergent pathways. DOS tries to develop maximal diversity, starting from carefully chosen starting materials and reagents, and hence demands a chemist to think in terms of forward synthesis. Utilising complexity-creating reactions (such as multi-component reactions, cycloadditions, ring-opening and ring-closing metathesis) and divergent pathways can maximise the diversity of structures that can be obtained in a few steps from given starting materials. Each product should therefore preferentially be able to act as a substrate for subsequent reactions, allowing further divergent pathways *via* split-pool synthesis and/or combinatorial chemistry.[28]

1.2.3.   *Obtaining diversity*

In DOS, diversity can be obtained on three levels:[28]

1) Appendage diversity is obtained by decorating a common core scaffold using combinatorial chemistry. Differentiation *via* appendages does not change the basic structure of the scaffold.

---

[a] Figure adapted from Burke *et al*.[28]

In this way, various chemical functionalities may be appended to a scaffold, but all are similarly displayed in three-dimensional space, making this approach less attractive for prospecting libraries.[a] To achieve a more diverse display of chemical information, stereochemical and skeletal diversity need to be employed.[28]

2) Stereochemical diversity is achieved by increasing the number of possible relative orientations of potentially target-interacting elements, often by using diastereo- and/or enantioselective reactions. Stereochemical diversity can also be introduced in a combinatorial manner, by using different stereoisomeric precursors which can be combined with the use of chiral catalysts or reagents to overwrite possible substrate biases.[33] For example, the Schreiber group synthesised all four possible stereoisomers of α,β-acetylenic alcohol **2**, starting from the *R*- and *S*- enantiomers of phenylalanine analogue **1** (Scheme 1).[33] By using chiral Me-CBS-oxazaborolidine **3** as a catalyst, the stereoselectivity of the ketone reduction was dictated by the oxazaborolidine enantiomer used, overriding the steric influence of the adjacent benzyl-substituted stereogenic centre. For comparison, a 5:1 mixture of *anti*:*syn* diastereomers **2b:2a** was obtained upon ketone reduction of (***R***)-1 with $NaBH_4$ in MeOH.[33]
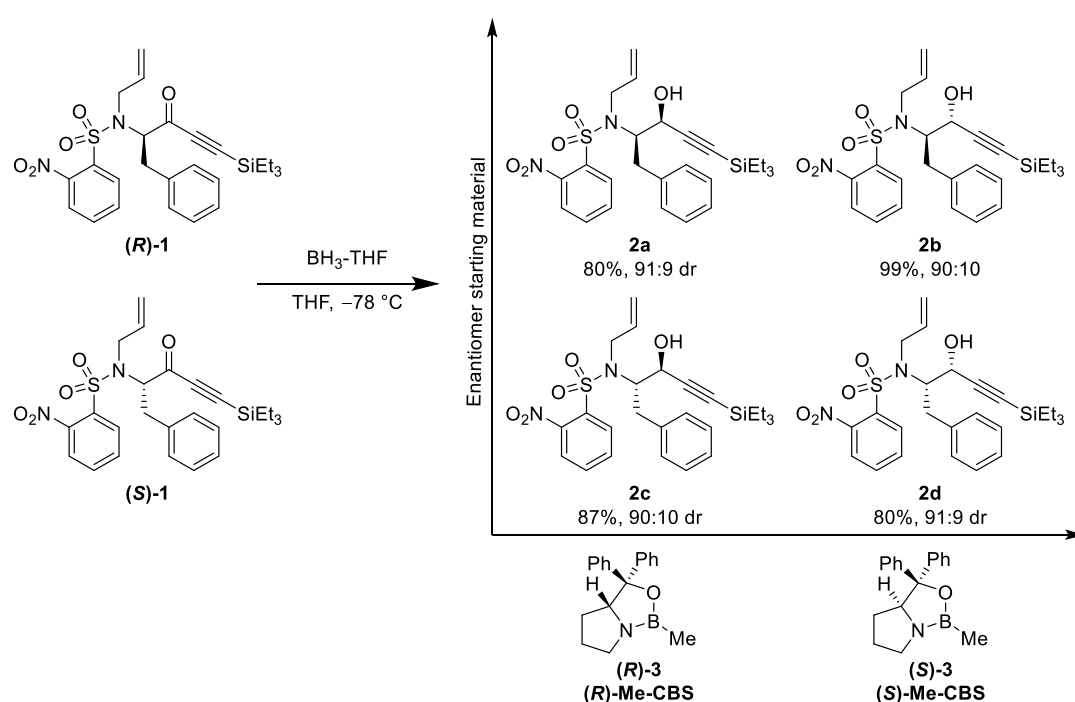
Scheme 1: An example of stereochemical diversity generated using a combinatorial approach, yielding four stereoisomeric products by using enantiomeric building blocks and both enantiomers of a chiral catalyst. [b]

---

[a] Nevertheless, once a hit has been identified, combinatorial chemistry and appending processes are important for exploring structure-activity relationships and optimising the drug-like properties of the hit molecule (Figure 7).
[b] Scheme adapted from Pizzirani *et al*.[33]

3) Skeletal diversity focuses on the generation of novel scaffolds, shapes and frameworks. One way to obtain skeletal diversity is to subject one substrate to different reactions, yielding different connections, functional groups and/or frameworks. This approach is termed 'differentiation' (Scheme 2). It can be difficult to obtain products using a differentiation approach which all have similar chemical reactivity and so can act as substrates for a subsequent general reaction. Therefore, another synthetic strategy is used more often: using different reactive appendages (σ, Scheme 2) on the same scaffold, a broad diversity of skeletons and frameworks can be obtained from a common reaction pathway, in a combinatorial manner. Since the structural information of the product is pre-encoded in the appendages, this approach is referred to as 'folding' (Scheme 2).[28]
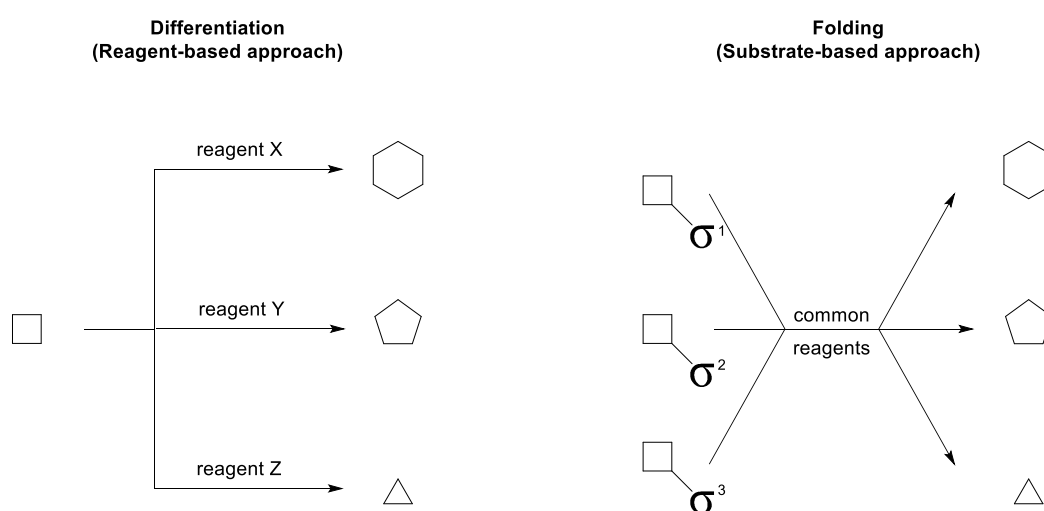
Scheme 2: Schematic representation of two approaches to skeletal diversity: either by differentiating or folding processes.[a]

---

[a] Figure adapted from Burke *et al*.[28]

A good example of the differentiation approach can be seen in the work of Sellstedt *et al.* who differentiated the peptidomimetic 2-pyridone **4**, using two electrophilic sites (Scheme 3).[34] First, nucleophilic substitution of the chloride moiety by *N*-Boc-Cys-OMe, Boc deprotection and reductive amination of the aldehyde gave fused eight-membered ring analogue **5**. Following a similar approach, nucleophilic substitution with NaN₃ and reductive amination with *N*-methyl propargylamine yielded 3-8-fused triazole analogue **6** after a thermal intramolecular Huisgen cyclisation. Finally, functionalised pyrroles **7** and **8** could be obtained using primary amines under mildly basic conditions.[34]
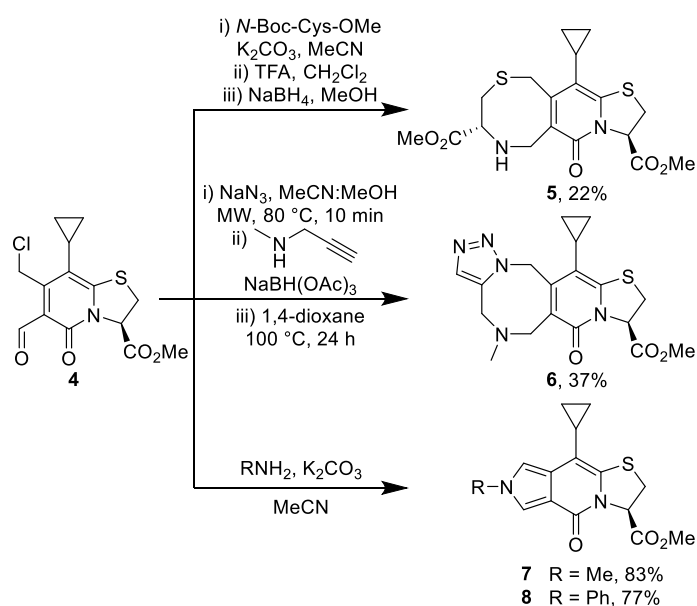
*Scheme 3: Differentiation of 2-pyridone analogue **4**, yielding various ring systems.[a]*

Folding can be achieved by identifying a relatively unreactive molecular core, which can react with its appendages after they have been transformed with a reagent. Folding strategies allow late-stage generation of new skeletons which facilitate the synthesis of functionalised scaffolds that may be difficult to obtain otherwise.[28] For example, using *N*-bromosuccinimide (NBS) and pyridinium *p*-toluenesulfonate (*p*PTS), furan **9** can undergo oxidative ring opening, yielding a *cis*-enedione intermediate (Scheme 4, A). Different molecular appendages can then react with the resulting carbonyl moieties, leading to skeletally distinct products. In this way, furan analogues **9–11** have been used to generate skeletally diverse products using solid-phase synthesis and a set of common reagents (Scheme 4).[35] First, furan **9** underwent NBS-mediated

---

[a] Scheme adapted from Sellstedt *et al.*.[34]

oxidative ring expansion, followed by bicycloketalisation, yielding the [3.2.1] bicycle **12**. Methyl analogue **10**, containing only one hydroxyl moiety, yielded an intermediate cyclic hemiketal following the same oxidative ring expansion reaction, which was then followed by a *p*PTS-catalysed dehydration, resulting in alkylidene pyran-3-one **13** as a single isomer. Since no hydroxyl group was present in acetylated analogue **11**, cyclisation was not possible after oxidative opening of the furan ring, resulting in isolation of the *trans*-enedione **14** after olefin isomerisation.[35]
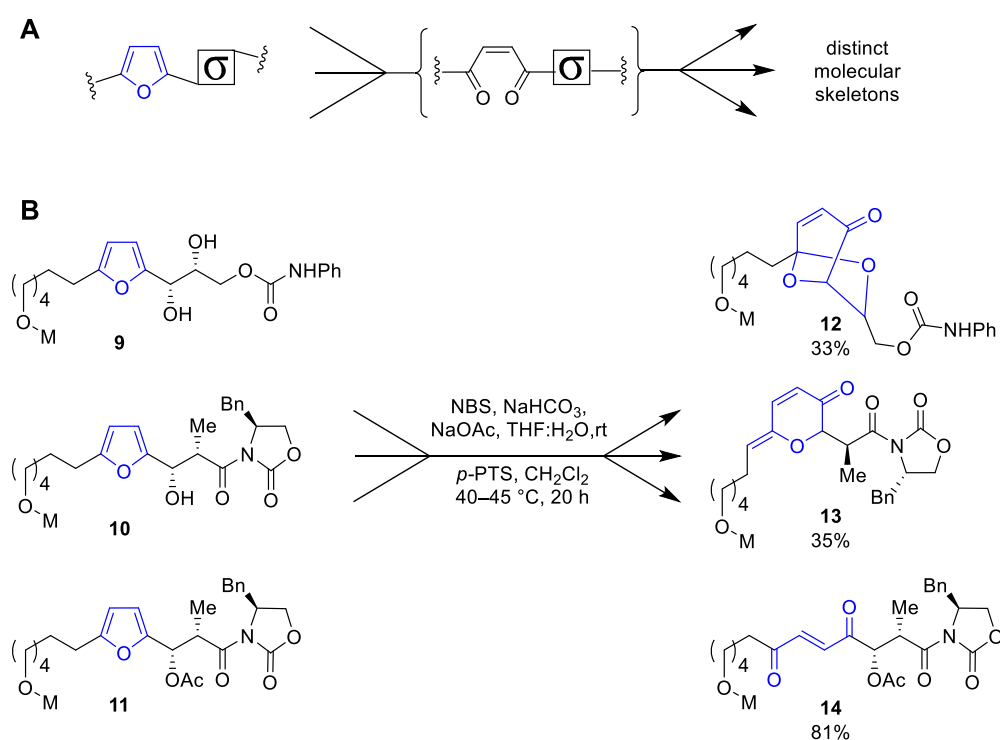
Scheme 4: A: General folding strategy: appended σ elements that pre-encode skeletal information yield skeletally diverse products under common reaction conditions. B: Example of a folding process. NBS: N-bromosuccinimide, p-PTS: pyridinium p-toluenesulfonate, M: polystyrene macrobead.[a]

Given that folding is substrate-dependent, at least two different appendages should be coupled to the core at different sites and functionalities, in order to pre-encode for a combinatorial matrix of skeletal structures.[28] Hence, the 'build-couple-pair' strategy is often followed, wherein appendages are added to the scaffold (build-couple), followed by intramolecular cyclisation (pair).[24] This approach was applied effectively by Lowe *et al*. to synthesise various fused azetidine scaffolds from parent scaffold **15** (Scheme 5).[36] During the build-couple phase, azetidine analogue **15** was synthesised bearing three reactive appendages, yielding multiple

---

cyclisation products during the pair phase. First, after trityl deprotection and subsequent mesylation of the alcohol, 4-6 fused scaffold **16** was obtained by nucleophilic substitution using the nosylamine (Scheme 5).[36] Alternatively, fused lactam **17** was synthesised *via* allyl deprotection using Pd(PPh$_3$)$_4$ and 1,3-dimethylbarbituric acid (1,3-DMBA) as an allyl group scavenger,[37] followed by cyclisation using BrCH$_2$COCl. Lastly, *N*-allylation of the nosylamine, followed by ring-closing metathesis yielded 4-8 fused azetidine **18** (Scheme 5).[36] Worth noting is that four stereoisomers of the azetidine starting material **15** were synthesised, allowing for simultaneous stereochemical diversification of the scaffold products, depending on which stereoisomer of **15** was used.
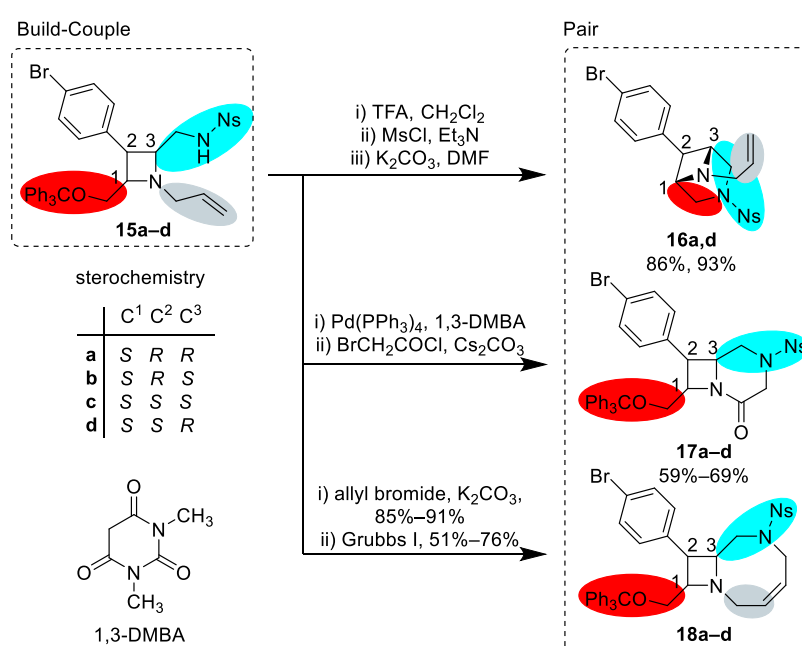
Scheme 5: Synthesis of diverse fused azetidine scaffolds, using the build-couple-pair strategy.[a]

As mentioned in Section 1.2.2, prospecting libraries obtained *via* DOS can be used to discover novel drugs, targets and modes of action. In order to discover these new targets and modes of action, a different screening method is required that is distinct from target-based screening methods.

---

[a] Scheme adapted from Lowe *et al*.[36]

1.3. Changing the screening paradigm

1.3.1. Target-based screening: concept and limitations

For over 25 years, target-based screening methods have been the primary approach in drug discovery.[38] Target-based screening methods start by identifying and validating a target, which plays a key role in the development and maintenance of a disease. Based on this chosen target, an assay is developed and applied in high-throughput screening methods. A hit is selected from the screened compound library and optimised by obtaining a structure-activity-relationship for analogues of the hit compound. The resulting lead compound(s) can then be further optimised for optimum drug properties such as absorption, distribution, metabolism, excretion and toxicity (ADME-tox), yielding a candidate molecule for further tests and clinical trials.[38]

Target-based methods have a few key limitations. Since target-based methods typically focus on the interaction with a single target, using *in vitro* assays, the chosen enzyme or interaction may not be the optimal target in the complex network of disease-causing drivers. Poor target validation can thus translate into unwanted side-effects upon inhibition of the target or an unforeseen bypass mechanism which allows for continuation of the targeted pathway despite inhibition of the target protein. Alternatively, the lead compound can exert undesired off-target activity, which does not often show up until undertaking *in vivo* assays.[39,40] Therefore, compounds obtained from target-based screening methods often suffer from high attrition rates in phase II and III clinical trials.[38] Bunnage even proposed that improved validation and selection of drug targets is the most important factor in decreasing the attrition rate of new drug molecules.[4]

Focusing on a single validated target on its own also limits the discovery of new targets. An analysis of all FDA-approved drugs in 2011 identified only 435 effective drug targets.[3] In contrast, the human genome consists of approximately 20,000–30,000 genes of which 3,000 have been linked to disease. Up to 1,500 of those genes are thought to express proteins which bind with small-molecule drugs,[41,42] indicating that there are plenty of opportunities to identify novel drug targets *via* an alternative screening strategy. Hence, instead of using biology as a starting point to identify compounds which can inhibit a potentially poorly validated target protein, the approach can be swapped around. Using chemistry as the starting point, (novel) targets can be identified which are inhibited by a compound from a diverse screening collection, potentially yielding not only novel drugs, but also novel targets. For this chemistry-first approach to hit identification, phenotypic screenings are the method of choice.

1.3.2. Phenotypic screening

Phenotypic screening methods do not rely on a single target and are therefore not limited by the need for a prior established mechanism of action. In this screening approach, a specific phenotype is identified which is characteristic for the chosen disease. Subsequently, an assay is developed which uses this phenotype to assess the progress and development of the disease, for example through parameters such as cell death, gene expression or increased bodyweight. The assay can then be used to screen for potential drug candidates.[38] A hit compound will change the observed phenotype in this assay, indicating its influence on the disease. Once a hit has been identified, elucidation of its mechanism of action is used to identify the affected biological target. In this way, phenotypic screening methods identify the target after hit identification, as opposed to target-based screening methods (Figure 8). Phenotypic screening methods are thus important for diseases where new targets are needed to reduce pressures of resistance generation, for example in antimicrobial-resistant bacteria, or for diseases which are currently hard to drug, such as Alzheimer's and Parkinson's disease.[38,43]

Target-based screening

| disease selection | target identification | develop assay | hit identification | lead optimisation |

Phenotypic screening

| disease selection | develop assay | hit identification | target identification | lead optimisation |

Figure 8: Comparison of target-based and phenotypic screening approaches.[a]

Phenotypic screening methods typically use cell-based assays, which means that any possible target-drug interaction occurs in a native cellular environment, making this approach more physiologically relevant than traditional *in vitro* target-based methods.[43] In an animal-based phenotypic screen, compounds are typically tested in small-animal disease models. This *in vivo* method can provide a lot of information on ADME-tox and the efficacy of a drug.[44] However, compounds with good lead properties (which could be optimised in a later stage) may not pass the primary screening.[38] Furthermore, the throughput of animal-based screening is low and ethical considerations regarding the use of animals can prevent or slow approval for the

---

[a] Figure adapted from Zheng et al.[38]

planned screening.[44] Hence, cell-based phenotypic screenings are favoured as the primary screening method.

Cell-based phenotypic screenings can combine the relevant biological complexity with a high-throughput screening (HTS) method.[45] Screenings can be performed in primary cells, cell lines or differentiated stem cells, and phenotypes can be assessed in three ways:

- Cell viability: an active compound may kill pathogens or cancer cells
- The expression of a reporter gene, such as β-galactosidase, green fluorescent protein and luciferase.[45] Reporter genes are used to assess signalling pathways, which allow interactions at any point in the pathway, with a single or multiple targets.[38]
- Specific disease phenotypes such as morphological change of cells or differential intracellular localisation of proteins.[38]

In 2011, Swinney and Anthony analysed the new molecular entities (NMEs) that were approved by the FDA between 1999 and 2008. Focusing on the first-in-class[a] small-molecule drugs, they found that 28 were obtained from phenotypic screenings, while only 17 came from target-based approaches (Figure 9).[47] Since target-based screening methods were the dominant strategy during this period, this analysis showed that phenotypic screening methods are more fit for first-in-class drug discovery.[47]
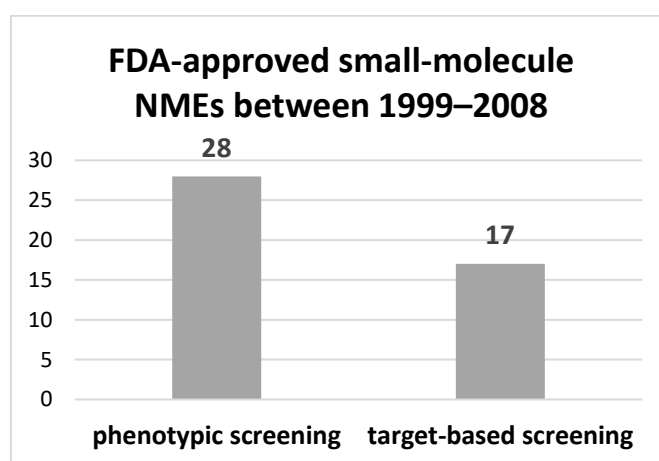
Figure 9: New FDA-approved small-drugs between 1999 and 2008, categorised by the used screening approach. NMEs: new molecular entities.[b]

---

[a] Drugs that have a new and unique mechanism of action for treatment of a medical condition are reported as 'first-in-class'.[46]
[b] Figure adapted from Swinney and Anthony.[47]

1.4.   Drug discovery in the last decade: increased innovation

The publication by Swinney and Anthony in 2011 led to a resurgence in phenotypic screening approaches in academia and industry (Figure 9),[47] and increased efforts to identify novel medicines and new mechanisms of action.[48] A particularly relevant example can be found in the identification of remdesivir **19** and chloroquine **20** as *in vitro* inhibitors of infection by the novel coronavirus (2019-nCoV) by Wang *et al.*: these compounds were tested in a phenotypic screen, which used Vero E6 cells infected with nCoV-2019BetaCoV/Wuhan/WIV04/2019.[48,49]
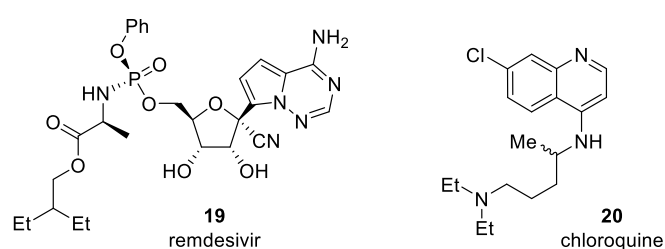
Figure 10: Structures of remdesivir and chloroquine, identified as inhibitors of 2019-nCoV infection through phenotypic screening methods.[49]

Whilst a superior screening method may maximise the chances of identifying a hit, the quality and nature of the compound library screened is also crucial for hit identification. The observed decline in R&D efficiency from 1950–2012 and established biases in drug discovery discussed in Section 1.1 illustrated that there was a need for more chemically diverse, sp^3-rich compound libraries for biological screening. In this light, the European Lead Factory (ELF) was set up in 2013 with the aim of delivering novel starting points for drug discovery.[50] Over the course of five years, this public-private partnership amassed over 500,000 compounds from pharmaceutical companies and small- and medium-sized enterprises (SMEs), including over 200,000 novel compounds synthesised through the ELF synthesis programme.[51] This compound collection was made available to SMEs, academia and charities for biological screening, overall generating a significant number of outputs: between 2013 and 2018, ELF yielded 8649 qualified hits, contributed to over 80 scientific articles and many patents on compounds for treatment of cancer, pain, infection and multi-resistant bacteria, and amassed over 40 crystal structures of target–compound complexes.[52] ELF has thus illustrated that continued efforts to synthesise novel molecules with drug-like properties can still be very successful.

In the past decade, new synthetic strategies have emerged for small-molecule drugs, aiming to produce more natural product-like drugs by building further on the principles introduced by DOS (Section 1.2.3, page 10). Privileged-substructure-based-DOS (pDOS), a strategy proposed by Kim *et al.*, aims to apply DOS principles whilst incorporating into the molecules privileged structures, which are frequently observed substructural motifs (*e.g.,* pyrimidines) found in various bioactive compounds with different modes of action.[53,54] Biology-oriented synthesis (BIOS), coined by Waldmann and co-workers, instead uses the core structure of a natural product as a scaffold for the synthesis of drug-like compound libraries.[55,56] Furthermore, Hergenrother and co-workers introduced the complexity-to-diversity strategy (CtD), which uses a natural product as a starting material for the production of semi-synthetic small-molecule compound libraries.[57] An interesting example of a bioactive semi-synthetic molecule is lefamulin **22**, an antibiotic for bacterial pneumonia, approved by the FDA in 2019 (Scheme 6).[58] Production of the natural product pleuromutilin cyclooctanol core **21** *via* fermentation allows for the scalable and economical synthesis of lefamulin **22**, requiring only three steps starting from the cyclooctanol.[59,60]

21
obtained by fermentation

22
lefamulin
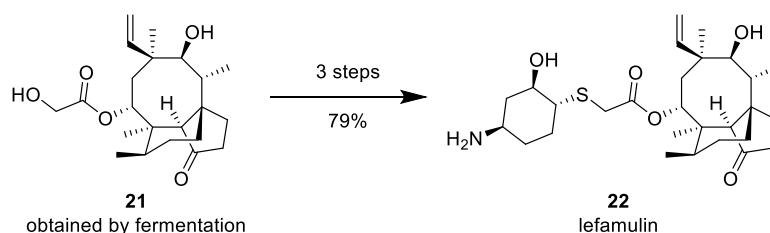
*Scheme 6: FDA-approved antibiotic lefamulin **22** is synthesised from natural product **21**, obtained by fermentation.[58–60]*

Initiatives like the European Lead Factory, new emerging synthetic strategies and a renewed interest in phenotypic screening have contributed to innovative approaches to drug development in the last decade, producing good results. Between 2009 and 2019 the median number of FDA approvals increased by 60%, from 25 to 40 new drugs per year compared to the previous decade, with first-in class drugs accounting for 37% of new approved drugs on average, compared to only 17% in 2009.[61] These numbers indicate that continued efforts to innovate in drug discovery can translate into an increased number of marketed drugs, assisting in averting the previously observed decrease in drug discovery efficiency.

1.5.   iDESIGN: generating novel compound libraries for drug discovery

In the previous sections, it has been shown that there are significant biases in drug discovery; increased pressure to progress and deliver safe and effective medicines has resulted in an over-reliance on classical chemistry and established frameworks, limiting the structural and chemical diversity in compound libraries. Inspired by the underexplored biologically relevant chemical space of natural products, diversity-oriented synthesis has emerged as a novel approach to library synthesis, maximising the functional, stereochemical and skeletal diversity of a library by subjecting well-chosen building blocks to complexity-generating reactions. Phenotypic screenings have proven to provide a suitable method for screening DOS-based compound libraries, as these do not require a known target or mechanism of action. The increased number of recent FDA approvals shows that there is still plenty of opportunity for new first-in-class drugs. New compound collections from collaborative platforms like ELF, built on innovative approaches to small-molecule drug synthesis, may facilitate continuation of this uptrend. Thus, diversity-oriented synthesis combined with phenotypic screening methods could provide the pharmaceutical sector with novel drugs and new targets, relieving medicinal chemistry from its bias by delivering first-in-class drugs which exploit currently underexplored chemical space. This conclusion resulted in the formation of iDESIGN, an EU-funded European Industrial Doctorate Innovative Training Network (EU-EID-ITN) involving The University of Birmingham, Symeres and AnalytiCon Discovery, which provided the framework and funding for the author's PhD research.

1.5.1.   *Overall project aims*

iDESIGN aims to design and synthesise novel compound libraries of structurally and functionally diverse, three-dimensional molecules with attractive physicochemical properties as starting points for drug discovery.[62] Library compounds made in the iDESIGN project will be added to the Haworth Chemically Enabled Compound Collection (HC[3]), which is maintained by the Birmingham Drug Discovery Hub. The Haworth Compound Collection collects together novel compounds made by researchers at The University of Birmingham, with the aim of supporting biological screening and hit generation for both internal and external collaborators.[63] By providing attractive novel compounds which probe underexplored chemical space, the iDESIGN project seeks to make a significant contribution to the Collection.

1.6.   Medium-sized rings: exploiting underexplored chemical space

One part of underexplored chemical space is occupied by medium-sized rings, defined here as eight- to eleven-membered ring structures. Given medium-sized rings are small enough to experience significant ring strain and destabilising transannular interactions, but large enough to experience significant entropy loss upon cyclisation,[64,65] their synthesis *via* cyclisation of linear precursors is often challenging.[66,67] As a result, medium-sized rings are under-represented in drug screening libraries, including the Haworth Compound Collection, and consequentially rarely found in marketed drugs.[67–69] For example, an FDA-approved subset of the DrugBank database comprising 632 compounds (used as a reference in Section 8.2, see Appendix 5.1) contains only one azocane derivative, whilst the virtual Haworth Chemically Enabled Compound Collection (5688 virtual compounds) contains only four azocane derivatives so far. Therefore, medium-sized rings present significant potential for the discovery of novel drug scaffolds and bioactive compounds.

Despite their under-representation in drug screening libraries, medium-sized rings occur frequently in natural products, including a range of bioactive eight-membered nitrogen heterocycle analogues such as cytotoxic lycopladine H **23**,[70] hepatotoxic otonecine **24**,[71] antimalarial (+)-decursivine **25**,[72] and actinophyllic acid **26**, an alkaloid which is used to treat cardiovascular disorders (Figure 11).[73] Although rarer, there are also examples of synthetic bioactive medium-sized ring analogues, which include the antiproliferative NB-IX-Gly44 **27**[74,75] and ROCK inhibitor H-0106 **28**,[76] illustrating that medium-sized rings can also yield bioactive molecules without having natural product analogues.
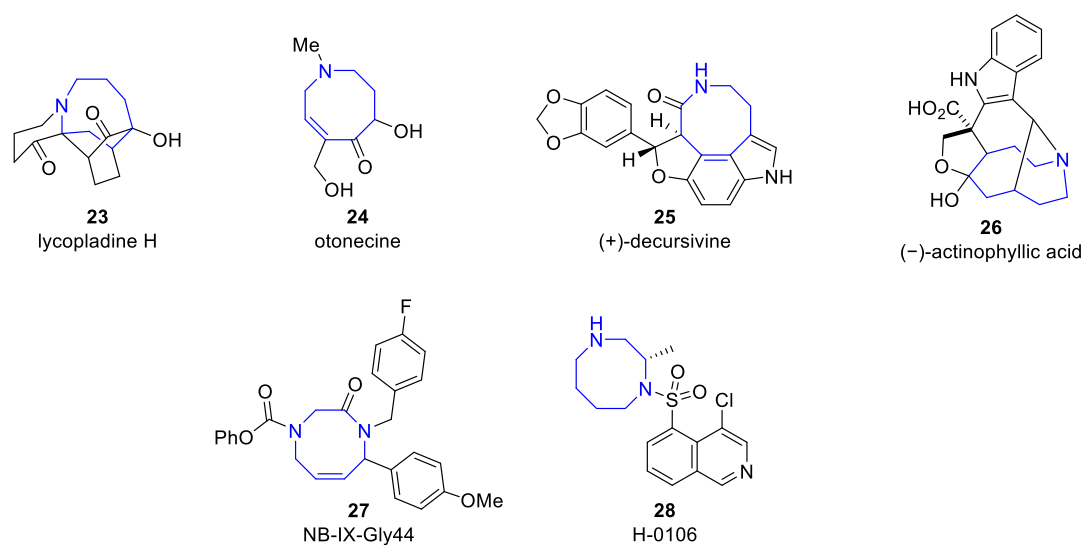
Figure 11: Bioactive natural and synthetic products containing medium-sized nitrogen heterocycles.

Medium-sized rings have specific properties that make them advantageous when considering compounds for biological screening. They are conformationally more flexible than three- to seven-membered rings. In this way, they can adopt more low-energy conformations than are available to smaller rings without big losses in free energy (Figure 12, A).[77,78] Incorporation of a heteroatom in a medium-sized ring or ring fusion will introduce a conformational bias: for example, azacyclooctanes prefer a boat-chair conformation, minimising transannular repulsion through pseudo-equatorial orientation of the N*H* proton (Figure 12, B).[79–81] However, the calculated 'gas-phase' lowest energy conformer of medium-sized heterocycles can differ significantly from the bioactive conformation, as the interaction energy upon binding a biological target may overcome conformational energy barriers.[82] Hence, a medium-sized ring can allow its appendages (and heteroatoms incorporated in the ring) to probe an overall larger volume of 3D space, increasing the probability for favourable interactions with a potential target and hence the chance of discovering new targets in phenotypic screenings. For these reasons, compound libraries of medium-sized ring analogues were considered an attractive addition to the iDESIGN project and Haworth Compound Collection, and so a suitable central medium-sized ring scaffold was sought.
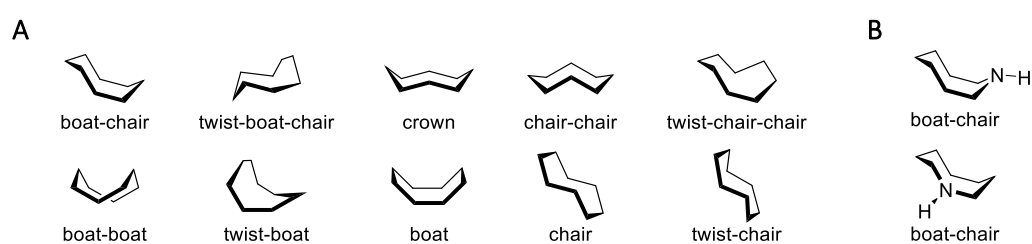
Figure 12: A: Ten theoretical conformations that can be adopted by an eight-membered ring.[77,78a] B: Low-energy boat-chair conformations of azacyclooctane.[80,81]

---

[a] Figure adapted from Pérez *et al*.[77]

1.7.   Azacyclooctenone: an attractive parent scaffold

In order to perform DOS on a medium-sized ring, a readily available core structure with multiple reactive sites was required. Using these reactive sites, skeletal diversity would be introduced from a common core *via* reagent-based differentiation approaches (see Section 1.2.3), yielding structurally diverse scaffolds with multiple reactive appendable handles. Functionalisation of these handles *via* parallel chemistry would then introduce appendage diversity, yielding diverse library compounds.

Azacyclooctenone **29** (Scheme 7) met this requirement as it was hypothesised the protected amine, ketone and double bond would allow for the synthesis of multiple diverse scaffolds. For example, the enone provides a polarised double bond, allowing for 1,4-additions and cycloadditions; the ketone can undergo direct nucleophilic attack, functional group conversion or yield fused bicycles through enol or haloketone intermediates, whilst the deprotected 2° amine can be functionalised to afford a diverse range of products, including sulfonamides, amides, 3° amines and ureas, all of which abound in therapeutic agents (Scheme 7). Given the synthesis of azacyclooctenone **29** had recently been reported by Morales-Chamorro and Vázquez in four high-yielding steps (see Section 2),[83] it was considered a suitable and valuable parent scaffold for diverse library synthesis.
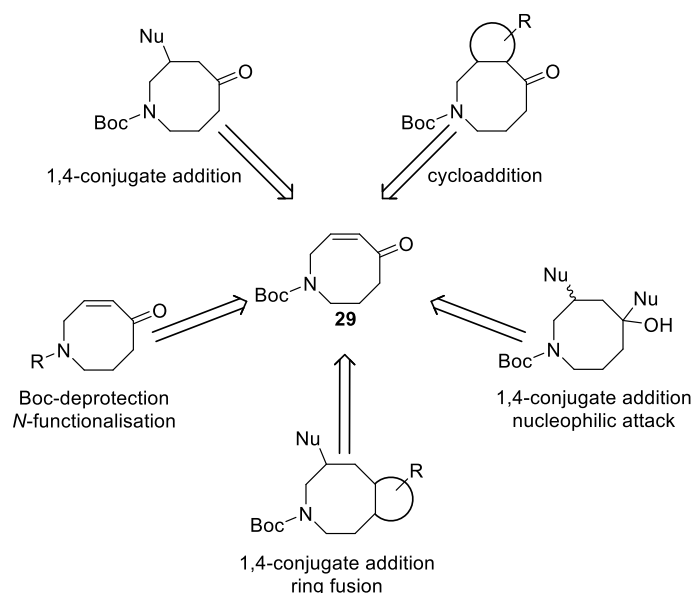
*Scheme 7: Some of the possible diversification strategies for parent scaffold **29**.*

1.8. Aims and objectives

With literature precedent for the synthesis of the selected parent scaffold **29**, our first aim was to reproduce the reported synthesis and scale up to gramme scale, to yield sufficient precursor for further derivatisation studies and library synthesis. Aiming to generate diverse compound libraries, *in silico* library design and validation would guide the choice of appendages and precursor scale-up, maximising the diversity obtained during library synthesis. Finally, experimental validation of the synthesised library compounds was planned to demonstrate their physicochemical and toxicological properties, illustrating their value as novel starting points for drug discovery.

Hence, the planned research had the following objectives:

- Establish a scalable synthesis of parent scaffold **29**
- Achieve skeletal diversification of parent scaffold **29** through exploration of possible chemistry on the embedded functionality
- Undertake *in silico* design and validation of diverse compound libraries
- Conduct library synthesis *via* parallel synthesis
- Validate library compounds experimentally

Once synthesised and validated, the obtained compound library would be submitted to the Haworth Compound Collection for screening against biological targets in the future, with screening against antimicrobial-resistant pathogens (the ESKAPE pathogens) and *Mycobacteria* envisaged as the first screens to be undertaken.

1.9. References

1   J. W. Scannell, A. Blanckley, H. Boldon and B. Warrington, *Nat. Rev. Drug Discov.*, 2012, **11**, 191–200.
2   B. C. Doak, J. Zheng, D. Dobritzsch and J. Kihlberg, *J. Med. Chem.*, 2016, **59**, 2312–2327.
3   M. S. Almen, H. B. Schioth, M. Rask-Andersen, M. S. Almén and H. B. Schiöth, *Nat. Rev.*, **10**, 579–590.
4   M. E. Bunnage, *Nat. Chem. Biol.*, 2011, **7**, 335–339.
5   B. C. Doak, B. Over, F. Giordanetto and J. Kihlberg, *Chem. Biol.*, 2014, **21**, 1115–1142.
6   C. A. Lipinski, F. Lombardo, B. W. Dominy and P. J. Feeney, *Adv. Drug Deliv. Rev.*, 2001, **46**, 3–26.
7   O. of the Commissioner, Step 3, https://www.fda.gov/patients/drug-development-process/step-3-clinical-research, (accessed 13 December 2021).
8   E. M. Driggers, S. P. Hale, J. Lee and N. K. Terrett, *Nat Rev Drug Discov*, 2008, **7**, 608–624.
9   G. W. Bemis and M. A. Murcko, *J Med Chem*, 1996, **39**, 2887–2893.
10   M. G. Siegel and M. Vieth, *Drug Discov. Today*, 2007, **12**, 71–79.
11   J. Wang and T. Hou, *J. Chem. Inf. Model.*, 2010, **50**, 55–67.
12   FDA, Orange Book Preface, https://www.fda.gov/drugs/development-approval-process-drugs/orange-book-preface, (accessed 1 May 2021).
13   R. D. Taylor, M. MacCoss and A. D. G. Lawson, *J. Med. Chem.*, 2017, **60**, 1638–1647.
14   R. D. Taylor, M. MacCoss and A. D. G. Lawson, *J. Med. Chem.*, 2014, **57**, 5845–5859.
15   R. Visini, J. Arus-Pous, M. Awale and J. L. Reymond, *J. Chem. Inf. Model.*, 2017, **57**, 2707–2718.
16   W. R. Pitt, D. M. Parry, B. G. Perry and C. R. Groom, *J. Med. Chem.*, 2009, **52**, 2952–2963.
17   F. Lovering, J. Bikker and C. Humblet, *J. Med. Chem.*, 2009, **52**, 6752–6756.
18   Y. A. Ivanenkov, B. A. Zagribelnyy and V. A. Aladinskiy, *J. Med. Chem.*, 2019, **62**, 10026–10043.
19   W. H. B. Sauer and M. K. Schwarz, *J. Chem. Inf. Comput. Sci.*, 2003, **43**, 987–1003.
20   D. G. Brown and J. Boström, *J. Med. Chem.*, 2016, **59**, 4443–4458.
21   J. Boström, D. G. Brown, R. J. Young and G. M. Keserü, *Nat. Rev. Drug Discov.*, 2018, **17**, 709.
22   C. M. Dobson, *Nature*, 2004, **432**, 824.
23   G. M. Cragg and D. J. Newman, *Biochim. Biophys. Acta Gen. Subj.*, 2013, **1830**, 3670–3695.
24   C. J. Gerry and S. L. Schreiber, *Nat. Rev. Drug Discov.*, 2018, **17**, 333.
25   S. L. Schreiber, *Science*, 2000, **287**, 1964.
26   P. Arya, R. Joseph, Z. Gan and B. Rakic, *Chem. Biol.*, 2005, **12**, 163–180.
27   D. S. Tan, *Nat. Chem. Biol.*, 2005, **1**, 74.
28   M. D. Burke and S. L. Schreiber, *Angew. Chem. Int. Ed.*, 2004, **43**, 46–58.
29   I. Collins and A. M. Jones, *Molecules*, 2014, **19**, 17221–17255.
30   C. J. Gerry and S. L. Schreiber, *Curr. Opin. Chem. Biol.*, 2020, **56**, 1–9.
31   J. P. Maianti, G. A. Tan, A. Vetere, A. J. Welsh, B. K. Wagner, M. A. Seeliger and D. R. Liu, *Nat. Chem. Biol.*, 2019, **15**, 565–574.
32   N. Kato, E. Comer, T. Sakata-Kato, A. Sharma, M. Sharma, M. Maetani, J. Bastien, N. M. Brancucci, J. A. Bittker, V. Corey, D. Clarke, E. R. Derbyshire *et al.*, *Nature*, 2016, **538**, 344–349.
33   D. Pizzirani, T. Kaya, P. A. Clemons and S. L. Schreiber, *Org. Lett.*, 2010, **12**, 2822–2825.
34   M. Sellstedt, G. Krishna Prasad, K. Syam Krishnan and F. Almqvist, *Tetrahedron Lett.*, 2012, **53**, 6022–6024.

35   M. D. Burke, E. M. Berger and S. L. Schreiber, *Science*, 2003, **302**, 613–618.

36   J. T. Lowe, M. D. Lee, L. B. Akella, E. Davoine, E. J. Donckele, L. Durak, J. R. Duvall, B. Gerard, E. B. Holson, A. Joliton, S. Kesavan, B. C. Lemercier *et al.*, *J. Org. Chem.*, 2012, **77**, 7187–7211.

37   F. Garro-Helion, A. Merzouk and F. Guibe, *J. Org. Chem.*, 1993, **58**, 6109–6113.

38   W. Zheng, N. Thorne and J. C. McKew, *Drug Discov. Today*, 2013, **18**, 1067–1073.

39   D. C. Swinney, *Clin. Pharmacol. Ther.*, 2013, **93**, 299–301.

40   J. G. Moffat, J. Rudolph and D. Bailey, *Nat. Rev. Drug Discov.*, 2014, **13**, 588.

41   M.-S. Kim, S. M. Pinto, D. Getnet, R. S. Nirujogi, S. S. Manda, R. Chaerkady, A. K. Madugundu, D. S. Kelkar, R. Isserlin, S. Jain, J. K. Thomas, B. Muthusamy *et al.*, *Nature*, 2014, **509**, 575–581.

42   A. L. Hopkins and C. R. Groom, *Nat. Rev. Drug Discov.*, 2002, **1**, 727–730.

43   M. Schenone, V. Dančík, B. K. Wagner and P. A. Clemons, *Nat. Chem. Biol.*, 2013, **9**, 232.

44   A. G. Atanasov, B. Waltenberger, E.-M. Pferschy-Wenzig, T. Linder, C. Wawrosch, P. Uhrin, V. Temml, L. Wang, S. Schwaiger, E. H. Heiss, J. M. Rollinger, D. Schuster *et al.*, *Biotechnol. Adv.*, 2015, **33**, 1582–1614.

45   E. Michelini, L. Cevenini, L. Mezzanotte, A. Coppa and A. Roda, *Anal. Bioanal. Chem.*, 2010, **398**, 227–238.

46   J. Lexchin, *Healthc. Policy*, 2016, **12**, 65–75.

47   D. C. Swinney and J. Anthony, *Nat. Rev. Drug Discov.*, 2011, **10**, 507–519.

48   D. C. Swinney, in *Phenotypic Drug Discovery*, RSC, 2020, ch. 4, pp. 1–19.

49   M. Wang, R. Cao, L. Zhang, X. Yang, J. Liu, M. Xu, Z. Shi, Z. Hu, W. Zhong and G. Xiao, *Cell Res.*, 2020, **30**, 269–271.

50   H. Laverty, K. M. Orrling, F. Giordanetto, M. Poinot, E. Ottow, T. W. Rijnders, D. Tzalis, S. Jaroch, H. Laverty, K. M. Orrling, F. Giordanetto, M. Poinot *et al.*, *J. Med. Dev. Sci.*, 2016, **1**, 20–33.

51   H. van Vlijmen, J.-Y. Ortholand, V. M.-J. Li and J. S. B. de Vlieger, *Drug Discov. Today*, 2021, **26**, 2406–2413.

52   Results | European Lead Factory, https://www.europeanleadfactory.eu/elf-2013-2018/results, (accessed 18 February 2022).

53   J. Kim, H. Kim and S. B. Park, *J. Am. Chem. Soc.*, 2014, **136**, 14629–14638.

54   H. Kim, T. T. Tung and S. B. Park, *Org. Lett.*, 2013, **15**, 5814–5817.

55   S. Wetzel, R. S. Bon, K. Kumar and H. Waldmann, *Angew. Chem. Int. Ed.*, 2011, **50**, 10800–10826.

56   M. Kaiser, S. Wetzel, K. Kumar and H. Waldmann, *Cell. Mol. Life Sci.*, 2008, **65**, 1186–1201.

57   R. W. Huigens III, K. C. Morrison, R. W. Hicklin, T. A. Flood Jr, M. F. Richter and P. J. Hergenrother, *Nat. Chem.*, 2013, **5**, 195–202.

58   A. C. Flick, C. A. Leverett, H. X. Ding, E. McInturff, S. J. Fink, S. Mahapatra, D. W. Carney, E. A. Lindsey, J. C. DeForest, S. P. France, S. Berritt, S. V. Bigi-Botterill *et al.*, *J. Med. Chem.*, 2021, **64**, 3604–3657.

59   W. Heilmayer, L. Spence and P. Hinsmann, Purification of pleuromutilin, US10913703B2, 2021.

60   R. Riedl, W. Heilmayer and L. Spence, Process for the preparation of pleuromutilins, US9120727B2, 2015.

61   D. G. Brown and H. J. Wobst, *J. Med. Chem.*, 2021, **64**, 2312–2338.

62   University of Birmingham, iDESIGN, https://www.birmingham.ac.uk/research/activity/chemistry/projects/idesign/idesign.aspx, (accessed 18 February 2022).

63   About the Haworth Collection, https://www.birmingham.ac.uk/research/birmingham-drug-discovery-hub/about-the-haworth-collection.aspx, (accessed 18 February 2022).

64   G. Illuminati and L. Mandolini, *Acc. Chem. Res.*, 1981, **14**, 95–102.

65   C. Galli and L. Mandolini, *Eur. J. Org. Chem.*, 2000, **2000**, 3117–3125.

66   R. L. Reyes, T. Iwai and M. Sawamura, *Chem. Rev.*, 2021, **121**, 8926–8947.

67   A. K. Clarke and W. P. Unsworth, *Chem. Sci.*, 2020, **11**, 2876–2881.

68   C. Zhao, Z. Ye, Z. Ma, S. A. Wildman, S. A. Blaszczyk, L. Hu, I. A. Guizei and W. Tang, *Nat. Commun.*, 2019, **10**, 4015.

69   A. Hussain, S. K. Yousuf and D. Mukherjee, *RSC Adv.*, 2014, **4**, 43241–43257.

70   K. Ishiuchi, T. Kubota, S. Hayashi, T. Shibata and J. Kobayashi, *Tetrahedron Lett.*, 2009, **50**, 6534–6536.

71   H. Niwa, Y. Uosaki and K. Yamada, *Tetrahedron Lett.*, 1983, **24**, 5731–5732.

72   D. Sun, Q. Zhao and C. Li, *Org. Lett.*, 2011, **13**, 5302–5305.

73   A. R. Carroll, E. Hyde, J. Smith, R. J. Quinn, G. Guymer and P. I. Forster, *J. Org. Chem.*, 2005, **70**, 1096–1099.

74   J.-P. H. Perchellet, E. M. Perchellet, K. R. Crow, K. R. Buszek, N. Brown, S. Ellappan, G. Gao, D. Luo, M. Minatoya and G. H. Lushington, *Int. J. Mol. Med.*, 2009, **24**, 633–643.

75   N. Brown, B. Xie, N. Markina, D. VanderVelde, J.-P. H. Perchellet, E. M. Perchellet, K. R. Crow and K. R. Buszek, *Bioorg. Med. Chem. Lett.*, 2008, **18**, 4876–4879.

76   K. Sumi, Y. Inoue, M. Nishio, Y. Naito, T. Hosoya, M. Suzuki and H. Hidaka, *Bioorg. Med. Chem. Lett.*, 2014, **24**, 831–834.

77   J. Perez, K. Nolsoe, M. Kessler, L. Garcia, E. Perez and J. L. Serrano, *Acta Crystallogr. Sect. B*, 2005, **61**, 585–594.

78   D. G. Evans and J. C. A. Boeyens, *Acta Crystallogr. Sect. B*, 1988, **44**, 663–671.

79   L. A. de Ceuninck van Capelle, J. M. Macdonald and C. J. T. Hyland, *J. Org. Biomol. Chem.*, 2021, **19**, 7098–7115.

80   F. A. L. Anet, P. J. Degen and I. Yavari, *J. Org. Chem.*, 1978, **43**, 3021–3023.

81   J. B. Lambert and S. A. Khan, *J. Org. Chem.*, 1975, **40**, 369–374.

82   M. Habgood, *J. Comput. Aided Mol. Des.*, 2017, **31**, 1073–1083.

83   M. Morales-Chamorro and A. Vázquez, *Synthesis*, 2019, **51**, 842–847.

CHAPTER II: RESULTS AND DISCUSSION

2. Scalable synthesis of the azacyclooctenone parent scaffold *via* ring-closing metathesis

The four-step synthesis of parent scaffold **29**, reported by Morales-Chamorro and Vázquez, started from readily available Boc-γ-aminobutyric acid **30** (Boc-GABA) and included a ring-closing metathesis (RCM) reaction as the final step (Scheme 8).[1] Medium-sized ring closure reactions *via* RCM are often unsuccessful or low-yielding, due to competing cross-metathesis and polymerisation reactions (see Section 1.6).[2,3] In fact, the reported cyclisation provides one of the few examples of using RCM to access eight-membered cyclic amines; Listratova's 2017 review on the synthesis of azocines reported only 23 examples in which RCM was used to access this class of cyclic amine, and only four of these did not exploit ring fusion to facilitate the cyclisation reaction.[4] Ring fusions can greatly improve the success of RCM when they introduce conformational restrictions that bring the reacting olefinic groups into closer proximity.[5,6] The high yield of Morales-Chamorro and Vázquez's RCM reaction (Scheme 8) thus made azacyclooctenone **29** an attractive scaffold, and its reported synthesis was deemed worthwile to reproduce and scale-up.
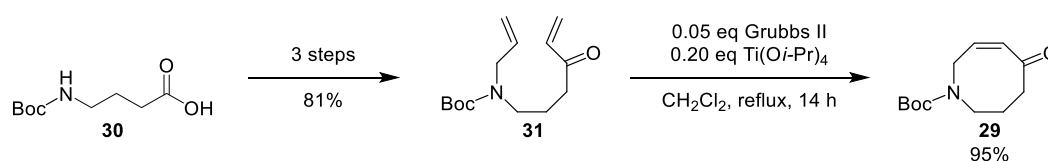
*Scheme 8: High-yielding synthesis of parent scaffold **29** via RCM, reported by Morales-Chamorro and Vázquez.*[1]

2.1. Towards a gramme-scale synthesis of parent scaffold 29

Following the synthetic route towards parent scaffold **29**, reported by Morales-Chamorro and Vázquez,[1] GABA **32** was sequentially Boc-protected, *N*-allylated and then converted into Weinreb amide **34** under standard EDC coupling conditions. Subsequent reaction with vinylmagnesium bromide afforded diene **34** (Scheme 9), alongside β-amine ketone **35** as a major byproduct, resulting from conjugate addition of the *N*-methyl-*N*-methoxy amine into enone **31**.[7–11] Acidifying the vinylation reaction at 0 °C with 1.0 M hydrochloric acid until pH = 3, rather than using $NH_4Cl_{sat.\ aq.}$ solution as described in the literature work-up procedure,[1] significantly increased the yield of enone product **31** by minimising the amount of byproduct **35**. No retro 1,4-addition of β-amino ketone **35** was observed *via* LCMS analysis of the mixture at pH = 3, indicating that cooling the reaction mixture to 0 °C prior to work-up and the use of

the stronger acid to quench the reaction prevented the formation of the byproduct **35**, rather than converted the β-amino ketone byproduct to diene **31**.
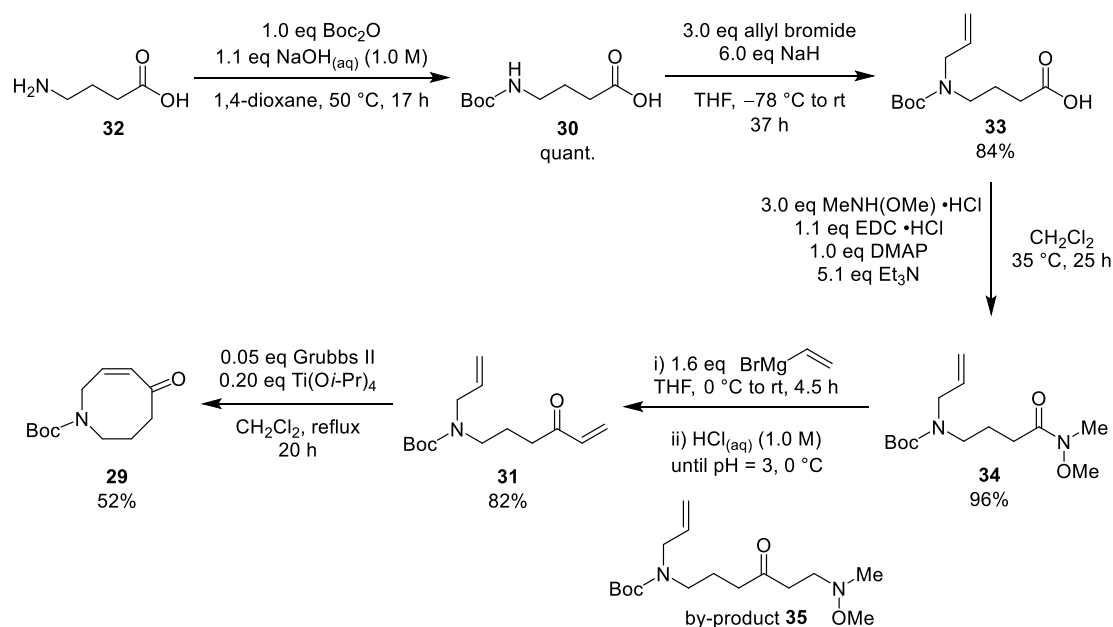
*Scheme 9: Synthesis of parent scaffold **29**.*

The route described above provided a high-yielding, gramme-scale synthesis of diene **31** (8.10 g). Unfortunately, yields for the key RCM step did not exceed 52% when the literature conditions were applied,[1] posing a significant bottleneck in the envisioned gramme-scale synthesis of the target parent scaffold **29**; this called for an optimisation of the RCM reaction.

2.2.   RCM optimisation

2.2.1.   Optimisation strategies: literature precedent

Although the success of an RCM reaction can depend heavily on the nature of the diene starting material, there are many reaction parameters that can be varied to improve the yield of an RCM reaction. For example, the RCM reaction conditions, reported to furnish our target scaffold **29** (Scheme 9), included Ti(O*i*-Pr)$_4$ as an additive, which was shown to be necessary to achieve full conversion of the starting material (Figure 13).[1] This mild Lewis acid coordinates preferentially to Lewis basic centres in the substrate (ketone, Boc-carbamate), preventing competing complexation of the ruthenium carbene intermediate, which can affect the efficiency of RCM reactions.[12,13]

Figure 13: Complexation of the ruthenium-carbene intermediate could hamper ring-closing metathesis. Addition of Ti(Oi-Pr)₄ as Lewis acid can prevent this complexation.[7,12,13]

The nature of the catalyst, solvent, temperature and active ethylene removal can also increase the success of an RCM reaction.[5] An example of the effect of catalyst choice on the success of RCM is provided by the total synthesis of natural product teubrevin G **38** by Paquette and Efremov (Scheme 10). Switching from Grubbs I to the Grubbs II catalyst provided cyclooctenone **37** in higher yields and faster reaction times, even with lower catalyst loading.[14] Therefore, we postulated that RCM of our diene **36** might also benefit from next-generation catalysts.
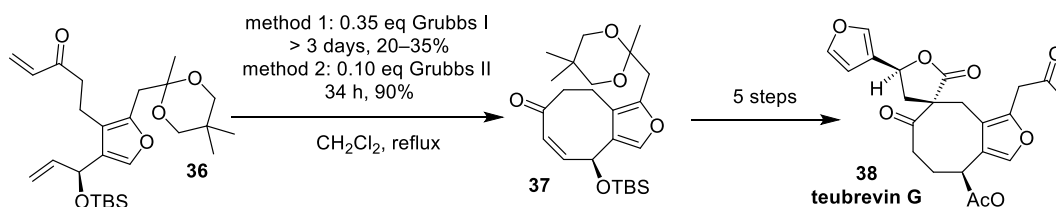
*Scheme 10: RCM reaction in the total synthesis of teubrevin G **38**. Switching to Grubbs II catalyst significantly improved the reaction time, yield of cyclooctenone **37** and allowed lower catalyst loading.[14]*

Temperature and reaction concentration can all play an important role in RCM reactions. Ring-closing metathesis is the only metathesis reaction which produces two olefins (the RCM product and ethylene) from one precursor molecule, which results in a positive entropy contribution, favouring ring-closing over intermolecular cross-metathesis.[a] However, the relatively large entropic loss upon cyclisation of medium-sized ring precursors contributes negatively to the entropy factor.[15] Dilution can provide a positive entropy contribution to favour RCM, since the ring-closed product displays greater translational mobility than an oligomer formed by cross metathesis; this contribution increases with increased dilution.[15] Therefore, at low reaction concentrations, elevated temperatures should decrease ΔG by increasing the entropic factor contribution, promoting RCM.[5]

Solvents can be used to perform the reaction over different reaction temperature ranges; they can also significantly affect catalyst activity and RCM yields. For example, Grela and co-workers

---

[a] For example, linear dimerisation affords two olefinic products (the linear dimer and ethylene) from two substrate molecules, which results in a lower entropic contribution.

used HG-II at 70 °C to access cyclopentene **40** by RCM. The yield of this reaction increased from 4% to 33% when toluene was used in place of DCE (Scheme 11).[16] Hence, we chose to use CH$_2$Cl$_2$, DCE and toluene to probe the effect of solvent and temperature on our RCM reaction, whilst increased dilution was considered to decrease possible dimer formation.

solvent	yield (%)
PhMe	33
DCE	4
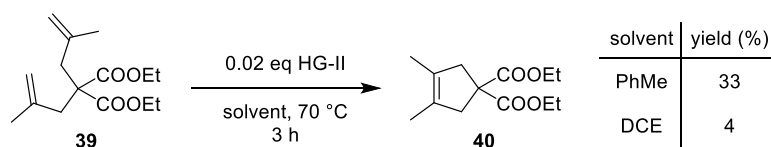
*Scheme 11: The yield of cyclopentene **40** increased upon using toluene instead of DCE as a solvent. [16]*

Active removal of ethylene from the reaction mixture, by continuously purging the reaction mixture with an inert gas, can also have a significant effect on RCM yields.[5] Not only does ethylene suppress RCM reactions (ethylene is typically more reactive towards the catalyst than other olefins in the reaction mixture and can cause ring-opening metathesis side reactions),[17] it can also form ruthenacyclobutane species, which decompose readily (reducing active catalyst lifetime),[18] and ruthenium hydride species,[19] which can themselves catalyse side reactions.[5,20] Active ethylene removal was key in the optimisation of kilogramme-scale syntheses of some marketed drugs, including a hepatitis C protease inhibitor and other antivirals.[5,21,22]

An example illustrating the influence of temperature and active ethylene removal on RCM is found in the synthesis of the antiproliferative library compound NB-IX-Gly44 **27**.[23] Brown *et al.* studied the RCM of diene intermediate **41**, using Grubbs II to afford lactam **42**.[24] They reported no reaction at temperatures up to 100 °C; only upon heating in toluene at reflux did the RCM proceed (Scheme 12). A continuous purge of the reaction mixture with N$_2$ or Ar, followed by addition of the ruthenium scavenger, tris(hydroxymethyl)phosphine, in the workup further increased the isolated yield of lactam **42** to 57%. Under these optimised conditions, the lactam could be produced on 10–20 gramme scale.[24]
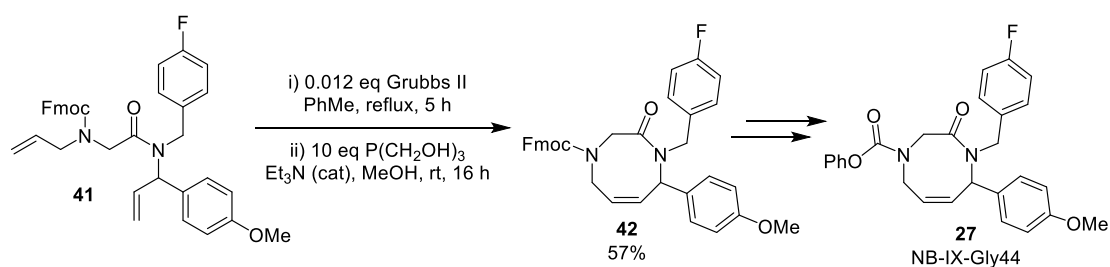
*Scheme 12: Brown's synthesis of lactam **42**.[a, b]*

Equipped with different strategies to improve the yield of RCM reactions, we turned towards optimising the RCM of diene **31**, in order to facilitate a gramme-scale synthesis of parent scaffold **29**.

2.2.2.   RCM optimisation through minimisation of dimerisation

Analysis of crude RCM reaction mixtures by ^{1}H-NMR spectroscopy and LCMS revealed the presence of a dimer **43** (Scheme 13, see Appendix 9).[c] The stereoisomeric structure of the dimer was not determined, but with molar ratios of monomer **29** : dimer **43** up to 1.0 : 0.3, efforts were directed towards minimising this byproduct. To this end, the influence of different catalysts, solvents, reaction temperature, active ethylene removal and reaction concentration on the RCM yield was investigated. Each reaction was monitored by TLC, ^{1}H-NMR spectroscopy and HPLC,[d] which gave a semi-quantitative measure of the relative generation of the desired product **29** and dimer **43**, and disappearance of starting material **31**.
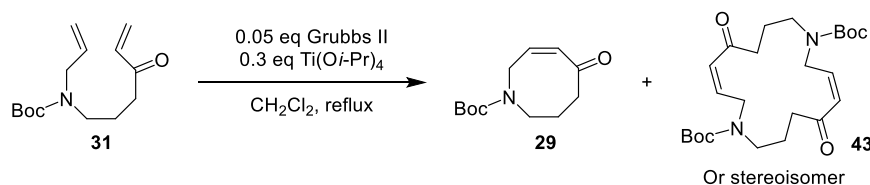
*Scheme 13: Crude RCM reaction mixtures revealed the presence of a dimer side-product **43**.*

---

[a] Scheme adapted from Brown *et al*.[24]

[b] The role of Et$_3$N is not explained in the publication,[24] nor in the paper by Maynard and Grubbs, in which this purification method was first introduced.[25] P(CH$_2$OH)$_3$ is reported to decompose at low pH,[26] so Et$_3$N could be added to maintain basic conditions.

[c] During flash column chromatography, dimer **43** co-eluted with the target ring-closed monomer **29** when hexane:EtOAc was used as the eluent. Using CH$_2$Cl$_2$:heptane:EtOAc 5:4:1 improved the separation of the two, with only 3 mol% dimer **43** observed in isolated fractions containing target RCM product **29**. (Calculated mol% *via* ^{1}H-NMR spectroscopy, using integration values of the olefinic hydrogen resonances: mol% = I_{dimer} / (I_{dimer} + $I_{monomer}$)) dimer peak: CDCl$_3$ δ_H 6.72 − 6.59 (m, 2H), monomer peak: CDCl$_3$ δ_H 5.66 (dt, 1H). Selected data for **43**: ESI-LRMS (+): m/z 473.2 ([M+Na]$^+$, 25%), 351.2 (90, [M− C$_5$H$_8$O$_2$ + H]$^+$), 295.1 (100, [M− C$_5$H$_8$O$_2$ − C$_4$H$_8$ + H]$^+$).

[d] HPLC performed using a Waters 2695 Separations Module, gradient (H$_2$O 0.1% HCOOH/MeCN 0.1% HCOOH); flow: 1 mL min^{-1}; run time: 30 min. The HPLC chromatogram showed dimer **43** as a single peak. The isomeric structure of dimer **43** was not investigated *via* 2D-NMR spectroscopy, so no claim is made about which stereoisomer was formed, nor whether a single isomer of **43** was formed, acknowledging possible co-elution of multiple *E/Z*-isomers.

First, three catalysts were tested: Grubbs II (G-II), Hoveyda-Grubbs II (HG-II) and nitro-Grela-I_2 (Figure 14). HG-II is tolerant of moisture and air, recyclable and has a broad substrate scope.[5] With literature precedent for its use in eight-ring synthesis and its high stability potentially reducing side-reactions, this catalyst was an attractive candidate.[27] The nitro-Grela-I_2 catalyst is another effective RCM catalyst that is less sensitive to the presence of impurities.[28] However, using this catalyst in the RCM reaction of diene **31** yielded more byproducts than were observed using Grubbs II and HG-II catalysts. Nitro-Grela-I_2 was therefore not used in further optimisation reactions.[a] Grubbs II showed a faster initial rate of reaction than HG-II; however, both showed a similar ratio of monomer and dimer, despite full consumption of the starting material after 28 h.
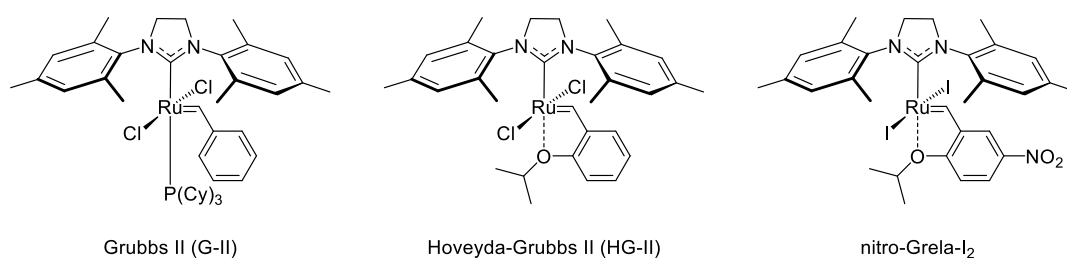
*Figure 14: Three ruthenium catalysts were tested in the RCM reaction of diene **31**.*

Different reaction temperatures and solvents were screened next. At 40 °C, HG-II catalyst showed an initial faster reaction rate in toluene, compared to HG-II in DCE and CH_2Cl_2 (Table 1, Entries 1, 2, 3); however, both Grubbs II and HG-II catalysts showed no significant change in the relative amounts of diene **31**, monomer **29** and dimer **43** after 6 h in toluene and DCE (Entries 1, 2, 4, 5). Moreover, at this temperature, only reactions in CH_2Cl_2 showed full consumption of the starting diene after 42 h (Entry 6). When RCM reactions were performed at reflux temperatures in toluene (111 °C), use of Grubbs II and HG-II catalysts led to full consumption of the diene after 1.5 h and 2.5 h, respectively. However, ^{1}H-NMR spectroscopic analysis of the crude reaction mixtures revealed complete decomposition, showing no monomer **29** nor any dimer **43** (Entries 7 and 8). In refluxing DCE (84 °C), Grubbs II showed a mixture of starting diene **31**, monomer **29** and dimer **43** after 26 h (Entry 9), but after 53.5 h, complete degradation was observed by ^{1}H-NMR spectroscopic analysis (Entry 10).

---

[a] Three reactions performed in parallel on 50 mg (0.20 mmol) scale (0.025 M), 0.05 eq catalyst, 0.3 eq Ti(O*i*-Pr)$_4$, CH_2Cl_2, 40 °C.

Table 1: Solvent and temperature screening of the RCM reaction of diene 31.[a]
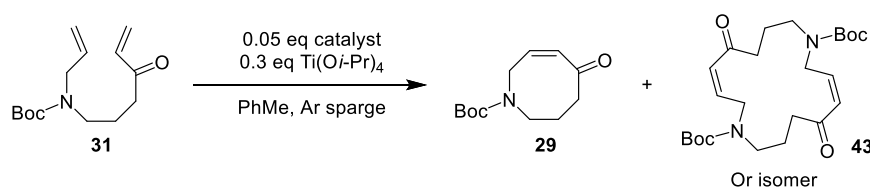
Entry	Catalyst	Temperature (°C)	Solvent	Reaction time (h)	31:29:43 [b]
1	G-II	40	toluene	6.0	1:1:2
2	G-II	40	DCE	6.0	2:1:1
3	G-II	39 (reflux)	CH_2Cl_2	42.0	0:4:1
4	HG-II	40	toluene	6.0	1:3:6
5	HG-II	40	DCE	6.0	1:5:5
6	HG-II	39 (reflux)	CH_2Cl_2	42.0	0:9:1
7	G-II	111 (reflux)	toluene	1.5	degradation
8	HG-II	111 (reflux)	toluene	2.5	degradation
9	G-II	84 (reflux)	DCE	26.0	5:8:9[c]
10	G-II	84 (reflux)	DCE	53.5	degradation

[a]Reactions were performed on 50 mg (0.20 mmol) scale, reaction concentration: 0.025 M. [b]Calculated by relative integrations on HPLC chromatogram. [c]Calculated by ^{1}H-NMR spectroscopy, using relative integration values of the olefinic hydrogen resonances.

The results of the solvent and temperature screening (Table 1) indicated degradation or polymerisation of the starting material and/or products upon prolonged exposure to high temperatures in both toluene and DCE. However, given full consumption of the diene was only observed when the reaction mixture was heated at reflux,[a] it was postulated that active removal of ethylene was important for this reaction, albeit within certain temperature limits. Using an Ar sparge led to a striking observation: at 40 °C in toluene, starting diene 31 was fully consumed in minutes rather than hours (Table 2, Entries 1 and 2).

---

[a] In addition, in a preliminary test reaction in a closed reaction vessel (0.05 eq Grubbs II, 0.20 eq Ti(O*i*-Pr)$_4$, CH_2Cl_2, 39 °C, 17 h) LCMS analysis of the reaction mixture still showed diene 31 after 17 h, yielding ring-closed enone 29 in <10% yield.

*Table 2: Optimisation of the RCM reaction of diene **31**.[a]*
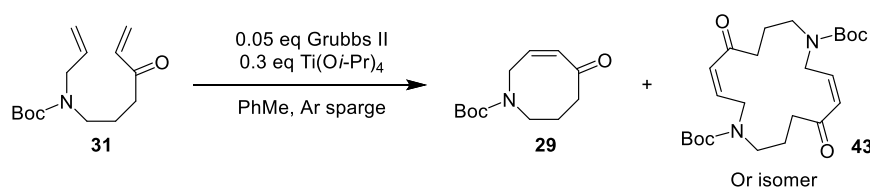
Entry	Temperature (°C)	Reaction concentration (M)	Reaction time (min)	Isolated yield 29 (%)	29:43[b]
1	40 (no sparge)	0.025	3090	-	1.0:0.5
2	40	0.025	31	-	1.0:0.5
3	80	0.025	21	53	1.0:0.2
4	rt	0.010	270	48	1.0:0.4
5	40	0.010	36	-	1.0:0.3
6	**80**	**0.010**	**16**	**67**	**1.0:0.1**
7[c]	80	0.010	34	69	1.00:0.07

[a]Reactions were performed on 50 mg (0.20 mmol) scale. [b]Calculated by ^{1}H-NMR spectroscopic analysis of the crude reaction mixture before purification, using relative integration values of the olefinic hydrogen resonances. [c]N_2 gas was used instead of Ar gas when the reaction was performed on larger scale (4.1 g, 16 mmol).

When the reaction temperature was increased to 80 °C, the reaction time reduced further, but more importantly, the ratio of desired monomer **29** to dimer **43** improved significantly (Table 2, Entry 3). Performing the reaction at lower concentrations (Table 2, Entries 4–6) increased this ratio further, while the same temperature-dependent trend in dimer formation was observed, supporting the notion that the intramolecular reaction is entropically favoured and that dilution reduces competition from oligomerisation pathways.[5] With the RCM reaction now proceeding in good yields (Table 2, Entry 6), these improved conditions were repeated on larger scale (Table 2, Entry 7), enabling access to our target enone **29** on gramme scale and with reproducible yields between 60% and 70%.

2.3. Substrate influence on success of RCM: α-amino acid analogues

Inspired by the work of Liskamp, Brown and Miller,[6,24,29,30] it was hypothesised that α-amino acids such as glycine and proline would provide quick access to RCM substrates, whilst giving an opportunity to compare the influence of the substrate on the outcome of the RCM reaction, using our optimised conditions (Scheme 14). We postulated that structural pre-organisation by

ring-fusion in proline derivative **48** or by conformational restriction *via* an amide **44** or ester **46**, would facilitate RCM,[5,6] while ketone **50** would provide a less conformationally restricted analogue for a comparison. For amide **44**, we proposed that steric repulsion, introduced by the Bn moiety, would favour the adoption of an RCM-favourable *Z*-conformation, or at minimum reduce the energy barrier to interconvert between the *E*- and *Z*-conformer.[6,31] Whilst ester **46** was considered to exist primarily as the *Z*-conformer,[31] coordination of the carbonyl oxygen to the catalyst upon complexation of the *N*-allyl group (Scheme 14, **46-[Ru]**) could bring the *O*-allyl group into proximity to the active [Ru] complex.[12] Alternatively, if the reaction conditions could overcome the energy barrier between the preferred *Z*-ester and *E*-ester ($\sim$10 kcal mol^{-1}),[32] the *E*-conformation would also favour RCM.
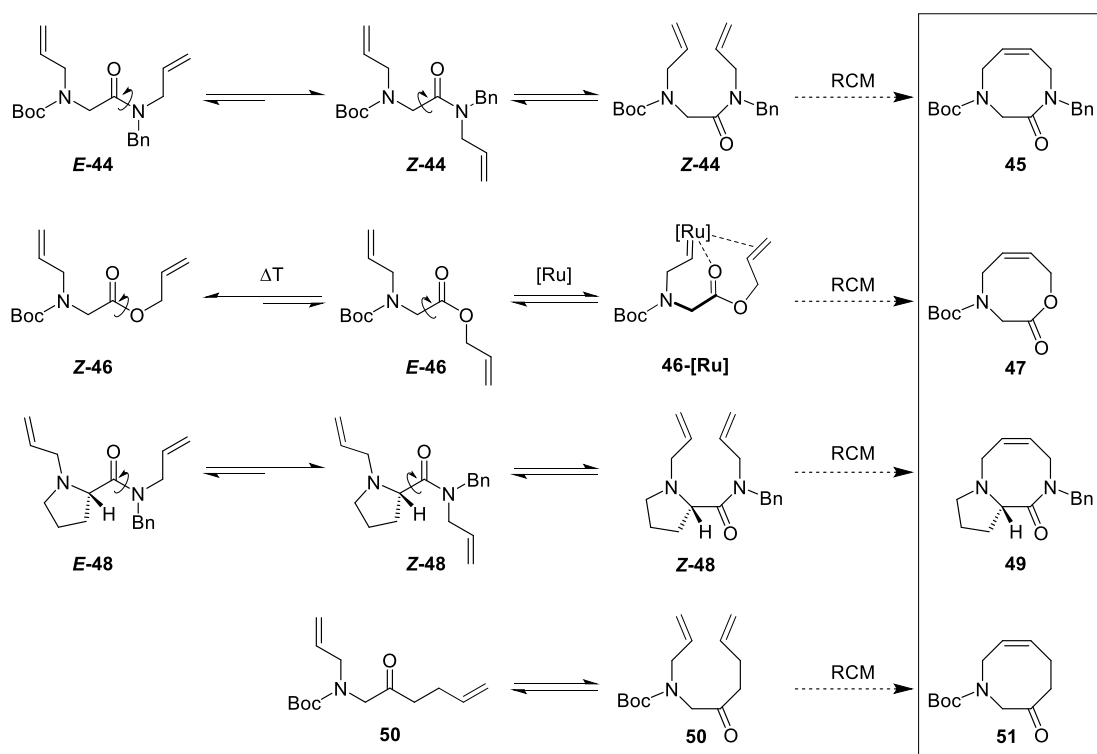
Scheme 14: Envisioned α-amino acid-derived rings and their diene precursors.

The synthesis of Boc-glycine and proline precursors, **44** and **48**, respectively, followed a similar pathway (Scheme 15): sequential *N*-allylation and saponification of the resulting Boc-protected methyl esters afforded *N*-allyl amino acids **53** and **55**. Benzylallylamine was prepared *via* reductive alkylation of allylamine with benzaldehyde and NaBH$_4$ in quantitative yield, and subsequent amide coupling with amino acids **53** and **55** •**HCl** afforded RCM precursors **44** and **48**.
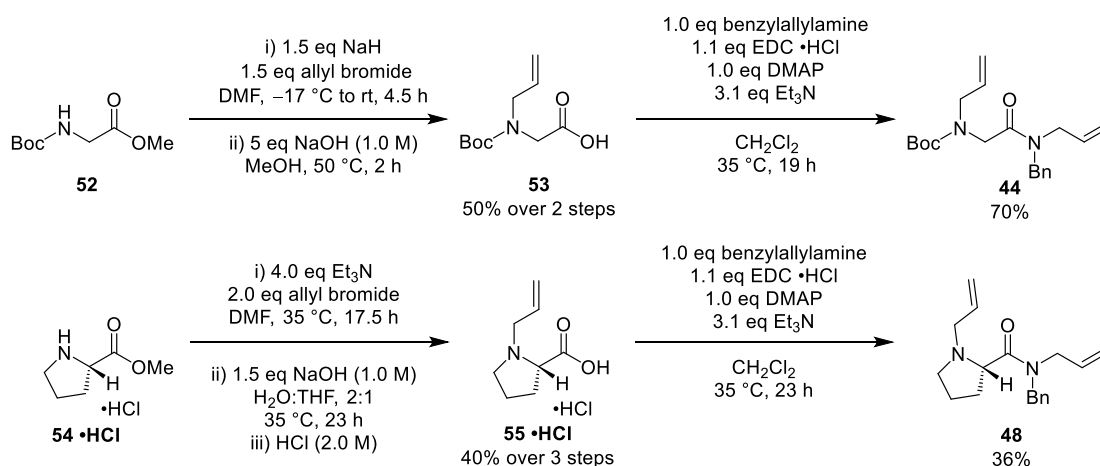
*Scheme 15: Synthesis of RCM precursors **44** and **48**.*

Diene **46** was obtained in a single step, by *N,O*-allylation of Boc-glycine **56**, while RCM precursor **50** was synthesised in an analogous fashion to the GABA ring precursor, involving conversion of *N*-allyl glycine **53** into its corresponding Weinreb amide **57**, followed by reaction with 1-butenylmagnesiumbromide, which was prepared *in situ* (Scheme 16).
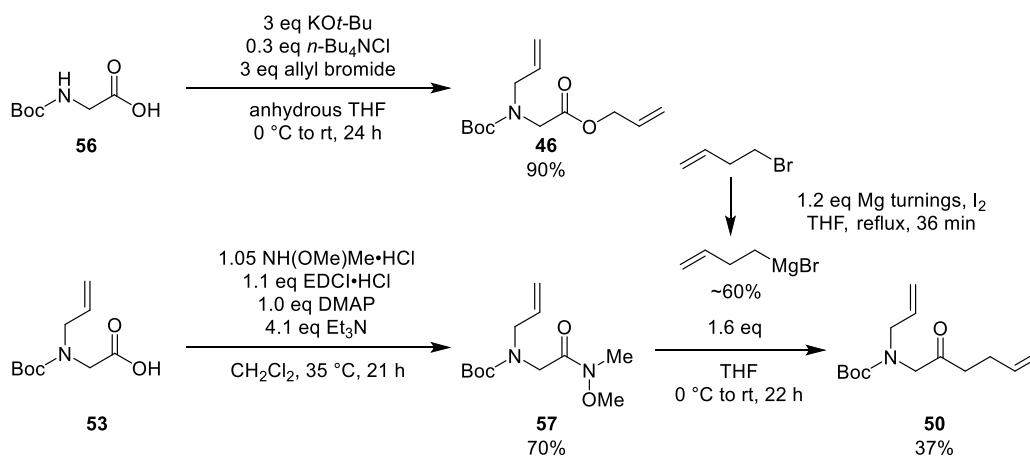
*Scheme 16: Synthesis of RCM precursors **46** and **50**.[a]*

Using our optimised conditions, RCM reactions were attempted on dienes **44**, **46**, **48** and **50** (Scheme 17). A 50 mg-scale test reaction with amide **44** using 0.3 eq Ti(O*i*-Pr)$_4$ afforded lactam **45** in only 44% isolated yield. However, without addition of Ti(O*i*-Pr)$_4$, amide **44** underwent ring-closure in 6–13 min, providing the lactam product **45** in yields of 80–86%.

---

[a] The Grignard reagent was titrated using menthol and 1,10-phenanthroline, following the literature procedure by Lin and Paquette.[33]

When performed on 50 mg scale, ester **46** was fully consumed after 12 min under the optimised RCM conditions, without the addition of Ti(O*i*-Pr)$_4$.[a] However, the reaction appeared to form two isomeric dimers **58** and **59** (Scheme 17), evidenced by stacked resonances in the ^{1}H-NMR spectrum, which did not coalesce during HT-^{1}H-NMR spectroscopic analysis, and the observation of more carbon resonances in the ^{13}C-NMR spectrum than would be expected for the monomer. LCMS and HRMS analysis also showed two peaks with m/z values corresponding to [M–Boc–*t*-Bu+H]$^+$, a fragment which could not be rationalised *via* the monomer. The regiochemistry of the dimers and stereochemistry of the double bonds was not investigated further. However, these results suggest that the used reaction conditions did not overcome the energy barrier between the preferred *Z*-ester and *E*-ester conformation,[32] required for intramolecular cyclisation of ester **46**,[34] favouring dimerisation instead.
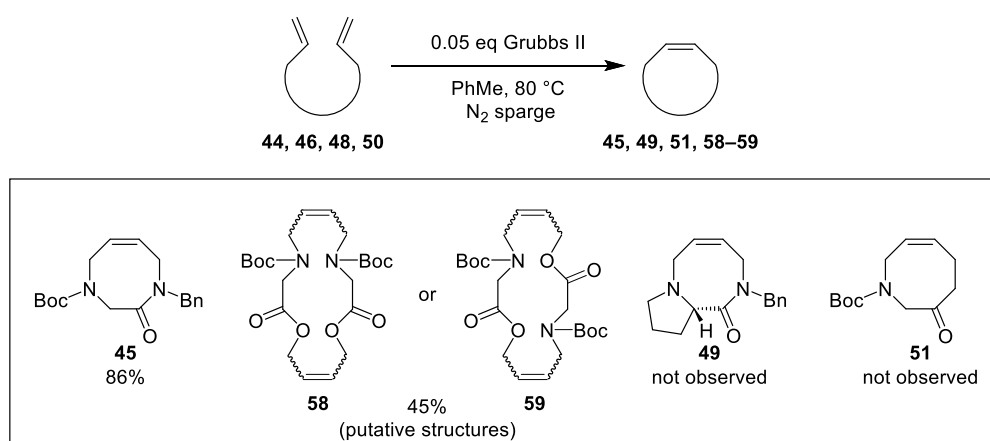
Scheme 17: Lactam **45** was synthesised on gramme-scale, while ester **46** formed two putative dimers. **49** and **51** were not identified in the reaction mixture.

Proline derivative **48** showed no reaction under our optimised RCM conditions, with or without the use of Ti(O*i*-Pr)$_4$. It is interesting to note that tri- up to hexapeptides, synthesised by Liskamp and co-workers, containing proline with analogous double *N*-allyl functionalities were also not found to afford RCM products. The authors found that *n*-butenyl appendages in place of allyl groups were required for these oligopeptides to undergo cyclisation, with a 13-membered ring being the smallest ring size obtained. Since the *n*-butenyl proline analogues showed increased yields compared to valine analogues, the authors suggested that incorporation of proline did promote cyclisation, but that *N*-allyl proline analogues could not adopt the conformation that was required for medium-sized ring closure.[29] Unfortunately, butenyl precursor **50** yielded

---

[a] 2.5 h reaction time on gramme scale.

polymers and isomers instead of the desired RCM product, illustrating once more the dependence of RCM success on the nature of the precursor.[5]

Although lactam **45** could provide novel scaffolds for drug discovery, eight-membered cyclic enone **29** was considered more attractive for further diversification, given the enone moiety provided more possibilities for further chemistry. In addition, lactam **45** was structurally similar to the reported antiproliferative agent NB-IX-Gly44 **27** (Section 1.6, page 22 and Scheme 12, page 34), decreasing further the novelty of this lactam ring system.

2.4. References

1   M. Morales-Chamorro and A. Vázquez, *Synthesis*, 2019, **51**, 842–847.
2   G. Illuminati and L. Mandolini, *Acc. Chem. Res.*, 1981, **14**, 95–102.
3   C. Galli and L. Mandolini, *Eur. J. Org. Chem.*, 2000, **2000**, 3117–3125.
4   A. V. Listratova and L. G. Voskressensky, *Synthesis*, 2017, **49**, 3801–3834.
5   M. Yu, S. Lou and F. Gonzalez-Bobes, *Org. Process Res. Dev.*, 2018, **22**, 918–946.
6   S. J. Miller, S.-H. Kim, Z.-R. Chen and R. H. Grubbs, *J. Am. Chem Soc.*, 1995, **117**, 2108–2109.
7   N. Papaioannou, J. T. Blank and S. J. Miller, *J. Org. Chem.*, 2003, **68**, 2728–2734.
8   N. Papaioannou, C. A. Evans, J. T. Blank and S. J. Miller, *Org. Lett.*, 2001, **3**, 2879–2882.
9   J. D. Firth, P. G. E. Craven, M. Lilburn, A. Pahl, S. P. Marsden and A. Nelson, *Chem. Commun.*, 2016, **52**, 9837–9840.
10   P. G. M. Wuts, S. R. Putt and A. R. Ritter, *J. Org. Chem.*, 1988, **53**, 4503–4508.
11   A. Gomtsyan, *Org. Lett.*, 2000, **2**, 11–13.
12   A. Fürstner and K. Langemann, *J. Am. Chem. Soc.*, 1997, **119**, 9130–9136.
13   Q. Yang, W.-J. Xiao and Z. Yu, *Org. Lett.*, 2005, **7**, 871–874.
14   L. A. Paquette and I. Efremov, *J. Am. Chem. Soc.*, 2001, **123**, 4492–4501.
15   S. Monfette and D. E. Fogg, in *Green Metathesis Chemistry*, eds. V. Dragutan, A. Demonceau, I. Dragutan and E. Sh. Finkelshtein, Springer Netherlands, Dordrecht, 2010, pp. 129–156.
16   C. Samojłowicz, M. Bieniek, A. Zarecki, R. Kadyrov and K. Grela, *Chem. Commun.*, 2008, 6282–6284.
17   E. F. van der Eide, P. E. Romero and W. E. Piers, *J. Am. Chem. Soc.*, 2008, **130**, 4485–4491.
18   P. E. Romero and W. E. Piers, *J. Am. Chem. Soc.*, 2005, **127**, 5032–5033.
19   W. Janse van Rensburg, P. J. Steynberg, W. H. Meyer, M. M. Kirk and G. S. Forman, *J. Am. Chem. Soc.*, 2004, **126**, 14332–14333.
20   C. S. Higman, L. Plais and D. E. Fogg, *ChemCatChem*, 2013, **5**, 3548–3551.
21   T. Nicola, M. Brenner, K. Donsbach and P. Kreye, *Org. Process Res. Dev.*, 2005, **9**, 513–515.
22   J. Kong, C. Chen, J. Balsells-Padros, Y. Cao, R. F. Dunn, S. J. Dolman, J. Janey, H. Li and M. J. Zacuto, *J. Org. Chem.*, 2012, **77**, 3820–3828.
23   J.-P. H. Perchellet, E. M. Perchellet, K. R. Crow, K. R. Buszek, N. Brown, S. Ellappan, G. Gao, D. Luo, M. Minatoya and G. H. Lushington, *Int. J. Mol. Med.*, 2009, **24**, 633–643.
24   N. Brown, G. Gao, M. Minatoya, B. Xie, D. VanderVelde, G. H. Lushington, J.-P. H. Perchellet, E. M. Perchellet, K. R. Crow and K. R. Buszek, *J. Comb. Chem.*, 2008, **10**, 628–631.

25   H. D. Maynard and R. H. Grubbs, *Tetrahedron Lett.*, 1999, **40**, 4137–4140.

26   B. R. James and F. Lorenzini, *Coord. Chem. Rev.*, 2010, **254**, 420–430.

27   J. M. Curto and M. C. Kozlowski, *J. Org. Chem.*, 2014, **79**, 5359–5364.

28   A. Tracz, M. Matczak, K. Urbaniak and K. Skowerski, *Beilstein J. Org. Chem.*, 2015, **11**, 1823–1832.

29   J. F. Reichwein, C. Versluis and R. M. J. Liskamp, *J. Org. Chem.*, 2000, **65**, 6187–6195.

30   J. F. Reichwein and R. M. J. Liskamp, *Eur. J. Org. Chem.*, 2000, **2000**, 2335–2344.

31   D. M. Pawar, A. A. Khalil, D. R. Hooks, K. Collins, T. Elliott, J. Stafford, L. Smith and E. A. Noe, *J. Am. Chem. Soc.*, 1998, **120**, 2108–2112.

32   E. B. Pentzer, T. Gadzikwa and S. T. Nguyen, *Org. Lett.*, 2008, **10**, 5613–5615.

33   H.-S. Lin and L. A. Paquette, *Synth. Commun.*, 1994, **24**, 2503–2506.

34   S. Monfette and D. E. Fogg, *Chem. Rev.*, 2009, **109**, 3783–3816.

3. Towards a first compound library

With access to gramme-scale quantities of parent scaffold **29**, the stage was set for further diversification, using the reactivity of the embedded enone and protected amine moieties, to yield novel scaffolds bearing multiple appendable sites. Using parallel synthesis, these sites would then be functionalised with a diverse set of reagents to generate a compound library (Scheme 18).
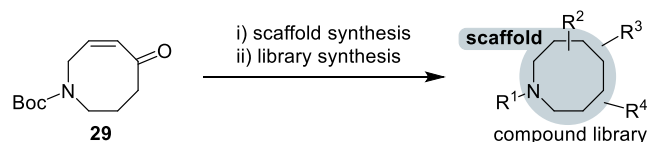
*Scheme 18: Schematic representation of diversification of parent scaffold **29** to yield an appendable scaffold for library synthesis. (Amount of R-groups drawn non-exhaustively, positions of the R-groups on the scaffold may vary.*

3.1. Functionalising the parent scaffold 29
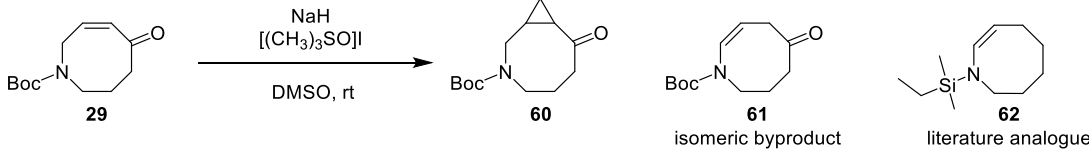
As the saturated azocine analogue of **29** is a literature compound,[1] further diversification of the ring, prior to library synthesis, would increase the novelty of the final scaffolds and library compounds derived therefrom.

3.1.1. Cyclopropanation

Furnishing what would be a novel bicyclo[6,1,0] system, cyclopropanations were an attractive starting point for diversification. Attempts to cyclopropanate enone **29** *via* Corey-Chaykovsky conditions[2] (Table 3, Entry 1) failed to produce the desired bicycle **60**. TLC analysis of the crude reaction mixture confirmed the consumption of starting material **29**, but LCMS analysis showed ions with the same m/z as the starting material. NMR spectroscopic analysis of the crude reaction mixture showed the emergence of resonances for a new double bond, which suggested that the starting material was isomerising under the basic reaction conditions: resonances in the ^{1}H-NMR spectrum (CDCl$_3$) at δ_H [6.70 (br s, 0.5H), 6.49 (br s, 0.5H)], 4.89 (dt, J = 9.5, 6.2 Hz, 1H) were similar (in chemical shift and J values) to those observed for an analogous eight-membered cyclic enamine **62** reported in the literature (Table 3).[3] To test this hypothesis, enone **29** was subjected to identical reaction conditions without the addition of [(CH$_3$)$_3$SO]I (Table 3, Entry 2). After following the same workup procedure, analysis of the crude reaction mixture showed the same putative alkene isomer **61**. Using an excess of [(CH$_3$)$_3$SO]I

relative to NaH[a] (Table 3, Entry 3) did not yield the potential isomer **61** nor the desired cyclopropane **60** as evidenced by ^{1}H-NMR spectroscopy and LCMS, either in the crude reaction mixture or column fractions. Using a small excess of NaH relative to [(CH$_3$)$_3$SO]I (Table 3, Entry 4), the putative alkene regioisomer **61** was also not observed but since the desired cyclopropane **60** was not identified either, the Corey-Chaykovsky cyclopropanation was abandoned.

*Table 3: Attempted Corey-Chaykovsky cyclopropanation of enone **29**.[a]*

Entry	Eq NaH	Eq [(CH$_3$)$_3$SO]I	Outcome
1	3.0	1.2	Isomer **61** observed
2	3.0	-	Isomer **61** observed
3	1.4	2.0	No isomer, product **60** not observed
4	1.4	1.1	No isomer, product **60** not observed

[a] Reactions performed on 50 mg (0.22 mmol) scale, reaction concentration 0.2 M.

3.1.2.   Luche reduction

Since allyl alcohol **63** could provide a useful substrate for further elaboration, such as directed cyclopropanation and Tsuji-Trost reactions, the Luche reduction of the enone **29** was investigated. The allyl alcohol **63** was furnished in good yield under standard conditions (Scheme 19).
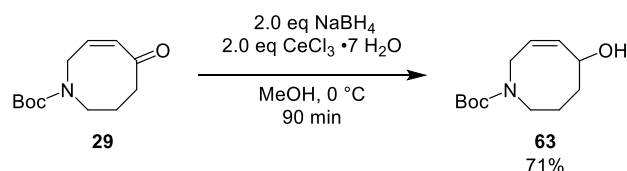
*Scheme 19: Luche reduction of enone **29**.*

---

[a]As NaH is consumed by [(CH$_3$)$_3$SO]I to form the reactive ylide, an excess of [(CH$_3$)$_3$SO]I should result in full consumption of NaH.

3.1.3.   Photochemical 1,4-addition

1,4-Additions to enone **29** were next explored to introduce another point of diversity. An early attempt to perform a conjugate addition on enone **29** following a procedure by Kilic *et al.* used indoline and DMAP in CH$_2$Cl$_2$ at 35 °C; however, this did not yield the desired 1,4-addition product **76**.[4] In 2007, Beauchemin and co-workers reported the UVA-activated conjugate addition of aromatic heterocycles on seven- and eight-membered cyclic enones **64** and **65** (Scheme 20).[5] In these instances, UVA irradiation (*ca* 350 nm) isomerises the double bond to its more strained (and therefore more reactive) *E*-isomer **75**;[6] upon conjugate addition of the nucleophile, this strain is released. The reaction scope within Beachemin's paper was however limited to heteroaromatic nucleophiles.[5] Small nucleophiles such as methanol, isopropanol and Et$_2$NH have been reported to yield analogous adducts in moderate yields, but only when these nucleophiles are used as the solvent.[7,8]
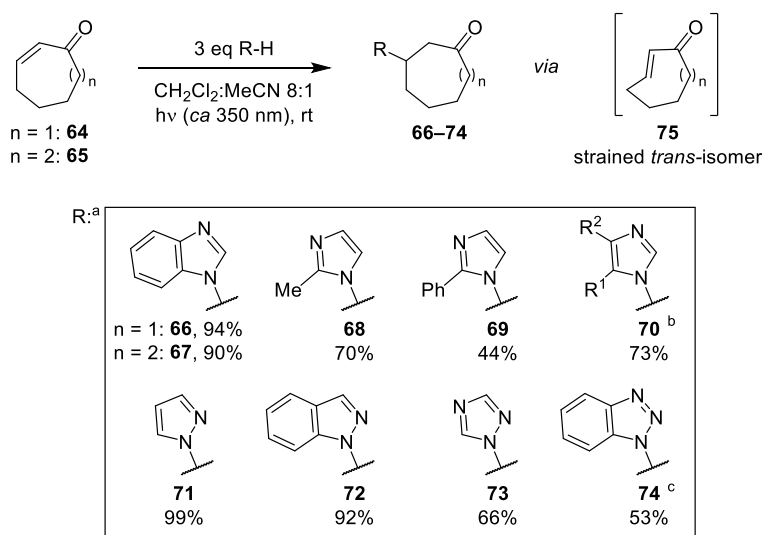
Scheme 20: UV-activated 1,4-addition of medium-sized cyclic enones reported by Beauchemin and co-workers. [a] All yields reported for n = 1, unless stated otherwise. [b] Inseparable mixture of regioisomers obtained, 7:1 ratio of (R^1 = H, R^2 = Me):(R^1 = Me, R^2 = H).[c] 11% of the N-2 regioisomer was also isolated.[5]

Applying Beauchemin's conditions in a Pyrex tube (UV cutoff ~285 nm) to enone **29**, using benzimidazole, 1,2,3-triazole and pyrazole as nucleophiles and a medium-pressure mercury lamp (125 W) as the light source, yielded adducts **77, 78** and **79**, respectively, in good yields (Scheme 21). Indoline adduct **76** was not formed under the same conditions. No reaction was observed for pyrazole and 1,2,3-triazole in the absence of UV irradiation.[a]

---

[a] Reaction of benzimidazole with enone **29** in the absence of UV irradiation was not tested.
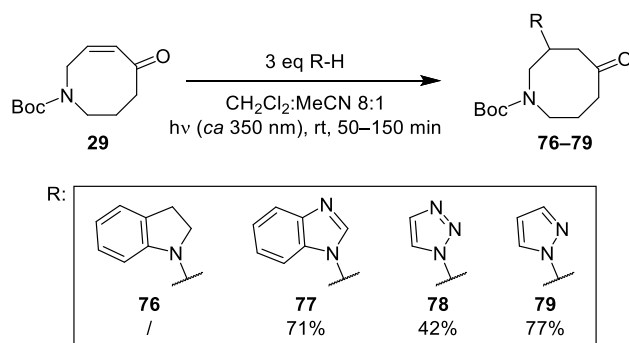
Scheme 21: UV-irradiation allowed enone **29** to undergo 1,4-addition chemistry with nitrogen heteroaromatic nucleophiles.

3.1.4. Boc deprotection: incompatibility with transannular carbonyl

With reductive aminations envisioned as a library step on the azocanone, Boc deprotection of the conjugate addition products was tested, as the deprotected amine could then be functionalised before manipulation of the ketone. Unfortunately, neither reaction of Boc amide with $HCl_{(aq)}$ or TFA on both pyrazole adduct **79** and enone **29** yielded the desired HX salts of Boc-deprotected analogues of **79** and **29** (Scheme 22). Instead, LCMS analysis of the crude reaction mixtures showed ions which correlated with pyrrolizidine analogues **81** and **83**, resulting from intramolecular nucleophilic addition of the deprotected amine into the ketone, followed by dehydration.
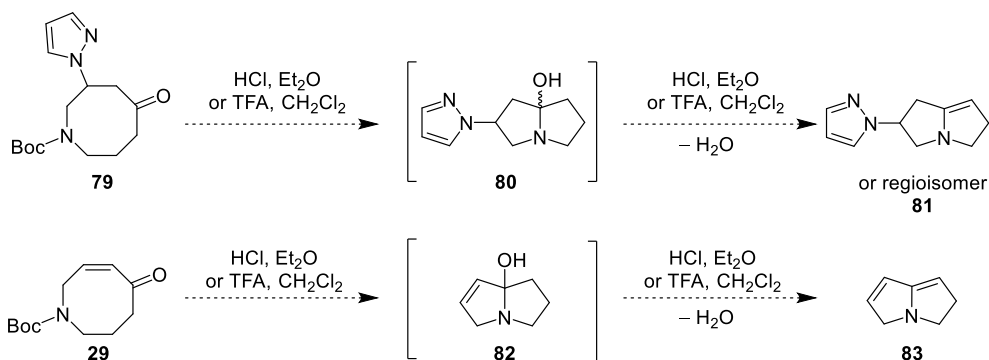
Scheme 22: Postulated pyrrolizidine formation upon Boc deprotection of ketone **79** and enone **29** (pututive structure drawn for **81**).

An analogous cyclic ketone **85** was used by Miller and co-workers as a precursor for pyrrolizidines **84** and **86** (Scheme 23).[9,10] XRD analysis of the enone precursor **87** to ketone **85** not only showed that the olefin and carbonyl were twisted out of conjugation, which may explain the lack of reactivity of enone **29** towards standard conjugate additions, but also that the nitrogen was presented at an angle of 112 °C (N-C=O) with respect to the transannular carbonyl. As the nitrogen in our azocanones may be aligned with the transannular C-O π^*

antibonding molecular orbital, this orientation would favour transannular cyclisation after deprotection of the amine.[10]
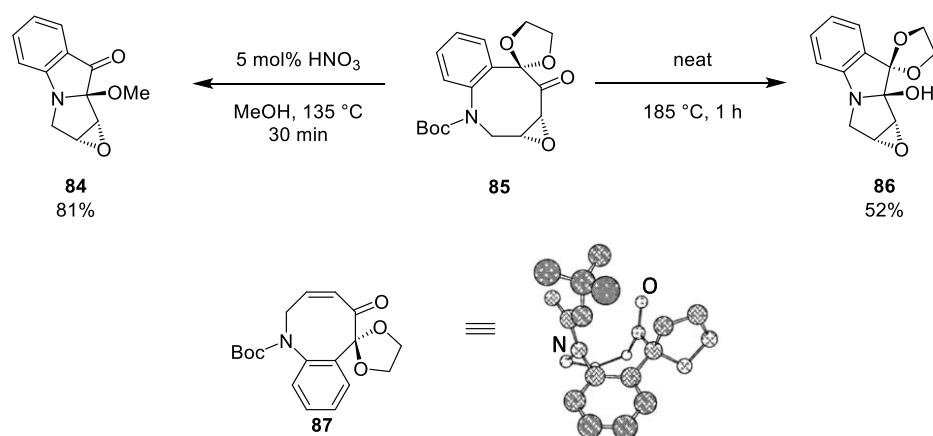
Scheme 23: Pyrrolizidine synthesis by Miller and co-workers.[9,10, a]

In light of these results (Scheme 22), we hypothesised that the carbonyl would need to be protected or converted to a less electrophilic moiety before Boc deprotection of the amine, in order to prevent transannular cyclisation. This hypothesis was confirmed by Boc deprotection of **63**, which did yield the deprotected amine **88** •HCl, although this product could not be obtained in analytically pure form (Scheme 24).[b]
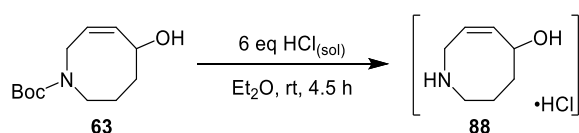
Scheme 24: Allyl alcohol **63** underwent Boc deprotection, but the isolated amine product was not analytically pure.

3.1.5.   Reductive amination

As Boc deprotection could not proceed in the presence of the transannular ketone, reductive amination was considered to first convert the carbonyl in ketone **79** and enone **29**. All attempts to perform reductive amination of ketone **79** with morpholine, a privileged structure in drug discovery,[11] using NaBH(OAc)$_3$, failed to afford the desired amine product **89**, although the [M+H]$^+$ ion for desired product **89** was observed in the crude reaction mixtures but never as the major peak. No reaction was observed without the addition of AcOH (Table 4, Entry 3), but

---

[a] Crystal structure reprinted with permission from Papaioannou et al.[10] Copyright 2022 American Chemical Society.
[b] Selected data: ^{1}H-NMR (300 MHz, CDCl$_3$) δ_H 10.22 (br s, 1H), 6.05 − 5.94 (m, 1H), 5.86 − 5.70 (m, 1H), 4.80 − 4.69 (m, 1H), 4.07 − 3.92 (m, 1H), 3.32 − 3.01 (m, 1H), 2.84 − 2.30 (m, 2H), 2.15 − 1.77 (m, 4H). LCMS (ESI+): m/z 255.4 ([2M+H]$^+$, 100%), 128.2 (100, [M+H]$^+$)

inclusion of this additive led to the formation of a salt, presumably with morpholine, which precipitated in THF (Table 4, Entry 1). Although this salt displayed better solubility in DCE and DMF (Table 4, Entries 2 and 4), ketone **79** was never fully consumed.

*Table 4: Attempted reductive amination of ketone **79** with morpholine.*
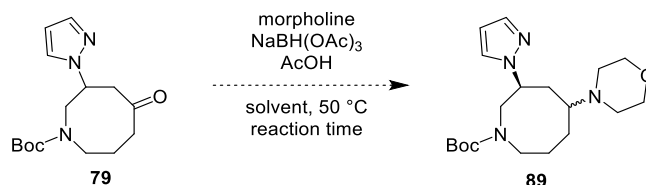
Entry	Solvent	Eq morpholine	Eq NaBH(OAc)$_3$	Eq AcOH	Reaction time (h)
1	THF	4.0	3.0	3.0	48
2	DCE	2.0	4.0	4.0	30
3	DMF	1.1	1.4	-	23
4	DMF	2.1	2.1	6.0	20

Given the Luche reduction of parent scaffold **29** had worked well (Scheme 19, page 44), a reductive amination was also attempted on the enone.[12] However, instead of yielding the allylic amine **90**, the 1,4-conjugate addition adduct **91** was observed. In this way, conjugate addition product **91** was synthesised on gramme-scale and in good yields (Scheme 25).
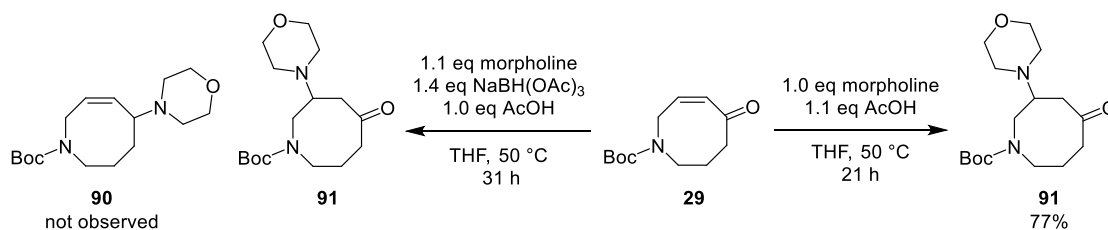
*Scheme 25: Reductive amination of enone **29** did not yield the desired amine **90** but conjugate addition product **91** instead.*

Given the synthesis of morpholine adduct **91** was amenable to scale-up, further chemistry was explored on this product. Since reductive aminations with morpholine had not proven successful on ketone **79** (Table 4) and enone **29** (Scheme 25), the primary amine BnNH$_2$ and NH$_3$ were investigated instead to further test the possibility of using a reductive amination to convert the ketone into an amine (Scheme 26). The target benzylamine **92** could not be isolated nor identified in the crude reaction mixture. Although application of a literature procedure for Lewis acid-activated reductive alkylation of NH$_3$ in EtOH did result in the formation of amine

93,[13] the desired product could not be isolated in more than 30% yield. In addition, because Ti(O*i*-Pr)$_4$ posed filtering and phase separation issues during the workup, an alternative approach was investigated.
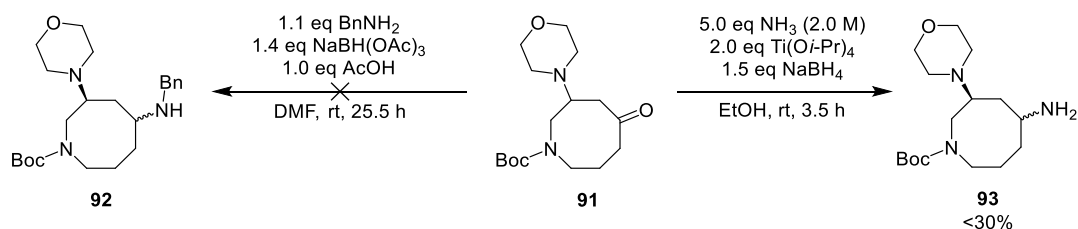
Scheme 26: Reductive amination of ketone **91** did not yield 2° amine **92**. Although 1° amine **93** could be obtained using NH$_3$, Ti(Oi-Pr)$_4$ and NaBH$_4$, low yields and workup issues called for an alternative approach.

3.1.6.   Oxime synthesis and reduction

The ketone was converted non-stereoselectively into the corresponding oxime **94**, which was subsequently reduced to primary amine **93**. Although the oxime synthesis could be performed on gramme-scale in excellent yields (98%), optimisation of the subsequent reduction was necessary (Table 5). Of all the reactions investigated, only Raney nickel (Table 5, Entry 6) showed clean conversion of the oxime **94** to amine **93**. LCMS chromatograms of the screened reduction mixtures (Entries 1 – 6) showed no emergence of a peak with the same mass as the oxime **94**, but with a different retention time, indicating no competition from a Beckmann ring expansion reaction. LCMS analysis of the LiAlH$_4$ reaction mixture (Table 5, Entry 3) showed the Boc-deprotected *N*-methyl oxime **95** as a major byproduct. This observation was not unexpected as LiAlH$_4$ has been reported to convert Boc-carbamates into *N*-methylamines.[14–16] Since the use of sodium (Table 5, Entry 1) and NiCl$_2$ (Table 5, Entry 2) could pose significant safety risks on scale-up, the reduction was scaled up with Raney nickel, allowing access to the 1° amine **93** on gramme-scale.

*Table 5: Optimisation of the reduction of oxime **94**.*
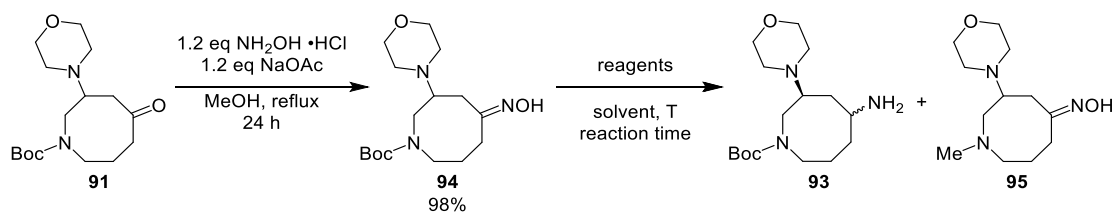
Entry	Reagents	Solvent	Temperature (°C)	Reaction time (h)	Outcome
1	Na, H$_2$ (1 atm)	*n*-PrOH	97	23	**93** + **94** in crude mixture
2	NaBH$_4$, NiCl$_2$•6H$_2$O	MeOH	65	21	**93** + **94** in crude mixture
3	LiAlH$_4$	THF	rt	24	**93** + **94** + **95** in crude mixture
4	PtO$_2$, H$_2$ (1 atm), AcOH	EtOH	rt	23	No reaction
5	Pd/C, H$_2$ (1 atm)	MeOH (7 M NH$_3$)	55	20	No reaction
6	Raney Ni, H$_2$ (1 atm)	MeOH (7 M NH$_3$)	rt	25	Full conversion of **94** to **93** 74% isolated yield

3.2. Diastereomer separation and characterisation

As expected, the reduction of oxime **94** with Raney Ni did not proceed stereoselectively (Table 5, Entry 6), and amine **93** was isolated as a mixture of diastereomers, whose ratio could not be determined *via* ^{1}H-NMR spectroscopy because of overlapping resonances. Unfortunately, these diastereomers proved inseparable: LCMS and SFC traces showed no separation using an achiral SFC column and only partial separation of the two diastereoisomers using a chiral SFC column. Since the amine **93** was not a solid, selective recrystallisation was not possible, and separation *via* diastereomeric salt formation was not explored. Hence, functionalisation of the amine to provide separable diastereomers was investigated.

3.2.1. *Synthesising separable diastereomers*

An initial approach was to synthesise library building blocks as a mixture of diastereomers; this would obviate the need for a protection/deprotection step of the free amine. However, attempted synthesis of aminopyridine **96** using 2-fluoropyridine in an S$_N$Ar reaction showed incomplete consumption of the starting material **93** after 51 h *via* LCMS and TLC analysis, and yielded none of the desired product mass and an unidentified byproduct with [M+H]$^+$ and

[2M+H]$^+$ ions for M = 326 Da. Reductive amination using amine **93** and formaldehyde did yield the desired 3° amine **97** (74% crude mass recovery) and showed separation on an LCMS chromatogram (reverse phase, basic). However, subsequent Boc deprotection of the crude reaction mixture resulted in degradation of the product, with LCMS analysis showing a major product with an m/z value corresponding to [M+H]$^+$ for M = 196 Da. As this result indicated deprotection issues with dimethylamine **97**, possibly due to intramolecular nucleophilic substitution of the deprotected amine on the protonated dimethylamine which could produce 5-5 bicycle **99**, the dimethylamine intermediate **97** was not resynthesised nor characterised (Scheme 27).
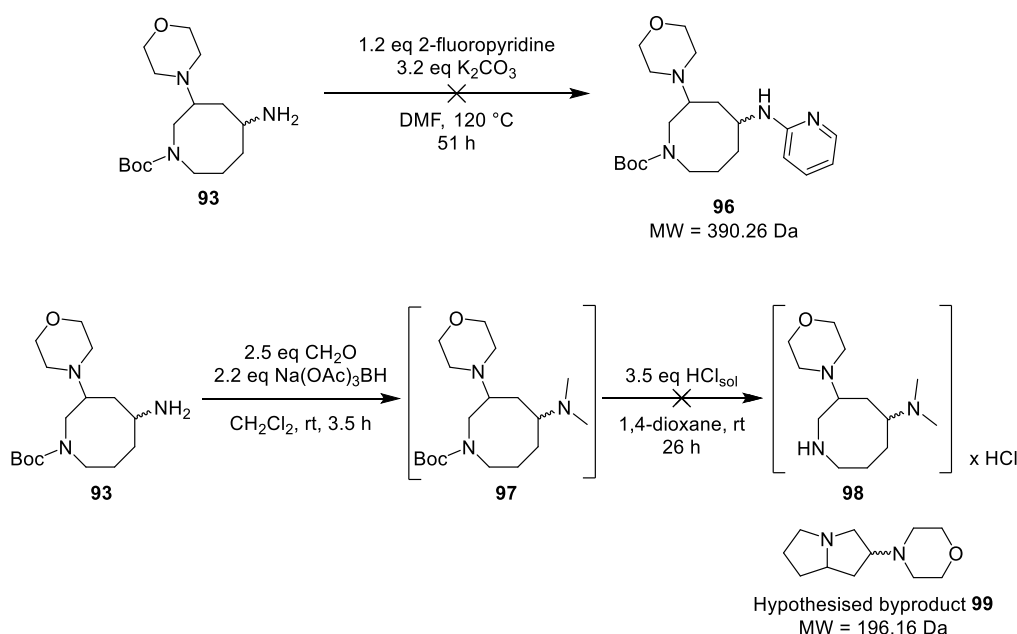
*Scheme 27: Initial attempts to synthesise separable diastereomers. S$_N$Ar using 2-fluoropyridine was unsuccessful, while dimethylamine **97** degraded upon Boc deprotection with HCl, which yielded putative pyrrolizidine **99**.*

Instead of trying to separate building block diastereomers, orthogonal protecting groups were next considered, since diastereomer separation of the protected intermediate would only require one separation step instead of multiple separations for multiple building blocks. Furthermore, the installment of an orthogonal protecting group on the primary amine would facilitate the synthesis of a combinatorial library, adding extra value to the synthesised scaffold.

Cbz protection with Cbz-Cl showed full consumption of the amine **93** after 3 h;[a] however, TLC and LCMS analysis showed no separation of the diastereomers and therefore the Cbz-protected

---

[a] Reaction conditions: 0.66 mmol starting material **93**, 1.1 eq DIPEA, 1.1 eq CbzCl in THF (0.5 molar), rt.

amine was not purified nor characterised. We hypothesised that functionalisation of the primary amine with NsCl could produce separable diastereomers. Preliminary models, using a molecular model kit, suggested that by lowering the pK_a of the amine proton by nosylation[17–19] an intramolecular H-bond could be obtained for the *cis* diastereomer **cis-100** but not in the *trans* diastereomer **trans-100** (Figure 15). This difference could increase the difference in polarity between the two diastereomers and thereby facilitate separation *via* chromatographic methods. Literature precedent for a sulfonamide acting as an intramolecular H-bond donor was provided by Harter *et al.*, who found that the rigidified peptide analogue **101** displayed improved potency towards caspase-1 inhibition.[20]
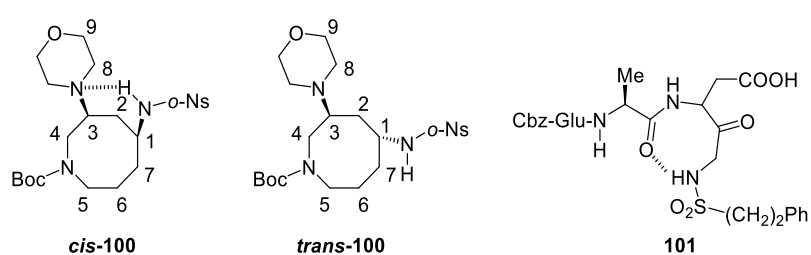
*Figure 15: Hypothesised intramolecular H-bond in cis diastereomer **cis-100**. Peptide analogue **101** showed precedent for sulfonamides as intramolecular H-bond donors.[20]*

Gratifyingly, nosylation of primary amine **93** with *o*-NsCl yielded separable diastereomers: both LCMS and SFC chromatograms showed separation of the two diastereomers, allowing for separation *via* chromatographic methods. Consequently, the synthesis of *o*-Ns protected amine diastereomers **a-100** and **b-100** was performed on gramme scale, followed by separation of the diastereomers *via* automatic reverse-phase chromatography (MeCN 0.1% HCOOH : H$_2$O 0.1% HCOOH). Since the acidic eluent yielded the separated diastereomers as formate salts, an additional aqueous workup with NaOH$_{aq}$ was performed to yield sulfonamides **a-100** and **b-100** in acceptable yields (Scheme 28).
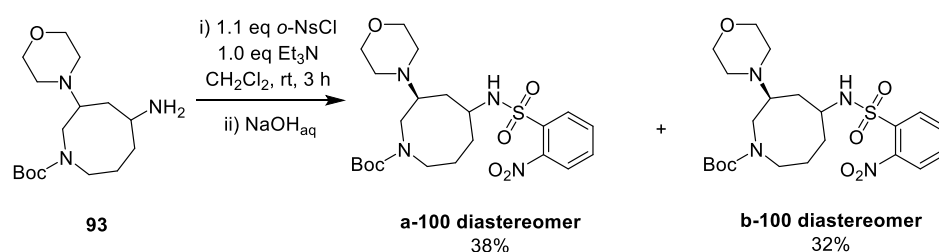
Scheme 28: Synthesis and separation of o-Ns protected amines.

3.2.2. Tentative assignment of nosylsulfonamide stereochemistry via NMR spectroscopy

Although the two nosyl diastereomers **a-100** and **b-100** were separable, their relative stereochemistry was yet unassigned. Whilst XRD analysis of a crystalline analogue would likely be necessary to confirm definitively the relative stereochemistry, we first turned to NMR spectroscopy to attempt a putative assignment of the relative stereochemistry. An interesting observation was that the two diastereomers showed very different chemical shifts for the N*H* proton resonances in CDCl$_3$ (400 MHz). The N*H* proton of more polar diastereomer **a-100** appeared under the stack at δ_H 1.40 – 2.03 ppm, while that for the less polar diastereomer **b-100** appeared at δ_H 5.35 ppm (Figure 16). A NOESY experiment did not give much information; cross peaks were observed between H-8 and the stack containing N*H* for **a-100**, but this cross peak could equally arise from an NOE between H-8 and H-2, as the H-2 resonance was also buried in this stack (Figure 16). The N*H* resonance in diastereomer **b-100** did not show NOESY cross peaks with H-8 nor H-9 (cross peaks which might be expected if the N*H* proton forms a H-bond with the morpholine nitrogen,) only with H-1, H-3 and the H-2, H-6, H-7 stack. These results indicate that the N*H* proton of diastereomer **b-100** is not in proximity to the morpholine protons.
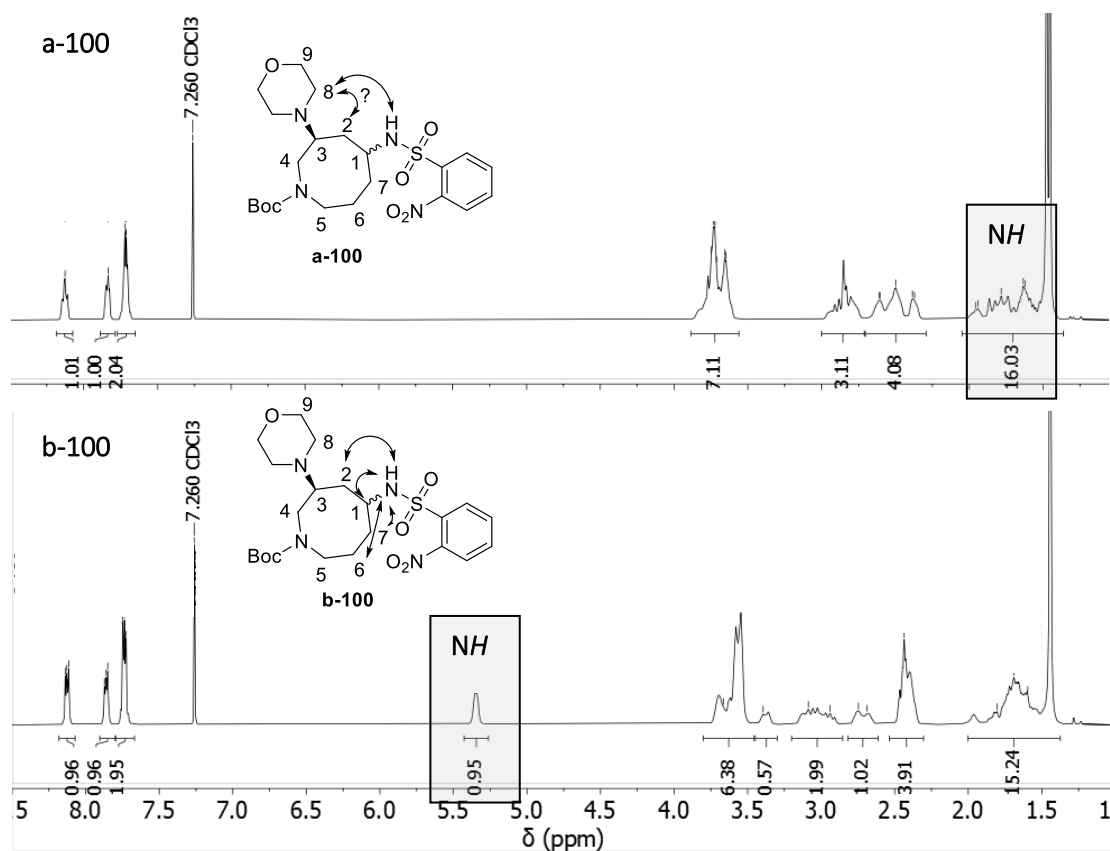
*Figure 16: ^{1}H-NMR spectroscopic analysis of diastereomers **a-100** and **b-100** revealed a significant difference in NH chemical shift (CDCl$_3$, 400 MHz, 298 K). Observed NOESY cross peaks with NH proton shown.*

Abraham *et al*. found that the difference in the ^{1}H chemical shift of an N*H* proton, in various amines, (acet)amides, anilines and sulfonamides, in DMSO-d_6 and CDCl$_3$ could be correlated to its 'solute H-bond acidity' (A), which is a quantitative indicator of how well an N*H* proton can form H-bonds with an external H-bond acceptor.[21,22] An N*H* proton with a high A-value has a high propensity to bond with an external hydrogen bond acceptor, in this case DMSO-d_6. An N*H* group which already participates in an intramolecular H-bond has a low A-value; it is less able to form a H-bond with DMSO-d_6 and therefore will not show a large change in the ^{1}H chemical shift between experiments in CDCl$_3$ (which is not an H-bond acceptor) and DMSO-d_6 (Δppm = 0 – 1.45 ppm). An acidic N*H* proton which is not involved in an intramolecular H-bond can thus form a H-bond with DMSO-d_6, showing a higher 'solute H-bond acidity' and will therefore display a larger difference in ^{1}H chemical shift in the two solvents (Δppm > 1.45 ppm).[21,22]

Compared to samples in CDCl$_3$, both diastereomers showed a downfield shift in the N*H* proton resonance upon ^{1}H-NMR spectroscopic analysis in DMSO-d_6, whilst samples in CDCl$_3$: DMSO-d_6 9:1 illustrated the downfield migration of the N*H* resonance (Figure 17). Given the higher chemical shift for the N*H* resonance of **b-100** in CDCl$_3$, the difference in its ^{1}H chemical shift in CDCl$_3$ and DMSO-d_6 (Δppm = ~6.5 ppm) was smaller than that observed for **a-100** (Δppm = ~3.0 ppm).
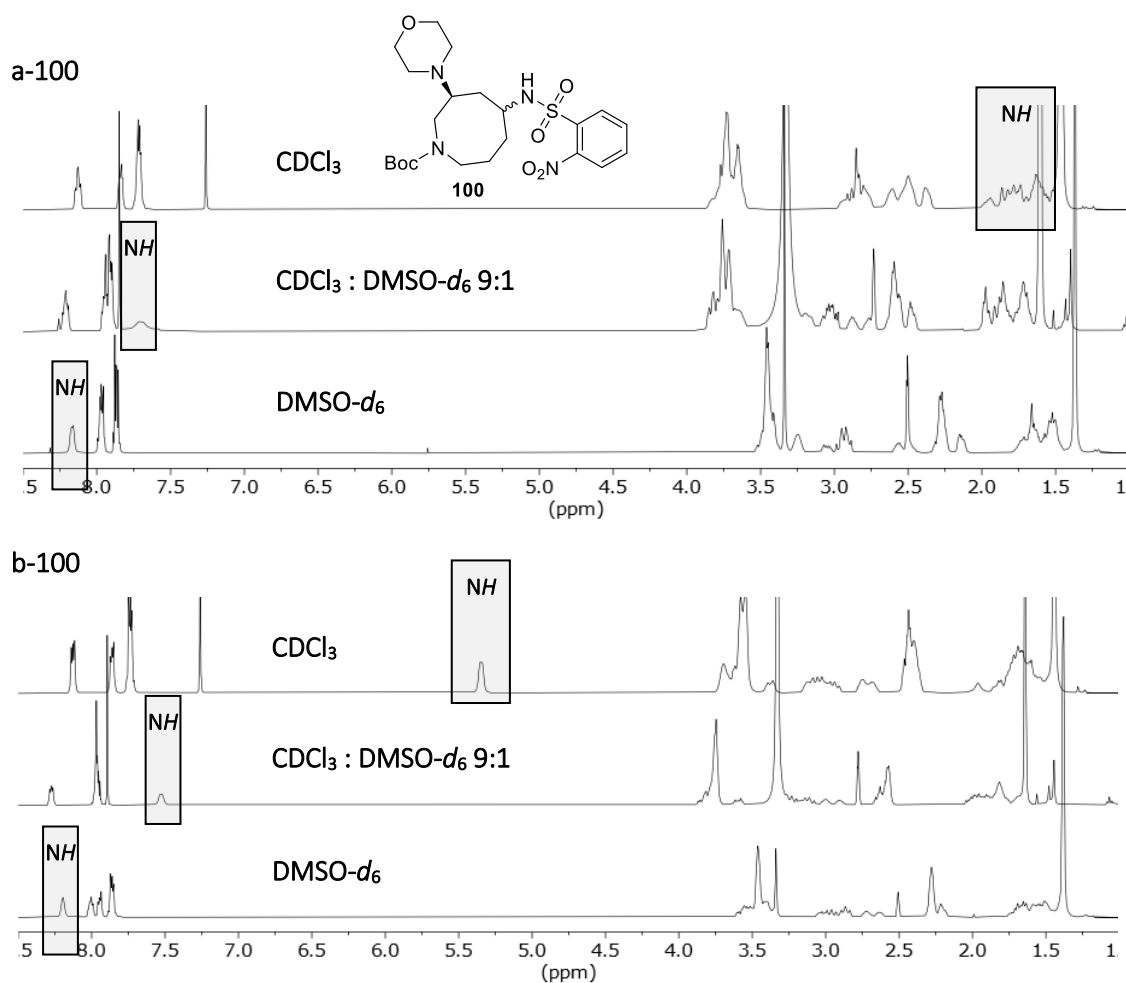
*Figure 17: The NH proton resonance of **a-100** shows a difference in chemical shift of roughly 6.5 ppm between ^{1}H-NMR spectra in CDCl$_3$ and DMSO-d$_6$, whilst for **b-100** the difference is only about 3.0 ppm. The ^{1}H-NMR spectrum in CDCl$_3$: DMSO-d$_6$ 9:1 shows large downfield migration of the NH resonances already. (NMR spectroscopy performed at 400 MHz, 297 K).*

Based on these results, we postulated that the N*H*-proton in **b-100** forms an intramolecular H-bond. Therefore, diastereomer **b-100** was tentatively assigned as the *cis*-diastereomer, but this assignment came with a few caveats: the observed differences in N*H* chemical shifts of roughly 6.5 ppm for **a-100** and 3.0 ppm for **b-100** were much larger than reported for N*H* protons participating in intramolecular H-bonds (< 1.45 ppm).[21] Furthermore, since no NOESY cross peaks were observed between H-8 and the N*H* proton in **b-100**, the assignment remained tentative and a crystal structure was therefore necessary to confirm definitively the relative stereochemistry of the two diastereomers. Unfortunately, nosylsulfonamides **a-100** and **b-100** were both isolated as colourless oils.

Reaction of 1° amine **93** with *p*-NsCl was attempted on 150 mg scale (Scheme 29). The resulting diastereomers **a-102** and **b-102** were also separable *via* preparative LC and showed similar

^{1}H-NMR and ^{13}C-NMR spectra to the *o*-nosyl diastereomers **a-102** and **b-102**, including the characteristic N*H* peak chemical shifts (see Appendix 1.1). As a result, **b-102** was also tentatively assigned as the *cis*-diastereomer by analogy.
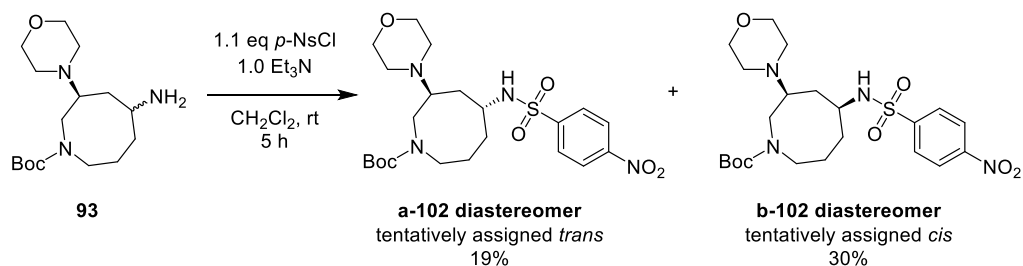
*Scheme 29: Synthesis of p-nosylsulfonamide diastereomers **a-102** and **b-102**.*

3.2.3. Crystal structure of p-nosylsulfonamide 102: revisiting the hypothesised stereochemistry

Although initial recrystallisation attempts on both *p*-nosylsulfonamide diastereomers (slow cooling in EtOAc, diisopropyl ether, *i*-PrOH or MeCN, supersaturation by slow evaporation of EtOAc or heptane/EtOAc solution) were unsuccessful, slow cooling of a solution of **a-102** in EtOH provided small colourless prisms.[a] The tentatively assigned *cis*-diastereomer **b-102** did not crystallise under these conditions. The crystals of **a-102** were submitted for XRD analysis by the University of Birmingham analytical staff.

XRD analysis of the obtained EtOH-cocrystal **a-102** disproved the tentative stereochemistry assignment that we had made by NMR spectroscopy as the structure of **a-102** proved to be the *cis* diastereomer (Figure 18). In addition, no intramolecular H-bond was observed in the crystal, as both the morpholine and sulfonamide moieties were oriented pseudo-equatorially on the eight-membered ring, which adopts a chair-boat conformation in the solid state. The morpholine ring adopts a chair conformation, while the sp^2 nitro moiety was twisted 31.5° out of the aromatic phenyl ring plane. All quaternary and secondary carbons and heteroatoms comprising the Boc-amide and its neighbouring ring-carbons were almost completely coplanar (the four possible torsion angles between C-4, C-5, Boc-N, C-10, (C-10)*O* and (C-10)=*O* were larger than 177.7° or smaller than 2.9°, see Appendix 7) illustrating the sp² character of the atoms that make up the carbamate.

---

[a] Attempted fractional crystallisation of **a-102** from a purified mixture of diastereomers in EtOH was unsuccessful.
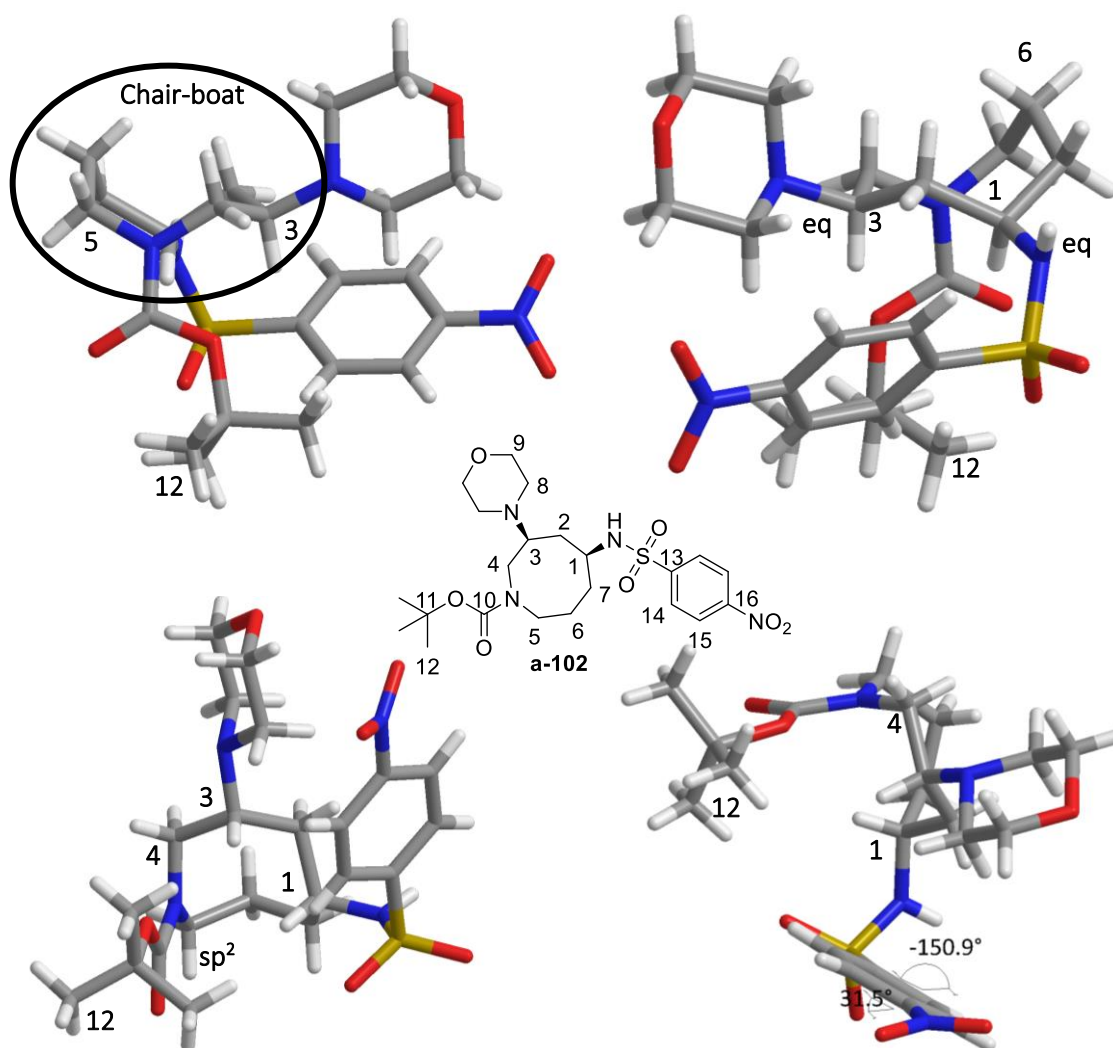
*Figure 18: Crystal structure of p-nosylsulfonamide **a-102**, generated using Chem3D. Hydrogens are not shown. Co-crystallised EtOH omitted for clarity. For full experimental data and 50% probability ellipsoid representations at 100 K, see Appendix 7.*

Although the crystal structure of **a-102** did not show the hypothesised intramolecular H-bond, this does not mean that the previously reported NMR spectroscopic experiments may not indicate a (weak) intramolecular H-bond: if the *p*-nosyl group were to be grafted on the pseudo-axial position whilst keeping all other conformations locked, a H-bond could be possible in the *trans* diastereomer between the sulfonamide proton and the Boc carbonyl (Figure 19). However, the trans diastereomer may adopt a different conformation than its *cis* analogue, both in the solid state and in solution. Therefore, no solid claims can be made on the possibility of a H-bond without additional experimental data.
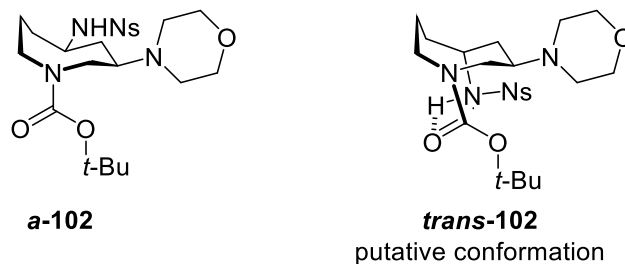
Figure 19: Possible H-bond in **trans-102**, based on X-ray structure of **a-102**.

Given the high degree of similarity observed in the ^{1}H-NMR and ^{13}C-NMR spectra between *o*-nosyl precursors **100** and *p*-nosyl precursors **102**, including the different N*H* proton resonance shift between the *cis* and *trans* diastereomers (see Appendix 1.1), the assigned stereochemistry of *p*-nosyl precursor **102** was applied to *o*-nosyl precursor **100** by analogy.

Having synthesised and separated the *o*-nosyl diastereomers **cis-100** and **trans-100** on gramme scale, each bearing two orthogonal protecting groups for the embedded 1° and 2° amine groups, a set of library compounds was now only two deprotections and two functionalisation steps away. The common core structure, shared by all library compounds was coined the SACE1 scaffold and the derivative compound library shares this name (Figure 20).
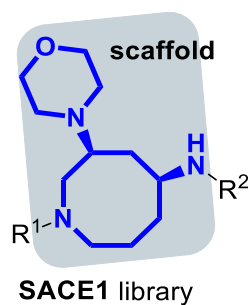
Figure 20: The SACE1 library, built on the SACE1 scaffold.

3.3. Compound library synthesis: terminology

A compound library often contains several analogues of a library precursor. These analogues are usually generated in the final steps of library synthesis, which means that many (if not all) compounds in a compound library share the same precursors. As these library precursors advance through the synthetic pathway towards the final library compounds, some terminology is used in this thesis to describe the synthesised products and precursors, depending on their place in the pathway towards the final compound library (Scheme 30). Since these terms are sometimes used subjectively, their use in this thesis is defined as follows:

- **Parent scaffold**: azacyclooctenone **29**, the common precursor for all synthesised library compounds.

- **Scaffold**: the core skeleton shared by all final compounds in a compound library. The compound libraries reported in this thesis are distinguished based on their scaffold (*e.g.,* SACE1 library, SACE2 library).

- **Protected scaffold**: contains the scaffold, but the appendable sites are functionalised with protecting groups. The protected scaffold has no structural analogues.

- **Building block:** the direct precursor to a library compound, it serves as the starting material for parallel synthesis. Building blocks are structural analogues, sharing a common scaffold.

- **Protected building block**: direct precursor to a building block. The appendable site for library synthesis is functionalised with a protecting group.

- **Library compound**: the product formed after functionalisation of a building block *via* parallel synthesis. Library compounds are the end products of library synthesis.
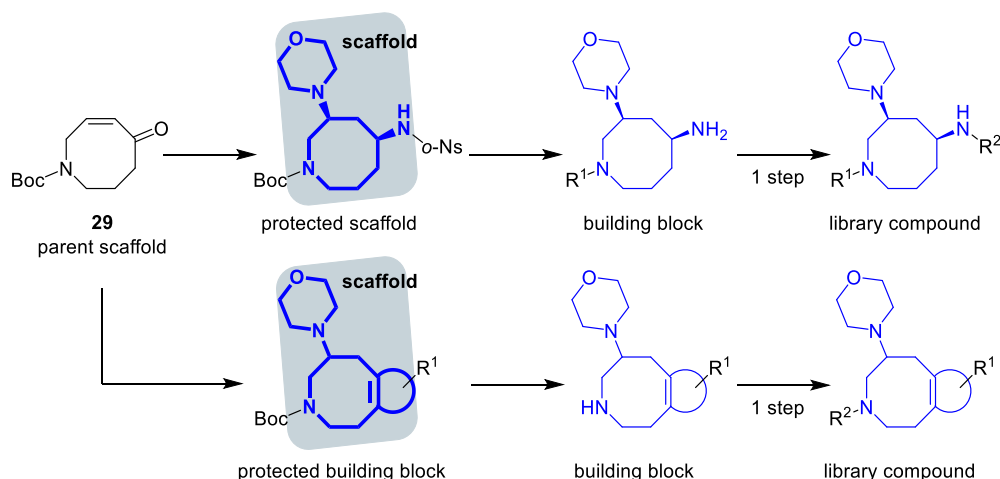
Scheme 30: Exemplar synthetic pathways towards compound libraries. The shared core skeleton (blue) is called a scaffold.

Building blocks and other library precursors are also included in the final compound library whenever deemed appropriate (*vide infra*).

3.4. Functionalising the SACE1 scaffold

o-Nosyl deprotection of a mixture of diastereomers **100** was achieved in quantitative yield using PhSH / K$_2$CO$_3$ in MeCN (Scheme 31). An aqueous workup involving saturated aqueous K$_2$CO$_3$ solution and EtOAc or CH$_2$Cl$_2$ only partly removed the excess PhSH and aromatic byproduct. However, a subsequent washing step over a silica plug allowed for complete removal of aromatic impurities by eluting with CH$_2$Cl$_2$, after which the deprotected amine could be eluted with CH$_2$Cl$_2$:NH$_3$ (7 M in MeOH) 9:1 solution. The separated *cis* and *trans* diastereomers were deprotected on 500 mg scale in yields of 96% and 87%, respectively (Table 7, Entries 5 and 6, *vide infra*). Given *cis*-*p*-nosylsulfonamide **cis-102** was obtained as a crystalline solid, we also attempted deprotection of this sulfonamide, as this crystalline compound could facilitate large-scale purifications. Deprotection of *p*-nosylsulfonamide **cis-102** under analogous conditions showed only partial deprotection after 24 h, and after subsequent heating for 29 h under reflux conditions, only 72% of deprotected amine was isolated (Scheme 31). Given the shorter reaction times and higher yields, synthetic work proceeded using *o*-nosylsulfonamide **100**.
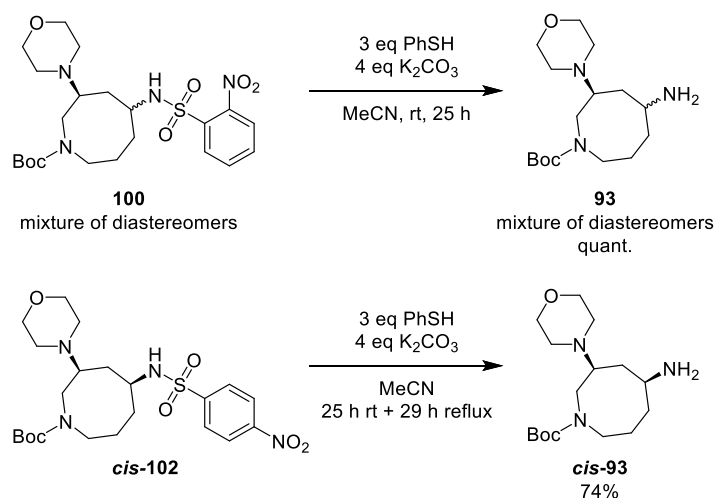
*Scheme 31: Deprotection of nosylsulfonamides **100** and **cis-102**.*

Although PhSH is a well-known reagent for nosyl deprotections,[17,23] it is also volatile, has a pungent odour and is (repro)toxic. Therefore, less toxic mercaptoacetic acid was investigated as an alternative, also because the aromatic byproduct from this deprotection is water-soluble.[17,23] Two conditions were tested,[23,24] but neither was as efficient in deprotecting the nosyl group as was the PhSH method: both reaction mixtures still showed starting material after 3 days at rt, after which overnight heating under reflux conditions yielded multiple unidentified side products for the mixture in MeCN and degradation in DMF, respectively, as observed *via* LCMS (Scheme 32). Hence, Ns deprotection using PhSH was the method of choice.
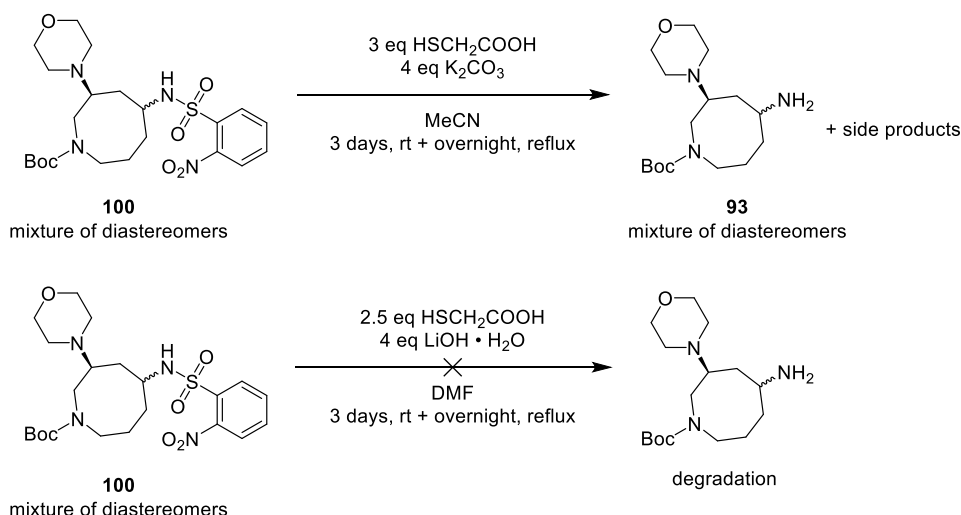
*Scheme 32: Attempted deprotections of nosylsulfonamide **100** using HSCH₂COOH.*

The Boc-protected amine of nosylsulfonamide **100** was decorated with a mesyl and ethylurea group, small representatives of common functional groups in medicinal chemistry, by performing a telescoped Boc deprotection/functionalisation step, which allowed for quick, high-yielding syntheses of sulfonamides **103** and ureas **104** (Table 6). Preliminary Boc deprotections using HCl in 1,4-dioxane yielded the deprotected crude product but required 10 equivalents of HCl. The crude mixture resulting from deprotection in *i*-PrOH formed a homogeneous mixture upon treatment with Et₃N in the next step to generate the free base, while the crude mixture dried from 1,4-dioxane remained a brown milk upon introduction to Et₃N in DMF. Therefore, *i*-PrOH was the solvent of choice for performing the Boc deprotection.

Table 6: Telescoped deprotection-functionalisation of the secondary amine. Relative stereochemistry of the starting material is shown in the table.
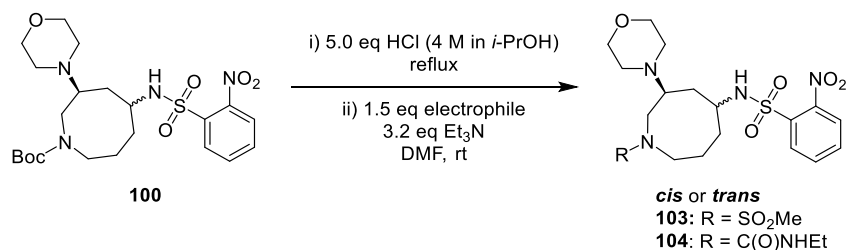
Entry	Product	Electrophile	Diastereomer	Step 1 rxn[a] time (min)	Step 2 rxn[a] time (min)	Isolated yield (%)
1	*cis*-**103**	MsCl	*cis*	100	120	90
2	*trans*-**103**	MsCl	*trans*	100	120	96
3	*cis*-**104**	EtNCO	*cis*	90	210	92
4	*trans*-**104**	EtNCO	*trans*	390	120	93

[a] rxn time: reaction time.

The high yields obtained for functionalisation of the secondary amine in the presence of the nosyl group illustrated the stability of the *o*-Ns protecting group under the used reaction conditions, which was in accordance with earlier reported stability of nosylsulfonamides under acidic and basic reaction conditions.[23]

Using the optimised deprotection and workup conditions (Scheme 31, page 60), all protected sulfonamides, ureas and carbamates were *o*-Ns deprotected in high yields, providing six building blocks **93**, **105** and **106** for validation reactions and library synthesis (Table 7).

*Table 7: Nosyl deprotection of intermediates **93, 105** and **106**.*

100: R = Boc
103: R = SO₂Me
104: R = C(O)NHEt

93: R = Boc
105: R = SO₂Me
106: R = C(O)NHEt
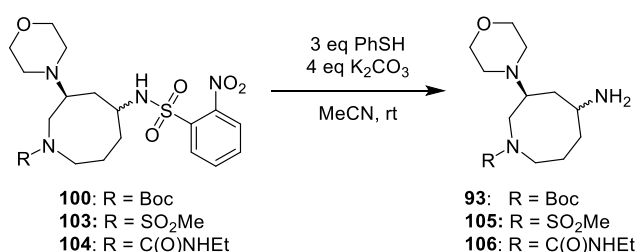
Entry	Product	R	Diastereomer	Time (h)	Isolated yield (%)
1	*cis*-105	SO₂Me	*cis*	18	90
2	*trans*-105	SO₂Me	*trans*	25	82
3	*cis*-106	C(O)NHEt	*cis*	22	98
4	*trans*-106	C(O)NHEt	*trans*	21	92
5	*cis*-93	Boc	*cis*	18	98
6	*trans*-93	Boc	*trans*	25	96

3.5.   Scaffold validation and library synthesis

With sufficient quantities of the six building blocks in hand (0.4 – 0.7 g each), the SACE1 scaffold could now be validated for library synthesis. Given that library synthesis proceeds *via* parallel chemistry, running dozens of reactions at once, validation of the planned library reactions was important to assess the feasibility of the library synthesis and to prevent the loss of precious time and resources. Following the planned library synthesis steps for a small selection of compounds would give an idea of what yields to expect (important to inform the reaction scale, since a minimum of 10 mg final product was desired) and whether the reaction and purification procedures used would need to be optimised before starting high-throughput library synthesis.

3.5.1. Parallel library synthesis: procedures and caveats

Performing a parallel synthesis of several dozens of library compounds requires careful planning and specialised equipment. The in-house expertise and facilities present at Symeres enabled efficient synthesis of the library compounds reported in this thesis, following procedures which have been previously developed at the company.

3.5.1.1. Parallel synthesis at Symeres

In general, parallel library synthesis at Symeres was performed in 8 mL capped vials, loaded in a 4 × 6-well heat-conducting reaction block, with each vial equipped with a stirrer bar. In order to efficiently set up reactions in a short time frame, stock solutions were made of the reagents (*e.g.*, amide coupling reagents) or free-based building blocks, which were then dispensed by a dispenser pipette, allowing for quick dispensing of equal volumes. The 4 × 6-well reaction blocks provided a visual aid for planning parallel syntheses, as every row can be filled with a single building block, or every column with a single reagent (Figure 21). Once set up, the reactions were monitored *via* LCMS, taking aliquots in parallel with automatic multichannel pipettes, which were then loaded onto 96-well plates.

Figure 21: Pictorial representation of an exemplar parallel synthesis experiment running in a 4 × 6 reaction block. Using dispenser pipettes, stock solutions can be added quickly per row or per column.

Upon completion of the reaction, the reaction mixtures were pushed through a syringe filter (solvent from reactions performed in CH_2Cl_2 was first evaporated under an open atmosphere and then re-dissolved in a polar solvent (DMSO, MeOH, DMF, MeCN, H_2O) prior to filtering) and submitted for preparative reverse-phase LC, which was executed by members of the analytical facility team at Symeres. The collected fractions were received in labelled tubes and the fractions were dried overnight in a Genevac^{TM} centrifugal evaporator. Subsequently, the residues were redissolved in a minimal amount of MeCN:H_2O (no set volumetric ratio, usually 1:1) and combined in a tared and barcoded 8 mL vial. The combined fractions were dried overnight once more in a Genevac^{TM} centrifugal evaporator, after which time every vial was weighed. All analytical data, including weights and compound names were linked to barcodes, which allowed for efficient archiving and tracking of compound data.

3.5.1.2.   *Parallel chemistry caveats*

Factors inherent to the parallel synthesis method used contribute to the loss of product (Table 8). For example, a library compound may behave differently on the preparative LC column than during reaction monitoring on a different instrument. Hence, the isolated yields were not as representative of the success of the reaction as single experiments performed on a larger scale: yields of 40% for library compounds were no exception and generally considered to be good. Nevertheless, the aim of library synthesis is to obtain adequate amounts of library compounds for future biological screening (> 1 mg is often considered enough for biological screening, so we aimed for 10 mg), rather than optimising every individual reaction.

Table 8: Common causes of product loss during parallel synthesis.

Parallel synthesis step	Cause of product loss
Reaction monitoring	For small reaction volumes (*e.g.*, 0.4 mL), several aliquots of 10 µL can result in loss of >10% yield
Syringe filter	Product may be retained on the filter
Preparative LC	<u>Tailing peaks</u>: maximum amount of collection tubes reached before end of peak <u>Early elution:</u> product elutes through the column before time threshold for compound collection (product in injection peak) <u>Co-elution with reagents/byproducts:</u> only pure fractions are collected, or additional round of preparative LC may be necessary <u>Solubility issues:</u> compound precipitates or crystallises on column <u>Poor UV absorption:</u> compound collected based on mass detection, but less sensitive to co-eluted products
Product/reaction mix transfer	Not entire volume injected on preparative LC, solubility issues in MeCN/H_2O during transfer to barcoded vial

3.5.2. Validation set

The validation study for parallel synthesis of Boc-protected building block **93** was prioritised as the synthesis of urea and sulfonamide building blocks **106** and **105** (Section 3.4) had already illustrated the reactivity of the secondary amine towards a representative isocyanate (EtNCO) and sulfonyl chloride (MsCl). The alternative approach, obtaining a set of primary amine building blocks, would require performing multiple nosyl deprotections in a parallel fashion (Scheme 33). Because of its smell and toxicity, reaction mixtures containing PhSH were not amenable to preparative LC and therefore not ideal for parallel synthesis. If *in silico* library design were to show significant advantages of a parallel nosyl deprotection step of the primary amine building blocks, the deprotection step and further validation could always be revisited.
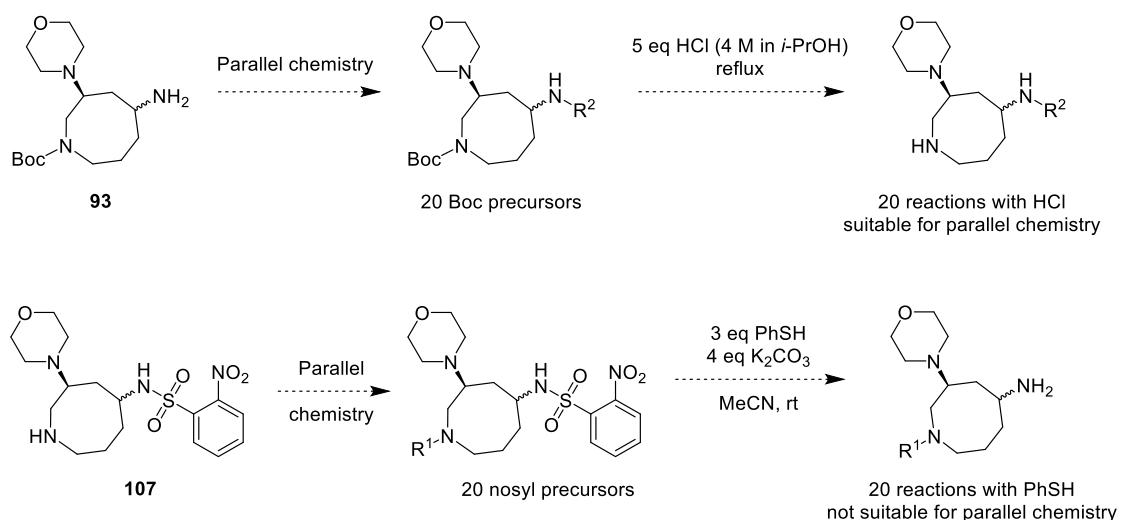
Scheme 33: Parallel nosyl deprotection would require reaction mixtures containing PhSH, which were not amenable to preparative LC.

In-house procedures were followed for reactions of the primary amine **93** with sulfonyl chlorides, AcCl and EtNCO, reagents which were chosen based on *in silico* library design (see Section 4.6, page 89), on a 50 mg scale. DMF was chosen as the reaction solvent, because it allowed the reaction mixtures to be submitted directly to preparative LC (after pushing the mixture through a syringe filter), instead of having to dry the mixtures first and then redissolve them (Section 3.5.1.1). The *trans* diastereomer ***trans*-93** showed isolated product yields well over 40%, with EtNCO showing lower yields than the sulfonyl chlorides and AcCl (Scheme 34). Reactions involving the *cis* diastereomer were consistently lower yielding.
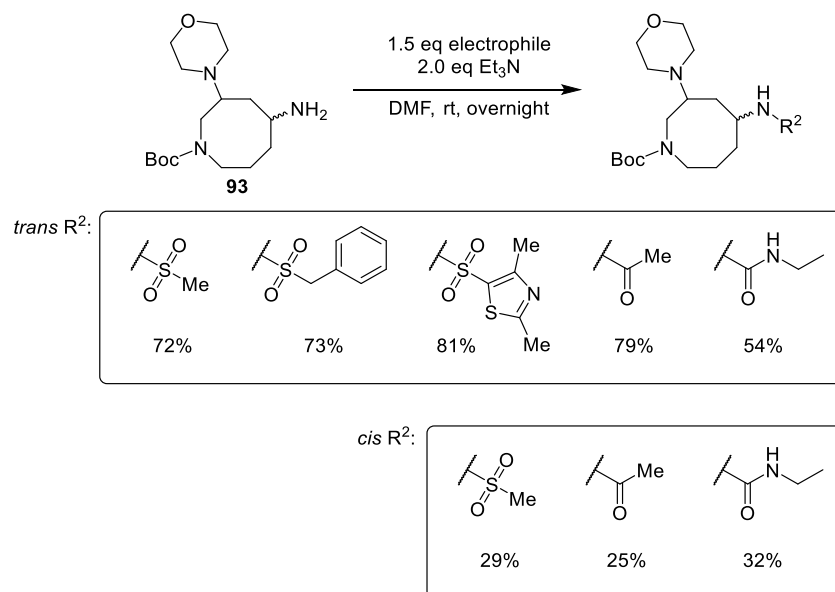
Scheme 34: Validation chemistry on 1° amine **93** using sulfonyl chlorides, AcCl and EtNCO.

Reaction of *cis*-diastereomer **cis-93** with EtNCO afforded the corresponding urea in comparable yields, compared to its reaction with MsCl and AcCl, so the 1° amine in **cis-93** was not considered to be less reactive towards isocyanates (Scheme 34). Worth noting is that LCMS analysis of both reaction mixtures with AcCl showed the presence of a compound with m/z corresponding to that of a doubly acylated product. Based on peak areas on the PDA chromatogram, the ratio of single:doubly acylated product was 9:1 for the *trans* diastereomer and 1:1 for the *cis* diastereomer. However, the obtained acetamide yields were satisfactory, yielding >4 mg product, so the reaction conditions were not optimised.

Parallel amide couplings were performed following in-house procedures, using EDC •HCl and Oxyma Pure (Scheme 35). EDC •HCl was the coupling agent of choice, since DCC and its urea analogue could pose solubility issues during preparative LC, whilst PF_6^- salts derived from HATU were known to contaminate the preparative LC column, requiring multiple flushing steps. Oxyma Pure was used as a less toxic and non-explosive alternative for DMAP, HOAt or HOBt.[25] Both amide couplings proceeded with acceptable yields (Scheme 35), so no further validation was deemed necessary before setting up the planned library reactions.
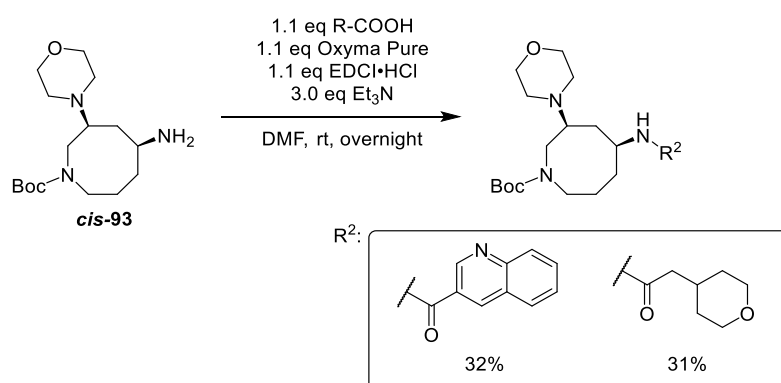
Scheme 35: Amide coupling validation chemistry on SACE1 cis-building block **cis-93**.

Boc deprotection of the validation compounds proceeded readily with HCl in *i*-PrOH (Scheme 36). Since the Boc-precursors had already been purified by preparative LC, another round of purification *via* preparative LC was not deemed necessary for the Boc-deprotected HCl salts. Although these products were not purified, the isolated yields were between 71% and 95%. This observed drop in yield can be explained by the aliquots taken during reaction monitoring (Table 8, page 64): since the reactions were performed in small reaction volumes (0.4 mL), taking multiple aliquots of >10 µL can decrease the yields significantly. Given the small scale of the reactions (10–53 mg), small weighing errors and pipette errors could further explain the

range in the observed yields. Chromatographic chloride ion content determination by the Symeres Analytical staff on the two Boc-deprotected *cis* amides (see Experimental Section 13) indicated that the tetrahydropyran analogue exists as a 2 HCl salt, while the quinoline analogue existed as a 3 HCl salt, showcasing the basicity of the morpholine amine, the secondary amine and quinoline moiety. Later salt determination of library analogues also showed 2 HCl salts for a sulfonamide and urea compound without basic decorations.
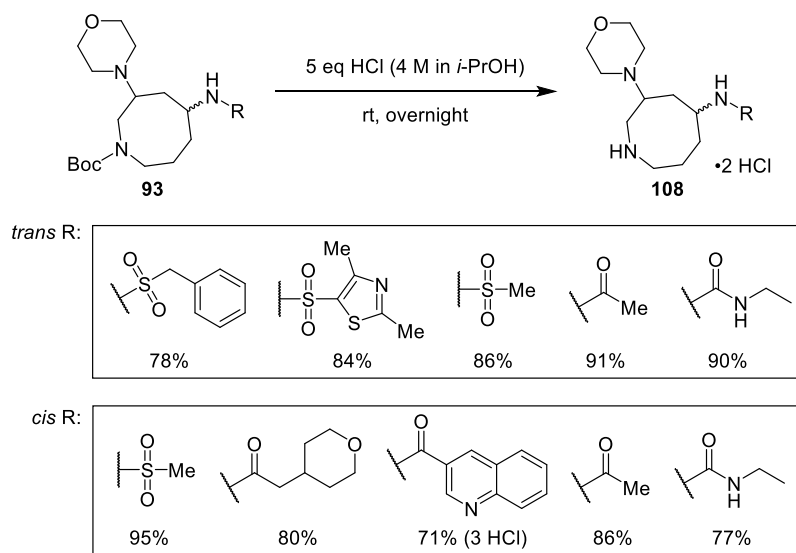
Scheme 36: Validation set for parallel Boc deprotection.

3.5.3.   Library synthesis

Using the reaction conditions validated in the previous section, we were set to synthesise a library with a diverse set of reagents and building blocks, informed by *in silico* library design (see Section 4.6, page 89). 78 parallel reactions were set up, containing either *cis* or *trans* diastereomers derived from building blocks **105**, **106** and **108** (Scheme 37). Since literature precedent exists for bioactive Boc carbamates,[26–29] Boc-protected precursors were also included in the library.
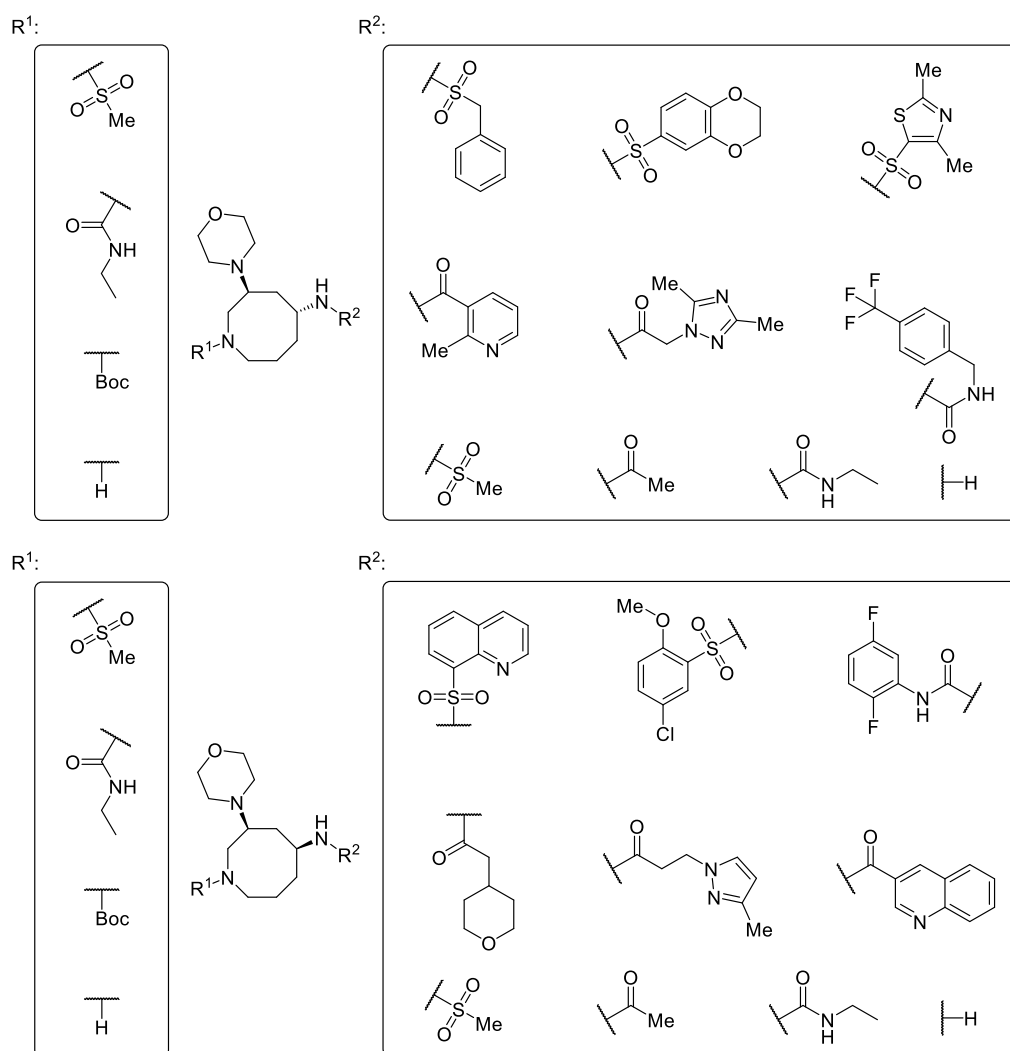
Scheme 37: The SACE1 library plan, consisting of 2 × 4 × 10 library molecules.

Of the 78 library reactions, only five reactions failed, including all three reactions with quinolinesulfonylchloride **a6**[a] and Boc deprotections of the Boc-building blocks *cis*-**93** and *trans*-**93** (for tables including yields, UPLC retention times and purity, see Experimental Section 6). Only three of the final compounds displayed a UV purity below 95%, which is the typical industry standard for compound purity required for biological screening. Boc deprotection of the *cis* chloromethoxyphenyl sulfonamide *cis*-**93a1**[b] was not executed, because the amount of available precursor was deemed too low. Given the synthesis of *cis* Boc-quinolinesulfonamide precursor *cis*-**93a6** failed, no subsequent Boc deprotection was performed either. An

---

[a] All appending reagents used in parallel synthesis reactions throughout the thesis are assigned a letter (depending on the reagent type) and a number. For the complete list of reagents and their assigned letters and numbers, see Experimental Section 4.1.

[b] All products of parallel synthesis reactions have been assigned the number of their building block precursor, followed by the letter and number of the used appending reagent.

69

interesting trend was that reactions with sulfonyl chlorides gave consistently lower yields than amide couplings and urea formations, while the analogues from Ms building blocks *cis*-**105** and *trans*-**105** showed lower yields for amide couplings and urea formations than the other building blocks. Given most compounds bearing a sulfonamide were solids, these low yields could be attributed to solubility issues during purification by preparative LC since submitted building blocks *cis*-**105** and *trans*-**105** only showed mass recoveries from preparative LC of 28% and 67%, respectively.

In the case of reactions with sulfonyl chlorides, it is also possible that DMF partly quenched the sulfonyl chloride reagents, forming an iminium species **109** (Scheme 38).[30] Even though this iminium species could act as a sulfonyl transfer reagent, yielding desired sulfonamides nonetheless, competing side reactions such as the generation of a Vilsmeier reagent[31] or an amidinium species[30] could have contributed to decreased sulfonamide yields (Scheme 38). Furthermore, possible dimethylamine contamination, resulting from decomposition of DMF,[32] could have also reacted with the sulfonyl chlorides. The set-up parallel reactions with sulfonyl chlorides did not show full consumption of the starting material upon submission to preparative LC, but no m/z signals were observed that could correspond with *N,N*-dimethylsulfonamides, nor with hypothetical iminium compounds, although these would likely have degraded on the LC column.
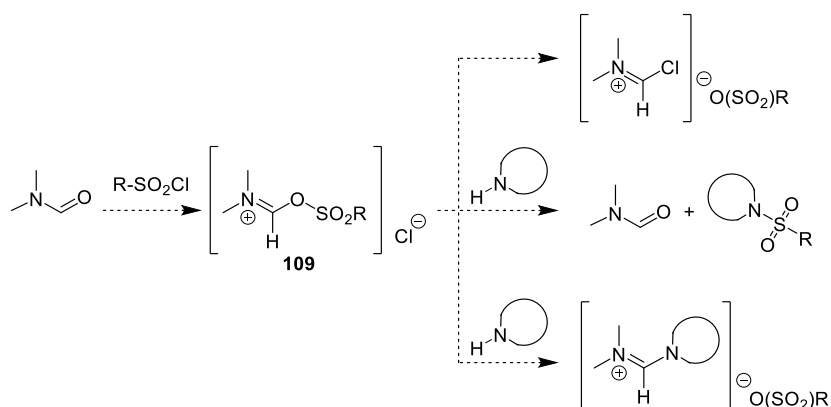
Scheme 38: Hypothesised R-SO₂Cl quench by DMF, potentially forming iminium species **109**.[30]

Both Boc deprotections of building blocks *cis*-93 and *trans*-93 yielded no product, but instead LCMS analysis showed a cation with m/z = 197, indicating possible intramolecular transannular attack of the deprotected amine with loss of the primary amine moiety, yielding putative pyrrolizidine **110** (Scheme 39). This intramolecular attack was also hypothesised during Boc-protection of ketone **79** (Scheme 22, page 46). However, the putative pyrrolizidine **110** could not be recovered from preparative LC.
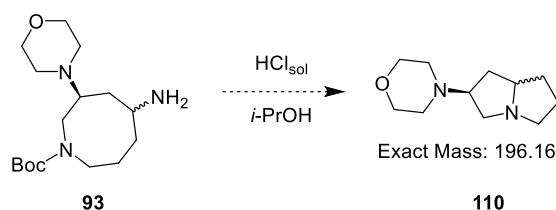
Scheme 39: LCMS chromatograms of the Boc deprotection mixtures of cis-93 and trans-93 showed a product with m/z = 197, which could be the pyrrolizidine 110, originating from intramolecular attack of the deprotected amine.

Overall, with a success rate of 73/78 reactions and 54 final compounds yielding more than 10 mg, the SACE1 library synthesis was considered a successful first round of parallel synthesis.

3.6.   Conclusion

A scalable route has been developed towards amine **93**. Nosyl protection of the primary amine **93** enabled separation of the two diastereomers, whilst XRD analysis of the crystalline *p*-Ns analogue *cis*-102 confirmed the relative stereochemistry of *o*-nosylsulfonamide **100**. Having shown that both protected primary and secondary amines could be deprotected and functionalised, the eight-membered cyclic amine **93** was used as a scaffold for library synthesis, generating 73 novel compounds *via* parallel synthesis, following a $2 \times 3 \times 10^a$ *in silico* library design supplemented with 2×10 Boc-carbamates (Scheme 40).
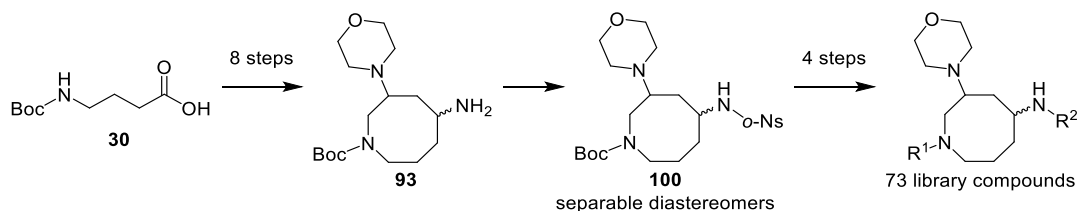
Scheme 40: Synthesis of the SACE1 library.

---

[a] 2 (cis & trans diastereoisomers) $\times$ 3 (R^1 decoration) $\times$ 10 (R^2 decoration)

3.7. References

1   M. Morales-Chamorro and A. Vázquez, *Synthesis*, 2019, **51**, 842–847.

2   E. A. Mash, T. M. Gregg and J. A. Baron, *J. Org. Chem.*, 1997, **62**, 8513–8521.

3   A. D. Bolig and M. Brookhart, *J. Am. Chem. Soc.*, 2007, **129**, 14544–14545.

4   H. Kilic, S. Bayindir, E. Erdogan and N. Saracoglu, *Tetrahedron*, 2012, **68**, 5619–5630.

5   J. Moran, P. Dornan and A. M. Beauchemin, *Org. Lett.*, 2007, **9**, 3893–3896.

6   P. E. Eaton and K. Lin, *J. Am. Chem. Soc.*, 1964, **86**, 2087–2088.

7   H. Hart and E. Dunkelblum, *J. Am. Chem. Soc.*, 1978, **100**, 5141–5147.

8   N. Ryoji and K. Masao, *Bull. Chem. Soc. Jpn.*, 1974, **47**, 1460–1466.

9   N. Papaioannou, C. A. Evans, J. T. Blank and S. J. Miller, *Org. Lett.*, 2001, **3**, 2879–2882.

10 N. Papaioannou, J. T. Blank and S. J. Miller, *J. Org. Chem.*, 2003, **68**, 2728–2734.

11 A. P. Kourounakis, D. Xanthopoulos and A. Tzara, *Med. Res. Rev.*, 2020, **40**, 709–752.

12 J. Zhang, Z.-X. Chen, T. Du, B. Li, Y. Gu and S.-K. Tian, *Org. Lett.*, 2016, **18**, 4872–4875.

13 B. Miriyala, S. Bhattacharyya and J. S. Williamson, *Tetrahedron*, 2004, **60**, 1463–1471.

14 J. K. Horner and W. A. Skinner, *Can. J. Chem.*, 1966, **44**, 315–319.

15 B. Yang, M. M. Vasbinder, A. W. Hird, Q. Su, H. Wang, Y. Yu, D. Toader, P. D. Lyne, J. A. Read, J. Breed, S. Ioannidis, C. Deng *et al.*, *J. Med. Chem.*, 2018, **61**, 1061–1073.

16 F. Schlauderer, K. Lammens, D. Nagel, M. Vincendeau, A. C. Eitelhuber, S. H. L. Verhelst, D. Kling, A. Chrusciel, J. Ruland, D. Krappmann and K.-P. Hopfner, *Angew. Chem. Int. Ed.*, 2013, **52**, 10384–10387.

17 T. Kan and T. Fukuyama, *Chem. Commun.*, 2004, 353–359.

18 C. Guisado, J. E. Waterhouse, W. S. Price, M. R. Jorgensen and A. D. Miller, *Org. Biomol. Chem.*, 2005, **3**, 1049–1057.

19 D. L. Hughes, in *Organic Reactions*, American Cancer Society, 2004, pp. 335–656.

20 W. G. Harter, H. Albrect, K. Brady, B. Caprathe, J. Dunbar, J. Gilmore, S. Hays, C. R. Kostlan, B. Lunney and N. Walker, *Bioorg. Med. Chem. Lett.*, 2004, **14**, 809–812.

21 M. H. Abraham and R. J. Abraham, *New J. Chem.*, 2017, **41**, 6064–6066.

22 M. H. Abraham, R. J. Abraham, J. Byrne and L. Griffiths, *J. Org. Chem.*, 2006, **71**, 3389–3394.

23 T. Fukuyama, C.-K. Jow and M. Cheung, *Tetrahedron Lett.*, 1995, **36**, 6373–6374.

24 W. Li, Z. Chen, D. Yu, X. Peng, G. Wen, S. Wang, F. Xue, X.-Y. Liu and Y. Qin, *Angew. Chem. Int. Ed.*, 2019, **58**, 6059–6063.

25 R. Subirós-Funosas, R. Prohens, R. Barbas, A. El-Faham and F. Albericio, *Chem. Eur. J.*, 2009, **15**, 9394–9403.

26 I. Ojima, S. Chakravarty, T. Inoue, S. Lin, L. He, S. B. Horwitz, S. D. Kuduk and S. J. Danishefsky, *Proc. Natl. Acad. Sci. U.S.A.*, 1999, **96**, 4256–4261.

27 D. Su, X. Hu, C. Dong and J. Ren, *Anal. Chem.*, 2017, **89**, 9788–9796.

28 M. S. L. Lim, E. R. Johnston and C. A. Kettner, *J. Med. Chem.*, 1993, **36**, 1831–1838.

29 S. Venkatraman, *Trends Pharmacol. Sci.*, 2012, **33**, 289–294.

30 J. D. Albright, E. Benz, A. E. Lanzilotti and L. Goldman, *Chem. Commun. Lond.*, 1965, 413–414.

31 S. V. Vinogradova, V. A. Pankratov, V. V. Korshak and L. I. Komarova, *Bull. Acad. Sci. USSR Div. Chem. Sci.*, 1971, **20**, 450–455.

32 Y. E. Jad, G. A. Acosta, S. N. Khattab, B. G. de la Torre, T. Govender, H. G. Kruger, A. El-Faham and F. Albericio, *Org. Biomol. Chem.*, 2015, **13**, 2393–2398.

4. *In silico* library design: method selection and SACE1 virtual library

Since this thesis aimed to provide multiple diverse physical compound libraries, built on different molecular scaffolds, a broadly applicable and reproducible method for *in silico* library design was envisioned. Once established, this method could be used consistently for the design of every library in this thesis. Furthermore, the method was aimed to minimise subjective decisions, limiting any personal biases and increasing its transferability to future projects. The goal was therefore to generate diverse virtual libraries, to inform the choice of building blocks and reagents for subsequent library synthesis.

4.1. Generating 'diverse' libraries

To generate a diverse chemical library, the aim is to maximise its chemical space coverage. For a library derived from a single scaffold, the chemical space that can be probed can be considered as the collection of compounds, derived from decorating the core scaffold with all possible combinations of appendages, which is called an enumeration of the scaffold. Depending on the size of the appendage database, chemical enumerations can reach an enormous size: a 2012 enumeration by Reymond *et al.* of all possible molecules with synthetic feasibility and chemical stability up to thirteen atoms, consisting of N, C, O, S and Cl alone, yielded 977 million structures.[1] In practice, the size of a scaffold enumeration will depend on the size of the used reaction and reagent set. For practical reasons, instead of synthesising the entire enumerated library, a physical diverse library typically consists of a representative selection, which still covers the enumerated chemical space as well as possible. At the basis of this selection lies the 'neighbourhood principle', which states that similar compounds (depending on the used descriptor, for example, similar structures) tend to have similar biological properties.[2,3] For example, compounds in a lead optimisation project will be structurally similar; although they may exhibit varying potency, they are typically all active against the biological target (Figure 22).[3] Thus, in order to maximise the chances of identifying new hits and novel targets, one approach is to pick the most dissimilar compounds from an enumeration. This can be achieved by clustering structurally similar compounds, and choosing a representative compound from each cluster (Figure 22).[3]
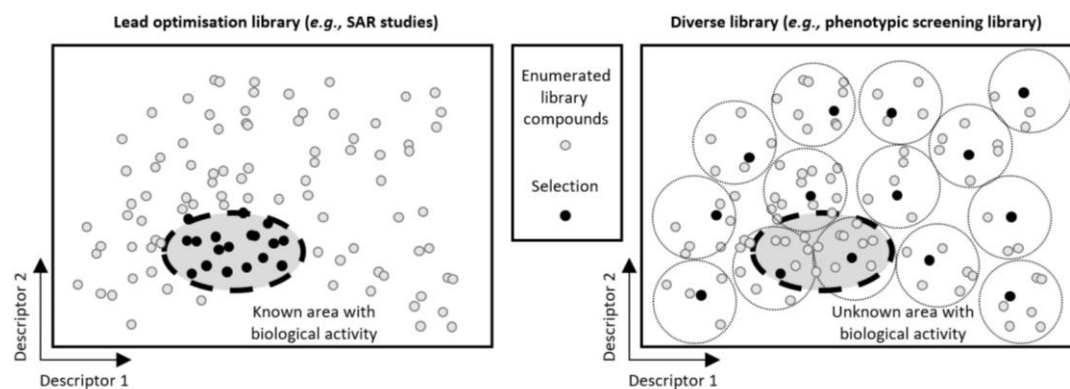
Figure 22: Graphical representation of probed chemical space, depending on the nature of the library. A selection for lead optimisation studies will yield predominantly close analogues (left), while a diverse library will select the most dissimilar compounds (right).[a]

The neighbourhood principle does not apply to every chemical descriptor as not every physicochemical parameter shows a clear correlation with biological activity. Patterson *et al.* investigated the neighbourhood behaviour of 11 molecular descriptors, by comparing the change in molecular descriptor to changes in biological activity for 20 datasets. They found that neighbourhood behaviour was most pronounced for hydrogen-bonding molecular fields, steric molecular fields and 2D fingerprints, validating them as good molecular diversity descriptors.[3] This gave us confidence to base our clustering and compound selection of the library compounds on molecular fingerprints. Prior to exploring fingerprint-based library design methods (see Section 4.3, page 76), we first investigated how to assess and compare different virtual libraries.

4.2. Assessing diversity

Given the plethora of 2D and 3D descriptors used to assess the molecular and chemical properties of a drug molecule, the diversity of a library can be assessed in many different ways.[3–6] Therefore, in order to find a suitable library design method, it was necessary to first identify the variables which would be used to assess the actual design.

---

[a] Figure adapted with permission from Patterson *et al.*[3] Copyright 2021 American Chemical Society.

4.2.1. Defining library variables

4.2.1.1. Physicochemical descriptors

We chose to assess the molecular weight (MW), lipophilicity (clogP)[a] and polar surface area (PSA) of the library compounds, as these descriptors generally play a crucial role in the absorption and distribution of a drug. The permeability of orally bioavailable small-molecule drugs through the gastrointestinal tract wall and blood brain barrier (BBB) typically decreases with increasing molecular weight.[7–9] This is a problem if the drug target lies beyond these barriers. Conversely, such poorly permeable compounds with higher molecular weights may act extracellularly or on a cell surface and avoid central nervous system side-effects.[10] A similar argument can be made for lipophilicity: for small-molecule drugs, gastrointestinal and BBB permeability generally increases as the clogP increases,[7,11] with an optimum for clogP between 0 and 5.[6,9] On the other end, drugs administered *via* subcutaneous, inhalation, ocular and topical routes, typically have low clogP values (clogP < 1) with even lower values observed for drugs with intramuscular (−1.75) and intravenous (−2.7) administration routes. PSA also influences the potency, distribution and permeability of a drug molecule. Several studies have highlighted how a change in PSA during lead optimisation phases increased cellular activity and oral bioavailability, although no clear correlation could be found.[12] However, an increase in PSA does lead to decreased BBB permeability.[12]

4.2.1.2. Physicochemical descriptors: filter values

Our envisioned compound libraries were intended to be orally bioavailable,[b] so we imposed filter values on the physicochemical descriptors of our virtual enumerations to ensure coverage of orally bioavailable chemical space. A preliminary enumeration of the target scaffold **93** using the Symeres in-house reagent database (1450 compounds, comprising 3° amines, (sulfon)amides and ureas; see Figure 23, page 77) yielded predominantly compounds which complied with Lipinski's Rule of Five (Ro5) (1440 out of 1450, 99%). These results indicated that future enumerations on analogous scaffolds using the Symeres reagent database were likely to yield mainly Ro5-compliant compounds too. Having a portion of the library that extended beyond the Rule of Five was not considered a problem; a study of oral druggable space beyond

---

[a] Acknowledging that source papers may quote different units for lipophilicity, based on the calculation method (*i.e.,* clogP, Slogp, AlogP) or measurement (ElogD), the calculated logP (clogP) is used consistently in this section for clarity purposes, as the calculated logP is most often used to assess compound libraries.
[b] Notwithstanding, other administration routes could always be considered if a promising hit is identified in future biological screenings.

the Ro5 (bRo5) shows that the majority of orally bioavailable bRo5 drugs (MW > 500 Da) fall in a much larger physicochemical space (93%, dataset of 226 compounds), with MW ≤ 1000 g/mol, −2 ≤ cLogP ≤ 10 and PSA ≤ 250 Å².[6]

Hence, the physicochemical descriptor filters applied in the virtual library design were installed with potential for future elaboration in mind, (adding MW or lipophilic groups onto existing library compounds in further stages of drug discovery,) rather than worrying about any rules for drug-likeness: MW was cut off above 600 Da, while clogP was kept within a range of −1.0 − 6.0 and no filters were imposed on PSA.

4.2.1.3. Shape space and functional group diversity

As discussed above (Section 4.1), topological descriptors including 2D fingerprints and hydrogen-bonding molecular fields are good molecular diversity descriptors. Hence, it seemed fit to assess the library design also by topological descriptors. Therefore, a broad shape space coverage was desired with ample functional group diversity, aiming to probe different H-bond donors and acceptors into a large 3D space. Apart from assessing the enumerated libraries visually *via* a PMI plot,[5] the shape space was also assessed in terms of sphericity, which is calculated as $(npr_1 + npr_2 - 1)$.[13, a] Considering the over-representation of rod- and disk-like drug molecules in medicinal chemistry,[14,15] priority was given to more coverage of the sphere-like space. Doak *et al.* found that flat and groove shaped binding sites, often considered difficult to drug, had more disk- and sphere-like ligands compared to pocket and internal binding site shapes.[16] In contrast, Koutsoukas *et al.* observed no visible correlation between bioactivity space and PMI shape space, showing examples of compounds in similar shape space which bind to different protein families and compounds in different shape spaces that bind to the same protein.[4] However, Sauer and Schwarz stated that this does not need to contradict the goal of achieving maximum shape diversity: after all, identifying several distinct chemical series with comparable bioactivity is desirable as it provides options for further research and drug optimisation.[5]

With proven relevance in drug discovery, PMI shape space, MW, clogP, TPSA and functional group diversity were chosen to assess future virtual libraries. Hence, the principal aims were to

---

[a] npr values for a PMI plot are calculated as follows: the lowest-energy conformer of a molecule is rotated around the x, y and z axis in 3D space, yielding calculated moments of inertia in the x, y and z axis, respectively I_x, I_y and I_z ($I_x < I_y < I_z$). $npr_1 = I_x / I_z$; $npr_2 = I_y / I_z$. In a PMI plot, the calculated sphericity ($npr_1 + npr_2 - 1$) can be interpreted visually as the distance to the flat-disk line ($npr_1 + npr_2 = 1$).[5]

achieve a maximum coverage of shape space, with enrichment in high-sphericity compounds and broad functional group diversity, whilst covering maximum MW/clogP/PSA space within the applied limits (MW < 600 Da, −1.0 < clogP < 6.0, no PSA filter). Having established these parameters and criteria, the library design method could now be tested and optimised.

4.3. Establishing a library design method

Four different library design methods were compared. Starting from a common enumerated library, these four methods each yielded a unique selection of compounds, which were plotted in DataWarrior, an open-source program for chemical data analysis and visualisation.[17] Using our library criteria, the best performing method would then be used for library design.

The enumerated library was built in KNIME, an open-source platform which allows for modular construction of data-processing workflows. Each module, called a node, performs a defined operation, such as sorting or filtering data, calculating molecular descriptors or *in silico* chemical reactions. Linking multiple nodes allows for sequential execution of every node, which can be used to establish complex workflows, such as library enumeration and clustering.[18] Using the Symeres in-house reagent database and the RDKit nodes,[19] a library was enumerated on scaffold **93**, yielding a 5 × 290 virtual library of amides (94 R-groups), sulfonamides (99 R-groups) and ureas (107 R-groups), all common functional groups in compound screening libraries (Figure 23).[a] This enumeration was next used to compare three clustering methods (two in KNIME, one in DataWarrior,) and the 'diverse selection' algorithm in DataWarrior, all which use different molecular fingerprints.
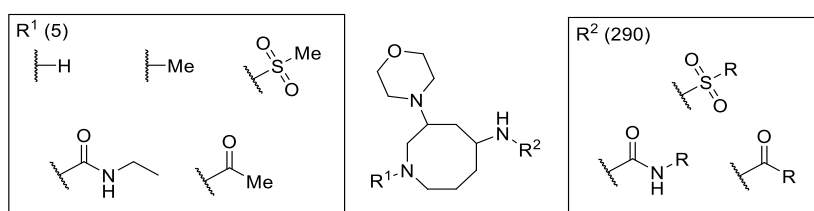
Figure 23: Enumerated library of amides, sulfonamides and ureas, used to compare different library design methods.

---

[a] For an example KNIME enumeration workflow, see Appendix 6.1.1.

4.3.1.   KNIME

4.3.1.1.   Molecular fingerprints in KNIME

Molecular fingerprints are molecular descriptors, which contain the structural information of a molecule in the form of a unique numerical string. Every number on this string is called a 'bit'. These fingerprints allow for fast searching and comparison of molecule structures, which enables virtual screening, structure-activity relationship studies, and representative selection of enumerated library compounds.[2,20] Depending on the properties of interest, fingerprints may describe the structural information of a molecule in different ways, such as pharmacophore features, 3D information or molecule fragments.[2,21]

Using the CDK toolkit available in KNIME,[22] two types of fingerprints were assigned to the enumerated molecules, ECFP6 and FCFP6. Both are circular fingerprints, which means that they describe the atom neighbourhoods within a defined radius.[2,21,23] The extended connectivity fingerprint (ECFP6) is specifically designed for studying structure-activity relationships and describes individual atoms in terms of atomic numbers, masses and charges. The functional-class fingerprint (FCFP6) indexes atoms by their role in a pharmacophore, like "hydrogen bond donor", "positively ionisable", "aromatic" or "halogen".[21,23] In this way, FCFP6 can produce functionally equivalent features which would be distinguished by the ECFP6 fingerprint. This form of abstraction makes FCFP6 attractive for pharmacophore studies,[23] so both fingerprints were investigated to see how they influenced the library selection.

4.3.1.2.   Clustering in KNIME

In order to quantify the similarity between two compounds, we calculated the Tanimoto distance. This distance is based on the amount of bits the two fingerprints have in common.[21] Calculating these distances between all members of a virtual library created a distance matrix, which enabled compounds to be grouped in clusters, with cluster sizes depending on set Tanimoto distance cutoffs (Figure 24).
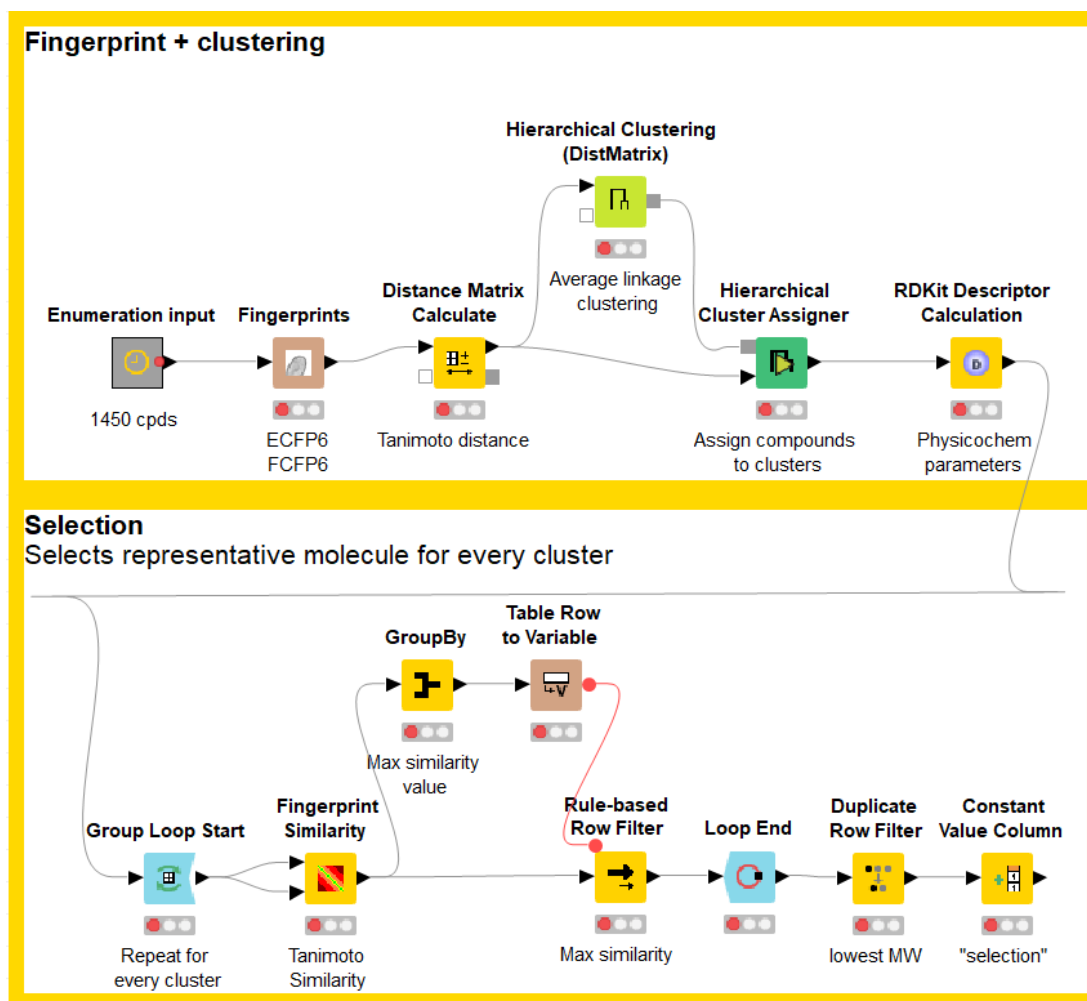
Figure 24: KNIME workflow used for clustering and selection from the enumerated library, using nodes from KNIME, RDKit, CDK and Erl Wood.[22,24]

For every cluster, a representative molecule was chosen by selecting the molecule with the highest average similarity score, based on intra-cluster Tanimoto distances. However, applying this method in KNIME yielded two or three selected molecules per cluster whenever the cluster contained, respectively, two or three molecules, as intra-cluster Tanimoto distances were equal for every cluster member in this instance. Therefore, an extra filter was applied, passing the compound with lowest molecular weight (interpreted as 'the smallest common denominator',) whenever multiple molecules passed the similarity selection. With a KNIME clustering and compound selection workflow in place (Figure 24, see Appendix 6.1.5), the influence of ECFP6 and FCFP6 fingerprints on library design could now be compared to each other, and to the DataWarrior selection algorithms.

4.3.2.   *DataWarrior selection algorithms and fingerprints*

DataWarrior has two selection algorithms, one of which, 'cluster compounds or reactions', is a clustering algorithm with built-in selection of representative molecules, and one called 'select diverse set'. The DataWarrior user manual gives little insight into the details of these algorithms, although both are based on Tanimoto distances calculated from molecular fingerprints.[25] DataWarrior uses its own set of fingerprints; the clustering algorithm uses 'SkelSpheres', a non-binary fingerprint,[26] while the 'select diverse set' algorithm uses 'SpheresFp', a circular fingerprint.[25] SkelSpheres has a greater resolution than 'SpheresFp', making it the more accurate descriptor for similarity calculations of chemical graphs.[25] Both DataWarrior (DW) algorithms were compared to the KNIME methods, ensuring a judicious choice of method for future library design. The 'select diverse set' algorithm was deemed especially interesting, since it selects the most dissimilar compounds first and ranks their 'dissimilarity'.[25]

4.4.   Comparing selection methods

The descriptors assessed in Section 4.2 were calculated for every enumerated compound in KNIME.[27, a] From the enumerated library of 1450 compounds, representative compounds were selected using ECFP6 and FCFP6 fingerprint-based cluster methods in KNIME (Figure 24), the DataWarrior (DW) clustering algorithm and DW's 'select diverse set' algorithm. The obtained selections were then plotted in DataWarrior, allowing for a comparison of their coverage of descriptor space. From a pragmatic viewpoint, smaller compound libraries were preferred. However, as the size of a selection decreases, it becomes increasingly difficult to obtain a representative selection for the enumerated library. Therefore, we also investigated whether a small selection of 50 compounds using the different selection methods would still be able to cover as much descriptor space as a larger selection of 250 compounds.

---

[a] MW, SlogP and TPSA were calculated using the 'RDKit Descriptor calculation' node, using the SlogP calculation reported by Wildman and Crippen.[28] PMI parameters npr1, npr2 and sphericity were calculated using the 'Principal Moment of Intertia (PMI)-Derived properties' (*sic*) node by Vernalis.

4.4.1. Comparing covered descriptor space

Whilst assessing the covered descriptor space, the principal aims were to achieve a maximum coverage of shape space, with enrichment in high-sphericity compounds, whilst covering maximum MW/SlogP/PSA space. Given the small differences in covered descriptor space between the selection methods, box plots were chosen to compare the different methods, since obtained 2D scatter plots (especially for the selection size of 250 compounds) did not allow for easy and unambiguous visual comparison. For the selection size of 250 compounds, both ECFP6 and FCFP6 fingerprints showed comparable coverage of MW and SlogP, though FCFP6 yielded slightly larger ranges and a lower average SlogP. A lower average SlogP was deemed attractive, since the increase of SlogP in future optimisation studies (for example by introduction of extra/longer alkyl functionality) is deemed more straightforward than trying to lower the SlogP of a given compound. FCFP6 also showed a larger TPSA range than ECFP6. Although both fingerprints yielded selections with equal sphericity maxima, the ECFP6 selection showed more compounds with higher sphericity (Figure 25), while a PMI plot showed that the high sphericity ECFP6 compounds covered a broader rod-disk space than the FCFP6 compounds (Figure 26). In terms of MW, SlogP and TPSA, DataWarrior's diverse selection consistently showed longer whiskers than the DW clustering method (Figure 25). Furthermore, in comparison to the DW cluster selection, the DW diverse selection showed a higher average sphericity (Figure 25) and covered some unique spaces on the PMI plot (Figure 26).
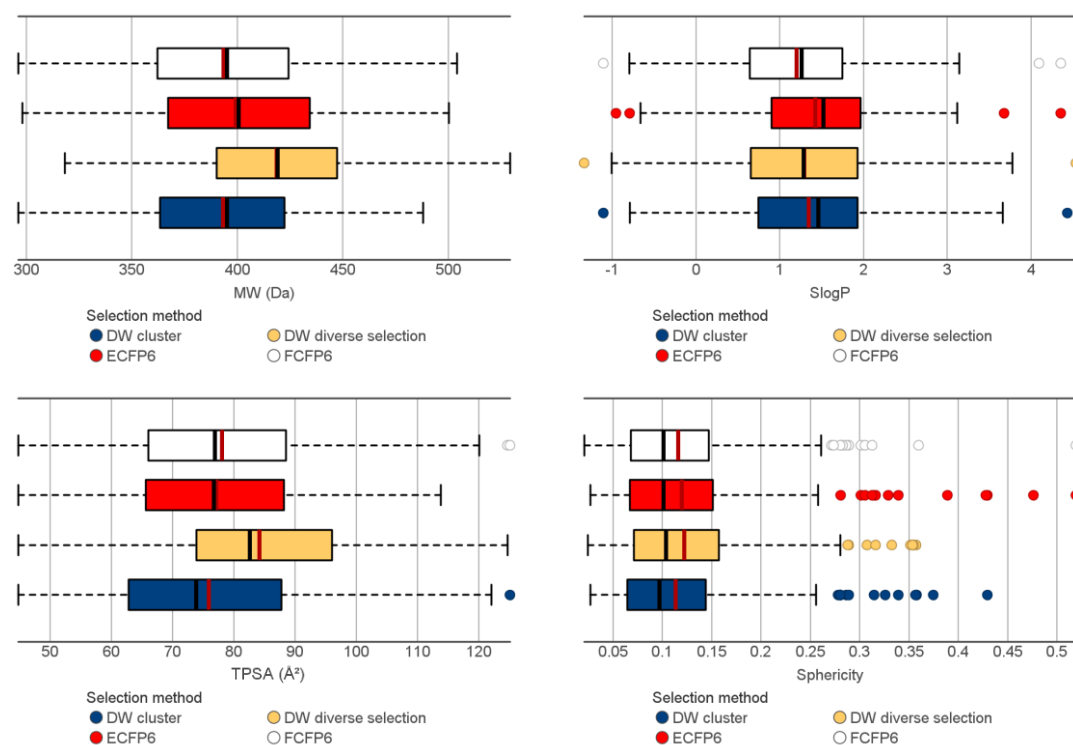
Figure 25: Molecular descriptor ranges covered by compound selections (size: 250 compounds). Mean: red line. Median: black line. For statistical values, see Appendix 1.1.

In comparison to the KNIME methods, the DW diverse selection also showed longer whiskers in MW, SlogP and TPSA space. Although the selection *via* ECFP6 fingerprint clustering included a few more outliers with higher sphericity (Figure 25), exploring some more sphere-like space on the PMI plot (Figure 26), the DW diverse algorithm showed a slightly higher average sphericity with longer whiskers in the boxplot. Overall, the DW diverse algorithm performed consistently well in the coverage of all four descriptor spaces, although none of the other three methods were particularly bad.
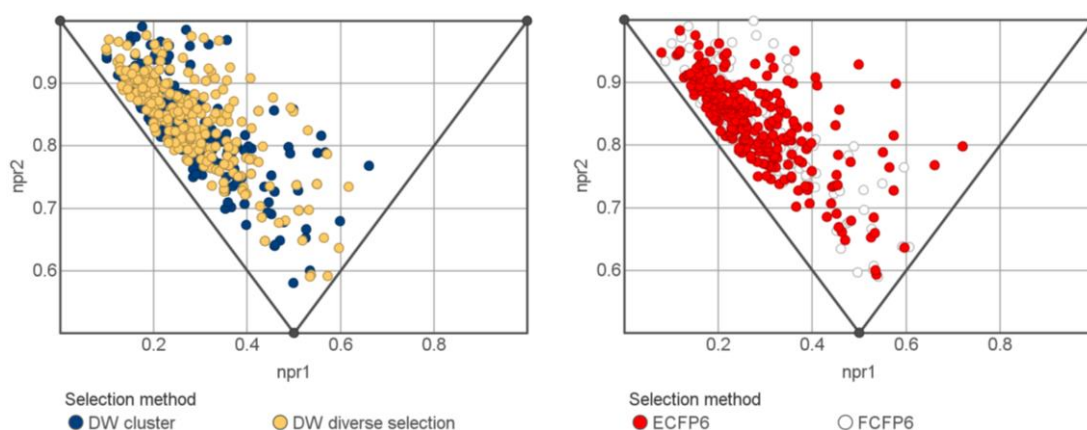
Figure 26: PMI analysis of the compound selections (size: 250 compounds).

In general, the smaller selection size covered slightly less low-MW and low-SlogP space, less high-TPSA space and less high-sphericity space. Comparing the four methods, FCFP6 displayed the largest MW, SlogP and TPSA ranges but covered the narrowest sphericity range (Figure 27).
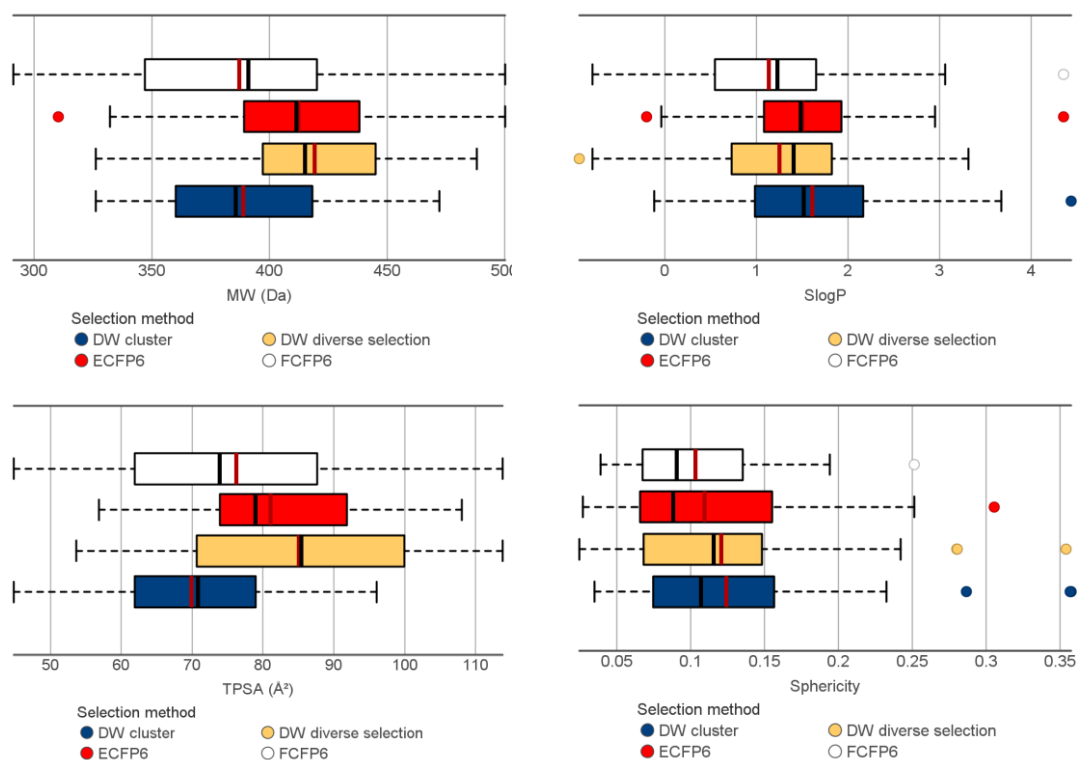
Figure 27: Molecular descriptor ranges covered by compound selections (size: 50 compounds). Mean: red line. Median: black line. For statistical values, see Appendix 2.1.

The DW diverse selection showed broader ranges than the DW cluster selection in all four one-dimensional descriptor spaces (Figure 27), covering a unique area of higher sphericity on the PMI plot while the DW cluster selection covered a more disk-like space (Figure 28). Nonetheless, the DW cluster selection showed the highest average sphericity of all four selections. ECFP6 and the DW diverse selection covered similar sphericity space (Figure 27) but the PMI plot reveals why the DW diverse selection has a higher mean sphericity; more compounds from the DW diverse selection reside in a space with higher sphericity, while the ECFP6 selection shows a few more disk-like compounds (Figure 28).
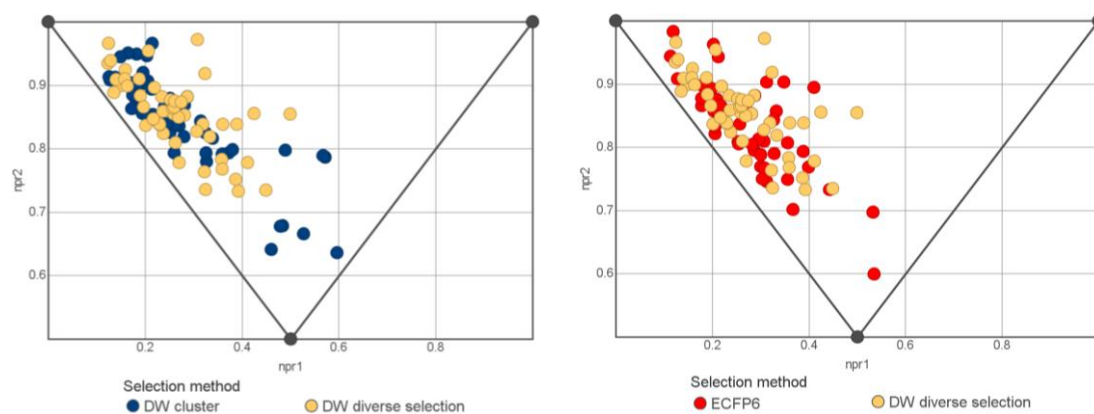
Figure 28: PMI plot showing compound selections (size: 50 compounds) obtained using ECFP6 fingerprints in KNIME, clustering in DataWarrior and DataWarrior's 'select diverse set' algorithm.

Overall, the ECFP6 fingerprint was chosen in preference to the FCFP6 fingerprint, as shape space was prioritised over MW, SlogP and TPSA. Both for large and small selection sizes, the ECFP6 selection yielded more spherical compounds than did the FCFP6 fingerprint, although FCFP6 showed better coverage of MW, SlogP and TPSA space for both selection sizes. Although the differences between the DW cluster and DW diverse selection were smaller for the large selection size of 250 compounds, the DW diverse selection method outperformed the DW cluster method for the smaller selection size (except for the DW cluster selection's higher mean sphericity), making it the DW method of choice.

4.4.2.   Comparing functional group diversity

One metric had remained uninvestigated, which was functional group diversity of the R-groups (Figure 23). Since functional groups can facilitate key interactions with possible targets, the outcome of the investigation would significantly influence the choice of the selection method. Although ECFP6 was chosen over FCFP6 based on the four descriptors above, its selection showed a significant over-representation of an acetyl group on R^1 for both selection sizes. The DW clustering method displayed analogous behaviour for its 50-compound selection, showing over-representation of a methyl group on R^1. For substitution on R^2, such over-representations were not observed for the three types of functional groups among the four selection methods, although the DW diverse selection did pick more sulfonyl chlorides. This effect was more strongly pronounced for the 50-compound selection size (Figure 29).
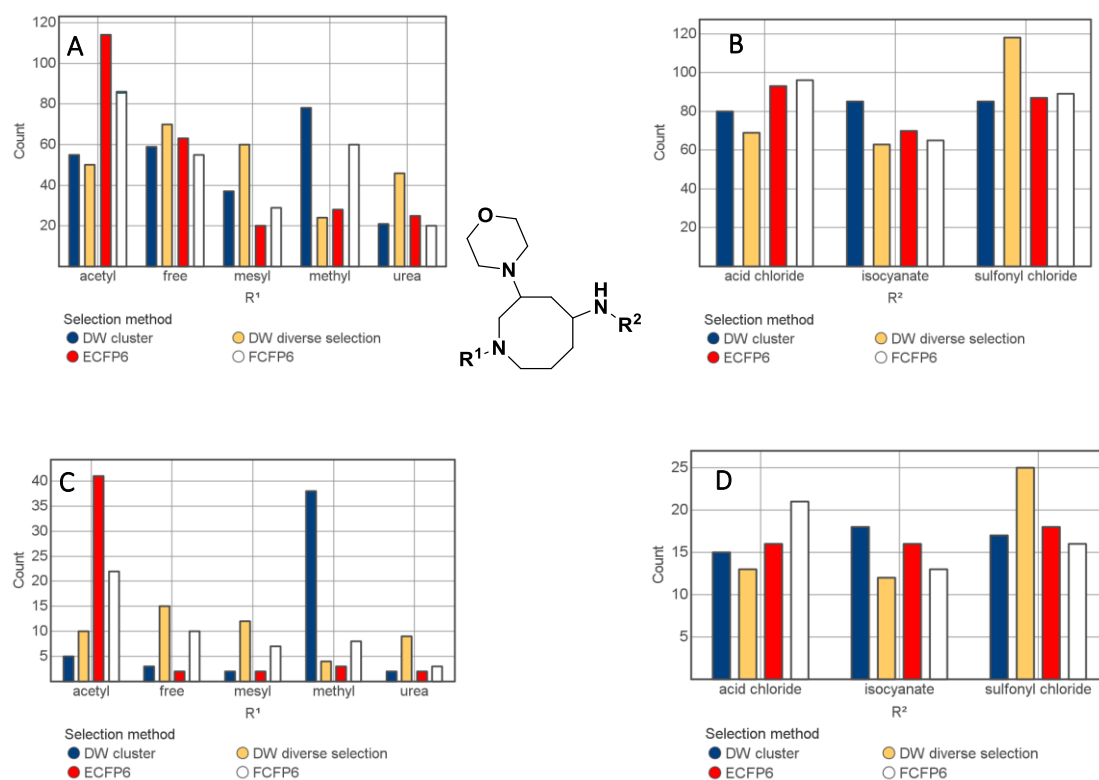
Figure 29: R-group count for compound selections obtained using ECFP6 and FCFP6 fingerprints in KNIME, clustering in DataWarrior and DataWarrior's 'select diverse set' algorithm. Selection sizes: A, B 250 compounds; C, D 50 compounds.

4.4.3.   Method of choice

Although the details of the DW 'diverse selection' algorithm are not provided in the DW user manual, this algorithm was chosen for future library design; not only did it give good coverage of shape space, MW, SlogP, TPSA and functional groups, it was also easier to use, providing quick access to diverse selections of enumerated libraries, thereby enabling quick assessment of future virtual libraries.[a] As a result, the selected workflow involved enumerating the scaffold of choice and calculating its molecular descriptors in KNIME, followed by compound selection and assessment of the selection in DataWarrior.
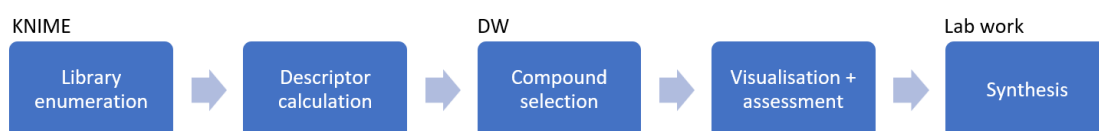
Figure 30: Selected workflow. DW: DataWarrior

---

[a] In addition, clustering *via* KNIME turned out to require more computational power, as the author's PC crashed significantly less whilst using the 'diverse selection' algorithm.

4.5.   Reagent selection – Practical Considerations

Preliminary attempts to make a diverse selection from a combinatorially enumerated scaffold with a large set of R-groups (Figure 23, page 77) often resulted in compound sets containing over 50 different R-groups, of which many were used only once. Since these outcomes were not amenable to parallel synthesis, a more pragmatic approach was required, which would allow for combinatorial synthesis, without significantly compromising chemical diversity. Therefore, the used reagent pool was reduced, since a diverse selection of a smaller enumerated library would increase the number of shared reagents between selected compounds.

In order to make a diverse and representative selection of the used reagent database, a selection from a virtual enumeration was preferred over making a selection from the actual reagent database, since the reagents display different functional groups compared to when they are reacted with the scaffold (*e.g.*, carboxylic acids yielding amides). Hence, cyclooctylamine was enumerated with a collection of 559 reagents containing carboxylic acids, isocyanates, sulfonyl chlorides and aryl halides (Figure 31). Cyclooctylamine was chosen as a simple representative of an appended eight-membered ring, providing quick access to an enumerated library.[a] A representative selection from this enumeration, covering the majority of the enumerated descriptor space, then yielded a set of R-groups, of which the accompanying reagents were chosen for future library design.
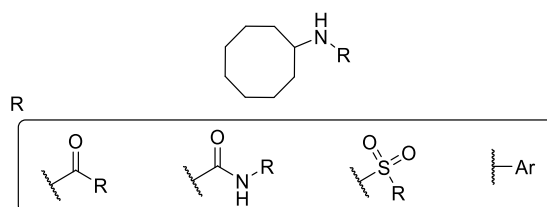
Figure 31: Enumeration of cyclooctylamine with a collection of 559 reagents, yielding amides, ureas, sulfonamides and aromatic amines.

Assessment of the enumerated library in a SlogP/MW plot revealed that urea products occupied a higher SlogP space and sulfonamides a lower SlogP space. In a PMI plot, both functional groups also occupied significantly different corners: the sulfonamides ventured into more sphere- and disk-like space while the ureas resided in the rod-like corner of the plot (Figure 32). With different functional groups residing in different corners of both the SlogP/MW

---

[a] Acknowledging that the SACE1 scaffold could also have been used for this enumeration, the core scaffold was not expected to influence reagent selection as by definition, the scaffold is not variable in the enumerated library.

and PMI plots, the diverse selections were compared in terms of their shape space coverage, since a broad shape space coverage was expected to translate in both functional group diversity and broad SlogP/MW coverage.
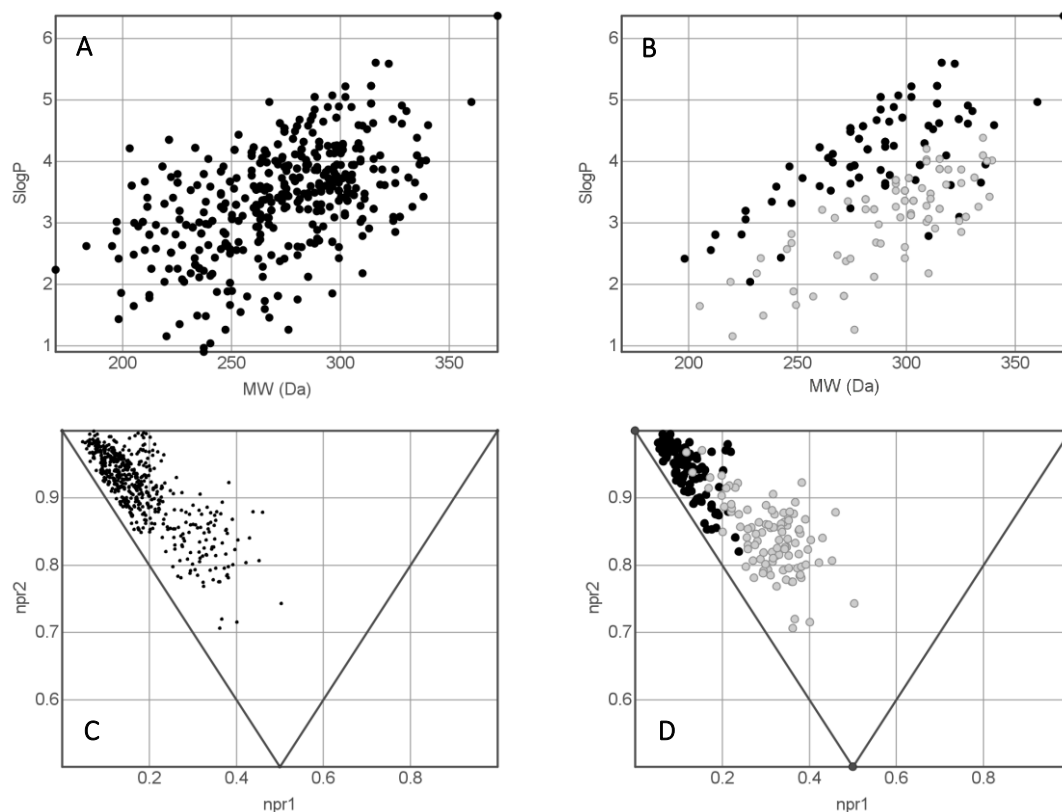
Figure 32: Assessing the cyclooctylamine enumeration via its chemical descriptors. A) SlogP/MW plot for the entire enumeration (559 compounds). B) Sulfonamides (grey) occupy a lower SlogP space than ureas (black). C) PMI plot for the entire enumeration (559 compounds). D) Sulfonamides (grey) venture more into sphere- and disk-like shape space, while ureas (black) reside in the rod-like corner.

DataWarrior's 'select diverse set' algorithm was used to obtain a representative selection of the enumerated library. Since the algorithm ranks the dissimilarity of enumerated compounds, larger selection sizes would always contain the same compounds from a smaller selection. For example, a 200-compound diverse selection would always contain the 100 compounds from a 100-compound diverse selection, since these are 'the 100 most dissimilar compounds' in the enumerated set. This enabled a quick selection size screen, which would help identify a reasonable minimum selection size.

As expected, it became increasingly difficult to cover the same areas in 2D plots as the selection size decreased. However, a diverse selection of 200 compounds did still manage to give a good representation of the enumerated library on the PMI plot (Figure 33, A). As soon as the selection size dropped to 100 compounds and below, gaps appeared on the PMI plot (B, C).

With maximum shape space coverage prioritised, this was undesirable. However, a reagent pool of 200 compounds was still too much for the envisioned library design, so a compromise had to be sought.
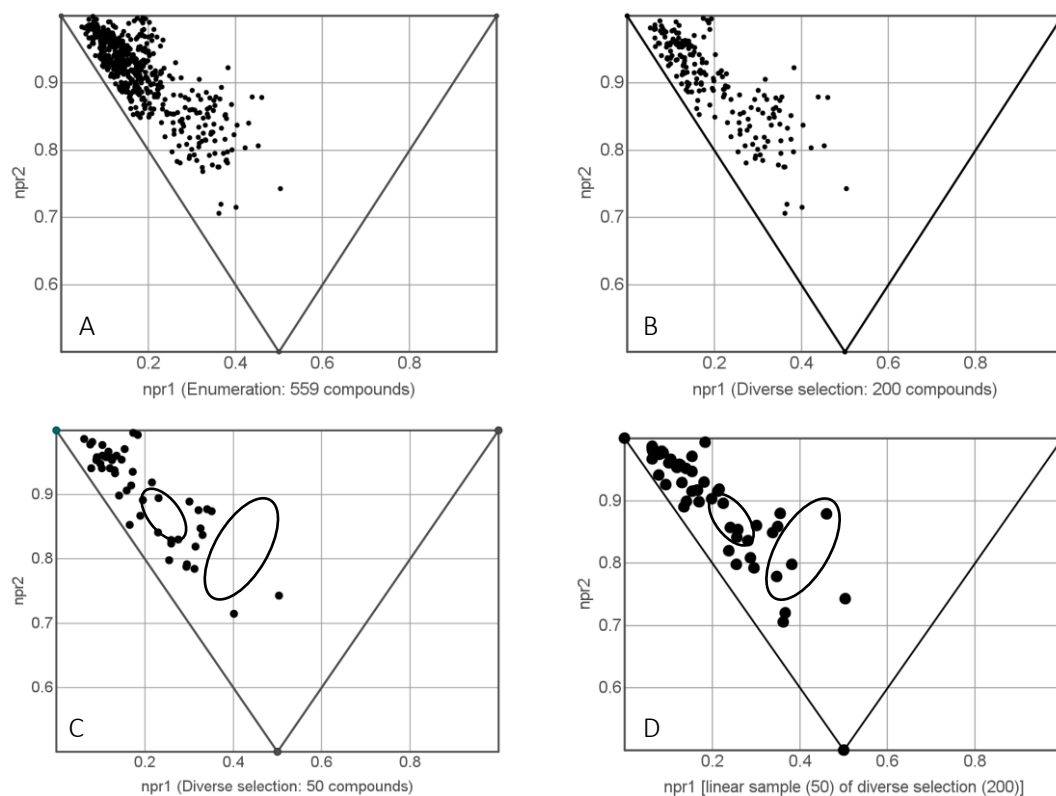
Figure 33: PMI analysis of the enumerated library (A), diverse selections (B, C) and a linear sample of a diverse selection (D). The linear selection (50 cpds) occupied areas which the diverse selection (50 cpds) didn't cover (circled).

Fortunately, the dissimilarity ranking assigned by the 'select diverse set' algorithm allowed for a KNIME-based solution to the selection size: using the 'linear sampling' node, the 200-compound diverse selection could be reduced four times, by ranking every compound by its dissimilarity and systematically choosing every fourth entry. Not only did this approach avoid human bias (cherry-picking 50 compounds), the linear selection of 50 compounds also proved to fill a few gaps on the PMI plot, which were observed for the diverse selection of 50 compounds (Figure 33, D). Different combinations of linear sample sizes and diverse selection sizes were tested but did not yield significant improvements compared to the current set of 50 compounds.

Unfortunately, analysis of MW, SlogP and TPSA coverage showed that the linear sampling did not achieve complete coverage of the enumerated library space. Although the linear sample did manage to cover most of the ranges one-dimensionally, the 2D plots showed that the linear

sample lacked compounds in the low MW/low SlogP space, as well as some corners in MW/TPSA space (Figure 34). It became clear that a trade-off had to be made between the quest for 'maximal diversity' and practical feasibility for library synthesis. Hence, the linear sample of 50 compounds (comprising 18 carboxylic acids, 9 isocyanates, 20 sulfonyl chlorides and 3 aryl halides, see Appendix 2.2) was chosen as the reagent pool for future library design.
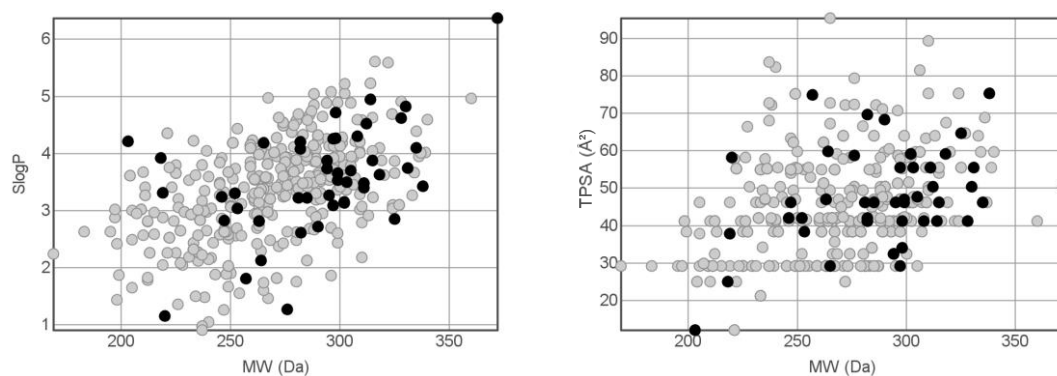
Figure 34: Analysis of MW/SlogP/TPSA space coverage by the enumerated library (grey) and linear sample (50) of diverse selection (black). The linear sample did not cover low MW/low SlogP space.

4.6.   SACE1 Library design

With a small reagent pool chosen, the SACE1 library was now ready for design. Given the reduction of oxime **94** did not proceed stereoselectively (see Section 3.2, page 50), the core scaffold would be available as both *cis* and *trans* diastereomers. Since each diastereomer would display the appendages spatially differently on R^2 in respect to the morpholine moiety, the library was divided into a *cis* and a *trans* subset.

4.6.1.   10 × 10 combinatorial libraries

A 51 × 51 combinatorial library was enumerated on the *cis*-scaffold, using the 50-reagent pool established in the previous chapter and an unfunctionalised amine entry (Figure 35).
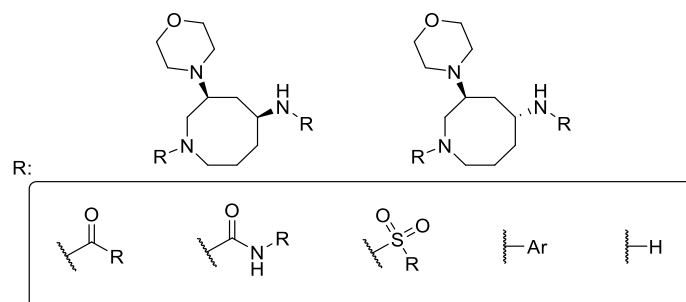
Figure 35: Combinatorially enumerated SACE1 library, consisting of 2 × 51 × 51 compounds, built from cis and trans diastereomers of the core scaffold.

The initial enumeration of 51 × 51 (2601) compounds was filtered using the ranges set in Section 4.2.1. S$_N$Ar reactions on the primary amine were also filtered out, since experimental attempts to effect nucleophilic aromatic substitution were unsuccessful (see Section 3.2.1, page 50). These filters yielded a virtual library of 2256 compounds with MW < 600 Da and −1.0 < SlogP < 6.0. From this enumeration, a diverse set of 200 compounds was picked using the DataWarrior 'select diverse set' algorithm (Figure 36).
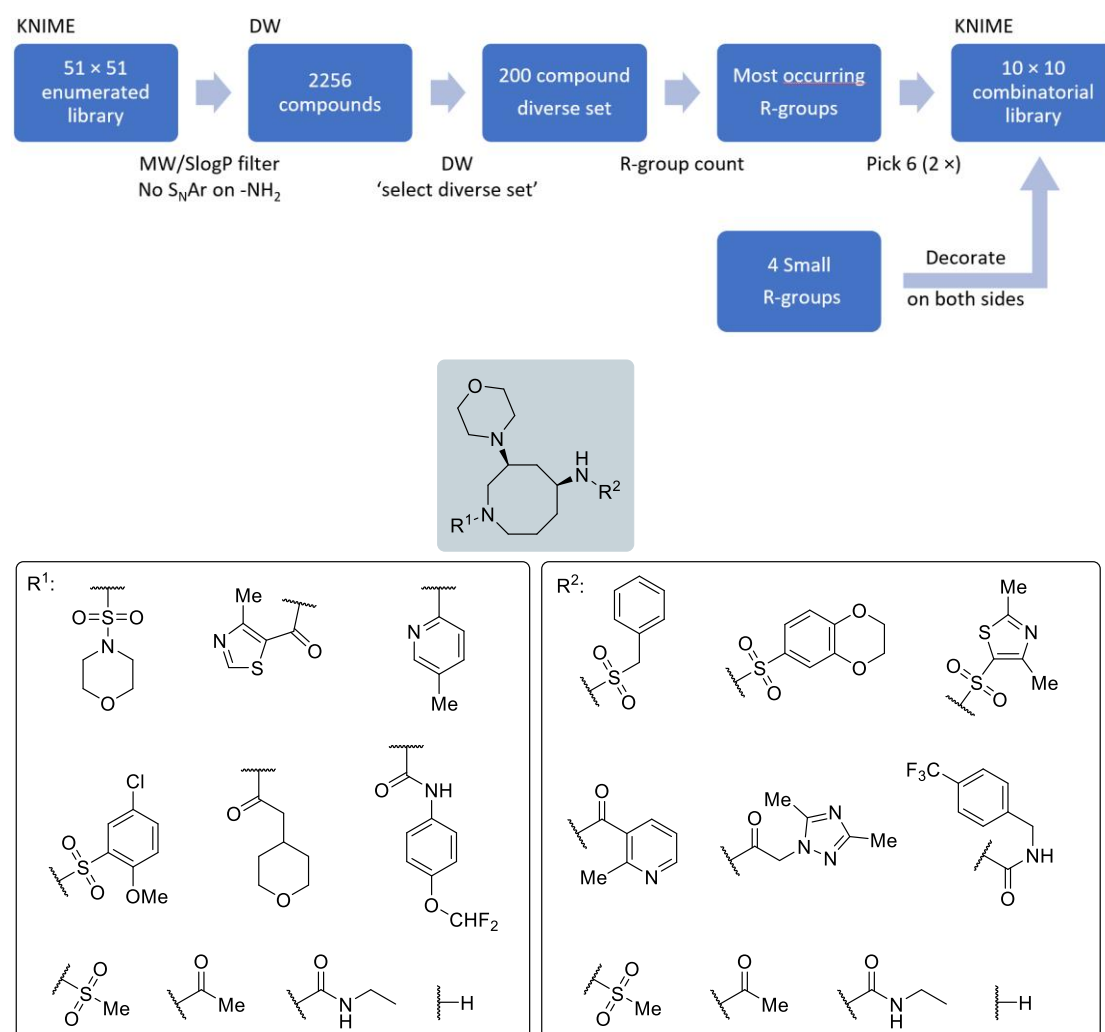
Figure 36: Workflow followed for SACE1 cis-library design, yielding a 10 × 10 combinatorial library.

Subsequently, the most frequently occurring R-groups on the secondary and primary amine were chosen from this selection. In this way, two sets of reagents were obtained, (1° amine: 15 reagents + unfunctionalised amine; 2° amine: 14 reagents + unfunctionalised amine, see Appendix 2.3) from which six reagents were chosen from each set. Since the 51 × 51

enumeration showed a high average MW, four small R-groups were added to the design, yielding acetamide, mesyl, ethylurea and unfunctionalised amine analogues, which could take advantage of smaller binding pockets and provided low-SlogP/MW entries. The chosen R-groups then yielded a 10 × 10 combinatorial library on the *cis*-scaffold (Figure 36).

In silico analysis of the virtual 10 × 10 library showed that it covered a large portion of the chemical space covered by the initial 51 × 51 enumerated library. In addition, inclusion of the four small R-groups resulted in coverage of a unique MW/SlogP/TPSA space, which was not covered by the 51 × 51 enumerated library (Figure 37). Pleasingly, the 10 × 10 *cis*-library still covered a substantial portion of the more disk- and sphere-like space on the PMI plot. Hence, the 10 × 10 library successfully probed a large area of descriptor space, including low MW entries. All in all, the first practical application of the established library design workflow was deemed successful.
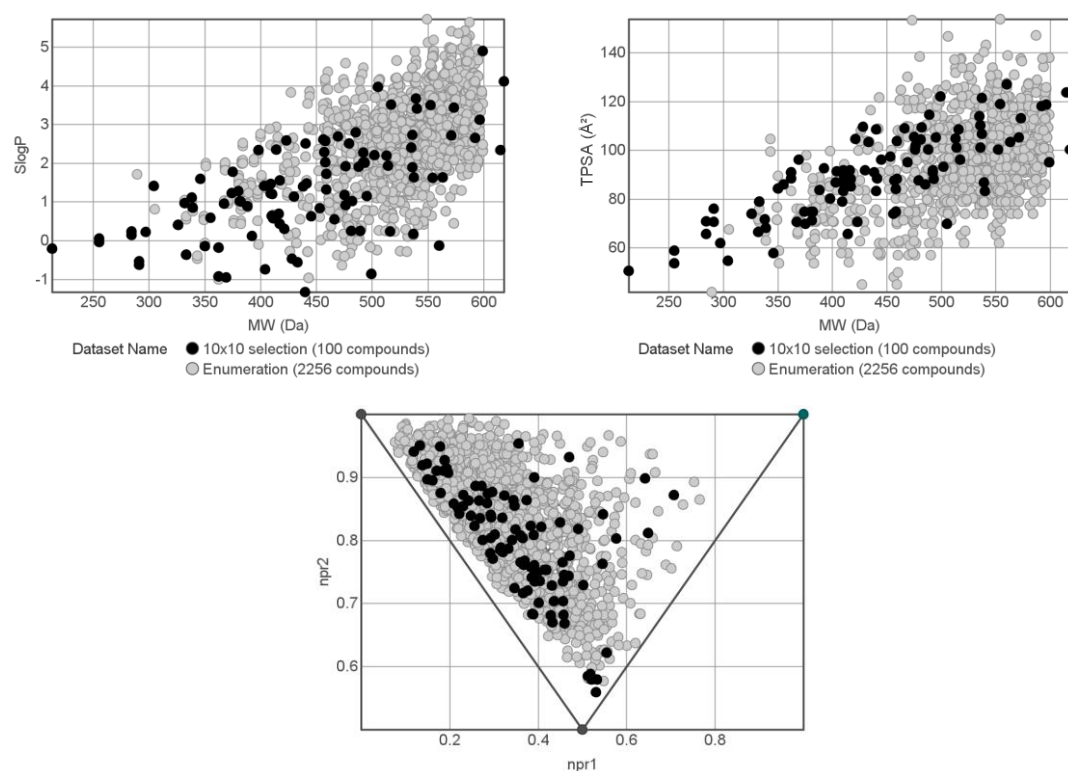
Figure 37: Analysis of descriptor space coverage by the cis 10 × 10 combinatorial library.

An analogous approach was followed for the *trans*-library (Figure 36), but a preliminary selection using the same reagent pool yielded the same large R-groups as for the *cis*-library. Hence, in order to increase the overall R-group diversity of the envisioned 2 × 10 × 10 library (*cis* + *trans*), all large R-groups that occurred in the 10 × 10 *cis*-library were filtered out of the *trans*-enumeration. Imposing the same filters on the enumeration as for the *cis*-library then resulted in an enumeration of 1695 compounds, on which the same workflow was applied as for the 10 × 10 *cis*-library (Figure 38, see Appendix 2.4).
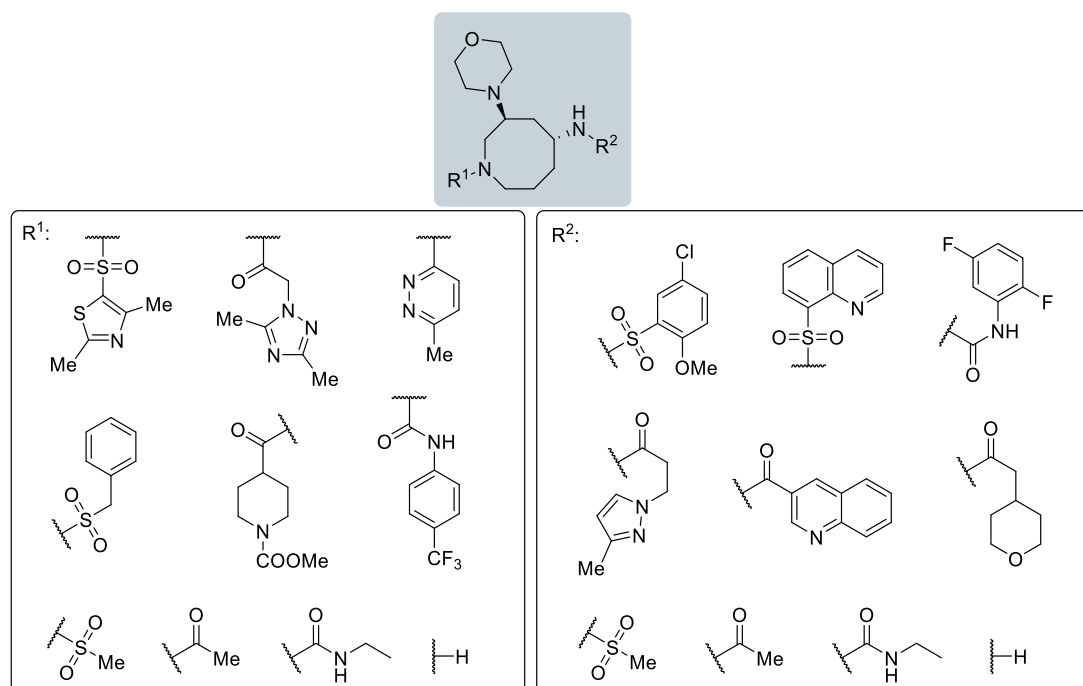
Figure 38: 10 × 10 trans virtual library.

Just like the 10 × 10 *cis*-library, the resulting 10 × 10 *trans*-library covered a unique low MW/SlogP/TPSA area which wasn't covered by the 51 × 51 enumerated *trans*-library. However, it still managed to cover a sizeable portion of the descriptor space defined by the 51 × 51 enumerated library, including compounds with higher sphericity (Figure 39).
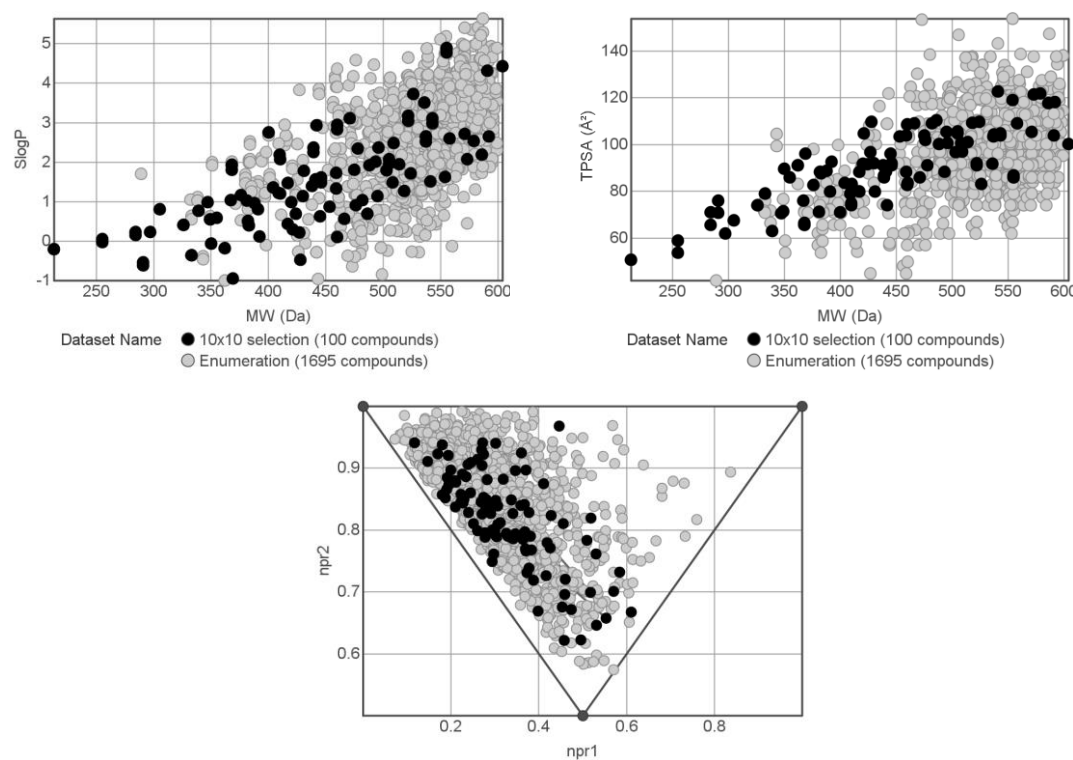
Figure 39. Analysis of descriptor space coverage by the trans 10 × 10 combinatorial library.

Although both 10 × 10 libraries showcased a broad coverage of chemical space, practical considerations had to be made once more: not only would the 2 × 10 × 10 design require a significant amount of starting material and 27 different reagents (4 × 6 chosen by selection + MsCl, EtNCO, AcOH), it would also require a laborious building block synthesis process. Since the laboratories at the University of Birmingham and Symeres were not equipped for larger combinatorial parallel synthesis, the 2 × 10 × 10 approach would demand for the synthesis of 20 separate building blocks. Hence, the library design size was reduced further.

4.6.2.   Towards a smaller virtual library

Since building block synthesis was the bottleneck for time-efficient library synthesis, the dimensions of the library were reduced to 2 × 3 × 10, using the same large R-groups from the 10 × 10 virtual libraries (Figure 40). Given the chemical moieties on each building block would be present in all their library analogues, small R-groups were chosen for the building block synthesis step to provide low-MW/SlogP analogue series. Furthermore, EtNCO was chosen over AcOH as a building block reagent because the resulting urea contains a H-bond donor and acceptor while the 3° amide would only contain a H-bond acceptor. In addition, both sulfonamides and ureas are known bioisosteres for amides.[29] Finally, functionalisation of the primary amine was chosen as the parallel synthesis step, since appendages on the primary amine would take greater advantage of the flexibility of the eight-membered ring, probing a larger 3D-space. Indeed, *in silico* PMI-analysis of the analogous 3 × 10 *cis*-library with the parallel step on the secondary amine showed less coverage of the more sphere-like shape space (Figure 41). In addition, a library step on the secondary amine would require a parallel Ns deprotection step to obtain the free primary amine. As this deprotection was currently performed with the toxic and rather smelly thiophenol (see Section 3.4, page 60), a parallel Boc deprotection step on the secondary amine in the alternative library was considered far more practical and safe.
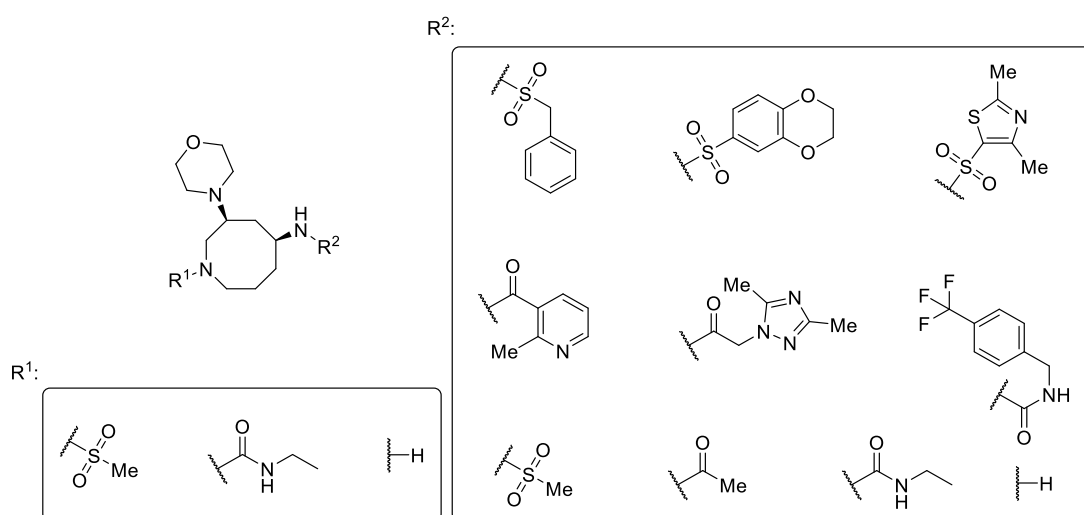
Figure 40: 3 × 10 SACE1 cis library design
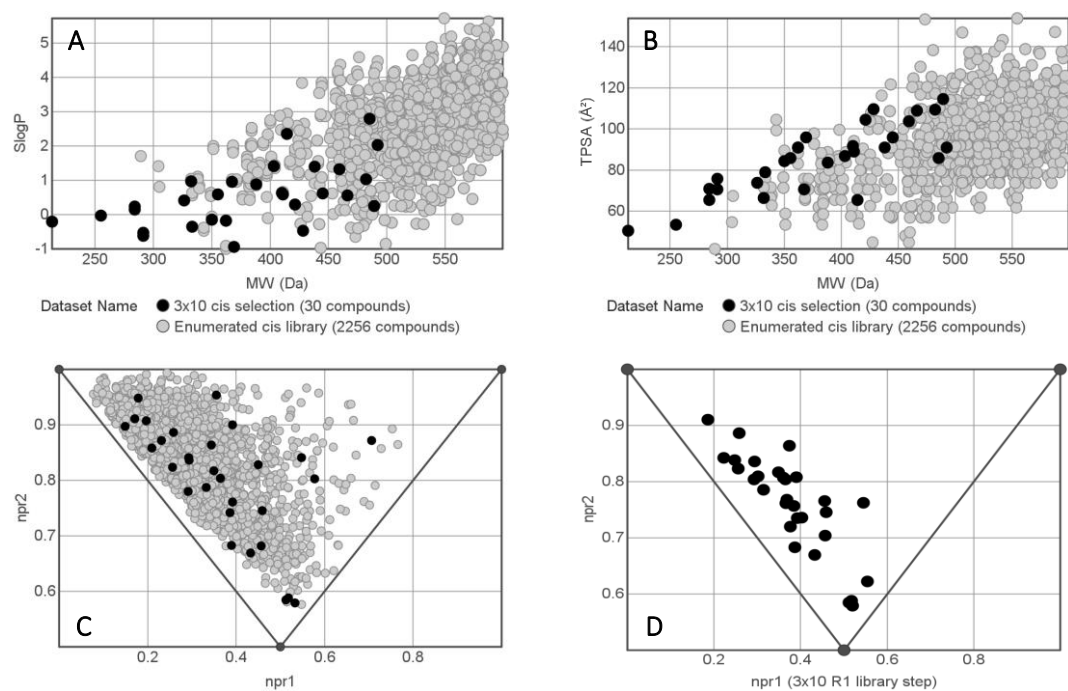
Figure 41. Analysis of the cis 3 × 10 selection (A, B, C). An analogous 3 × 10 cis library with the library step on the secondary amine showed less coverage of more spherical PMI space (D).

Analogously for the *trans*-isomer, a 3 × 10 virtual library with the library step on the primary amine covered a larger shape space, including compounds with higher average sphericity than the 3 × 10 equivalent with the library step on the secondary amine (Figure 41). As was established during the development of the design method earlier (Section 4.4), it was expected that it would become increasingly difficult for a smaller library to cover the same ranges in descriptor space as a larger alternative; indeed, both 3 × 10 libraries did not cover the same area of descriptor space as did their larger 10 × 10 libraries (Figure 37, Figure 39,Figure 41, Figure 42). The choice for small R-groups in building block synthesis did increase the bias for low MW but also resulted in less coverage of the descriptor spaces defined by the 51 × 51 enumerated libraries. However, the compounds in both 3 × 10 libraries were still well distributed in SlogP and PMI shape space within the limitations of low MW. In particular, both 3 × 10 libraries retained a set of more spherical compounds, which was considered to outweigh the loss in MW/SlogP/TPSA space coverage (Figure 41 and 42).
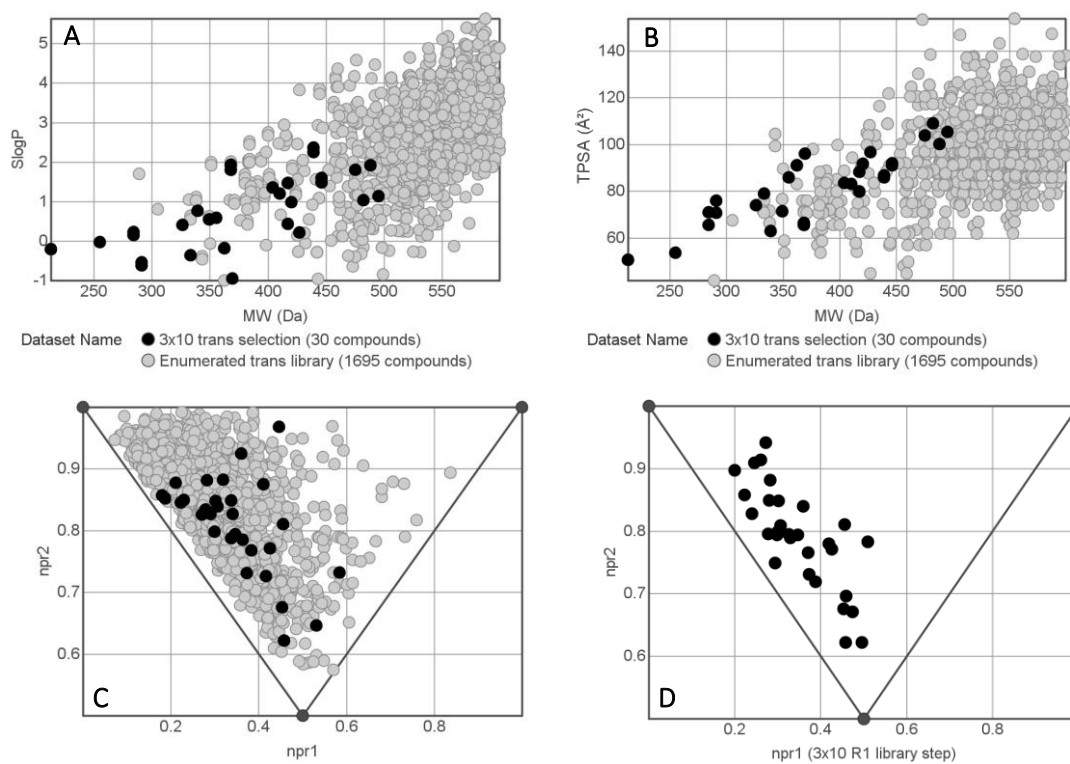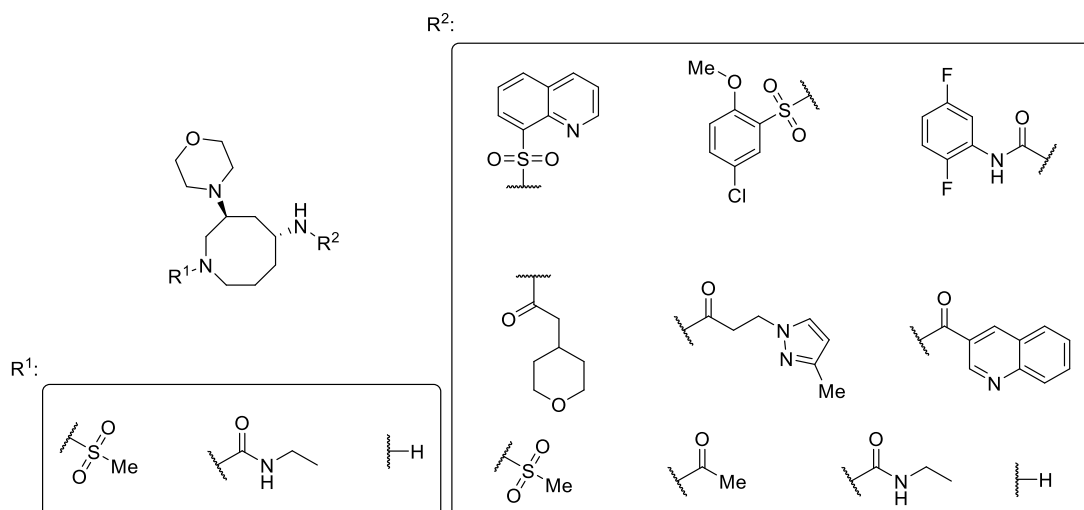
Figure 42: Analysis of trans 3 × 10 selection (A, B, C). An analogous 3 × 10 trans library with the library step on the secondary amine showed less coverage of more spherical PMI space (D).

The 2 × 3 × 10 virtual library was considered a pragmatic trade-off between maximising diversity and practical limitations in the lab and research schedule. Investing time and resources in other libraries based on different scaffolds would ultimately yield greater diversity, rather than focusing on a large single-scaffold library.[5] Nonetheless, the 2 × 10 × 10 virtual library was not made in vain; if any compound from the 2 × 3 × 10 set proves to be bio-active in future assays, the 2 × 10 × 10 combinatorial library could be used immediately to provide a set of analogues.

4.7.   Implications of X-ray diffraction analysis

The two 3 × 10 libraries were synthesised before definitive assignment of relative stereochemistry in the precursors. At this stage, tentative assignment of the relative stereochemistry of the precursors was based on the hypothesis of an intramolecular H-bond in the *cis*-diastereomer, which was supported by NMR spectroscopic analysis of *o*-nosyl sulfonamide **100** (see Section 3.2.2, page 53). X-ray analysis of recrystallised *p*-nosyl sulfonamide **102** ultimately disproved this hypothesis (see Section 3.2.3); thus, the relative stereochemistry of the products in our two 3 × 10 libraries needed revision: all initially *cis*-assigned compounds are therefore in fact *trans*-diastereomers, while the initially *trans*-assigned compounds are *cis* (Figure 43). Given these structural reassignments to the library compounds, we investigated how the swapped stereochemistry assignments influenced the library properties as the two libraries used different R-groups.

NMR spectroscopy based hypothesis: *trans*
XRD analysis: *cis*

NMR spectroscopy based hypothesis: *cis*
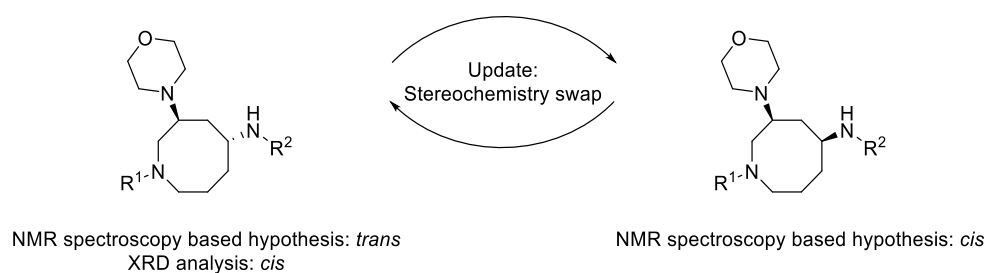
*Figure 43: XRD analysis of sulfonamide **102** disproved the tentative stereochemistry assignments of library precursors, so the assigned stereochemistry of the diastereomer subsets had to be updated.*

In terms of MW, SlogP and TPSA, the stereochemistry swap had no influence. Although this is evident for MW, it did illustrate that our SlogP and TPSA calculations did not take stereochemistry into account. However, the changes in stereochemistry did influence the occupied shape space. The updated *trans*-library had a lower average sphericity (0.160) compared to its *cis* parent library (0.170), while the updated *cis*-library had a higher average sphericity (0.166) than its parent *trans* library (0.157) (Figure 44). An interesting parallel to draw is that for the libraries with putative (disproven) stereochemistry, the *cis*-library also had a higher sphericity than the *trans*-library, illustrating that the SACE1 *cis*-scaffold will yield more spherical compounds in general. Fortunately, the stereochemistry swap had little influence on the overall sphericity of both sets combined as the relative increase and decrease in sphericity evened each other out.
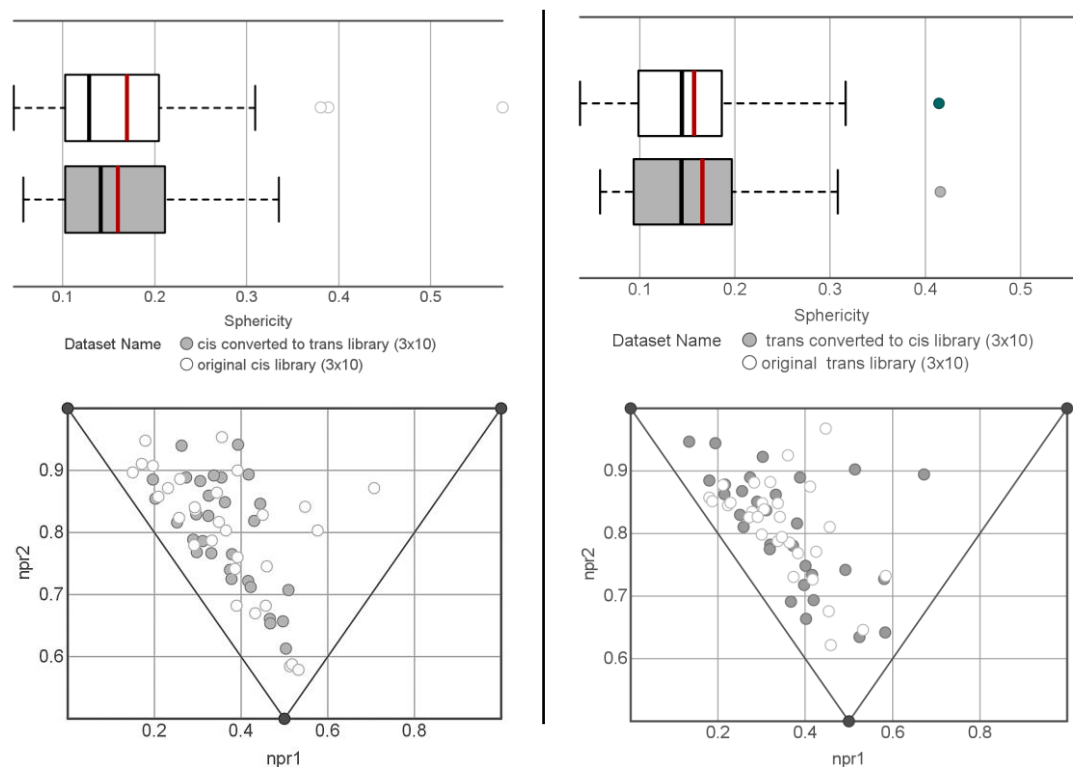
Figure 44: Analysis of the two 3 × 10 libraries with updated stereochemistry. Mean: red line. Median: black line. For statistical values, see Appendix 2.5.

In conclusion, the SACE1 library design provided a challenging but nonetheless successful first application of the established library design method. The initial 10 × 10 library designs showed excellent coverage of the enumerated 51 × 51 libraries, whilst also covering a unique low MW/SlogP/TPSA space. The pragmatic decision to reduce the library sizes to 3 × 10 showed how decreased library size comes at the cost of narrower descriptor space coverage, increasing the bias of the used building blocks when their relative amount is decreased. Finally, the reassignment of library stereochemistry showed that *cis*-diastereomers showed an overall higher sphericity than their *trans*-analogues, although this stereochemistry swap in the 1/1 diastereomeric library had little effect on the overall sphericity of the combined library.

4.8. References

1   J.-L. Reymond, L. Ruddigkeit, L. Blum and R. van Deursen, *WIREs Comput. Mol. Sci.*, 2012, **2**, 717–733.

2   I. Muegge and P. Mukherjee, *Expert Opin. Drug Discov.*, 2016, **11**, 137–148.

3   D. E. Patterson, R. D. Cramer, A. M. Ferguson, R. D. Clark and L. E. Weinberger, *J. Med. Chem.*, 1996, **39**, 3049–3059.

4   A. Koutsoukas, S. Paricharak, W. R. J. D. Galloway, D. R. Spring, A. P. IJzerman, R. C. Glen, D. Marcus and A. Bender, *J. Chem. Inf. Model.*, 2014, **54**, 230–242.

5   W. H. B. Sauer and M. K. Schwarz, *J. Chem. Inf. Comput. Sci.*, 2003, **43**, 987–1003.

6   B. C. Doak, B. Over, F. Giordanetto and J. Kihlberg, *Chem. Biol.*, 2014, **21**, 1115–1142.

7   M. A. Navia and P. R. Chaturvedi, *Drug Discov. Today*, 1996, **1**, 179–189.

8   C. A. Lipinski, F. Lombardo, B. W. Dominy and P. J. Feeney, *Adv. Drug Deliv. Rev.*, 2001, **46**, 3–26.

9   C. R. W. Guimarães, A. M. Mathiowetz, M. Shalaeva, G. Goetz and S. Liras, *J. Chem. Inf. Model.*, 2012, **52**, 882–890.

10   F. Roth-Walter, I. M. Adcock, C. Benito-Villalvilla, R. Bianchini, L. Bjermer, G. Caramori, L. Cari, K. F. Chung, Z. Diamant, I. Eguiluz-Gracia, E. F. Knol, A. G. A. Kolios *et al.*, *Allergy*, 2019, **74**, 432–448.

11   V. A. Levin, *J. Med. Chem.*, 1980, **23**, 682–684.

12   D. E. Clark, *Future Med. Chem.*, 2011, **3**, 469–484.

13   M. Wirth, A. Volkamer, V. Zoete, F. Rippmann, O. Michielin, M. Rarey and W. H. B. Sauer, *J. Comput. Aided Mol. Des.*, 2013, **27**, 511–524.

14   D. G. Brown and J. Boström, *J. Med. Chem.*, 2016, **59**, 4443–4458.

15   J. Meyers, M. Carter, N. Y. Mok and N. Brown, *Future Med. Chem.*, 2016, **8**, 1753–1767.

16   B. C. Doak, J. Zheng, D. Dobritzsch and J. Kihlberg, *J. Med. Chem.*, 2016, **59**, 2312–2327.

17   T. Sander, J. Freyss, M. von Korff and C. Rufener, *J. Chem. Inf. Model.*, 2015, **55**, 460–473.

18   M. R. Berthold, N. Cebron, F. Dill, T. R. Gabriel, T. Kötter, T. Meinl, P. Ohl, C. Sieb, K. Thiel and B. Wiswedel, in *Data Analysis, Machine Learning and Applications*, eds. C. Preisach, H. Burkhardt, L. Schmidt-Thieme and R. Decker, Springer, Berlin, Heidelberg, 2008, pp. 319–326.

19   RDKit, https://www.rdkit.org/, (accessed 16 January 2022).

20   A. Capecchi, D. Probst and J.-L. Reymond, *J. Cheminformatics*, 2020, **12**, 43.

21   A. Cereto-Massagué, M. J. Ojeda, C. Valls, M. Mulero, S. Garcia-Vallvé and G. Pujadas, *Methods*, 2015, **71**, 58–63.

22   C. Steinbeck, Y. Han, S. Kuhn, O. Horlacher, E. Luttmann and E. Willighagen, *J. Chem. Inf. Comput. Sci.*, 2003, **43**, 493–500.

23   D. Rogers and M. Hahn, *J. Chem. Inf. Model.*, 2010, **50**, 742–754.

24   Erl Wood Cheminformatics nodes for KNIME (trusted extension), https://www.knime.com/community/erlwood, (accessed 22 November 2021).

25   Molecule or Reaction Similarity and Descriptors, https://openmolecules.org/help/similarity.html, (accessed 22 November 2021).

26   C. Boss, J. Hazemann, T. Kimmerlin, M. von Korff, U. Lüthi, O. Peter, T. Sander and R. Siegrist, *Chimia*, 2017, **71**, 667–677.

27   D. R. Stephen, *Curr. Med. Chem.*, 2020, **27**, 6495–6522.

28   S. A. Wildman and G. M. Crippen, *J. Chem. Inf. Comput. Sci.*, 1999, **39**, 868–873.

29   S. Kumari, A. V. Carmona, A. K. Tiwari and P. C. Trippier, *J. Med. Chem.*, 2020, **63**, 12290–12358.

5. SACE2 library
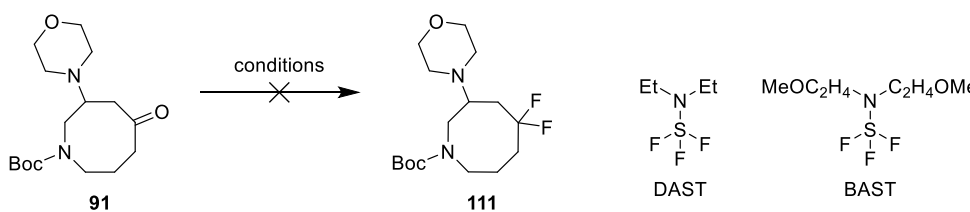
Given the synthesis, characterisation and separation of the diastereomeric SACE1 library precursors was not straightforward, a simpler, more atom-economical synthesis was envisioned for the second library (SACE2). Starting from ketone precursor **91**, the aim was to yield a new set of building blocks in relatively few steps, as racemic mixtures of enantiomers or single diastereomers. Since the 2° amine embedded in the eight-membered ring was hypothesised to attack the transannular carbonyl upon Boc deprotection, manipulation of the ketone was once again required. Therefore, difluorination of the ketone and its incorporation into an aromatic heterocycle were investigated (Scheme 41).
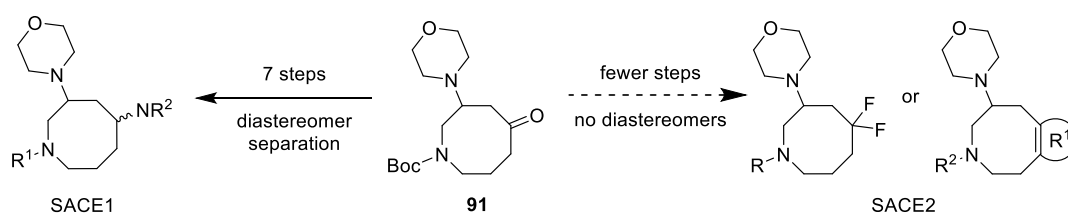
*Scheme 41: Synthesis of the SACE1 library required 7 steps from ketone **91**, including a diastereomer separation step. A simpler synthesis was envisioned for the SACE2 library.*

With the introduction of fluorine reported to positively influence the potency and pharmacokinetics properties of a drug,[1] difluorination of the ketone **91** would yield racemic Boc-protected building block **111** in one step, providing a quick and attractive entry into a racemic library with one decoration site. Unfortunately, literature procedures using diethylaminosulfur trifluoride (DAST)[2] and the more thermally stable deoxofluor (BAST)[3,4] did not yield the difluorinated compound **111**. No reaction was observed when a solution of ketone **91** in CH_2Cl_2 was treated with DAST and BAST (Table 9, Entries 1 and 2), whilst extensive degradation was observed when BAST was used in toluene at 90 °C (Table 9, Entry 3), evidenced by multiple peaks in the LCMS chromatogram of the reaction mixture and no identified products in the ^{1}H-NMR spectrum of the crude mass obtained after workup. Given previous reductive amination attempts on ketone **91** had also proven unsuccessful (see Section 3.1.5), ketone **91** appears to display limited reactivity. Hence, the difluorination was not explored further and the focus shifted towards the synthesis of fused aromatic heterocycles.

*Table 9: Attempted difluorination of ketone **91**.[a]*

Entry	Reagents	Solvent	T (°C)	Time (h)	Outcome
1	DAST (2 eq), EtOH (0.5 eq)	CH_2Cl_2	−15 to rt to reflux	46	No reaction
2	BAST (2 eq)	CH_2Cl_2	−4 to rt to reflux	24	No reaction
3	BAST (2 eq)	toluene	0 to 90	25	Degradation

[a]Reactions performed on 0.19 mmol scale, 0.2 M reaction concentration.

5.1.   Fused aromatic heterocycles

Aromatic heterocycle fusion to the azocanone **91** was considered an attractive route towards a new series of library compounds. Besides being a common motif in drug discovery (Figure 45),[5–9] fused heterocycles introduce sp^2 centres and conformational restriction into the molecular framework. This will significantly alter the preferred conformation of the eight-membered ring, compared to SACE1 library molecules, giving access to new shape space and increasing the overall diversity obtained through diversification of parent scaffold **29**.
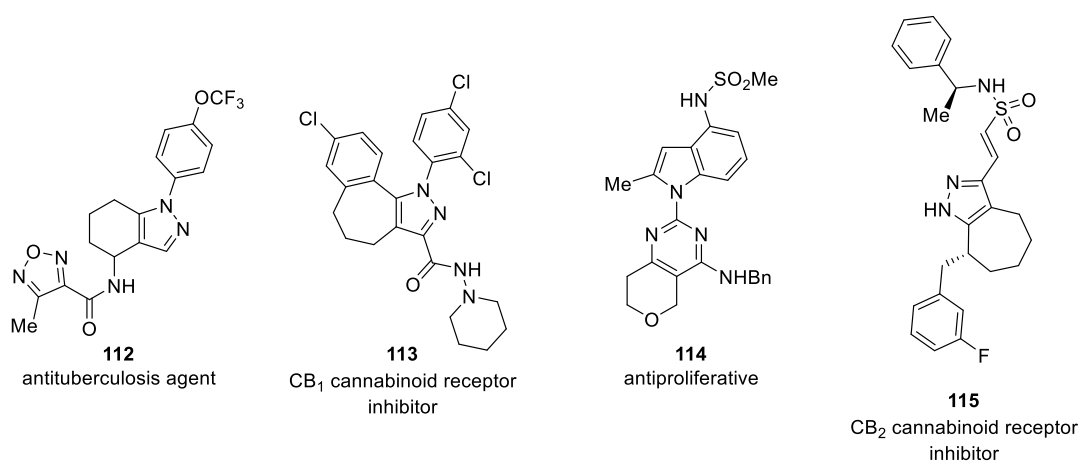
Figure 45: Biologically active fused heterocycles.[6–9]

5.1.1. Entropic considerations regarding conformational flexibility

Although the conformational flexibility of the eight-membered ring may facilitate molecular recognition (see Section 1.6, page 22), it is possible that the SACE1 library compounds may suffer from significant entropic penalties upon interaction with a biological target. Binding to a biological target results in a reduction in the ligand's rotational, translational and vibrational degrees of freedom.[10,11] This loss in conformational entropy decreases the overall binding free energy, contributing negatively to the potency of the ligand.[11] For example, Sager *et al*. found that a septanose analogue **117** of α-D-mannopyranoside **116** displayed nine times lower affinity for bacterial protein FimH, although co-crystal structures of the two protein-bound inhibitors showed identical interactions with the target protein (Figure 46). This loss in affinity was attributed to a loss in conformational entropy, as the more flexible seven-membered ring **117** showed a higher entropic penalty upon binding.[12]
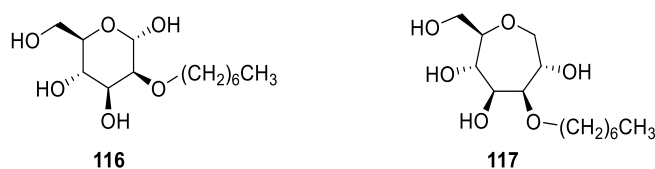
*Figure 46: The more flexible septanose analogue **117** displayed lower affinity for bacterial protein FimH, because of an increased entropic penalty upon binding.[12]*

The entropic penalty upon binding a target protein can be decreased by reducing the conformational flexibility of the ligand. Therefore, fused heterocycles were considered a valuable addition to our collection of eight-membered cyclic amine analogues; conformationally restricting the eight-membered ring would not only yield novel analogues in a different region of chemical space, but could also potentially yield more potent molecules,[a] compared to the SACE1 library compounds. Hence, a suitable intermediate for fused aromatic heterocycle synthesis was sought.

---

[a] Although high potency is not essential during the hit identification stage, compounds are often considered a hit when they show inhibition above a certain threshold (*e.g.*, in high-throughput single-concentration assays). Increased potency may influence whether this threshold is met or not.

5.1.2. Finding a suitable intermediate for fused aromatic heterocycle synthesis: α-bromoketones and β-keto-enamines

Initially, the synthesis of α-haloketones was considered, since they are important precursors for a variety of fused heterocycles, including isoxazoles, pyrroles, carbazoles and thiazoles.[13] Two literature conditions for α-bromination were tested using NBS[14] and CuBr$_2$.[15a] LCMS analysis of the reaction mixtures showed disappearance of the starting material after overnight stirring; however, no mass signals showing the characteristic [79]Br: [81]Br 1:1 ratio were observed in the chromatogram (Table 10).

Table 10: Attempted α-bromination of ketone **91**.
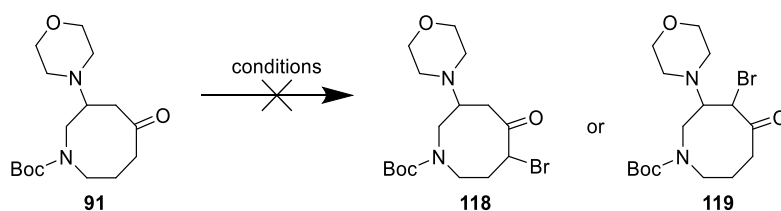
Entry	Reagent	Solvent	T (°C)	Time (h)	Outcome[a]
1	NBS (1.2 eq), SiO$_2$ (10% w/w)	MeOH	rt	19	m/z of product observed (trace) after 25 min, but disappeared overnight; after 19 h, no more SM or Br-containing products observed
2	CuBr$_2$ (2.2 eq)	EtOAc:CHCl$_3$ (1:1)	70 (reflux)	25	Br-containing products not observed in RM aliquots, full consumption of SM

[a] SM: starting material. RM: reaction mixture.

β-Ketoenamines provide another attractive entry into fused aromatic heterocycles. These precursors are typically synthesised from ketones using *N,N*-dimethylformamide dimethyl acetal (DMF-DMA) or Bredereck's reagent (Figure 47).[16,17] Starting from cyclic β-keto-enamines, the syntheses of many fused aromatic heterocycles have been reported, including pyrazoles, isoxazoles, pyridines and pyrimidines.[16]

---

[a] Bromination using Br$_2$ in AcOH was not attempted, because of the toxicity of Br$_2$ and lack of literature precedent for bromination of Boc-protected cyclic aminoketones using this procedure, indicating a risk of Boc deprotection.
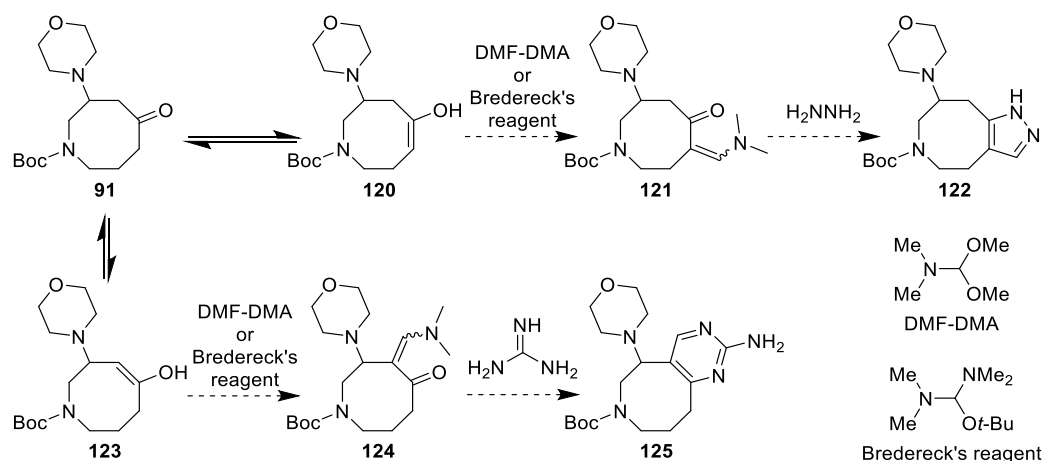
Figure 47: Potential heterocycle fusion routes using DMF-DMA or Bredereck's reagent.

A key criterion for successful scaffold synthesis was the regioselectivity of the enamine formation. Given enamine formation is assumed to proceed via an enol, the asymmetrically substituted ketone **91** can yield two possible regioisomers (Figure 47), which would yield structurally distinct fused heterocycles. Both enamine regioisomers **121** and **124** would represent attractive ring precursors, but a regioselective enamine synthesis was preferred to avoid possible regioisomer separation issues. Initial attempts to synthesise β-ketoenamines using DMF-DMA in DMF solvent failed; although LCMS analysis of the reaction mixture showed the $[M+H]^+$ ion for the target enamine **121/124** in trace amounts after 1 h, no relative increase of this product was observed after 19 h and no starting material nor desired product was observed after 44 h (Table 11, Entry 1). No reaction was observed when the reaction was performed in THF at 65 °C (Table 11, Entry 2). Although a reaction performed in DMF-DMA as the solvent[18] (Table 11, Entry 3) yielded enamine **121/124** ([M+H]+ observed *via* LCMS) as the major compound in the crude mass after aqueous workup, the long reaction time and use of a large excess of DMF-DMA were not ideal.

*Table 11: Attempted synthesis of β-ketoenamine **121** (putative regioisomer is drawn).[a]*
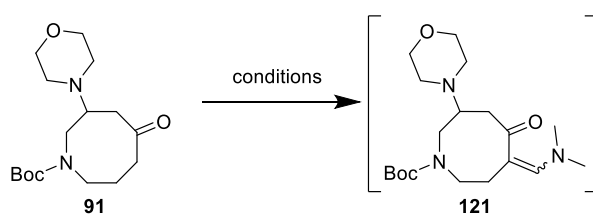
Entry	Reagent	Solvent	T (°C)	Time (h)	Outcome
1	DMF-DMA (1.2 eq)	DMF	153 (reflux)	44	m/z of **121** observed (trace) after 1 h, but extensive degradation upon prolonged reaction
2	DMF-DMA (3 eq)	THF	65	168	no reaction
3	DMF-DMA (10 eq)	neat	103 (reflux)	72	no clean conversion 91% crude mass recovery
4	Bredereck's reagent (1.1 eq)	DMF	90	72	conversion to **121**, but **93** still present after 48 h, while **121** degraded
5	Bredereck's reagent (2.0 eq)	1,4-dioxane	100 (reflux)	2	clean conversion 35% crude mass recovery ^{1}H-NMR analysis: unidentified aliphatic impurity
6	Bredereck's reagent (2.0 eq)	DMF	153 (reflux)	2	clean conversion 68% crude mass recovery ^{1}H-NMR analysis: residual DMF present. Product not recovered from column, assumed to be unstable on SiO_2

[a] Reaction performed on 100 mg scale in a closed vessel. Reaction mixtures monitored *via* LCMS.

Instead of using DMF-DMA, a small excess of Bredereck's reagent[19] resulted in around 50% conversion to the enamine **121**[a] after 6 h according to LCMS analysis, but the ketone **91** was still present after two days and after three days, almost complete degradation of enamine **121** was observed (Table 11, Entry 4). Using a larger excess of Bredereck's reagent in refluxing 1,4-dioxane or DMF (Table 11, Entries 5 and 6) resulted in clean conversion of the ketone **91** to enamine **121** according to LCMS analysis. The enamine **121** was observed as a single peak on the LCMS chromatogram, which gave a first indication that this reaction was regioselective. However, the low crude mass recoveries after aqueous workup and the instability of enamine **121** towards purification by silica chromatography, encouraged us to consider using the enamine directly without purification, to yield fused heterocycles in a one-pot fashion or by telescoping.

---

[a] Although the structure of the enamine was not yet determined at this point, putative regioisomer **121** is used to denote the target enamine in the following discussion instead of **121/124** for clarity.

The reactivity of intermediate **121** (Table 11, Entry 3) was tested by redissolving the crude mixture in DMF and adding 4-fluorophenylhydrazine •HCl and heating at 90 °C (Scheme 42). Pleasingly, LCMS analysis of the reaction mixture showed full consumption of intermediate enamine **121** after 36 min. Subsequent concentration under reduced pressure followed by purification by column chromatography (CH$_2$Cl$_2$:7 M NH$_3$ in MeOH) yielded fused pyrazole **126** in good yield. This showed that the enamine **121** could be used as an intermediate and that the resulting fused pyrazole **126** could be purified by column chromatography, yielding enough material for characterisation.
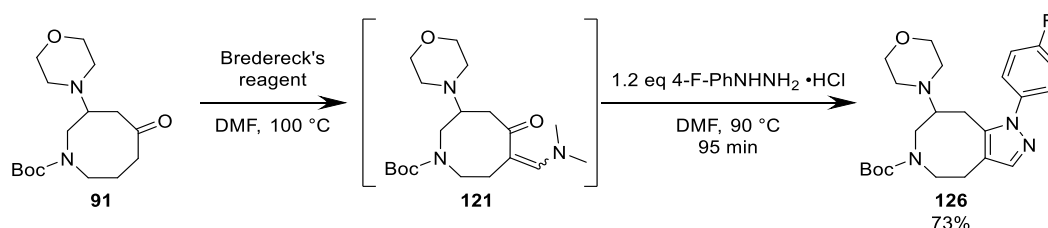
*Scheme 42: A test reaction on crude ketoenamine **121** yielded fused pyrazole **126** in good yield.*

The regioselectivity of the reaction was confirmed by NMR spectroscopic analysis: HMBC experiments on pyrazole **126** showed cross peaks between the carbon and proton resonances of C(2)H$_2$ and C(4)H$_2$, and between H-10 and C-6 (Figure 48). Furthermore, no HMBC cross peaks were observed between C(3)H and C(10)H, further supporting the location of the ring fusion and therefore the regioselectivity of enamine formation, which is likely explained by steric hindrance from the morpholine group.
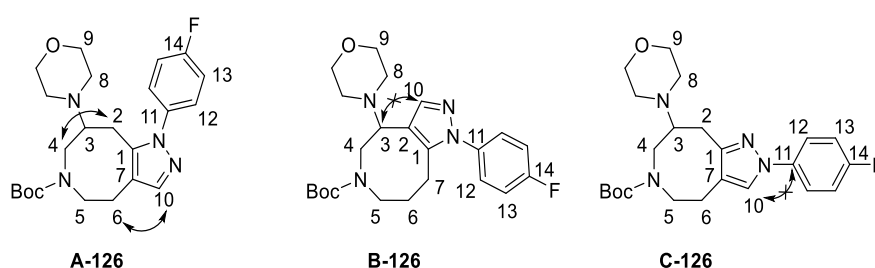
*Figure 48: Relevant HMBC cross peaks observed for possible regioisomers of pyrazole **126**, confirming that **A-126** is the obtained regioisomer.*

Attack of the hydrazine reagent and subsequent cyclisation also posed regioselectivity concerns, although the regioselectivity for fused pyrazole syntheses, starting from β-ketoenamines, is generally reported to yield only the N(1)-R isomer.[16] HMBC cross peaks were

observed between H-10 and C-11, supporting the formation of pyrazole regioisomer **A-126** and not **C-126**, consistent with the generally reported regioselectivity for these types of reactions.[16]

The good yield and regioselectivity of this test reaction (Scheme 42) encouraged us to explore one-pot procedures and telescoping. First, a one-pot conversion of the ketone **91** to fused pyrazole was tested in 1,4-dioxane; however, LCMS analysis of the reaction mixture showed no enamine intermediate **121** nor pyrazole **126** after adding the hydrazine reagent. Instead, multiple unidentified products were formed, one of which showed an m/z value which could correspond to the [M+H]$^+$ ion of the hydrazone **127** (Scheme 43). After 18 h, ketone starting material **91** was still present in the mixture, indicating that the hydrazine may have also reacted with Bredereck's reagent. Since hydrazines are known to react with ketones to form hydrazones,[20,21] the observed results were not completely unexpected and hence the one-pot approach was deprioritised.
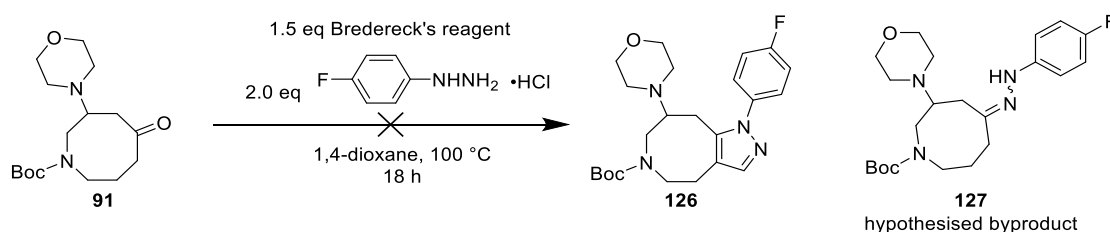
Scheme 43: Attempted one-pot synthesis of fused pyrazole 126 yielded no enamine intermediate 121, nor pyrazole 126. Instead, multiple byproducts were formed.

Since the pyrazole synthesis test reaction had worked in DMF (Scheme 42), a telescoped synthesis of pyrazole **126** from ketone **91** was attempted in DMF.[a] Given Bredereck's reagent has a low boiling point (50 – 55 °C), we hypothesised the excess reagent present in the reaction mixture after the first step could be removed selectively under reduced pressure at rt. Retaining the enamine product as a solution in DMF, hydrazine was added subsequently. In a first test reaction performed on 75 mg scale, full consumption of ketone **91** in step 1, and intermediate **121** in step 2, was achieved in short reaction times (Table 12, Entry 1). The reaction mixture was loaded directly on to a normal phase SiO$_2$ column (heptane:EtOAc), but column chromatography had to be performed twice to obtain pure product. This was attributed to the presence of DMF and HCl salts in the mixture, hampering the separation on the first

[a]A telescoped reaction on 50 mg scale in 1,4-dioxane at 100 °C (step 1: 1.5 eq Bredereck's reagent, 1 h, step 2: 3.0 eq 4-fluorophenylhydrazine •HCl, 1 h) also yielded pyrazole **126** (17% after column chromatography (heptane/EtOAc)), but after 1 h, step 1 did not show full consumption of the ketone **91**. The presence of unreacted starting material in step 2 was therefore attributed to the low yield of pyrazole **126**.

column. Repeating the reaction on 300 mg scale, followed by loading the reaction mixture on a reverse phase column (10 mM NH_4HCO_3 in H_2O:MeCN) resulted in better separation of the reaction mixture, and furnished the pyrazole **91** in 68% yield (Table 12, Entry 2). In a final attempt at reaction optimisation, an aqueous workup using $NaHCO_3$ sat. aq. and Et_2O, prior to normal phase column chromatography (CH_2Cl_2:7M NH_3 in MeOH), yielded the pyrazole **126** in 60% yield (Table 12, Entry 3). Although this aqueous workup now allowed the purification with one round of column chromatography, purification *via* reverse-phase chromatography was preferred (Table 12, Entry 2) since it obviated the need for any workup and also showed a slightly higher yield.

*Table 12: Optimisation of the isolation procedure for the telescoped synthesis of pyrazole **126**.[a]*
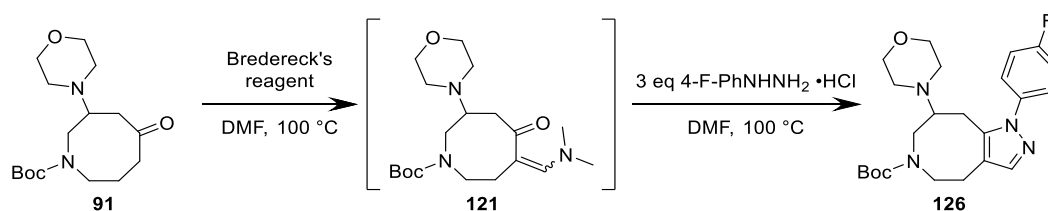
Entry	Bredereck's reagent (equiv.)	Step 1 reaction time (min)	Step 2 reaction time (min)	Purification	Isolated yield (%)
1	3	40	22	normal phase column (heptane:EtOAc)	33
2	3	60	20	reverse phase column	68
3	6[b]	210	15	$NaHCO_3$/Et_2O aqueous work-up + normal phase column (CH_2Cl_2:7 M NH_3 in MeOH)	60

[a]Reactions were performed in a closed vessel. [b]The reaction was performed in a larger closed vessel than Entry 2 (40 mL instead of 20 mL), so extra equivalents of Bredereck's reagent were added to compensate for the larger headspace as reactions were performed at temperatures above the boiling point of this reagent.

The β-ketoenamine **121** was now shown to be a good intermediate for fused aromatic heterocycles: by telescoping two short reactions, fused pyrazole **126** could be obtained regioselectively in good yields, which paved the way for synthesising other pyrazole analogues.

5.1.3. Fused pyrazoles

5.1.3.1. Facile analogue generation

With a quick route for pyrazole synthesis in hand, a series of pyrazoles were synthesised, each on 0.1 mmol scale. The choice of pyrazole substituents was informed by *in silico* library design (Scheme 44, see Section 6). Using the optimised telescoped reaction conditions (Table 12), five fused pyrazoles were obtained in good yields. All displayed analogous HMBC cross peaks to pyrazole **126** (Figure 48), thereby confirming the regioselectivity of the reactions.
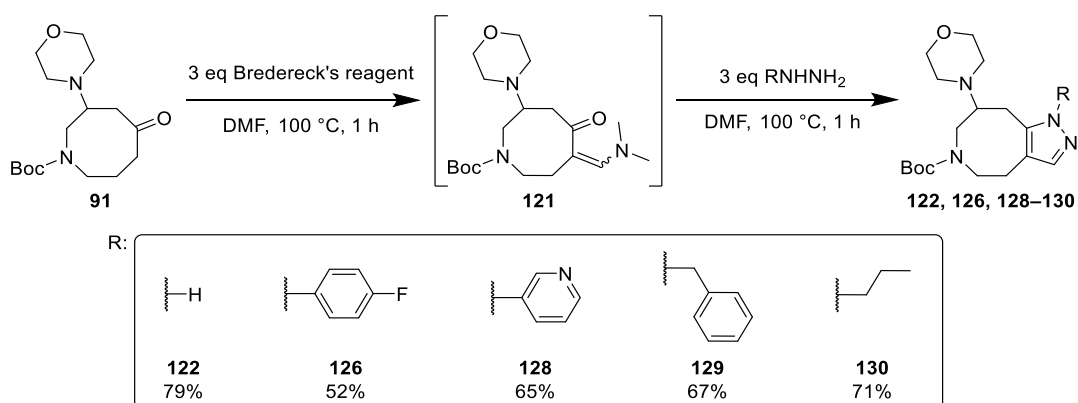
Scheme 44: Using a telescoped approach, five fused pyrazoles were synthesised regioselectively in good yields.

Synthesis of the corresponding *N*-Me pyrazole did not proceed in a regioselective fashion: ^{1}H-NMR spectroscopic analysis of the crude mixture showed a 2:1 ratio of the 1-methyl- and 2-methyl regioisomers, based on relative integration of the pyrazole H-10 resonances (Scheme 45). Fortunately, the regioisomers could be separated *via* SFC (BEH column, CO_2:20 mM NH_3 in MeOH), yielding regioisomers **131** in 51% yield (809 mg) and **132** in 30% yield (478 mg). The regioisomers were assigned *via* HMBC experiments; thus, the 1-methylpyrazole regioisomer **131** showed cross peaks between NCH_3 and C-1 and no cross peaks between C(10)H and NCH_3, while 2-methylpyrazole analogue **132** showed HMBC cross peaks between NCH_3 and H-10, but not between NCH_3 and C-1. Analogous non-regioselective pyrazole fusions starting from β-ketoenamines and methylhydrazine have been reported, with the 1-methylpyrazole also formed as the major regioisomer.[22–24] These findings suggest the two nitrogens in methylhydrazine display a more similar reactivity compared to the other substituted hydrazines, which reacted regioselectively.
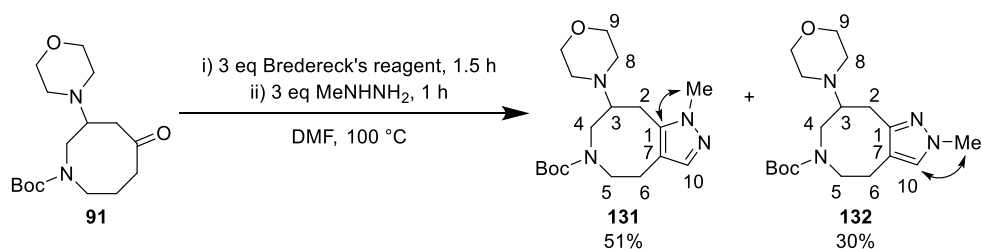
Scheme 45: Synthesis of N-Me pyrazoles did not proceed regioselectively. Relevant HMBC interactions shown (arrows).

Attempted synthesis of cyclopropyl analogue **133** using 2 eq of cyclopropylhydrazine •2 HCl at 100 °C yielded a crude mixture (96% crude mass recovery) containing cyclopropyl analogue **133** and the H-pyrazole **122** in a ∼2:1 ratio.[a] Repeating the cyclisation step at rt again showed the generation of H-pyrazole **122** (85% crude mass recovery, **133**:**122** ∼2:1), excluding the unlikely possibility of thermal cleavage of the cyclopropyl group (Scheme 46).
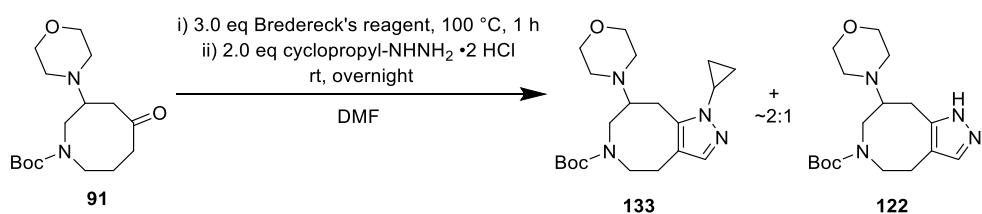
*Scheme 46: Attempted synthesis of cyclopropyl analogue **133** yielded H-pyrazole **122** as well.*

Quantitative NMR (Q-NMR) spectroscopic analysis[b] of the cyclopropyl-NHNH$_2$ •2 HCl used in the reaction showed only 88 wt% purity. If the remaining 12 wt% were H$_2$NNH$_2$ (0–2 HCl salt), this would mean that the batch of reagent used was only 84 − 63 mol% cyclopropyl-NHNH$_2$. H$_2$NNH$_2$ has two equivalent reactive sites, which we hypothesised would react more readily with the ketoenamine intermediate **121**, to yield relatively more of pyrazole **122** as the amount of used reagent (88 wt% purity) were increased. Hence, the reaction was repeated with only 1.1 eq cyclopropylhydrazine •2HCl (88 wt% purity), which resulted in lower amounts of pyrazole **122** in the crude ^{1}H-NMR spectrum (**133**:**122** ∼5:1). However, still only 36% (26 mg) of cyclopropyl analogue **133** was obtained (Scheme 47). Since Q-NMR spectroscopic analysis of a newly bought batch of cyclopropylhydrazine •2 HCl from a different supplier yielded no better weight purity, cyclopropylpyrazole **133** was not scaled up for future library synthesis, and *n*-

---

[a] Ratio based on integration of the pyrazole C*H* resonances in the ^{1}H-NMR spectrum of the crude product after aqueous workup.

[b] Quantitative ^{1}H-NMR (400 MHz, DMSO-d_6), dimethyl malonic acid used as internal standard.

propyl analogue **130** was synthesised instead without any issues, serving as an aliphatic alternative (Scheme 44, page 109).
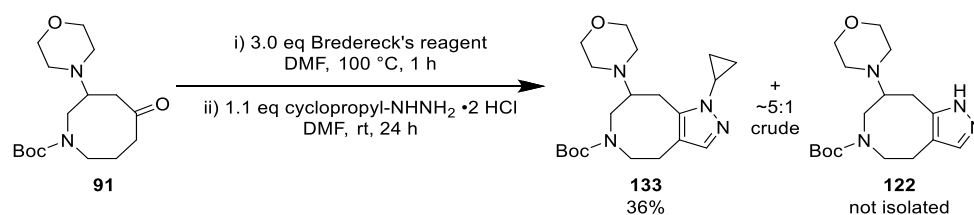
*Scheme 47: Reducing the number of equivalents of cyclopropylhydrazine •2HCl (88 wt%) decreased the relative amount of H-pyrazole **122**, but **133** was obtained in low yield nonetheless.*

5.1.3.2.　Alkylation of H-pyrazole 122

It was worth investigating alkylation of the unsubsituted pyrazole **122** using alkyl halides, since literature precedent suggested a preference for regioselective reaction on the N(2)-position.[25–27] As alkylation of this nitrogen would position appendages in a different orientation compared to the building blocks already synthesised (Scheme 44, page 109), a series of analogues with this substitution pattern would make for a valuable addition to the envisioned SACE2 library. Since a heterocyclic benzyl analogue had not yet been synthesised (Scheme 44), 5-(chloromethyl)-2,4-dimethyl-1,3-thiazole was chosen as the reagent to test pyrazole alkylation, noting the N(1)-R regioisomer would still provide a valuable precursor for library synthesis. Following a literature procedure,[28] pyrazole **122** was alkylated on 700 mg scale to afford a 1:2 mixture of regioisomers **134** and **135**, after purification by column chromatography (CH$_2$Cl$_2$:7 M NH$_3$ in MeOH) (Scheme 48). The regioisomers were separable *via* SFC and although the recovered yields were rather low, enough of each compound was obtained to synthesise a few analogues (Section 5.2.4, page 122) and provided a proof of concept for future alkylation of pyrazole **122**.[a] The regioisomers were assigned *via* COSY and HMBC experiments: isomer **134** showed HMBC cross peaks between H-11 and C-1, but no cross peaks between C(10)H and C(11)H$_2$, while isomer **135** showed HMBC cross peaks between H-10 and C-11 as well as COSY cross peaks between H-10 and H-11.

---

[a] Although there is limited literature precedent for the synthesis of fused pyrroles,[32,33] this option was not pursued as the synthesis of 2-functionalised analogues **134** and **135** was deemed sufficient to explore 2-functionalised analogues.
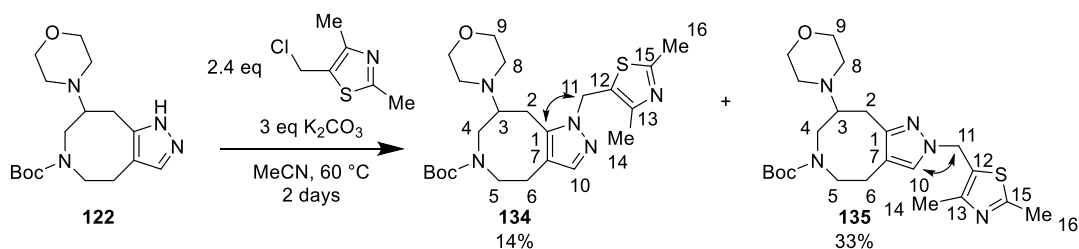
Scheme 48: Alkylation of pyrazole **122** was not regioselective; the 2-functionalised product **135** was isolated as the major product.

Having synthesised nine pyrazole analogues, the synthesis of other aromatic heterocycles *via* ketoenamine intermediate **121** was now explored as these heterocycles would provide different structural motifs with different H-bonding properties.

5.1.4.   Isoxazoles

Attempted synthesis of fused isoxazole **137** using hydroxylamine •HCl and the previously developed telescoping procedure for pyrazole synthesis (Scheme 44, page 109) led to none of the desired product. Instead, the reaction yielded an intermediate, which we hypothesise is *N*-hydroxy enamine **136** according to LCMS analysis of the reaction mixture, which revealed a m/z value corresponding to the [M+H]$^+$ ion. Under the pyrazole synthesis conditions, this intermediate failed to react further over the course of 3 h; however, upon addition of a large excess of AcOH (22 eq), following literature precedent by Barraja *et al.*,[29] the target isoxazole product **137** was observed. Using these modified cyclisation conditions, isoxazole **137** was synthesised on 600 mg scale in good yields. Isoxazole **137** showed analogous HMBC cross peaks to 4-fluorophenyl pyrazole analogue **126** (Figure 48), while a comparable chemical shift of the isoxazole C*H* proton resonance to pyrazole **137** ruled out the alternative isomer **138**, for which the isoxazole C*H* proton would appear further downfield.[30]
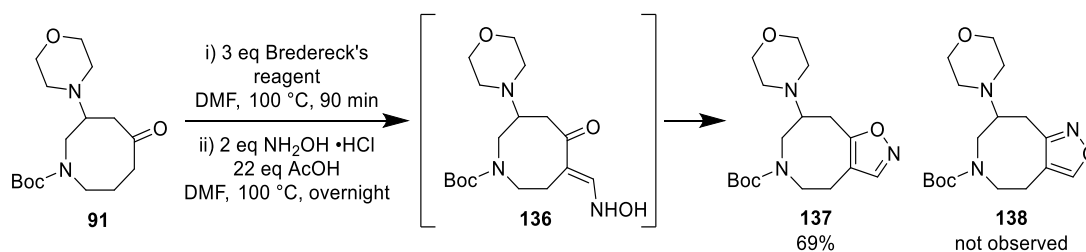
Scheme 49: Synthesis of isoxazole **137** required the addition of AcOH to drive the conversion of the hypothesised intermediate **136**.

Literature precedent for the hypothesised *N*-hydroxy enamine intermediate was provided by Al-Afaleq *et al.*, who attributed the inability of *N*-hydroxy enamine **140** to undergo cyclisation

to the desired isoxazole **141**, to the *trans* stereochemistry, which was indicated by ^{1}H-NMR spectroscopic analysis (Scheme 50).[31] We hypothesise that intermediate **136** is similarly formed as the *trans* isomer, which prevents cyclisation to form isoxazole **137**. On the other hand, Barraja *et al*. reported no issues during their synthesis of [1,2]oxazolo[5,4-*e*]indazoles from **142** and analogues, which used a MeOH:AcOH 2:1 mixture as solvent (Scheme 50).[29] Addition of AcOH presumably facilitates interconversion between the *cis* and *trans* isomers of **143**, allowing for annelation of the oxazole ring to yield **144**.
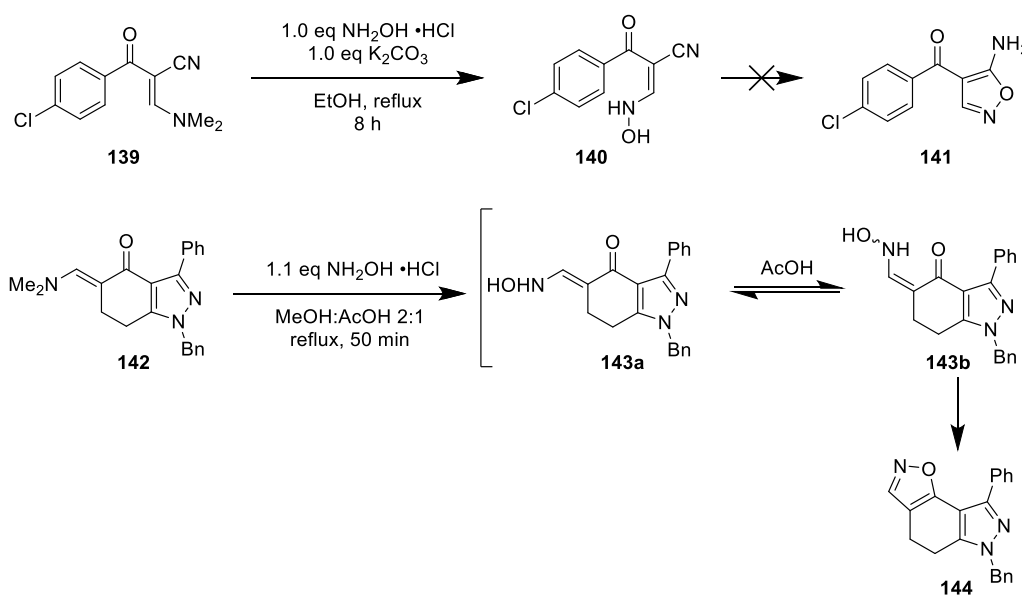
*Scheme 50: Literature precedent for a trans N-hydroxy enamine intermediate **136**, which did not cyclise to the desired isoxazole **141**,[31] and a successful isoxazole synthesis after including AcOH.[29]*

Having performed a variety of regioselective (Scheme 44, page 109) and non-regioselective (Scheme 45) fused pyrazole syntheses, including an alkylation of H-pyrazole **122** (Scheme 48) and synthesis of isoxazole analogue **137** (Scheme 49, page 112), synthetic efforts turned towards 8-6 fused ring systems.

5.1.5. Fused pyrimidines

With literature precedent available for the synthesis of fused 8-6 heterocycles from β-ketoenamines,[32–34] fused pyrimidines and analogues were explored as potential library building blocks. We hypothesise that these structurally different scaffolds may orientate appendages in a slightly different direction to those appended to the earlier synthesised 8-5 fused heterocycles. Examples of biologically active fused six-membered heterocycles can be found in

cytotoxic compound **145**[33], RORγt[a] inhibitor **146**[35] and acetylcholinesterase inhibitor **147**[36] (Figure 49). In fact, pyrimidines and pyrazoles share the fourth position in the top five most frequent nitrogen heterocycles in FDA-approved drugs from 2015–2020, after pyridines, piperidines and piperazines, highlighting their relevance for drug discovery.[5]
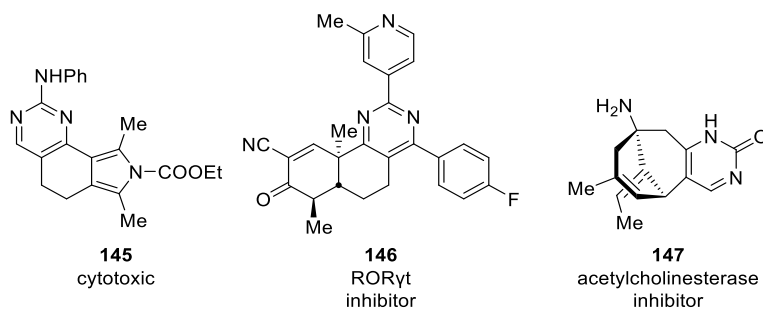
Figure 49: Examples of biologically active fused six-membered heterocycles.[33,35,36]

Initially, a method reported by Appell *et al*. was used for fused pyrimidine synthesis using acetamidine (Table 13, Entry 1).[34] After 2 days, LCMS analysis of the reaction mixture showed only partial conversion to pyrimidine **150**; β-ketoenamine intermediate **121** was still present along with a major product with m/z = 340. This product was not identified but its mass would correspond to enamine **149**, which could be a fragment of hypothesised intermediate **148**, which (in an analogous fashion to the synthesis of isoxazole **137** (Scheme 49) could not cyclise (Scheme 51).
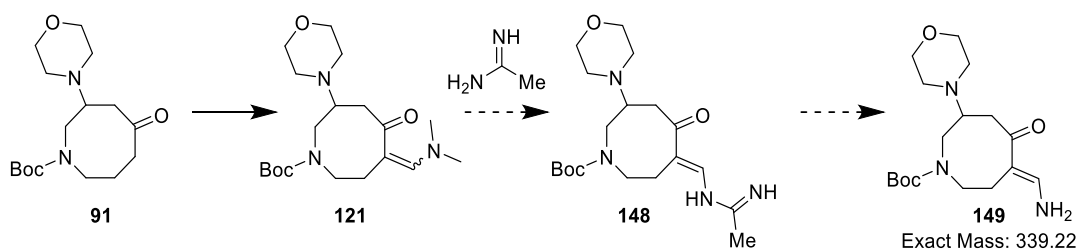
*Scheme 51: LCMS analysis of the reaction mixture showed a peak with m/z = 340, which could correspond to a fragment ion of hypothesised intermediate **148**.*

Given the comparatively low reflux temperature of MeOH, the experiment was repeated in DMF at 100 °C (Table 13, Entry 2). These conditions yielded full consumption of β-ketoenamine **121** after 22 h, with LCMS analysis of the reaction mixture showing pyrimidine **150** as the major compound, although the putative intermediate **148** was also present. Work-up and purification by column chromatography (CH$_2$Cl$_2$:7 M NH$_3$ in MeOH) afforded pyrimidine **150** in 21% yield.

---

[a] RORγt: retinoic acid receptor-related orphan receptor γt, a target for treating autoimmune diseases.

Increasing the temperature further to 150 °C resulted in a cleaner LCMS chromatogram of the reaction mixture after 22 h (Table 13, Entry 3), showing pyrimidine **150** as the major product and no evidence for intermediates **121** nor **148**. However, this improved procedure was not reflected in a higher yield as pyrimidine **150** was isolated in 20% yield after purification *via* reverse-phase chromatography. Since the fused pyrazoles were obtained from hydrazine HCl-salts without using NaOMe (Scheme 44), we checked whether the inclusion of NaOMe was necessary (Table 13, Entry 4). This was confirmed, as LCMS analysis of the reaction mixture showed no pyrimidine **150** after 27 h and acetamide **148** as the major compound. After 44 h, pyrimidine **150** was present as a minor compound, but enamine **148** still predominated and degradation was now evident on the chromatogram.

*Table 13: Conditions for the synthesis of fused pyrimidine **150**.[a]*
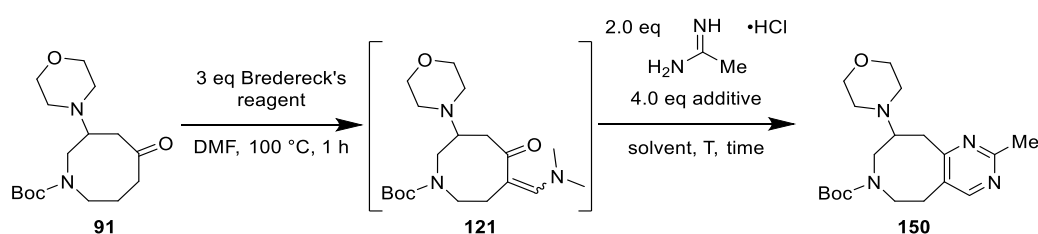
Entry	Additive	Solvent	T (°C)	Time (h)	Outcome
1	NaOMe	MeOH	65 (reflux)	120	Partial conversion to **150**, byproduct/intermediate **148**
2	NaOMe	DMF	100	21	Full consumption of **121**, **148** minor, 21% isolated yield
3	NaOMe	DMF	150	22	Full consumption of **121**, **148** not observed, 20% isolated yield
4	No additive	DMF	100	41	**148** major compound, **150** minor, degradation

[a]Reactions performed on 50 mg scale. Reaction mixtures monitored *via* LCMS analysis.

Given Appell *et al.* reported even lower yields (2%) for their synthesis of pyrimidine **152a** (Scheme 52),[34] no further optimisation was attempted. Since they reported higher yields for the synthesis of phenylpyrimidine **152b** (47%) and aminopyrimidine **152c** (27%),[34] the reaction conditions in DMF (Table 13, Entry 2) were repeated only with benzamidine and guanidine salts.
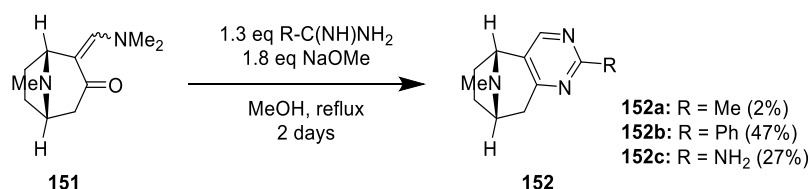
Scheme 52: Fused pyrimidine synthesis reported by Appell et al.[34]

Pleasingly, both phenylpyrimidine **153** and aminopyrimidine **154** were obtained in moderate yields of 48% and 56%, respectively (Scheme 53),[a] indicating that these reagents may be more reactive than acetamidine under the reaction conditions, which is in accordance with analogous 6-6 ring fusion yields reported in the literature.[37–39]
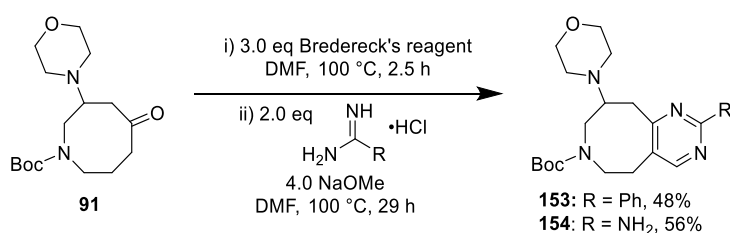
*Scheme 53: Synthesis of 2-phenylpyrimidine **153** and 2-aminopyrimidine **154**, following the optimised conditions (Table 13, Entry 2).*

Appell *et al.* did not report the synthesis of phenylaminopyrimidines (a privileged structure in medicinal chemistry),[40] so a procedure by Spanò *et al.* was followed.[33] Since this paper reported the use of NaOMe (10 eq) with guanidine •HNO_3 (5 eq) to synthesise fused aminopyrimidine **156** but no base with phenylguanidine (3 eq) to afford phenylaminopyrimidine **157**, it was worth trying the synthesis of phenylaminopyrimidine **158** without a large excess of base.[b] This approach provided phenylaminopyrimidine **158** in 50% yield (Scheme 54).

---

[a] An earlier synthesis of aminopyrimidine **154** on smaller scale (0.51 mmol) under analogous reaction conditions yielded 159 mg mass recovery (86%) but was not analytically pure (LCMS analysis showed 94% UV purity, calculated by relative peak integrations).
[b] Phenylguanidine was not in stock at the time of synthesis, so Et_3N was added to the reaction mixture to render the available phenylguanidine •H_2CO_3 as the free base.
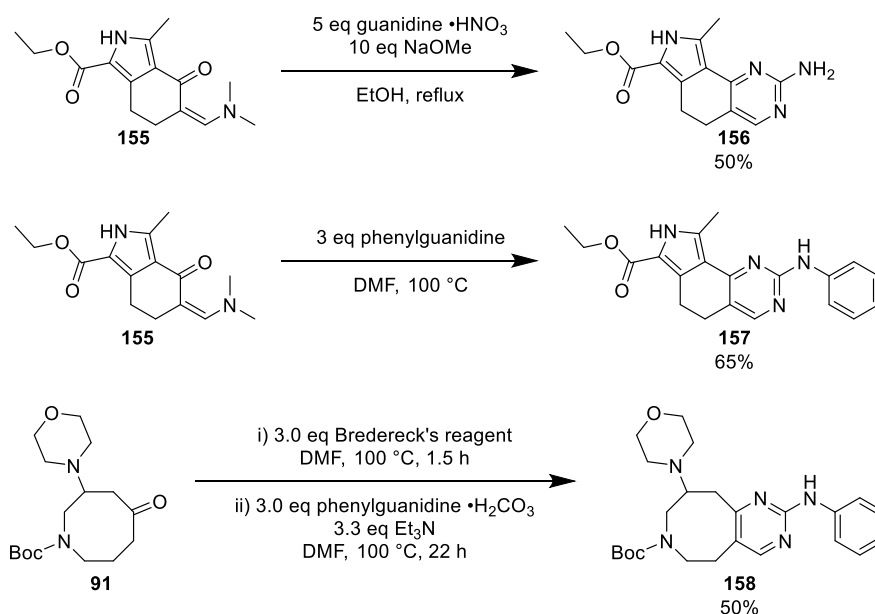
Scheme 54: Synthesis of (phenyl)aminopyrimidines.[33]

5.2. Scaffold validation and library synthesis

Having prepared a series of Boc-protected fused aromatic heterocycles, deprotection and validation of the deprotected compounds as library precursors needed to be performed, to ensure a successful library synthesis.

5.2.1. Building block preparation: Boc deprotection

TFA effected Boc deprotection of the SACE2 building blocks (Scheme 55). Although no issues were reported for these deprotection reactions, conditions were switched to hydrogen chloride in isopropanol since the analytical staff at Symeres were able to determine chloride ion content *via* chromatographic methods (see Experimental Section 13), which allowed for confirmation of the salt multiplicities.
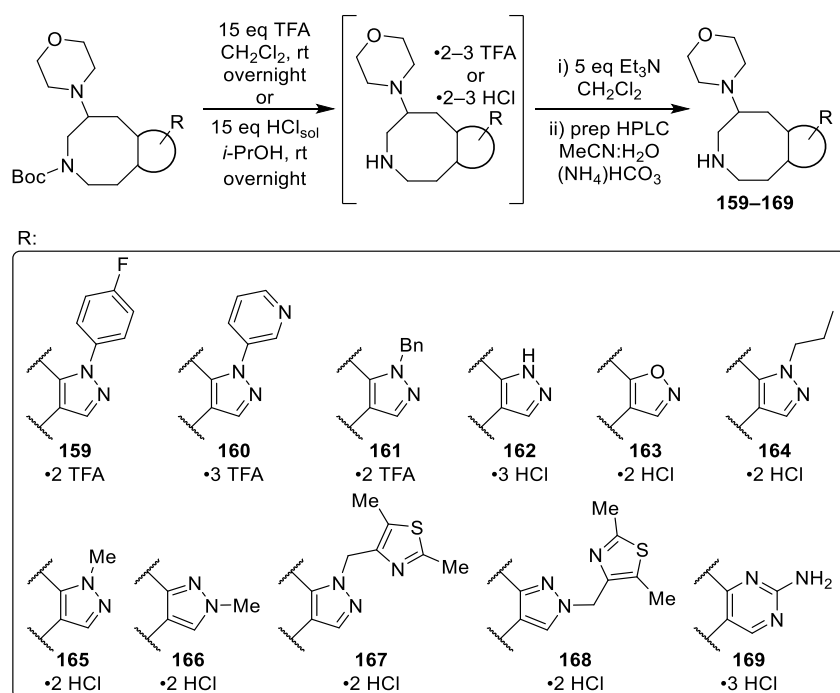
Scheme 55: Boc deprotection of SACE2 building blocks proceeded initially with TFA, but HCl was chosen later to enable determination of chloride ion content.[a]

The crude HCl salt of isoxazole **163** showed a chloride ion content of 2.1 eq per base, while the crude HCl salt of *n*-propyl pyrazole **164** contained 2.6 eq chloride ion per base. These observations were in accordance with the obtained quantitative mass recoveries for the double HCl salts, indicating that the morpholine and deprotected amine were both protonated in these cases. By analogy, the salts of fused heterocyclic analogues **160**, **162** and **169**, which all contained an extra basic nitrogen were reported as triple salts, which was in accordance with their quantitative mass recoveries after deprotection (Scheme 55). Given all eleven Boc-deprotected building blocks showed quantitative mass recoveries based on their experimentally determined (or deduced by analogy) salt multiplicities, all deprotection yields were assumed quantitative.

Although LCMS analysis of the crude salts showed >95% purity (calculated by relative peak integrations, 210–320 nm), ^{1}H-NMR spectroscopic analysis showed baseline impurities. The salts also proved to be poorly soluble in CD$_3$OD and DMSO-d_6. Because of the low SlogP values

---

[a] H-pyrazole **162** is assumed to exist as a mixture of tautomers with the aromatic N*H* proton on both the 1- and 2-position. However, to keep the schemes and figures concise, pyrazole **162** and analogues are drawn as only the 1-*H* tautomer. All deprotection yields are assumed to be quantitative. For yield after prep HPLC step, see Experimental Section 8.4.

calculated for the free amines (–0.2 to 1.4), there was a risk of product loss *via* basic aqueous workup through inefficient extraction (aqueous solubility). Therefore, a more pragmatic approach was followed: a fraction of the crude salt was treated with Et₃N using library synthesis conditions to afford the free base, followed by purification *via* preparative HPLC (MeCN:10 mM (NH₄)HCO₃ in H₂O). In this way, a purified, free-based amine was obtained for characterisation, whilst providing a reference yield for the synthesised library analogues (Scheme 55).

The increased basicity of the unsubstituted pyrazole **162** (3 HCl salt) compared to *N*-Me analogues **165** and **166** (2 HCl salt) (Scheme 55) is in accordance with studies performed by Abboud *et al.* (pK_a pyrazole = 2.48, pK_a *N*-Me pyrazole = 2.06)[41] and can be attributed to the loss of the pyrazole proton upon methylation, which is an active centre for solvation. Upon protonation, the protonated *N*-Me analogues **165** and **166** are thus less stabilised by solvent interactions, which results in decreased basicity (Figure 50).[41,42]
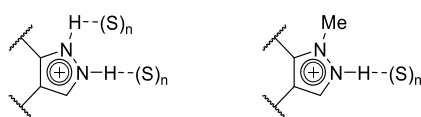
Figure 50: Loss of an active solvation centre could account for the loss of basicity upon N-methylation.[41,42]

5.2.2. Validation set

Synthesis of a validation set of compounds followed the same parallel approach as for the SACE1 validation set (Section 3.5.2, page 65), but with some minor changes. Since DMF was postulated to have played a role in the low-yielding reactions with sulfonyl chlorides during SACE1 library synthesis (Section 3.5.3, Scheme 38), all SACE2 library reactions were performed in CH₂Cl₂, including amide couplings and urea formations.[a] This, however, required evaporation of the chlorinated solvent and re-dissolution in DMSO before submitting the reaction mixtures for preparative HPLC purification, since CH₂Cl₂ was incompatible with the used reverse-phase column conditions. Furthermore, decorations with AcCl were swapped for amide couplings with AcOH, which is less sensitive to trace water and other impurities. Although the yields for mesylation were still low, all other reactions including sulfonylation gave adequate yields, validating the reaction conditions used for parallel library chemistry (Scheme 56).

---

[a] This allowed for the use of one stock solution per building block, otherwise every building block batch would have to be divided for separate DMF and CH₂Cl₂ stock solutions.
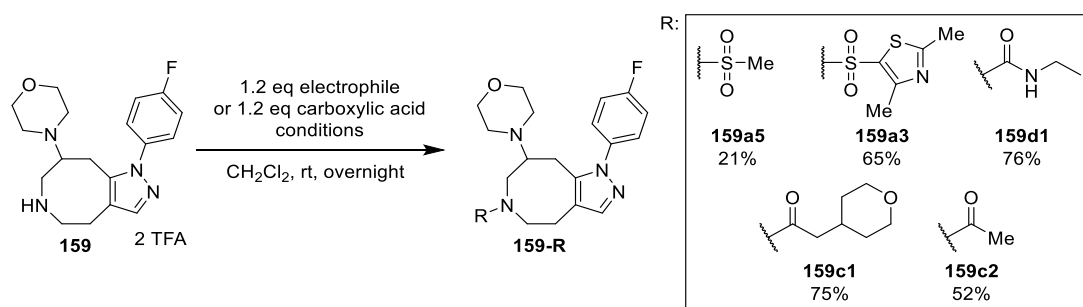
*Scheme 56: Validation chemistry performed on building block **159** •2 TFA. Conditions for sulfonamides and ureas: 5 eq Et₃N; Conditions for amides: 1.2 eq EDC •HCl, 1.2 eq Oxyma Pure, 6.0 eq Et₃N.*

5.2.3.   Reactivity of the H-pyrazole building block

Since the unsubstituted pyrazole **122** was successfully alkylated with dimethylthiazolylmethyl chloride (Scheme 48, page 112), validation of the pyrazole building block **162** •**3 TFA** in particular was necessary to investigate whether the pyrazole moiety would remain un-decorated upon introduction to library synthesis conditions. In a 40 mg scale test reaction, 1.8 eq MsCl was added to building block **162** •**3 TFA** at rt. After 7 min, LCMS analysis of the reaction mixture showed no more starting material and a mixture of the single and doubly mesylated products, with the doubly mesylated product **170** as the major compound[a] (Scheme 57).
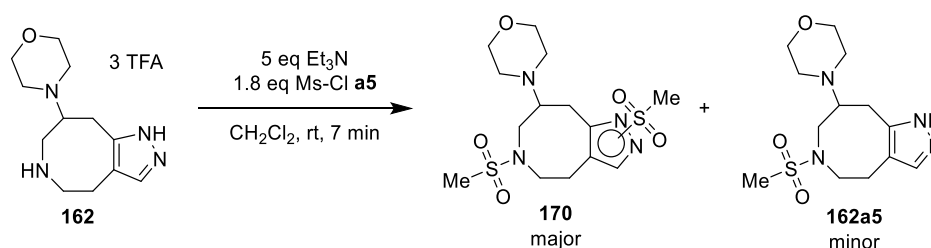
*Scheme 57: Adding an excess of MsCl to pyrazole building block **162** •3 TFA yielded a mixture of singly and doubly mesylated products.*

---

[a] Selected data: LCMS (ESI+): m/z = 393.1. (100%, [M+H]⁺). Observation of a single peak on the LCMS chromatogram supports formation of a single regioisomer, but the structure of the regioisomer was not investigated further.

Konradi *et al.* reported that sulfonylated pyrazole **171** could be selectively hydrolysed (Scheme 58),[43] so this procedure was extended to the crude mixture of pyrazoles **170** and **162a5**.
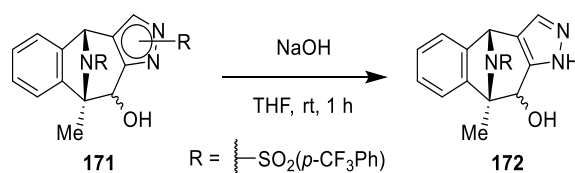
*Scheme 58: Selective hydrolysis of pyrazole **171**, reported by Konradi et al.[43]*

Konradi's selective hydrolysis conditions were indeed applicable to the crude mixture of **170** and **162a5**; LCMS analysis of the reaction mixture showed the absence of the doubly mesylated product **170** after 2 days in a 1:1 volumetric mixture of NaOH (50 wt% in H$_2$O) and THF (Scheme 59). However, the large excess of NaOH (307 eq) would require post-reaction processing before purification by preparative HPLC, so this methodology was not applied to parallel library synthesis.
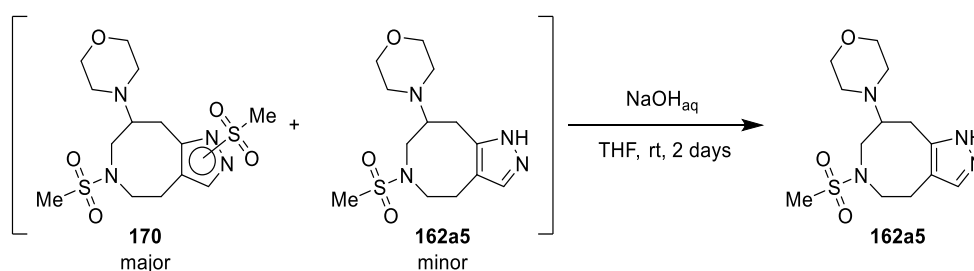
*Scheme 59: Hydrolysis of doubly mesylated compound **170** , applying the conditions by Konradi et al.[43]*

We expected a smaller excess of reagent would decrease the amount of doubly functionalised product, whilst preferentially functionalising the 2° amine. Hence, three parallel validation experiments were set up using 1.2 eq of coupling partner. LCMS analysis of the reaction mixtures still showed the presence of doubly functionalised product (13% for **162a3**, 30% for urea **162d1** and 23 % for **162c1**, based on relative UV peak area), but the monofunctionalised product could be obtained in satisfactory yields (Scheme 60). HMBC cross peaks between the carbonyl carbon and neighbouring ring methylene proton resonances in urea **162d1** and amide **162c1** confirmed preferential functionalisation of the 2° amine.
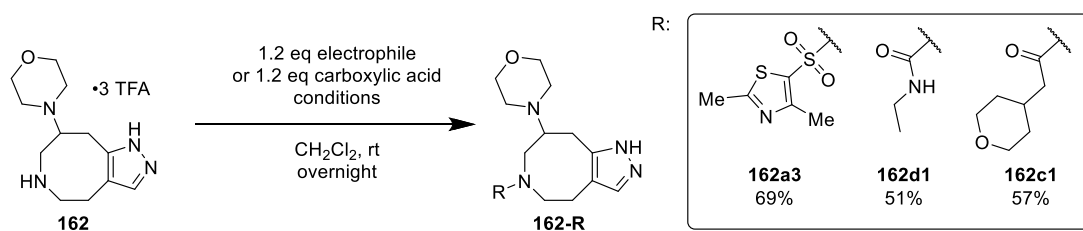
*Scheme 60: Validation chemistry on pyrazole building block **162** using a small excess of reagent. Conditions for **162a3** and **162d1**: 5 eq Et₃N; Conditions for **162c1**: 1.2 eq EDC •HCl, 1.2 eq Oxyma Pure, 6.0 eq Et₃N.*

Since monofunctionalised analogues of pyrazole building block **162** could be obtained in sufficient yields by applying only a small excess of reagent, building block **162** could be used as a valid precursor for the SACE2 library.

5.2.4.   Library synthesis

Having validated the fused heterocycle scaffold as an appropriate precursor for library synthesis, a diverse library could now be synthesised. Following the same *in silico* approach as for the first library (see Section 6), eleven fused heterocyclic building blocks (R^2) were chosen along with eleven R^1-groups, which yielded an 11×11 combinatorial library design (Figure 51).
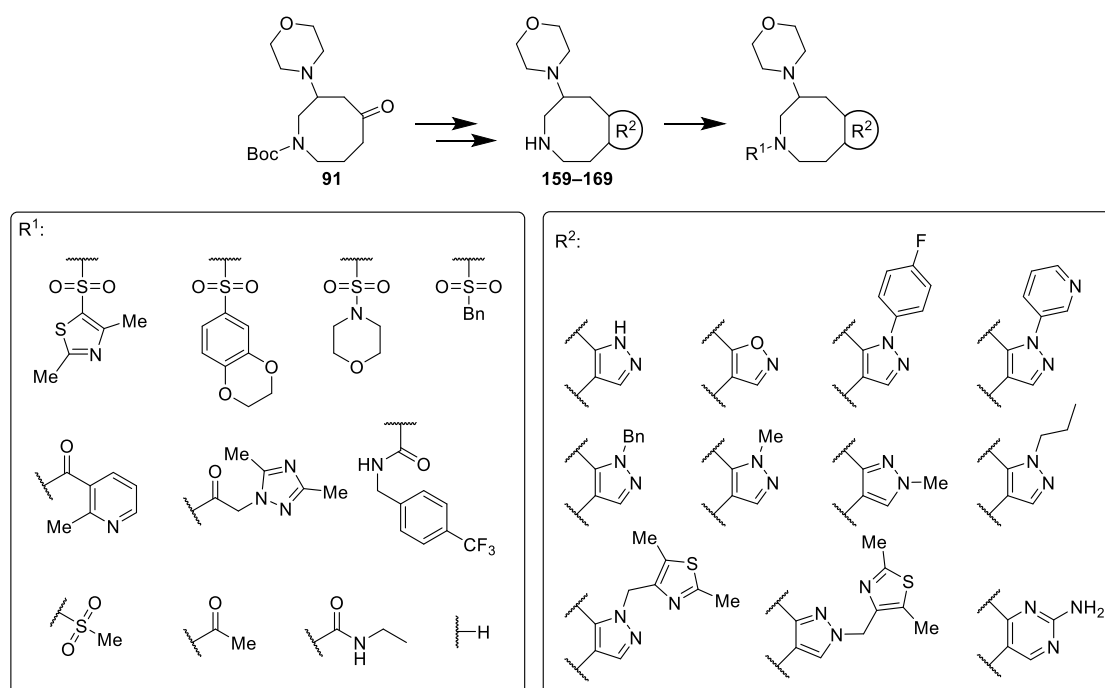
Figure 51: The 11 × 11 SACE2 library design.

In total, 98 parallel reactions were set up,[a] while the 11 Boc-deprotected building blocks were treated with Et$_3$N, purified *via* preparative HPLC and added to the library as well. Pleasingly, all of the parallel experiments were successful (for tabulated yields and purity values, see Experimental Section 9), with the majority of parallel reactions yielding above 40% (65 reactions out of 98). However, 19% of the library compounds (19 out of 98) showed a UV purity <95%, which was comparatively more than for the SACE1 library (4%): eight compounds showed UV purity between 95%–90%, seven between 90%–80% and four below 80%. No clear building block trends were observed for these obtained purities, although only one urea compound out of 20 had a UV purity <95%. In terms of yields, the aminopyrimidine building block **169** •3 HCl gave the lowest-yielding analogues; eight of the ten reactions with aminopyrimidine **169** •3 HCl showed yields below 44%, of which five were below 24%. It is noteworthy that the mass recovery of building block **169** after preparative LC was already only 15% and since all obtained aminopyrimidine analogues were solids, the low yields could be attributed to poor solubility of the compounds under the HPLC conditions (Section 3.5.1.2). Seven of the nine mesylation reactions yielded <35%; reactions with the other sulfonyl chlorides showed no trends. LCMS analysis of the mesylation reaction mixtures showed incomplete conversion of the building blocks before purification, so it is likely that either the sulfene intermediate was less reactive towards the used building blocks or degraded in the reaction,[44] or that the used batch of mesyl chloride was of poor quality. For the amide couplings, reactions with (3,5-dimethyl-[1,2,4]triazol-1-yl)-acetic acid **c3** were consistently lower yielding (<43%), a trend which was also observed for the SACE1 library analogues (see Experimental Section 6).

5.3. Conclusion

The β-ketoenamine intermediate **121** obtained from reaction with Bredereck's reagent allowed rapid access to a variety of fused heterocycles in good yields and short reaction times. Functionalised pyrazoles and isoxazoles were synthesized readily whilst fused pyrimidine syntheses proved to be more challenging and lower yielding. Unfunctionalised pyrazole analogue **122** was alkylated non-regioselectively. For this analogue, validation studies showed that the aliphatic 2° amine reacted preferentially under the library synthesis conditions. Using eleven fused heterocycle analogues as building blocks for library synthesis, 98 library compounds were synthesised in good yields. This demonstrated a successful synthesis of the

---

[a] Not all of the 2 x 11 analogues of the two dimethylthiazolyl building blocks **167** and **168** in the library design were synthesised, because of the limited amount of building block available.

SACE2 library, requiring fewer reaction steps than the SACE1 library and obviating the need for diastereomer separation (Scheme 61).
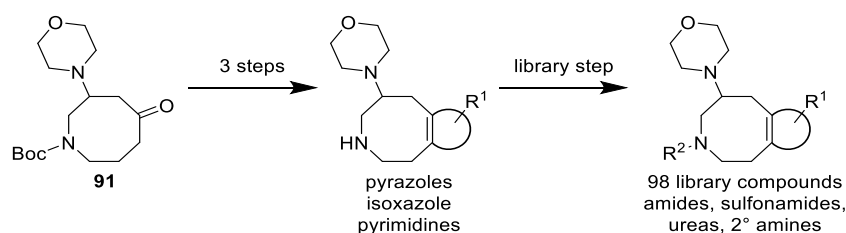
Scheme 61: The SACE2 library synthesis required few steps, yielding various fused heterocyclic analogues.

5.4. References

1   E. P. Gillis, K. J. Eastman, M. D. Hill, D. J. Donnelly and N. A. Meanwell, *J. Med. Chem.*, 2015, **58**, 8315–8359.

2   L. P. Stasi, L. Rovati, R. Artusi, C. BOVINO, F. Colace and S. Mandelli, 4,4-difluoro-piperidine-compounds, WO2013127913A1, 2013.

3   G. S. Lal, G. P. Pez, R. J. Pesaresi, F. M. Prozonic and H. Cheng, *J. Org. Chem.*, 1999, **64**, 7048–7054.

4   K. Miura and Y. Nishikimi, Dihydro Pyrroloquinoline Derivatives, US2011112133 (A1), 2011.

5   P. Bhutani, G. Joshi, N. Raja, N. Bachhav, P. K. Rajanna, H. Bhutani, A. T. Paul and R. Kumar, *J. Med. Chem.*, 2021, **64**, 2339–2381.

6   S. Han, J. Thatte, D. J. Buzard and R. M. Jones, *J. Med. Chem.*, 2013, **56**, 8224–8256.

7   P. Lazzari, R. Distinto, I. Manca, G. Baillie, G. Murineddu, M. Pira, M. Falzoi, M. Sani, P. Morales, R. Ross, M. Zanda, N. Jagerovic *et al.*, *Eur. J. Med. Chem.*, 2016, **121**, 194–208.

8   S. Guo, Y. Song, Q. Huang, H. Yuan, B. Wan, Y. Wang, R. He, M. G. Beconi, S. G. Franzblau and A. P. Kozikowski, *J. Med. Chem.*, 2010, **53**, 649–659.

9   X. Wang, E. Bai, H. Zhou, S. Sha, H. Miao, Y. Qin, Z. Liu, J. Wang, H. Zhang, M. Lei, J. Liu, O. Hai *et al.*, *Bioorg. Med. Chem.*, 2019, **27**, 533–544.

10   D. L. Mobley and K. A. Dill, *Structure*, 2009, **17**, 489–498.

11   F. Peccati and G. Jiménez-Osés, *ACS Omega*, 2021, **6**, 11122–11130.

12   C. P. Sager, B. Fiege, P. Zihlmann, R. Vannam, S. Rabbani, R. P. Jakob, R. C. Preston, A. Zalewski, T. Maier, M. W. Peczuh and B. Ernst, *Chem. Sci.*, 2018, **9**, 646–654.

13   A. W. Erian, S. M. Sherif and H. M. Gaber, *Molecules*, 2003, **8**, 793–865.

14   B. Mohan Reddy, V. Venkata Ramana Kumar, N. Chinna Gangi Reddy and S. Mahender Rao, *Chin. Chem. Lett.*, 2014, **25**, 179–182.

15   H. Quast, C. Becker, E. Geißler, K. Knoll, E.-M. Peters, K. Peters and H. G. von Schnering, *Liebigs Ann. Chem.*, 1994, **1994**, 109–120.

16   F. A. Abu-Shanab, S. M. Sherif and S. A. S. Mousa, *J. Heterocycl. Chem.*, 2009, **46**, 801–827.

17   G. B. Rosso, *Synlett*, 2006, **2006**, 809–810.

18   K. A. Ali, H. M. Hosni, E. A. Ragab and S. I. A. El-Moez, *Arch. Pharm.*, 2012, **345**, 231–239.

19   K. Wang, Y.-C. Wu, J.-C. Yang, M.-H. Zhang, M. El-Shazly, D.-Y. Zhang and X.-M. Wu, *Synthesis*, 2016, **48**, 2245–2254.

20   E. Fischer and F. Jourdan, *Chem. Ber.*, 1883, **16**, 2241–2245.

21   E. Fischer and O. Hess, *Chem. Ber.*, 1884, **17**, 559–568.

22   D. N. Deaton, C. D. Haffner, B. R. Henke, M. R. Jeune, B. G. Shearer, E. L. Stewart, J. D. Stuart and J. C. Ulrich, *Bioorg. Med. Chem.*, 2018, **26**, 2107–2150.

23   H. Imura and N. Takada, Method for Producing Pyrazole Compound, JP2013006780 (A), 2013.

24   H. Chu, B. A. Z. Gonzalez, H. Guo, X. Han, L. Jiang, J. Li, M. L. Mitchell, H.-J. Pyun, S. D. Schroeder, G. M. Schwarzwalder, N. D. Shapiro, D. M. Shivakumar *et al.*, Bridged Tricyclic Carbamoylpyridone Compounds and Their Pharmaceutical Use, WO2020197991 (A1), 2020.

25   J.-P. Salvador, F. Sánchez-Baeza and M.-P. Marco, *Anal. Biochem.*, 2008, **376**, 221–228.

26   N. Kratena, V. Enev, G. Gmeiner and P. Gärtner, *Monatsh. Chem.*, 2019, **150**, 843–848.

27   S. Casati, R. Ottria and P. Ciuffreda, *Molecules*, 2020, **25**, 2019.

28   S.-P. Hong, K. G. Liu, G. Ma, M. Sabio, M. A. Uberti, M. D. Bacolod, J. Peterson, Z. Z. Zou, A. J. Robichaud and D. Doller, *J. Med. Chem.*, 2011, **54**, 5070–5081.

29   P. Barraja, V. Spanò, D. Giallombardo, P. Diana, A. Montalbano, A. Carbone, B. Parrino and G. Cirrincione, *Tetrahedron*, 2013, **69**, 6474–6477.

30   T. A. Farghaly, N. A. Abdel Hafez, E. A. Ragab, H. M. Awad and M. M. Abdalla, *Eur. J. Med. Chem.*, 2010, **45**, 492–500.

31   E. I. Al-Afaleq, *Synth. Commun.*, 2000, **30**, 1985–1989.

32   L. Peterlin-Mašič, G. Mlinšek, T. Šolmajer, A. Trampuš-Bakija, M. Stegnar and D. Kikelj, *Bioorg. Med. Chem. Lett.*, 2003, **13**, 789–794.

33   V. Spanò, A. Montalbano, A. Carbone, B. Parrino, P. Diana, G. Cirrincione, I. Castagliuolo, P. Brun, O.-G. Issinger, S. Tisi, I. Primac, D. Vedaldi *et al.*, *Eur. J. Med. Chem.*, 2014, **74**, 340–357.

34   M. Appell, W. J. Dunn, M. E. A. Reith, L. Miller and J. L. Flippen-Anderson, *Bioorg. Med. Chem.*, 2002, **10**, 1197–1206.

35   X. Jiang, I. Dulubova, S. A. Reisman, M. Hotema, C.-Y. I. Lee, L. Liu, L. McCauley, I. Trevino, D. A. Ferguson, Y. Eken, A. K. Wilson, W. C. Wigley *et al.*, *Bioorg. Med. Chem. Lett.*, 2020, **30**, 126967.

36   A. P. Kozikowski, G. Campiani, V. Nacci, A. Sega, A. Saxena and B. P. Doctor, *J. Chem. Soc., Perkin Trans. 1*, 1996, 1287.

37   Y. Zhang, W. Yuan, X. Wang, H. Zhang, Y. Sun, X. Zhang and Y. Zhao, *Med. Chem. Commun.*, 2018, **9**, 1910–1919.

38   S. Ananthan, H. S. Kezar, R. L. Carter, S. K. Saini, K. C. Rice, J. L. Wells, P. Davis, H. Xu, C. M. Dersch, E. J. Bilsky, F. Porreca and R. B. Rothman, *J. Med. Chem.*, 1999, **42**, 3527–3538.

39   L. Herrera, H. Feist, M. Michalik, J. Quincoces and K. Peseke, *Carbohydr. Res.*, 2003, **338**, 293–298.

40   L. C. F. Pimentel, A. C. Cunha, L. V. B. Hoelz, H. F. Canzian, D. I. L. F. Marinho, N. Boechat and M. M. Bastos, *Curr. Top. Med. Chem.*, **20**, 227–243.

41   J. L. M. Abboud, P. Cabildo, T. Canada, J. Catalan, R. M. Claramunt, J. L. G. De Paz, J. Elguero, H. Homan and R. Notario, *J. Org. Chem.*, 1992, **57**, 3938–3946.

42   J. Catalan, P. Cabildo, J. Elguero, J. Gómez and J. Laynez, *J. Phys. Org. Chem.*, 1989, **2**, 646–652.

43   A. W. Konradi, X. M. Ye, S. Bowers, A. W. Garofalo, D. L. Aubele, D. Dressen, R. Ng, G. Probst, C. M. Semko, M. Sun, A. P. Truong and M. S. Dappen, *N*-sulfonamido polycyclic pyrazolyl compounds, US8283358B2, 2012.

44   W. E. Truce, R. W. Campbell and J. R. Norell, *J. Am. Chem. Soc.*, 1964, **86**, 288.

6. SACE2 library design

With the primary amine of the SACE1 scaffold decorated and a telescoped pyrazole synthesis deemed less amenable to parallel synthesis, the secondary amine on the eight-membered ring was considered an attractive point of diversity for the synthesis of the second library (Figure 52).

SACE1
library step on 1° amine

SACE2
library step on 2° amine
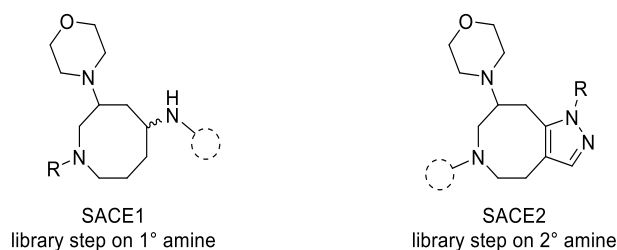
Figure 52: Parallel synthesis performed on the SACE1 scaffold and planned on the SACE2 scaffold.

In silico design of the SACE2 library proceeded in four phases (Figure 53). Analogous to the SACE1 library, KNIME and DataWarrior were used in phases 1 and 2 to generate an initial set of seven fused pyrazole building blocks (prior to their synthesis) and eleven reagents were used for functionalisation of the 2° amine, yielding a 7 × 11 library design. Whereas phase 1 informed which building blocks to synthesise, phases 3 and 4 started from a set of already synthesised five- and six-membered fused heterocycle analogue building blocks; KNIME and DataWarrior were then used to assess the added value of these analogues, when functionalised with the same reagent set. This approach provided an 11 × 11 *in silico* library, in which eleven building blocks were combinatorially reacted with eleven reagents.
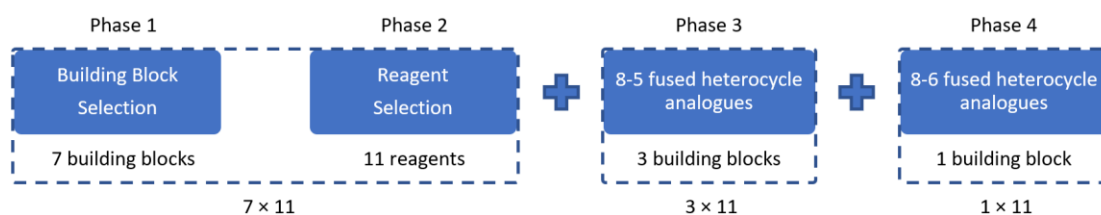
Figure 53: Followed workflow to establish the 11 × 11 SACE2 virtual library.

6.1. Phase 1: building block selection

Before enumerating the secondary amine, appropriate hydrazine reagents needed to be selected in order to provide the library with a diverse set of pyrazole building blocks. Analogous to the reagent selection described in Section 4.5 (page 86), an *N*-acyl capped morpholino-azocine was enumerated using all 104 hydrazines present in the Symeres database, yielding 104 fused pyrazoles built on a simple, *N*-functionalised eight-membered ring.[a] The resulting pyrazoles were filtered for molecular weight (MW < 450),[b] leading to a subset of 98 compounds. Two selections of 10 representative compounds were made using the DataWarrior 'select diverse set' algorithm and the DataWarrior clustering algorithm. As expected, both algorithms did not fully cover the same ranges and areas as the enumerated library in terms of MW, SlogP and shape space, given the small sample size of the selection; however, both selections yielded heteroaromatic, aromatic carbocyclic, benzylic and aliphatic R-groups, as well as the free pyrazole moiety (see Appendix 3.1). With experienced chemists often choosing their substrate scope or building blocks to cover all of these categories, the outcome of the selection algorithms gave us confidence to do the same. A selection of five hydrazines was chosen manually (Figure 54), representing all five R-group types. *N*-Methyl pyrazole was added to the list, as literature precedent has shown that methylhydrazine does not always form pyrazoles regioselectively.[1] Should the regioisomers be separable (confirmed in Section 5.1.3, page 109), both would yield interesting building blocks for a future library.
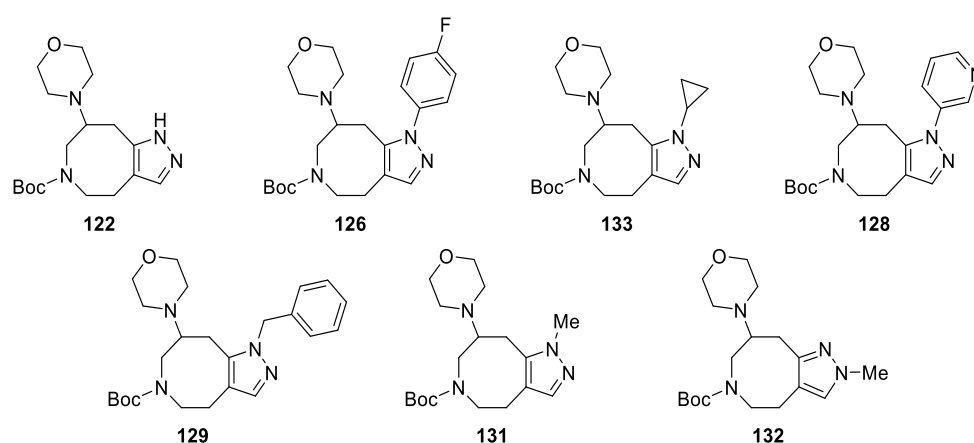
Figure 54: Selection of pyrazole building blocks.

---

[a] Acknowledging that the SACE2 scaffold could have been used for this enumeration, the core scaffold was not expected to influence the hydrazine selection, since it was not variable in the enumerated pyrazole library. The *N*-acyl functionalisation was chosen as an exemplar 2° amine functionalisation, common in compound screening sets.
[b] Accounting for the MW of large substituents on the 2° amine, this threshold was chosen to prevent *N*-functionalised final compounds from excessively exceeding the MW = 600 Da threshold set in Section 4.2.

6.2.   Phase 2: reagent selection and initial 7 × 11 design

With an initial selection of seven building blocks in hand, library design now followed the workflow established in Section 4. Using the same reagent pool used for the first library, the seven building blocks were enumerated with sulfonyl chlorides, isocyanates and carboxylic acids. Reductive alkylations and S_NAr reactions were not attractive since introduction of an extra basic amine was thought to increase the chances of potential hERG inhibition, which is not desired and is an important flag during early toxicology studies.[a] The resulting enumerated library consisted of 336 compounds of sulfonamides, amides and ureas, with 236 < MW < 578 Da and −1.1 < SlogP < 5.8. Given these ranges were within the cutoff ranges defined in Section 4, no extra filters were applied. Since this enumerated library consisted of 7 × 48 compounds, compared to the combinatorial 51 × 51 library enumerated for our first scaffold (Section 4.6), a smaller enumeration size allowed for a smaller representative diverse selection. Even a diverse selection of 100 compounds provided a representative selection for the enumerated library (Figure 55). Hence, the diverse selection of 100 compounds was used for R-group comparison.
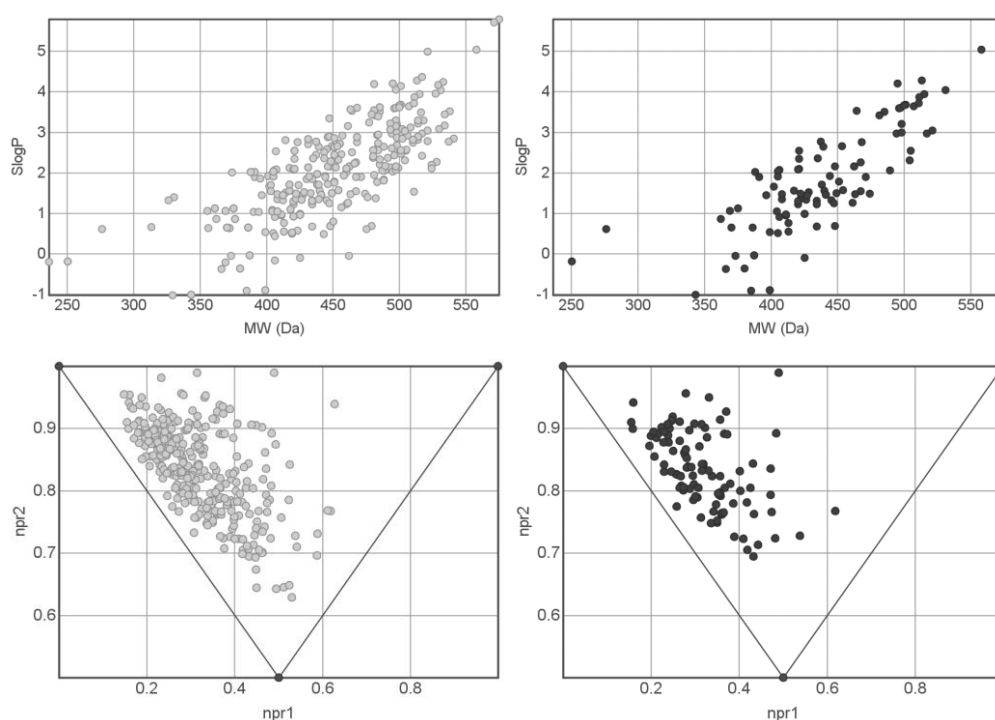
Figure 55: A diverse selection of 100 compounds (black) provided a representative selection for the enumerated library (7 × 48 compounds, grey).

---

[a] For a detailed discussion of hERG inhibition, see Section 8.3.3.

Since the *N*-Me pyrazole building blocks had not yet been synthesised at the time of library design and their successful synthesis and separation not yet guaranteed, a separate 100-compound diverse selection was made from a subset of the enumerated library without the two *N*-Me pyrazole building blocks. Comparing the most often recurring R-groups between both selections showed great overlap, which gave us confidence to base the R-group selection on the diverse selection without *N*-Me pyrazole building blocks. From the most recurring R-groups (15 R-groups, see Appendix 3.2) in this set, seven R-groups were chosen for the virtual library, reflecting the functional group diversity of the set, ensuring the presence of aliphatic, heteroaromatic and aromatic carboxylic R-groups. An acetyl, mesyl, ethylurea and unfunctionalised 2° amine moiety were added to this set. This resulted in a 7 × 11 virtual library, which combined a very good coverage of the descriptor space defined by the 7 × 48 initial enumeration with low MW/SlogP/TPSA coverage, governed by the addition of the small R-groups (Figure 56).
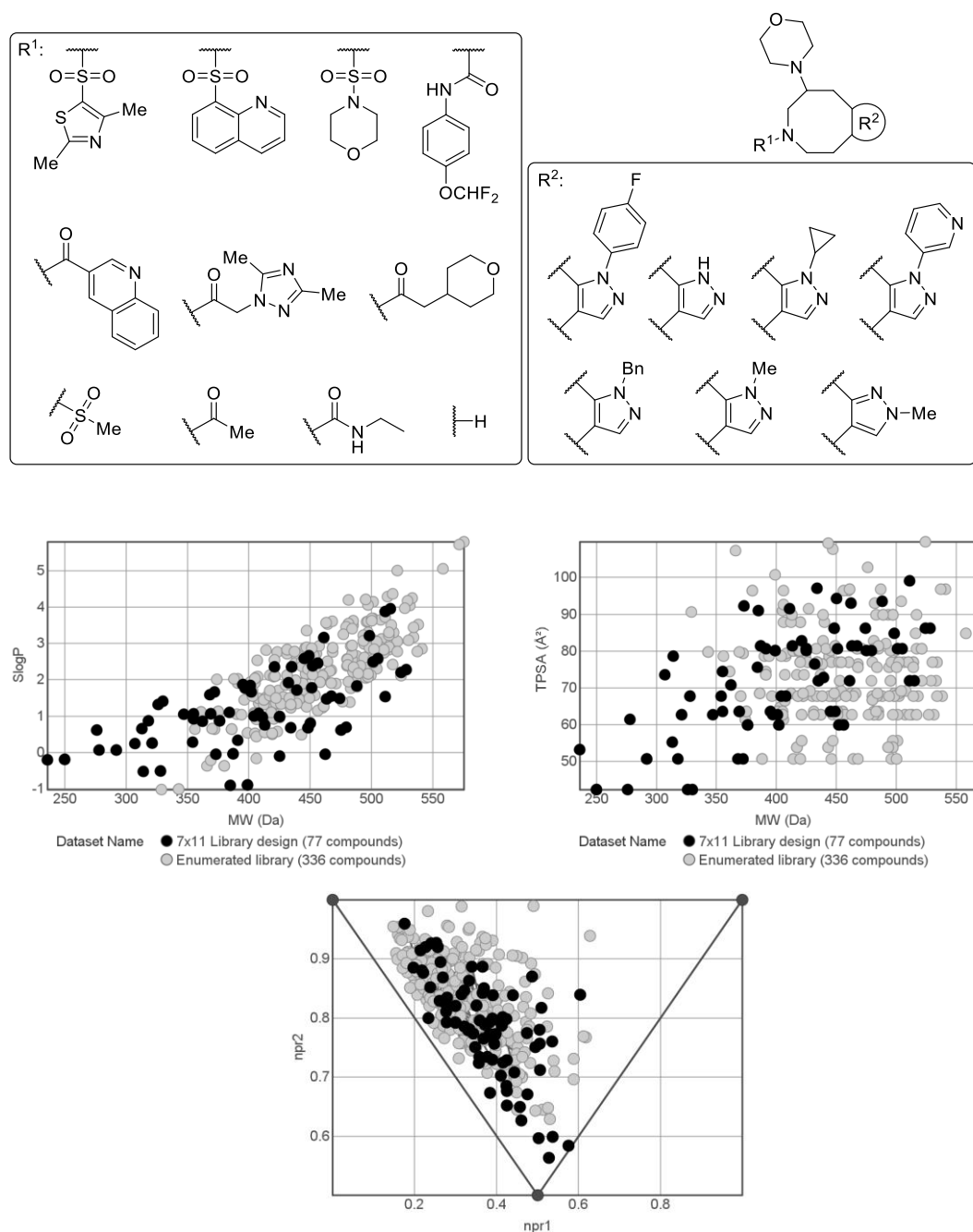
Figure 56: Analysis of the 7 × 11 pyrazole library in chemical descriptor space covered by the 7 × 48 enumerated library.

As was observed in the SACE1 library, introduction of the small R-groups resulted in a bias for low MW compounds, but the 7 × 11 library nevertheless gave a relatively better coverage of the enumerated descriptor space in comparison to the SACE1 library. This can be attributed to the fact that the 7 × 11 library still contains 7 × 7 compounds (no acetamides, Ms-amines, ethylureas and 2° amines) which are also members of the 7 × 48 enumerated library, while the 2 × 3 × 10 SACE1 library contains no members of the 51 × 51 enumerated libraries, after only allowing small R-groups for building block synthesis in the last iteration (Section 4.6.2). In a final

iteration, the cyclopropyl pyrazole was swapped with the *n*-propyl pyrazole in the 7 × 11 library, given synthesis of the *n*-propyl pyrazole proved to be more reliable than its cyclopropyl analogue (see Section 5.1.3, page 109). This change had little impact on the covered descriptor space.

6.3.   Phase 3: 3 × 11 expansion with analogous 8-5 fused heterocycles

Once the synthesis and scale-up of isoxazole **135** and thiazole-functionalised pyrazoles **143** and **144** had been established (see Section 5.1.4, page 112), the library design was extended to 10 × 11, decorating the three new building blocks with the same set of 11 reagents (Figure 57).
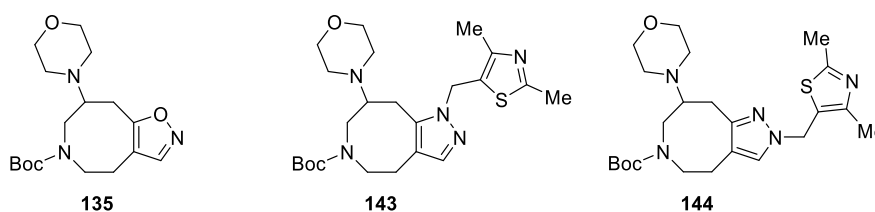
Figure 57: The 3 × 11 library expansion protected building blocks, encompassing isoxazole and dimethylthiazolyl analogues.

Analysis of the descriptor space covered by the 3 × 11 library expansion showed that most of the occupied space was already covered by the 7 × 11 library. Worth noting is that the 2-dimethylthiazolyl subset yielded significantly flatter molecules than its 1-dimethylthiazolyl analogous subset (Figure 58). Despite the apparent redundancy in terms of descriptor space shown below (Figure 58), the 3 × 11 library expansion was still considered a valuable addition to the 7 × 11 library: although the free pyrazole and isoxazole subsets yield similar MW/SlogP/TPSA values and occupy similar shape space, the isoxazole moiety swaps a H-bond donor for a H-bond acceptor compared to the free pyrazole, which could play an essential role in key interactions with potential targets. Furthermore, the 2-dimethylthiazolyl subset, albeit relatively flat, shows a significantly different skeletal structure compared to the other entries. Although the 2-Me subset also occupied the 2-position on the pyrazole, the 2-dimethylthiazolyl moiety extends further away from the pyrazole, probing different 3D-space. Hence, the 3 × 11 library expansion was added to the 7 × 11 library, yielding a 10 × 11 library.
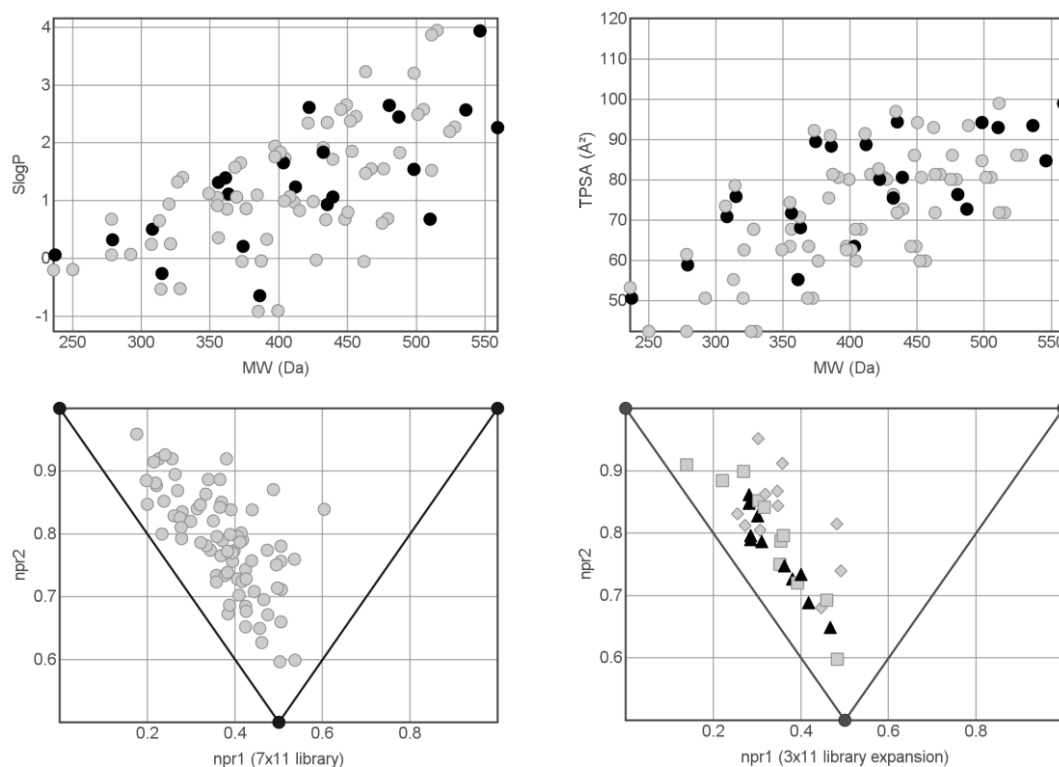
Figure 58: Top: Analysis of the 3 × 11 library expansion (black) and comparison with the 7 × 11 library (grey). Bottom left: PMI analysis of the 7 × 11 library. Bottom right: PMI analysis of the 2-dimethylthiazolyl subset (▲), isoxazole subset (■) and 1-dimethylthiazolyl subset (◆).

6.4. Phase 4: 8-6 fused pyrimidine subset

With only modest yields obtained in the synthesis of the 8-6 fused pyrimidine building blocks **150**, **153**, **154** and **158** (see Section 5.1.5, page 113), plenty of possibilities for diversification of enone parent scaffold **29** and only a limited amount of research time left, we considered whether adding fused pyrimidine entries to the existing virtual library would add significant value. Therefore, *in silico* analysis of three 8-6 fused pyrimidine subsets and comparison with the 10 × 11 library was performed, to inform whether an 8-6 fused pyrimidine subset was worth the synthetic effort.
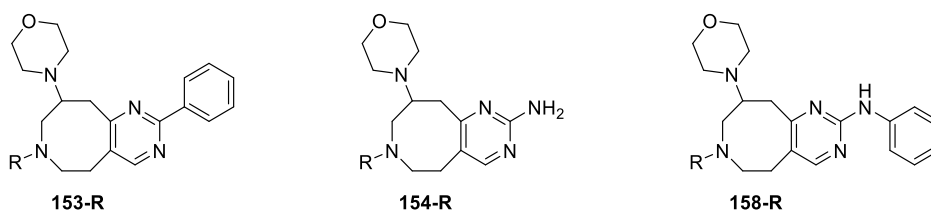
Figure 59: Three 8-6 fused pyrimidine subsets were analysed and compared against the 10 × 11 library.

Considering MW, SlogP and shape space, the 8-6 subset did not cover any space, not already covered by the 10 × 11 library. Interestingly, the 8-6 subset produced mainly rod-disk-like compounds, occupying a shape space which was already covered by the 2-dimethylthiazolyl subset (Figure 58). Furthermore, the aminopyrimidine subset occupied a lower SlogP space, while both phenylpyrimidine and phenylaminopyrimidine subsets showed coverage of a higher SlogP space (Figure 60). On this basis, the 8-6 fused pyrimidines would not add much value to the existing virtual library in terms of MW/SlogP/shape space coverage.
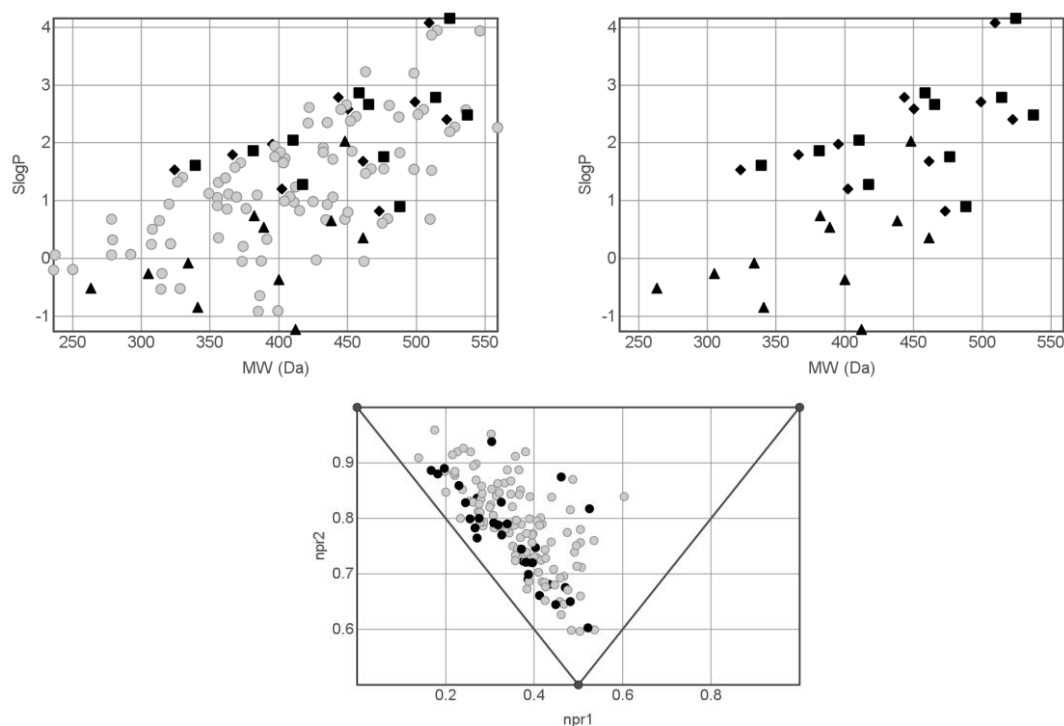
Figure 60: The 8-6 fused pyrimidine subset (black) resided in a MW/SlogP/TPSA and shape space which was covered already by the current 10 × 11 library (grey). The aminopyrimidine subset (▲) occupied a lower SlogP space than the phenylpyrimidines (◆) and phenylaminopyrimidines (■).

However, the aminopyrimidines did cover a unique MW/TPSA space, which wasn't explored by the 10 × 11 library (Figure 61). Given the TPSA cutoff for brain penetration has been reported to be 90 Å²,[2] the nine aminopyrimidines with TPSA > 90 Å² could display different BBB penetration properties, compared to the majority of the 10 × 11 library (TPSA < 90 Å²). Therefore, the aminopyrimidine was considered a valuable addition to the virtual library, while the other two pyrimidine subsets were not pursued.
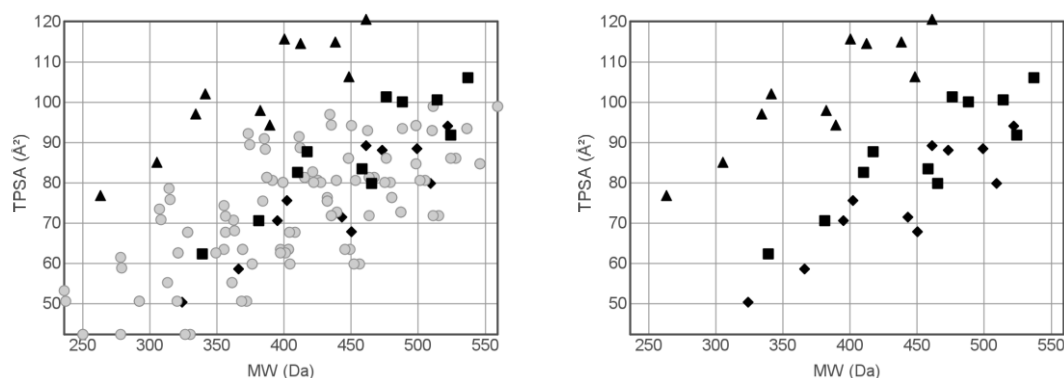
Figure 61: MW/TPSA analysis of the 8-6 pyrimidine subset. The aminopyrimidine (▲) showed coverage of a unique MW/TPSA space, while the phenylpyrimidine (◆) and phenylaminopyrimidine (■) covered space which was already occupied by the current 10 × 11 library.

The final SACE2 virtual library thus consisted of 11 building blocks, with each subset adding specific value to the library in terms of descriptor space, H-bond donors or acceptors, moiety diversity and skeletal diversity. In terms of MW/SlogP/TPSA space, the resulting library achieved a good distribution, covering almost three SlogP units and 30 — 60 Å² TPSA for every MW range of 50 Da (> 300 Da) (Figure 62). PMI analysis of the virtual library showed a satisfying amount of more sphere-like compounds, with no occupation of the flat rod-disk line. Although this library of 121 compounds may contribute almost insignificantly to the overall bias for flat drug molecules in massive drug molecule databases, it does show that it is possible to steer away from synthesising flat molecules.[3,4]

Figure 62: The final 11 × 11 fused heterocycle library. Grey boxes highlight the broad SlogP/TPSA ranges obtained within a small MW range (50 Da).

6.5.   Conclusion

Overall, the quick generation of building blocks facilitated by the efficient telescoped synthesis of fused aromatic heterocycles allowed for a more 2D-combinatorial library profile compared to the SACE1 library. Given that every building block could be synthesised easily and assessed quickly in DataWarrior, the library could be built incrementally, increasing chemical space coverage with every new introduced building block. Since it had been shown that adding extra building blocks to the set did not significantly increase the descriptor space coverage, the library was deemed to have arrived at a sufficient size, having probed a broad range of numerical descriptor space with a diverse set of chemical moieties.

6.6.   References

1   D. N. Deaton, C. D. Haffner, B. R. Henke, M. R. Jeune, B. G. Shearer, E. L. Stewart, J. D. Stuart and J. C. Ulrich, *Bioorg. Med. Chem.*, 2018, **26**, 2107–2150.
2   H. van de Waterbeemd, G. Camenisch, G. Folkers, J. R. Chretien and O. A. Raevsky, *J. Drug Target.*, 1998, **6**, 151–165.
3   D. G. Brown and J. Boström, *J. Med. Chem.*, 2016, **59**, 4443–4458.
4   F. Lovering, J. Bikker and C. Humblet, *J. Med. Chem.*, 2009, **52**, 6752–6756.

7. SACE3 library

Having performed library synthesis using both the secondary amine (SACE2, see Section 5) and the ketone of precursor **93** (after functional group conversion to a 1° amine, SACE1, see Section 3), we considered using the alkene of parent scaffold **29** to install a diversification site, amenable to parallel synthesis (Figure 63). Introducing a fused aromatic heterocycle in the SACE2 series had reduced the average Fsp^3 of the resulting compound library.[a] The SACE3 series aimed to reconcile conformational restriction whilst retaining high Fsp^3, just as sp^3-bridged and fused rings are found in many biologically active natural products.[1] Once again, we envisaged scaffold synthesis would focus on highly stereoselective transformations to avoid difficulties with diastereomer separation and characterisation, as was experienced for the SACE1 series. A 1,3-dipolar cycloaddition on the enone functionality embedded in **29** satisfied all criteria, as it would install an extra point of diversity in a stereoselective fashion, whilst conformationally restricting the eight-membered ring without any loss in Fsp^3 (Figure 63). Pyrrolidine *cis* ring fusion was also expected to control the stereoselectivity of subsequent functional group conversion of the resulting ketone, allowing for stereoselective installation of R^3-groups. The envisioned 1,3-dipolar cycloaddition would also deliver a different scaffold shape, further expanding our exploration of chemical space. To our knowledge, the envisioned pyrrolo[3,4-*c*]azocine scaffold structure has not been reported in the literature.[b]
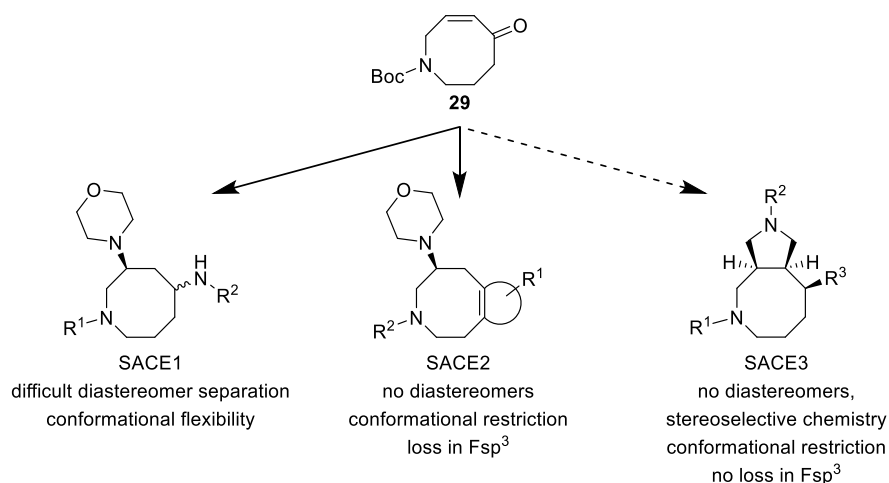
Figure 63: The SACE3 series aimed to reconcile conformational restriction with high Fsp³, using stereoselective chemistry to avoid difficult diastereomer separation.

---

[a] Average Fsp^3 of SACE1 library: 0.80. Average Fsp^3 of SACE2 library: 0.63.
[b] A Reaxys search performed on 16-03-2022 yielded no matches.

7.1. Fused pyrrolidine synthesis *via* 1,3-dipolar cycloaddition

The pyrrolidine ring is a common structural motif in drug molecules; two comparative studies of FDA-approved pharmaceuticals in 2014 by Taylor *et al.* and the Njardarson group found pyrrolidine to be the fifth most commonly used nitrogen heterocycle[2,3] and the eighth most frequently recurring ring structure.[3] Among these bioactive pyrrolidines are various fused pyrrolidine bicycles, such as telaprevir **173**,[4] moxifloxacin **174**[5] and seltorexant **175** (Figure 64).[6–8]

173
telaprevir
hepatitis C drug

174
moxifloxacin
antibacterial agent

175
seltorexant
anti-insomnia, antidepressant
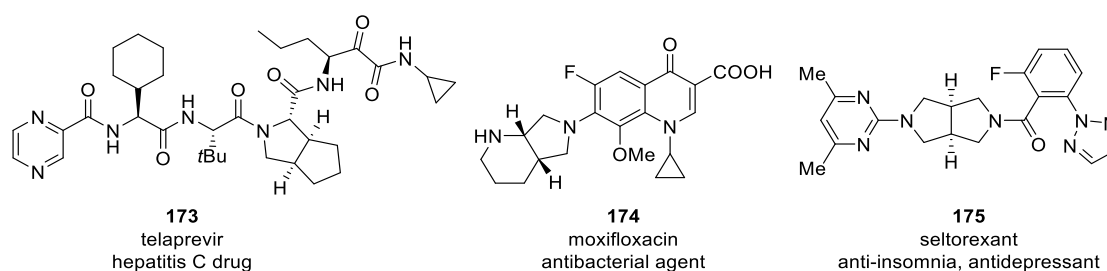
Figure 64: Examples of bioactive fused pyrrolidines.[4–8]

Fused pyrrolidines can be obtained *via* 1,3-dipolar cycloadditions using azomethine ylides, such as symmetrical ylide **177** (Scheme 62). By definition, these [3+2] cycloadditions proceed *via* a concerted reaction mechanism, which yields the *syn*-adduct specifically.[9a] A commonly used ylide precursor for pyrrolidine synthesis is *N*-methoxymethyl-*N*-(trimethylsilylmethyl) benzylamine **176** (Scheme 62), which forms ylide **177** in the presence of catalysts like TFA, ZnCl$_2$ and LiF.[11–13] Ylide **177** was an attractive dipole for a [3+2] cycloaddition, since its symmetry would avoid possible regioselectivity issues.[14] An example of its use can be found in the total synthesis of conessine **180**, an alkaloid natural product used in the treatment of dysentery (Scheme 62).[15] During this synthesis, a [3+2] cycloaddition allowed the installation of the stereochemistry of C-1 in the conessine **180** framework in s*yn*-adduct **179**. Presumably because of a steric clash with the Me and *i*-Pr moieties on the convex side, the azomethine ylide **177** approached fused lactam **178** predominantly on the concave side, (15:1 *anti*:*syn* relative to Me), yielding a diastereomeric mixture which was readily separated *via* column chromatography.[15] In our parent scaffold **29**, facial selectivity was not relevant as enone **29** contains no stereocentres, and *syn* addition of symmetrical ylide **177** was thus expected to yield a racemic mixture of cycloadducts.

---

[a] There are examples of stepwise and therefore non-stereospecific formal 1,3-dipolar cycloadditions,[9,10] but these examples lie beyond the scope of this thesis.
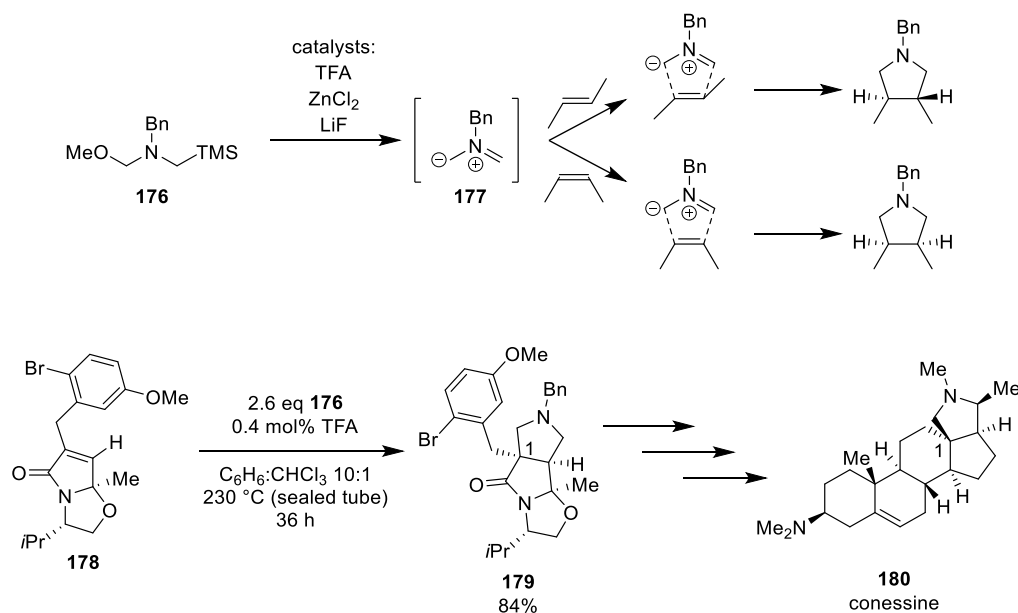
*Scheme 62: 1,3-dipolar cycloadditions using ylide precursor **176**. This reagent was used in the total synthesis of conessine **180**.[15]*

1,3-Dipolar cycloaddition on enone **29**, using symmetrical ylide **177** was thus considered an attractive route towards our final scaffold and SACE3 library. In order to provide a robust synthesis, the stereoselectivity of the 1,3-dipolar cycloaddition and subsequent reactions was a key criterion for successful scaffold synthesis. With this in mind, we investigated the synthetic route towards our envisioned 5-8 fused pyrrolidine analogues.

7.1.1.   5-8 fused pyrrolidines: reaction optimisation and epimerisation

Using established Symeres in-house reaction conditions based on work by Terao *et al.*,[12] enone **29** was reacted with ylide precursor **176**. A test reaction on 100 mg scale using 1.1 eq of ylide precursor **176** and 0.1 eq TFA resulted in incomplete conversion to fused pyrrolidine **181** after 6 h. This was evidenced by ^{1}H-NMR spectroscopic analysis of the crude mixture after workup, which showed the presence of enone **29** and desired pyrrolidine **181** as a 1:1 mixture. A subsequent reaction, performed on 5.5 mmol scale, using 2.0 eq of ylide precursor **176**, led to full conversion of enone **29** after 28 h. The target cycloaddition product, *cis*-**181** was observed *via* TLC and LCMS analysis of the reaction mixture; however, chromatographic purification (heptane:EtOAc) of the crude product after aqueous workup yielded a mixture of *cis*-**181** and *trans*-**181** diastereoisomers (82% combined yield) in a ∼5:1[a] − 4:1[b] ratio (Scheme 63). 325 mg

---

[a]Ratio based on *cis* H-4 min peak integration and stacked Boc-peak integration in ^{1}H-NMR spectrum (CDCl$_3$, 400 MHz, 298 K) at δ_H 3.35 and 1.45 ppm.

[b] Ratio based on relative peak integrations on LCMS chromatogram at 210 nm.

of this mixture of diastereomers was submitted for separation *via* SFC (BEH column, CO_2:20 mM NH_3 in MeOH), and the isolated ratio of *cis*-**181**:*trans*-**181** cycloaddition products was in accordance with that observed in the ^{1}H-NMR spectrum of the mixture (*cis*-**181**: 214 mg, *trans*-**181***:* 45 mg). NMR spectroscopic analysis of the diastereomers confirmed the connectivity expected for fused pyrrolidine **181**, but overlapping resonances prevented assignment of the relative stereochemistry of the ring junction. However, since [3+2] cycloadditions are concerted processes, we postulated the major product to be *cis*-**181**. Both epimers existed as an oil, preventing crystal structure analysis, but the postulated stereochemistry was later confirmed *via* XRD analysis of a derivative (see Section 7.6).
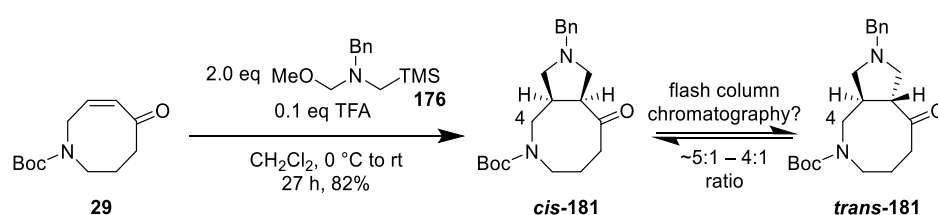
*Scheme 63: 1,3-dipolar cycloaddition on enone **29** using ylide precursor **176**.*

Given that the postulated *trans* diastereomer was not observed in the reaction mixture and crude product, it was hypothesised that *cis*-**181** had epimerised during purification by silica chromatography. Given the presence of the ketone next to the ring junction, epimerisation to *trans*-**181** could have occurred *via* keto-enol tautomerism or a retro-Mannich mechanism (Scheme 64).
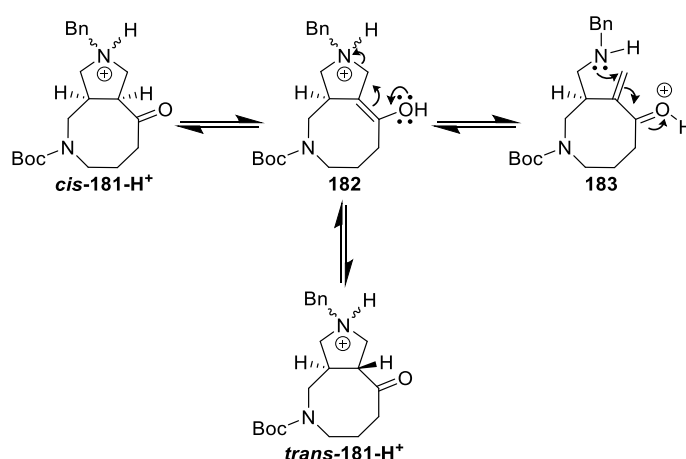
*Scheme 64: Possible epimerisation mechanisms of **cis**-**181** via enol **182** under acidic conditions.*[a]

---

[a] Epimerisation through keto-enol tautomerism can proceed with or without protonation of the pyrrolidine amine.

Literature precedent for epimerisation of analogous 5-8 fused ring systems was provided by Umehara *et al.*;[16] under both acidic and basic methanolic conditions, fused octanone **cis-184** epimerised completely to **trans-184** diastereomer upon long reaction times (Scheme 65). A control experiment starting from the **trans-184** diastereomer under identical basic conditions yielded no **cis-184** epimer, indicating that the *trans* epimer is more thermodynamically stable.[16] This example illustrates how *cis* ring fusion is not necessarily thermodynamically favoured in larger ring systems; because of the increased conformational flexibility of larger ring systems, *trans* ring fusion can occur without imposing significant ring strain. Hence, the hypothesised epimerisation of **cis-181** was considered plausible and was investigated further.
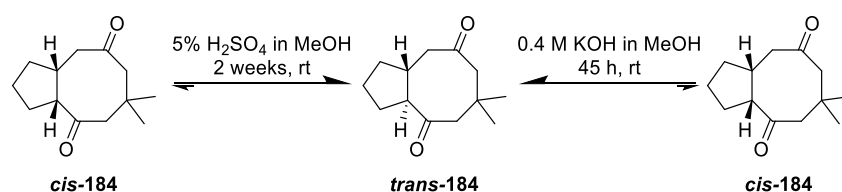
*Scheme 65: Epimerisation of octanone **cis-184** to **trans-184** under acidic and basic conditions.[16]*

^{1}H- and ^{13}C-NMR spectroscopic analysis of our purified diastereomers in CDCl$_3$ did not show epimerisation after 7 h in solution. LCMS analysis of these samples in CDCl$_3$ after 7 days in solution also showed no epimerisation from **trans-181** to **cis-181** and <5% of **cis-181** to **trans-181** (based on relative peak integrations on the LCMS chromatogram at 210 nm). Hence, NMR spectroscopic data and LCMS data were considered to give reliable diastereomeric ratios and could therefore be used to test the hypothesis that SiO$_2$ was mediating epimerisation.[a] SiO$_2$ (60 eq) was added to a solution of the ~4:1[b] mixture of **cis-181** and **trans-181** diastereomers in different column eluents. LCMS analysis of these solutions showed a significant shift of the equilibrium towards **trans-181** in those mixtures containing SiO$_2$ (Table 14, Entries 1 – 4), whereas a reference mixture in MeOH without SiO$_2$ showed no change in the *cis*:*trans* ratio (Entry 5). Observation of a 3:2 *cis*:*trans* mixture of a sample in CH$_2$Cl$_2$, 40 min after addition of SiO$_2$, showed that the rate of epimerisation is fast enough to yield a significant amount of **trans-181** if large amounts of **cis-181** are kept on SiO$_2$ for less than an hour. These observations

---

[a] Although **cis-181** could slowly epimerise to **trans-181** in CDCl$_3$ or on an LCMS column, this process was assumed too slow to interfere significantly with the analyses, as samples for NMR spectroscopy were measured within hours and LCMS samples remained on the LCMS column for <3 min.
[b] Ratio based on relative peak integrations on LCMS chromatogram at 210 nm.

supported the hypothesis that **trans-181** was obtained by epimerisation of **cis-181** during flash column chromatography, as this purification method can take up to 30 min and longer, when performed on gramme-scale. Given that epimerisation was postulated to occur *via* an enol intermediate, facilitated by Brønsted acid SiO_2, NH_3 was added to the column eluent in an effort to suppress epimerisation of **cis-181** to **trans-181** (Table 14, Entry 2). However, this was not the case and a similar *cis*:*trans* ratio was observed. The equilibrium shifts towards **trans-181** (Table 14) indicate that **trans-181** is the more thermodynamically stable epimer. Acknowledging that **cis-181** could potentially fully convert to **trans-181** on a longer time scale, this equilibrium was not investigated further.

*Table 14: LCMS analysis of **cis-181** to **trans-181** epimerisation in mixtures containing SiO_2.*
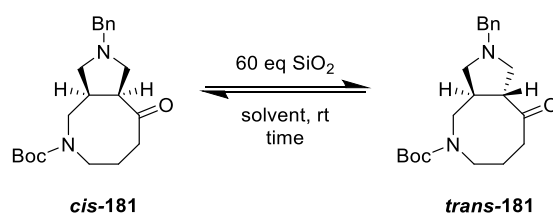
Entry	Conditions	Time (h)	*cis*:*trans* ratio[a]
1	CH_2Cl_2, SiO_2	17	3:7
2	(CH_2Cl_2:MeOH 7 M NH_3) 9:1, SiO_2	21	3:7
3	heptane, SiO_2	30	2:3
4	MeOH, SiO_2	3.5	2:3
5	MeOH, no SiO_2	3.5	4:1

Since the **trans-181** epimer could also provide a novel scaffold with a different skeleton and shape, base-catalysed epimerisation of **cis-181** was also explored; literature precedent for intentional epimerisation of structurally related 8-5 bicyclic ketones under basic conditions appeared to be more common. An intermediate in their total synthesis of (±)-asterisca-3(15),6-diene **186**, Mehta and Umarye epimerised *cis*-fused bicycle **cis-185** to the *trans*-fused diastereoisomer **trans-185** by addition of KO*t*-Bu, yielding a 1:4 *cis*:*trans* mixture after 20 min (Scheme 66).[17]

---

[a] Ratio based on relative peak integrations on LCMS chromatogram at 210 nm.
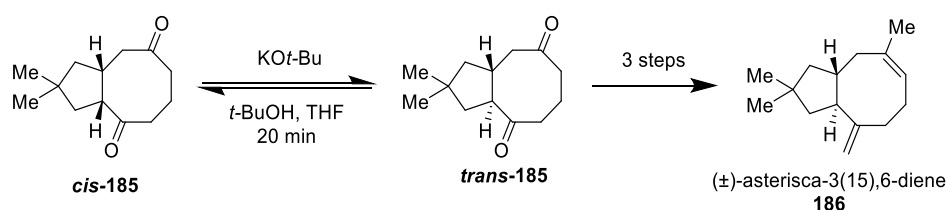
*Scheme 66: Epimerisation of **cis-185** to **trans-185** using KOt-Bu, as reported by Mehta and Umarye.[17]*

Trost and Parquette reported the epimerisation of 8-5 bicyclic ketone **cis-187** to **trans-187** using DBU in CHCl₃ in their total synthesis of (±)-11-hydroxyjasionone **188**, a natural product with antifungal and antibacterial activity (Scheme 67).[18] The epimerised analogue **trans-187** was obtained in 51% after column chromatography (heptane:EtOAc).[18]
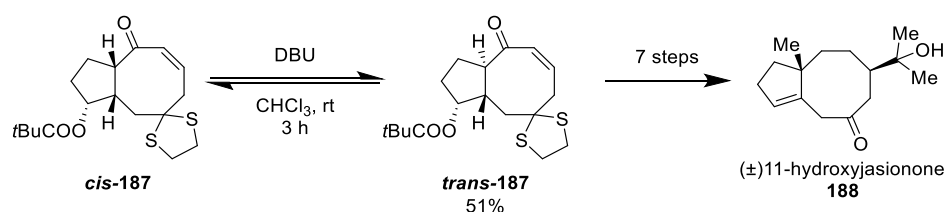
*Scheme 67: Epimerisation of **cis-187** to **trans-187** using DBU, reported as part of the total synthesis of (±)-11-hydroxyjasionone **188** by Trost and Parquette.[18]*

Based on Mehta's and Umarye's epimerisation conditions, the ~4:1[a] mixture of diastereomers **cis-181** and **trans-181** was treated with KOt-Bu in t-BuOH and in THF.[17] However, LCMS analysis of both reaction mixtures showed complete degradation of both diastereomers after 1 h (Table 15, Entries 1 and 2). The slightly weaker base NaOMe in MeOH did not lead to degradation and the equilibrium was again shifted towards **trans-181** (Table 15, Entries 3 and 4), although the reaction mixtures in THF (Table 15, Entries 2 and 4) contained an unknown byproduct, which co-eluted with the *cis* epimer during LCMS analysis. This byproduct was not investigated further.

---

[a] Ratio based on relative peak integrations on LCMS chromatogram at 210 nm.

Table 15: Epimerisation conditions using KOtBu and NaOMe.

cis-181   trans-181
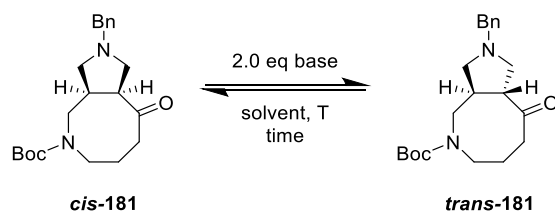
Entry	Base	Solvent	T (°C)	Time (h)	cis : trans ratio[a]
1	KO*t*-Bu	*t*-BuOH	65[b]	1.0	Degradation
2	KO*t*-Bu	THF	rt	1.0	Degradation, unknown byproduct
3	NaOMe	MeOH	rt	2.5	1:3
4	NaOMe	THF	rt	1.0	3:7, but co-elution with unknown byproduct

Although **trans-181** would yield a series of analogues with a unique skeletal structure, preventing epimerisation of **cis-181** was deemed easier than maximising **trans-181** yields and with limited research time left, further chemistry on the **cis-181** diastereomer was therefore prioritised.

In order to prevent the epimerisation of **cis-181** during flash column chromatography (Table 14), our attention turned to processing the crude **cis-181** product directly in a next step. Therefore, the 1,3-dipolar cycloaddition reaction conditions were optimised to reduce the minor byproducts that persisted in the crude mixture after workup. One of these byproducts showed an m/z value which corresponded to diamine **191**. Padwa and Dent reported the formation of diamine **191** whilst generating ylide **177** using $ZnCl_2$ as the catalyst in the absence of a dipolarophile (Scheme 68).[11] Reaction of the ylide **177** with its precursor **189** was hypothesised to yield iminium species **190**, which hydrolysed to form the secondary amine **191**. This byproduct was not reported for reactions which employed LiF as the catalyst.[11]

---

[a] Ratio based on relative peak integrations on LCMS chromatogram at 210 nm.
[b] The reaction mixture became solid at rt upon addition of KO*t*-Bu but returned to liquid upon heating.
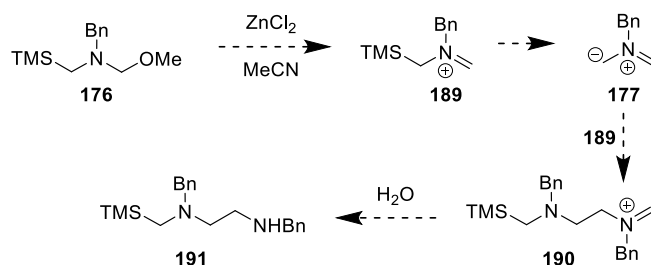
*Scheme 68: Formation of byproduct **191** reported by Padwa and Dent, with hypothesised pathway.[11]*

Building on the observations made by Padwa and Dent,[11] an excess of ylide **177** and precursor **176** could increase the chances of forming the 2° amine byproduct **191**. Given TFA is reported as a catalyst for generation of ylide **177**,[12] TFA could have facilitated the formation of byproduct **191** observed during the 1,3-cycloaddition on enone **29**. Therefore, we performed the cycloaddition under alternative conditions, using LiF[11] and no additive[19] in MeCN. LCMS analysis of test reaction mixtures after 23 h (50 mg scale) showed that *cis*-**181** was formed in MeCN, even in the absence of any additive (Table 16). The reaction with TFA led to the formation of byproduct **191** (Table 16, Entry 1). This byproduct was not observed in the reactions with LiF and no additive, which showed similar LCMS chromatograms (Table 16, Entries 2 and 3). Hence, the reaction conditions using no additive in MeCN (Table 16, Entry 3) were scaled up and yielded the crude pyrrolidine *cis*-**181** on gramme scale, which was used in subsequent telescoped reactions.

*Table 16: All reaction conditions yielded **cis-181**, regardless of the additive.*
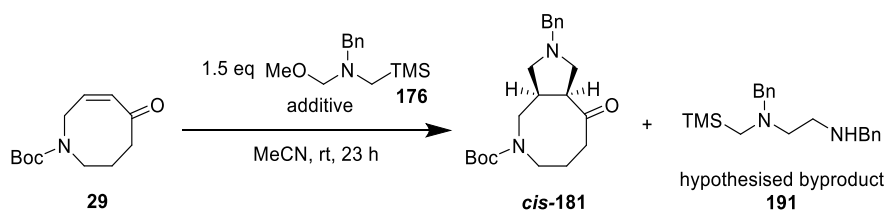
Entry	Additive	Observation (LCMS analysis)
1	0.10 eq TFA	*cis*-**181** present, **191** present
2	1.25 eq LiF	*cis*-**181** present, no **191**
3	No additive	*cis*-**181** present, no **191**

In conclusion, a 1,3-dipolar cycloaddition using ylide precursor **176** allowed for synthesis of the fused pyrrolidine *cis*-**181** on gramme scale. We confirmed that fused pyrrolidine *cis*-**181** epimerises to *trans*-**181** on SiO$_2$ and under basic conditions. By optimising the [3+2] reaction

conditions, the presence of byproduct **191** could be avoided in the crude product, allowing for diversification of the fused pyrrolidine *cis*-**181** without further purification of the starting material. With three reactive sites present on the 8-5 ring system, diversification strategies were now explored on the ketone, the Bn-protected pyrrolidine and the Boc-protected amine.

7.2.   Intramolecular attack

Revisiting the lack of orthogonality between the Boc-protected amine and carbonyl in SACE1 precursor **91** (see Section 3.1.4, page 46), it was worth investigating whether the conformational restriction imposed by the fused pyrrolidine would facilitate the hypothesised attack of the deprotected amine on the transannular carbonyl. Literature precedent for intramolecular cyclisation was provided by Papaioannou *et al.*: Boc deprotection of eight-membered ring analogue **85** using 5 mol% HNO_3 in MeOH yielded methoxy-pyrrolizidine **84**, while deprotection under thermolysis conditions yielded hydroxy-pyrrolizidine **86** (Scheme 69).[20]

84
81%

5 mol% HNO_3
MeOH, 135 °C
30 min

85

neat
185 °C, 1 h

86
52%
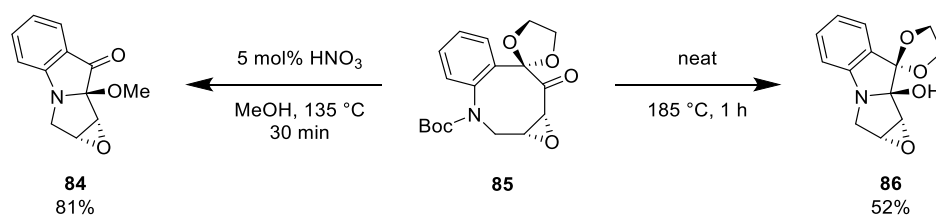
Scheme 69: Pyrrolizidine synthesis reported by Papaioannou et al.[20]

When we deprotected Boc-amine *cis*-**181** with HCl in MeOH, the iminium salt *cis*-**192** was obtained as the end product after 6 days (Scheme 70), showing a characteristic resonance in the ^{13}C-NMR spectrum at δ_C 196.8 ppm (C, C-1)[a] and an m/z value in the LCMS chromatogram which corresponds to the iminium cation ([M]$^+$ = 241.1). The isolation and characterisation of iminium salt *cis*-**192** allowed for confirmation of the hypothesised intramolecular attack, supporting the decision to convert the carbonyl before Boc deprotection of SACE1 library precursor **91** to keep the eight-membered ring intact. Unlike Papaioannou *et al.*, no methoxy- or hydroxypyrrolizidine analogue masses were observed during LCMS analysis of the deprotection mixture of Boc-amine *cis*-**181**, although these could have converted to the iminium species on the LC column.[b]

---

[a] ^{13}C-NMR spectrum recorded at 101 MHz, 296 K in CD$_3$OD.
[b] The observation of a single peak with the m/z value of iminium *cis*-**192** on the LCMS chromatogram indicated that if any expected methoxy- or hydroxypyrrolizidine analogue were stable on the LC column (which would show up as an extra peak), these compounds do not produce the iminium fragment upon ESI+.
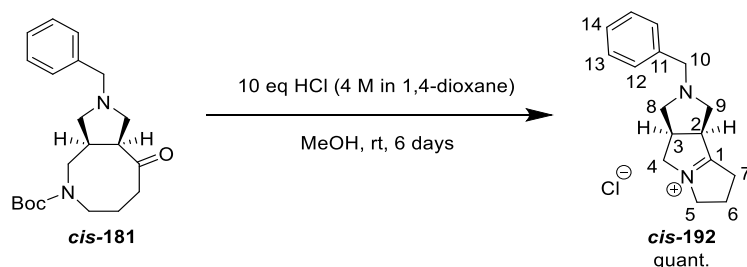
*Scheme 70: Boc deprotection of ketone **cis-181** yielded iminium salt **cis-192**, resulting from intramolecular attack of the deprotected amine on the transannular ketone.*

LCMS analysis of the Boc deprotection mixture (Scheme 70) showed an interesting conversion route of ketone **cis-181** towards iminium ion **cis-192** (Scheme 71). After 14 h, four peaks were observed whose m/z values corresponded to Boc-protected epimers **cis-181** and **trans-181**, a Boc-deprotected compound and iminium salt **cis-192**. After 6 days, only the iminium **cis-192** peak remained. Based on these observations, we postulate the following pathway: Boc amide **cis-181** epimerises under acidic conditions to **trans-181**. Both epimers undergo Boc deprotection to afford 2° amines **cis-193** and **trans-193**. Since the ring strain in *trans*-fused pyrrolizidine **trans-192** and its hemiaminal precursor **trans-194** disfavours intramolecular cyclisation of deprotected epimer **trans-193**, the deprotected epimer **trans-193** epimerises instead to afford **cis-193**, which rapidly undergoes cyclisation and dehydration to form the iminium salt **cis-192** (Scheme 71). **Trans-193** is then the second Boc-deprotected peak observed in the LCMS chromatogram.
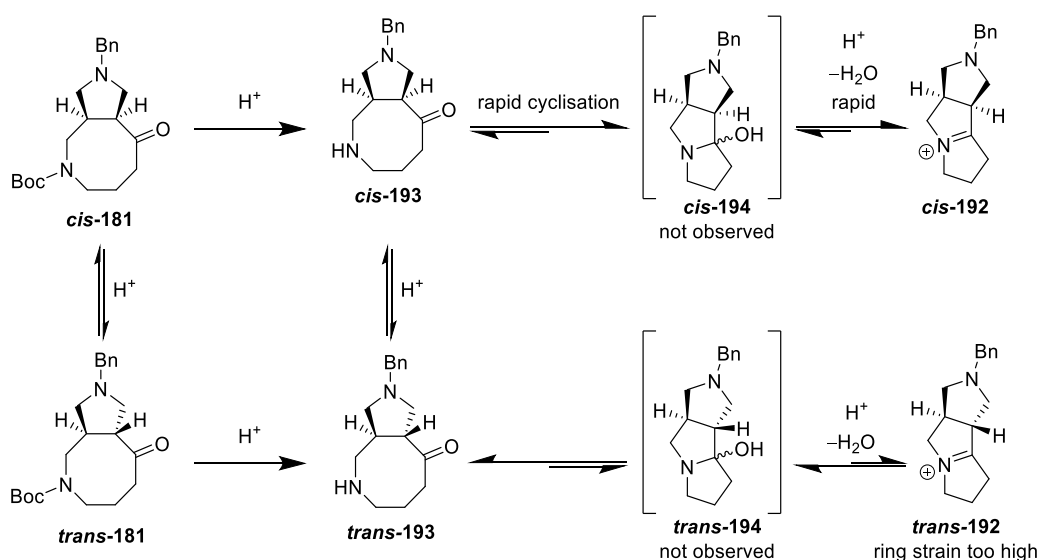
*Scheme 71: Hypothesised pathway towards iminium species **cis-192**.*

Since pyrrolizidine alkaloids are known natural products with broad-ranging bioactivity, often used in traditional Chinese medicine,[21] we attempted to reduce pyrrolizidinium salt **cis-192** to

generate 5-5-5 fused pyrrolizidine analogue **197** (Scheme 73). Iminium salt **cis-192** was reduced using conditions by Saha *et al.*, reported in their synthesis of cytotoxic alkaloid (±)-crispine A **196** (Scheme 72).[22]
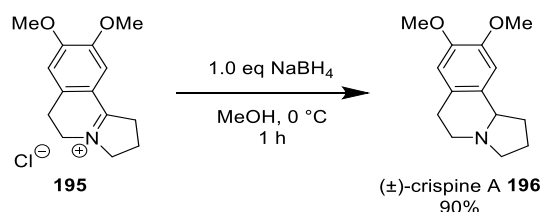
*Scheme 72: Synthesis of natural product crispine A **196**, using NaBH₄ to reduce iminium salt **cis-192**.[22]*

Although 80 mg of pyrrolizidinium salt **cis-192** was completely reduced in a short time (2 h), the reduction did not proceed diastereoselectively as both fused pyrrolizidine diastereomers were obtained in a **cis-197**:**trans-197** ratio of 3:2 (Scheme 73).[a]

Tentative assignment	δ_C trans-197 (ppm)	δ_C cis-197 (ppm)
C-7	30.5	24.7
C-2	49.2	45.0
C-1	72.2	69.3

$J_{1-2} = 6.6$ Hz $J_{1-2} = 9.2$ Hz
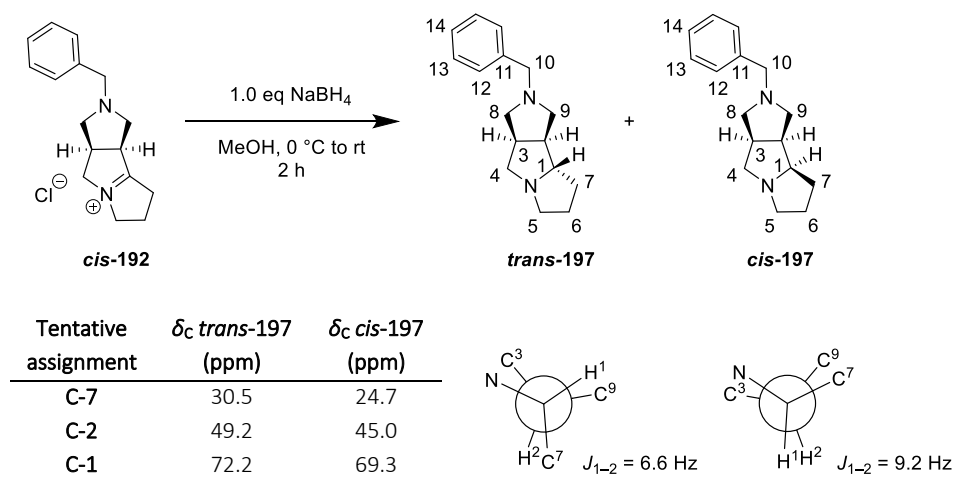
*Scheme 73: Reduction of iminium salt **cis-192** with NaBH₄ did not proceed diastereoselectively.*

Both diastereomers were separated from each other *via* flash column chromatography but were not obtained analytically pure. However, the amount of impurity[b] was sufficiently small to distinguish the two pyrrolizidines. 2D-NMR spectroscopic analysis allowed for tentative assignment of the observed resonances, by analogy with pyrrolizidine diastereomers **199** reported by Pearson *et al.*[23] and diastereomers **201** reported by Tsuge *et al.* (Scheme 74).[24] In accordance with the reported ¹³C-NMR resonances, C-1, C-2 and C-7 resonances appeared further upfield in the *cis*-diastereomer **cis-197**, compared to the *trans*-analogue **trans-197**

---

[a] Ratio based on relative integration values for H-1 in the crude ¹H NMR spectrum.
[b] The nature of the impurity was unknown, both diastereomers showed different impurities.

(Scheme 73, see Appendix 4.1).[a] Furthermore, the larger J_{1-2}-value observed for H-1 in the **cis-197** diastereomer (J_{1-2} = 9.2 Hz) compared to **trans-197** (J_{1-2} = 6.6 Hz) could indicate a smaller dihedral angle, which is expected for the *cis* diastereomer (Scheme 73).
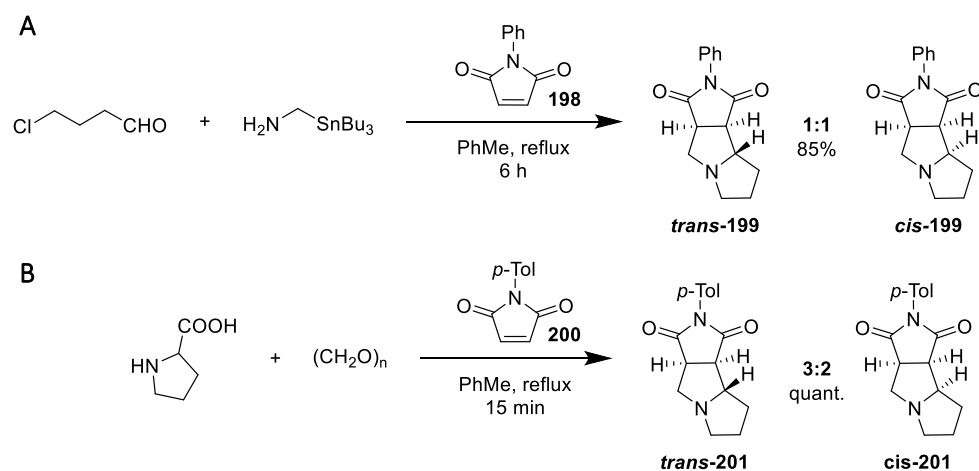
Scheme 74: 5-5-5 fused pyrrolizidine synthesis by Pearson et al. (A) and Tsuge et al. (B).[23,24]

Apart from providing a reference for tentative assignment of the resonances of pyrrolizidine diastereomers **cis-197** and **trans-197**, the reported syntheses by Pearson *et al.* and Tsuge *et al.* also provided a more elegant and economical approach to synthesising 5-5-5 fused pyrrolizidines: for example, pyrrolizidines **199** and **201** were prepared in a one-pot process, generating the azomethine ylides *in situ*, followed by 1,3-dipolar cycloaddition with *N*-phenylmaleimide **198** or *N*-(*p*-tolyl)maleimide **199** (Scheme 74).[23,24] Hence, no further efforts were made towards the synthesis and diversification of pyrrolizidine **197**, and the focus was shifted towards functional group conversion of the ketone moiety of Boc-protected amine **cis-181**.

7.3. Functional group conversion of the ketone

The formation of the 5-5-5 fused ring system **cis-192** highlighted the need to manipulate the ketone moiety of **cis-181** prior to Boc deprotection. In order to facilitate library synthesis, chemistry on the carbonyl was required to be stereoselective or complexity-reducing, as non-stereoselective generation of an sp^3 centre would yield diastereomers.

---

[a] The ^{1}H-NMR spectroscopic data provided by Pearson *et al.* and Tsuge *et al.* were not reported with sufficient detail (*i.e.*, multiple resonances reported as one broad multiplet, not assigned) to enable comparison with the ^{1}H-NMR spectra of diastereomers **cis-197** and **trans-197**.[23,24]

7.3.1. Difluorination

As was experienced with SACE2 precursor **91** (Table 9, page 101), attempted difluorination of **cis-181** using DAST or BAST was unsuccessful; LCMS analysis of the reaction mixtures showed no reaction and the ketone **cis-181** starting material was recovered (Table 17).

*Table 17: Attempted difluorination of **cis-181** using DAST or BAST.[a]*
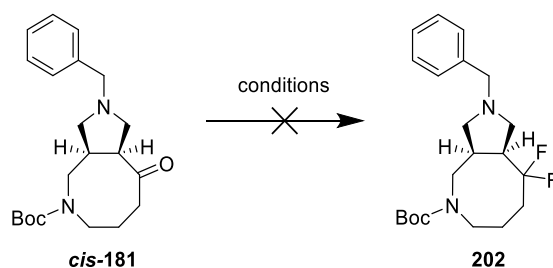
Entry	Reagent	Solvent	Temperature	Time	Outcome
1	DAST (4 eq)	CH_2Cl_2	rt	overnight	No reaction
2	BAST (4 eq, 2.7 M in toluene)	CH_2Cl_2	rt to reflux	3 days	No reaction

[a] Reactions performed on 30 mg scale.

7.3.2. Reductive amination

In an attempt to effect reductive amination, ketone **cis-181** was treated with $HNMe_2$ and $Na(OAc)_3BH$ (Scheme 75). After 4 h at room temperature, no reaction was observed *via* LCMS analysis. However, upon addition of 1.2 eq AcOH, LCMS analysis of the reaction mixture showed epimerisation of the pyrrolidine **cis-181**. No desired amine product **203** was observed after 5 days and after addition of extra $HNMe_2$ (1.2 eq) and $Na(OAc)_3BH$ (1.5 eq), the reaction was stopped after 7 days in total.
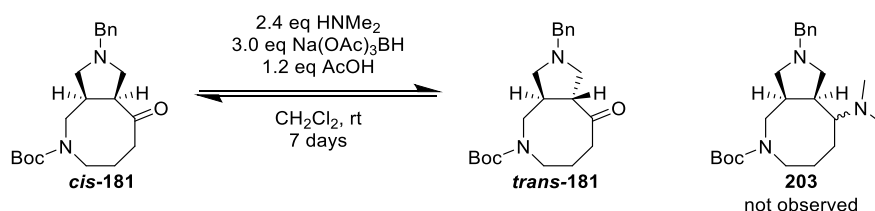
*Scheme 75: An attempt to reductively aminate ketone **cis-181** resulted in epimerisation, rather than formation of tertiary amine **203**.*

Reductive amination using primary amines was not explored, since the resulting secondary amine was expected to give selectivity issues upon functionalisation of the Boc- or Bn-deprotected amines in the library step. Nonetheless, it was deemed worthwhile to probe the reactivity of the ketone, as earlier reductive amination attempts using a primary amine on SACE1 precursor **91** had proven unsuccessful (see Section 3.1.5, page 47).

In contrast with the previous reductive amination attempt, LCMS analysis of the reaction mixture under initial conditions (1.2 eq cyclopropylamine, 1.5 eq Na(OAc)$_3$BH, 1.2 eq AcOH) showed no epimerisation of the ketone **cis-181** after 42 h. However, LCMS analysis did show two peaks with m/z values corresponding to amine **204**,[a] indicating that the reductive amination may not proceed stereoselectively. After addition of an extra 0.3 eq Na(OAc)$_3$BH, ketone **cis-181** did begin to epimerise and even though the reaction was finally driven towards full consumption of the ketone **cis-181** by addition of extra cyclopropylamine and Na(OAc)$_3$BH, LCMS analysis of the obtained crude mixture still showed at least two isomers, which were not purified nor characterised (Scheme 76).
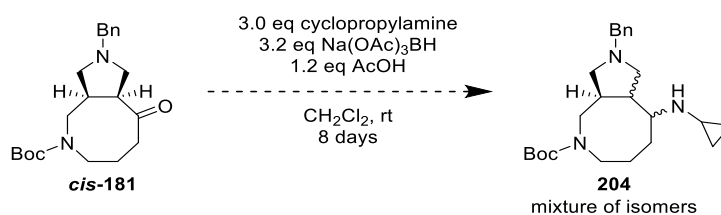
*Scheme 76: Attempted reductive amination of ketone **cis-181** using cyclopropylamine yielded a mixture of isomers.*

7.3.3.   Stereoselective reduction

Stereoselective reduction of the ketone **cis-181** was worth exploring, as the resulting alcohol could be functionalised, serving as another point of diversity. Literature precedent for the reduction of – or nucleophilic attack on – analogous 5,8-fused cyclic ketones (carbocyclic and heterocyclic) was not found,[b] which highlights the novelty of the planned reaction and envisioned alcohol product, but this also required an extended literature survey to identify precedent for the planned reduction.

---

[a] Selected data for amine isomers **204**: ESI-LRMS (+): m/z 400.2 ([M+H]$^+$, 100%).
[b] One literature reference was found which reported ketone reduction, but no comment was made about the stereoselectivity of the reduction, as the alcohol was oxidised in the next step.[17]

Poli and Giambastiani reported a stereoselective reduction of ketone **205** using NaBH$_4$ in MeOH.[25] However, Daubié and Mutti did not obtain diastereopure alcohols from pyrrolidinohexanone **207** using NaBH$_4$ (Scheme 77). Hence, the fused pyrrolidine in azocanone *cis*-**181** gave no guarantee for a stereoselective reduction using NaBH$_4$.
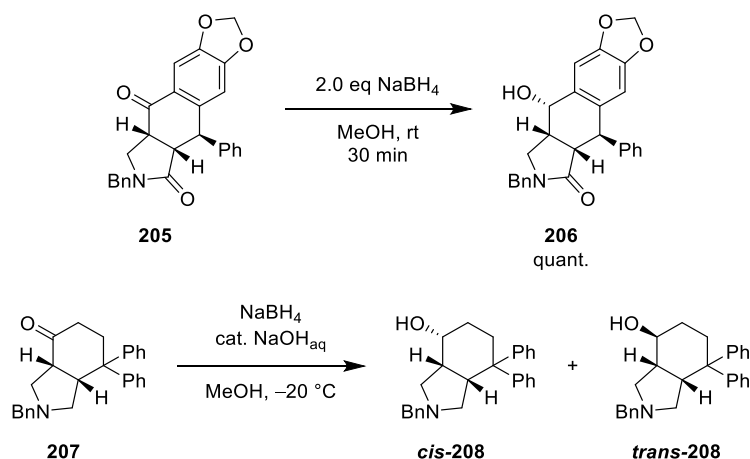
*Scheme 77: Ketone reductions reported for analogous fused ring systems **205** and **207** do not always proceed stereoselectively.[25,26]*

Applying the conditions by Poli and Giambastiani to azocanone *cis*-**181**,[25] using NaBH$_4$ on 100 mg scale yielded the desired alcohol product, but as a mixture of diastereomers; LCMS analysis of the crude product after workup (using NH$_4$Cl $_{sat. aq.}$, CHCl$_3$:*i*-PrOH 3:1 solution) showed two peaks with equal mass in a ∼1:9 ratio.[a] Purification *via* flash column chromatography afforded diastereomer *cis*-**209** in 61% yield while the other diastereomer *trans*-**209** was not obtained in sufficient purity and yield to allow full characterisation (Scheme 78).[b]
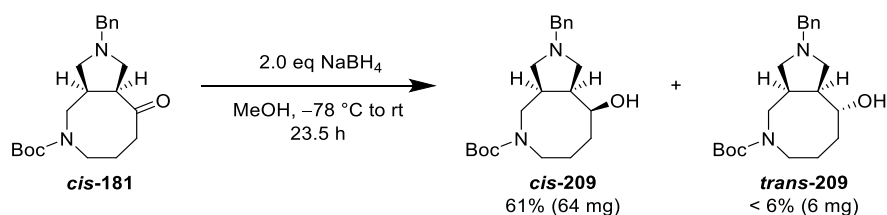
*Scheme 78: Reduction of ketone **cis-181** using NaBH$_4$ yielded both diastereomers.*

Whilst a 9:1 diastereomeric ratio of alcohol **209** was not bad, the bulky reducing agent L-selectride was next explored, postulating that increased steric hindrance between the substrate and reducing agent would better differentiate the diastereotopic faces of the

---

[a] Ratio based on relative peak integrations on LCMS chromatogram at 210 nm.
[b] Selected data: R$_f$ (CH$_2$Cl$_2$: 7 M NH$_3$ in MeOH 9:1): *cis*-**207** 0.8, *trans*-**207** 0.6.

ketone.[27] This has been proven successful on analogous fused pyrrolidine **210** in a patent by Casimiro-Garcia *et al.*[28] and on fused cyclopentyl analogue **212** in a paper by Dragojlovic[27] (Scheme 79). An interesting observation was the reversal in diastereoselectivity when tricyclic ketone **212** was reduced with NaBH$_4$, yielding ***trans*-213** as the major alcohol product, albeit less stereoselectively. This reversal was attributed to steric hindrance of the carbonyl group being the determining factor for stereoselectivity using L-selectride, whilst the reduction with smaller NaBH$_4$ was controlled by torsional strain in the transition state.[27]

L-selectride: 92% ***cis*-213**,   *cis:trans* = 96:4
NaBH$_4$: 97% diast. mixture, *cis:trans* = 25:75
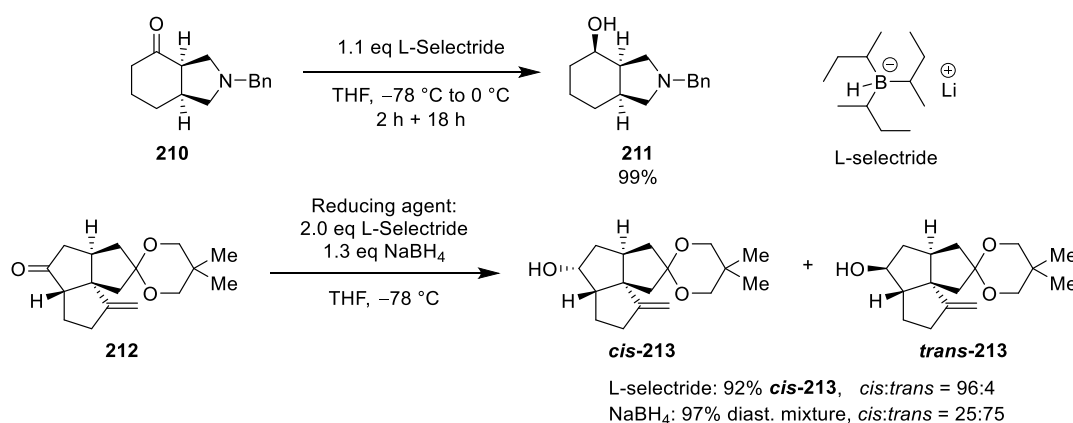
Scheme 79: Literature precedent for stereoselective ketone reduction using L-Selectride.[27,28]
[a]Calculated via ^{1}H-NMR spectroscopic analysis.

In accordance with the reported reduction of ketones **210** and **212**,[27,28] reduction of the crude azocanone ***cis*-181** with L-selectride proceeded with high stereoselectivity, as LCMS analysis of the reaction mixture showed only one peak with the desired product mass and only one diastereomeric alcohol product was isolated (Scheme 80). This result supported our approach to perform a stereoselective 1,3-dipolar cycloaddition followed by a stereoselective ketone reduction to provide a single diastereoisomeric product. The telescoped 1,3-dipolar cycloaddition of enone **29** – ketone reduction was scaled up to yield alcohol ***cis*-209** on gramme scale (Scheme 80).
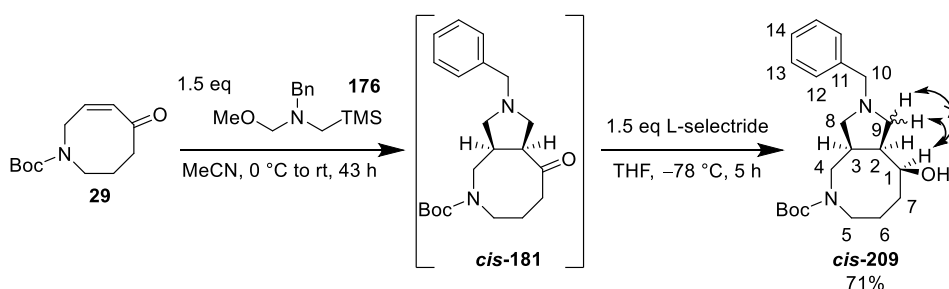
*Scheme 80: Telescoped 1,3-dipolar cycloaddition and ketone reduction with L-selectride yielded one diastereomer **cis-209**. NOESY showed cross peaks between H-1 and only one H-9 proton.*

Thus far, the relative stereochemistry in alcohol *cis*-209 had not been confirmed definitively. The NOESY spectrum showed cross peaks between H-1 and only one H-9 proton, but because of the conformational flexibility of the eight-membered ring, this observation could not be correlated to a particular diastereomer (Scheme 80). Since alcohol *cis*-209 was a yellow oil, determination of the relative stereochemistry of alcohol *cis*-209 was not possible *via* XRD analysis. However, crystal structure determination of a derivative compound (see Section 7.6) later confirmed the stereochemistry of the alcohol to be *cis* in regards to the fused pyrrolidine, which was in accordance with the stereoselectivity reported for L-selectride reduction by Casimiro-Garcia[28] and Dragojlovic (Scheme 79).[27] Having reduced the ketone *cis*-181 stereoselectively, the hydroxyl moiety was probed as a third point of diversity on the SACE3 scaffold.

7.4. Functionalising the alcohol

Conversion of the alcohol to an azide would provide access to 1,2,3-triazoles using a CuAAC reaction as introduced by the Sharpless group.[29] Hence, alcohol *cis*-209 was subjected to diphenylphosphoryl azide (DPPA) following literature conditions reported by Thompson et al. (Scheme 81).[30] LCMS analysis of the reaction mixture showed no evidence for the desired azide 214. After 3 days, the alcohol *cis*-209 had been fully consumed, but multiple unidentified byproducts were present and the reaction was discarded.
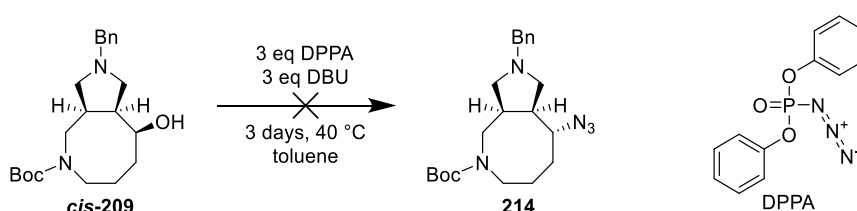
Scheme 81: Attempted azide synthesis using Mitsunobu chemistry.

Another approach to convert alcohol *cis*-209 to the azide 214 was by mesylation of the alcohol, followed by nucleophilic substitution with NaN_3. This approach was used by Jung *et al.* to synthesise a range of small-molecule inhibitors of the mitochondrial permeability transition pore (mPTP) for treatment of Alzheimer's disease (Scheme 82).[31]
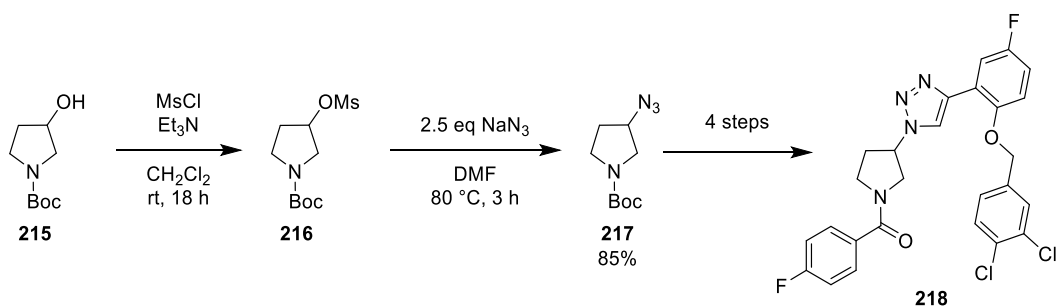
Scheme 82: Alcohol mesylation-azidation approach used by Jung et al. MsCl/Et₃N equivalents and mesylation yield not specified.[31]

Although LCMS analysis of the mesylation reaction mixture did show the desired mesylate **219**, an extra product was observed with an m/z value that could correspond to the 5-5-5 fused pyrrolizidine analogue *cis*-**197** (Scheme 83).[a] Although this hypothesised byproduct *cis*-**197** was found in the aqueous layer after workup (using NaHCO₃ $_{sat. aq.}$, CH₂Cl₂), the mesylate **219** appeared to degrade on SiO₂, as no desired product was recovered after flash column chromatography (CH₂Cl₂:MeOH, 9:1).
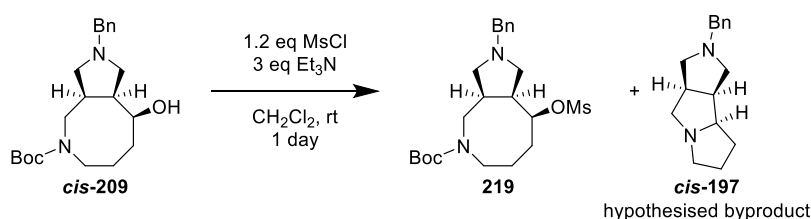
*Scheme 83: LCMS analysis of the reaction mixture did show desired mesylate **219** and hypothesised byproduct* cis-***197**, but mesylate **219** was not recovered after flash column chromatography. Reaction scale: 60 mg* cis-**209**.

The observation of hypothesised byproduct *cis*-**197** was in line with a publication by Papaioannau *et al.*,[20] who reported a similar intramolecular attack of a Boc-protected amine in a Mitsunobu reaction mixture, which yielded pyrrolizidine **221** instead of the envisioned *p*-NO₂-benzoyl ester **222** (Scheme 84, A and B). They hypothesised that this cyclisation occurred upon activation of the alcohol.[20] Given that their crystal structure of ketone precursor **87** showed alignment of the Boc-nitrogen lone pair with the transannular C-O π^* orbital (Scheme 84, B), we considered the possibility that the Boc-protected amine *cis*-**209** could cyclise before Boc-cleavage: if the mesylated alcohol *cis*-**209** adopts an analogous conformation to ketone **87**, the

---

[a] This reaction was monitored on a different LCMS machine, so exact retention times could not be compared against the synthesised pyrrolizidine **197** diastereomers. However, m/z values (243.1) and similar retention times (t_R = 2.2 min and t_R = 2.4 min, both in basic conditions, run time 3.0 min) strongly suggest that pyrrolizidine **197** is formed.

pseudo-axial orientation of the OMs moiety would favour SN$_2$, losing the Boc-group after intramolecular attack of the transannular nitrogen (Scheme 84, C).
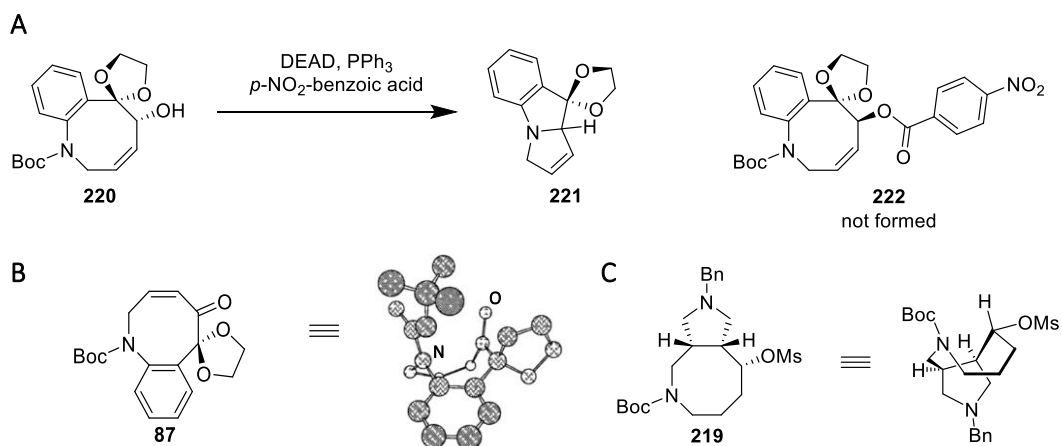
Scheme 84: (A) Literature precedent for reaction of an alcohol under Mitsunobu conditions yielding a pyrrolizidine instead of ester **222**. (B) Crystal structure of literature ketone **87**.[20, a] (C) Hypothesised analogous conformation of mesyl alcohol **219**.

Given the apparent instability of mesylate **219** to purification, a subsequent experiment telescoped the mesylation and subsequent substitution with NaN$_3$ on 60 mg scale; thus, the work-up from the mesylation involved removal of the CH$_2$Cl$_2$ solvent under reduced pressure before addition of DMF and NaN$_3$ (Scheme 85). Although LCMS analysis of the reaction mixture and crude product after aqueous workup did show the expected azide mass signal as a minor peak and disappearance of the mesylate **219**, the hypothesised byproduct **cis-197** was still present. Furthermore, the azide was not recovered after flash column chromatography (CH$_2$Cl$_2$:MeOH 9:1), indicating that the azide either degraded on the column, or was only formed in very low quantities. It was possible that other attempts at functionalisation of **cis-209** via alcohol activation would be as cumbersome, even whilst the transannular amine was Boc-protected. Therefore, this synthetic strategy was abandoned and alkylation of the alcohol was considered.
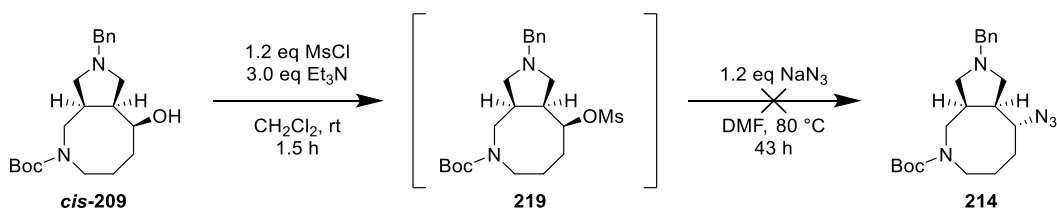
Scheme 85: A telescoped attempt at synthesising azide **214** was unsuccessful.

A preliminary attempt at *O*-methylation using MeI (1.2 eq) and NaH (2.0 eq) on 100 mg scale (Scheme 86) showed double methylation as a side-reaction; LCMS analysis of the reaction mixture showed a mixture of the starting material and a doubly methylated product as the major product, which was hypothesised to be quaternary ammonium species **223**. To confirm the hypothesis, the reaction was driven to full conversion to the doubly methylated product **223** by addition of extra MeI (3.6 eq) and NaH (6.0 eq). ^{13}C-NMR spectroscopic analysis of the crude product showed downfield shifts of C-1, C-8, C-9 and C-10 compared to precursor *cis-209*, consistent with the generation of a quaternary ammonium species, and the appearance of two new CH$_3$ peaks, indicating *O*-methylation of the alcohol and *N*-methylation of the pyrrolidine. The product was not purified further. Since *O*-alkylation with haloalkanes was thus expected to require optimisation, this route was not pursued further.[a]
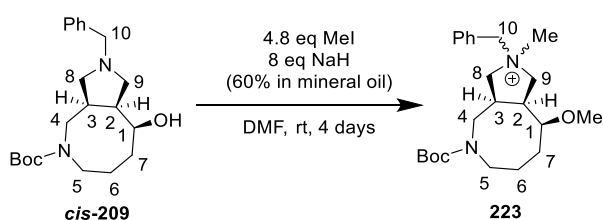
assignment *cis-209*	*cis-209* δ_C (ppm)	223 δ_C (ppm)	assignment 223
C-1	74.9	80.8	C-1
C-8	62.4		
C-9	55.9, 55.8	68.3, 66.4	C-8, C-9, C-10
C-10	60.0		

*Scheme 86: Methylation of precursor **cis-209** using MeI yielded doubly methylated product **223**.*

Since attempts to functionalise the alcohol were unsuccessful, Bn- and Boc-protected alcohol *cis-209* was used as the core scaffold for the SACE3 library, using the orthogonally protected 2° amines as appendable handles, while keeping the alcohol unfunctionalised.

---

[a] Selected data for dimethylated product **223**: ^{13}C-NMR (101 MHz, CDCl$_3$) (tentative assignments based on analogy with precursor *cis-209*) δ_C 155.7 (C, Boc *C*O), [132.7, 130.5, 129.1 (CH, Ph)], 128.0 (C, Ph), 80.8 (CH, C-1), 79.8 (C, Boc *C*(CH$_3$)$_3$), [68.3, 66.4 (CH$_2$, C-8, C-9, C-10, resonance overlap)], 57.3 (CH$_3$, Me), 50.8 (CH$_3$, Me), 47.7 (CH$_2$, C-5), 43.9 (CH$_2$, C-4), 42.5 (CH, C-2), 36.7 (CH, C-3), 28.3 (CH$_3$, Boc), 27.8 (CH$_2$, C-7), 22.1 (CH, C-6). ESI-LRMS (+): m/z 389.3 ([M]$^+$, 100%).

7.5.   Scaffold validation

With a limited amount of research time left, the size of the SACE3 library was limited to a small set of validation compounds, with the main aim of showcasing the functionalisation potential of protected pyrrolidine scaffold *cis*-**209**. In order to demonstrate that the SACE3 scaffold can provide access to a combinatorial library, the 2° amines of building blocks **224** and **225** were functionalised, followed by subsequent deprotection (Scheme 87). These planned reactions would validate both 2° amines as appendable sites and the tolerance of the functionalised sites towards subsequent deprotection, enabling combinatorial library synthesis.
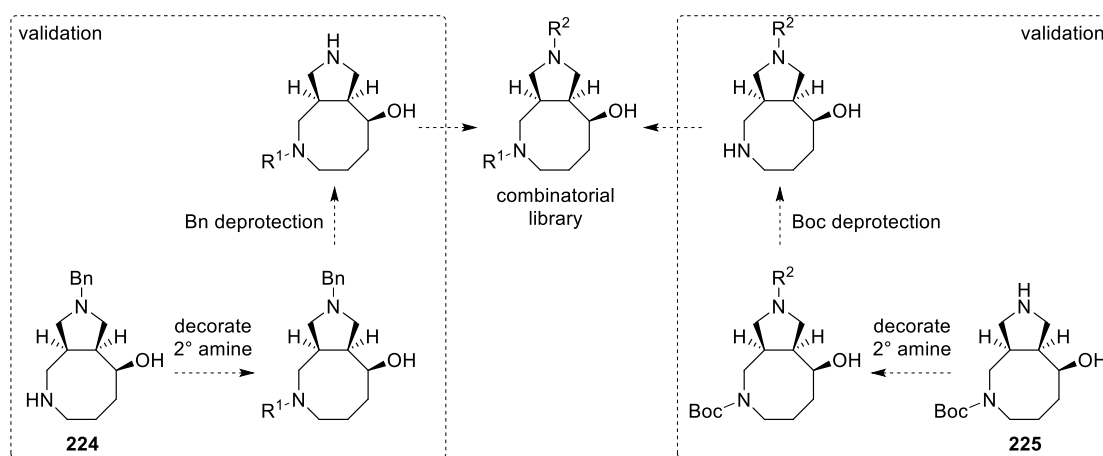
Scheme 87: Possible synthetic routes towards a SACE3 combinatorial library.

7.5.1.   Building block preparation: Bn and Boc deprotection

The presence of both a Bn and Boc protecting group should enable orthogonal deprotection of precursor *cis*-**209**, which would allow for the generation of a two-dimensional combinatorial library. This was confirmed by successfully Boc and Bn deprotecting precursor *cis*-**209** in good yields on gramme scale, using hydrogen chloride and hydrogenolysis on Pd/C, respectively (Scheme 88). Analysis of the Bn deprotection reaction by LCMS showed multiple unidentified byproducts; however, the desired deprotected 2° amine product **225** appeared as a baseline spot on a TLC plate (CH_2Cl_2:7 M NH_3 MeOH 9:1, $KMnO_4$). In this way, deprotected amine **225** could be isolated by pouring the reaction mixture onto a bed of SiO_2 and flushing the byproducts through with CH_2Cl_2:7 M NH_3 MeOH 9:1 solution, after which the desired product **225** was eluted with 7 M NH_3 in MeOH solution without the need for further purification.
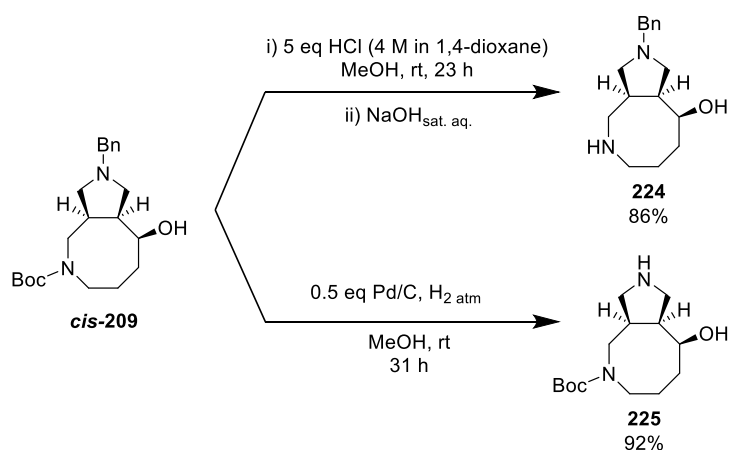
*Scheme 88: Selective Boc and Bn deprotection of precursor **cis-209**.*

7.5.2.　Validation set

To validate 2° amines **224** and **225** as two-dimensional library building blocks, both precursors were functionalised and subsequently deprotected. With no more basic morpholine nitrogen present in the precursors, as opposed to the SACE1 and SACE2 building blocks, reductive amination was considered as a parallel reaction step: as is discussed in more detail in Section 8.3.3, the presence of a basic amine is common in pharmacophores of hERG, an ion channel, which if inhibited can result in cardiac arrest.[32] Therefore, the number of basic amines was kept to a minimum for all library precursors. However, the presence of SACE3 library compounds both with and without any basic amines would make for an interesting comparison of their bioactivity and more specifically, hERG inhibition. Hence, two reductive alkylations were performed using acetaldehyde and picolinaldehyde and Na(OAc)$_3$BH, yielding tertiary amines **224e1** and **225e2** in good yields.[a] Aldehyde precursors for **224e1** and **225e2** were chosen to complement the appendage diversity, by adding a small, saturated alkyl group (**e1**) and a heteroaromatic benzyl analogue (**e2**). For sulfonamide, urea and amide syntheses, the same reaction conditions were used as for the SACE2 library synthesis, using reagents which had successfully yielded library compounds on the SACE2 scaffold. All parallel syntheses yielded the desired products in satisfactory yields, validating the secondary amines in **224** and **225** as points of diversification (Scheme 89). In addition, no *O*-functionalised products were observed *via* LCMS, as only 1 product peak with the desired m/z signals was observed and collected. No significant differences in the chemical shift for the ^{13}C and ^{1}H resonances were observed for

---

[a] The numbers assigned to compounds obtained *via* parallel synthesis contain the used building block, followed by a letter and number which is assigned to the reagent used to install the R-group. For example, **224e1** was obtained by reacting building block **224** with acetaldehyde **e1**. For reagent codes, see Experimental Section 4.1.

159

the α-hydroxyl-CH before and after functionalisation, whereas HMBC analysis showed cross peaks between the *C*=O resonances and the neighbouring ring *C*H$_2$ resonances for amides **224c1**, **225c5** and ureas **224d1**, **225d3**. Tertiary amines **224e1** and **225e2** showed cross peaks between the alkyl *C*H$_2$ and neighbouring ring *C*H$_2$ resonances, confirming chemoselective functionalization of the 2° amine.
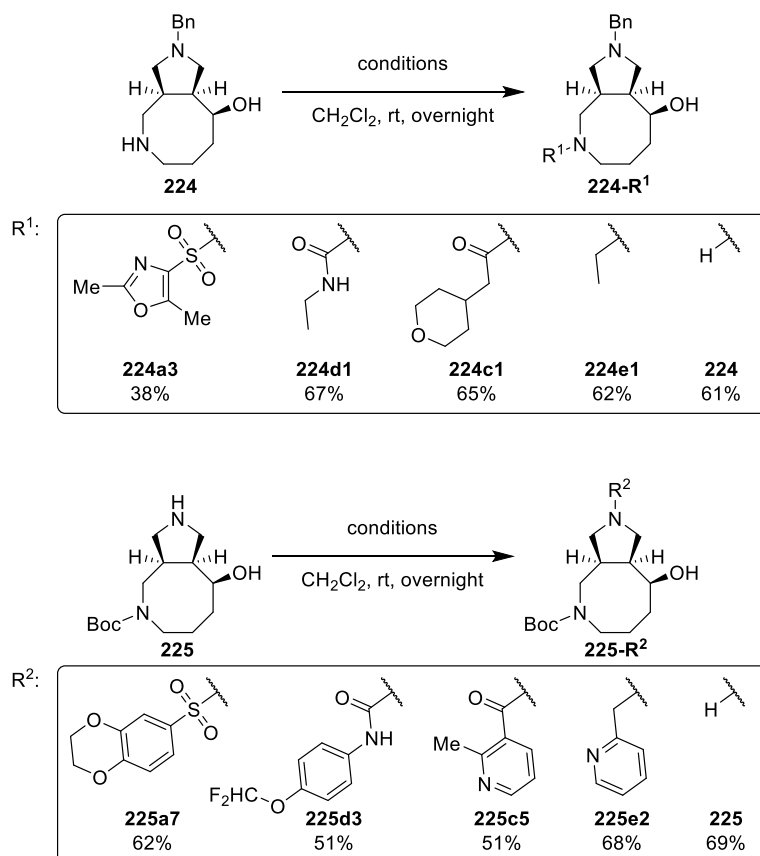
Scheme 89: Validation chemistry on SACE3 scaffold. Sulfonamides and ureas: 1.2 eq electrophile, 2.0 eq Et$_3$N; amide couplings: 1.2 eq carboxylic acid, 1.2 eq EDC •HCl, 1.2 eq Oxyma Pure, 3.0 eq Et$_3$N; reductive alkylations: 1.2 eq aldehyde, 1.2 eq Na(OAc)$_3$BH. Mass recovery from preparative LC reported for deprotected building blocks **224** and **225**.

In order to validate Boc and Bn deprotections as the penultimate reaction step for two-dimensional library synthesis, the functionalised Boc- and Bn-protected compounds (Scheme 89) were deprotected using the same conditions for the synthesis of building blocks **224** and **225** (Scheme 88). Only three out of five benzyl pyrrolidine precursors were successfully Bn-deprotected. LCMS analysis of the reaction mixture containing sulfonamine **224a3** showed no Bn deprotection after 2 days while the Bn deprotection of urea **224d1** only showed a fraction of deprotected amine **226d1**. However, upon addition of 2.0 eq HCl (4 M in 1,4-dioxane),[33] full conversion towards 2° amine **2226d1** was observed after 2.5 h, at which point the mixture containing **226d1** was submitted for preparative LC. The observed increased debenzylation rate

was in accordance with work by Studer and Blaser,[33] as protonation of the nitrogen facilitates attack of a Pd-bound hydride on the benzyl position.[33] 19 h after the addition of HCl, the reaction with oxazole **224a3** showed Bn-deprotected product **226a3**, but no full deprotection was observed *via* LCMS when the reaction mixture was submitted for preparative LC. This resulted in a low yield for Bn-deprotected sulfonamide **226a3** (4%) (Scheme 90). All Boc-precursors showed full Boc deprotection after overnight stirring under acidic conditions.
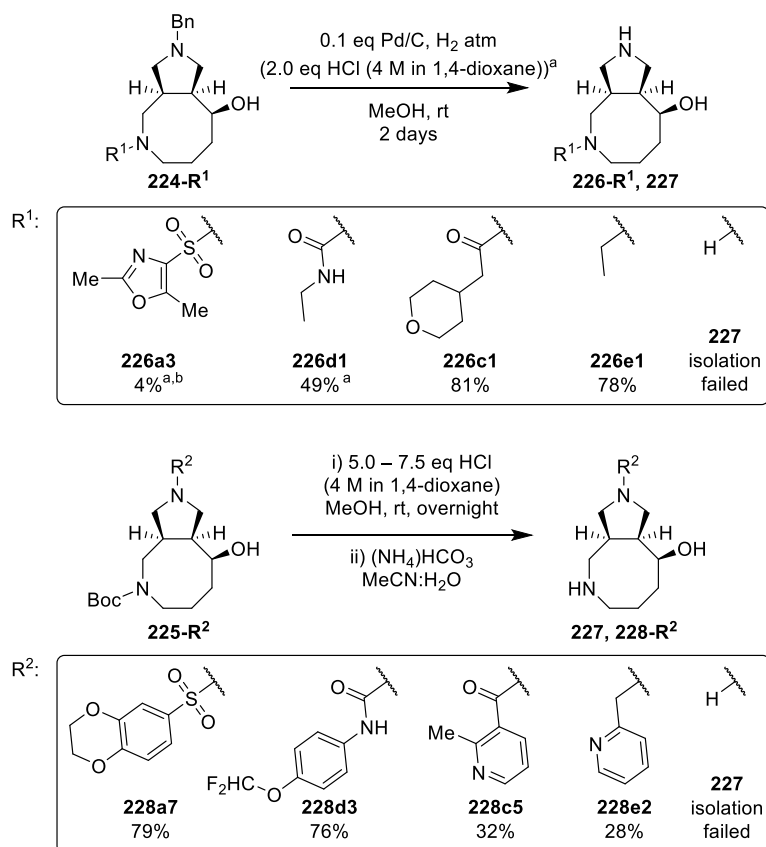
Scheme 90: Validation of deprotection chemistry on SACE3 scaffold. *[a]After 2 days, LCMS analysis of the reaction mixture showed no deprotection and 2.0 eq HCl (4 M in 1,4-dioxane) was added. [b]No complete deprotection observed via LCMS analysis before purification.*

The lower yields for urea **226d1**, amide **228c5**, tertiary amine **228e2** and the failure to isolate naked scaffold **227** were attributed to their short retention times on the preparative column used. Therefore, the products had already (partly) eluted before the collection time threshold, resulting in no collection or collection of only the tail of the peak (Table 8, page 64). In addition, the length of the tail of amide **228c5** exceeded the set fraction collection time limit, as a maximum of collection tubes was filled. Naked scaffold **227** eluted entirely before the collection time threshold and hence was not collected, although LCMS analysis of the deprotection of both Boc-protected **224** and Bn-protected **225** precursors did show complete deprotection.

7.6. X-ray structure validation

Due to previous inconclusive NMR spectroscopic analyses (see Section 7.1 and 7.3.3), a crystal structure was necessary to confirm the relative stereochemistry of the 5-8 fused pyrrolidine and alcohol for all SACE3 library compounds and precursors. Since no library precursors were found to be crystalline solids, an initial attempt was to protect the 8-5 core scaffold with a *p*-nosyl group, since this protecting group had yielded crystalline compounds for *cis*-diastereomer *cis*-**102** (see Section 3.2.3). Both *p*-nosyl analogues **229** and **230** were obtained in acceptable yields (Scheme 91). Benzylamine **229** was isolated as a yellow oil and whilst Boc-amine **230** was isolated as a white solid foam, slow cooling in *i*-PrOH, EtOAc or MeCN did not yield any crystals, nor did oversaturation in these solvents by slow evaporation or slow evaporation of a heptane:EtOAc solution.
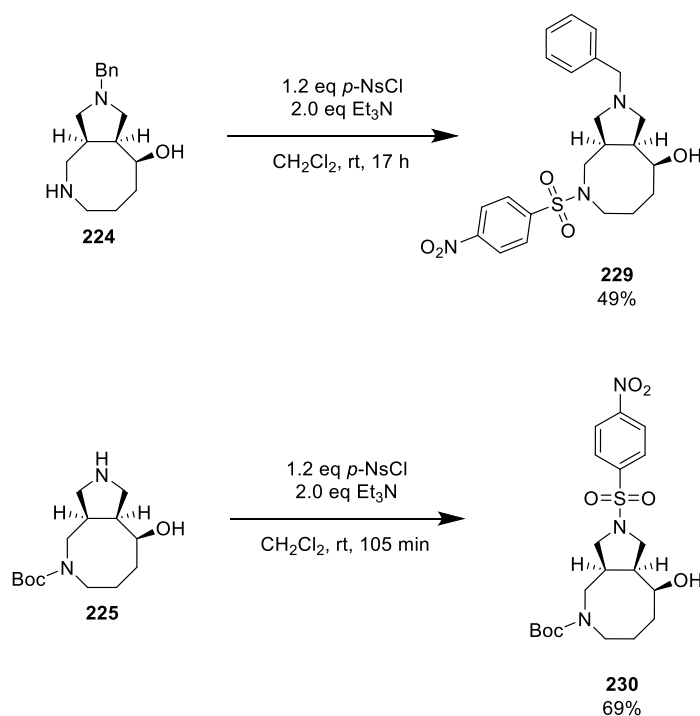
*Scheme 91: Synthesis of p-nosylamines **229** and **230** did not yield crystalline material.*

Fortuitously, one of the compounds synthesised in the validation set was crystalline: Boc-deprotected urea **228d3** could be recrystallised in an NMR tube by slow cooling in *i*-PrOH; this yielded sufficiently large prisms for X-ray structure determination (Figure 65).
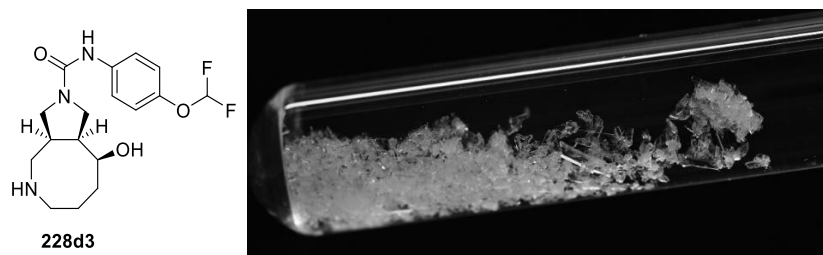
*Figure 65: NMR tube containing recrystallised urea **228d3**.*

The crystal structure of bicycle **228d3** confirmed the *cis* ring fusion (Figure 66, Section 7.1.1), which is in accordance with the concerted nature of 1,3-dipolar cycloadditions.[9] The ring junction C-2 next to the alcohol was oriented pseudo-axially on the eight-membered ring and the other ring junction C-3 pseudo-equatorially, which resulted in the fused pyrrolidine facing a convex face of the chair-boat. As was expected, reduction of the ketone from the convex face was consistent with the observed alcohol stereochemistry. Interestingly, the alcohol forms an intramolecular H-bond with the transannular secondary nitrogen (Figure 66, B). Although this observation does not guarantee the presence of an intramolecular H-bond in solution, it does make these types of Boc-deprotected 8-5 fused rings interesting for biological testing: pre-organisation of the ring conformation by an intramolecular H-bond could increase biological potency by lowering its conformational entropy.[34–36] Furthermore, an intramolecular H-bond can increase the solubility and permeability of a compound:[37,38] in aqueous media, the intramolecular H-bond is likely to break, enabling the exposed polar moieties to interact with the solvent and thereby increase its solubility; in the 'closed' form, intramolecular H-bonding may shield the polar moieties from the environment, increasing the lipophilicity and membrane permeability.[37,38] Just like the *cis*-diastereomeric *p*-nosylamine ***cis*-102** discussed earlier (see Section 3.2.3), the eight-membered ring in urea **228d3** adopts a chair-boat conformation (Figure 66, A). However, the three connected secondary ring carbons C-5, C-6 and C-7 in **228d3** occupy the chair part of the ring, instead of the boat part observed in urea ***cis*-102**. The phenyl ring is not coplanar with the F_2HC-O-C plane (C-15 – O – C-14 – C-13 dihedral angle = 30.0 °), nor with the urea moiety (C-10 – N – C-11 – C-12 dihedral angle = 29.0 °, (C-10)=O – C-10 – N – C-11 dihedral angle = 47.0°), presumably relieving a steric interaction between the C-15 hydrogen/fluorine and the C-13 *ortho* hydrogen, and between the C-10 carbonyl and the C-12 *ortho* hydrogen (Figure 66, C, D, E).
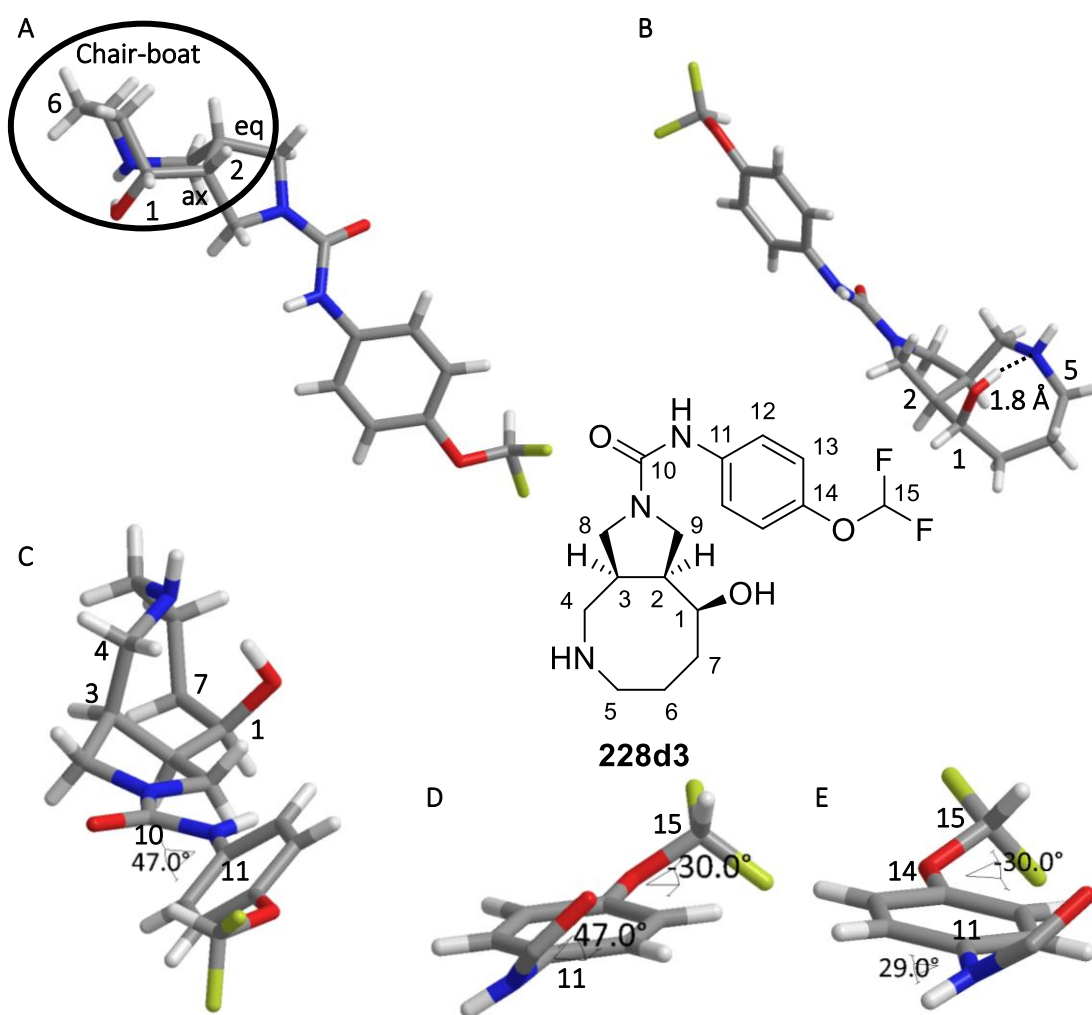
*Figure 66: Crystal structure of urea **228d3**, generated using Chem3D. The 5-8 fused ring is omitted in D and E for clarity. For full experimental data and 50% probability ellipsoid representations at 100 K, see Appendix 8.*

7.7.   Conclusion

An optimised telescoped 1,3-cycloaddition using ylide precursor **176** followed by ketone reduction with L-selectride, allowed the synthesis of fused pyrrolidinyl-hydroxyazocine *cis*-**209** on gramme scale as a single diastereoisomer. Using the ketone cycloaddition product without purification avoided epimerisation of ketone intermediate *cis*-**181**, which was otherwise observed during flash chromatography (Scheme 92). Conformational restriction *via* the fused pyrrolidine facilitated intramolecular attack of the deprotected amine upon Boc deprotection of ketone *cis*-**181** (Scheme 92). The isolated iminium salt *cis*-**195** and its reduced 5-5-5 fused pyrrolizidine diastereomers *cis*-**197** and *trans*-**197** provided experimental proof for this intramolecular attack, which had remained but a hypothesis during the synthesis of the SACE1

library. Initial attempts to derivatise the ketone *cis-181* *via* difluorination and reductive aminations were unsuccessful or non-stereoselective, and attempts to convert the alcohol to an azide or to chemoselectively *O*-methylate also failed. Nevertheless, the alcohol *cis-209* still provided a useful precursor for library synthesis: 18 validation compounds were prepared in good yields using parallel synthesis procedures. Single crystal X-ray diffraction of validation compound **228d3** confirmed the relative configuration of the SACE3 molecules, and the expected stereoselectivity of the 1,3-dipolar cycloaddition and subsequent ketone reduction.
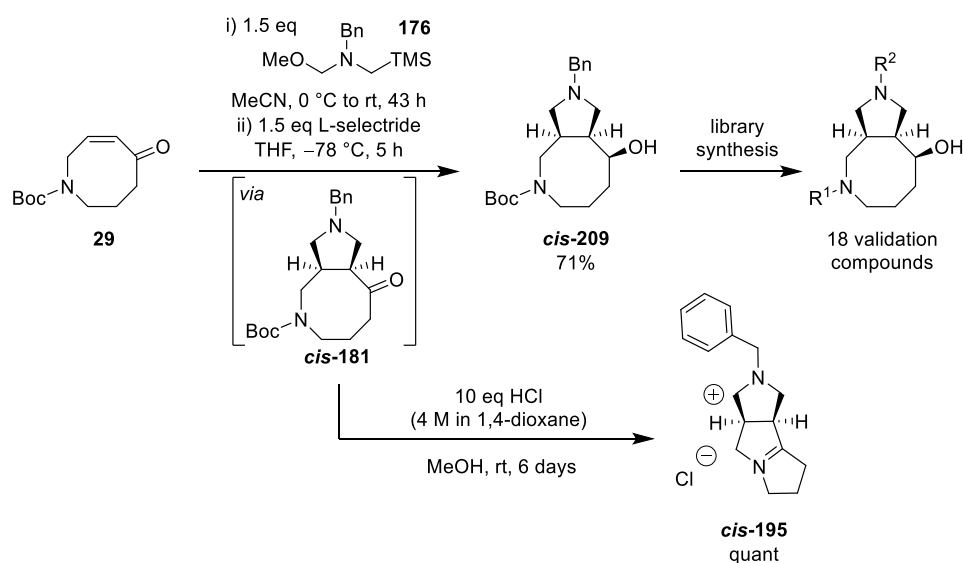
Scheme 92: Overview of the synthetic pathway from parent scaffold **29** towards SACE3 validation compounds and intramolecular cyclisation of ketone **cis-181**, which afforded iminium salt **cis-195**.

7.8.   References

1   C. A. Chang, W. Chen and M. K. Gilson, *Proc. Natl. Acad. Sci. U.S.A.*, 2007, **104**, 1534–1539.

2   E. Vitaku, D. T. Smith and J. T. Njardarson, *J. Med. Chem.*, 2014, **57**, 10257–10274.

3   R. D. Taylor, M. MacCoss and A. D. G. Lawson, *J. Med. Chem.*, 2014, **57**, 5845–5859.

4   L. Moni, L. Banfi, A. Basso, L. Carcone, M. Rasparini and R. Riva, *J. Org. Chem.*, 2015, **80**, 3411–3428.

5   D. R. Rao, R. N. Kankan, P. L. Srinivas, P. Ravikumar, M. Gangrade and S. Kanathala, Process for the synthesis of moxifloxacin hydrochloride, WO2008059223A2, 2008.

6   M. A. Letavic, P. Bonaventure, N. I. Carruthers, C. Dugovic, T. Koudriakova, B. Lord, T. W. Lovenberg, K. S. Ly, N. S. Mani, D. Nepomuceno, D. J. Pippel, M. Rizzolio *et al.*, *J. Med. Chem.*, 2015, **58**, 5620–5636.

7   S. Brooks, G. E. Jacobs, P. de Boer, J. M. Kent, L. Van Nueten, G. van Amerongen, R. Zuiker, I. Kezic, R. Luthringer, P. van der Ark, J. M. van Gerven and W. Drevets, *J. Psychopharmacol.*, 2019, **33**, 202–209.

8   A. Savitz, E. Wajs, Y. Zhang, H. Xu, M. Etropolski, M. E. Thase and W. C. Drevets, *Int. J. Neuropsychopharmacol.*, 2021, **24**, 965–976.

9   M. Breugst and H.-U. Reissig, *Angew. Chem. Int. Ed.*, 2020, **59**, 12293–12307.

10   S. A. Siadati, *Prog. React. Kinet. Mech.*, 2016, **41**, 331–344.

11   A. Padwa and W. Dent, *J. Org. Chem.*, 1987, **52**, 235–244.

12   Y. Terao, H. Kotaki, N. Imai and K. Achiwa, *Chem. Pharm. Bull.*, 1985, **33**, 2762–2766.

13   V. I. Savych, V. L. Mykhalchuk, P. V. Melnychuk, A. O. Isakov, T. Savchuk, V. M. Timoshenko, S. A. Siry, S. O. Pavlenko, D. V. Kovalenko, O. V. Hryshchuk, V. A. Reznik, B. A. Chalyk *et al.*, *J. Org. Chem.*, 2021, **86**, 13289–13309.

14   A. Padwa, Y. Y. Chen, W. Dent and H. Nimmesgern, *J. Org. Chem.*, 1985, **50**, 4006–4014.

15   M. E. Kopach, A. H. Fray and A. I. Meyers, *J. Am. Chem. Soc.*, 1996, **118**, 9876–9883.

16   M. Umehara, S. Hishida, K. Fujieda, H. Ogura and H. Takayanagi, *Bull. Chem. Soc. Jpn.*, 1978, **51**, 2449–2450.

17   G. Mehta and J. D. Umarye, *Tetrahedron Lett.*, 2001, **42**, 8101–8104.

18   B. M. Trost and J. R. Parquette, *J. Org. Chem.*, 1994, **59**, 7568–7569.

19   V. J. Santora, J. A. Covel, R. Hayashi, B. J. Hofilena, J. B. Ibarra, M. D. Pulley, M. I. Weinhouse, D. Sengupta, J. J. Duffield, G. Semple, R. R. Webb, C. Sage *et al.*, *Bioorganic Med. Chem. Lett.*, 2008, **18**, 1490–1494.

20   N. Papaioannou, J. T. Blank and S. J. Miller, *J. Org. Chem.*, 2003, **68**, 2728–2734.

21   E. Roeder, *Pharmazie*, 2000, **55**, 711–726.

22   S. Saha, Ch. Venkata Ramana Reddy and B. Patro, *Tetrahedron Letters*, 2011, **52**, 4014–4016.

23   W. H. Pearson, P. Stoy and Y. Mi, *J. Org. Chem.*, 2004, **69**, 1919–1939.

24   O. Tsuge, S. Kanemasa, M. Ohe and S. Takenaka, *Bull. Chem. Soc. Jpn.*, 1987, **60**, 4079–4089.

25   G. Poli and G. Giambastiani, *J. Org. Chem.*, 2002, **67**, 9456–9459.

26   C. Daubié and S. Mutti, *Tetrahedron Lett.*, 1996, **37**, 7743–7744.

27   V. Dragojlovic, *Molecules*, 2000, **5**, 674–698.

28   A. Casimiro-Garcia, J. W. Strohbach, D. Hepworth, F. E. Lovering, C. Choi, C. P. Allais and S. W. Wright, Novel pyrimidine carboxamides as inhibitors of vanin-1 enzyme, WO2018011681A1, 2018.

29   V. V. Rostovtsev, L. G. Green, V. V. Fokin and K. B. Sharpless, *Angew. Chem. Int. Ed.*, 2002, **41**, 2596–2599.

30   A. S. Thompson, G. R. Humphrey, A. M. DeMarco, D. J. Mathre and E. J. J. Grabowski, *J. Org. Chem.*, 1993, **58**, 5886–5888.

31   S. hwa Jung, K. Choi, A. Nim Pae, J. Kyun Lee, H. Choo, G. Keum, Y. Seo Cho and S.-J. Min, *Org. Biomol. Chem.*, 2014, **12**, 9674–9682.

32   W. Wang and R. MacKinnon, *Cell*, 2017, **169**, 422-430.e10.

33   M. Studer and H.-U. Blaser, *J. Mol. Catal. Chem.*, 1996, **112**, 437–445.

34   L. Chan, G. M. Morris and G. R. Hutchison, *J. Chem. Theory Comput.*, 2021, **17**, 2099–2106.

35   W. G. Harter, H. Albrect, K. Brady, B. Caprathe, J. Dunbar, J. Gilmore, S. Hays, C. R. Kostlan, B. Lunney and N. Walker, *Bioorg. Med. Chem. Lett.*, 2004, **14**, 809–812.

36   T. Honda, H. Nagahara, H. Mogi, M. Ban and H. Aono, *Bioorg. Med. Chem. Lett.*, 2011, **21**, 1782–1785.

37   B. Kuhn, P. Mohr and M. Stahl, *J. Med. Chem.*, 2010, **53**, 2601–2611.

38   G. Caron, J. Kihlberg and G. Ermondi, *Med. Res. Rev.*, 2019, **39**, 1707–1729.

8. Validation of SACE library compounds

8.1. Library compounds: overview

Having synthesised two libraries and a validation set for a third, we compared the three sets to see if they displayed different coverage and ranges of the discussed descriptor space. In terms of MW/SlogP, the SACE3 validation set covered a uniquely high SlogP space for low MW values, which was attributed to compounds containing the Bn-protected amine (Figure 67, A, B, D). Moreover, despite the presence of an alcohol and free amine moieties, the SACE3 validation set did not cover the same low SlogP ranges as the SACE1 and SACE2 libraries. Overall, the SACE2 library covered the largest areas of MW/SlogP and MW/TPSA. At first sight, this would be explained by the larger size of the SACE2 library, but careful analysis shows that a 4 × 11 subset consisting of the 4-fluorophenyl, benzyl, pyridinyl and unsubstituted pyrazole series already covers a significant part of the MW/SlogP space defined by the 11 × 11 library (Figure 67, C). Furthermore, the high TPSA space covered by the SACE2 aminopyrimidine series was not covered by the SACE1 and SACE3 libraries, consolidating the added value of this series.
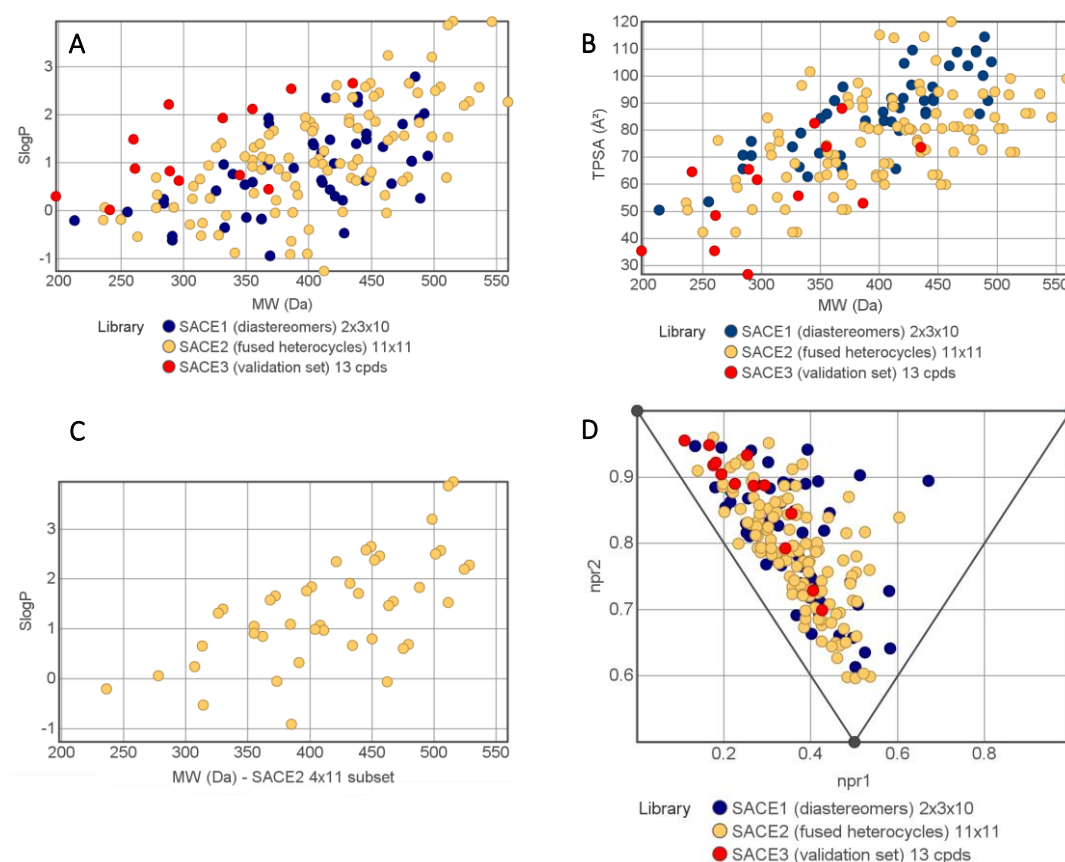
Figure 67: Comparison of the three virtual libraries (A, B, D). MW/SlogP area covered by the SACE2 4 × 11 library subset (C).

167

An explanation for the superior descriptor space coverage by the SACE2 library may be found in its building blocks. In contrast to the SACE1 library, the SACE2 library contained 11 diverse building blocks of different sizes with different chemical moieties, while the SACE1 library had only three small R-groups for its six building blocks. These findings are in accordance with the observed loss in descriptor space coverage, when the 2 × 10 × 10 SACE1 library design was reduced to 2 × 3 × 10 for practical reasons. Nevertheless, this does not mean that more building blocks will always lead to better coverage of descriptor space, as the *in silico* experiments in Section 6.4 showed that extra 8-6 fused pyrimidine series did not cover extra descriptor space for the SACE2 library.

In conclusion, these results indicate that a well-chosen set of building blocks and reagents can maximise the diversity obtained for a combinatorial library built around one scaffold, limited by the nature of the scaffold. This supports the argument for focusing on diverse scaffold design instead of synthesising excessively large combinatorial libraries,[1] which is illustrated by the SACE1 and SACE2 libraries covering unique spaces with higher sphericity in the PMI plot.

8.2.   *In silico* validation of SACE libraries

In order to showcase the relevance of the SACE libraries for drug discovery, the three libraries were combined and compared to a subset of FDA-approved small-molecule drugs in the DrugBank database (see Appendix 5.1).[2] In order to compare like with like, the subset was filtered for compounds with 190 Da < MW < 560 Da, so that only molecules of similar size were compared. A first observation was that the SACE libraries were situated in the same descriptor space as the DrugBank database (Figure 68). However, the SACE libraries showed a few characteristic trends, which are noteworthy. The SACE libraries covered a low SlogP area in comparison with the DrugBank subset, which is in accordance with an often observed increase in logP as molecules progress from hit to lead.[3] In this way, the SACE library compounds allow for tailoring SlogP values by addition of lipophilic groups, whilst providing a low SlogP limit. This is not undesirable as studies have shown that more lipophilic compounds have a higher attrition rate in both drug discovery and drug development.[4] Over two thirds of the DrugBank subset (432 compounds) showed a TPSA below 90 $Å^2$, whilst the SACE libraries contained 143 compounds with TPSA < 90 $Å^2$ (74%). This may indicate a relative increase in potential for BBB penetration by SACE compounds, as the threshold for BBB penetration is generally set at < 90 $Å^2$.[5] Analysis of the PMI plot showed that 173 compounds of the DrugBank subset have npr1 < 0.2 and npr2 > 0.9, which is a significant portion of the used subset (27%). By contrast, only 9

compounds of the SACE combined library design (5%) occupy this space, demonstrating the relative enrichment in more disk- and sphere-like compounds.
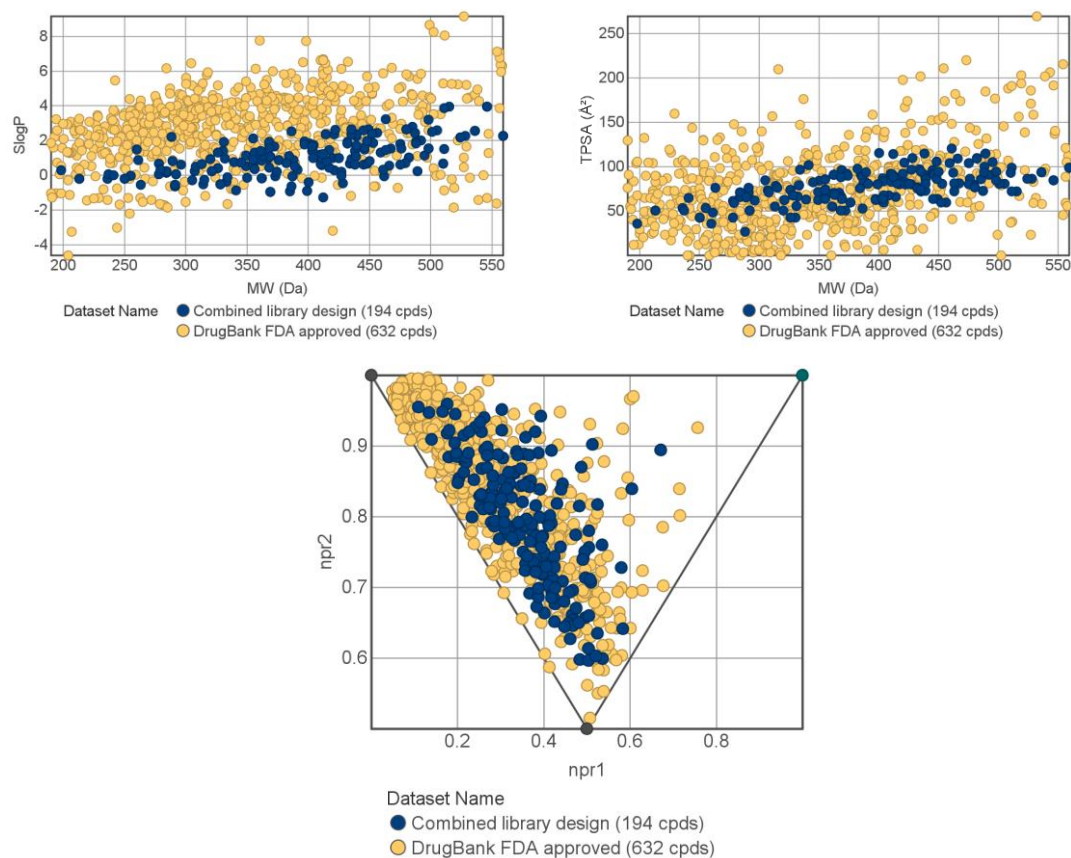
Figure 68: The combined library design covered space occupied by FDA-approved drugs, while showing a lower average SlogP and significantly more disk- and sphere-like compounds than the DrugBank subset.

8.2.1.   Principal component analysis

Since the SACE libraries were designed using Symeres' in-house reagent database, it was expected that a small scaffold consisting of C, N and O without any exotic functional groups would be situated in a similar MW/SlogP/TPSA space compared to other small-molecule drugs. However, this does not mean that the SACE libraries might not cover a unique multidimensional space (*e.g.,* a unique combination of MW/SlogP/TPSA/Fsp^3/sphericity/#H-bond donors/#H-bond acceptors). In order to investigate this possibility, principal component analysis (PCA) was performed on the SACE libraries and DrugBank subset, allowing for a representation of

multidimensional descriptor space in a 3D plot.[a,6] In this way, the DrugBank subset and SACE libraries were compared in multidimensional MW/SlogP/TPSA/Fsp^3/#H-bond donors/#H-bond acceptors/npr1/npr2 space. Important to note is that the resulting PCA space for both analyses is no longer chemically interpretable and therefore will only be used to show similarity or difference between the two sets.[8]
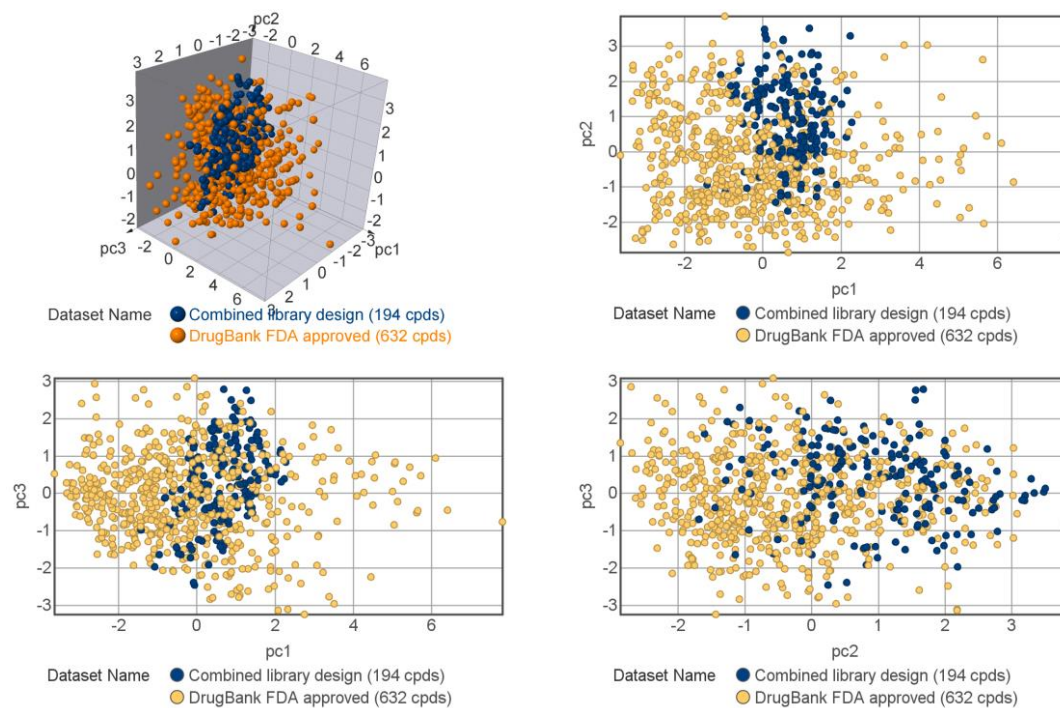
Figure 69: Principal component analysis of the DrugBank subset and SACE libraries, giving a 3D representation of the multidimensional MW/SlogP/TPSA/Fsp^3/#H-bond donors/#H-bond acceptors/npr1/npr2 space. For statistical values, see Appendix 5.2.

The PCA plots show that the SACE combined library occupies a similar MW/SlogP/TPSA/Fsp^3/#H-bond donors/#H-bond acceptors/npr1/npr2 space to the DrugBank subset. This means that the properties of the SACE library in this space are similar to FDA-approved molecules, which makes them relevant for drug discovery and may indicate their potential for biological activity according to the neighbourhood principle.[9–11]

---

[a] PCA constructs a new set of variables (principal components, pcs) as linear combinations of the existing set of variables (which may be highly correlated), which maximise the perceived variance in multidimensional space. Calculation of these pcs is stepwise, so pc1 will explain the largest amount of variance.[6,7] Performing principal component analysis in DataWarrior yields the explained variance percentages for every pc and the contributions of every variable to every pc, expressed in eigenvalues.

8.2.2.   Molecular similarity

Whilst physicochemical properties play a significant role in the ADME profile of a drug, specific interactions with biological targets are governed by the precise spatial organisation of interacting H-bond donors/acceptors, hydrophobic or aromatic moieties, or covalent binders. Therefore, our compounds were designed to show similar physicochemical properties with marketed drugs, illustrating their drug-like properties (assessed in the PCA plot above) whilst also being structurally dissimilar to marketed drugs. In this way, the synthesised library compounds would represent structurally novel molecules with drug-like properties, making them attractive for novel hit discovery and novel target identification. Assessment of similarity was made by calculating the maximum Tanimoto similarity (Tc_{max}) between every SACE library compound and the FDA-approved DrugBank subset, based on ECFP6 fingerprints. The maximum Tanimoto similarity (which is the Tanimoto similarity between a SACE compound and its most similar neighbour in the DrugBank subset)[12] was chosen over the average Tanimoto similarity to mitigate possible bias introduced by over-representation of structurally similar compounds in the compared sets.[a] For comparison of a random dataset with a reference dataset of bioactive compounds using ECFP fingerprints, a Tc_{max} value lower than 0.4 has been reported to yield subsets which are enriched with similarly bioactive, but structurally distinct scaffolds.[13] Hence, using the DrugBank subset of FDA-approved drugs as a reference set, synthesised compounds with Tc_{max} values lower than 0.4 were considered to show increased potential of delivering structurally novel bioactive compounds.

The SACE physical library showed significant structural novelty. Compared to the DrugBank subset, Tc_{max} values no higher than 0.3 were observed, whilst the majority of SACE compounds displayed Tc_{max} values between 0.15 and 0.21 (Figure 70). The physical iDESIGN compound library (which comprises 651 compounds from six different PhD projects) (Figure 71), including 186 of SACE library compounds, showed similar Tanimoto similarity with the DrugBank subset ranging between $Tc_{max} = 0.12 - 0.36$.

---

[a] The presence of one very similar compound in the DrugBank subset would not be noticed if the average Tanimoto distance is used, while this would have implications for the novelty of our compounds.

SACE vs DrugBank similarity

iDESIGN vs DrugBank similarity
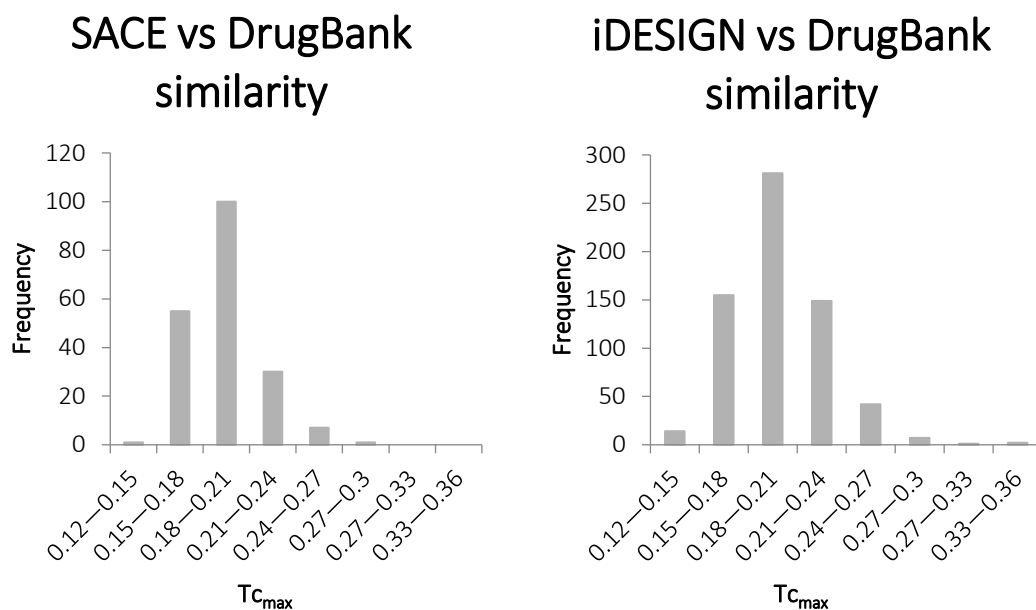
Figure 70: Tc_{max} distribution for the synthesised SACE library (194 compounds) and physical iDESIGN library (651 compounds), using the FDA-approved DrugBank subset (632 compounds) as reference.

Comparison of the SACE and iDESIGN histograms shows that the SACE library compounds display relatively more dissimilarity to the DrugBank dataset than to the iDESIGN library (Figure 70). Nonetheless, the calculated Tanimoto similarities confirm the structural novelty of the iDESIGN compounds, fulfilling the aim of providing novel starting points for drug discovery.
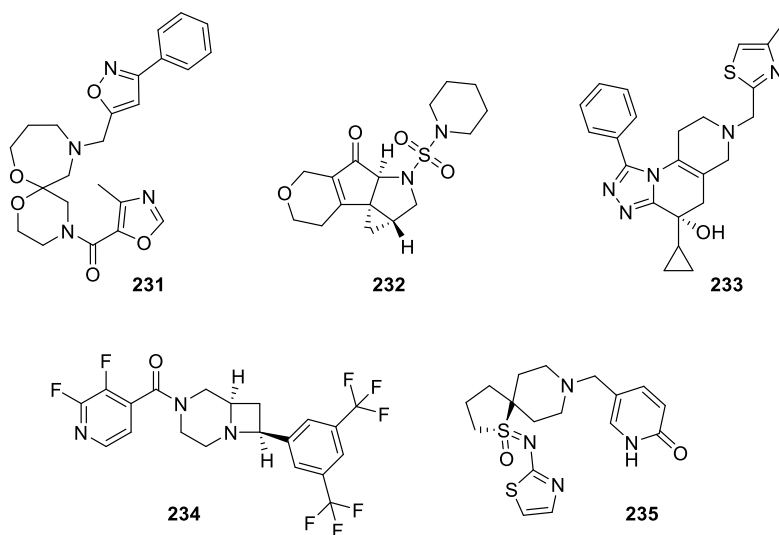
Figure 71: Exemplar compounds present in the iDESIGN library.

In conclusion, the SACE library occupies similar physicochemical property space to FDA-approved molecules of similar molecular weight, whilst combining this similar space coverage

with a relative enrichment in disk- and sphere-like molecules, low SlogP and low TPSA. Tanimoto distance calculations showed significant structural dissimilarity with the FDA-approved reference set, validating the compounds as structurally novel compounds with drug-like properties. Therefore, the SACE library was deemed an attractive compound set for biological screening.

8.3. Experimental validation of SACE libraries

8.3.1. Experimental logD measurement

Calculated logP values can differ significantly from pH-dependent experimental logD values.[14,15] Since logP does not take into account the protonation state of basic amines under physiological conditions, which decreases the lipophilicity of a compound, lower ElogD (7.4) values, compared to logP values, were expected for our library compounds.[16] Therefore, a representative selection of library compounds[a] was therefore submitted for ElogD (7.4) determination by the Symeres Analytical Department to assess the calculated SlogP values used for *in silico* validation of the synthesised compound libraries.[b]

The ElogD (7.4) values determined for the 20 compounds submitted for analysis (Figure 72), were indeed generally lower than their calculated SlogP values (Table 18). The calculated SlogP showed the same relative trends as ElogD (7.4) for both SACE1 and SACE2 libraries with only one exception, namely SACE2 thiazole **144c1**, which could not be rationalised (pK_a thiazole-H$^+$ = 2.5). Furthermore, the obtained ElogD (7.4) values still covered a large range (<0.2 to 3.5), which reflected our efforts to maximise SlogP coverage (–0.9 to 3.9). The largest difference between calculated SlogP and ElogD (7.4) was observed for the SACE3 compounds, with [SlogP] – [ElogD (7.4)] values ranging from –1.1 to > 2.0. For Bn-protected SACE3 compounds **224d1** and **224e1**, and *N*-alkylated amine **228e2**, the large difference between SlogP and ElogD (7.4) can be explained by the basicity of the alkylated amines [pK_a (R_3NH)$^+$ ~ 11]. Benzodioxane sulfonamides **129a7** and **225a7** showed significantly higher ElogD (7.4) values than SlogP, which could be attributed to overestimation of the hydrophilicity of the heteroatoms.

---

[a] The compounds were chosen manually to reflect the MW/SlogP range and functional group diversity of their library.
[b] SlogP was calculated using the 'RDKit Descriptor calculation' node in KNIME, using the SlogP calculation reported by Wildman and Crippen.[17]

trans-108d1   *trans*-105a3   *trans*-106d4

cis-105d1   *cis*-106c4   *cis*-108c6

132a4   122   154c5

130d1   135a3   144c1

129a7   126d3   226c1

228e2   224d1

225c5   224e1   225a7
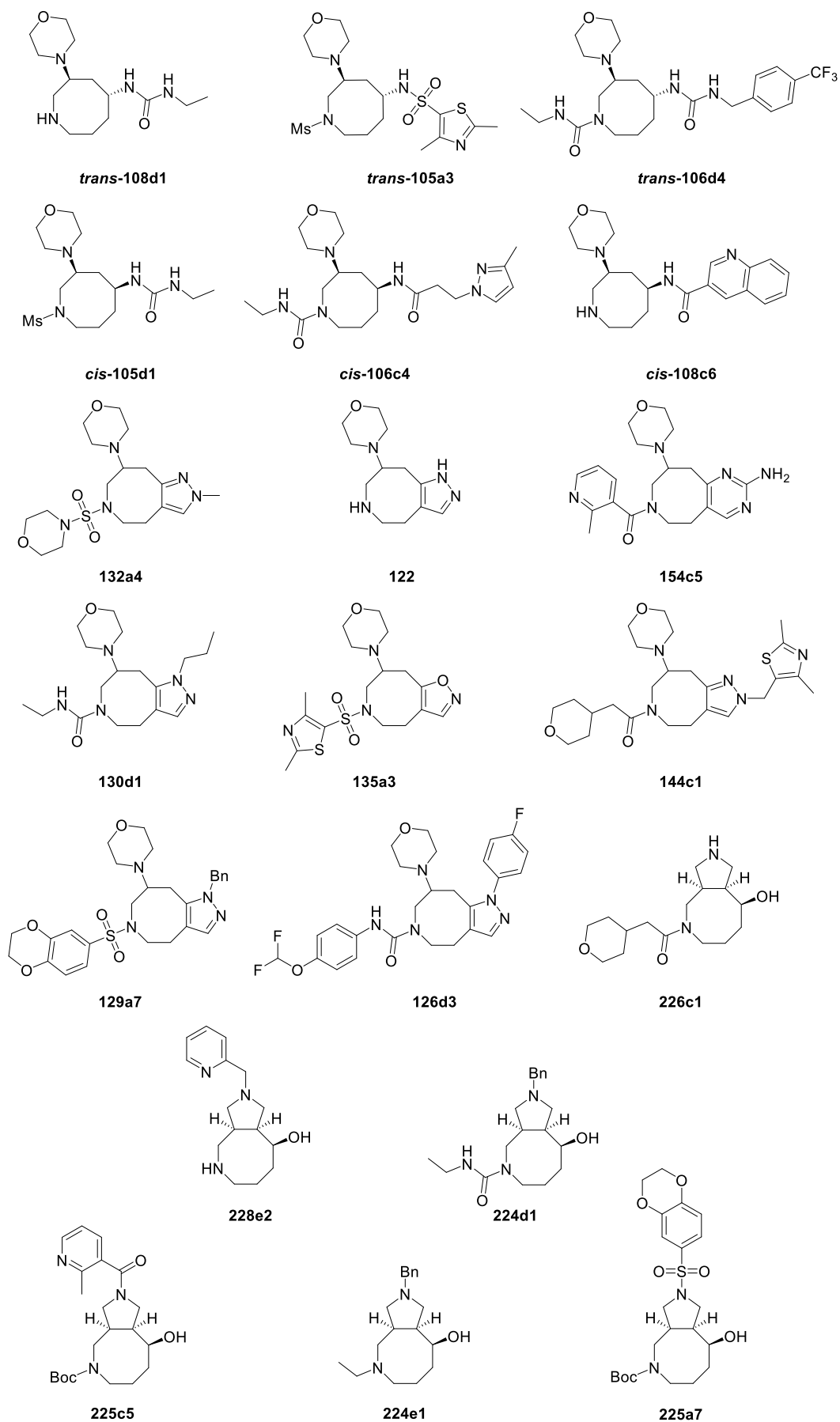
Figure 72: 20 compounds submitted for ElogD measurement

174

Table 18: ElogD values measured for 20 representative library compounds.

Library	Compound	Calculated SlogP	Average ElogD (7.4) (n = 3)	[SlogP] – [ElogD (7.4)][a]
SACE1	*trans*-105a3	0.6	0.8	−0.2
SACE1	*trans*-106d4	2.8	3.1	−0.3
SACE1	*trans*-108d1	0.2	<0.2[b]	<0.0
SACE1	*cis*-105d1	−0.2	<0.2[b]	n.a.
SACE1	*cis*-106c4	1	0.4	0.6
SACE1	*cis*-108c6	1.8	0.7	1.1
SACE2	122	−0.2	<0.2[b]	n.a.
SACE2	126d3	3.9	3.5	0.4
SACE2	129a7	2.2	3.2	−1.0
SACE2	130d1	1.1	0.7	0.4
SACE2	132a4	−0.9	<0.2[b]	n.a.
SACE2	135a3	1.2	1.3	−0.1
SACE2	144c1	1.6	0.5	1.1
SACE2	154c5	0.7	<0.2[b]	>0.5
SACE3	224d1	1.9	<0.2[b]	>1.7
SACE3	224e1	2.2	<0.2[b]	>2.0
SACE3	225a7	2.1	3.2	−1.1
SACE3	225c5	2.5	1.4	1.1
SACE3	226c1	0.6	1.3	−0.7
SACE3	228e2	0.9	0.2	0.7

[a] n.a., not applicable. [b] Compounds with ElogD <0.2 produced data points which fell below the range of the calibration curve or co-eluted with the internal standard, preventing accurate measurement of ElogD.

Hence, the SlogP values were considered useful to compare relative lipophilicity between compounds sharing a common scaffold, with an additional flag, noting the presence of basic amines can be expected to result in lower ElogD values. With ElogD (7.4) values well below 5.0, our synthesised compounds should be amenable to functionalisation or analogue generation with lipophilic moieties without impairing their oral bioavailability.[16]

8.3.2. Storage stability test

As compound libraries are often stored indefinitely in stock solutions at low temperatures, it is important to assess the stability of these compounds as degradation of the compound will interfere with biological screening assays. Performing a stability test at room temperature over the course of a month was deemed a sufficient indicator of compound stability in DMSO solution upon long-term storage in a fridge or freezer, given lower storage temperatures will decrease the rate of any possible degradation reaction. Hence, 5 mM solutions of our compounds (Figure 73) in DMSO were stored at rt in a closed cupboard. The solutions were not

purged with inert gasses, nor stored under an inert atmosphere. Providing a semi-quantitative[a] measurement of compound purity (and hence stability) *via* analysis of the UPLC PDA chromatogram (210 – 320 nm), 16 out of the 18 library compounds measured showed little (<5%) to no degradation, whilst two compounds showed <20% degradation (Table 19). However, since compounds *cis*-105d1 and **228e2** both were poorly UV active, there is a chance that more UV-active trace impurities may have interfered with the UV purity measurement. These results indicated no serious stability concerns for the synthesised compound libraries upon long-term storage in DMSO at low temperatures, which is an attractive property for members of a compound screening collection.

Table 19: Compound stability upon storage in DMSO (5 mM) under ambient conditions.

Library	Compound	UV Purity (%)[a] t = 0	UV Purity (%)[a] t = 30 days
SACE1	*trans*-105a3	100	99
SACE1	*trans*-106d4	100	100
SACE1	*cis*-105d1	100	84
SACE1	*cis*-108c6	96	96
SACE1	*cis*-106c4	97	97
SACE2	126d3	100	100
SACE2	129a7	100	99
SACE2	122	100	94
SACE2	135a3	100	100
SACE2	132a4	100	100
SACE2	154c5	100	99
SACE2	130d1	100	100
SACE2	144c1	86	100
SACE3	224d1	100	95
SACE3	224e	100	100
SACE3	255a7	100	100
SACE3	225c5	100	100
SACE3	228e2	99	83

[a]Purity measured *via* UPLC (reverse-phase, basic) calculated as product peak AUC fraction in the total absorbance chromatogram (210 – 320 nm).

---

[a] Acknowledging that degradation products may have different absorption coefficients, preventing quantitative interpretation of relative area under the curve without further investigation and calibration.
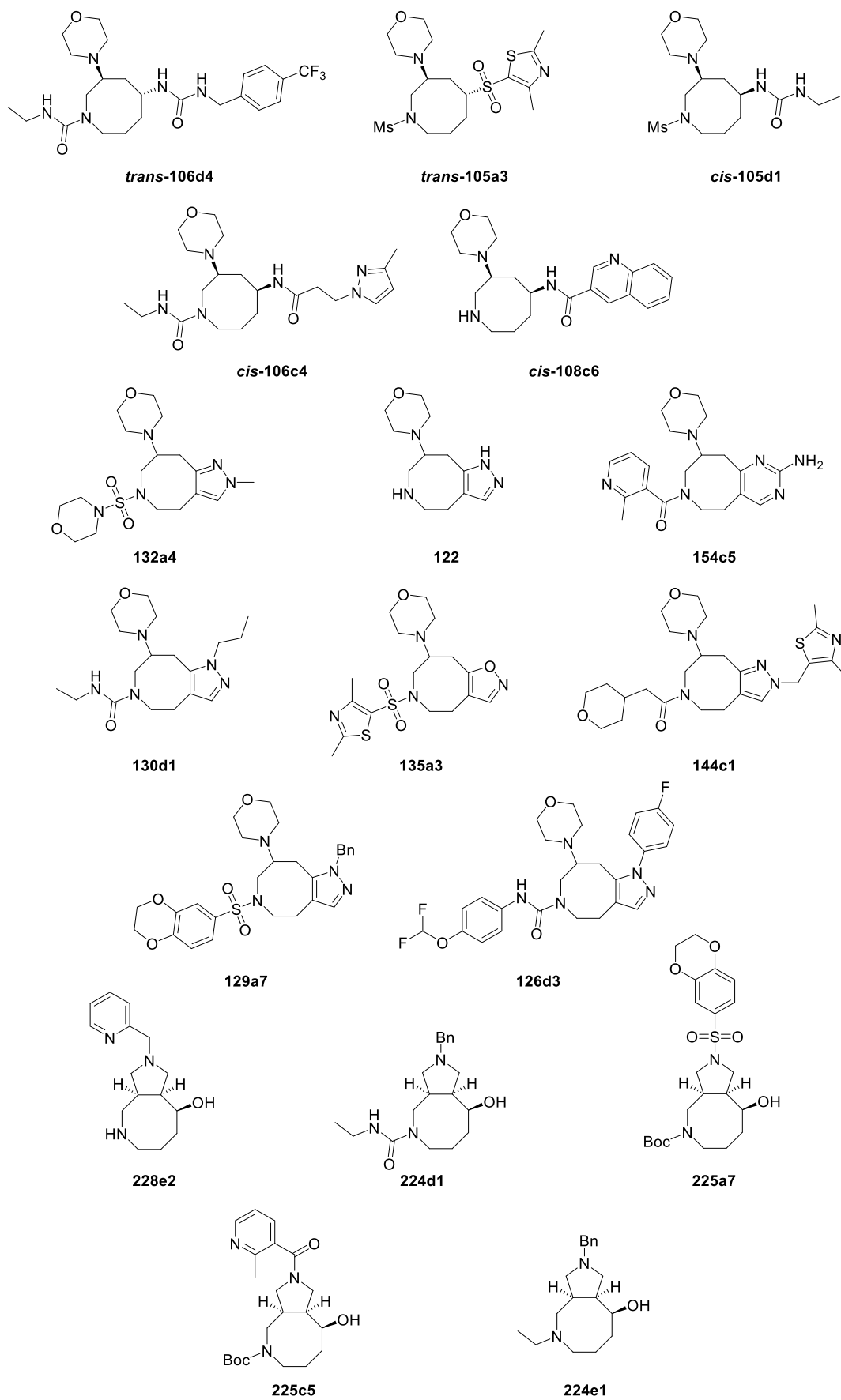
Figure 73: Compounds tested for stability upon storage in DMSO.

8.3.3. hERG screening

Besides its potency against a clinical target, it is of utmost importance that a drug molecule is well tolerated by the patient. Since off-target interactions of a drug molecule (or its metabolites) may cause adverse side-effects or even death, critical assessment of a compound's toxicity plays a key role in drug discovery. In fact, drug safety is a major cause of drug attrition.[18] Therefore, early identification of safety risks decreases the chance of late-stage attrition and concomitantly saves time and resource.[19] Hence, it was attractive to screen a selection of our compounds for a major liability in cardiovascular safety, namely hERG inhibition.[18,20]

The human ether-à-go-go (hERG) channel (also known as Kv11.1)[21,22] is a transmembrane potassium channel, involved in the regulation of cardiac action potentials.[20,23] Inhibition of this channel results in prolongation of the QT interval on the electrocardiogram, which can result in a type of cardiac arrhythmia called Torsades des Pointes (TdP) and ultimately cardiac arrest.[18,20,21,23–25] Therefore, hERG activity is a critical safety concern, and was responsible for approximately one third of drug attrition between 1990 and 2006.[18,26] Although several hypotheses exist regarding the binding mode and pharmacophore of hERG inhibitors,[23] it is generally accepted that the presence of a basic nitrogen surrounded by hydrophobic and aromatic groups is likely to facilitate hERG inhibition,[22] as illustrated by the pharmacophore models generated by Ekins et al.,[27] Cavalli et al.[28,29] and Kratz et al.[30] (Figure 74). Wang and MacKinnon determined the structure of the hERG channel via cryo-electron microscopy. This structure reveales three hydrophobic pockets which extend from a central cavity with negative electrostatic potential.[21] Since a basic nitrogen is protonated under physiological conditions, the resulting cation can favourably interact with the central cavity.[21]
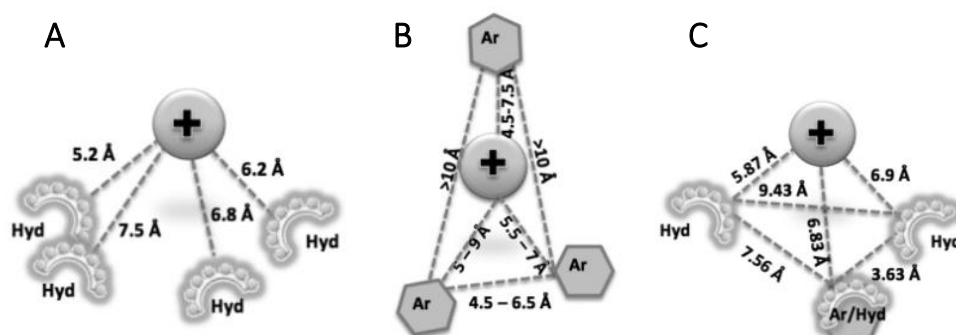
Figure 74: hERG inhibitor pharmacophore models by Ekins et al. (**A**),[27] Cavalli et al (**B**).[28,29] and Kratz et al. (**C**).[30] "+" denotes a positively ionisable group, "Ar" aromatic groups, "Hyd" hydrophobic moieties.[a]

---

[a] Figure reprinted with permission from Kalyaanamoorthy and Barakat.[22]

Examples of hERG inhibitors can be found in drugs which were discontinued by the FDA, due to observed prolongation of the QT interval; these include cisapride **237**,[31] domperidone **236**[32] (formerly used in antinausea medicine Motilium) and prenylamine **238** (Figure 75).[22,33]

236
domperidone

237
cisapride

238
prenylamine
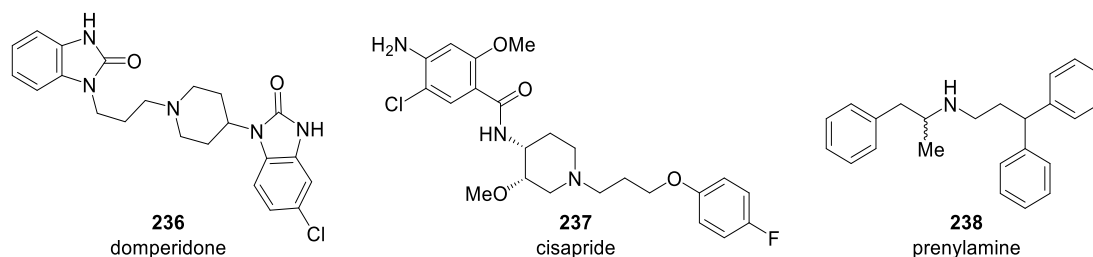
Figure 75: Drug molecules ultimately withdrawn by the FDA owing to hERG inhibition.[22]

In 2016, Yu *et al.* screened approximately 300,000 compounds for hERG inhibition and found that hERG inhibitors typically displayed higher lipophilicity, higher molecular weight and more rotatable bonds than non-inhibitors.[34] Inversely, hERG potency can be mitigated through lowering the logP of a drug,[35] rigidifying the compound structure[36] or decreasing the basicity of the amine.[37] Hence, identification of a hERG inhibitor early in the drug development process can still allow for optimisation towards maximum potency against the primary target and decreased hERG inhibition. In fact, as a guide, hERG inhibition is typically tolerated if the drug is at least thirty times more potent against its primary target:[38] If the drug concentration in the body remains well below the IC_{50} of hERG (the concentration at which 50% of all hERG activity is inhibited), hERG inhibition does not lead to adverse safety effects.

Seven library compounds were selected for hERG screening (Figure 76), representing the diversity of the synthesised compound libraries through different scaffolds, functional groups and appendages. One compound was chosen per scaffold type which was expected to have a higher chance of showing hERG inhibition based on its structural and physicochemical properties: urea *trans*-**106d4** displayed an ethyl group and benzylic moiety on both sides relative to the basic morpholine nitrogen and represented a high-MW subset of the SACE1 library (MW = 485 Da). Phenylurea **126d3** also displayed relatively high MW (515 Da) in the SACE2 library and the presence of two phenyl groups in the vicinity of the basic morpholine nitrogen was postulated to increase the chance of hERG inhibition. Furthermore, the fluorophenyl fragment has been reported to significantly contribute to hERG binding affinity.[39] Benzyl-pyrrolidine **224e1** contained two basic nitrogens and the presence the benzyl and ethyl appendages was hypothesised to increase hERG affinity. In addition, pyrrolidine **224e1** would present a unique low-lipophilicity hERG inhibitor if found active, with ElogD < 0.2.
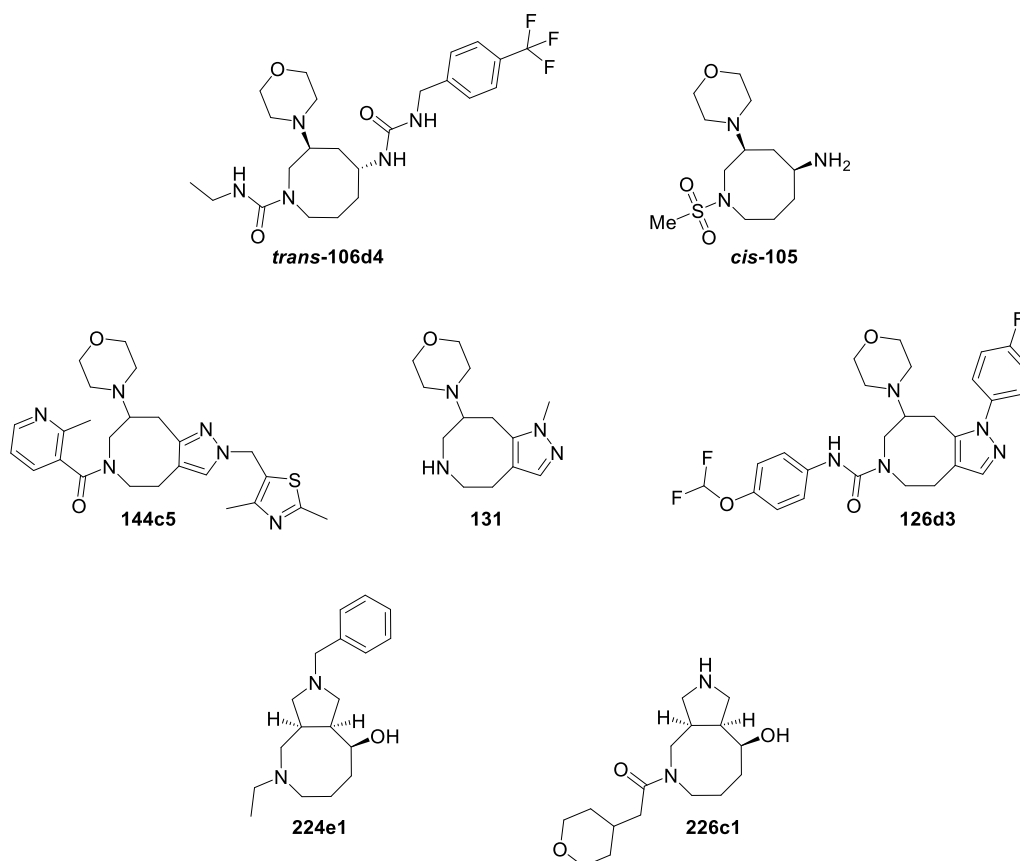
Figure 76: Selected library compounds for hERG screening.

8.3.3.1. *hERG activity assay*

The submitted compounds were screened for hERG activity by Dr Michael Morton, Director and co-founder of ApconiX.[a] The screening was performed at ambient room temperature, using an IonWoks Quattro automated patch-clamp system and CHO-K1 cell line. By measuring the relative decrease in ionic current in whole-cell systems before and 3 minutes after incubation with the screened compound, the percentage of hERG inhibition was determined.[40] Although hERG inhibition can also be measured *via* fluorescence-based assays or radioligand binding assays,[25] the used IonWorks high-throughput electrophysiological assay is considered the gold-standard.[20]

Every compound was divided over four wells containing hERG-expressing cells, which were each measured *in duplo*. A maximum of eight datapoints can therefore be obtained for each compound; however, measurements can fail due to cell debris or air bubbles in the well,

---

[a] For more information, visit www.ApconiX.com.

unstable current amplitudes or poor cell quality.[40] The percentage of hERG inhibition was measured at 30 µM compound concentration. Although single-concentration measurements provide a quick assessment of hERG activity, the obtained average %inhibition values were only interpreted qualitatively. Given the sigmoidal nature of the dose response curve of an inhibitor (Figure 77), concentrations close to the IC_{50} may display significant differences in measured % inhibition. Therefore, average % inhibition values lower than 30% were considered inactive, while values above 50% were considered active and potentially biologically significant.
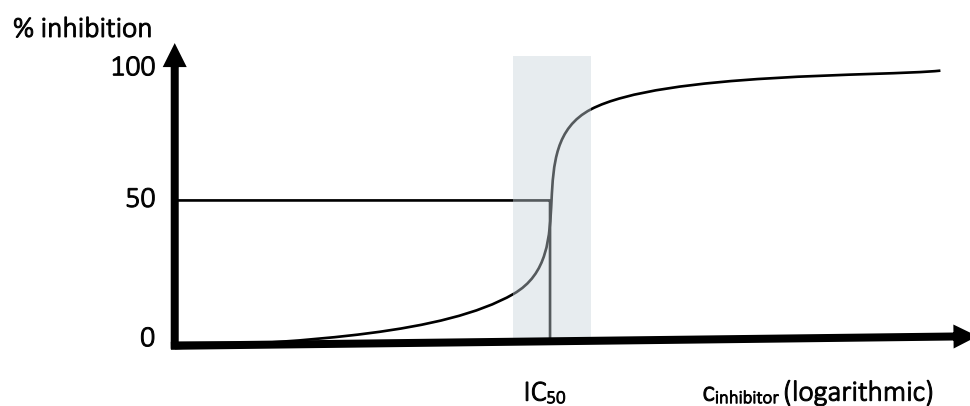
Figure 77: Graphical representation of a dose-response curve. Inhibitor concentrations close to the IC_{50} (highlighted in grey) may display significant differences in measured %inhibition.

Five out of seven screened library compounds displayed low hERG inhibition (Figure 78), while fused 4-fluorophenylpyrazole **126d3** and benzylamine **224e1** showed an average hERG inhibition of 96% and 79%, respectively, confirming their hypothesised hERG activity. Given both of these hERG inhibitors had library analogues which showed low hERG inhibition, these results indicate that the synthesised library scaffolds are not intrinsic hERG inhibitors and that hERG inhibition is likely to be mitigated through optimisation of the appendages. For example, thiazole analogue **144c5** also displayed two aromatic rings and a basic hydrogen, but its lower hERG activity suggests that hERG activity of phenylpyrazole **126d3** could possibly be mitigated by synthesising heteroaromatic analogues or by introducing the aromatic group on the 2-position of the pyrazole moiety (Scheme 93).
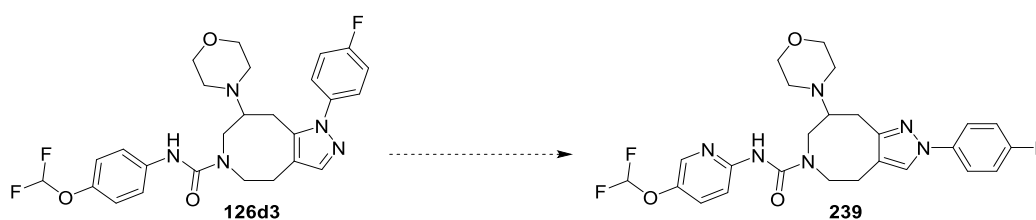
*Scheme 93: Possible modification of **126d3** to mitigate hERG activity.*

Thiazole analogue **144c5** and pyrrolidine **226c1** showed a large spread in recorded % inhibition, 38% and 27% respectively. Given % inhibition is measured on whole cell systems, it is possible that these two compounds are cytotoxic and that the measured currents are influenced by deterioration of the cell during the measurement. The data presented highlights the attractive properties of the synthesised compound libraries for hit screening and the value of recording this safety information early.
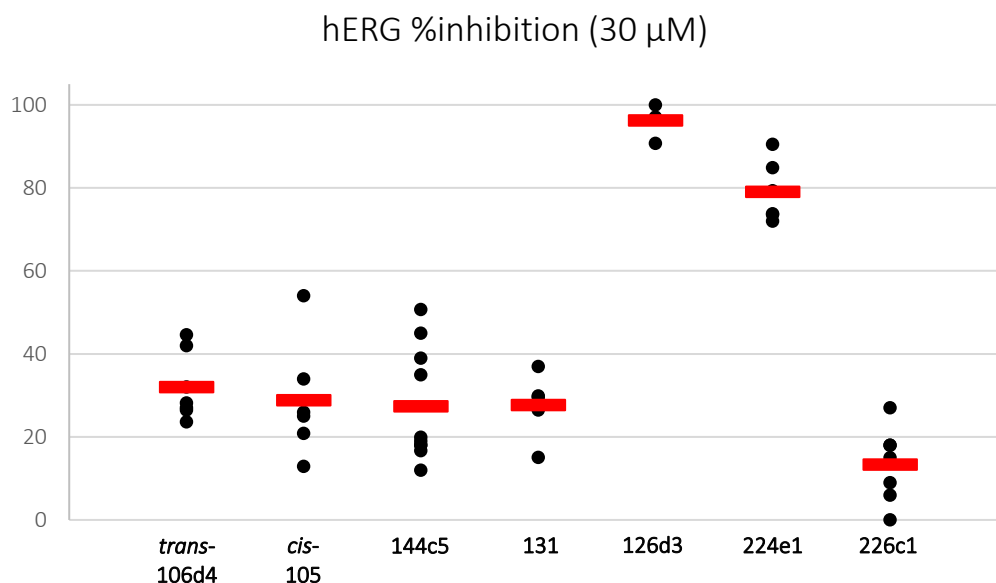
Figure 78: hERG inhibition assay results. Measured data points shown as black dots, average values shown as red bars. For numerical data, see Appendix 5.3.

8.4.   References

1   W. H. B. Sauer and M. K. Schwarz, *J. Chem. Inf. Comput. Sci.*, 2003, **43**, 987–1003.
2   D. S. Wishart, C. Knox, A. C. Guo, S. Shrivastava, M. Hassanali, P. Stothard, Z. Chang and J. Woolsey, *Nucleic Acids Res.*, 2006, **34**, D668-672.
3   G. M. Keserü and G. M. Makara, *Nat. Rev. Drug Discov.*, 2009, **8**, 203–212.
4   S. Lobo, *Expert Opin. Drug Discov.*, 2020, **15**, 261–263.
5   H. van de Waterbeemd, G. Camenisch, G. Folkers, J. R. Chretien and O. A. Raevsky, *J. Drug Target.*, 1998, **6**, 151–165.
6   R. Bro and A. K. Smilde, *Anal. Methods*, 2014, **6**, 2812–2831.
7   Principal Component Analysis, https://openmolecules.org/help/ml.html, (accessed 20 November 2021).
8   L. B. Akella and D. DeCaprio, *Curr. Opin. Chem. Biol.*, 2010, **14**, 325–330.
9   I. Muegge and P. Mukherjee, *Expert Opin. Drug Discov.*, 2016, **11**, 137–148.
10   D. E. Patterson, R. D. Cramer, A. M. Ferguson, R. D. Clark and L. E. Weinberger, *J. Med. Chem.*, 1996, **39**, 3049–3059.
11   V. J. Gillet, *Curr. Opin. Chem. Biol.*, 2008, **12**, 372–378.

12   J. Hert, P. Willett, D. J. Wilton, P. Acklin, K. Azzaoui, E. Jacoby and A. Schuffenhauer, *J. Chem. Inf. Comput. Sci.*, 2004, **44**, 1177–1185.

13   M. Vogt, D. Stumpfe, H. Geppert and J. Bajorath, *J. Med. Chem.*, 2010, **53**, 5707–5715.

14   M. D. Shultz, *J. Med. Chem.*, 2019, **62**, 1701–1714.

15   D. Eros, I. Kövesdi, L. Orfi, K. Takács-Novák, G. Acsády and G. Kéri, *Curr. Med. Chem.*, 2002, **9**, 1819–1829.

16   S. K. Bhal, K. Kassam, I. G. Peirson and G. M. Pearl, *Mol. Pharm.*, 2007, **4**, 556–560.

17   S. A. Wildman and G. M. Crippen, *J. Chem. Inf. Comput. Sci.*, 1999, **39**, 868–873.

18   H. Laverty, C. Benson, E. Cartwright, M. Cross, C. Garland, T. Hammond, C. Holloway, N. McMahon, J. Milligan, B. Park, M. Pirmohamed, C. Pollard *et al.*, *Br. J. Pharmacol.*, 2011, **163**, 675–693.

19   R. A. Roberts, *Drug Discov. Today*, 2018, **23**, 1925–1928.

20   T. Hanser, F. P. Steinmetz, J. Plante, F. Rippmann and M. Krier, *J. Cheminformatics*, 2019, **11**, 9.

21   W. Wang and R. MacKinnon, *Cell*, 2017, **169**, 422-430.

22   S. Kalyaanamoorthy and K. H. Barakat, *Med. Res. Rev.*, 2018, **38**, 525–555.

23   S. Kalyaanamoorthy and K. H. Barakat, *Expert Opin. Drug Discov.*, 2018, **13**, 207–210.

24   G. Y. Di Veroli, M. R. Davies, H. Zhang, N. Abi-Gerges and M. R. Boyett, *Am. J. Physiol. Heart Circ. Physiol.*, 2013, **304**, H104–H117.

25   B. Priest, I. M. Bell and M. Garcia, *Channels*, 2008, **2**, 87–93.

26   R. R. Shah, *Pharmacogenomics*, 2006, **7**, 889–908.

27   S. Ekins, W. J. Crumb, R. D. Sarazan, J. H. Wikel and S. A. Wrighton, *J. Pharmacol. Exp. Ther.*, 2002, **301**, 427–434.

28   A. Cavalli, E. Poluzzi, F. De Ponti and M. Recanatini, *J. Med. Chem.*, 2002, **45**, 3844–3853.

29   A. Cavalli, R. Buonfiglio, C. Ianni, M. Masetti, L. Ceccarini, R. Caves, M. W. Y. Chang, J. S. Mitcheson, M. Roberti and M. Recanatini, *J. Med. Chem.*, 2012, **55**, 4010–4014.

30   J. M. Kratz, D. Schuster, M. Edtbauer, P. Saxena, C. E. Mair, J. Kirchebner, B. Matuszczak, I. Baburin, S. Hering and J. M. Rollinger, *J. Chem. Inf. Model.*, 2014, **54**, 2887–2901.

31   S. Mohammad, Z. Zhou, Q. Gong and C. T. January, *Am. J. Physiol. Heart Circ. Physiol.*, 1997, **273**, H2534–H2538.

32   S. Claassen and B. J. Zünkler, *Pharmacology*, 2005, **74**, 31–36.

33   A. N. Katchman, J. Koerner, T. Tosaka, R. L. Woosley and S. N. Ebert, *J. Pharmacol. Exp. Ther.*, 2006, **316**, 1098–1106.

34   H. Yu, B. Zou, X. Wang and M. Li, *Acta Pharmacol. Sin.*, 2016, **37**, 111–123.

35   J. G. Cumming, H. Tucker, J. Oldfield, C. Fielding, A. Highton, A. Faull, M. Wild, D. Brown, S. Wells and J. Shaw, *Bioorg. Med. Chem. Lett.*, 2012, **22**, 1655–1659.

36   J. F. S. Carvalho, J. Louvel, M. L. J. Doornbos, E. Klaasse, Z. Yu, J. Brussee and A. P. IJzerman, *J. Med. Chem.*, 2013, **56**, 2828–2840.

37   C. Jamieson, E. M. Moir, Z. Rankovic and G. Wishart, *J. Med. Chem.*, 2006, **49**, 5029–5046.

38   W. S. Redfern, L. Carlsson, A. S. Davis, W. G. Lynch, I. MacKenzie, S. Palethorpe, P. K. S. Siegl, I. Strang, A. T. Sullivan, R. Wallis, A. J. Camm and T. G. Hammond, *Cardiovasc. Res.*, 2003, **58**, 32–45.

39   M. Song and M. Clark, *J. Chem. Inf. Model.*, 2006, **46**, 392–400.

40   A. Finkel, A. Wittel, N. Yang, S. Handran, J. Hughes and J. Costantin, *J. Biomol. Screen.*, 2006, **11**, 488–496.

9. Conclusion and Future Work

Azacyclooctenone **29** has been demonstrated to be an attractive starting point for scaffold synthesis. Through an optimised pathway, using RCM as a key step, enone **29** was synthesised on gramme scale, providing sufficient precursor for the synthesis of three compound libraries, comprising 200 novel small molecules with attractive physicochemical properties for drug discovery. The structural diversity of the three synthesised compound libraries illustrated the diversification potential of all reactive sites on this parent scaffold, providing not only novel scaffold structures based on the eight-membered ring, but also different orientation options for appendages relative to the 2° amine embedded within the eight-membered ring 5 (Scheme 94).
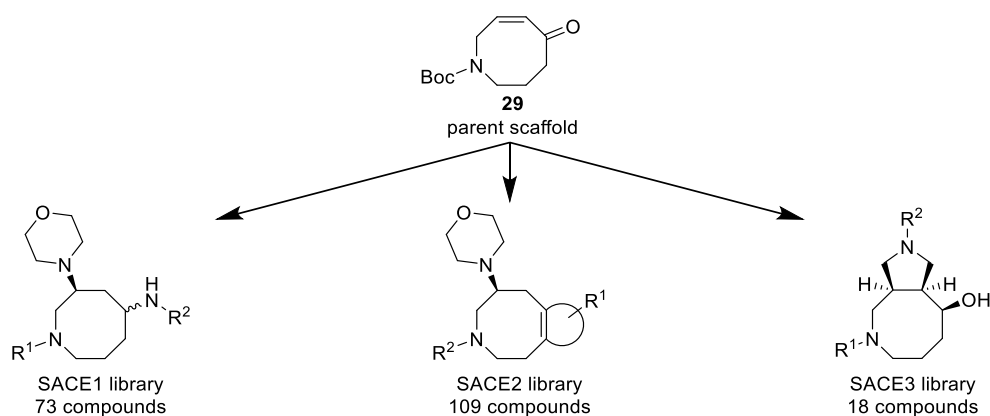
*Scheme 94: Diversification of parent scaffold **29**.*

Following a reagent-based differentiation approach, parent scaffold **29** yielded the three novel scaffolds in three steps or fewer (Scheme 94); this highlights the attractive potential of the parent scaffold to provide quick access to both structurally distinct scaffolds, which are useful for exploratory studies, and more similar scaffold analogues, which can be useful for structure-activity analysis and scaffold hopping, for example by switching a fused pyrazole for a fused aminopyrimidine in the SACE2 library.

During the course of this PhD research, Nelson and Marsden published the synthesis of 53 diverse screening compounds, obtained *via* reagent-based differentation of tropane analogue **237** (Scheme 95).[1] Besides performing 1,4-additions, fused heterocycle synthesis *via* a haloketone intermediate and 1,3-dipolar cycloadditions on enone **29**, similar to our synthetic routes, validating the relevance of the chemistry reported in this thesis, they demonstrated that the combination of an enone moiety on a cyclic amine provides many more possibilities

for diversification. Two transformations, reported on tropane analogue **237**,[1] are viable options for further diversification of our azacyclooctenone **29** (Scheme 95). Reaction of enone **237** with *p*-Tol-SO₂CH₂NC and KO*t*-Bu yielded fused pyrrole **236**.[1] Applying this reaction to our parent scaffold **29** would generate the unsaturated analogue *cis*-**181** of the SACE3 fused pyrrolidine scaffold. A Baylis-Hillman reaction on enone **29**, yielding hydroxymethyl-substituted enone **238**,[1] was also deemed interesting, since the 1° alcohol provides a site for covalent attachment of a linker for solid-phase synthesis, enabling combinatorial library synthesis after functionalisation of the enone using the diversification strategies discussed in this thesis.
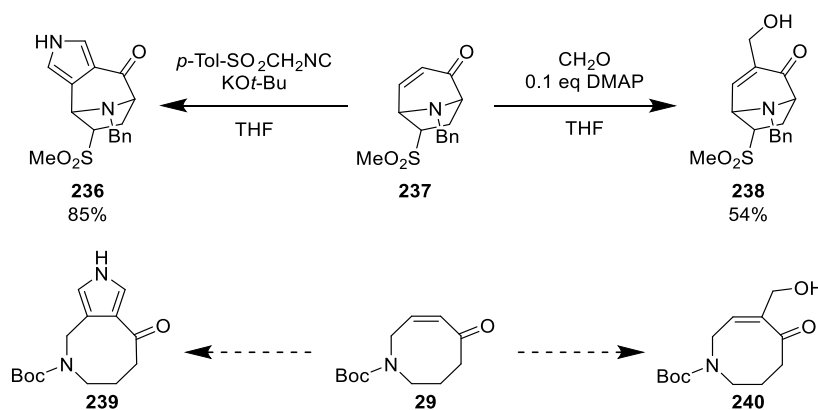
Scheme 95: Diversification of tropane analogue **237**,[1] *which could be applied to parent scaffold* **29**.

Whilst the three synthesised compound libraries illustrated the diversification potential of parent scaffold **29**, each diversification strategy still provides routes for further investigation, which allows for further expansion of the obtained diversity (Scheme 96). For example, the scope of the 1,4-addition on the enone could be expanded to other nitrogen nucleophiles, alcohols, thiols, or organocuprates. Use of azide nucleophile[2] to provide azide adduct **241**, would allow for rapid 1,2,3-triazole analogue synthesis *via* CuAAC chemistry.[3] Taking advantage of the demonstrated regioselectivity of enolisation of the ketone of morpholine adduct **91**, Claisen condensation with anhydrides or esters,[4] would afford 1,3-diketone intermediates. Subsequent reaction with functionalised hydrazines would then yield 1,3- or 2,3-functionalised pyrazoles **245** or **246**, exploring appendages on the thus far unfunctionalised 3-carbon of 8-5 fused pyrazole derivatives.[4] Furthermore, given the reactivity of the alcohol moiety in the SACE3 protected scaffold towards MeI, alkylation of the alcohol should be possible without quaternisation of the pyrrolidine nitrogen by first converting the pyrrolidine amine to an amide **243** for example. This route would validate the hydroxyl group as an appendable handle for future library synthesis, enabling late-stage diversification of the SACE3 scaffold on all three appendable sites.
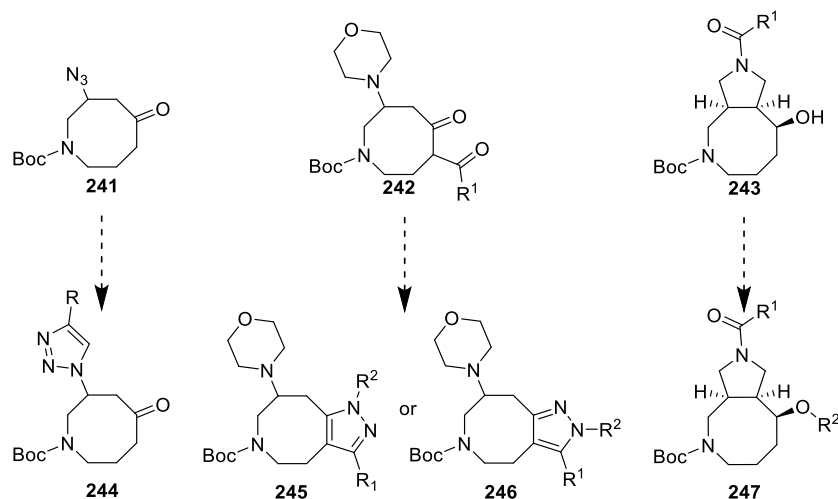
Scheme 96: Possible next steps, elaborating on previously established chemistry.

As an early-stage researcher, identifying a suitable choice of reagents for diverse library synthesis *via* parallel synthesis can be challenging. Whilst experienced medicinal chemists may have their preferred set of, for example, carboxylic acids, primary amines or sulfonyl chlorides, the argument for using these specific reagents is often vague or limited to ensuring the presence of an aliphatic analogue, a (hetero)cyclic analogue, a sterically bulky analogue and a small analogue in the library. The *in silico* library design used in this thesis thus provided a useful guide for reagent choice, with the bias of the experienced medicinal chemist limited to the in-house reagent collection from which reagents were chosen. Given the fingerprint-based selection method used, yielded reagent sets which aligned with the intuition of experienced chemists, the *in silico* approach provided support for the choices of an experienced medicinal chemist, whilst providing a transparent reference for the early-stage researcher. Furthermore, the inclusion of less common structures and moieties (like a morpholine sulfamide product from a sulfonyl chloride reagent pool) as an output of the *in silico* approach could provide alternatives or expansions for over-represented reagent sets, which may inspire (biased) chemists in future exploratory studies.

In silico validation of the SACE compound library showed that we have successfully synthesised compounds with drug-like physicochemical properties, displaying significant dissimilarity (and hence novelty) against FDA-approved drugs. Experimental validation through ElogD determination indicated that although experimental values may differ from calculated SlogP values for individual compounds (for example, basic amines), the effort to maximise physicochemical space coverage *in silico* does translate into a broad range in experimentally determined physicochemical parameters. hERG screening of a representative selection of

186

synthesised compounds showed that none of the three SACE scaffolds were inherently hERG inhibitors; however, the identification of two hERG inhibitors illustrated both the diversity of the synthesised compound library, whilst indicating possible molecular motifs or appendages that may lead to hERG inhibition.

Having validated the attractive properties of our synthesised compounds both *in silico* and experimentally, the most compelling measure of success would now be to provide a hit against a known or novel target in biological screening. The recent paper by the Nelson and Marsden groups illustrates that diversification strategies like ours can discover new hits, as their efforts yielded new inhibitors of the Hedgehog signalling pathway (an oncology target), such as indotropane **248**, and compounds with activity against *Plasmodium falciparum*, a parasite which causes malaria (Figure 79).[1] Of note is the structural resemblance of antimalarial compounds **249** and **250** with the SACE1 and SACE3 scaffolds, respectively, which makes our compounds attractive for screening against this target. Currently, our compounds are being tested against antibiotic resistant bacteria (ESKAPE pathogens) and *Mycobacteria* at the University of Birmingham.
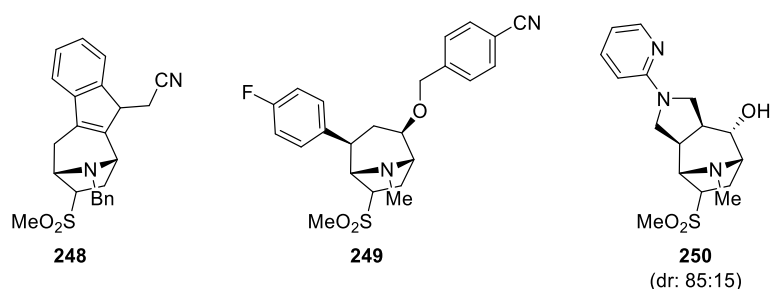
Figure 79: Bioactive tropane analogues, synthesised by the Nelson and Marsden groups.[1]

Although exploratory studies like the research described in this thesis may be high-risk, the possibly high reward makes this approach worth pursuing. As our understanding of diseases increases, molecular motifs established decades ago, but which proved inactive in past target-based assays, may find their way into novel drugs which act on new targets. Similarly, if our compounds do not show activity in the currently planned assays, their reported synthesis may provide a valuable reference for future analogue generation or scaffold hopping. The success of the European Lead Factory demonstrates that collaborative compound collections and screening projects such as the Haworth Compound Collection have the potential to provide necessary innovation in small-molecule drugs and targets, allowing the pharmaceutical sector to benefit from Novel Scaffolds for Drug Discovery.

9.1. References

1   R. A. Lowe, D. Taylor, K. Chibale, A. Nelson and S. P. Marsden, *Bioorg. Med. Chem.*, 2020, **28**, 115442.
2   D. J. Guerin, T. E. Horstmann and S. J. Miller, *Org. Lett.*, 1999, **1**, 1107–1109.
3   Y. Sajja, S. Vanguru, L. Jilla, H. R. Vulupala, R. Bantu, P. Yogeswari, D. Sriram and L. Nagarapu, *Bioorg. Med. Chem. Lett.*, 2016, **26**, 4292–4295.
4   D. N. Deaton, C. D. Haffner, B. R. Henke, M. R. Jeune, B. G. Shearer, E. L. Stewart, J. D. Stuart and J. C. Ulrich, *Bioorg. Med. Chem.*, 2018, **26**, 2107–2150.

CHAPTER III: EXPERIMENTAL SECTION

1. General experimental section

Unless stated otherwise, all reactions were carried out in oven-dried glassware under an Ar atmosphere using anhydrous solvents. Anhydrous THF and CH_2Cl_2 were collected from a PureSolv^{TM} solvent purification system and stored over 4 Å molecular sieves, which were activated by heating at 250 °C under high vacuum (< 2 mbar) for at least 6 h prior to use following a procedure by Williams *et al.*[1] Anhydrous DMF was supplied by Acros and stored on sieves (size not specified) in an AcroSeal™ Winchester bottle. All other reagents and solvents used were purchased from commercial suppliers and used without further purification unless stated otherwise. Water used in reactions and workup procedures was deionised and dispensed from an Elga Purelab Option DV35 Water Filtration System. Room temperature refers to a temperature range of 17–25 °C. Reaction temperatures of 0 °C were maintained using an ice-water bath. Whenever reaction mixtures were degassed, this was done by continuously bubbling Ar gas through the mixture for a specified amount of time.

R_f values and reaction progress were determined by thin-layer chromatography (TLC) which was performed on Merck silica gel 60 F_{254} plates, which were visualised under UV irradiation (254 nm) and staining with either potassium permanganate, ninhydrin or vanillin solutions. Flash column chromatography was performed using silica gel (Aldrich Silica Gel 60, 230–400 mesh, 40–63 μm) and the indicated eluent. All solutions are aqueous and saturated unless stated otherwise. Automatic flash column chromatography was performed using a Reveleris X2 flash chromatography purification system (equipped with an ELSD/UV-vis detector) and the indicated eluent. For automatic flash column chromatography using heptane:EtOAc as eluent, a gradient of 1–100% EtOAc was used; when CH_2Cl_2:MeOH was used as eluent, a 0.1–10% MeOH gradient was applied. General methods have been written for frequently recurring experimental procedures; any deviations from the general method (*e.g.,* different reaction conditions, different order of addition) is specified when discussing the synthesised compound.

The concentration of vinylmagnesium bromide was determined by titration with menthol and phenanthroline, following a procedure published by Lin *et al.*[2]

The gas flow rate of the N_2 sparge, used in RCM reactions, was determined by measuring the volume of displaced water in an inverted graduated cylinder over time. The gas flow was measured to displace on average 360 mL water / min.

HCl salt multiplicities were experimentally determined for a representative selection of compounds by the Symeres Analytical Facility (see Section 13). The salt multiplicities reported

for each compound are thus experimentally determined or based on analogy with a compound whose Cl⁻ content was experimentally determined.

^{1}H-NMR and proton-decoupled ^{13}C-NMR spectra were recorded in commercially available deuterated solvents on a Bruker AVIII 300 (^{1}H = 300 MHz), AVIII 400 (^{1}H = 400 MHz, ^{13}C = 101 MHz) or AVANCE NEO 400 (^{1}H = 400 MHz, ^{13}C = 101 MHz) spectrometer. All NMR spectra were recorded at room temperature, unless stated otherwise. Chemical shifts are reported in ppm and coupling constants, J, in Hz, to the nearest 0.1 Hz. Spectra recorded in CDCl$_3$ were calibrated using the solvent resonance, δ_H = 7.26 ppm and δ_C = 77.16 ppm. Spectra recorded in CD$_3$OD were calibrated using the solvent resonance, δ_H = 3.31 ppm and δ_C = 49.00 ppm. The following abbreviations are used to describe the multiplicity (and appearance) of resonances in ^{1}H-NMR spectra: s (singlet), d (doublet), t (triplet), q (quartet), p (pentet/quintet), m (multiplet), br (broad) and app (apparent). Stack is used to describe resonances from two or more protons that are in different environments but which are coincident (including rotamer resonances of protons attached to the same carbon). For ease of interpretation, coupling constants in ^{1}H-NMR spectra are reported as the average of the separately measured coupling constants. It is acknowledged that in ABX and ABXY systems, the experimentally measured and reported J_{A-X}, J_{B-X}, J_{A-Y} and J_{B-Y} are approximations of their true values. For apparent multiplets, the reported J values are those measured as if the observed resonance truly had this multiplicity. Proton-decoupled ^{13}CNMR spectra were recorded using the PENDANT pulse sequence and/or the UDEFT pulse sequence. Carbon multiplicities are derived from JMOD/DEPT experiments, or *via* gradient HSQC experiments. Proton and carbon assignments were determined on the basis of unambiguous chemical shift or coupling pattern, by patterns observed in 2D experiments or by analogy with fully interpreted spectra for structurally related compounds. Whenever 2D-NMR data are not available and assignment by analogy cannot be done with certainty, recorded spectra are not or only partially assigned. Approximate rotamer ratios are stated for ^{1}H-NMR spectra whenever possible, based on relative integrations of rotamer resonances observed in the ^{1}H-NMR spectrum. When rotamers are observed, and rotamer peaks can be distinguished and assigned, proton and carbon peaks that belong to the same rotamer are marked with 'maj' and 'min', denoting, respectively, the major rotamer and minor rotamer. This notation (*e.g.*, H-1 maj, H-1 min, Boc C(C*H*$_3$)$_3$ maj) is used consistently in both ^{1}H- and ^{13}C-NMR spectra (*e.g.*, H-1 maj and C-1 maj show a cross-peak in the HSQC spectrum). For 1:1 rotameric mixtures, the notation 'rot A' and 'rot B' is used to distinguish rotamers, analogously to the 'maj/min' notation reported above. Resonances that cannot be assigned to a single rotamer, or that contain multiple rotamer signals, are reported without any

assignment. For rotamers and conformational isomers, fractional integration is used for the reported proton count, with values rounded to one decimal place (*e.g.*, 0.2H). For 2:1 and 3:1 rotameric mixtures, proton counts are rounded to two decimal places to facilitate interpretation (*e.g.*, 0.67H:0.33H, 0.75H:0.25H). Numbering of the compounds for assignment of proton and carbon peaks is arbitrary. All obtained ^{1}H-NMR, ^{13}C-NMR and ^{19}F-NMR spectra reported in this thesis are compiled in a separate document (NMR spectra PhD thesis SXC 2022.docx), sorted per compound, and consistently numbered in accordance with the compound numbers assigned in this thesis. This document is stored in a secure RDS folder, which can be accessed by authorised members of the University of Birmingham (see below).

Melting points were recorded on a Büchi B-540 melting point apparatus. Infrared spectra were recorded on a Perkin-Elmer Spectrum 100 FTIR spectrometer. Wavelengths (*v*) are reported in cm^{-1}. ESI LRMS spectra were recorded on a Micromass LCT time-of-flight mass spectrometer. LCMS spectra were obtained using a Waters e2695 separations module and recorded on a Waters SQ Detector 2, using MassLynx software for processing. High-resolution mass spectrometry on all instruments was run with a tolerance of 5.0 ppm and calculated to find a monoisotopic mass.

Preparative basic HPLC was performed by the Symeres Analytical Facility using a Waters Modular Preparative HPLC System with the following specifications: MS instrument type: ACQ-SQD2; column: Waters XSelect (C18, 100 × 30mm, 10 μm); flow rate: 55 mL min^{-1}; column temperature: rt; eluent A: 100% MeCN, eluent B: 10 mM $(NH_4)HCO_3$ in H_2O pH=9.5; detection: DAD (220 – 320 nm); detection: MSD (ESI pos/neg); mass range: 100 – 800; fraction collection based on MS and DAD.

Preparative SFC was performed by the Symeres Analytical Facility using a Waters Prep 100 SFC UV/MS directed system equipped with a Waters 2998 Photodiode Array (PDA) Detector, a Waters Acquity QDa MS detector and the Waters 2767 Sample Manager. Further specifications of the system: column: Waters Viridis BEH Prep OBD (250 × 19 mm, 5 μm); column temperature: 35 °C; flow rate: 70 mL min^{-1}; ABPR: 120 bar; eluent A: CO_2, eluent B: 20 mM NH_3 in MeOH; linear gradient: t=0 min 10% B, t=5 min 40% B; detection: PDA (210 – 400 nm); Fraction collection based on PDA and TIC.

Purity analysis and retention time (t_R) determination *via* UPLC was performed using a Waters IClass apparatus, with the following specifications: binary pump: UPIBSM, SM: UPISMFTN with SO; UPCMA, PDA: UPPDATC, 210 – 320 nm, MS: QDA ESI, pos/neg 100 – 800; column: Waters XSelect CSH C18, (50 × 2.1 mm, 2.5 μm), temperature: 25 °C, flow rate: 0.6 mL min^{-1}, gradient:

t_0 = 5% B, $t_{2.0\,min}$ = 98% B, $t_{2.7\,min}$ = 98% B, post-time: 0.3 min, eluent A: 10 mM $(NH_4)HCO_3$ in H_2O (pH=9.5), eluent B: MeCN.

For library compounds synthesised *via* parallel synthesis, at least 20 compounds or 5% of the library (whichever is greater) were fully characterised, while the retention time (t_R), UV purity (determined *via* UPLC) and yields were reported for the whole library. This is in accordance with the Author Guidelines set for ACS Combinatorial Science.[a3]

1.1. Purification *via* preparative basic HPLC

Dry reaction mixtures were redissolved in DMSO (1 − 2 mL), while reaction mixtures in DMF and MeOH were used as such. The reaction mixture was pushed through a syringe filter (pore size 22 µm) and loaded onto a preparative basic HPLC purification system. Collected product fractions were concentrated under reduced pressure using a Genevac HT-12 centrifugal evaporator. The dried fractions were redissolved in MeCN:H_2O 1:1 solution, combined in a tared and barcoded 8 mL vial, and concentrated under reduced pressure in a Genevac centrifugal evaporator, yielding the purified library compound.

1.2. Data management

Raw data for all experiments carried out in Birmingham can be found in a secure RDS folder, with file names in accordance with their lab notebook experiment code (*e.g.*, SXC4-152).

For all experiments carried out in Nijmegen, all processed data are archived in a secure RDS folder, named in accordance with the lab notebook experiment code (*e.g.*, SACE01-037) and can be traced back to its raw data file *via* the Data File Name (*e.g.*, RUN_0305_162452_560.D), reported in the Parameter box for NMR spectra and MS data. Experimental procedures and observations are reported in an electronic lab notebook; scanned copies of the accompanying physical lab notebook are stored in the RDS folder.

The RDS folder can be accessed by authorised members of the University of Birmingham (\\its-rds.bham.ac.uk\rdsprojects\c\coxlr-idesign-ceusters).

---

[a] https://publish.acs.org/publish/author_guidelines?coden=acsccc, last accessed 13th February 2022.

2. Parent scaffold synthesis

(*tert*-Butoxycarbonylamino)butanoic acid (30)
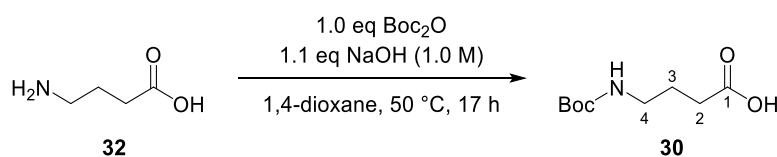
NaOH solution (1.0 M, 55 mL, 55 mmol) was added to a solution of 4-aminobutanoic acid **32** (5.16 g, 50.0 mmol) in 1,4-dioxane (100 mL). The resulting solution was stirred and cooled to 0 °C. After addition of Boc_2O (12 mL, 51 mmol), the reaction mixture was stirred at 50 °C until TLC analysis of the reaction mixture showed full conversion of the starting material. 1,4-Dioxane was then evaporated under reduced pressure and the concentrated reaction mixture was acidified with $KHSO_4$ solution (20 mL) until pH = 3. The mixture was extracted with EtOAc (3 × 200 mL). The organic phases were combined, dried over anhydrous Na_2SO_4, filtered and concentrated under reduced pressure[4] to yield Boc amide **30** as a colourless oil, which solidified upon storage in the fridge (10.11 g, quant.).

R_f (hexane:EtOAc 6:4 + 0.5% v/v AcOH): 0.2.

v_{max} **(neat / cm^{-1}):** 3361 s (OH, NH), 2973 m, 2936 m, 1682 v s (C=O), 1528 s, 1440 m.

^{1}H-NMR (400 MHz, CDCl$_3$) (2:1 mixture of rotamers)[a] δ_H 11.54 (br s, 1H, OH), [6.10 (br s, 0.33H, NH min), 4.77 (br s, 0.67H, NH maj)], 3.24 − 3.00 (m, 2H, H-4), 2.36 (t, J = 7.2 Hz, 2H, H-2), 1.79 (tt, J = 7.2, 6.8 Hz, 2H, H-3), 1.41 (br s, 9H, Boc).

^{13}C-NMR (101 MHz, CDCl$_3$) (mixture of rotamers) δ_C 178.5 (C, C-1), [157.9, 156.3 (C, Boc *C*=O)], [80.9, 79.6 (C, Boc (CH$_3$)$_3$*C*O)], [41.0, 39.9 (CH$_2$, C-4)], 31.4 (CH$_2$, C-2), 28.5 (CH$_3$, Boc C(*C*H$_3$)$_3$), 25.2 (CH$_2$, C-3).

ESI-LRMS (+): m/z 226 ([M+Na]$^+$, 100%), 170 (15, [M−C$_4$H$_8$ + Na]$^+$).

^{1}H-NMR and ^{13}C-NMR spectroscopic data were in accordance with those reported in the literature.[5]

---

[a] Ratio based on NH peak integrations in the reported ^{1}H-NMR spectrum.

4-(Allyl(*tert*-butoxycarbonyl)amino)butanoic acid (33)
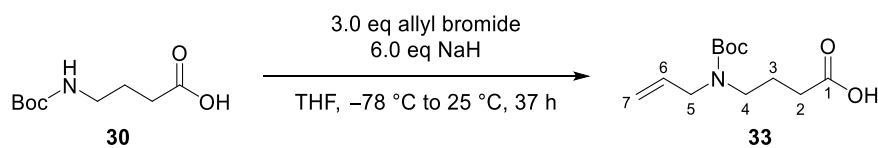
In a 1 L round-bottom flask, NaH (7.09 g of a 60% dispersion in mineral oil, 148 mmol) was washed with hexane (3 × 50 mL) to remove the mineral oil. Any residual hexane was removed from the washed NaH under high vacuum. The flask was backfilled with Ar gas and anhydrous THF (123 mL) was added. The resulting dispersion was cooled to −78 °C. A solution of Boc-GABA-OH **30** (5.00 g, 24.6 mmol) in anhydrous THF (123 mL) was added dropwise over 15 min to the cooled and vigorously stirred dispersion.[a] After stirring the cooled mixture for 30 min, allyl bromide (6.4 mL, 74 mmol) was added dropwise over 1 min. The resulting grey reaction mixture was stirred for 37 h with the dry ice-acetone cooling bath in place, leaving the bath and reaction mixture to warm to rt. The reaction mixture was then cooled to 0 °C, before quenching with deionised water (35 mL).[b] The resulting clear solution was washed with hexane (2 × 250 mL) and then acidified with hydrochloric acid (1.0 M, 50 mL) until pH = 3. The product was extracted with EtOAc (3 × 270 mL). The combined organic extracts were dried over anhydrous Na$_2$SO$_4$, filtered and concentrated under reduced pressure to yield allyl carbamate **33** as a yellow oil, which was used without further purification (5.02 g, 84%).

R$_f$ (hexane:EtOAc 6:4 + 0.5% v/v AcOH): 0.3.

v_{max} (neat / cm^{-1}): 2934 w, 1736 m (C=O), 1692 s (C=O), 1411 s, 1366 m, 1248 s, 1158 v s.

^{1}H-NMR (400 MHz, CDCl$_3$) δ_H 10.94 (br s, 1H, O*H*), 5.78 – 5.61 (m, 1H, H-6), 5.10 – 4.99 (stack, 2H, H-7), 3.90 – 3.59 (m, 2H, H-5), 3.29 – 3.21 (m, 2H, H-4), 2.32 (t, *J* = 7.3 Hz, 2H, H-2), 1.81 (tt, *J* = 7.3, 7.3 Hz, 2H, H-3), 1.42 (s, 9H, Boc).

^{13}C-NMR (101 MHz, CDCl$_3$) (mixture of rotamers) δ_C 178.7 (C, C-1), 155.9 (C, Boc *C*=O), 134.0 (CH, C-6), [116.7, 116.4 (CH$_2$, C-7)], 80.0 (C, Boc (CH$_3$)$_3$*C*O), [49.9, 49.4 (CH$_2$, C-5)], 45.7 (CH$_2$, C-4), 31.3 (CH$_2$, C-2), 28.4 (CH$_3$, Boc C(*C*H$_3$)$_3$), 23.4 (CH$_2$, C-3).

ESI-LRMS (+): m/z 509.3 ([2M+Na]$^+$, 33%), 266.1 (100, [M+Na]$^+$), 210.1 (8, [M−C$_4$H$_8$ + Na]$^+$).

---

[a] Addition of Boc-GABA-OH was stopped temporarily when foaming or effervescence was observed, maintaining the reaction mixture as a grey suspension.
[b] On gramme scale, cooling, stirring and slow addition was increasingly important, as the generated hydrogen gas caused heavy effervescence and foaming of the reaction mixture if water was added too quickly.

IR, ^{1}H-NMR and ^{13}C-NMR spectroscopic data were in accordance with those reported in the literature,[6] although Morales-Chamorro and Vázquez do not report rotamers.

tert-Butyl allyl(4-(methoxy(methyl)amino)-4-oxobutyl)carbamate (34)
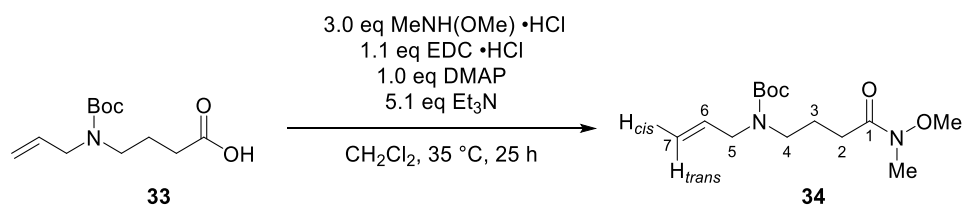
Et$_3$N (28.4 mL, 204 mmol), DMAP (4.88 g, 39.9 mmol), MeNH(OMe) •HCl (11.68 g, 120 mmol) and EDC •HCl (8.42 g, 43.9 mmol) were added sequentially to a solution of carboxylic acid **33** (9.71 g, 39.9 mmol) in anhydrous CH$_2$Cl$_2$ (400 mL). The reaction mixture was stirred under an Ar atmosphere at 35 °C for 25 h, at which point, analysis of the reaction mixture by TLC showed complete conversion of the starting material.[a] After diluting the reaction mixture with CH$_2$Cl$_2$ (100 mL), the mixture was washed sequentially with citric acid solution (5 w/v%, 3 × 500 mL) and NaHCO$_3$ solution (3 × 500 mL). The organic phase was dried over anhydrous Na$_2$SO$_4$, filtered and concentrated under reduced pressure. The crude compound was purified by flash column chromatography (hexane:EtOAc 6:4) to yield Weinreb amide **34** as a colourless oil (10.97 g, 96%).

R$_f$ (hexane:EtOAc 6:4): 0.3.

v_{max} (neat / cm^{-1}): 2974 w, 2936 w, 1678 br, s (C=O), 1462 m, 1410 s.

^{1}H-NMR (400 MHz, CDCl$_3$) δ_H 5.74 (ddt, J = 16.8, 10.5, 5.7 Hz, 1H, H-6), 5.08 (d, J = 16.8 Hz, 1H, H-7$_{trans}$), 5.07 (d, J = 10.5 Hz, 2H, H-7$_{cis}$), 3.86 – 3.69 (m, 2H, H-5), 3.64 (s, 3H, OMe), 3.21 (t, J = 7.3 Hz, 2H, H-4), 3.13 (s, 3H, NMe), 2.38 (t, J = 7.5 Hz, 2H, H-2), 1.80 (tt, J = 7.5, 7.3 Hz, 2H, H-3), 1.41 (s, 9H, Boc).

^{13}C-NMR (101 MHz, CDCl$_3$) (mixture of rotamers) δ_C 174.0 (C, C-1), 155.5 (C, Boc *C*=O), 134.2 (CH, C-6), [116.4 (CH$_2$, C-7), 116.0 (CH$_2$, C-7)], 79.4 (C, Boc (CH$_3$)$_3$*C*O), 61.1 (CH$_3$, OMe), [49.5 (CH$_2$, C-5), 49.2 (CH$_2$, C-5)], 45.9 (CH$_2$, C-4), 32.2 (CH$_3$, N-Me), 29.1 (CH$_2$, C-2), 28.4 (CH$_3$, Boc C(*C*H$_3$)$_3$), 23.2 (CH$_2$, C-3).

---

[a]Conversion of EDC •HCl could be monitored *via* IR spectroscopy, observing disappearance of the characteristic carbodiimide peak at 2125 cm^{-1}.

IR, ^{1}H-NMR and ^{13}C-NMR spectroscopic data were in accordance with those reported in the literature,[6] although Morales-Chamorro and Vázquez do not report the presence of rotamers.

tert-Butyl allyl(4-oxohex-5-en-1-yl)carbamate (31)
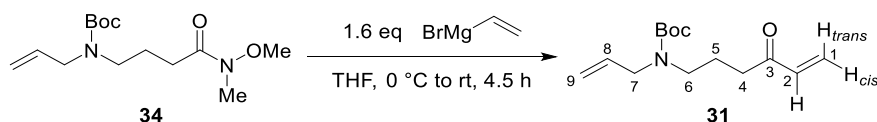
Vinylmagnesium bromide (0.7 M in THF, 89 mL, 63 mmol) was added dropwise over 9 min to a solution of Weinreb amide **34** (11.2 g, 39.1 mmol) in anhydrous THF (390 mL) under an Ar atmosphere at 0 °C. The reaction mixture was stirred for 4.5 h while allowing the cooling bath to warm to rt. The reaction was quenched by addition of hydrochloric acid (1.0 M, 150 mL) until pH = 3. The THF was removed under reduced pressure and the residue was extracted with CH_2Cl_2 (3 × 500 mL). The combined organic extracts were dried over anhydrous Na_2SO_4, filtered and concentrated under reduced pressure. Purification of the residue by flash column chromatography (hexane:EtOAc 4:1) yielded diene **31** as a colourless oil (8.10 g, 82%).

R_f (hexane:EtOAc 8:2): 0.3.

v_{max} (neat / cm^{-1}): 2976 w, 2933 w, 1683 s (C=O), 1407 s.

^{1}H-NMR (400 MHz, CDCl$_3$) δ_H 6.33 (A of ABX, J_{A-B} = 17.7, J_{A-X} = 10.5 Hz, 1H, H-2), 6.19 (B of ABX, J_{A-B}= 17.7, J_{B-X} = 1.2 Hz, 1H, H-1$_{trans}$), 5.83 − 5.69 (stack, 2H, [including 5.81 (X of ABX, J_{A-X} = 10.5 Hz, 1H, H-1$_{cis}$)], H-1$_{cis}$, H-8), 5.15 − 5.04 (stack, 2H, H-9), 3.88 − 3.69 (m, 2H, H-7), 3.20 (t, J = 7.2 Hz, 2H, H-6), 2.58 (t, J = 7.2 Hz, 2H, H-4), 1.82 (tt, J = 7.2, 7.2 Hz, 2H, H-5), 1.43 (s, 9H, Boc).

^{13}C-NMR (101 MHz, CDCl$_3$) (mixture of rotamers) δ_C 200.2 (C, C-3), 155.7 (C, Boc *C*=O), 136.6 (CH, C-2), 134.2 (CH, C-8), 128.2 (CH$_2$, C-1), [116.7, 116.2 (CH$_2$, C-9)], 79.6 (C, Boc (CH$_3$)$_3$*C*O), [49.7, 49.3 (CH$_2$, C-7)], 45.8 (CH$_2$, C-6), 36.6 (CH$_2$, C-4), 28.5 (CH$_3$, Boc C(*C*H$_3$)$_3$), 22.4 (CH$_2$, C-5).

ESI-LRMS (+): m/z 276.1 ([M+Na]$^+$, 5%), 154.1 (100, [M−C$_5$H$_8$O$_2$ + H]$^+$).

IR, ^{1}H-NMR, and ^{13}C-NMR spectroscopic data were in accordance with those reported in the literature.[6]

tert-Butyl (*Z*)-5-oxo-3,4,5,8-tetrahydroazocine-1(2*H*)-carboxylate (29)
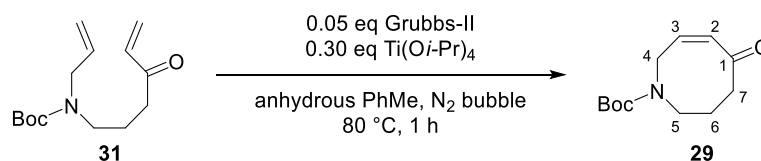
Ti(O*i*-Pr)$_4$ (0.99 mL, 3.4 mmol) was added to a heated (40 °C) solution of diene **31** (2.852 g, 11.26 mmol) in anhydrous PhMe (1.1 L) under a N$_2$ atmosphere. After heating to 80 °C (30 min), Grubbs II catalyst (45 mg, 0.053 mmol) was added. N$_2$ gas was bubbled through the stirred solution for 1 h, after which time, the mixture was immediately concentrated under reduced pressure and adsorbed onto Celite. The dry-loaded crude mixture was separated using automatic flash column chromatography (CH$_2$Cl$_2$:heptane:EtOAc 5:4:1), which yielded the ring-closed product **29** as a pale brown oil, which solidified upon overnight storage in a fridge (1.59 g, 63%).[a]

R$_f$ (hexane:EtOAc:CH$_2$Cl$_2$ 4:1:5): 0.2.

Melting point: 59 – 61 °C.

v_{max} (neat / cm^{-1}): 2929 w, 1686 s (C=O), 1668 s (C=O), 1437 s, 1401 s, 1240 s.

^{1}H-NMR (400 MHz, CDCl$_3$) (5:4 mixture of rotamers)[b] δ_H 5.97 – 5.83(stack, 1H, H-3), 5.66 (dt, *J* = 12.0, 2.4 Hz, 1H, H-2), 3.93 – 3.81 (stack, 2H, H-4), 3.47 – 3.36 (stack, 2H, H-5), 2.42 – 2.32 (stack, 2H, H-7), 2.07 – 1.94 (stack, 2H, H-6), [1.39 (s, 5H, Boc maj), 1.36 (s, 4H, Boc min)].

^{13}C-NMR (101 MHz, CDCl$_3$) (mixture of rotamers) δ_C 208.1 (C, C-1), 154.7 (C, Boc *C*=O), [135.3, 135.2 (CH, C-3)], 126.7 (CH, C-2), [80.6, 80.5 (C, Boc (CH$_3$)$_3$*C*O)], [48.9, 48.6 (CH$_2$, C-4)], [47.6, 47.3 (CH$_2$, C-5)], [42.3, 42.0 (CH$_2$, C-7)], 28.4 (CH$_3$, Boc C(*C*H$_3$)$_3$) [25.1, 24.4 (CH$_2$, C-6)].

ESI-LRMS (+): m/z 473.4 ([2M+Na]$^+$, 46%), 225.9 (100, [M+H]$^+$).

IR, ^{1}H-NMR and ^{13}C-NMR data were in accordance with those reported in the literature.[6]

For a ^{1}H-NMR spectrum of a mixture of dimer **43** and monomer **29**, see Appendix 9.

---

[a] A yield of 71% after 16 min reaction time was achieved in another reaction on 2 g scale, but used heptane:EtOAc 4:1 as chromatography eluent. Hence, a mixture of dimer **43** and monomer **29** was isolated (7 mol% dimer), and the yield for **29** was calculated *via* ^{1}H-NMR spectroscopy.
[b] Ratio based on Boc peak integrations in the reported ^{1}H-NMR spectrum.

tert-Butyl (*Z*)-5-hydroxy-3,4,5,8-tetrahydroazocine-1(2*H*)-carboxylate (63)
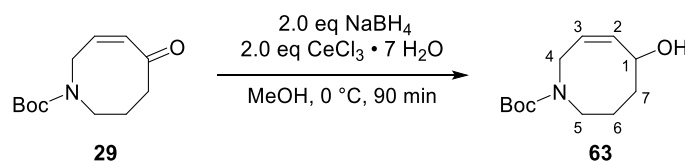
Following a procedure reported by El-Mansy et al.:[7] $CeCl_3 \cdot 7 H_2O$ (1.10 g, 2.97 mmol) was added to a solution of enone **29** (335 mg, 1.49 mmol) in anhydrous MeOH (11 mL). The resulting mixture was stirred at rt until all of the material was fully dissolved and subsequently cooled to 0 °C. $NaBH_4$ (113 mg, 2.97 mmol) was added and the reaction mixture was stirred for 90 min at 0 °C, at which point TLC analysis showed full consumption of the starting material. The reaction mixture was quenched with H_2O (10 mL) and the aqueous layer was extracted with EtOAc (3 × 10 mL). The combined organic extracts were dried over anhydrous Na_2SO_4, filtered and concentrated under reduced pressure. Purification of the residue by flash column chromatography (hexane:EtOAc 7:3) yielded allylic alcohol **63** as a brown oil (240 mg, 71%).

R_f (hexane:EtOAc 3:2): 0.3.

v_{max} (neat / cm^{-1}): 3411 w br (O–H), 2974 w, 2931 w, 1670 s (C=O), 1412 s, 1159 s.

^{1}H-NMR (400 MHz, CDCl$_3$)[a] δ_H 5.82 − 5.14 (stack, 2H, H-2, H-3), 5.05 − 4.67 (m, 1H, H-1), 4.55 − 4.28 (m, 1H, H-4), 4.13 − 3.74 (m, 1H, H-5), 3.40 − 3.25 (m, 1H, H-4), 3.00 −2.85 (m, 1H, H-5), 2.13 (br s, 1H, O*H*), 2.02 − 1.86 (m, 1H, H-7), 1.87 − 1.64 (stack, 2H, H-6), 1.63 − 1.33 (stack, 10H, [including 1.44 (s, 9H, Boc)], H-7, Boc).

^{13}C-NMR (101 MHz, CDCl$_3$) (mixture of rotamers) δ_C 155.5 (C, Boc *C*=O), [134.2, 133.8 (CH, C-2)], 126.2 (CH, C-3), 79.9 (C, Boc (CH$_3$)$_3$*C*O), 68.0 (CH, C-1), 47.3 (CH$_2$, C-4, C-5, resonance overlap), 36.4 (CH$_2$, C-7), 28.6 (CH$_3$, Boc C(*C*H$_3$)$_3$), [24.22, 24.15 (CH$_2$, C-6)].

ESI-LRMS (+): m/z 477.29 ([2M+Na]$^+$, 20%), 250.14 (100, [M+Na]$^+$).

HRMS: Found [M+Na]$^+$ 250.1418. C$_{12}$H$_{22}$NNaO$_3$ requires M+Na, 250.1419.

---

[a] reported *J* values for apparent broad doublets are only to be interpreted as an approximate distance between the observed maxima: broadening of the peaks led to plateaus on the maxima, demanding manual peak picking. Both resonances for H-5 showed coupling with H-6 *via* COSY analysis, which led to the other apparent broad doublet at 4.37 ppm being assigned to H-4 (assigned H-4 protons did not show this coupling). Geminal coupling observed (COSY analysis) between diastereotopic protons on C-4 and C-5.

tert-Butyl 3-(1*H*-benzo[*d*]imidazol-1-yl)-5-oxoazocane-1-carboxylate (77)
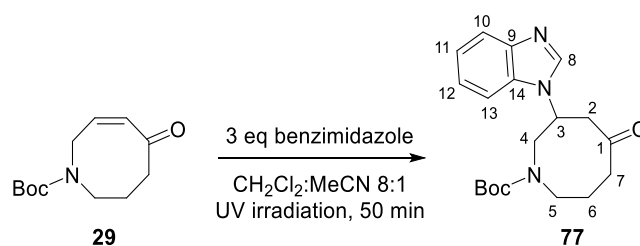
Following a procedure reported by Moran *et al*.:[8] In a Pyrex tube, enone **29** (50 mg, 0.22 mmol) and benzimidazole (81 mg, 0.68 mmol) were dissolved in a mixture of CH_2Cl_2 (4.0 mL) and MeCN (0.5 mL). The resulting mixture was degassed with Ar gas for 20 min and irradiated under an Ar atmosphere with a medium-pressure 125 W Hg lamp for 50 min. The volatiles were removed under reduced pressure and the crude mixture was separated using flash column chromatography (CH_2Cl_2:MeOH 95:5) to yield the 1,4-adduct **77** as a colourless oil (54 mg, 71%).

R$_f$ (CH_2Cl_2:MeOH 9:1): 0.4.

v_{max} (neat / cm^{-1}): 2976 w, 2934 w, 1689 s (C=O), 1408 m, 1155 s.

^{1}H-NMR (400 MHz, CDCl$_3$) (5:4 mixture of rotamers)[a] δ_H 7.98 − 7.92 (stack, 1H [including 7.97 (s, 0.6H, H-8 maj), 7.96 (s, 0.4H, H-8 min)], H-8), 7.88 − 7.77 (stack, 1H, H-13), [7.71 (d, *J* = 8.1 Hz, 0.6H, H-10 maj), 7.58 − 7.52 (m, 0.4H, H-10 min)], 7.38 − 7.27 (stack, 2H, H-11, H-12), [5.33 (app tt, *J* = 12.1, 4.5 Hz, 0.6H, H-3 maj), 5.22 (app tt, *J* = 12.2, 4.2 Hz, 0.4H, H-3 min)], 4.19 − 3.71 (stack, 2H, H-4, H-5), 3.45 (dd, *J* = 12.2, 12.2 Hz, 1H, H-2), 3.35 − 2.95 (stack, 2H, H-4, H-5), 2.73 − 2.63 (stack, 1H, H-2), 2.62 − 2.32 (stack, 3H, H-6, H-7), 2.22 − 2.04 (stack, 1H, H-6), [1.56 (s, 4H, Boc min), 1.51 (s, 5H, Boc maj)].

^{13}C-NMR (101 MHz, CDCl$_3$) (mixture of rotamers) δ_C [207.23, 207.20 (C, C-1)], [155.1, 154.9 (C, Boc *C*=O)], [143.9 (C, C-9b), 143.8 (C, C-9a)], [140.5, 140.3 (CH, C-8)], [133.3 (C, C-14a), 133.0 (C, C-14b)], [123.5, 123.4 (CH, C-11)], [122.8, 122.7 (CH, C-12)], [120.9 (CH, H-13b), 120.5 (CH, C-13a)], [110.8 (CH, C-10a), 110.1 (CH, C-10b)], [81.7, 81.4 (C, Boc (CH$_3$)$_3$*C*O)], [54.9 (CH, C-3b), 53.7 (CH, C-3a)], [51.7, 51.5 (CH$_2$, C-4)], [48.0, 47.0 (CH$_2$, C-5)], [43.8, 43.3 (CH$_2$, C-2)], [42.5, 42.4 (CH$_2$, C-7)], [28.6, 28.5 (CH$_3$, Boc C(*CH$_3$*)$_3$)], [26.3, 25.2 (CH$_2$, C-6)].

ESI-LRMS (+): m/z 344.20 ([M+H]$^+$, 100%).

HRMS: Found [M+H]$^+$ 344.1972. $C_{19}H_{26}N_3O_3$ requires M+H, 344.1974.

---

[a] Ratio based on Boc peak integrations in the reported ^{1}H-NMR spectrum.

tert-Butyl 5-oxo-3-(1*H*-1,2,3-triazol-1-yl)azocane-1-carboxylate (78)
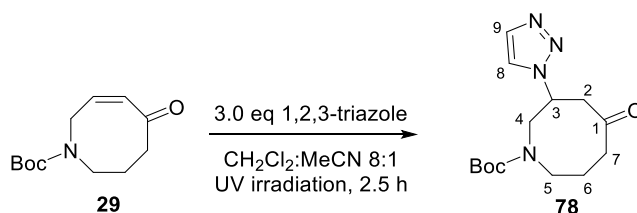
Following a procedure reported by Moran *et al.*:[8] In a Pyrex tube, enone **29** (201 mg, 0.89 mmol) and 1,2,3-triazole (189 mg, 2.73 mmol) were dissolved in a mixture of CH_2Cl_2 (16.0 mL) and MeCN (2.0 mL). The resulting mixture was degassed with Ar gas for 30 min and irradiated under an Ar atmosphere with a medium-pressure 125 W Hg lamp for 2.5 h. The volatiles were removed under reduced pressure and the crude mixture was redissolved in EtOAc (20 mL). The organic phase was washed with $NaHCO_3$ solution (3 × 40 mL), dried over anhydrous Na_2SO_4, filtered and concentrated under reduced pressure. The crude product was purified using flash column chromatography (CH_2Cl_2:MeOH 99:1 – 95:5) to yield 1,4-adduct **78** as a yellow oil, which solidified upon overnight storage in a fridge (110 mg, 42%).

R$_f$ (hexane:EtOAc 4:1): 0.5.

v_{max} (neat / cm^{-1}): 3114 w, 2935 w, 1692 s (C=O), 1405 m, 1367 m, 1158 s.

^{1}H-NMR (400 MHz, CDCl$_3$) (2:3 mixture of rotamers)[a] δ_H 7.70 − 7.47 (stack, 2H, H-8, H-9), 5.23 (stack, 1 H, [including 5.29 (app tt, *J* = 11.9, 4.1 Hz, 0.6H, H-3 maj), 5.18 (app tt, *J* = 11.9, 4.0 Hz, 0.4H, H-3 min)], H-3), 4.05 − 3.89 (m, 0.4H, H-5 min), 3.88 − 3.69 (stack, 1.6H, H-4, H-5 maj), 3.57 − 3.27 (m, 2H, H-2, H-4), [3.10 − 3.00 (m, 0.6H, H-5 maj), 2.99 − 2.88 (m, 0.4H, H-5 min)], 2.61 − 2.26 (stack, 4H, H-2, H-6, H-7), 2.10 − 1.91 (stack, 1H, H-6), [1.44 (s, 3.8H, Boc min), 1.42 (s, 5.2H, Boc maj)].

^{13}C-NMR (101 MHz, CDCl$_3$) (mixture of rotamers) δ_C [207.8, 207.8 (C, C-1)], [155.2, 154.7 (C, Boc *C*=O)], [133.7 (CH, triazole min), 133.5 (CH, triazole maj)], [123.7 (CH, triazole maj), 123.0 (CH, triazole min)], [81.5, 81.4 (C, Boc (CH$_3$)$_3$*C*O)], [59.2 (CH, C-3 min), 57.8 (CH, C-3 maj)], 52.1 (CH$_2$, C-4), [48.0 (CH$_2$, C-5 maj), 46.7 (CH$_2$, C-5 min)], [44.6, 43.9 (CH$_2$, C-2)], [42.7, 42.6 (CH$_2$, C-7)], 28.4 (CH$_3$, Boc C(*C*H$_3$)$_3$), [25.9, 24.8 (CH$_2$, C-6)].

ESI-LRMS (+): m/z 295.18 ([M+H]$^+$, 100%).

---

[a] Ratio based on H-5 peak integrations in the reported ^{1}H-NMR spectrum at δ_H 4.05 − 3.89, 3.88 − 3.69, 3.10 − 3.00 and 2.99 − 2.88 ppm.

HRMS: Found [M+H]$^+$ 295.1758. $C_{14}H_{22}N_4O_3$ requires M+H, 295.1765.

tert-Butyl 5-oxo-3-(1*H*-pyrazol-1-yl)azocane-1-carboxylate (79)
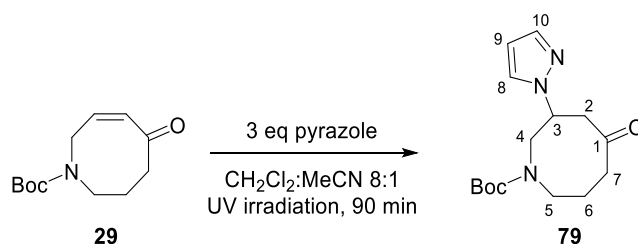
Following a procedure reported by Moran *et al.*:[8] In a Pyrex tube, enone **29** (201 mg, 0.89 mmol) and pyrazole (186 mg, 2.73 mmol) were dissolved in a mixture of CH_2Cl_2 (16.0 mL) and MeCN (2.0 mL). The resulting mixture was degassed with Ar for 20 min and irradiated under an Ar atmosphere with a medium-pressure 125 W Hg lamp for 90 min. The volatiles were removed under reduced pressure and the crude mixture was redissolved in EtOAc (20 mL). The organic phase was washed with NaHCO$_3$ solution (5 × 40 mL), dried over anhydrous Na$_2$SO$_4$, filtered and concentrated under reduced pressure. The crude product was purified using flash column chromatography (CH_2Cl_2:MeOH 99:1 – 98:2) to yield 1,4-adduct **79** as a yellow oil, which solidified upon overnight storage in a fridge (202 mg, 77%).

R*f* (hexane:EtOAc 4:1): 0.5.

***v*$_{max}$ (neat / cm^{-1}):** 2975 w, 2933 w, 1692 s (C=O), 1406 m, 1152 s.

^{1}H-NMR (400 MHz, CDCl$_3$) (1:1 mixture of rotamers)[a] δ_H 7.50 – 7.45 (stack, 1H, H-10), [7.43 (d, *J* = 2.1 Hz, 0.5H, H-8 rot A), 7.32 (d, *J* = 2.1 Hz, 0.5H, H-8 rot B)], [6.18 (dd, *J* = 2.1, 2.1 Hz, 0.5H, H-9 rot B), 6.15 (dd, *J* = 2.1, 2.1 Hz, 0.5 H-9 rot A)], [5.06 (app tt, *J* = 11.8, 4.2 Hz, 0.5H, H-3 rot A), 4.91 (app tt, *J* = 11.8, 4.1 Hz, 0.5H, H-3 rot B)], 3.79 – 3.62 (m, 0.5H, H-5 rot B), 3.81 – 3.61 (stack, 1.5H, H-4, H-5 rot A), 3.48 – 3.24 (stack, 2H, H-2, H-4), [3.04 – 2.95 (m, 0.5H, H-5 rot A), 2.94 – 2.82 (m, 0.5H, H-5 rot B)], 2.48 – 2.25 (stack, 4H, H-2, H-6, H-7), 2.04 – 1.91 (stack, 1H, H-6), [1.44 (s, 4.5H, Boc), 1.41 (s, 4.5H, Boc)].

^{13}C-NMR (101 MHz, CDCl$_3$) (mixture of rotamers) δ_C [208.49, 208.47 (C, C-1)], [155.1 (C, Boc *C*=O rot A), 154.9 (C, Boc *C*=O rot B)], [140.0, 139.9 (CH, C-10)], [129.2 (CH, C-8 rot A), 128.6 (CH, C-8 rot B], [105.3 (CH, C-9 rot B), 105.1 (CH, C-9 rot A)], [80.9, 80.8 (C, Boc (CH$_3$)$_3$*C*O)], [60.1 (CH, C-3 rot B), 58.7 (CH, C-3 rot A)], 52.1 (CH$_2$, C-4), [47.9 (CH$_2$, C-5 rot A), 46.6 (CH$_2$, C-5 rot

---

[a] Ratio based on H-8 peak integrations in the reported ^{1}H-NMR spectrum.

B)], [44.8 (CH$_2$, C-2 rot A), 44.0 (CH$_2$, C-2 rot B)], [42.61, 42.56 (CH$_2$, C-7)], [28.38, 28.36 (CH$_3$, Boc C(CH_3)$_3$)], [25.7 (CH$_2$, C-6 rot A), 24.6 (CH$_2$, C-6 rot B)].

ESI-LRMS (+): m/z 294.18 ([M+Na]$^+$, 48%), 294.18 (100, [M+H]$^+$).

HRMS: Found [M+H]$^+$ 294.1818. C$_{15}$H$_{24}$N$_3$O$_3$ requires M+H, 294.1818.

tert-Butyl 3-morpholino-5-oxoazocane-1-carboxylate (91)
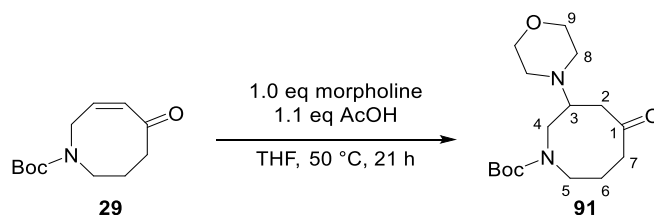
Morpholine (0.20 mL, 2.2 mmol) was added to a solution of enone **29** (500 mg, 2.22 mmol) in anhydrous THF (22 mL). AcOH (0.13 mL, 2.3 mmol) was added and the resulting mixture was stirred at 50 °C for 21 h. The volatiles were then removed under reduced pressure and the crude mixture was redissolved in CH_2Cl_2 (50 mL). The resulting mixture was washed sequentially with $NaHCO_3$ solution (50 mL) and H_2O (3 × 50 mL). The organic phase was dried over Na_2SO_4, filtered and concentrated under reduced pressure. Purification of the residue by automatic column chromatography (CH_2Cl_2:MeOH, 0.5% − 1% MeOH gradient) yielded the conjugate adduct **91** as a viscous amber oil (536 mg, 77%).

R_f (hexane:EtOAc 4:1): 0.5.

v_{max} **(neat / cm⁻¹):** 2966 w, 1697 s (C=O), 1412 m, 1162 m.

¹H-NMR (400 MHz, CDCl₃) (3:2 mixture of rotamers)[a] δ_H 3.89 − 3.70 (m, 0.6H, H-5 maj), 3.68 − 3.23 (stack, 6.4H, [including 3.68 − 3.57 (stack, 4H, H-9), 3.64 − 3.45 (stack, 1H, H-4), 3.45 − 3.35 (m, 0.4H, H-5 min), 3.45 − 3.23 (stack, 1H, H-3)], H-3, H-4, H-5 min, H-9), 3.12 − 2.95 (stack, 0.8H, H-4 min, H-5 min), 2.93 − 2.71 (stack, 1.2H, H-4 maj, H-5 maj), 2.70 − 2.41 (stack, 5H, H-2, H-8), 2.40 − 2.19 (stack, 3H, H-2, H-7), 2.19 − 2.05 (stack, 1H, H-6), 1.94 − 1.76 (stack, 1H, H-6), 1.40 − 1.35 (stack, 9H, [including 1.38 (s, 5H, Boc maj), 1.37 (s, 4H, Boc min)], Boc).

¹³C-NMR (101 MHz, CDCl₃) (mixture of rotamers) δ_C [210.7, 210.6 (C, C-1)], [155.3, 155.2 (C, C, Boc *C*=O)], 80.5 (C, Boc (CH₃)₃*C*O), [67.39, 67.36 (CH₂, C-9)], [64.1, 62.6 (CH, C-3)], 50.0 (CH₂, C-4), [49.9, 49.8, 49.7 (CH₂, C-4, C-8)], [48.1 (CH₂, C-5 min), 47.0 (CH₂, C-5 maj)], [42.3 (CH₂, C-7 maj), 41.6 (CH₂, C-7 min)], [40.1, 39.1 (CH₂, C-2)], 28.5 (CH₃, Boc C(*C*H₃)₃), [26.7, 25.0 (CH₂, C-6)].

ESI-LRMS (+): m/z 313.21 ([M+H]⁺, 100%), 257.15 (12, [M−C₄H₈ + H]⁺).

HRMS: Found [M+H]⁺ 313.2136. $C_{16}H_{29}N_2O_4$ requires M+H, 313.2127.

---

[a] Ratio based on H-4 and H-5 peak integrations in the reported ¹H-NMR spectrum at δ_H 3.89 − 3.70, 3.12 − 2.95 and 2.93 − 2.71 ppm.

tert-Butyl 5-(hydroxyimino)-3-morpholinoazocane-1-carboxylate (94)
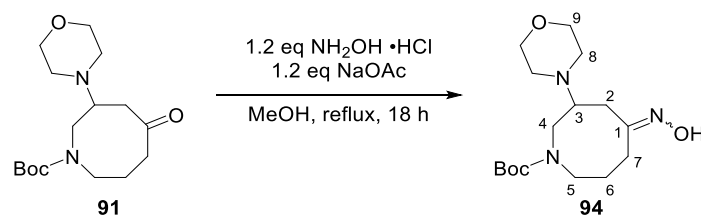
Following a procedure reported by Zaveri *et al*.:[9] NH$_2$OH •HCl (0.542 g, 7.79 mmol) and NaOAc (0.639 g, 7.79 mmol) were added sequentially to a stirred solution of ketone **91** (2.029 g, 6.49 mmol) in MeOH (32.5 mL). After heating for 18 h under reflux, the volatiles were removed under reduced pressure and the mixture was redissolved in CH$_2$Cl$_2$ (20 mL). The organic phase was washed with K$_2$CO$_3$ solution (1 × 20 mL), after which the aqueous phase was back-extracted with CH$_2$Cl$_2$ (3 × 20 mL). The organic phases were combined, dried over Na$_2$SO$_4$, filtered and concentrated under reduced pressure. Purification of the residue by automatic column chromatography (CH$_2$Cl$_2$:MeOH, 0.5% − 4% MeOH gradient) yielded oxime **94** as a colourless oil (2.083 g, 98%).

R*$_f$* (hexane:EtOAc 4:1): 0.5.

***v*$_{max}$ (neat / cm^{-1}):** 3334 br m (OH), 2930 m, 2855 m, 1662 s (C=O), 1424 m, 1364 m, 1249 m.

^{1}H-NMR (400 MHz, CDCl$_3$) (mixture of rotamers and isomers)[a] δ_H 8.72 − 8.13 (stack, 1H, O*H*), 4.01 − 3.87 (stack, 0.4H, H-5), 3.76 − 3.58 (stack, 4.8H, includes H-9), 3.57 − 3.44 (stack, 0.9H, includes H-3, H-4 or H-5), 3.38 − 3.20 (stack, 0.4H, includes H-4 or H-5), 3.17 − 3.03 (stack, 0.9H, includes H-2, H-3), 3.03 − 2.94 (stack, 0.6H, includes H-2, H-4 or H-5), 2.94 − 2.79 (stack, 0.9H, includes H-4 or H-5), 2.79 − 2.57 (stack, 4.3H, includes H-4 or H-5, H-8), 2.57 − 2.28 (stack, 2.1H, includes H-2, H-7), 2.28 − 2.16 (stack, 1H, includes H-7), 2.14 − 1.86 (stack, 1.8H, H-2, H-6), 1.86 − 1.71 (stack, 0.9H, H-6), 1.48 − 1.36 (stack, 9H, Boc).

^{13}C-NMR (101 MHz, CDCl$_3$) (mixture of rotamers and isomers) δ_C [159.9, 159.8, 159.8, 159.6 (C, C-1)], [155.3, 155.3, 155.2 (C, Boc *C*=O), resonance overlap], [79.9, 79.9, 79.8 (C, Boc (CH$_3$)$_3$*C*O, resonance overlap)], 67.5 (CH$_2$, C-9), [63.7, 62.0, 59.2, 58.5 (CH, C-3)], [50.2, 49.8, 49.6, 49.5, 49.5, 49.3, 48.9, 48.8, 48.7, 48.1, 47.0 (CH$_2$, C-4, C-5, C-8)], [33.7, 33.0, 32.6, 32.5 (CH$_2$, C-7)], [28.6, 28.5, 28.5, 28.4 (CH$_3$, Boc C(*C*H$_3$)$_3$)], [27.3, 27.2, 26.4, 26.4 (CH$_2$, C-2)], [26.0, 24.8, 24.2, 23.6 (CH$_2$, C-6)].

---

[a] Stacked rotamer resonances in the reported ^{1}H-NMR spectrum only allowed for partial assignment of peaks. Relative rotamer/isomer ratio could not be determined.

ESI-LRMS (+): m/z 328.22 ([M+H]$^+$, 100%), 272.16 (23, [M$-$C$_4$H$_8$ + H]$^+$).

HRMS: Found [M+H]$^+$ 328.2242. C$_{16}$H$_{30}$N$_3$O$_4$ requires M+H, 328.2236.

tert-butyl 5-amino-3-morpholinoazocane-1-carboxylate (93)
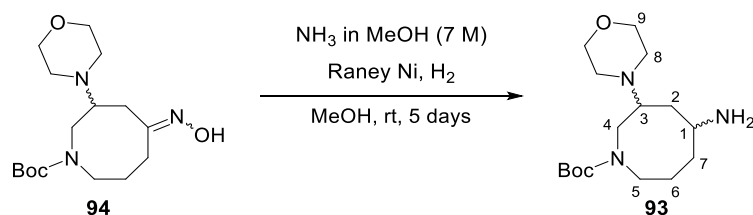
A 250 mL flask was loaded with oxime **94** (1.79 g, 5.48 mmol) in MeOH (110 mL) and purged with N_2. 7 M NH_3 in MeOH (110 mL, 770 mmol) and Raney Ni slurry (50 wt% in H_2O, 4.4 mL, 38 mmol) were subsequently added under a N_2 atmosphere. The resulting mixture was stirred at rt under a H_2 atmosphere (1 atm). After 4 days, an extra portion of Raney Ni was added (50 wt% in H_2O, 2.2 mL, 19 mmol) and the reaction mixture was stirred at rt for another 29 h under a H_2 atmosphere (1 atm). The flask was purged with N_2 before opening and the reaction mixture was filtered through a pad of Celite. The residue was washed with MeOH (3 × 100 mL) and the combined filtrates were concentrated under reduced pressure. Purification of the residue by automatic flash column chromatography (CH_2Cl_2:7.0 M NH_3 in MeOH 9:1) yielded amine **93** as a colourless oil and undetermined mixture of diastereoisomers (1.44 g, 84%).

R*f* (CH_2Cl_2:7.0 M NH_3 in MeOH 9:1): 0.5.

v_max (neat / cm⁻¹): 2926 m, 2855 m, 1681 v s (C=O), 1416 m, 1364 m, 1159 v s, 1115 v s.

¹H-NMR (400 MHz, CDCl₃) (mixture of rotamers and diastereomers)[a] δ_H 3.54 – 3.40 (stack, 5H, H-9, H-4 and/or H-5), 3.38 – 3.08 (stack, 1H, H-4 and/or H-5), 3.07 – 2.81 (stack, 2H, H-1, H-4 and/or H-5), 2.81 – 2.70 (stack, 1H, H-1, H-4 and/or H-5), 2.69 – 2.53 (stack, 1H, H-3), 2.46 – 2.28 (stack, 4H, H-8), 1.68 – 1.15 (stack, 17H, N*H*₂, H-2, H-6, H-7, Boc).

¹³C-NMR (101 MHz, CDCl₃) (mixture of rotamers and diastereomers) δ_C [155.82, 155.79, 155.7, 155.4 (C, Boc *C*=O)], [79.8, 79.7, 79.59, 79.57 (C, Boc *C*(CH₃))], [67.60, 67.57, 67.5, 67.4 (CH₂, C-9)], [61.8, 61.0, 58.5, 57.8 (CH, C-3)], [51.3, 50.5 (CH, C-1)], [50.1, 50.0, 49.8, 49.7, 49.3, 49.1, 48.9 (CH₂, C-4, C-5, C-8)], 48.5 (CH, C-1), 48.2 (CH₂, C-4 or C-5), 48.0 (CH, C-1), 47.9 (CH₂, C-4 or C-5), 47.5 (CH₂, C-4 or C-5), [39.22, 39.18, 36.6, 36.0, 35.7, 34.9, 33.4, 33.0 (CH₂, C-2, C-7)], [28.7, 28.63, 28.61 (CH₃, Boc C(*C*H₃)₃, resonance overlap)], [24.2, 23.5, 23.4, 22.7 (CH₂, C-6)].

ESI-LRMS (+): m/z 314.2 ([M+H]⁺, 100%).

---

[a] Due to stacked rotamer resonances in the reported ¹H-NMR spectrum, rotamer/diastereomer ratios could not be determined.

HRMS: Found [M+H]$^+$ 314.2439. $C_{16}H_{31}N_3O_3$ requires M+H, 314.2438.

Methyl *N*-allyl-*N*-(*tert*-butoxycarbonyl)glycinate (52a)
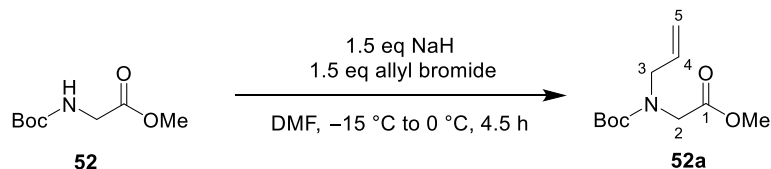
NaH (294 mg of a 60% dispersion in mineral oil, 6.12 mmol) was added over 4 min to a stirred solution of methyl ester **52** (772 mg, 4.08 mmol) in DMF (7.7 mL) in an ice:NaCl bath. After 15 min, allyl bromide (0.53 mL, 6.1 mmol) was added dropwise over 1 min to the cooled solution. After 4.5 h at 0 °C, NH$_4$Cl solution (7 mL) and H$_2$O (5 mL) were added sequentially. The resulting solution was extracted with Et$_2$O (3 × 15 mL). The organic phases were combined and washed with H$_2$O (3 × 40 mL). The organic phase was dried over anhydrous Na$_2$SO$_4$, filtered and concentrated under reduced pressure. The crude product was purified by flash column chromatography (hexane:EtOAc 95:5) to yield methyl ester **52a** as a colourless oil (631 mg, 68%).

R$_f$ (hexane:EtOAc 4:1): 0.3.

v$_{max}$ **(neat / cm^{-1}):** 2977 w, 1752 m (C=O), 1695 s (C=O), 1399 m, 1366 m.

^{1}H-NMR (400 MHz, CDCl$_3$) (1:1 mixture of rotamers)[a] δ_H 5.78 − 5.65 (m, 1H, H-4), 5.15 − 5.00 (stack, 2H, H-5), 3.91 − 3.86 (stack, 2H, H-2 rot A, H-3 rot B), 3.82 (d, *J* = 5.9 Hz, 1H, H-3 rot A), 3.78 (br s, 1H, H-2 rot B), 3.65 (br s, 3H, OMe), [1.40 (s, 4.5H, Boc), 1.36 (s, 4.5H, Boc)].

^{13}C-NMR (101 MHz, CDCl$_3$) (mixture of rotamers) δ_C [170.53, 170.48 (C, C-1)], [155.6 (C, Boc *C*=O rot A), 155.1 (C, Boc *C*=O rot B)], [133.7 (CH, C-4 rot B), 133.6 (CH, C-4 rot A)], [117.6 (CH$_2$, C-5 rot B), 116.8 (CH$_2$, C-5 rot A)], 80.3 (C, Boc (CH$_3$)$_3$*C*O), [51.90, 51.86 (CH$_3$, OMe)], [50.8 (CH$_2$, C-3 rot A), 50.3 (CH$_2$, C-3 rot B)], [47.9 (CH$_2$, C-2 rot B), 47.5 (CH$_2$, C-2 rot A)], [28.3, 28.2 (CH$_3$, Boc C(*C*H$_3$)$_3$)].

ESI-LRMS (+): m/z 252.1 ([M+Na]$^+$, 100%), 196.0 (25, [M−C$_4$H$_8$ + Na]$^+$).

^{1}H-NMR spectroscopic data were in accordance with those reported in the literature.[10]

---

[a] Ratio based on Boc peak integrations in the reported ^{1}H-NMR spectrum.

N-Allyl-*N*-(*tert*-butoxycarbonyl)glycine (53)
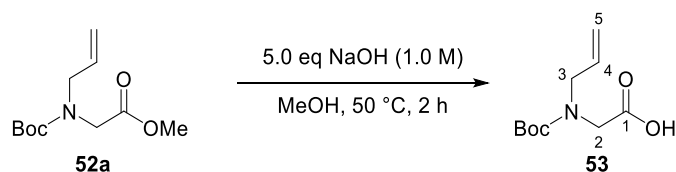
Following a procedure reported by Lawton *et al*.:[11] NaOH solution (1.0 M, 39.3 mL, 39.3 mmol) was added to a stirred solution of methyl ester **52a** (1.80 g, 7.85 mmol) in MeOH (19.6 mL). After stirring at rt for 5.5 h, hydrochloric acid (1.0 M) was added until pH = 2. The aqueous phase was extracted with EtOAc (3 × 200 mL). The combined organic extracts were dried over Na_2SO_4, filtered and concentrated under reduced pressure. Purification of the residue using automatic column chromatography (heptane:EtOAc, 0 – 100% EtOAc gradient) yielded carboxylic acid **53** as a colourless oil (1.26 g, 74%).

R*f* (hexane:EtOAc 3:2): 0.1.

***v*max (neat / cm⁻¹):** 2979 w, 1697 m (C=O), 1396 m, 1246 m, 1144 s.

¹H-NMR (400 MHz, CDCl₃) δ_H 11.49 (br s, 1H, O*H*), 5.77 – 5.61 (m, 1H, H-4), 5.14 – 4.99 (stack, 2H, H-5), 3.95 – 3.76 (stack, 4H, H-2, H-3), 1.37 (br s, 9H, Boc).

¹³C-NMR (101 MHz, CDCl₃) (mixture of rotamers) δ_C [175.9, 175.5 (C, C-1)], [156.0, 155.3 (C, Boc *C*=O)], [133.6, 133.4 (CH, C-4)], [118.0, 117.3 (CH₂, C-5)], [81.0, 80.9 (C, Boc (CH₃)₃*C*O)], [51.0, 50.4 (CH₂, C-3)], 47.7 (CH₂, C-2), [28.4, 28.3 (CH₃, Boc C(*C*H₃)₃)].

ESI-LRMS (+): m/z 238.0 ([M+Na]⁺, 10%), 115.9 (100, [M−C₅H₈O₂ + H]⁺).

¹H-NMR and ¹³C-NMR spectroscopic data were in accordance with those reported in the literature.[12]

N-benzylprop-2-en-1-amine (benzylallylamine)
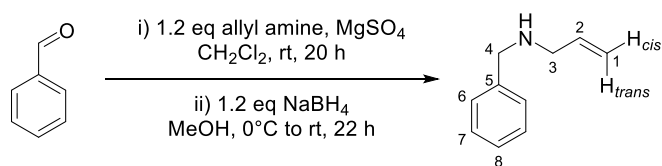
Allylamine (0.626 mL, 8.35 mmol) was added to a solution of benzaldehyde (0.71 mL, 6.96 mmol) in anhydrous CH_2Cl_2 (7 mL) on $MgSO_4$ (~2 g). After stirring at rt for 20 h, the mixture was filtered. The residue was washed with CH_2Cl_2 (3 × 5 mL) and the washings were added to the crude mixture. After removing CH_2Cl_2 under reduced pressure, MeOH (7 mL) was added and the mixture was cooled to 0 °C. $NaBH_4$ (0.316 g, 8.35 mmol) was added and the resulting mixture was stirred at rt for 22 h, after which time, the solvent was removed under reduced pressure. After addition of $CHCl_3$ (10 mL), the crude mixture was washed with $NaHCO_3$ solution (10 mL) and then H_2O (2 × 10 mL). The organic phase was dried over anhydrous Na_2SO_4, filtered and concentrated under reduced pressure, yielding benzylallylamine as a colourless oil (1.02 g, quant.).

R_f (hexane:EtOAc 3:2): 0.2.

¹H-NMR (400 MHz, CDCl₃) δ_H 7.28 − 7.23 (stack, 4H, H-6, H-7), 7.21 − 7.15 (m, 1H, H-8), 5.87 (ddt, J = 17.3, 10.3, 6.0 Hz, 1H, H-2), 5.13 (ddt, J = 17.3, 1.7, 1.4 Hz, 1H, H-1$_{cis}$), 5.05 (ddt, J = 10.3, 1.7, 1.4 Hz, 1H, H-1$_{trans}$), 3.72 (s, 2H, H-4), 3.20 (ddd, J = 6.0, 1.4, 1.4 Hz, 2H, H-3), NH not observed.

¹³C-NMR (101 MHz, CDCl₃) δ_C 140.3 (C, C-5), 136.8 (CH, C-2), [128.3, 128.1 (CH, C-6, C-7)], 126.9 (CH, C-8), 115.9 (CH₂, C-1), 53.2 (CH₂, C-4), 51.7 (CH₂, C-3).

ESI-LRMS (+): m/z 295.2 ([2M+H]⁺, 12%) 148.1 (100, [M+H]⁺).

¹H-NMR, ¹³C-NMR and LRMS data were in accordance with those reported in the literature.[13]

tert-Butyl allyl(2-(allyl(benzyl)amino)-2-oxoethyl)carbamate (44)
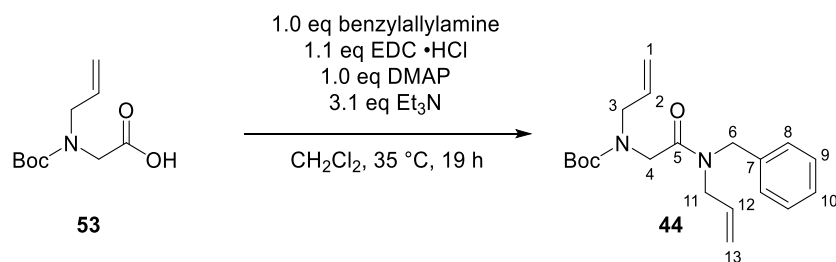
Et$_3$N (1.1 mL, 8.3 mmol), DMAP (331 mg, 2.71 mmol), benzylallylamine (470 mg, 3.19 mmol) and EDC •HCl (571 mg, 2.98 mmol) were added sequentially to a solution of *N*-allylated amino acid **53** (573 mg, 2.66 mmol) in CH$_2$Cl$_2$ (27 mL). After stirring for 17 h at rt, the reaction mixture was washed sequentially with 5% citric acid solution (3 × 30 mL) and NaHCO$_3$ solution (3 × 30 mL). The organic phase was dried over anhydrous Na$_2$SO$_4$, filtered and concentrated under reduced pressure. Purification of the residue by automatic flash column chromatography (heptane:EtOAc 4:1) yielded diene **44** as a yellow oil (607 mg, 70%).

R$_f$ (hexane:EtOAc 3:2): 0.6.

v_{max} (neat / cm^{-1}): 2932 w, 1694 s (C=O), 1663 s (C=O), 1166 s.

^{1}H-NMR (400 MHz, CDCl$_3$) (mixture of four rotamers, 2:2:3:3)[a] δ_H 7.46 − 7.12 (stack, 5H, [including 7.16 (app d, *J* = 7.5 Hz, 0.8 H, H-8], H-8, H-9, H-10), 5.91 − 5.60 (stack, 2H, H-2, H-12), 5.30 − 4.94 (stack, 4H, H-1, H-13), [4.58 (s, 1.2H, H-6), 4.50 (s, 0.4H, H-6), 4.44 (s, 0.4H, H-6)], 4.11 − 3.71 (stack, 6H, [including (3.95 (s, 1H, H-4), 3.84 − 3.71 (stack, 1.2H, H-11)], H-3, H-4, H-11), [1.46 (s, 3.2H, Boc), 1.43 (s, 5.8H, Boc)].

^{13}C-NMR (101 MHz, CDCl$_3$) (mixture of four rotamers) δ_C [169.3, 169.0, 168.6 (C, C-5, resonance overlap)], [155.9, 155.6 (C, Boc *C*=O)], [137.5, 137.3, 136.5, 136.4 (C, C-7)], [134.4, 134.1, 133.9 (CH, C-2, resonance overlap)], [132.8, 132.5, 132.4 (CH, C-12)], [129.0, 128.7, 128.44, 128.37, 127.8, 127.7, 127.6, 127.5 (CH, C-9, C-10)], [126.6, 126.4 (CH, C-8)], [117.94, 117.86 (CH$_2$, C-13)], [117.3, 117.2, 117.1 , 116.7, 116.6 (CH$_2$, C-1, C-13, resonance overlap)], [80.2, 80.1 (C, Boc (CH$_3$)$_3$*C*O)], [50.6, 50.4 (CH$_2$, C-3, resonance overlap)], [49.5, 49.3, 49.0, 48.8, 48.6, 48.4 (CH$_2$, C-6, C-11, resonance overlap)], [47.5, 47.3, 47.1 (CH$_2$, C-4, resonance overlap)], 28.4 (CH$_3$, Boc (*C*H$_3$)$_3$CO).

---

[a] Ratio based on H-6 peak integrations in the reported ^{1}H-NMR spectrum.

ESI-LRMS (+): m/z 367.20 ([M+Na]$^+$, 100%), 345.22 (10, [M+H]$^+$), 267.15 (25, [M−C$_5$H$_8$O$_2$ + Na]$^+$), 245.16 (25, [M−C$_5$H$_8$O$_2$ + H]$^+$).

HRMS: Found [M+Na]$^+$ 367.1991. C$_{20}$H$_{28}$N$_2$NaO$_3$ requires M+Na, 367.1992.

Methyl *N*-allyl-(L)-prolinate (54a)
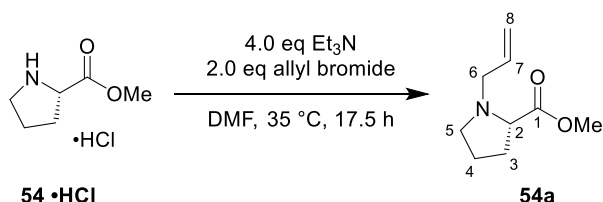
Et$_3$N (5.2 mL, 37 mmol) and allyl bromide (1.6 mL, 19 mmol) were added sequentially to a cooled (0 °C) solution of methyl ester **54 •HCl** (1.55 g, 9.33 mmol) in anhydrous DMF (20 mL). After stirring at 35 °C for 17.5 h, H$_2$O (10 mL) was added. The aqueous phase was extracted with EtOAc (6 × 30 mL). The combined organic extracts were washed with H$_2$O (3 × 150 mL) and then brine (1 × 150 mL), dried over anhydrous Na$_2$SO$_4$, filtered and concentrated under reduced pressure. Purification of the residue by flash column chromatography (hexane:EtOAc, gradient 4:1 − 3:2) yielded allylated amino ester **54a** as a pale yellow oil (628 mg, 40%).

R$_f$ (hexane:EtOAc 3:2): 0.3.

***v*$_{max}$ (neat / cm$^{−1}$):** 2952 w, 2797 w, 1732 s (C=O), 1196 s, 1168 s.

^{1}H-NMR (400 MHz, CDCl$_3$) δ_H 5.81 (dddd, *J* = 17.1, 10.1, 7.0, 6.4 Hz, 1H, H-7), 5.07 (app ddt, *J* = 17.1, 1.8, 1.2 Hz, 1H, H-8), 4.98 (ddt, *J* = 10.1, 1.8, 1.2 Hz, 1H, H-8), 3.61 (s, 3H, OMe), 3.21 (app ddt, *J* = 13.1, 6.4, 1.2 Hz, 1H, H-6), 3.09 − 2.97 (stack, 3H, [including 3.09 − 3.02 (m, 1H, H-6)], H-2, H-5, H-6), 2.35 − 2.18 (m, 1H, H-5), 2.12 − 1.94 (m, 1H, H-3), 1.92 − 1.62 (stack, 3H, [including 1.92 − 1.70 (m, 1H, H-3)], H-3, H-4).

^{13}C-NMR (101 MHz, CDCl$_3$) δ_C 174.6 (C, C-1), 135.2 (CH, C-7), 117.4 (CH$_2$, C-8), 65.2 (CH, C-2), 57.7 (CH$_2$, C-6), 53.4 (CH$_2$, C-5), 51.7 (CH$_3$, OMe), 29.5 (CH$_2$, C-3), 23.0 (CH$_2$, C-4).

ESI-LRMS (+): m/z 361.42 ([2M+Na]$^+$, 20%), 192.06 (100, [M+Na]$^+$), 170.05 (100, [M+H]$^+$).

^{1}H-NMR and ^{13}C-NMR spectroscopic data were in accordance with those reported in the literature.[14]

N-Allyl-(L)-proline hydrochloride (55 •HCl)
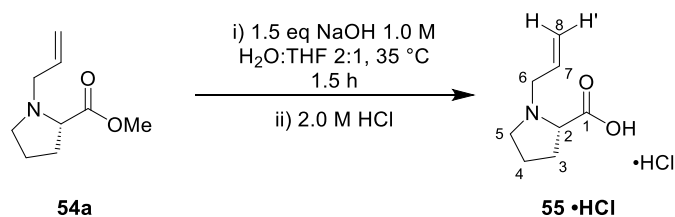
Following a procedure reported by Hung *et al.*:[15] NaOH (1.0 M, 4.7 mL, 4.7 mmol) was added to a solution of methyl ester **54a** (534 mg, 3.16 mmol) in H_2O:THF 2:1 (6.3 mL). The resulting clear solution was stirred at 35 °C for 1.5 h, after which time, the THF was removed under reduced pressure. The aqueous phase was acidified with hydrochloric acid (2.0 M, 2 mL) until pH = 4. *i*-PrOH (20 mL) and $CHCl_3$ (20 mL) were added to the mixture. Removal of the solvent under reduced pressure yielded carboxylic acid **55 •HCl** as a white amorphous solid, which was used without further purification (605 mg, quant.).

Melting point: 176 – 180 °C dec.

v_{max} (neat / cm^{-1}): 3010 w, 2850 w, 1716 s (C=O).

^{1}H-NMR (400 MHz, CD$_3$OD) δ_H 5.99 (app ddt, *J* = 17.1, 10.3, 7.2 Hz, 1H, H-7), 5.60 (app ddt, *J* = 17.1, 1.2, 1.0 Hz, 1 H, H-8) 5.52 (app ddt, *J* = 10.3, 1.2, 1.0 Hz, 1H, H-8), 4.11 (dd, *J* = 9.6, 6.7 Hz, 1H, H-2), 3.93 (app ddt, *J* = 13.1, 7.2, 1.0 Hz, 1H, H-6), 3.83 (app ddt, *J* = 13.1, 7.2, 1.0 Hz, 1H, H-6), 3.70 (ddd, *J* = 11.6, 8.3, 4.4 Hz, 1H, H-5), 3.23 (ddd, *J* = 11.6, 9.0, 7.4 Hz, 1H, H-5), 2.61 – 2.41 (m, 1H, H-3), 2.27 – 2.07 (stack, 2H, H-3, H-4), 2.06 – 1.93 (m, 1H, H-4), exchangeable protons not observed.

^{13}C-NMR (101 MHz, CD$_3$OD) δ_C 170.8 (C, C-1), 127.4 (CH, C-7), 124.4 (CH$_2$, C-8), 67.0 (CH, C-2), 57.0 (CH$_2$, C-6), 54.1 (CH$_2$, C-5), 28.5 (CH$_2$, C-4), 22.6 (CH$_2$, C-3).

ESI-LRMS (+): m/z 354.39 ([2M+Na]$^+$, 40%), 333.43 (70, [2M+H]$^+$), 178.33 (100, [M+Na]$^+$), 156.32 (100, [M+H]$^+$).

^{1}H-NMR and ^{13}C-NMR spectroscopic data were in accordance with those reported in the literature.[16]

(S)-N,1-Diallyl-N-benzylpyrrolidine-2-carboxamide (48)
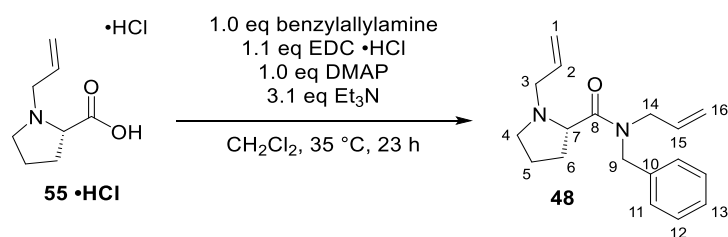
Et₃N (0.73 mL, 4.1 mmol), DMAP (124 mg, 1.02 mmol), benzylallylamine (147 mg, 1.00 mmol) and EDC •HCl (215 mg, 1.12 mmol) were added sequentially to a stirred solution of *N*-allyl-(L)-proline hydrochloride **55 •HCl** (192 mg, 1.00 mmol) in CH$_2$Cl$_2$ (10 mL). The resulting solution was stirred at 35 °C for 23 h. The volatiles were then removed under reduced pressure and the crude mixture was redissolved in EtOAc (20 mL) and washed with NaHCO$_3$ solution (3 × 20 mL).[a] The organic phase was dried over anhydrous Na$_2$SO$_4$, filtered and concentrated under reduced pressure. Purification of the residue by flash column chromatography (CH$_2$Cl$_2$:MeOH, gradient 99:1 − 9:1) yielded amide **48** as a pale yellow oil (102 mg, 36%).

R*ƒ* (CH$_2$Cl$_2$:MeOH 98:2): 0.3.

ν$_{max}$ (neat / cm⁻¹): 2974 w, 1639 s (C=O), 1417 m, 1213 m.

¹H-NMR (400 MHz, CDCl₃) (mixture of rotamers)[b] δ_H 7.35 − 7.09 (stack, 5H, H-11, H-12, H-13), 5.99 − 5.82 (m, 1H, H-2), 5.71 (dddd, *J* = 17.1, 15.1, 10.3, 4.5 Hz, 1H, H-15), 5.21 − 4.93 (stack, 4H, H-1, H-16), 4.71 − 4.39 (stack, 2H, H-9), 4.12 − 3.83 (stack, 2H, H-14), 3.36 − 3.27 (stack, 2H, H-3, H-7), 3.25 − 3.09 (stack, 1H, H-4), 3.04 − 2.92 (m, 1H, H-3), 2.38 − 2.22 (stack, 1H, H-4), 2.13 − 1.61 (stack, 4H, H-5, H-6).

¹³C-NMR (101 MHz, CDCl₃) (mixture of rotamers) δ_C [173.65, 173.55 (C, C-8)], [137.7, 137.0 (C, C-10)], 135.9 (CH, C-2), [133.1, 133.0 (CH, C-15)], [128.8, 128.5, 128.3, 127.5, 127.3 (CH, Ph)], 126.4 (CH, C-11), [117.5, 117.0, 116.9 (CH$_2$, C-1, C-16)], [63.8, 63.5 (CH, C-7)], 57.3 (CH$_2$, C-3), [53.3, 53.2 (CH$_2$, C-4)], 49.4 (CH$_2$, C-9), 48.3 (CH$_2$, C-14), 48.2 (CH$_2$, C-9), [29.74, 29.66 (CH$_2$, C-6)], [23.0, 22.9 (CH$_2$, C-5)].

ESI-LRMS (+): m/z 285.20 ([M+H]⁺, 100%).

HRMS: Found [M+H]⁺ 285.1978. C$_{18}$H$_{25}$N$_2$O requires M+H, 285.1967.

---

[a] Initial extraction of the organic phase with 0.5 M HCl$_{(aq)}$ resulted in protonation of the title compound. Neutralisation of the acidic aqueous phase with Na$_2$CO$_3$ (satd aq.) allowed the desired compound to be back-extracted with EtOAc.

[b] Due to stacked rotamer resonances in the reported ¹H-NMR spectrum, the rotamer ratio could not be determined.

Allyl *N*-allyl-*N*-(*tert*-butoxycarbonyl)glycinate (46)
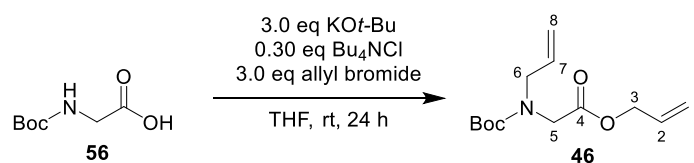
Following a procedure reported by Mouna *et al.*:[17] Boc-glycine **56** (491 mg, 2.80 mmol) was added to a cooled (0 °C) solution of KO*t*-Bu (943 mg, 8.40 mmol) and Bu$_4$NCl (257 mg, 0.92 mmol) in THF (15 mL). The resulting solution was stirred for 36 min, followed by dropwise addition of allyl bromide (0.72 mL, 8.4 mmol) over 2 min. After 24 h of stirring at rt, the solvent was removed under reduced pressure and the residue was redissolved in H$_2$O (20 mL). The aqueous phase was extracted with EtOAc (3 × 25 mL) and the combined organic extracts were dried over anhydrous Na$_2$SO$_4$, filtered and concentrated under reduced pressure. Purification of the residue by flash column chromatography (hexane:EtOAc, gradient 9:1 − 4:1) yielded diene **46** as a colourless oil (643 mg, 90%).

R$_f$ (hexane:EtOAc 4:1): 0.5.

v_{max} (neat / cm^{-1}): 2978 w, 1752 m (C=O), 1697 s (C=O), 1164 s, 1142 s.

^{1}H-NMR (400 MHz, CDCl$_3$) (4:5 mixture of rotamers)[a] δ_H 5.92 − 5.80 (m, 1H, H-2), 5.79 − 5.66 (m, 1H, H-7), 5.32 − 5.15 (stack, 2H, H-1), 5.15 − 5.02 (stack, 2H, H-8), 4.57 (d, *J* = 5.7 Hz, 2H, H-3), 3.94 − 3.79 (stack, 4H, [including 3.92 (s, 0.9H, H-5 min), 3.90 (d, *J* = 6.2 Hz, 1.1H, H-6 maj), 3.84 (d, *J* = 5.9 Hz, 0.9H, H-6 min), 3.81 (s, 1.1H, H-5 maj)], H-5, H-6), 1.41 (s, 4H, Boc min), 1.38 (s, 5H, Boc maj).

^{13}C-NMR (101 MHz, CDCl$_3$) (mixture of rotamers) δ_C [169.8 (C, C-4 maj), 169.7 (C, C-4 min)], [155.6 (C, Boc *C*=O min), 155.1 (C, Boc *C*=O maj)], [133.8 (CH, C-7 maj), 133.7 (CH, C-7 min)], [131.86, (CH, C-2 maj), 131.81 (CH, C-2 min)], [118.7 (CH$_2$, C-1 maj), 118.4 (CH$_2$, C-1 min)], [117.7 (CH$_2$, C-8 maj), 116.9 (CH$_2$, C-8 min)], 80.4 (C, Boc (CH$_3$)$_3$*C*O), 65.5 (CH$_2$, C-3), [50.8 (CH$_2$, C-6 min), 50.4 (CH$_2$, C-6 maj)], [48.0 (CH$_2$, C-5 maj), 47.7 (CH$_2$, C-5 min)], [28.33 (CH$_3$, Boc C(*C*H$_3$)$_3$ min), 28.27 (CH$_3$, Boc C(*C*H)$_3$ maj)].

ESI-LRMS (+): m/z 278.12 ([M+Na]$^+$, 100%), 533.24 (20, [2M−Na]$^+$).

HRMS: Found [M+Na]$^+$ 278.1361. C$_{13}$H$_{21}$NNaO$_4$ requires M+Na, 278.1363.

---

[a] Ratio based on Boc peak integrations in the reported ^{1}H-NMR spectrum.

tert-Butyl allyl(2-(methoxy(methyl)amino)-2-oxoethyl)carbamate (57)
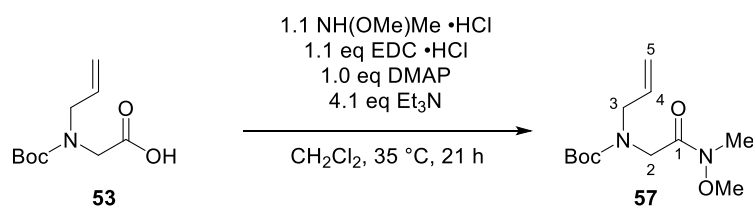
Et$_3$N (3.0 mL, 21 mmol), DMAP (650 mg, 5.32 mmol), NH(OMe)Me •HCl (562 mg, 5.76 mmol) and EDC •HCl (1.12 g, 5.87 mmol) were added sequentially to a solution of *N*-allyl-*N*-(*tert*-butoxycarbonyl)glycine **53** (1.13 g, 5.24 mmol) in anhydrous CH$_2$Cl$_2$ (52 mL). The reaction mixture was stirred under an Ar atmosphere at 35 °C for 21 h. The volatiles were removed under reduce pressure and the crude mixture was redissolved in EtOAc (50 mL). The mixture was washed sequentially with citric acid solution (aq., 5 w/v%, 3 × 30 mL), NaHCO$_3$ solution (3 × 30 mL) and both aqueous phases were back-extracted with EtOAc (1 × 50 mL). The combined organic phases were dried over anhydrous Na$_2$SO$_4$, filtered and concentrated under reduced pressure. Purification of the residue by flash column chromatography (hexane/EtOAc 7:3) yielded Weinreb amide **57** as a colourless oil (945 mg, 70%).

R$_f$ (hexane:EtOAc 3:2): 0.3.

v_{max} (neat / cm^{-1}): 2976 w, 1678 s (C=O), 1393 s, 1167 s.

^{1}H-NMR (400 MHz, CDCl$_3$) (4:5 mixture of rotamers)[a] δ_H 5.78 – 5.51 (stack, 1H, H-4), 5.15 – 4.85 (stack, 2H, H-5), [3.98 (s, 1.1H, H-2 maj), 3.88 (s, 0.9H, H-2 min)], [3.81 (d, *J* = 6.1 Hz, 0.9H, H-3 min), 3.76 (d, *J* = 5.8 Hz, 1.1H, H-3 maj)], [3.56 (s, 1.6H, OMe maj), 3.54 (s, 1.4H, OMe min)], [3.03 (s, 1.4H, NMe min), 3.02 (s, 1.6H, NMe maj)], [1.31 (s, 5H, Boc maj), 1.28 (s, 4H, Boc min)].

^{13}C-NMR (101 MHz, CDCl$_3$) δ_C [170.2 (C, C-1 min), 169.9 (C, C-1 maj)], [155.6 (C, Boc *C*=O maj), 155.2 (C, Boc *C*=O min)], [134.0 (CH, C-4 min), 133.8 (CH, C-4 maj)], [116.9 (CH$_2$, C-5 min), 116.1 (CH$_2$, C-5 maj)], [79.7, 79.6 (C, Boc (CH$_3$)$_3$*C*O)], 61.1 (CH$_3$, OMe), [50.6 (CH$_2$, C-3 maj), 50.0 (CH$_2$, C-3 min)], [46.7 (CH$_2$, C-2 min), 46.6 (CH$_2$, C-2 maj)], [32.2 (CH$_3$, NMe), 32.1 (CH$_3$, NMe)], [28.1, 28.0 (CH$_3$, Boc C(*C*H$_3$)$_3$)].

ESI-LRMS (+): m/z 281.16 ([M+Na]$^+$, 100%), 181.09 (10, [M+Na–C$_5$H$_8$O$_2$]$^+$).

HRMS: Found [M+Na]$^+$ 281.1470. C$_{12}$H$_{22}$N$_2$NaO$_4$ requires M+Na, 281.1472.

---

[a] Ratio based on Boc peak integrations in the reported ^{1}H-NMR spectrum.

^{1}H-NMR spectroscopic data were consistently shifted upfield (by 0.13 ppm) in respect to those reported in the literature.[18]

tert-Butyl allyl(2-oxohex-5-en-1-yl)carbamate (50)
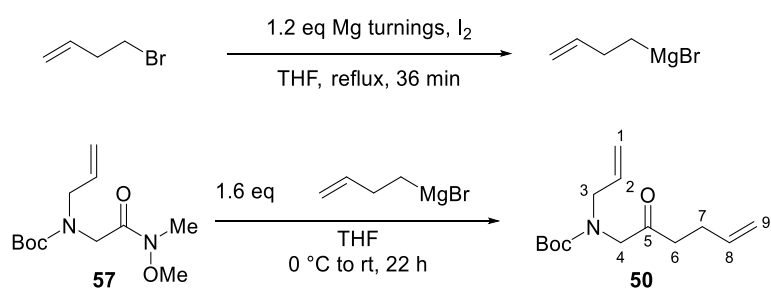
Three small crystals of iodine were added to Mg turnings (1.02 g, 42.0 mmol) in a two-necked flask, equipped with a reflux condenser and filled with crushed glass (10% volume). The flask was treated with a heat gun until the iodine vapours were evenly distributed inside the flask. A solution of bromobut-1-ene (4.73 g, 35.0 mmol) in THF (40 mL) was added over 10 min and the reaction mixture was heated under reflux for 2 h. Titration of the Grignard species with menthol and 1,10-phenanthroline[2] showed a 0.7 M concentration of Grignard reagent, which was used *in situ.*

The prepared Grignard solution (0.7 M in THF, 8.4 mL, 5.85 mmol) was added dropwise over 2 min to a solution of Weinreb amide **58** (945 mg, 3.66 mmol) in THF (37 mL) at 0 °C. The reaction mixture was stirred for 1.5 h at rt, whilst allowed to warm to rt. After dropwise addition of NH$_4$Cl solution (10 mL) over 5 min, THF was removed under reduced pressure and the aqueous phase was extracted with EtOAc (3 × 30 mL). The combined organic extracts were dried over anhydrous Na$_2$SO$_4$, filtered and concentrated under reduced pressure. Purification of the residue by flash column chromatography (hexane:EtOAc, 3:2) yielded diene **50** as a colourless oil (376 mg, 41%).

R*f* (hexane:EtOAc 3:2): 0.8.

ν$_{max}$ (neat / cm^{-1}): 2977 w, 2929 w, 1692 s (C=O), 1246 s, 1163 s.

^{1}H-NMR (400 MHz, CDCl$_3$) (1:1 mixture of rotamers)[a] δ_H 5.87 − 5.54 (stack, 2H, H-2, H-8), 5.20 − 4.49 (stack, 4H, H-1, H-9), 3.95 − 3.76 (stack, 4H, [including 3.93 (s, 1H, H-4 rot A), 3.87 (d, *J* =

---

[a] Ratio based on Boc peak integrations in the reported ^{1}H-NMR spectrum.

6.0 Hz, H-3 rot B), 3.82 (s, 1H, H-4 rot B), 3.79 (d, J = 5.8 Hz, H-3 rot A)], H-3, H-4), 2.48 – 2.37 (stack, 2H, H-6), 2.33 – 2.24 (stack, 2H, H-7), [1.41 (s, 4.5H, Boc), 1.37 (s, 4.5H, Boc)].

^{13}C-NMR (101 MHz, CDCl$_3$) (mixture of rotamers) δ_C [205.9 (C, C-5 rot A), 205.6 (C, C-5 rot B)], [155.6 (C, Boc C=O rot A), 155.1 (C, Boc C=O rot B)], [136.9, 136.8 (CH, C-8)], [133.8 (CH, C-2 rot B), 133.7 (CH, C-2 rot A)], [117.6 (CH$_2$, C-1 rot B), 116.8 (CH$_2$, C-1 rot A)], [115.6, 115.4 (CH$_2$, C-9)], 80.3 (C, Boc (CH$_3$)$_3$$C$O), [55.7 (CH$_2$, C-4 rot B), 55.4 (CH$_2$, C-4 rot A)], [50.9 (CH$_2$, C-3 rot A), 50.5 (CH$_2$, C-3 rot B)], [38.8, 38.6 (CH$_2$, C-6)], [28.33, 28.26 (CH$_3$, Boc C(CH$_3$)$_3$)], [27.5, 27.4 (CH$_2$, C-7)].

ESI-LRMS (+): m/z 208.17 ([M–C$_5$H$_8$O$_2$ + MeOH+Na]$^+$, 60%), 198.11 (100, [M–C$_4$H$_8$ + H]$^+$).

HRMS: Found [M+H–C$_5$H$_8$O$_2$]$^+$ 154.1245. C$_9$H$_{16}$NO requires M+H–C$_5$H$_8$O$_2$, 154.1232.

tert-Butyl (*Z*)-4-benzyl-3-oxo-3,4,5,8-tetrahydro-1,4-diazocine-1(2*H*)-carboxylate (45)
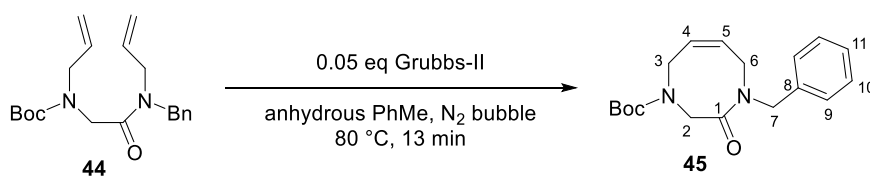
Grubbs II catalyst (45 mg, 0.053 mmol) was added to a heated (80 °C) solution of diene **44** (366 mg, 0.053 mmol) in anhydrous PhMe (112 mL) under a N_2 atmosphere. N_2 gas was bubbled through the stirred solution for 13 min, after which time, the mixture was immediately concentrated under reduced pressure and adsorbed on to Celite. The dry-loaded crude mixture was separated using automatic flash column chromatography (heptane:EtOAc 4:1 – 3:2), which yielded lactam **45** as a pale brown oil (290 mg, 86%).

R$_f$ (heptane:EtOAc 3:2): 0.2.

v_{max} (neat / cm^{-1}): 2974 w, 2931 w, 1692 s (C=O), 1635 s (C=O), 1246 s, 1160 s.

^{1}H-NMR (400 MHz, CDCl$_3$) (11:7 mixture of rotamers)[a] δ_H 7.36 – 7.10 (stack, 5H, Ph), 5.79 – 5.70 (stack, 1H, H-4), 5.70 – 5.57 (stack, 1H, H-5), [4.59 (s, 1.2H, H-7 maj), 4.54 (s, 0.8H, H-7 min)], [4.36 (s, 0.8H, H-2 min), 4.14 (s, 1.2H, H-2 maj)], [4.07 – 4.04 (m, 1.2H, H-3 maj), 3.97 – 3.92 (m, 0.8H, H-3 min)], 3.80 – 3.72 (stack, 2H, [including 3.78 (d, *J* = 8.1 Hz, 1.2H, H-6 maj), 3.75 (d, *J* = 7.0 Hz, 0.8H, H-6 min)], H-6), [1.42 (s, 5.5H, Boc maj), 1.39 (s, 3.5H, Boc min)].

^{13}C-NMR (101 MHz, CDCl$_3$) (mixture of rotamers) δ_C [169.7, 169.6 (C, C-1)], 154.8 (C, Boc *C*=O), [137.3, 137.0 (C, C-8)], [132.8, 131.5 (CH, C-4)], 128.6 (CH, Ph), 128.1 (CH, Ph), 127.5 (CH, Ph), 127.5 (CH, Ph), [125.6, 125.3 (CH, C-5)], [81.0, 80.6 (C, Boc (CH$_3$)$_3$*C*O)], [52.8 (CH$_2$, C-2 maj), 52.5 (CH$_2$, C-2 min)], [52.3 (CH$_2$, C-7 maj), 51.2 (CH$_2$, C-7 min)], [46.6 (CH$_2$, C-3 min), 46.4 (CH$_2$, C-3 maj)], [43.1 (CH$_2$, C-6 maj), 42.4 (CH$_2$, C-6 min)], [28.4, 28.3 (CH$_3$, Boc C(*C*H$_3$)$_3$)].

ESI-LRMS (+): m/z 317.19 ([M+H]$^+$, 25%), 261.13 (100, [M−C$_4$H$_8$ + H]$^+$), 217.14 (10, [M−C$_5$H$_8$O$_2$ + H]$^+$).

HRMS: Found [M+H]$^+$ 317.1862. C$_{18}$H$_{25}$N$_2$O$_3$ requires M+H, 317.1865.

tert-Butyl (*Z*)-2-oxo-2,3,5,8-tetrahydro-4*H*-1,4-oxazocine-4-carboxylate (47)

---

[a] Ratio based on Boc peak integrations in the reported ^{1}H-NMR spectrum.

di-tert-Butyl 2,11-dioxo-1,12-dioxa-4,9-diazacyclohexadeca-6,14-diene-4,9-dicarboxylate (58)

di-tert-Butyl 2,10-dioxo-1,9-dioxa-4,12-diazacyclohexadeca-6,14-diene-4,12-dicarboxylate (59)

58 45% 59
(putative structures)

47
(desired RCM product)
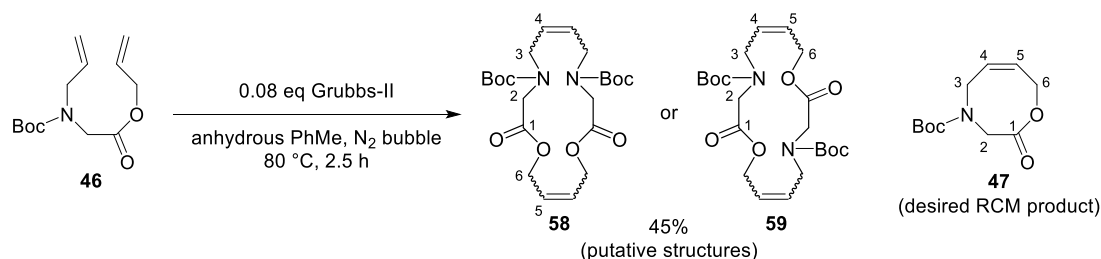
Grubbs II catalyst (794 mg, 0.935 mmol) was added to a heated (80 °C) solution of diene **46** (2.873 g, 11.25 mmol) in anhydrous PhMe (1.1 L) under a N_2 atmosphere. After bubbling N_2 gas the stirred solution for 2.5 h, the mixture was immediately concentrated under reduced pressure. The crude mixture was separated using automatic flash column chromatography (heptane:EtOAc 4:1 – 3:2) to yield a brown oil (1.14 g, 45%). The reported data most closely matches with a mixture of dimers **58** and **59**, whose regiochemistry and stereochemistry around the double bonds was not investigated further.

R*f* (hexane:EtOAc 4:1): 0.5.

***v*max (neat / cm⁻¹):** 2975 w, 2934 w, 1741 m (C=O), 1692 s (C=O), 1247 m, 1157 s.

¹H-NMR (400 MHz, CDCl₃) (mixture of rotamers and isomers)[a] δ_H 5.89 – 5.40 (stack, 4H, H-4, H-5), 4.66 – 4.52 (stack, 4H, H-6), 3.98 – 3.74 (stack, 8H, H-2, H-3), 1.49 – 1.37 (stack, 18H, Boc).

¹H-NMR (400 MHz, DMSO-*d₆*, 298 K) (mixture of rotamers and isomers) δ_H 5.87 – 5.60 (stack, 3.5H, H-4, H-5), 5.60 – 5.43 (stack, 0.5H, H-4, H-5), 4.66 – 4.41 (stack, 4H, H-6), 3.99 – 3.71 (stack, 8H, H-2, H-3), [1.41 (s, 2H, Boc), 1.40 (s, 1.5H, Boc), 1.39 (s, 1.5H, Boc), 1.34 (s, 13H, Boc)].

¹H-NMR (400 MHz, DMSO-*d₆*, 353 K) (mixture of isomers) δ_H 5.97 – 5.77 (stack, 0.5H, H-4, H-5), 5.77 – 5.62 (stack, 3H, H-4, H-5), 5.62 – 5.51 (stack, 0.5H, H-4, H-5), 4.71 – 4.57 (stack, 1H, H-6), 4.57 – 4.49 (stack, 3H, H-6), 4.02 – 3.78 (stack, 8H, H-2, H-3), 1.39 (br s, 18H, Boc).

¹³C-NMR (101 MHz, CDCl₃) (mixture of rotamers and isomers) δ_C [169.6, 169.5, 169.4 (C, C-1)], [155.3, 155.0 (C, Boc *C*=O)], [130.3, 130.0, 129.9, 129.0 (CH, C-4 or C-5)], [127.5, 127.4, 127.0,

---

[a] Due to stacked rotamer resonances in the reported ¹H-NMR spectrum, the rotamer ratio could not be determined.

126.7 (CH, C-4 or C-5)], [80.8, 80.7, 80.6 (C, Boc (CH$_3$)$_3$CO)], [64.2, 64.1, 63.9, 63.7 (CH$_2$, C-6)], [50.8, 50.6, 50.0, 49.4, 49.3, 49.2, 48.9, 48.7 (CH$_2$, C-2, C-3)], [28.41, 28.38, 28.3 (CH$_3$, Boc C(CH$_3$)$_3$)].

^{13}C-NMR (101 MHz, DMSO-d_6, 298 K) (mixture of rotamers and isomers) δ_C [169.54, 169.47, 169.4, 169.3 (C, C-1)], 154.4 (C, Boc C=O), [128.8, 127.7, 127.0, 126.9, 126.8, 126.2 (CH, C-4, C-5)], [79.8, 79.54, 79.50 (C, Boc (CH$_3$)$_3$CO)], [63.7, 63.6, 63.5 (CH$_2$, C-6)], [49.4, 49.23, 49.21, 49.15, 48.9 (CH$_2$, C-2, C-3)], [28.09, 28.06, 28.00, 27.97 (CH$_3$, Boc C(CH$_3$)$_3$)].

^{13}C-NMR (101 MHz, DMSO-d_6, 353 K) (mixture of isomers) δ_C [168.8, 168.7 (C, C-1)], 154.1 (C, Boc C=O), [128.5, 128.1, 126.5 (CH, C-4, C-5)], 79.2 (C, Boc (CH$_3$)$_3$CO), [63.1, 62.7 (CH$_2$, C-6)], [48.8, 48.4 (CH$_2$, C-2, C-3), 27.7 (CH$_3$, Boc C(CH$_3$)$_3$)].

ESI-LRMS (+): m/z 931.45 ([2M+Na]$^+$, 10%), 477.22 (35, [M+Na]$^+$), 299.13 (100, [M–C$_5$H$_8$O$_2$ –C$_4$H$_8$ + H]$^+$).

HRMS: Found [M+Na]$^+$ 477.2215. C$_{22}$H$_{34}$N$_2$NaO$_8$ requires M+Na, 477.2213.

Boc deprotection of the putative mixture of dimers was attempted for further structure elucidation (4 eq HCl in 1,4-dioxane, rt, 23 h). Selected data for the deprotected mixture is shown below.

^{1}H-NMR (400 MHz, CD$_3$OD) (mixture of isomers) δ_H 6.12 (app dt, J = 15.4, 5.9 Hz, 1.5H), 6.07 – 6.03 (m, 0.5H), 6.00 – 5.95 (m, 0.5H), 5.85 (app dt, J = 15.4, 7.4 Hz, 1.5H), 4.84 – 4.76 (stack, 4H), [4.07 (s, 1H), 4.00 (s, 3H)], [3.91 – 3.86 (m, 1H), 3.86 – 3.80 (m, 3H)].

ESI-LRMS (+): m/z 509.1 ([2M+H]$^+$, 25%), 255.1 (100, [M+H]$^+$), 128.1 (5, [M + 2H]$^{2+}$).

3. SACE1 library precursors

3.1. GENERAL PROCEDURE 1: Boc deprotection and subsequent functionalisation of protected building block
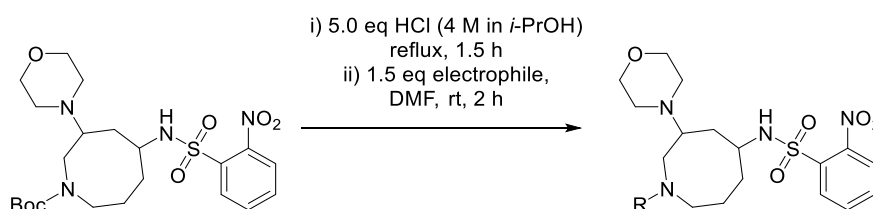
A mixture of HCl solution (4 M in *i*-PrOH, 5.0 eq) and the corresponding Boc-protected secondary amine was heated under reflux for 1.5 h, after which time, the volatiles were removed under reduced pressure. The resulting crude salt was redissolved in DMF (0.10 M). Et$_3$N (3.2 eq) and the corresponding electrophile (1.5 eq sulfonyl chloride or isocyanate) were added to the solution. After stirring at rt for 2 h, the reaction mixture was diluted with EtOAc (50 mL) and washed with NaHCO$_3$ solution (5 × 100 mL), yielding the desired sulfonamide or urea derivative.

3.2. GENERAL PROCEDURE 2: Nosyl deprotection
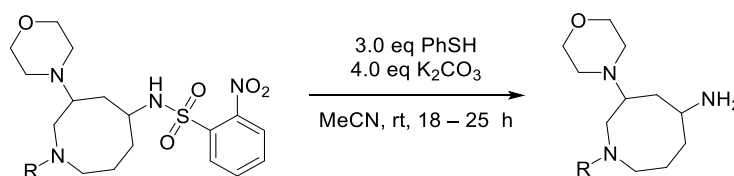
PhSH (3.0 eq) was added to a solution of nosyl-protected amine and K$_2$CO$_3$ (4.0 eq) in MeCN (0.1 M). After stirring for 18 − 25 h at rt, K$_2$CO$_3$ solution (50 mL) was added and the resulting mixture was extracted with CH$_2$Cl$_2$ (5 × 100 mL). The combined organic extracts were dried over anhydrous Na$_2$SO$_4$. Excess PhSH was removed by eluting with CH$_2$Cl$_2$ through a silica plug, after which the primary amine product was recovered by eluting with CH$_2$Cl$_2$:7 M NH$_3$ in MeOH 9:1 solution. Concentration of the eluted product fractions under reduced pressure yielded the free amine. Reaction times are specified for each individual product.

3.3. Compound synthesis and characterisation

tert-butyl (3*S**,5*S**)-3-morpholino-5-((2-nitrophenyl)sulfonamido) azocane-1-carboxylate (*cis*-100)

tert-butyl (3*S**,5*R**)-3-morpholino-5-((2-nitrophenyl)sulfonamido) azocane-1-carboxylate (*trans*-100)

93   *cis*-**100**   *trans*-**100**
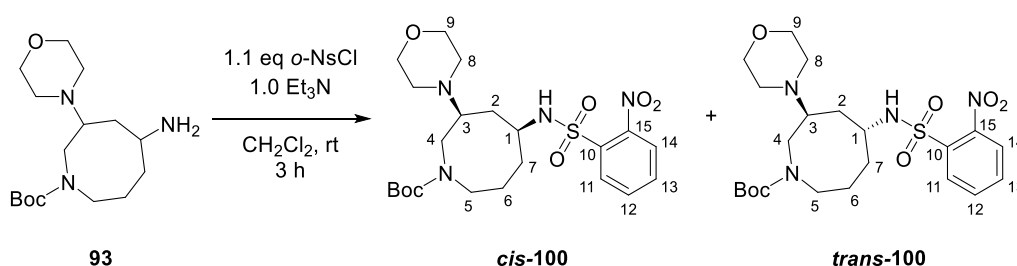
o-NsCl (4.57 g, 20.6 mmol) was added to a solution of 1° amine **93** (5.87 g, 18.7 mmol) and Et$_3$N (2.6 mL, 19 mmol) in CH$_2$Cl$_2$ (100 mL). After stirring at 30 °C for 3 h, H$_2$O (10 mL) was added and the resulting mixture was extracted with CH$_2$Cl$_2$ (3 × 150 mL). The combined organic extracts were dried over anhydrous Na$_2$SO$_4$, filtered and concentrated under reduced pressure. Purification of the resulting crude mixture *via* automatic reverse phase chromatography (0.1% HCOOH in MeCN:H$_2$O) yielded both diastereomers separately as their corresponding formate salts. The salts were each dissolved in CH$_2$Cl$_2$ (250 mL) and washed with NaOH solution (1 M, 3 × 250 mL). Removal of the solvent under reduced pressure yielded the two diastereomers as colourless oils (*cis*-**100**: 3.51 g, 38%. *trans*-**100**: 2.99 g, 32%).

(*cis*-**100**)

Melting point: 80 – 83 °C

R$_f$ (CH$_2$Cl$_2$:7 M NH$_3$ in MeOH, 9:1): 0.8

v$_{max}$ (neat / cm^{-1}): 2929 w, 2855 w, 1681 m (C=O), 1539 m (NO$_2$), 1364 m, 1163 s.

^{1}H-NMR (400 MHz, CDCl$_3$) (mixture of rotamers, 5:4)[a] δ_H 8.16 – 8.10 (stack, 1H, H-11 or H-14), 7.88 – 7.80 (stack, 1H, H-11 or H-14), 7.76 – 7.67 (stack, 2H, H-12, H-13), 3.86 – 3.57 (stack, 7H, H-1, H-4 or H-5, H-9), 2.99 – 2.73 (stack, 3H, H-3, H-4 or H-5), 2.69 – 2.29 (stack, 4H, H-8), 2.03 – 1.40 (stack, 16H, [including 1.48 (s, 5H, Boc maj), 1.45 (s, 4H, Boc min)], Boc, N*H*, H-2, H-6, H-7).

---

[a] Ratio based on Boc peak integrations in the reported ^{1}H-NMR spectrum.

13C-NMR (101 MHz, CDCl₃) (mixture of rotamers) δ_C [155.5, 155.4 (C, Boc *C*=O)], [148.0, 147.9 (C, C-15)], 135.7 (C, C-10), [133.4, 133.3 (CH, C-12 or C-13)], 133.0 (CH, C-12 or C-13), [130.8, 130.6 (CH, C-11 or C-14)], [125.39, 125.36 (CH, C-11 or C-14)], [80.2, 80.1 (C, Boc *C*(CH₃))], 67.1 (CH₂, C-9), [61.6, 60.5 (CH, C-3)], [53.9, 53.6 (CH, C-1)], [50.6, 50.1 (CH₂, C-8)], [48.9, 48.4, 47.5 (CH₂, C-4, C-5)], [33.5, 33.3 (CH₂, C-2, C-7)], [28.6, 28.6 (CH₃, Boc C(*C*H₃)], [23.2, 22.9 (CH₂, C-6)].

ESI-LRMS (+): m/z 499.4 ([M+H]⁺, 100%).

HRMS: Found [M+H]⁺ 499.2213. C₂₂H₃₅N₄O₇S requires M+H, 499.2221.

(*trans*-100)

Melting point: 81 – 84 °C

R*f* (CH₂Cl₂:7 M NH₃ in MeOH, 9:1): 0.8

***v*max (neat / cm⁻¹):** 2930 w, 2855 w, 1685 m (C=O), 1539 m (NO₂), 1364 m, 1163 s.

1H-NMR (400 MHz, CDCl₃) (mixture of rotamers: 3:2)[a] δ_H 8.16 – 8.09 (stack, 1H, H-11 or H-14), 7.90 – 7.83 (stack, 1H, H-11 or H-14), 7.78 – 7.69 (stack, 2H, H-12, H-13), 5.35 (app br d, *J* = 3.3 Hz, 1H, N*H*), 3.79 – 3.48 (stack, 6.4H, [including 3.79 – 3.65 (stack, 1H, H-1)], H-1, H-4, H-5 min, H-9), 3.42 – 3.33 (m, 0.6H, H-5 maj), 3.20 – 2.87 (stack, 2H, H-4, H-5), 2.81 – 2.63 (stack, 1H, H-3), 2.51 – 2.31 (stack, 4H, H-8), 1.89 – 1.38 (stack, 15 H, [including 1.44 (s, 9 H, Boc)], H-2, H-6, H-7, Boc).

13C-NMR (101 MHz, CDCl₃) (mixture of rotamers) δ_C [155.9, 155.6 (C, Boc *C*=O)], [148.3, 135.1 (C, C-10, C-15)], [134.0, 133.3 (CH, C-12, C-13)], [131.3, 131.2 (CH, C-11 or C-14)], 125.9 (CH, C-11 or C-14), [80.44, 80.35 (C, Boc *C*(CH₃)₃)], 67.6 (CH₂, C-9), [59.1, 58.3 (CH, C-3)], [52.6, 52.3 (CH, C-1)], [50.3, 50.2, 50.0, 49.7 (CH₂, C-4, C-5, C-8)], 48.2 (CH₂, C-5), [34.0, 33.9 (CH₂, C-2 or C-7)], [31.6, 31.3 (CH₂, C-2 or C-7)], 28.9 (CH₃, Boc C(*C*H₃)₃), [23.9, 22.8 (CH₂, C-6)].

ESI-LRMS (+): m/z 521.3 ([M+Na]⁺, 1%), 499.4 (100, [M+H]⁺).

HRMS: Found [M+H]⁺ 499.2214. C₂₂H₃₅N₄O₇S requires M+H, 499.2221.

---

[a] Ratio based on H-5 peak integrations in the reported ¹H-NMR spectrum at δ_H (CDCl₃) 3.79 – 3.48, 3.42 – 3.33 ppm.

tert-butyl (3*S**,5*S**)-3-morpholino-5-((4-nitrophenyl)sulfonamido)azocane-1-carboxylate (*cis*-102)

tert-butyl (3*S**,5*R**)-3-morpholino-5-((4-nitrophenyl)sulfonamido)azocane-1-carboxylate (*trans*-102)
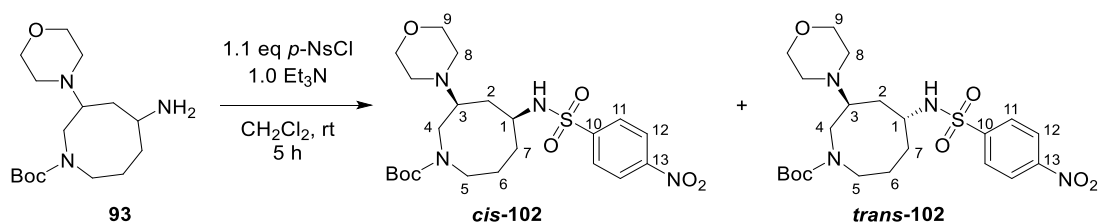
p-NsCl (138 mg, 0.625 mmol) was added to a solution of 1° amine **93** (178 mg, 0.568 mmol) and Et$_3$N (79 μL, 0.57 mmol) in CH$_2$Cl$_2$ (2.8 mL). After stirring at rt for 4.5 h, H$_2$O (5 mL) was added and the resulting mixture was extracted with CH$_2$Cl$_2$ (3 × 5 mL). The combined organic extracts were dried over anhydrous Na$_2$SO$_4$, filtered and concentrated under reduced pressure. The obtained diastereomeric mixture of sulfonamides was separated *via* preparative reverse-phase liquid chromatography (0.1% HCOOH in MeCN:H$_2$O), yielding sulfonamides **cis-102** as a white solid (53 mg, 19%) and **trans-102** as an off-white foam (83 mg, 30%).

The *cis*-diastereomer crystallised in EtOH after dissolving at elevated temperature, followed by slow cooling.[a]

(*cis*-102)

Melting point: 99 − 101 °C (EtOH).

R$_f$ (CH$_2$Cl$_2$:7 M NH$_3$ in MeOH, 9:1): 0.9.

v$_{max}$ (neat / cm^{-1}): 2937 m, 1662 s (C=O), 1536 s (NO$_2$), 1349 s, 1163 v s.

^{1}H-NMR (400 MHz, CDCl$_3$) (mixture of rotamers, 1:1)[b] δ_H 8.37 − 8.30 (AA' of AA'BB', 2H, H-12), 8.06 − 7.99 (stack, 2H, H-11), 3.92 − 3.45 (stack, 7H, [including 3.53 (app br s, 1 H, H-1)], H-1, H-4 or H-5, H-9), 2.93 − 2.72 (stack, 3H, H-3, H-4 or H-5), 2.62 − 2.34 (stack, 4H, H-8), 1.91 − 1.33 (stack, 16H, [including 1.46 (s, 4.5H, Boc), 1.44 (s, 4.5H, Boc)], N*H*, H-2, H-6, H-7, Boc).

^{13}C-NMR (101 MHz, CDCl$_3$) (mixture of rotamers) δ_C 155.5 (C, Boc *C*=O), 150.0 (C, C-13), 147.5 (C, C-10), 128.1 (CH, C-11), 124.5 (CH, C-12), [80.3, 80.2 (C, Boc *C*(CH$_3$)$_3$)], 67.2 (CH$_2$, C-9), [61.6,

---

[a] Crystallisation attempts in heptane:EtOAc and diisopropyl ether did not yield any crystals.
[b] Ratio based on observed Boc peak intensities in the reported ^{1}H-NMR spectrum.

60.2 (CH, C-3)], [53.4, 53.0 (CH, C-1)], 50.5 (CH$_2$, C-8), 48.8 (CH$_2$, C-4, C-5, resonance overlap), [34.2, 33.9 (CH$_2$, C-2, C-7)], 28.5 (CH$_3$, Boc C(CH$_3$)$_3$), 23.1 (CH$_2$, C-6).

ESI-LRMS (+): m/z 499.4 ([M+H]$^+$, 100%).

HRMS: Found [M+H]$^+$ 499.2225. C$_{22}$H$_{35}$N$_4$O$_7$S requires M+H, 499.2221.

(*trans*-102)

R$_f$ (CH$_2$Cl$_2$:7 M NH$_3$ in MeOH, 9:1): 0.9.

v_{max} (neat / cm^{-1}): 2930 m, 2855 w, 1684 s (C=O), 1528 s (NO$_2$), 1349 s, 1163 v s.

^{1}H-NMR (400 MHz, CDCl$_3$) (mixture of rotamers, 1:1)[a] δ_H 8.36 − 8.30 (AA' of AA'BB', 2H, H-12), 8.08 − 8.02 (BB' of AA'BB', 2H, H-11), 5.65 (br s, 1H, N*H*), 3.77 − 3.45 (stack, 6.5H, H-1, H-4, H-5, H-9), 3.45 − 3.31 (m, 0.5H, H-5), 3.16 − 2.94 (stack, 1H, H-4, H-5), 2.94 − 2.80 (stack, 1H, H-4, H-5), 2.78 − 2.59 (stack, 1H, H-3), 2.57 − 2.32 (stack, 4H, H-8), 1.83 − 1.35 (stack, 15H, [including 1.83 − 1.64 (stack, 2H, H-2), 1.70 − 1.60 (stack, 1H, H-6), 1.67 − 1.53 (stack, 2H, H-7), 1.55 − 1.47 (stack, 1H, H-6), 1.42 (s, 9H, Boc)], H-2, H-6, H-7, Boc).

^{13}C-NMR (101 MHz, CDCl$_3$) (mixture of rotamers) δ_C [155.6, 155.3 (C, Boc *C*=O)], 150.0 (C, C-10), 147.1 (C, C-13), 128.3 (CH, C-11), 124.5 (CH, C-12), 80.2 (C, Boc *C*(CH$_3$)$_3$), 67.2 (CH$_2$, C-9), [58.9, 57.8 (CH, C-3)], [51.8, 50.8 (CH, C-1)], [50.5, 50.2, 49.6 (CH$_2$, C-4 or C-5, C-8)], 48.4 (CH$_2$, C-4 or C-5), 47.8 (CH$_2$, C-5), [33.9, 33.2 (CH$_2$, C-2)], 31.3 (CH$_2$, C-7), 28.5 (CH$_3$, Boc C(*C*H$_3$)$_3$), [23.7, 22.5 (CH$_2$, C-6)].

ESI-LRMS (+): m/z 499.4 ([M+H]$^+$, 100%).

HRMS: Found [M+H]$^+$ 499.2213. C$_{22}$H$_{35}$N$_4$O$_7$S requires M+H, 499.2221.

---

[a] Ratio based on H-5 peak integrations in the reported ^{1}H-NMR spectrum at δ_H (CDCl$_3$) 3.77 − 3.45, 3.45 − 3.31 ppm.

N-((3S*,5S*)-1-methylsulfonyl-3-morpholinoazocan-5-yl)-2-nitrobenzenesulfonamide (cis-103)
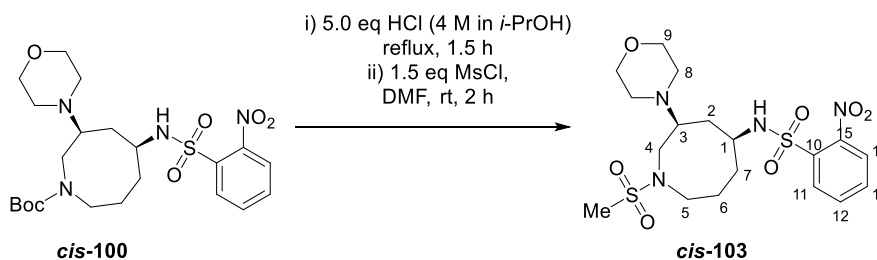
General procedure 1 (page 222) was followed, using nosylamine **cis-100** (900 mg, 1.81 mmol) as starting material and MsCl as the electrophile. The Boc-protected amine was dissolved in *i*-PrOH (2 mL) before adding HCl solution (4 M in *i*-PrOH, 2.3 mL, 9.0 mmol). Sulfonamide **cis-103** was obtained as a white foam (0.77 g, 90%).

R*f* (CH$_2$Cl$_2$:7 M NH$_3$ in MeOH, 9:1): 0.7.

v$_{max}$ (neat / cm^{-1}): 2922 m, 1539 s (NO$_2$), 1323 v s, 1148 v s, 1111 v s.

^{1}H-NMR (400 MHz, CDCl$_3$) δ_H 8.18 (X of ABX, J_{X-A} = 7.3, J_{X-A} = 1.9 Hz, 1H, H-14), 7.83 (Y of ABY, J_{Y-B}= 7.4, J_{Y-A} = 1.8 Hz, 1H, H-11),[a] 7.80 − 7.67 (stack, 2H, H-12, H-13), 3.94 − 3.80 (m, 1H, H-1), 3.75 − 3.57 (stack, 4H, H-9), 3.45 (dd, *J* = 14.0, 5.2 Hz, 1H, H-4), 3.41 − 3.31 (m, 1H, H-5), 3.03 − 2.87 (stack, 2H, H-4, H-5), 2.90 − 2.79 (m, 1H, H-3), 2.77 (s, 3H, Me), 2.65 − 2.34 (stack, 4H, H-8), 2.12 − 2.02 (m, 1H, H-2), 2.02 − 1.87 (m, 1H, H-2), 1.88 − 1.50 (stack, 5H, H-6, H-7, N*H*).

^{13}C-NMR (101 MHz, CDCl$_3$) δ_C [133.5, 133.2 (CH, C-12, C-13)], 131.5 (CH, C-14), 125.3 (CH, C-11), 67.1 (CH$_2$, C-9), 62.9 (CH, C-3), 53.2 (CH, C-1), 49.9 (CH$_2$, C-8), [49.5, 49.0 (CH$_2$, C-4, C-5)], 35.4 (CH$_3$, SO$_2$*C*H$_3$), 33.3 (CH$_2$, C-7), 23.2 (CH$_2$, C-6). C-2 and quaternary carbon resonances not observed, but HSQC shows a cross peak with H-2 at δ_C 31.6 ppm and HMBC shows cross peaks at δ_C 147.6 ppm, indicating C-10 or C-15.

ESI-LRMS (+): m/z 477.3 ([M+H]$^+$, 100%).

HRMS: Found [M+H]$^+$ 477.1463. C$_{18}$H$_{29}$N$_4$O$_7$S$_2$ requires M+H, 477.1472.

---

[a] The author acknowledges this is an ABX-type pattern. In this case, Y is used to distinguish this ABX system from the other one. A and B are used consistently for the reported ABX/ABY systems.

N-((3*S**,5*R**)-1-methylsulfonyl-3-morpholinoazocan-5-yl)-2-nitrobenzenesulfonamide (*trans*-103)

i) 5.0 eq HCl (4 M in *i*-PrOH)
reflux, 1.5 h
ii) 1.5 eq MsCl,
DMF, rt, 3.5 h
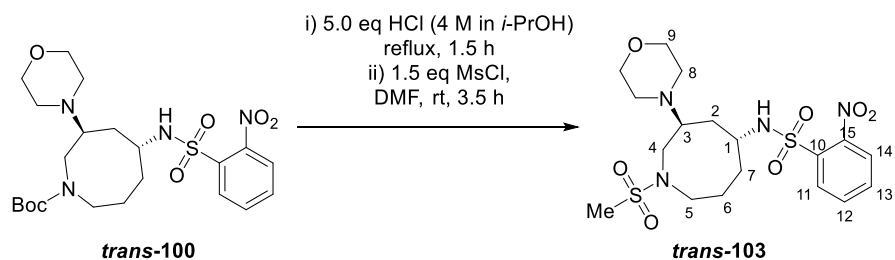
trans-100   *trans*-103

General procedure 1 (page 222) was followed, using nosylamine *trans*-100 (1.01 g, 2.01 mmol) as starting material and MsCl as the electrophile. The Boc-protected amine was dissolved in *i*-PrOH (3 mL) before adding HCl solution (4 M in *i*-PrOH, 2.5 mL, 10 mmol). After addition of the MsCl, the mixture was stirred at rt for 3.5 h before workup. Sulfonamide *trans*-103 was obtained as an off-white foam (0.92 g, 96%).

Melting point: 103 – 104 °C

R$_f$ (CH$_2$Cl$_2$:7 M NH$_3$ in MeOH, 9:1): 0.8.

v_{max} (neat / cm^{-1}): 2926 w, 1539 s (NO$_2$), 1323 v s, 1148 v s, 1118 v s.

^{1}H-NMR (400 MHz, CDCl$_3$) δ_H 8.20 – 8.12 (m, 1H, H-11 or H-14), 7.87 – 7.81 (m, 1H, H-11 or H-14), 7.79 – 7.71 (stack, 2H, H-12, H-13), 5.53 (br d, *J* = 6.4 Hz, 1H, N*H*), 3.88 – 3.77 (m, 1H, H-1), 3.71 – 3.56 (stack, 4H, H-9), 3.36 – 3.23 (stack, 3H, H-4, H-5), 3.16 – 3.07 (m, 1H, H-5), 3.06 – 2.93 (m, 1H, H-3), 2.80 (s, 3H, SO$_2$C*H*$_3$), 2.67 – 2.42 (stack, 4H, H-8), 2.06 – 1.96 (m, 1H, H-2), 1.92 – 1.57 (stack, 5H, [including 1.92 –1.82 (m, 1H, H-2), 1.82 – 1.74 (stack, 2 H, H-7), 1.74 – 1.57 (m, 2H, H-6)], H-2, H-6, H-7).

^{13}C-NMR (101 MHz, CDCl$_3$) δ_C 148.0 (C, C-15), 133.8 (C, C-10), 133.1 (CH, C-12, C-13, resonance overlap), 131.4 (CH, C-14), 125.5 (CH, C-11), 66.9 (CH$_2$, C-9), 59.2 (CH, C-3), 51.7 (CH, C-1), 49.9 (CH$_2$, C-4), 49.5 (CH$_2$, C-8), 49.0 (CH$_2$, C-5), 36.2 (CH$_3$, SO$_2$C*H$_3$), 32.5 (CH$_2$, C-2), 31.2 (CH$_2$, C-7), 24.0 (CH$_2$, C-6).

ESI-LRMS (+): m/z 477.2 ([M+H]$^+$, 100%).

HRMS: Found [M+H]$^+$ 477.1465. C$_{18}$H$_{29}$N$_4$O$_7$S$_2$ requires M+H, 477.1472.

(3S*,5S*)-N-ethyl-3-morpholino-5-((2-nitrophenyl)sulfonamido)azocane-1-carboxamide (cis-104)
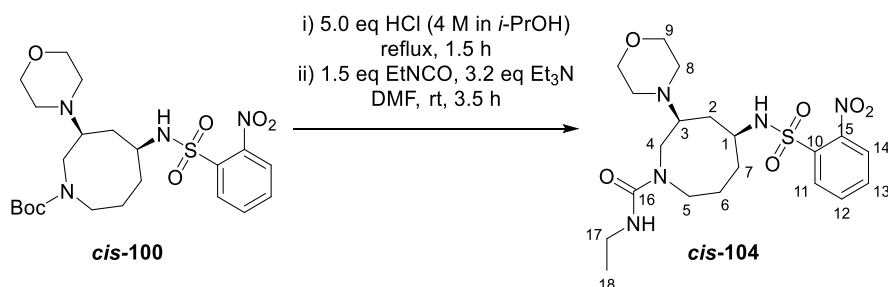
General procedure 1 (page 222) was followed, using nosylamine **cis-100** (900 mg, 1.81 mmol) as the starting material and EtNCO as the electrophile. After addition of the electrophile, the mixture was stirred at rt for 3.5 h before workup. Urea **cis-104** was obtained as a white foam (0.78 g, 92%).

Melting point: 96 − 97 °C.

v_{max} **(neat / cm^{-1})**: 2930 m, 2855 m, 1621 s (C=O), 1536 v s (NO$_2$), 1338 s, 1163 s, 1115 s.

^{1}H-NMR (400 MHz, CDCl$_3$) δ_H 8.17 − 8.08 (m, 1H, H-14), 7.90 − 7.80 (m, 1H, H-11), 7.79 − 7.69 (stack, 2H, H-12, H-13), 5.25 (br s, 1H, CN*H*CH$_2$), 3.76 − 3.55 (stack, 6H, H-1, H-4, H-9), 3.45 − 3.31 (m, 1H, H-5), 3.31 − 3.18 (stack, 3H, H-5, H-17), 3.13 (dd, *J* = 14.9, 8.4 Hz, 1H, H-4), 2.74 − 2.61 (m, 1H, H-3), 2.61 − 2.39 (stack, 4H, H-8), 1.93 − 1.60 (stack, 6H, H-2, H-6, H-7, SO$_2$N*H*CH), 1.60 − 1.44 (m, 1H, H-6), 1.14 (t, *J* = 7.2 Hz, 3H, H-18).

^{13}C-NMR (101 MHz, CDCl$_3$) δ_C 158.1 (C, C-16), 148.0 (C, C-15), 135.2 (C, C-10), [133.5, 133.0 (CH, C-12, C-13)], 130.8 (CH, C-14), 125.4 (CH, C-11), 67.1 (CH$_2$, C-9), 61.7 (CH, C-3), 53.8 (CH, C-1), 50.4 (CH$_2$, C-8), 49.7 (CH$_2$, C-4), 47.9 (CH$_2$, C-5), 35.8 (CH$_2$, C-17), 33.5 (CH$_2$, C-7), 32.0 (CH$_2$, C-2), 23.5 (CH$_2$, C-6), 16.0 (CH$_3$, C-18).

ESI-LRMS (+): m/z 470.1 ([M+H]$^+$, 100%).

HRMS: Found [M+H]$^+$ 470.2058. C$_{20}$H$_{32}$N$_5$O$_6$S requires M+H, 470.2068.

(3*S**,5*R**)-*N*-ethyl-3-morpholino-5-((2-nitrophenyl)sulfonamido)azocane-1-carboxamide (*trans*-104)
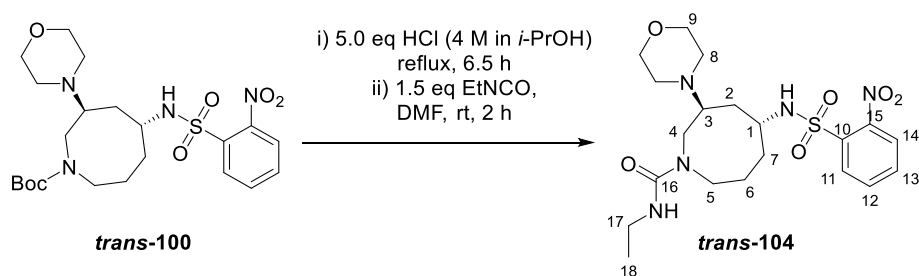
General procedure 1 (page 222) was followed, using nosylamine ***trans*-100** (1.00 g, 2.01 mmol) as the starting material and EtNCO as the electrophile. After the addition of HCl solution (4 M in *i*-PrOH), the mixture was heated at reflux for 6.5 h. Urea ***trans*-104** was obtained as a white foam (0.88 g, 93%).

Melting point: 95 − 96 °C.

R$_f$ (CH$_2$Cl$_2$:7 M NH$_3$ in MeOH, 9:1): 0.7.

***v*$_{max}$ (neat / cm^{-1}):** 2922 w, 1621 m (C=O), 1536 v s (NO$_2$), 1334 m, 1163 s, 1115 s.

^{1}H-NMR (400 MHz, CDCl$_3$) δ_H 8.16 − 8.11 (m, 1H, H-14), 7.90 − 7.85 (m, 1H, H-11), 7.80 − 7.71 (m, 2H, H-12, H-13), 6.40 (app br s, 1H, CON*H*CH$_2$), 5.36 (d, *J* = 7.2 Hz, 1iH, SO$_2$N*H*CH), 3.85 − 3.67 (stack, 2H, H-1, H-5), 3.67 − 3.56 (stack, 4H, H-9), 3.44 (A of ABX, *J*$_{A-B}$ = 15.3, *J*$_{A-X}$ = 5.2 Hz, 1H, H-4), 3.37 (B of ABX, *J*$_{B-A}$ = 15.3, *J*$_{B-X}$ = 5.2 Hz, 1H, H-4), 3.24 (dq, *J* = 7.4, 5.5 Hz, 2H, H-17), 3.06 − 2.86 (m, 1H, H-5), 2.69 − 2.59 (m, 1H, H-3), 2.53 − 2.38 (stack, 4H, H-8), 1.96 (ddd, *J* = 14.6, 6.2, 2.0 Hz, 1H, H-2), 1.85 − 1.63 (stack, 3H, H-2, H-6, H-7), 1.61 − 1.50 (m, 1H, H-7), 1.50 − 1.38 (m, 1H, H-6), 1.14 (t, *J* = 7.4 Hz, 3H, H-18).

^{13}C-NMR (101 MHz, CDCl$_3$) δ_C 158.6 (C, C-16), 134.3 (C, C-10), [133.8, 133.1 (CH, C-12, C-13)], 131.0 (CH, C-14), 125.6 (CH, C-11), 67.2 (CH$_2$, C-9), 59.1 (CH, C-3), 52.2 (CH, C-1), 51.3 (CH$_2$, C-4), 50.7 (CH$_2$, C-8), 48.3 (CH$_2$, C-5), 35.6 (CH$_2$, C-17), 32.2 (CH$_2$, C-7), 31.0 (CH$_2$, C-2), 24.1 (CH$_2$, C-6), 16.2 (CH$_3$, C-18). C-15 resonance not observed, but HMBC shows expected cross-peaks for C-15 at δ_C 147.8 ppm.

ESI-LRMS (+): m/z 470.1 ([M+H]$^+$, 100%).

HRMS: Found [M+H]$^+$ 470.2060. C$_{20}$H$_{32}$N$_5$O$_6$S requires M+H, 470.2068.

tert-butyl (3*S**,5*R**)-5-amino-3-morpholinoazocane-1-carboxylate (*trans*-93)
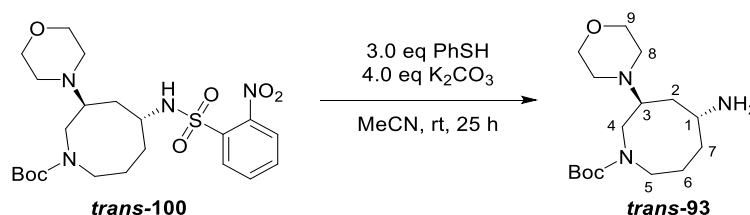
General procedure 2 (page 222) was followed, using nosylamine *trans*-100 (1.128 g, 2.262 mmol) as the starting material. The reaction mixture was stirred for 25 h. 1° amine *trans*-93 was isolated as a colourless oil (682 mg, 96%).

v_{max} (neat / cm^{-1}): 3370 m (N–H), 2930 m, 2859 m, 1674 s (C=O), 1416 s, 1364 s, 1159 v s, 1111 v s.

^{1}H-NMR (400 MHz, CDCl$_3$) (mixture of rotamers, 1:1)[a] δ_H 3.55 − 3.40 (stack, 5H, H-4, H-9), 3.41 − 3.30 (m, 0.5H, H-5), 3.20 − 3.10 (m, 0.5H, H-5), 3.10 − 2.87 (stack, 2.5H, H-1, H-4, H-5), 2.86 − 2.76 (m, 0.5H, H-4), 2.74 − 2.56 (stack, 1H, H-3), 2.56 − 2.26 (stack, 4H, H-8), 2.25 (app br s, 2H, N*H*$_2$), 1.74 − 1.19 (stack, 15H, H-2, H-6, H-7, Boc).

^{13}C-NMR (101 MHz, CDCl$_3$) (mixture of rotamers) δ_C [155.4, 155.0 (C, Boc *C*=O)], [79.3, 79.2 (C, Boc *C*(CH$_3$)$_3$], [67.13, 67.06 (CH$_2$, C-9)], [58.1, 57.4 (CH, C-3)], [49.74, 49.69, 49.44, 49.38 (CH$_2$, C-4, C-8)], 48.2 (CH, C-1), 47.8 (CH$_2$, C-5), 47.7 (CH, C-1), 47.6 (CH$_2$, C-5), [35.0, 34.8 (CH$_2$, C-2)], [32.5, 32.2 (CH$_2$, C-7)], 28.3 (CH$_3$, Boc C(*C*H$_3$)$_3$), [23.8, 22.4 (CH$_2$, C-6)].

ESI-LRMS (+): m/z 314.2 ([M+H]$^+$, 100%), 258.2 (1, [M–C$_4$H$_8$ + H]$^+$).

HRMS: Found [M+H]$^+$ 314.2433. C$_{16}$H$_{32}$N$_3$O$_3$ requires M+H, 314.2438.

---

[a] Ratio based on H-5 peak integrations in the reported ^{1}H-NMR spectrum at δ_H (CDCl$_3$) 3.41 − 3.30, 3.20 − 3.10 ppm.

tert-butyl (3*S**,5*S**)-5-amino-3-morpholinoazocane-1-carboxylate (*cis*-93)
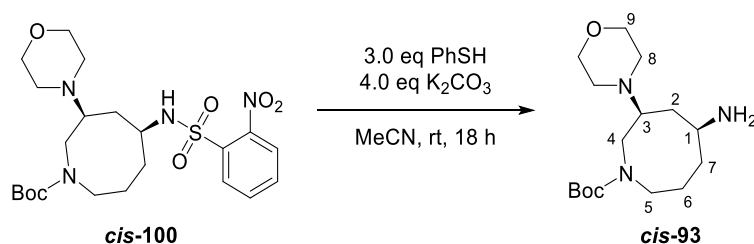
General procedure 2 (page 222) was followed, using nosylamine *cis*-100 (0.978 g, 1.96 mmol) as the starting material. The reaction mixture was stirred for 18 h. 1° amine *cis*-93 was isolated as a colourless oil (603 mg, 98%).

v_{max} (neat / cm^{-1}): 2930 m, 2855 m, 1685 v s (C=O), 1416 s, 1364 s, 1163 vs, 1115 v s.

^{1}H-NMR (400 MHz, CDCl$_3$) (mixture of rotamers, 1:1)[a] δ_H 3.71 − 3.54 (stack, 5.5H, H-4, H-5 rot A, H-9), 3.49 − 3.38 (m, 0.5H, H-5 rot B), 3.17 − 3.06 (m, 0.5H, H-5 rot B), 3.07 − 2.96 (stack, 1H, H-4, H-5 rot A), 2.97 − 2.86 (stack, 1.5H, H-1, H-4), 2.80 − 2.69 (stack, 1H, H-3), 2.67 − 2.45 (stack, 4H, H-8), 1.83 − 1.30 (stack, 17H, [including 1.43 (s, 4.5H, Boc), 1.42 (s, 4.5H, Boc)], H-2, H-6, H-7, N*H*$_2$, Boc).

^{13}C-NMR (101 MHz, CDCl$_3$) (mixture of rotamers) δ_C [155.7, 155.6 (C, Boc *C*=O)], (79.8, 79.6 (C, Boc *C*(CH$_3$)$_3$)], [67.53, 67.49 (CH$_2$, C-9)], [61.7, 60.9 (CH, C-3)], [51.2, 50.4 (CH, C-1)], [49.2, 49.1 (CH$_2$, C-8)], [48.8, 48.1, 47.9, 47.5 (CH$_2$, C-4, C-5)], [39.03, 38.97 (CH$_2$, C-2)], [36.4, 34.8 (CH$_2$, C-7)], [28.7, 28.6 (CH$_3$, Boc C(*C*H$_3$)$_3$)], [23.4, 23.3 (CH$_2$, C-6)].

ESI-LRMS (+): m/z 314.2 ([M+H]$^+$, 100%).

HRMS: Found [M+H]$^+$ 314.2432. C$_{16}$H$_{32}$N$_3$O$_3$ requires M+H, 314.2438.

---

[a] Ratio based on H-5 peak integrations in the reported ^{1}H-NMR spectrum.

(3S*,5R*)-1-methylsulfonyl-3-morpholinoazocan-5-amine (*trans*-105)
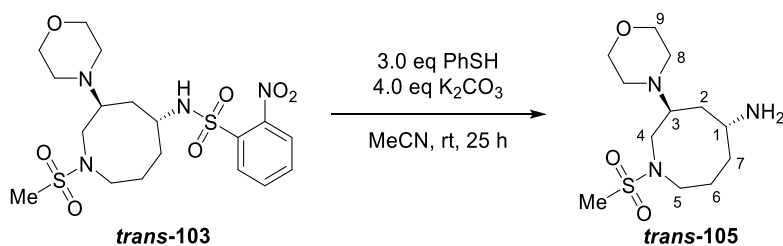
General procedure 2 (page 222) was followed, using nosylamine *trans*-103 (0.92 g, 1.9 mmol) as the starting material. The reaction mixture was stirred at rt for 25 h. The 1° amine *trans*-105 was isolated as an off-white foam (0.46 g, 82%).

v_{max} (neat / cm^{-1}): 3265 br w (N–H), 2937 m, 2859 w, 1439 m, 1320 s, 1144 s, 1114 s.

^{1}H-NMR (400 MHz, CD$_3$OD) δ_H 3.73 – 3.61 (stack, 4H, H-9), 3.49 – 3.19 (stack, 5H, H-1, H-4, H-5), 3.02 – 2.91 (m, 1H, H-3), 2.87 (s, 3H, Me), 2.71 – 2.52 (stack, 4H, H-8), 2.05 – 1.92 (m, 1H, H-2), 1.91 – 1.65 (stack, 5H, H-2, H-6, H-7), exchangeable protons not observed.

^{13}C-NMR (101 MHz, CD$_3$OD) δ_C 68.3 (CH$_2$, C-9), 60.3 (CH, C-3), 51.5 (CH$_2$, C-4), 50.8 (CH$_2$, C-8), 49.9 (CH$_2$, C-5), 49.7 (CH, C-1), 35.5 (CH$_3$, Me), 34.6 (CH$_2$, C-2), 32.1 (CH$_2$, C-7), 26.8 (CH$_2$, C-6).

ESI-LRMS (+): m/z 292.1 ([M+H]$^+$,100%).

HRMS: Found [M+H]$^+$ 292.1686. C$_{12}$H$_{26}$N$_3$O$_3$S requires M+H, 292.1689.

(3S*,5S*)-1-methylsulfonyl-3-morpholinoazocan-5-amine (cis-105)
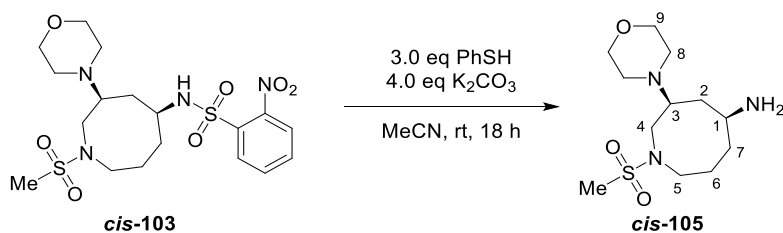
General procedure 2 (page 222) was followed, using nosylamine **cis-103** (0.77 g, 1.6 mmol) as the starting material. The reaction mixture was stirred at rt for 18 h. 1° amine **cis-105** was isolated as a yellow oil (0.42 g, 90%).

v_{max} (neat / cm^{-1}): 2922 w, 2859 w, 1323 s, 1148 s, 1109 s.

^{1}H-NMR (400 MHz, CDCl$_3$) δ_H 3.67 – 3.52 (stack, 4H, H-9), 3.32 – 3.15 (stack, 2H, H-4, H-5), 3.16 – 3.00 (stack, 3H, H-1, H-4, H-5), 2.89 – 2.77 (m, 1H, H-3), 2.73 (s, 3H, Me), 2.60 – 2.39 (stack, 4H, H-8), 1.93 – 1.71 (stack, 5H, H-2, H-6, H-7, NH$_2$), 1.70 – 1.53 (stack, 2H, H-2, H-6), 1.49 – 1.37 (m, 1H, H-7).

^{13}C-NMR (101 MHz, CDCl$_3$) δ_C 67.4 (CH$_2$, C-9), 62.8 (CH, C-3), 50.8 (CH, C-1), 49.3 (CH$_2$, C-8), [49.14, 49.09 (CH$_2$, C-4, C-5)], 36.6 (CH$_2$, C-2), 35.5 (CH$_3$, Me), 35.4 (CH$_2$, C-7), 23.9 (CH$_2$, C-6).

ESI-LRMS (+): m/z 292.1 ([M+H]$^+$, 100%).

HRMS: Found [M+H]$^+$ 292.1682. C$_{12}$H$_{26}$N$_3$O$_3$S requires M+H, 292.1689.

(3S*,5R*)-5-amino-N-ethyl-3-morpholinoazocane-1-carboxamide (*trans*-106)
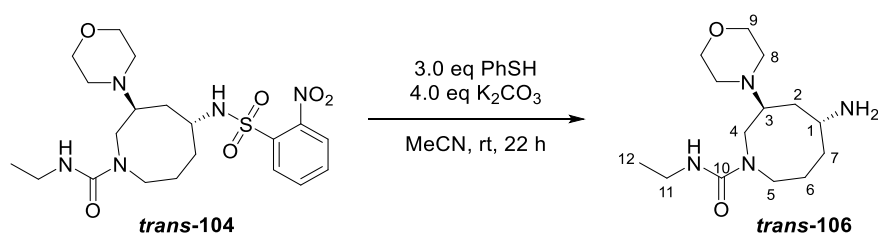
General procedure 2 (page 222) was followed, using nosylamine *trans*-104 (0.88 g, 1.9 mmol) as the starting material. The reaction mixture was stirred at rt for 22 h. 1° amine *trans*-106 was isolated as a yellow oil (0.49 g, 92%).

v_{max} (neat / cm^{-1}): 3347 br m (N–H), 2930 m, 1602 s (C=O), 1536 v s, 1111 s.

^{1}H-NMR (400 MHz, CDCl$_3$) δ_H 6.31 (br s, 1H, CON*H*CH$_2$), 3.80 − 3.63 (m, 1H, H-5), 3.64 − 3.44 (stack, 4H, H-9), 3.43 − 3.22 (stack, 2H, H-4), 3.22 − 2.99 (stack, 3H, H-1, H-11), 2.99 − 2.73 (m, 1H, H-5), 2.77 − 2.54 (m, 1H, H-3), 2.37 − 2.51 (stack, 4H, H-8), 1.75 − 1.53 (stack, 4H, H-2, H-6, H-7), 1.53 − 1.19 (stack, 4H, H-6, H-7, N*H$_2$*), 1.01 (t, *J* = 7.2 Hz, 3H, H-12).

^{13}C-NMR (101 MHz, CDCl$_3$) δ_C 158.5 (C, C-10), 67.1 (CH$_2$, C-9), 58.4 (CH, C-3), 51.3 (CH$_2$, C-4), 50.4 (CH$_2$, C-8), 48.2 (CH$_2$, C-5), 48.1 (CH, C-1), 35.2 (CH$_2$, C-11), 33.7 (CH$_2$, C-7), 32.7 (CH$_2$, C-2), 24.2 (CH$_2$, C-6), 16.0 (CH$_3$, C-12).

ESI-LRMS (+): m/z 285.2 ([M+H]$^+$, 100%).

HRMS: Found [M+H]$^+$ 285.2280. C$_{14}$H$_{29}$N$_4$O$_2$ requires M+H, 285.2285.

(3S*,5S*)-5-amino-N-ethyl-3-morpholinoazocane-1-carboxamide (cis-106)
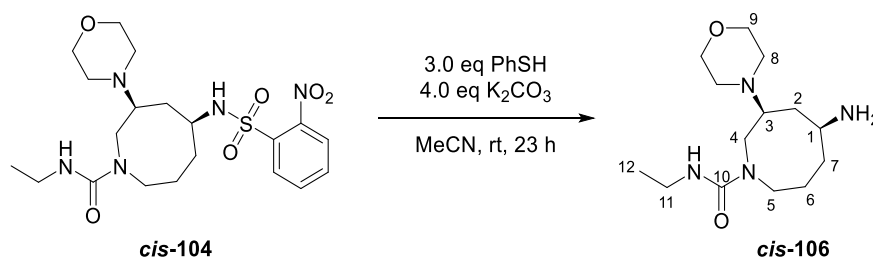
General procedure 2 (page 222) was followed, using nosylamine **cis-104** (0.78 g, 1.7 mmol) as the starting material. The reaction mixture was stirred at rt for 23 h. 1° amine **cis-106** was isolated as a yellow oil (0.46 g, 98%).

*v*_{max} (neat / cm⁻¹): 3347 br s (N–H), 2933 m, 1595 s (C=O), 1539 s, 1111 s.

¹H-NMR (400 MHz, CDCl₃) δ_H 6.51 − 5.98 (stack, 3H, N*H₂*, CON*H*CH₂), 3.76 − 3.54 (stack, 4H, H-9), 3.54 − 3.31 (stack, 2H, H-4, H-5), 3.31 − 3.05 (stack, 5H, H-1, H-4, H-5, H-11), 2.69 − 2.45 (stack, 5H, H-3, H-8), 2.25 − 2.06 (m, 1H, H-2), 2.02 − 1.73 (stack, 3H, H-2, H-6, H-7), 1.73 − 1.57 (stack, 2H, H-6, H-7), 1.09 (t, *J* = 7.3 Hz, 3H, H-12).

¹³C-NMR (101 MHz, CDCl₃) δ_C 158.7 (C, C-10), 67.3 (CH₂, C-9), 62.1 (CH, C-3), 51.3 (CH, C-1), 50.0 (CH₂, C-4 or C-5, C-8, resonance overlap), 47.8 (CH₂, C-4 or C-5), 35.7 (CH₂, C-11), [32.6, 32.4 (CH₂, C-2, C-6)], 23.8 (CH₂, C-7), 16.0 (CH₃, C-12).

ESI-LRMS (+): m/z 285.2 ([M+H]⁺, 100%).

HRMS: Found [M+H]⁺ 285.2279. C₁₄H₂₉N₄O₂ requires M+H, 285.2285.

4. SACE1 Library

4.1. Parallel synthesis reagents

Sulfonyl chlorides

a1   **a2**   **a3**   **a4**

a5   **a6**   **a7**

Acid chlorides, carboxylic acids

b1   **c1**   **c2**   **c3**

c4   **c5**   **c6**

Isocyanates

d1   **d2**   **d3**   **d4**

Aldehydes

e1   **e2**
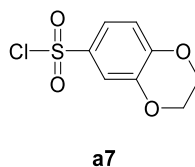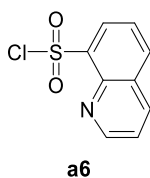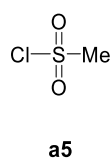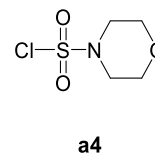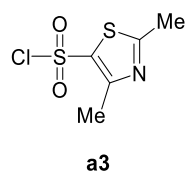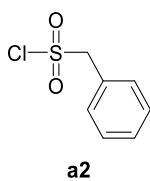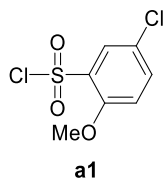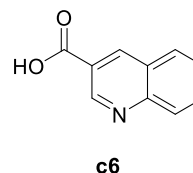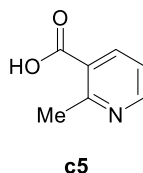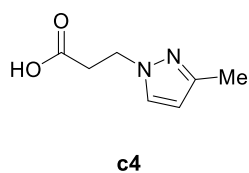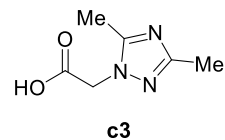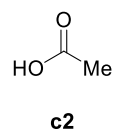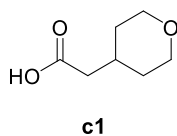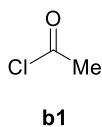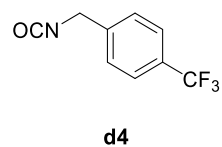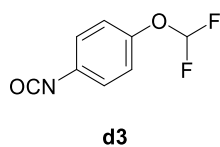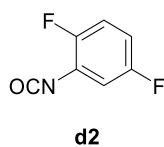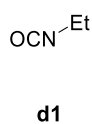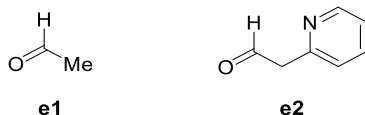
5. SACE1 Library: selected compound characterisation

5.1. GENERAL PROCEDURE 3: sulfonyl chlorides, acid chlorides and isocyanates
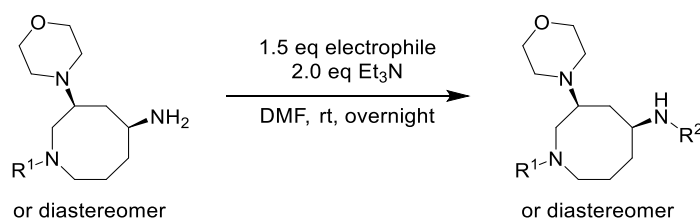
A solution of the building block (0.10 – 0.18 mmol) in DMF[a] and Et$_3$N (2.0 eq) were added sequentially to a solution of the electrophile (1.5 eq) in DMF (0.4 mL) in a capped 8 mL vial. After stirring overnight at rt, the reaction mixture was purified directly *via* preparative basic HPLC.

5.2. GENERAL PROCEDURE 4: amide couplings
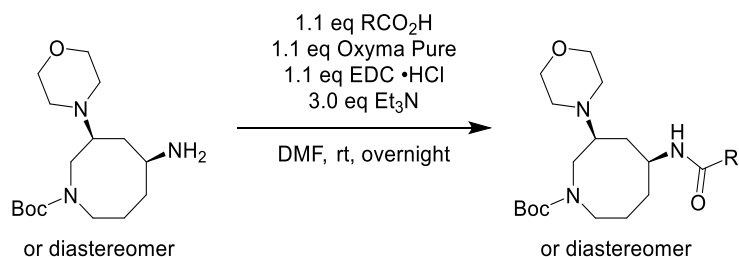
A solution of the building block (0.10 – 0.18 mmol) in DMF[b] and Et$_3$N (3.0 eq) were added sequentially to a solution of the carboxylic acid (1.1 eq), EDC •HCl (1.1 eq) and Oxyma Pure (1.1 eq) in DMF (0.4 mL) in a capped 8 mL vial. After stirring overnight at rt, the reaction mixture was purified directly *via* preparative basic HPLC.

---

[a] Volume of DMF calculated to yield a final reaction concentration of 0.1 M.
[b] Volume of DMF calculated to yield a final reaction concentration of 0.1 M.

5.3. GENERAL PROCEDURE 5: Boc deprotection
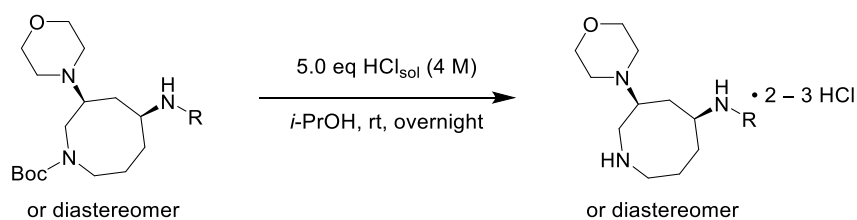
A solution of HCl (4 M in *i*-PrOH, 5.0 eq) was added to a solution of Boc-protected amine in *i*-PrOH (0.4 mL). After stirring overnight, the reaction mixture was concentrated under reduced pressure in a Genevac HT-12 centrifugal evaporator, yielding the deprotected amine salt.

5.4. Compound synthesis and characterisation

2,4-dimethyl-*N*-((3*S**,5*R**)-1-methylsulfonyl-3-morpholinoazocan-5-yl)thiazole-5-sulfonamide (*trans*-105a3)
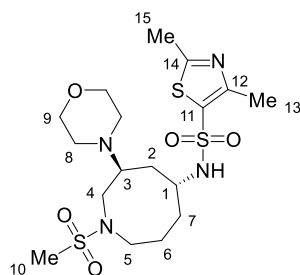
General procedure 3 (page 238) was followed, using building block **trans-105** (0.130 mmol) as the starting material and **a3** as the electrophile. Sulfonamide **trans-105a3** was obtained as an off-white solid (15.8 mg, 26%).

ν_{max} (neat / cm^{-1}): 3265 w (N–H), 2937 w, 2859 w, 1439 m, 1320 s, 1144 s.

^{1}H-NMR (400 MHz, CDCl$_3$) δ_H 5.00 (br d, *J* = 6.7 Hz, 1H, N*H*), 3.80 − 3.69 (m, 1H, H-1), 3.69 − 3.56 (stack, 4H, H-9), 3.40 (dd, *J* = 13.7, 5.7 Hz, 1H, H-4), 3.31 (app dt, *J* = 14.0, 5.2 Hz, 1H, H-5), 3.16 − 2.96 (stack, 2H, H-4, H-5), 2.85 − 2.76 (stack, 4H, [including 2.81 (s, 3H, H-10)], H-3, H-10), 2.68 (s, 3H, H-15), 2.61 (s, 3H, H-13), 2.55 − 2.36 (stack, 4H, H-8), 2.05 − 1.95 (m, 1H, H-2), 1.90 − 1.59 (stack, 5H, H-2, H-6, H-7).

^{13}C-NMR (101 MHz, CDCl$_3$) δ_C 168.7 (C, C-14), 155.9 (C, C-12), 130.3 (C, C-11), 67.2 (CH$_2$, C-9), 59.4 (CH, C-3), 50.8 (CH, C-1, CH$_2$, C-4, resonance overlap), 49.8 (CH$_2$, C-8), 49.5 (CH$_2$, C-5), 36.1 (CH$_3$, C-10), 32.7 (CH$_2$, C-2), 31.3 (CH$_2$, C-7), 24.0 (CH$_2$, C-6), 19.6 (CH$_3$, C-15), 16.5 (CH$_3$, C-13).

ESI-LRMS (+): m/z 489.1 ([M+Na]$^+$, 5%), 467.1 (100, [M+H]$^+$).

HRMS: Found [M+H]$^+$ 467.1446. $C_{17}H_{31}N_4O_5S_3$ requires M+H, 467.1451.

2-(3,5-dimethyl-1*H*-1,2,4-triazol-1-yl)-*N*-((3*S**,5*R**)-1-methylsulfonyl-3-morpholinoazocan-5-yl)acetamide (*trans*-105c3)
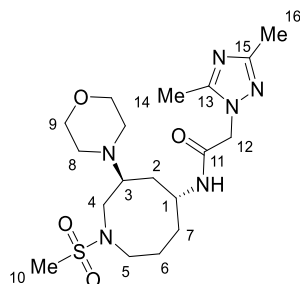
General procedure 4 (page 238) was followed, using building block *trans*-105 (0.130 mmol) as starting the material and **c3** as the carboxylic acid. Amide *trans*-105c3 was obtained as an off-white foam (15.1 mg, 27%).

v_{max} (neat / cm^{-1}): 3310 w (N–H), 2930 w, 1655 s (C=O), 1525 m, 1320 s, 1136 s.

^{1}H-NMR (400 MHz, CDCl$_3$) δ_H 6.50 (d, *J* = 7.8 Hz, 1H, N*H*), 4.65 (A of AB, J_{A-B} = 16.8 Hz, 1H, H-12), 4.63 (B of AB, J_{B-A} = 16.8 Hz, 1H, H-12), 4.31 − 4.21 (m, 1H, H-1), 3.71 − 3.59 (stack, 4H, H-9), 3.44 (dd, *J* = 13.8, 5.5 Hz, 1H, H-4), 3.34 (app dt, *J* = 13.8, 5.4 Hz, 1H, H-5), 3.14 (app dt, *J* = 13.8, 6.6 Hz, 1H, H-5), 3.05 (dd, *J* = 13.8, 10.4 Hz, 1H, H-4), 2.82 (s, 3H, H-10), 2.74 − 2.61 (m, 1H, H-3), 2.55 − 2.45 (m, 2H, H-8), 2.44 − 2.30 (stack, 8H, [including 2.41 (s, 3H, H-14), 2.35 (s, 3H, H-16)], H-8, H-14, H-16), 2.11 − 2.01 (m, 1H, H-2), 1.86 − 1.64 (stack, 5H, H-2, H-6, H-7).

^{13}C-NMR (101 MHz, CDCl$_3$) δ_C 165.0 (C, C-11), 161.0 (C, C-15), 153.8 (C, C-13), 67.3 (CH$_2$, C-9), 59.8 (CH, C-3), [51.3, 51.1 (CH$_2$, C-4, C-12)], [49.7, 49.5 (CH$_2$, C-5, C-8)], 46.7 (CH, C-1), 36.1 (CH$_3$, C-10), 30.8 (CH$_2$, C-7), 29.8 (CH$_2$, C-2), 24.2 (CH$_2$, C-6), 14.0 (CH$_3$, C-14), 12.0 (CH$_3$, C-16).

ESI-LRMS (+): m/z 451.2 ([M+Na]$^+$, 1%), 429.2 (100, [M+H]$^+$).

HRMS: Found [M+H]$^+$ 429.2273. $C_{18}H_{33}N_6O_4S$ requires M+H, 429.2279.

1-ethyl-3-((3*S**,5*R**)-1-methylsulfonyl-3-morpholinoazocan-5-yl)urea (*trans*-105d1)
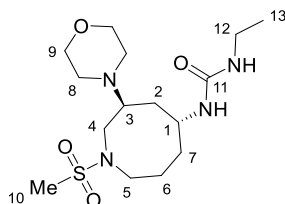
General procedure 3 (page 238) was followed, using building block **trans-105** (0.130 mmol) as the starting material and **d1** as the electrophile. Urea **trans-105d1** was obtained as an off-white solid (29.0 mg, 62%).

v_{max} (neat / cm^{-1}): 3347 w (N–H), 2922 w, 1633 s (C=O), 1562 s, 1312 s, 1141 s.

^{1}H-NMR (400 MHz, CDCl$_3$) (mixture of rotamers, 2:3)[a] δ_H 4.83 (d, J = 7.2 Hz, 0.4H, CHN*H*CO min), 4.66 (t, J = 5.7 Hz, 0.4H, CON*H*CH$_2$ min), 4.14 – 4.04 (m, 1H, H-1), 3.74 – 3.59 (stack, 4H, H-9), 3.59 – 5.54 (m, 1H, H-5), 3.52 – 3.40 (stack, 1H, H-4), 3.26 – 3.09 (stack, 2H, H-12), 3.09 – 2.98 (stack, 1H, H-4), 2.98 – 2.88 (stack, 1H, H-5), 2.83 (s, 3H, H-10), 2.78 – 2.69 (stack, 1H, H-3), 2.61 – 2.41 (stack, 4H, H-8), 2.17 – 2.06 (stack, 1H, H-2), 1.88 – 1.55 (stack, 5H, H-2, H-6, H-7), 1.10 (app t, J = 7.2 Hz, 3H, H-13), CHN*H*CO maj and CON*H*CH$_2$ maj not observed.

^{13}C-NMR (101 MHz, CDCl$_3$) (mixture of rotamers) δ_C [157.64, 157.61, 157.58, (C, C-11)], 67.3 (CH$_2$, C-9), 60.0 (CH, C-3), 51.8 (CH$_2$, C-5), [49.9, 49.8 (CH$_2$, C-4, C-8)], [46.3, 46.2 (CH, C-1)], 36.0 (CH$_3$, C-10), [35.3, 35.1 (CH$_2$, C-12)], 31.7 (CH$_2$, C-2), 30.7 (CH$_2$, C-7), 24.5 (CH$_2$, C-6), [15.69, 15.67 (CH$_3$, C-13)].

ESI-LRMS (+): m/z 385.2 ([M+Na]$^+$, 5%), 363.2 (100, [M+H]$^+$).

HRMS: Found [M+H]$^+$ 363.2056. C$_{15}$H$_{31}$N$_4$O$_4$S requires M+H, 363.2061.

---

[a] Ratio based on CHN*H*CO and C*H*NHCO peak integrations in the reported ^{1}H-NMR spectrum. Both peaks integrate for 0.4H. Since all other integrations measured yielded integer values, it is assumed that CHN*H*CO and C*H*NHCO signals have only been observed for one rotamer.

(3*S**,5*R**)-*N*-ethyl-3-morpholino-5-((phenylmethyl)sulfonamido)azocane-1-carboxamide (*trans*-106a2)
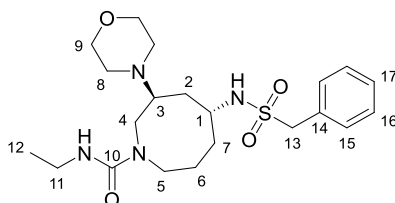
General procedure 3 (page 238) was followed, using building block **trans-106** (0.130 mmol) as the starting material and **a2** as the electrophile. Sulfonamide **trans-106a2** was obtained as a white solid (15.1 mg, 26%).

v_{max} (neat / cm^{-1}): 2930 m, 2855 m, 1618 s (C=O), 1528 s, 1316 s, 1267 s, 1115 v s.

^{1}H-NMR (400 MHz, CDCl$_3$) δ_H 7.43 – 7.34 (stack, 5H, H-15, H-16, H-17), 5.92 (s, 1H, N*H*CO), 4.34 (d, *J* = 7.5 Hz, 1H, N*H*SO$_2$), 4.25 (s, 2H, H-13), 3.75 – 3.54 (stack, 5H, H-5, H-9), 3.54 – 3.38 (stack, 2H, H-1, H-4), 3.37 – 3.19 (stack, 3H, H-4, H-11), 3.19 – 3.07 (m, 1H, H-5), 2.64 – 2.46 (stack, 5H, H-3, H-8), 2.01 – 1.93 (m, 1H, H-2), 1.93 – 1.76 (m, 1H, H-7), 1.76 – 1.60 (stack, 2H, H-2, H-6), 1.54 – 1.39 (stack, 2H, H-6, H-7), 1.13 (t, *J* = 7.2 Hz, 3H, H-12).

^{13}C-NMR (101 MHz, CDCl$_3$) δ_C 158.4 (C, C-10), 130.8 (CH, Ph), 129.4 (C, C-14), [129.0, 128.9 (CH, Ph)], 67.3 (CH$_2$, C-9), 59.8 (CH$_2$, C-13), 58.7 (CH, C-3), 52.1 (CH, C-1), 51.5 (CH$_2$, C-4), 50.4 (CH$_2$, C-8), 48.3 (CH$_2$, C-5), 35.7 (CH$_2$, C-11), 31.9 (CH$_2$, C-2, C-7, resonance overlap), 24.0 (CH$_2$, C-6), 16.1 (CH$_3$, C-12).

ESI-LRMS (+): m/z 461.2 ([M+Na]$^+$, 1%), 439.2 (100, [M+H]$^+$).

HRMS: Found [M+H]$^+$ 439.2368. C$_{21}$H$_{35}$N$_4$O$_4$S requires M+H, 439.2374.

(3S*,5R*)-N-ethyl-3-morpholino-5-(3-(4-(trifluoromethyl)benzyl)ureido)azocane-1-carboxamide (*trans*-106d4)
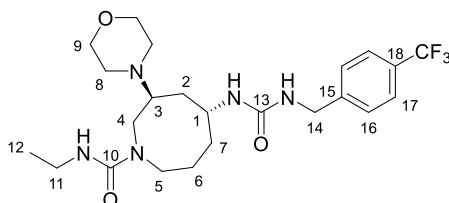
General procedure 3 (page 238) was followed, using building block *trans*-106 (0.130 mmol) as the starting material and **d4** as the electrophile. Urea *trans*-106d4 was obtained as an amber solid (48.1 mg, 76%).

v_{max} (neat / cm^{-1}): 3306 w (N–H), 2930 w, 2855 w, 1614 m (C=O), 1543 s, 1323 s, 1111 s.

^{1}H-NMR (400 MHz, CDCl$_3$) δ_H 7.55 − 7.48 (AA′ of AA′BB′, 2H, H-17), 7.39 − 7.32 (BB′ of AA′BB′, 2H, H-16), 5.94 (t, J = 6.0 Hz, 1H, NHCONHCH$_2$), 5.70 (d, J = 7.6 Hz, 1H, CHNHCO), 5.43 (app br s, 1H, EtNHCO), 4.41 (A of ABX, $J_{A–B}$ = 15.7, $J_{A–X}$ = 6.0 Hz, 1H, H-14), 4.34 (B of ABX, $J_{B–A}$ = 15.7, $J_{B–X}$ = 6.0 Hz, 1H, H-14), 3.98 (app br s, 1H, H-1), 3.72 − 3.57 (stack, 5H, H-4, H-9), 3.58 − 3.42 (m, 1H, H-5), 3.26 − 2.96 (stack, 4H, H-4, H-5, H-11), 2.57 − 2.31 (stack, 5H, H-3, H-8), 2.06 − 1.98 (m, 1H, H-2), 1.83 − 1.54 (stack, 3H, H-2, H-6, H-7), 1.54 − 1.36 (stack, 2H, H-6, H-7), 1.03 (t, J = 7.2 Hz, 3H, H-12).

^{13}C-NMR (101 MHz, CDCl$_3$) δ_C [158.3, 158.0 (C, C-10, C-13)], 144.6 (C, C-15), 129.3 (C, q, $J_{C–F}$ = 32.3 Hz, C-18), 127.5 (CH, C-16), 125.4 (CH, q, $J_{C–F}$ = 3.8 Hz, C-17), 124.3 (C, q, $J_{C–F}$ = 271.9 Hz, CF$_3$), 67.2 (CH$_2$, C-9), 59.3 (CH, C-3), 52.6 (CH$_2$, C-4), 50.2 (CH$_2$, C-8), 48.4 (CH$_2$, C-5), 47.0 (CH, C-1), 43.5 (CH$_2$, C-14), 35.7 (CH$_2$, C-11), 31.0 (CH$_2$, C-2), 30.2 (CH$_2$, C-7), 23.7 (CH$_2$, C-6), 15.9 (CH$_3$, C-12).

ESI-LRMS (+): m/z 508.2 ([M+Na]$^+$, 5%), 486.2 (100, M+H]$^+$).

HRMS: Found [M+H]$^+$ 486.2682. C$_{23}$H$_{35}$F$_3$N$_5$O$_3$ requires M+H, 486.2687.

(3*S**,5*R**)-*N*-ethyl-5-(2-methylnicotinamido)-3-morpholinoazocane-1-carboxamide (*trans*-106c5)
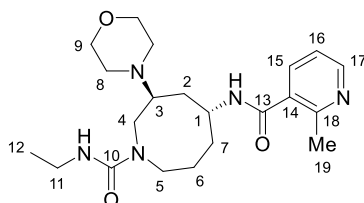
General procedure 4 (page 238) was followed, using building block *trans*-106 (0.130 mmol) as the starting material and **c5** as the carboxylic acid. Amide *trans*-106c5 was obtained as a yellow oil (36.7 mg, 70%).

v_{max} (neat / cm^{-1}): 3239 m (N–H), 2930 m, 2855 w, 1621 s (C=O), 1528 s, 1111 s.

^{1}H-NMR (400 MHz, CDCl$_3$) δ_H 8.49 (dd, *J* = 5.0, 1.8 Hz, 1H, H-17), 7.58 (dd, *J* = 7.7, 1.8 Hz, 1H, H-15), 7.12 (dd, *J* = 7.7, 5.0 Hz, 1H, H-16), 6.22 (d, *J* = 7.8 Hz, 1H, CHN*H*CO), 5.63 (br s, 1H, EtN*H*CO), 4.39 – 4.25 (m, 1H, H-1), 3.76 – 3.45 (stack, 6H, H-4, H-5, H-9), 3.34 – 3.10 (stack, 4H, H-4, H-5, H-11), 2.67 – 2.44 (stack, 8H, [including 2.62 (s, 3H, H-19)], H-3, H-8, H-19), 2.21 – 2.10 (m, 1H, H-2), 2.03 – 1.87 (m, 1H, H-7), 1.87 – 1.71 (stack, 2H, H-2, H-6), 1.67 – 1.51 (stack, 2H, H-6, H-7), 1.08 (t, *J* = 7.2 Hz, 3H, H-12).

^{13}C-NMR (101 MHz, CDCl$_3$) δ_C 167.9 (C, C-13), 158.3 (C, C-10), 156.0 (C, C-18), 150.2 (CH, C-17), 134.7 (CH, C-15), 132.0 (C, C-14), 120.9 (CH, C-16), 67.3 (CH$_2$, C-9), 59.3 (CH, C-3), 51.4 (CH$_2$, C-4), 50.5 (CH$_2$, C-8), 48.4 (CH$_2$, C-5), 47.4 (CH, C-1), 35.6 (CH$_2$, C-11), 30.7 (CH$_2$ C-2), 30.3 (CH$_2$, C-7), 24.2 (CH$_2$, C-6), 23.1 (CH$_3$, C-19), 16.0 (CH$_3$, C-12).

ESI-LRMS (+): m/z 426.3 ([M+Na]$^+$, 5%), 404.3 (100, [M+H]$^+$).

HRMS: Found [M+H]$^+$ 404.2648. C$_{21}$H$_{34}$N$_5$O$_3$ requires M+H, 404.2656.

5-chloro-2-methoxy-*N*-((3*S**,5*S**)-1-methylsulfonyl-3-morpholinoazocan-5-yl)benzenesulfonamide (*cis*-105a1)

General procedure 3 (page 238) was followed, using building block *cis*-105 (0.100 mmol) as the starting material and **a1** as the electrophile. Sulfonamide *cis*-105a1 was obtained as an amber glass (4.4 mg, 9%).

***v*~max~ (neat / cm⁻¹):** 3183 m (N–H), 2889 m, 1480 m, 1316 s, 1271 s, 1162 s, 1107 s.

¹H-NMR (400 MHz, CDCl₃) δ_H 7.91 (d, *J* = 2.6 Hz, 1H, H-12), 7.50 (dd, *J* = 8.8, 2.6 Hz, 1H, H-14), 7.00 (d, *J* = 8.8 Hz, 1H, H-15), 5.21 (app br s, 1H, N*H*), 4.00 (s, 3H, H-17), 3.66 − 3.52 (stack, 4H, H-9), 3.45 − 3.33 (m, 1H, H-1), 3.32 − 3.20 (m, 1H, H-5), 3.20 − 3.14 (stack, 2H, H-4), 3.13 − 3.03 (m, 1H, H-5), 2.77 (s, 3H, H-10), 2.75 − 2.65 (m, 1H, H-3), 2.41 − 2.30 (m, 2H, H-8), 2.29 − 2.18 (m, 2H, H-8), 1.95 − 1.47 (stack, 6H, H-2, H-6, H-7).

¹³C-NMR (101 MHz, CDCl₃) δ_C 154.9 (C, C-16), 134.2 (CH, C-14), [130.2, 130.0 (C, CH, C-12, C-11 or C-13)], 126.3 (C, C-11 or C-13), 113.9 (CH, C-15), 67.2 (CH₂, C-9), 62.3 (CH, C-3), 57.0 (CH₃, C-17), 54.7 (CH, C-1), [49.3, 49.1, 49.0 (CH₂, C-4, C-5, C-8)], 36.2 (CH₃, C-10), 33.0 (CH₂, C-7), 31.8 (CH₂, C-2), 23.8 (CH₂, C-6).

ESI-LRMS (+): m/z 518.1 ([M+Na]⁺, 5%, ³⁵Cl isotope), 498.1 (50, [M+H]⁺, ³⁷Cl isotope), 496.1 (100, [M+H]⁺, ³⁵Cl isotope).

HRMS: Found [M+H]⁺ 496.1331. C₁₉H₃₁³⁵ClN₃O₆S₂ requires M+H, 496.1337.

1-ethyl-3-((3*S**,5*S**)-1-methylsulfonyl-3-morpholinoazocan-5-yl)urea (*cis*-105d1)
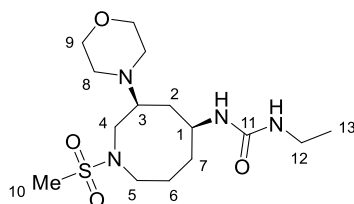
General procedure 3 (page 238) was followed, using building block *cis*-105 (0.100 mmol) as the starting material and **d1** as the electrophile. Urea *cis*-105d1 was obtained as a white solid (31.6 mg, 87%).

v_{max} (neat / cm^{-1}): 3351 m (N–H), 2922 m, 2855 m, 1629 s (C=O), 1558 s, 1323 s, 1144 s, 1115 s.

^{1}H-NMR (400 MHz, CDCl$_3$) (mixture of rotamers, 9:1)[a] δ_H 4.64 – 4.51 (stack, 1H, CHN*H*CO), 4.36 (t, *J* = 5.4 Hz, 0.1H, CON*H*Et min), 4.29 (t, *J* = 5.6 Hz, 0.9H, CON*H*Et maj), 3.83 – 3.71 (stack, 1H, H-1), 3.71 – 3.53 (stack, 4H, H-9), 3.46 – 3.29 (stack, 2H, H-4, H-5), 3.25 – 3.11 (stack, 3H, H-4, H-12), 3.11 – 3.01 (stack, 1H, H-5), 3.00 – 2.88 (stack, 1H, H-3), 2.84 (s, 0.3H, H-10 min), 2.82 (s, 2.7H, H-10 maj), 2.71 – 2.53 (stack, 2H, H-8), 2.53 – 2.40 (stack, 2H, H-8), 2.18 – 1.91 (stack, 2H, H-2, H-7), 1.91 – 1.75 (stack, 1H, H-6), 1.75 – 1.52 (stack, 3H, H-2, H-6, H-7), 1.13 (t, *J* = 7.2 Hz, 2.7H, H-13 maj), 1.12 (t, *J* = 7.1 Hz, 0.3H, H-13 min).

^{13}C-NMR (101 MHz, CDCl$_3$) δ_C 157.3 (C, C-11), 67.3 (CH$_2$, C-9), 62.3 (CH, C-3), 50.7 (CH, C-1), [49.3, 49.2, 49.1 (CH$_2$, C-4, C-5, C-8)], 36.2 (CH$_3$, C-10), 35.5 (CH$_2$, C-12), 32.7 (CH$_2$, C-2), 32.1 (CH$_2$, C-7), 24.1 (CH$_2$, C-6), 15.6 (CH$_3$, C-13).

ESI-LRMS (+): m/z 385.2 ([M+Na]$^+$, 10%), 363.2 (100, [M+H]$^+$).

HRMS: Found [M+H]$^+$ 363.2053. C$_{15}$H$_{31}$N$_4$O$_4$S requires M+H, 363.2061.

---

[a] Ratio based on CON*H*Et peak integrations in the reported ^{1}H-NMR spectrum.

N-((3*S**,5*S**)-1-methylsulfonyl-3-morpholinoazocan-5-yl)quinoline-3-carboxamide (*cis*-105c6)
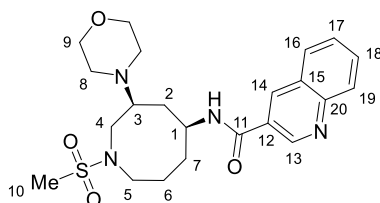
General procedure 4 (page 238) was followed, using building block *cis*-105 (0.100 mmol) as the starting material and **c6** as the carboxylic acid. Amide *cis*-105c6 was obtained as an off-white solid (21.6 mg, 48%).

v$_{max}$ (neat / cm^{-1}): 3329 w (N–H), 2930 w, 2855 w, 2814 w, 1644 s (C=O), 1517 s, 1320 s, 1148 s, 1107 s.

^{1}H-NMR (400 MHz, CDCl$_3$) (mixture of rotamers, 9:1)[a] δ_H 9.33 − 9.27 (stack, 1H, H-13), 8.64 (d, *J* = 2.3 Hz, 0.1H, H-14 min), 8.60 (d, *J* = 2.3 Hz, 0.9H, H-14 maj), 8.15 − 8.06 (stack, 1H, H-16), 7.92 − 7.83 (stack, 1H, H-19), 7.82 − 7.72 (stack, 1H, H-17), 7.58 (app dd, *J* = 7.5, 7.5 Hz, 1H, H-18), [4.73 − 4.62 (m, 0.1H, H-1 min), 4.33 − 4.19 (m, 0.9H, H-1 maj)], 3.73 − 3.54 (stack, 4H, H-9), 3.49 − 3.32 (stack, 2H, H-4, H-5), 3.32 − 3.20 (stack, 1H, H-4), 3.21 − 3.10 (stack, 1H, H-5), 3.10 − 3.00 (stack, 1H, H-3), [2.87 (s, 0.3H, H-10 min), 2.84 (s, 2.7H, H-10 maj)], H-10, 2.76 − 2.63 (stack, 2H, H-8), 2.55 − 2.44 (stack, 2H, H-8), 2.24 − 1.79 (stack, 5H, H-2, H-6, H-7), 1.79 − 1.64 (stack, 1H, H-6), NH not observed.

^{13}C-NMR (101 MHz, CDCl$_3$) (mixture of rotamers) δ_C [165.0 (C, C-11 min), 164.7 (C, C-11 maj)], 149.3 (C, C-12), 148.5 (CH, C-13), 135.6 (CH, C-14), 131.3 (CH, C-17), 129.4 (CH, C-16), 128.9 (CH, C-19), 127.6 (CH, C-18), [127.3, 127.0 (C, C-15, C-20)], 67.2 (CH$_2$, C-9), 62.6 (CH, C-3), 50.6 (CH, C-1), [49.5, 49.3, 49.2 (CH$_2$, C-4, C-5, C-8)], 36.2 (CH$_3$, C-10), 31.4 (CH$_2$, C-2, C-7, resonance overlap), 24.2 (CH$_2$, C-6).

ESI-LRMS (+): m/z 469.3 ([M+Na]$^+$, 1%), 447.3 (100, [M+H]$^+$).

HRMS: Found [M+H]$^+$ 447.2057. C$_{22}$H$_{31}$N$_4$O$_4$S requires M+H, 447.2061.

---

[a] Ratio based on H-1 and H-14 peak integrations in the reported ^{1}H-NMR spectrum.

(3S*,5S*)-N-ethyl-5-(methylsulfonamido)-3-morpholinoazocane-1-carboxamide (*cis*-106a5)
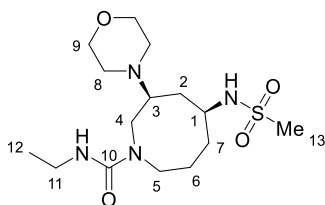
General procedure 3 (page 238) was followed, using building block *cis*-106 (0.120 mmol) as the starting material and **a5** as the electrophile. Sulfonamide *cis*-106a5 was obtained as an off-white solid (8.0 mg, 18%).

v_{max} **(neat / cm^{-1}):** 3250 w (N–H), 2930 m, 2855 m, 1618 s (C=O), 1528 s, 1305 s, 1141 s, 1111 s.

^{1}H-NMR (400 MHz, CDCl$_3$) (mixture of rotamers, 9:1)[a] δ_H 5.47 (br s, 1H, EtN*H*CO), 3.77 − 3.66 (stack, 4H, H-9), 3.66 − 3.50 (stack, 2H, H-1, H-5), 3.46 − 3.33 (stack, 2H, H-4), 3.33 − 3.17 (stack, 3H, H-5, H-11), [2.98 (s, 0.3H, H-13 min), 2.94 (s, 2.7H, H-13 maj)], 2.81 − 2.71 (stack, 1H, H-3), 2.71 − 2.51 (stack, 4H, H-8), 2.03 − 1.85 (stack, 2H, H-2, H-7), 1.85 − 1.51 (stack, 4H, H-2, H-6, H-7), 1.14 (t, *J* = 7.2 Hz, 3H, H-12), CHN*H*SO$_2$ not observed.

^{13}C-NMR (101 MHz, CDCl$_3$) δ_C 158.3 (C, C-10), 67.2 (CH$_2$, C-9), 61.8 (CH, C-3), 53.1 (CH, C-1), 50.6 (CH$_2$, C-8), 49.9 (CH$_2$, C-5), 48.2 (CH$_2$, C-4), 41.8 (CH$_3$, C-13), 35.8 (CH$_2$, C-11), 34.1 (CH$_2$, C-2), 32.2 (CH$_2$, C-7), 23.6 (CH$_2$, C-6), 16.0 (CH$_3$, C-12).

ESI-LRMS (+): m/z 385.2 ([M+Na]$^+$, 1%), 363.2 (100, [M+H]$^+$).

HRMS: Found [M+H]$^+$ 363.2050. C$_{15}$H$_{31}$N$_4$O$_4$S requires M+H, 363.2061.

---

[a] Ratio based on H-13 peak integrations in the reported ^{1}H-NMR spectrum.

(3S*,5S*)-N-ethyl-3-morpholino-5-(2-(tetrahydro-2H-pyran-4-yl)acetamido)azocane-1-carboxamide (cis-106c1)
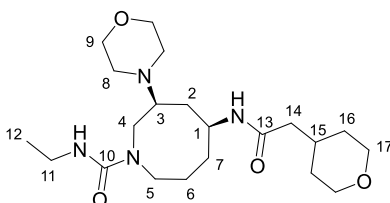
General procedure 4 (page 238) was followed, using building block **cis-106** (0.120 mmol) as the starting material and **c1** as the carboxylic acid. Amide **cis-106c1** was obtained as an amber oil (38.3 mg, 78%).

v_{max} **(neat / cm^{-1}):** 3295 w (N–H), 2930 m, 2848 m, 1625 s (C=O), 1528 s, 1115 s.

^{1}H-NMR (400 MHz, CDCl$_3$) (mixture of rotamers, 9:1)[a] δ_H 6.48 (br s, 0.9H, CHNHCO maj), 6.28 (br s, 1H, EtNHCO), 5.83 (d, J = 7.7 Hz, 0.1H, CHNHCO min), 3.98 − 3.83 (stack, 3H, H-1, H-17), 3.78 − 3.57 (stack, 5H, H-5, H-9), 3.46 − 3.30 (stack, 4H, H-4, H-17), 3.30 − 3.13 (stack, 2H, H-11), 3.13 − 2.99 (stack, 1H, H-5), 2.69 − 2.48 (stack, 5H, H-3, H-8), 2.11 − 1.94 (stack, 3H, H-14, H-15), 1.94 − 1.85 (m, 1H, H-2), 1.84 − 1.42 (stack, 7H, H-2, H-6, H-7, H-16), 1.37 − 1.17 (stack, 2H, H-16), 1.11 (t, J = 7.2 Hz, 3H, H-12).

^{13}C-NMR (101 MHz, CDCl$_3$) (mixture of rotamers) δ_C 170.5 (C, C-13), 158.9 (C, C-10), 67.9 (CH$_2$, C-17), 67.3 (CH$_2$, C-9), 62.5 (CH, C-3), 50.6 (CH$_2$, C-8), 50.3 (CH$_2$, C-4), 48.9 (CH, C-1), 48.2 (CH$_2$, C-5), 44.1 (CH$_2$, C-14), 35.5 (CH$_2$, C-11), [32.9, 32.8, 32.62, 32.56 (CH, C-15, CH$_2$, C-7, C-16)], 31.5 (CH$_2$, C-2), 24.4 (CH$_2$, C-6), 16.2 (CH$_3$, C-12).

ESI-LRMS (+): m/z 433.4 ([M+Na]$^+$, 5%), 411.4 (100, [M+H]$^+$).

HRMS: Found [M+H]$^+$ 411.2957. C$_{21}$H$_{39}$N$_4$O$_4$ requires M+H, 411.2966.

---

[a] Ratio based on CHNHCO peak integrations in the reported ^{1}H-NMR spectrum.

tert-butyl (3*R**,5*S**)-3-morpholino-5-((phenylmethyl)sulfonamido)azocane-1-carboxylate (*trans*-93a2)
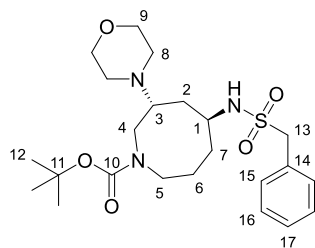
General procedure 3 (page 238) was followed, using building block **trans-93** (0.130 mmol) as the starting material and **a2** as the electrophile. Sulfonamide **trans-93a2** was obtained as an amber oil (15.1 mg, 26%).

*v*max (neat / cm⁻¹): 3255 w (N–H), 2930 m, 2855 m, 2818 w, 1677 s (C=O), 1416 s, 1152 s, 1115 v s.

¹H-NMR (400 MHz, CDCl₃) (mixture of rotamers, 1:1)[a] δ_H 7.44 − 7.35 (stack, 5H, H-15, H-16, H-17), 4.28 (app A of AB, $J_{A–B}$ = 14.0 Hz, 1H, H-13), 4.25 (app B of AB, $J_{B–A}$ = 14.0 Hz, 1H, H-13), 4.07 (app d, J = 7.3 Hz, 1H, N*H*), 3.78 − 3.59 (stack, 5.5H, H-9, H-4, H-5), 3.59 − 3.48 (stack, 1H, H-1), 3.47 − 3.34 (stack, 0.5H, H-5), 3.18 − 2.99 (stack, 1H, H-4, H-5), 2.99 − 2.83 (stack, 1H, H-4, H-5), 2.75 − 2.57 (stack, 1H, H-3), 2.57 − 2.41 (stack, 4H, H-8), 1.89 − 1.39 (stack, 15H, [including 1.46 (s, 9H, H-12)], H-2, H-6, H-7, H-12).

¹³C-NMR (101 MHz, CDCl₃) (mixture of rotamers) δ_C 155.0 (C, C-10), 130.8 (CH, C-15 or C-16 or C-17), 128.92 (C, C-14), 128.91 (CH, C-15 or C-16 or C-17), 80.1 (C, C-11), 67.4, (CH₂, C-9), [60.2, 60.1 (CH₂, C-13)], [58.8, 57.9 (CH, C-3)], [52.2, 51.6 (CH, C-1)], [50.2, 49.7, 48.3, 47.8 (CH₂, C-4, C-5, C-8)], [34.6, 34.3 (CH₂, C-2)], [31.5, 31.2 (CH₂, C-7)], 28.6 (CH₃, C-12), 23.7 (CH₂, C-6).[b]

ESI-LRMS (+): m/z 490.2 ([M+Na]⁺, 1%), 468.2 (100, [M+H]⁺).

HRMS: Found [M+H]⁺ 468.2519. C₂₃H₃₈N₃O₅S requires M+H, 468.2527.

---

[a] Ratio based on H-5 peak integration in the reported ¹H-NMR spectrum at δ_H (CDCl₃) 3.47 − 3.34 ppm.
[b] HSQC shows only cross peaks of phenylic proton resonances with δ_C 130.8 and 128.9 ppm carbon resonances. Hence, it is assumed that two aromatic *C*H resonances overlap.

tert-butyl (3*R**,5*S**)-5-(methylsulfonamido)-3-morpholinoazocane-1-carboxylate (*trans*-93a5)
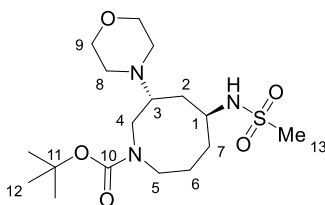
General procedure 3 (page 238) was followed, using building block **trans-93** (0.130 mmol) as the starting material and **a5** as the electrophile. Sulfonamide **trans-93a5** was obtained as a yellow solid (5.9 mg, 12%).

ν$_{max}$ (neat / cm^{-1}): 3269 w (N–H), 2933 m, 2855 w, 2818 w, 1685 s (C=O), 1416 s, 1320 s, 1152 s, 1118 s.

^{1}H-NMR (400 MHz, CDCl$_3$) (mixture of rotamers, 1:1)[a] δ_H 4.26 (app d, *J* = 6.9 Hz, 1H, N*H*), 3.80 – 3.62 (stack, 7H, H-1, H-4, H-5, H-9), 3.50 – 3.40 (m, 0.5H, H-5), 3.20 – 3.02 (stack, 1H, H-4, H-5), 3.00 (app s, 3H, H-13), 2.96 – 2.86 (m, 0.5H, H-4), 2.82 – 2.65 (stack, 1H, H-3), 2.65 – 2.49 (stack, 4H, H-8), 1.97 – 1.73 (stack, 4H, H-2, H-6, H-7), 1.72 – 1.54 (stack, 2H, H-6, H-7), 1.47 (app s, 9H, Boc).

^{13}C-NMR (101 MHz, CDCl$_3$) (mixture of rotamers) δ_C 155.7 (C, C-10), 80.0 (C, C-11), 67.4 (CH$_2$, C-9), [58.6, 57.6 (CH, C-3)], [51.8, 51.1 (CH, C-1), 50.1 (CH$_2$, C-8), 49.8 (CH$_2$, C-4 or C-5), 49.5 (CH$_2$, C-8), [49.2, 48.0, 47.6, (CH$_2$, C-4, C-5)], 41.8 (CH$_3$, C-13), [34.7, 34.3 (CH$_2$, C-2)], 31.1 (CH$_2$, C-7), 28.5 (CH$_3$, C-12), 23.6 (CH$_2$, C-6).

ESI-LRMS (+): m/z 392.3 ([M+H]$^+$, 100%).

HRMS: Found [M+H]$^+$ 392.2205. C$_{17}$H$_{34}$N$_3$O$_5$S requires M+H, 392.2214.

---

[a] Ratio based on H-5 and H-4 peak integrations in the reported ^{1}H-NMR spectrum at respectively δ_H (CDCl$_3$) 3.50 – 3.40 ppm and 2.96 – 2.86 ppm.

tert-butyl (3*R**,5*S**)-5-(3-ethylureido)-3-morpholinoazocane-1-carboxylate (*trans*-93d1)
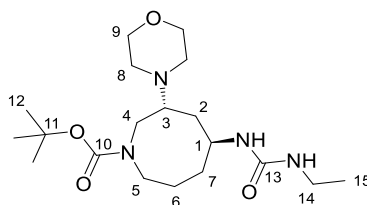
General procedure 3 (page 238) was followed, using building block *trans*-93 (0.130 mmol) as the starting material and **d1** as the electrophile. Urea *trans*-93d1 was obtained as a colourless liquid (40.7 mg, 81%).

v_{max} (neat / cm⁻¹): 3351 w (N–H), 2930 m, 2855 w, 1685 s (C=O), 1625 s, 1558 s, 1416 s, 1241 s, 1163 s, 1115 s.

¹H-NMR (400 MHz, CDCl₃) (mixture of rotamers, 1:1)[a] δ_H δ 4.95 − 4.62 (stack, 2H, CHN*H*CO, CON*H*CH₂), 4.02 − 3.73 (stack, 2H), 3.73 − 3.56 (stack, 4H, H-9), 3.54 − 3.41 (m, 0.5H), 3.24 − 3.01 (stack, 2.5H), 3.01 − 2.74 (stack, 1.5H), 2.72 − 2.33 (stack, 5.5H, including H-8), 1.97 − 1.49 (stack, 5.5H, H-2, H-6, H-7), 1.49 − 1.31 (stack, 9.5H, H-2 or H-6 or H-7, H-12), 1.13 − 0.99 (stack, 3H, H-15).

¹³C-NMR (101 MHz, CDCl₃) (mixture of rotamers) δ_C [157.6, 157.4 (C, C-13)], [155.8, 155.5 (C, C-10)], [80.0, 79.8 (C, C-11)], 67.4 (CH₂, C-9), [59.6, 58.2 (CH, C-1)], [51.0, 50.5, 49.7, 49.1, 48.0, 47.7, 46.0 (CH, C-3, CH₂, C-4, C-5, C-8)], 35.3 (CH₂, C-14), [33.2, 31.8 (CH₂, C-2)], [31.1, 30.1 (CH₂, C-7)], 28.6 (CH₃, C-12), [24.0, 22.8 (CH₂, C-6)], 15.7 (CH₃, C-15).[b]

ESI-LRMS (+): m/z 407.3 ([M+Na]⁺, 10%), 385.3 (100, [M+H]⁺).

HRMS: Found [M+H]⁺ 385.2800. C₁₉H₃₇N₄O₄ requires M+H, 385.2809.

---

[a] Ratio based on peak integrations in the reported ¹H-NMR spectrum at δ_H (CDCl₃) 3.54 − 3.41, 3.24 − 3.01, 3.01 − 2.74, 2.72 − 2.33, 1.97 − 1.49 and 1.49 − 1.31 ppm.
[b] No 2D data available, nor DEPT experimental data. Resonances partially assigned in analogy with *cis*-analogue *cis*-93d1.

tert-butyl (3*S**,5*S**)-5-(methylsulfonamido)-3-morpholinoazocane-1-carboxylate (*cis*-93a5)
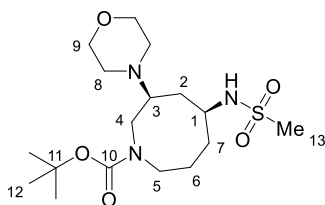
General procedure 3 (page 238) was followed, using building block *cis*-93 (0.180 mmol) as the starting material and **a5** as the electrophile. Sulfonamide *cis*-93a5 was obtained as a colourless liquid (12.4 mg, 18%).

v_{max} (neat / cm^{-1}): 3265 w (N–H), 2933 m, 2859 m, 2818 m, 1685 s (C=O), 1416 s, 1320 s, 1148 s, 1115 s.

^{1}H-NMR (400 MHz, CDCl$_3$) (mixture of rotamers, 1:1)[a] δ_H 3.96 – 3.84 (m, 0.5H, H-4 or H-5), 3.84 – 3.63 (stack, 5.5H, H-4, H-5, H-9), 3.63 – 3.51 (stack, 1H, H-1), 3.07 – 2.85 (stack, 6H, H-3, H-4, H-5, H-13), 2.74 – 2.59 (stack, 2H, H-8), 2.58 – 2.45 (stack, 2H, H-8), 2.00 – 1.52 (stack, 6H, H-2, H-6, H-7), [1.47 (s, 4.5H, H-12), 1.46 (s, 4.5H, H-12)], NH not observed.

^{13}C-NMR (101 MHz, CDCl$_3$) (mixture of rotamers) δ_C 155.5 (C, C-10), [80.3, 80.2 (C, C-11)], 67.3 (CH$_2$, C-9), [61.6, 60.7 (CH, C-3)], [53.3, 52.8 (CH, C-1)], [50.5, 50.2 (CH$_2$, C-8)], [48.9, 48.4, 47.6 (CH$_2$, C-4, C-5)], [41.9, 41.7 (CH$_3$, C-13)], 34.4 (CH$_2$, C-2), 28.6 (CH$_3$, C-12), [23.4, 23.2 (CH$_2$, C-6, C-7)].[b]

ESI-LRMS (+): m/z 414.2 ([M+Na]$^+$, 5%), 392.3 (100, [M+H]$^+$).

HRMS: Found [M+H]$^+$ 392.2205. C$_{17}$H$_{34}$N$_3$O$_5$S requires M+H, 392.2214.

---

[a] Ratio based on H-4 or H-5 peak integrations in the reported ^{1}H-NMR spectrum at δ_H (CDCl$_3$) 3.96 – 3.84, 3.84 – 3.63 ppm.
[b] The resonance of C-7 in other *cis*-analogous sulfonamides appears typically at 33 – 32 ppm. Therefore, it is possible that resonances at 23.4 and 23.2 ppm correspond to C-6 rotamers, and that the C-7 signal isn't observed. HSQC cross peaks for these two C-resonances span across the entire ^{1}H-NMR stack 1.80 – 1.52 (stack, 4H, H-6, H-7).

tert-butyl (3*S**,5*S**)-5-acetamido-3-morpholinoazocane-1-carboxylate (*cis*-93b1)
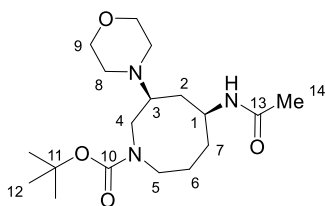
General procedure 3 (page 238) was followed, using building block *cis*-93 (0.180 mmol) as the starting material and **b1** as the electrophile. Amide *cis*-93b1 was obtained as a colourless oil (19.5 mg, 30%).

v_{max} **(neat / cm^{-1}):** 3295 w (N–H), 2930 m, 2855 m, 2814 w, 1685 s (C=O), 1416 s, 1364 s, 1163 s, 1115 s.

^{1}H-NMR (400 MHz, CDCl$_3$) (mixture of rotamers, 1:1)[a] δ_H [6.26 (s, 0.5H, N*H*), 6.14 (s, 0.5H, N*H*)], 3.97 − 3.86 (stack, 1H, H-1), 3.76 − 3.59 (stack, 5.5H, H-4, H-5, H-9), 3.59 − 3.44 (m, 0.5H, H-4 or H-5), 3.20 − 2.85 (stack, 3H, [including 2.97 − 2.85 (m, 1H, H-3)], H-3, H-4, H-5), 2.70 − 2.46 (stack, 4H, H-8), 1.97 − 1.52 (stack, 9H, H-2, H-6, H-7, H-14), [1.46 (s, 4.5H, H-12), 1.45 (s, 4.5H, H-12)].

^{13}C-NMR (101 MHz, CDCl$_3$) (mixture of rotamers) δ_C [168.94, 168.88 (C, C-13)], [155.8, 155.7 (C, C-10)], [80.2, 80.0 (C, C-11)], 67.4 (CH$_2$, C-9), [61.7, 61.1 (CH, C-3)], [49.9, 49.8, 49.6, 49.5, 49.0, 48.8, 48.4, 48.2, 47.6 (CH, C-1, CH$_2$, C-4, C-5, C-8)], [32.4, 31.9 (CH$_2$, C-2)], [28.63, 28.60 (CH$_3$, C-12)], [24.0, 23.7, 23.6, 23.4 (CH$_2$, CH$_3$, C-6, C-7, C-14)].[b]

ESI-LRMS (+): m/z 378.3 ([M+Na]$^+$, 1%), 356.3 (100, [M+H]$^+$).

HRMS: Found [M+H]$^+$ 356.2538. C$_{18}$H$_{34}$N$_3$O$_4$ requires M+H, 356.2544.

---

[a] Ratio based on H-4 or H-5 peak integrations in the reported ^{1}H-NMR spectrum at δ_H (CDCl$_3$) 3.76 − 3.59, 3.59 − 3.44 ppm.
[b] The ten ^{13}C-NMR resonances for C-1, C-4, C-5, C-8 exceed the expected number (eight) for two rotamers. This may be explained by additional rotamer effects originating from the acetyl group, yielding four rotamers instead of two. No DEPT/JMOD experimental data are available, so carbon multiplicities could not be distinguishedh .

tert-butyl (3S*,5S*)-5-(3-ethylureido)-3-morpholinoazocane-1-carboxylate (cis-93d1)
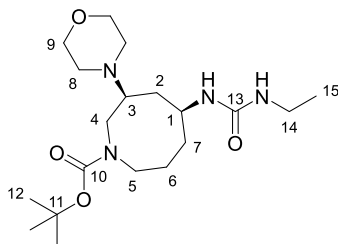
General procedure 3 (page 238) was followed, using building block **cis-93** (0.180 mmol) as the starting material and **d1** as the electrophile. Urea **cis-93d1** was obtained as a white solid (54.4 mg, 79%).

ν$_{max}$ (neat / cm^{-1}): 3351 w (N–H), 2929 m, 2857 m, 1685 s (C=O), 1625 s, 1416 s, 1163 s, 1115 s.

^{1}H-NMR (400 MHz, CDCl$_3$) (mixture of rotamers, 1:1)[a] δ_H 5.05 – 4.86 (stack, 1H, CHN*H*CO), 4.77 – 4.63 (stack, 1H, CON*H*CH$_2$), 3.75 – 3.34 (stack, 7H, [including 3.75 – 3.59 (stack, 1H, H-1)], H-1, H-4, H-5, H-9), 3.27 – 2.97 (stack, 4H, H-4, H-5, H-14), 2.89 – 2.74 (stack, 1H, H-3), 2.67 – 2.41 (stack, 4H, H-8), 1.98 – 1.86 (m, 1H, H-2), 1.86 – 1.54 (stack, 3H, H-6, H-7), 1.54 – 1.32 (stack, 11H, [including 1.43 (s, 4.5 H, H-12), 1.42 (s, 4.5H, H-12)], H-2, H-7, H-12), 1.17 – 1.00 (stack, 3H, H-15).

^{13}C-NMR (101 MHz, CDCl$_3$) (mixture of rotamers)[b] δ_C [157.7, 157.6 (C, C-13)], [155.9, 155.8 (C, C-10)], [80.1, 79.8 (C, C-11)], 67.3 (CH$_2$, C-9), [61.7, 61.1 (CH, C-3)], [50.2, 49.6, 49.4, 49.3, 48.9, 47.9, 47.4 (CH, C-1, CH$_2$, C-4, C-5, C-8)], 35.2 (CH$_2$, C-14), 34.5 (CH$_2$, C-2), [32.7, 32.0 (CH$_2$, C-7)], [28.6, 28.5 (CH$_3$, C-12)], [23.6, 23.2 (CH$_2$, C-6)], [15.7, 15.6 (CH$_3$, C-15)].

ESI-LRMS (+): m/z 407.3 ([M+Na]$^+$, 5%), 385.3 (100, [M+H]$^+$).

HRMS: Found [M+H]$^+$ 385.2802. C$_{19}$H$_{37}$N$_4$O$_4$ requires M+H, 385.2809.

---

[a] Ratio based on observed H-12 peak intensities in the reported ^{1}H-NMR spectrum.
[b] No DEPT experimental data available, so CH could not be distinguished from CH$_2$ signals.

N-((3*S**,5*R**)-3-morpholinoazocan-5-yl)-2,3-dihydrobenzo[*b*][1,4]dioxine-6-sulfonamide dihydrochloride (*trans*-108a7 •2 HCl)
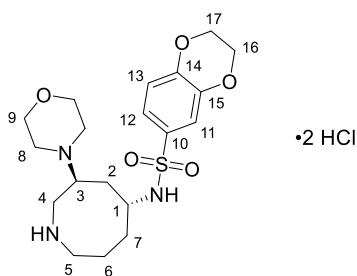
General procedure 5 (page 239) was followed, using Boc-amine *trans*-93 (0.035 mmol) as the starting material. Amine *trans*-108a7 •2 HCl was obtained as an off-white solid (13.3 mg, 78%).

***v*max (neat / cm⁻¹):** 3127 m (N–H), 3042 m, 1580 m, 1491 s, 1402 s, 1286 v s, 1252 s, 1062 s.

¹H-NMR (400 MHz, CD₃OD) δ_H 7.45 – 7.37 (stack, 2H, H-11, H-12), 7.02 (d, *J* = 9.1 Hz, 1H, H-13), 4.35 – 4.29 (stack, 4H, H-16, H-17), 4.11 – 3.89 (stack, 5H, H-3, H-9), 3.82 (dd, *J* = 14.7, 4.4 Hz, 1H, H-4), 3.64 (dd, *J* = 14.7, 7.8 Hz, 1H, H-4), 3.58 – 3.48 (m, 1H, H-1), 3.47 – 3.19 (stack, 6H, [including 3.28 (app t, *J* = 5.8 Hz, 2H, H-5)], H-5, H-8), 2.54 – 2.43 (m, 1H, H-2), 2.31 – 2.18 (m, 1H, H-2), 2.02 – 1.90 (m, 1H, H-6), 1.83 – 1.65 (stack, 3H, H-6, H-7), exchangeable protons not observed.

¹³C-NMR (101 MHz, CD₃OD) δ_C 149.2 (C, C-15), 145.3 (C, C-14), 133.6 (C, C-10), 121.8 (CH, C-11), 118.9 (CH, C-13), 117.6 (CH, C-12), [66.0, 65.6 (CH₂, C-16, C-17)], 65.2 (CH₂, C-9), 59.4 (CH, C-3), 50.9 (CH, C-1), 46.6 (CH₂, C-4), 31.8 (CH₂, C-2), 30.6 (CH₂, C-7), 21.0 (CH₂, C-6). C-5, C-8 resonances not observed, although HSQC cross peaks suggest they are stacked under the CD₃OD signal.

ESI-LRMS (+): m/z 434.2 ([M+Na]⁺, 5%), 412.2 (100, [M+H]⁺).

HRMS: Found [M+H]⁺ 412.1894. $C_{19}H_{30}N_3O_5S$ requires M+H, 412.1901.

2-methyl-*N*-((3*S**,5*R**)-3-morpholinoazocan-5-yl)nicotinamide dihydrochloride (*trans*-108c5 •2 HCl)
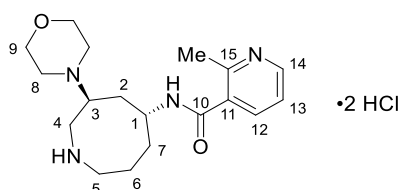
General procedure 5 (page 239) was followed, using Boc-amine *trans*-93 (0.099 mmol) as the starting material. Amine *trans*-108c5 •2 HCl was obtained as an off-white solid (33.5 mg, 83%).

v_{max} (neat / cm^{-1}): 3444 w (N–H), 3273 w (N–H), 2937 w, 1640 s (C=O), 1416 s, 1159 s, 1111 v s.

^{1}H-NMR (400 MHz, D$_2$O) δ_H 8.72 (dd, *J* = 5.9, 1.6 Hz, 1H, H-14), 8.56 (dd, *J* = 8.0, 1.6 Hz, 1H, H-12), 7.94 (dd, *J* = 8.0, 5.9 Hz, 1H, H-13), 4.44 (app ddt, *J* = 11.6, 7.8, 3.8 Hz, 1H, H-1), 4.09 − 3.92 (stack, 5H, H-3, H-9), 3.86 (A of ABX, J_{A-B} = 15.1, J_{A-X} = 3.3 Hz, 1H, H-4), 3.72 (B of ABX, J_{B-A} = 15.1, J_{B-X} = 7.9 Hz, 1H, H-4), 3.56 − 3.31 (stack, 6H, H-5, H-8), 2.82 (s, 3H, Me), 2.54 − 2.36 (stack, 2H, H-2), 2.19 − 1.97 (stack, 3H, H-6, H-7), 1.96 − 1.82 (m, 1H, H-7), exchangeable protons not observed.

^{13}C-NMR (101 MHz, D$_2$O) δ_C 168.3 (C, C-10), 155.2 (C, C-15), 147.0 (CH, C-12), 145.1 (CH, C-14), 136.6 (C, C-11), 127.4 (CH, C-13), 66.6 (CH$_2$, C-9), 61.3 (CH, C-3), 51.7 (CH$_2$, C-8), 48.9 (CH, C-1), 48.8 (CH$_2$, C-5), 45.8 (CH$_2$, C-4), 33.3 (CH$_2$, C-2), 32.1 (CH$_2$, C-7), 23.0 (CH$_2$, C-6), 20.5 (CH$_3$, Me).

ESI-LRMS (+): 355.3 ([M+Na]$^+$, 5%), 333.3 (100, [M+H]$^+$).

HRMS: Found [M+H]$^+$ 333.22806. C$_{18}$H$_{29}$N$_4$O$_2$ requires M+H, 333.2285.

1-ethyl-3-((3S*,5R*)-3-morpholinoazocan-5-yl)urea dihydrochloride (*trans*-108d1 •2 HCl)
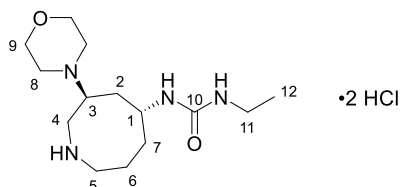
General procedure 5 (page 239) was followed, using Boc-amine *trans*-93 (0.087 mmol) as the starting material. Amine *trans*-108d1 •2 HCl was obtained as a white solid (27.9 mg, 90%).

v_{max} (neat / cm^{-1}): 3311 w (N–H), 2983 w, 2662 m, 1621 m (C=O), 1562 s, 1115 s.

^{1}H-NMR (400 MHz, CD₃OD) δ_H 4.16 – 3.85 (stack, 7H, [including 3.89 (dd, *J* = 14.5, 4.3 Hz, 1H)]), 3.69 (dd, *J* = 14.5, 8.9 Hz, 1H), 3.61 – 3.23 (stack, 6H), 3.17 (app q, *J* = 7.3 Hz, 2H), 2.41 (app ddd, *J* = 15.9, 6.5, 3.4 Hz, 1H), 2.26 (app ddd, *J* = 15.9, 7.6, 3.0 Hz, 1H), 2.17 – 2.04 (m, 1H), 2.04 – 1.87 (stack, 2H), 1.86 – 1.72 (m, 1H), 1.10 (t, *J* = 7.3 Hz, 3H), exchangeable protons not observed.

^{13}C-NMR (101 MHz, CD₃OD) δ_C 160.3 (C, C-10), 65.1 (CH₂), 60.5 (CH), 51.0 (CH₂), 48.2 (CH₂), 47.1 (CH), 45.1 (CH₂), 35.8 (CH₂), 32.5 (CH₂), 31.4 (CH₂), 21.6 (CH₂), 15.7 (CH₃, C-12).

ESI-LRMS (+): m/z 285.3 ([M+H]$^+$, 100%).

HRMS: Found [M+H]$^+$ 285.2285. $C_{14}H_{29}N_4O_2$ requires M+H, 285.2285.

1-((3S*,5R*)-3-morpholinoazocan-5-yl)-3-(4-(trifluoromethyl)benzyl)urea dihydrochloride (*trans*-108d4 •2 HCl)
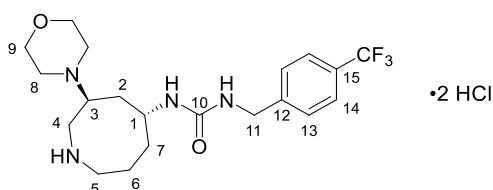
General procedure 5 (page 239) was followed, using Boc-amine *trans*-93 (0.094 mmol) as the starting material. Amine *trans*-108d4 •2 HCl was obtained as an off-white solid (42.3 mg, 93 %).

v$_{max}$ (neat / cm^{-1}): 3310 m (N–H), 2937 w, 2673 w, 1644 m (C=O), 1558 s, 1323 s, 1111 s, 1066 s.

^{1}H-NMR (400 MHz, CD$_3$OD) δ_H 7.66 − 7.56 (AA' of AA'BB', 2H, H-14), 7.54 − 7.41 (BB' of AA'BB', 2H, H-13), 4.43 (A of AB, $J_{A–B}$ = 16.1 Hz, 1H, H-11), 4.36 (B of AB, $J_{B–A}$ = 16.1 Hz, 1H, H-11), 4.07 − 3.77 (stack, 7H, H-1, H-3, H-4, H-9), 3.67 (B of ABX, J_{A-B} = 14.4, J_{B-X} = 8.8 Hz, 1H, H-4), 3.51 − 3.28 (stack, 6H, H-5, H-8), 2.41 (A of ABXY, J_{A-B} = 15.9, J_{A-X} = 6.4 , J_{A-Y} = 3.2 Hz, 1H, H-2), 2.24 (B of ABXY, J_{B-A} = 15.9, J_{B-X} = 7.5, J_{B-Y} = 2.9 Hz, 1H, H-2), 2.18 − 2.04 (m, 1H, H-6), 2.04 − 1.88 (stack, 2H, H-6, H-7), 1.88 − 1.73 (m, 1H, H-7), exchangeable protons not observed.

^{13}C-NMR (101 MHz, CD$_3$OD) δ_C 160.2 (C, C-10), 146.2 (C, C-12), 130.2 (C, q, $J_{C–F}$ = 31.6 Hz, C-15), 128.7 (CH, C-13), 126.4 (CH, q, $J_{C–F}$ = 3.5 Hz, C-14), 65.1 (CH$_2$, C-9), 60.4 (CH, C-3), 50.9 (CH$_2$, C-8), 48.2 (CH$_2$, C-5) , 47.1 (CH, C-1), 45.2 (CH$_2$, C-4) , 44.1 (CH$_2$, C-11), 32.4 (CH$_2$, C-2), 31.3 (CH$_2$, C-7), 21.6 (CH$_2$, C-6), *C*F$_3$ resonance not observed.

ESI-LRMS (+): m/z 437.3 ([M+Na]$^+$, 5%), 415.3 (100, [M+H]$^+$).

HRMS: Found [M+H]$^+$ 415.2311. C$_{20}$H$_{30}$F$_3$N$_4$O$_2$ requires M+H, 415.2315.

1-ethyl-3-((3S*,5S*)-3-morpholinoazocan-5-yl)urea dihydrochloride (*cis*-108d1 •2 HCl)
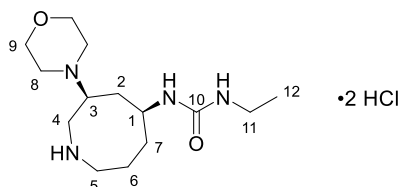
General procedure 5 (page 239) was followed, using Boc-amine *cis*-93 (0.125 mmol) as the starting material. Amine *cis*-108d1 •2 HCl was obtained as a white solid (34.5 mg, 77%).

v_{max} (neat / cm^{-1}): 3280 m (N–H), 2967 m, 2661 m, 2550 m, 1648 s (C=O), 1551 s, 1267 m.

^{1}H-NMR (400 MHz, D$_2$O) δ_H 4.11 − 3.86 (stack, 5H, H-3, H-9), 3.86 − 3.75 (stack, 2H, H-1, H-4), 3.58 (dd, J = 14.4, 9.0 Hz, 1H, H-4), 3.48 − 3.23 (stack, 6H, H-5, H-8), 3.09 (q, J = 7.3 Hz, 2H, H-11), 2.43 − 2.33 (m, 1H, H-2), 2.25 − 1.93 (stack, 3H, H-2, H-6, H-7), 1.91 − 1.78 (m, 1H, H-6), 1.78 − 1.65 (m, 1H, H-7), 1.05 (t, J = 7.3 Hz, 3H, H-12), exchangeable protons not observed.

^{13}C-NMR (101 MHz, D$_2$O) δ_C 159.3 (C, C-10), 63.9 (CH$_2$, C-9), 59.9 (CH, C-3), 48.61 (CH$_2$, C-8), 48.57 (CH, C-1), 47.0 (CH$_2$, C-5), 44.6 (CH$_2$, C-4), 34.9 (CH$_2$, C-11), 33.3 (CH$_2$, C-2), 30.5 (CH$_2$, C-7), 20.2 (CH$_2$, C-6), 14.5 (CH$_3$, C-12).

ESI-LRMS (+): m/z 285.3 ([M+H]$^+$, 100%).

HRMS: Found [M+H]$^+$ 285.2277. C$_{14}$H$_{29}$N$_4$O$_2$ requires M+H, 285.2285.

1-(2,5-difluorophenyl)-3-((3S*,5S*)-3-morpholinoazocan-5-yl)urea dihydrochloride (cis-108d2 •2 HCl)
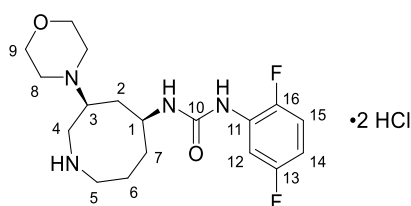
General procedure 5 (page 239) was followed, using Boc-amine **cis-93** (0.045 mmol) as the starting material. Amine **cis-108d2 •2 HCl** was obtained as a yellow solid (14.5 mg, 73%).

v_{max} (neat / cm^{-1}): 3418 w (N–H), 3276 m (N–H), 2866 w, 2445 w, 1677 m (C=O), 1543 s, 1439 s, 1234 m.

^{1}H-NMR (400 MHz, D$_2$O) δ_H 7.47 – 7.38 (m, 1H, H-12), 7.18 – 7.09 (m, 1H, H-15), 6.89 – 6.79 (m, 1H, H-14), 4.08 – 3.82 (stack, 6H, H-1, H-3, H-9), 3.78 (dd, J = 14.3, 3.9 Hz, 1H, H-4), 3.57 (dd, J = 14.4, 9.0 Hz, 1H, H-4), 3.44 – 3.24 (stack, 6H, H-5, H-8), 2.48 – 2.38 (m, 1H, H-2), 2.19 – 2.02 (stack, 3H, H-2, H-6, H-7), 1.95 – 1.72 (stack, 2H, H-6, H-7), exchangeable protons not observed.

^{13}C-NMR (101 MHz, D$_2$O) δ_C 156.3 (C, C-10), 126.9 (C, C-11), 116.1 (CH, dd, J = 22.4, 10.0 Hz, C-15), 110.7 (CH, dd, J = 24.3, 7.7 Hz, C-14), 110.1 (CH, d, J = 28.0 Hz, C-12), 64.2 (CH$_2$, C-9), 59.7 (CH, C-3), 48.6 (CH, C-1), 48.5 (CH$_2$, C-8), 47.0 (CH$_2$, C-5), 44.8 (CH$_2$, C-4), 33.1 (CH$_2$, C-2), 30.4 (CH$_2$, C-7), 20.2 (CH$_2$, C-6). C-13, C-16 signals not observed in ^{13}C-NMR spectrum, but HMBC crosspeaks between δ_C 153 – 147 ppm and 156 – 160 ppm with all three aromatic protons indicates their presence as doublets with $J_{C–F}$ > 250 Hz.

ESI-LRMS (+): m/z 391.3 ([M+Na]$^+$, 1%), 369.3 (100, [M+H]$^+$).

HRMS: Found [M+H]$^+$ 369.2093. C$_{18}$H$_{27}$F$_2$N$_4$O$_2$ requires M+H, 369.2097.

N-((3*S**,5*S**)-3-morpholinoazocan-5-yl)-2-(tetrahydro-2*H*-pyran-4-yl)acetamide dihydrochloride (*cis*-108c1 •2 HCl)
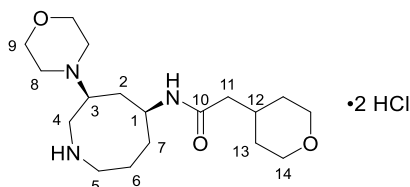
General procedure 5 (page 239) was followed, Boc-amine *cis*-93 (0.101 mmol) as the starting material. Amine *cis*-108c1 •2 HCl was obtained as an off-white solid (33.2 mg, 80%).

v$_{max}$ (neat / cm^{-1}): 3452 w (N–H), 2840 m, 2643 m, 2527 m, 2453 m, 1636 s (C=O), 1536 s, 1461 s, 1275 s, 1088 s.

^{1}H-NMR (400 MHz, CD$_3$OD) δ_H 4.14 − 3.84 (stack, 9H, H-1, H-3, H-4, H-9, H-14), 3.65 (dd, *J* = 14.3, 8.7 Hz, 1H, H-4), 3.54 − 3.32 (stack, 8H, H-5, H-8, H-14), 2.49 − 2.38 (m, 1H, H-2), 2.23 − 1.79 (stack, 8H, H-2, H-6, H-7, H-11, H-12), 1.68 − 1.58 (m, 2H, H-13), 1.39 − 1.25 (m, 2H, H-13), exchangeable protons not observed.

^{13}C-NMR (101 MHz, CD$_3$OD) δ_C 173.9 (C, C-10), [68.83, 68.80 (CH$_2$, C-14)], 65.0 (CH$_2$, C-9), 61.6 (CH, C-3), 50.4 (CH$_2$, C-5), 49.6 (CH, C-1), 48.2 (CH$_2$, C-8), 46.0 (CH$_2$, C-4), 44.0 (CH$_2$, C-11), 33.84 (CH, C-12), 33.75 (CH$_2$, C-13), 33.3 (CH$_2$, C-2), 31.4 (CH$_2$, C-7), 21.8 (CH$_2$, C-6).

ESI-LRMS (+): m/z 362.3 ([M+Na]$^+$, 5%), 340.3 (100, [M+H]$^+$).

HRMS: Found [M+H]$^+$ 340.2592. C$_{18}$H$_{34}$N$_3$O$_3$ requires M+H, 340.2595.

N-((3*S**,5*S**)-3-morpholinoazocan-5-yl)quinoline-3-carboxamide trihydrochloride (*cis*-108c6 •3 HCl)
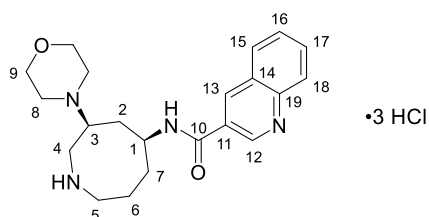
General procedure 5 (page 239) was followed, using Boc-amine *cis*-93 (0.101 mmol) as the starting material. Amine *cis*-108c6 •3 HCl was obtained as a beige solid (34.0 mg, 71%).

v$_{max}$ (neat / cm^{-1}): 3362 w (N–H), 3235 w (N–H), 2650 w, 1640 s (C=O), 1539 s, 1297 m, 1115 m.

1H-NMR (400 MHz, CD₃OD) δ_H 9.67 (s, 1H, H-12 or H-13), 9.65 (s, 1H, H-12 or H-13), 8.44 (d, *J* = 8.1 Hz, 1H, H-15), 8.34 – 8.29 (m, 1H, H-18), 8.29 – 8.22 (m, 1H, H-17), 8.07 – 8.01 (m, 1H, H-16), 4.36 – 4.29 (m, 1H, H-1), 4.21 – 4.11 (m, 1H, H-3), 4.11 – 3.92 (stack, 5H, H-4, H-9), 3.73 (dd, *J* = 14.3, 8.6 Hz, 1H, H-4), 3.64 – 3.35 (stack, 6H, H-5, H-8), 2.76 – 2.64 (m, 1H, H-2), 2.47 – 2.20 (stack, 3H, H-2, H-6, H-7), 2.20 – 1.98 (stack, 2H, H-6, H-7), exchangeable protons not observed.

13C-NMR (101 MHz, CD₃OD) δ_C 164.0 (C, C-10), [146.3, 146.0 (CH, C-12, C-13)], 141.0 (C, C-11), 137.4 (CH, C-17), [131.7, 131.5 (CH, C-15, C-16), [129.5, 129.3 (C, C-14, C-19)], 122.7 (CH, C-18), 65.1 (CH₂, C-9), 61.7 (CH, C-3), 50.7 (CH, C-1), 48.3 (CH₂, C-5 or C-8), 46.2 (CH₂, C-4), 33.3 (CH₂, C-2), 31.4 (CH₂, C-7), 22.0 (CH₂, C-6). The resonance for is C-5 or C-8 not observed, but HSQC cross peaks indicate its presence between δ_C 51 – 48 ppm.

ESI-LRMS (+): m/z 391.3 ([M+Na]⁺, 5%), 369.3 (80, [M+H]⁺), 185.2 (100, [M+2H]²⁺).

HRMS: Found [M+H]⁺ 369.2282. C₂₁H₂₉N₄O₂ requires M+H, 369.2285.

6. SACE1 Library summary

Cis library (36 compounds)

Table 20: SACE1 cis library compounds.

cis-93   **cis-105**   **cis-106**   **cis-108**
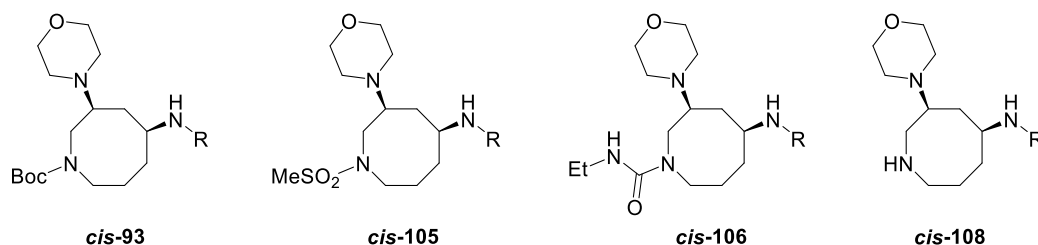
Product	Method	MW (Da)	Amount SM (mmol)[a]	Yield (mg)	Yield (%)	t_R (min)[b]	Purity (%)[b]	Comments[c]
cis-93	-	313.4	0.180	52.6	93	0.90	100	-
cis-93a1	3	518.1	0.180	2.3	2	1.52	100	-
cis-93a5	3	391.5	0.180	12.4	18	1.08	100	-
cis-93a6	3	504.7	0.180	-	-	-	-	Failed
cis-93b1	3	355.5	0.180	19.5	30	0.98	100	-
cis-93c1	4	439.6	0.180	53.2	67	1.05	95	-
cis-93c4	4	449.6	0.180	44.8	55	1.09	90	-
cis-93c6	4	468.6	0.180	49.5	59	1.27	92	-
cis-93d1	3	384.5	0.180	54.4	79	1.05	100	-
cis-93d2	3	468.5	0.180	27.0	32	1.50	100	-
cis-105	-	291.4	0.100	8.2	28	0.57	100	-
cis-105a1	3	496.0	0.100	4.4	9	1.17	100	-
cis-105a5	3	369.5	0.100	8.8	24	0.72	100	-
cis-105a6	3	482.6	0.100	-	-	-	-	Failed
cis-105b1	3	333.5	0.100	8.9	27	0.67	63	-
cis-105c1	4	417.6	0.100	29.6	71	0.76	95	-
cis-105c4	4	427.6	0.100	27.1	63	0.82	100	-
cis-105c6	4	446.6	0.100	21.6	48	0.99	99	-
cis-105d1	3	362.5	0.100	31.6	87	0.75	100	-
cis-105d2	3	446.5	0.100	12.5	28	1.18	100	-
cis-106	-	284.4	0.120	25.9	76	0.60	100	-
cis-106a1	3	489.0	0.120	1.9	3	1.11	100	-
cis-106a5	3	362.5	0.120	8.0	18	0.71	100	-
cis-106a6	3	475.6	0.120	-	-	-	-	Failed
cis-106b1	3	326.4	0.120	5.0	13	0.67	71	-
cis-106c1	4	410.6	0.120	38.3	78	0.74	100	-
cis-106c4	4	420.6	0.120	37.7	75	0.79	97	-
cis-106c6	4	439.6	0.120	38.2	72	0.93	99	-
cis-106d1	3	355.5	0.120	40.3	94	0.73	96	-
cis-106d2	3	439.5	0.120	8.7	16	1.11	100	-
cis-108	5	286.2	0.018	-	-	-	-	Failed
cis-108a5	5	364.3	0.041	14.4	95	0.64	100	2 HCl
cis-108b1	5	328.3	0.033	9.4	86	0.54	95	2 HCl
cis-108c1	5	412.4	0.101	33.2	80	0.61	94	2 HCl
cis-108c4	5	422.4	0.084	29.9	84	0.64	88	2 HCl
cis-108c6	5	477.9	0.101	34.0	71	0.75	99	3 HCl
cis-108d1	5	357.3	0.125	34.5	77	0.59	94	2 HCl

| cis-108d2 | 5 | 441.3 | 0.045 | 14.5 | 73 | 0.87 | 100 | 2 HCl |

[a]SM: starting material. [b]Retention time and purity measured using UPLC. Purity calculated as product peak AUC fraction in the total absorbance chromatogram (210 – 320 nm). [c]Deprotected compounds were obtained as HCl salts. HCl multiplicity was determined experimentally for a representative selection. (see Section 13)

Trans-library (39 compounds)

Table 21: SACE1 trans library compounds.

trans-93　　　　**trans-105**　　　　**trans-106**　　　　**trans-108**
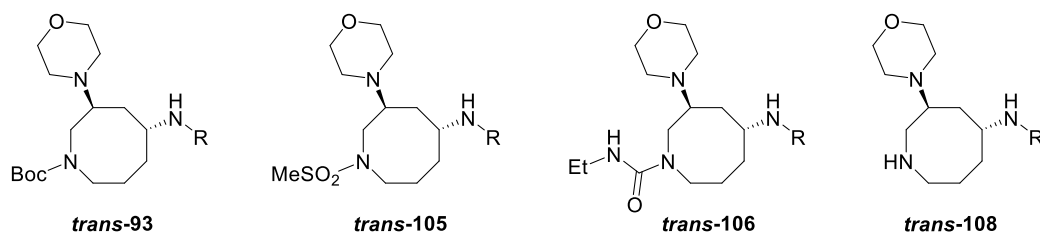
Product	Method	MW (Da)	Amount SM (mmol)[a]	Yield (mg)	Yield (%)	t_R (min)	Purity (%)[b]	Comments[c]
trans-93	-	313.4	0.130	38.5	94	0.96	100	-
trans-93a2	3	467.6	0.130	8.4	14	1.47	100	-
trans-93a3	3	488.7	0.130	6.0	9	1.34	100	-
trans-93a5	3	391.5	0.130	5.9	12	1.12	100	-
trans-93a7	3	511.6	0.130	20.5	31	1.44	98	-
trans-93b1	3	355.5	0.130	4.3	9	1.01	90	-
trans-93c3	4	450.6	0.130	25.0	43	1.01	97	-
trans-93c5	4	432.6	0.130	50.1	89	1.10	99	-
trans-93d1	3	384.5	0.130	40.7	81	1.06	100	-
trans-93d4	3	514.6	0.130	62.0	93	1.49	100	-
trans-105	-	291.4	0.130	25.4	67	0.59	100	-
trans-105a2	3	445.6	0.130	7.3	13	1.12	100	-
trans-105a3	3	466.6	0.130	15.8	26	0.99	100	-
trans-105a5	3	369.5	0.130	5.5	11	0.75	100	-
trans-105a7	3	489.6	0.130	6.1	10	1.10	100	-
trans-105b1	3	333.5	0.130	5.6	13	0.67	98	-
trans-105c3	4	428.6	0.130	15.1	27	0.71	100	-
trans-105c5	4	410.5	0.130	32.7	61	0.77	100	-
trans-105d1	3	362.5	0.130	29.0	62	0.73	100	-
trans-105d4	3	492.6	0.130	33.2	52	1.21	100	-
trans-106	-	284.4	0.130	33.9	92	0.61	100	-
trans-106a2	3	438.6	0.130	15.1	26	1.04	100	-
trans-106a3	3	459.6	0.130	11.4	19	0.94	100	-
trans-106a5	3	362.5	0.130	10.7	23	0.73	100	-
trans-106a7	3	482.6	0.130	12.8	20	1.04	98	-
trans-106b1	3	326.4	0.130	7.0	16	0.66	65	-
trans-106c3	4	421.5	0.130	21.1	39	0.69	100	-
trans-106c5	4	403.5	0.130	36.7	70	0.74	100	-
trans-106d1	3	355.5	0.130	36.1	78	0.71	100	-
trans-106d4	3	485.6	0.130	48.1	76	1.15	100	-
trans-108	5	213.3	0.018	-	-	-	-	Failed
trans-108a2	5	440.4	0.059	20.4	78	1.02	96	2 HCl
trans-108a3	5	461.5	0.108	42.0	84	0.89	98	2 HCl

trans-108a5	5	364.3	0.121	37.9	86	0.64	100	2 HCl
trans-108a7	5	484.4	0.035	13.3	78	0.83	58	2 HCl
trans-108b1	5	328.3	0.106	31.6	91	0.55	94	2 HCl
trans-108c3	5	423.4	0.034	12.4	86	0.57	97	2 HCl
trans-108c5	5	405.3	0.099	33.5	83	0.60	86	2 HCl
trans-108d1	5	357.3	0.087	27.9	90	0.57	98	2 HCl
trans-108d4	5	487.4	0.094	42.3	93	0.90	100	2 HCl

[a]SM: starting material. [b]Retention time and purity measured using UPLC. Purity calculated as product peak AUC fraction in the total absorbance chromatogram (210 − 320 nm). [c]Deprotected compounds were obtained as HCl salts. HCl multiplicity was determined experimentally for a representative selection. (see Section 13)

7. SACE2 library precursors

7.1. GENERAL PROCEDURE 6: Fused heterocycle synthesis
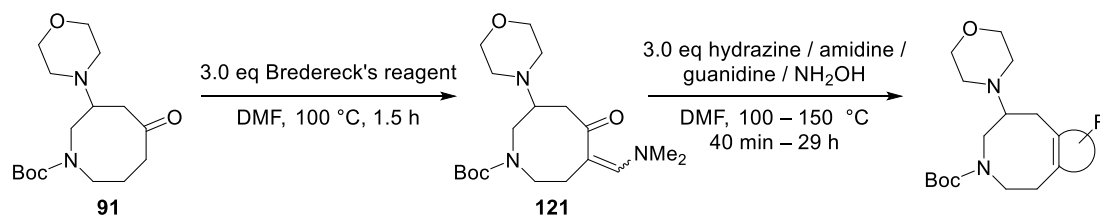
Bredereck's reagent (3.0 eq) was added to a solution of ketone **91** in DMF (0.4 M). After stirring for 1.5 h at 100 °C, unreacted Bredereck's reagent was removed under reduced pressure at rt and the desired hydrazine, amidine, guanidine or hydroxylamine (3.0 eq) was added to the reaction mixture. After stirring for 40 min − 29 h at 100 − 150 °C (specified in the reaction scheme for each compound), the volatiles were removed under reduced pressure. The resulting crude mixture was purified *via* aqueous workup and column chromatography to yield the fused heterocycle. Aqueous workup and column chromatography conditions are specified for each compound. Any deviations from this general procedure (*e.g.*, different amount of equivalents, extra reagents) are specified for each compound.

7.2. Compound synthesis and characterisation

tert-butyl 1-(4-fluorophenyl)-8-morpholino-1,4,5,7,8,9-hexahydro-6H-pyrazolo[4,3-d]azocine-6-carboxylate (126)
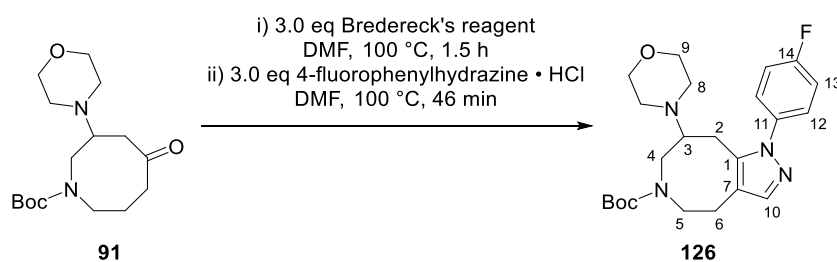
General procedure 6 (page 267) was followed, using ketone **91** (941 mg, 3.01 mmol) and 4-fluorophenylhydrazine hydrochloride. After removal of volatiles under reduced pressure, NaHCO$_3$ solution (100 mL) was added and the resulting mixture was extracted with Et$_2$O (5 × 100 mL). The combined organic extracts were concentrated under reduced pressure and the resulting crude mixture was purified using automatic reverse phase column chromatography (basic), yielding fused pyrazole **126** as an off-white powder (671 mg, 52%).

R$_f$ (CH$_2$Cl$_2$:MeOH, 4:1): 0.9.

v $_{max}$ **(neat / cm^{-1}):** 2930 w, 2855 w, 1681 s (C=O), 1513 v s, 1413 s, 1116 v s.

^{1}H-NMR (400 MHz, CDCl$_3$) (mixture of rotamers, 11:5)[a] δ_H 7.45 − 7.29 (stack, 3H, [including 7.43 (s, 0.3 H, H-10 min), 7.39 (s, 0.7 H, H-10 maj)], H-10, H-12), 7.19 − 7.08 (stack, 2H, H-13), 4.14 − 3.97 (m, 0.3H, H-5 min), 3.84 − 3.66 (stack, 1.7H, H-4, H-5 maj), [3.66 − 3.51 (stack, 2.7H, H-9 maj), 3.53 − 3.36 (stack, 1.3H, H-9 min)], 3.36 − 3.23 (m, 0.7H, H-3 maj), 3.21 − 3.09 (m, 0.7H, H-5 maj), 3.09 − 2.88 (stack, 1.3H, H-4 maj, H-5 min, H-3 min), 2.88 − 2.56 (stack, 4.3H, H-2, H-4 min, H-6), [2.56 − 2.41 (stack, 2.7H, H-8 maj), 2.42 − 2.25 (stack, 1.3H, H-8 min)], [1.38 (s, 2.8H, Boc min), 1.26 (s, 6.2H, Boc maj)].

^{13}C-NMR (101 MHz, CDCl$_3$) (mixture of rotamers) δ_C 162.1 (C, d, J_{C-F} = 248.5 Hz, C-14), [155.6 (C, Boc C=O maj), 155.5 (C, Boc C=O min)], [139.9 (CH, C-10 min), 139.5 (CH, C-10 maj)], [139.2 (C, C-1 maj), 138.5 (C, C-1 min)], [136.6 (C (br), C-11 min), 136.1 (C, d, J_{C-F} = 3.2 Hz, C-11 maj)], [127.7 (CH, d, J_{C-F} = 8.6 Hz, C-12 maj), 127.4 (CH, d, J_{C-F} = 8.6 Hz, C-12 min)], [117.9, (C, C-7 min), 116.5 (C, C-7 maj)], [116.13 (CH, d, J_{C-F} = 23.0 Hz, C-13 maj), 116.10 (CH, d, J_{C-F} = 22.8 Hz, C-13 min)], [79.9 (C, Boc C(CH$_3$)$_3$ min), 79.8 (C, Boc C(CH$_3$)$_3$ maj)], [67.14 (CH$_2$, C-9), 67.06 (CH$_2$, C-9], [62.9 (CH, C-3 min), 60.5 (CH, C-3 maj)], 50.1 (CH$_2$, C-8 min), [49.9 (CH$_2$, C-4 maj), 49.5 (CH$_2$, C-4 min)], 49.3 (CH$_2$, C-8 maj), [48.6 (CH$_2$, C-5 min), 48.2 (CH$_2$, C-5 maj)], [28.6 (CH$_3$, Boc C(CH$_3$)$_3$ min), 28.2 (CH$_3$, Boc C(CH$_3$)$_3$ maj)], [24.7 (CH$_2$, C-2 min), 24.6 (CH$_2$, C-2 maj)], [24.1 (CH$_2$, C-6 min), 23.7 (CH$_2$, C-6 maj)].

^{19}F NMR (376 MHz, DMSO-d_6) (mixture of rotamers) δ_F [−113.9 − (−114.1) (m), −114.3 − (−114.4) (m)].

ESI-LRMS (+): m/z 431.2 ([M+H]$^+$, 100%).

HRMS: Found [M+H]$^+$ 431.2443. C$_{23}$H$_{32}$FN$_4$O$_3$ requires M+H, 431.2453.

---

[a] Ratio based on Boc peak integrations in the reported ^{1}H-NMR spectrum.

tert-butyl 8-morpholino-1-(pyridin-3-yl)-1,4,5,7,8,9-hexahydro-6*H*-pyrazolo[4,3-*d*]azocine-6-carboxylate (128)
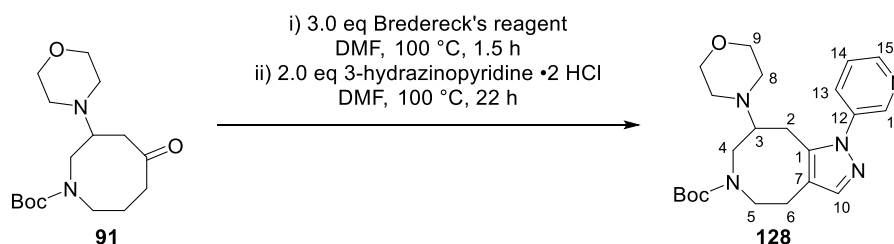
General procedure 6 (page 267) was followed, using ketone **91** (931 mg, 2.98 mmol) and 3-hydrazinopyridine dihydrochloride (121 mg, 0.666 mmol). After removal of volatiles under reduced pressure, NaHCO₃ solution (100 mL) was added and the resulting mixture was extracted with CH₂Cl₂ (3 × 100 mL). The combined organic extracts were dried over anhydrous Na₂SO₄, filtered and concentrated under reduced pressure. The resulting crude mixture was purified using automatic column chromatography (CH₂Cl₂:7 M NH₃ in MeOH), yielding fused pyrazole **128** as a yellow oil (0.80 g, 65%).

R*ƒ* (CH₂Cl₂:7 M NH₃ in MeOH, 9:1): 0.8.

***v*max (neat / cm⁻¹):** 2967 m, 2930 m, 2855 m, 1681 s (C=O), 1413 s, 1245 s, 1163 s, 1115 v s.

¹H-NMR (400 MHz, CDCl₃) (mixture of rotamers, 3:2)ᵃ δ$_H$ 8.69 − 8.62 (stack, 1H, H-11), 8.62 − 8.52 (stack, 1H, H-15), [7.80 − 7.73 (m, 0.4H, H-13 min), 7.73 − 7.65 (m, 0.6H, H-13 maj)], 7.50 − 7.32 (stack, 2H, [including 7.45 (s, 0.4H, H-10 min), 7.41 (s, 0.6H, H-10 maj)], H-10, H-14), 4.05 (ddd, *J* = 13.1, 7.8, 4.8 Hz, 0.4H, H-5 min), 3.79 − 3.66 (stack, 1.2H, H-4 maj, H-5 maj), 3.67 − 3.17 (stack, 5H, H-3 maj, H-4 min, H-9), 3.15 − 3.01 (m, 0.6H, H-5 maj), 3.01 − 2.78 (stack, 2.4H, H-2, H-3 min, H-4 maj, H-5 min), 2.78 − 2.64 (stack, 2.2H, H-2, H-4 min, H-6 min), 2.64 − 2.50 (stack, 1.2H, H-6 maj), [2.50 − 2.37 (stack, 2.4H, H-8 maj), 2.36 − 2.14 (stack, 1.6H, H-8 min)], [1.34 (s, 4H, Boc min), 1.22 (s, 5H, Boc maj)].

ᵃ Ratio based on H-13 peak integrations in the reported ¹H-NMR spectrum.

¹³C-NMR (101 MHz, CDCl₃) (mixture of rotamers) δ_C [155.4 (C, Boc C=O maj), 155.3 (C, Boc C=O min)], [148.8 (CH, C-15 maj), 148.6 (CH, C-15 min)], [146.4 (CH, C-11 maj), 146.0 (CH, C-11 min)], [140.8 (CH, C-10 min), 140.4 (CH, C-10 maj)], [139.4 (C, C-1 maj), 138.6 (C, C-1 min)], [137.0 (C, C-12 min), 136.7 (C, C-12 maj)], [132.73 (CH, C-13 min), 132.69 (CH, C-13 maj)], [123.8 (CH, C-14 min), 123.7 (CH, C-14 maj)], [118.6 (C, C-7 min), 117.4 (C, C-7 maj)], [79.9 (C, Boc C(CH₃) min), 79.7 (C, Boc C(CH₃) maj)], [67.1 (CH₂, C-9 maj), 66.9 (CH₂, C-9 min)], [62.8 (CH, C-3 min), 60.5 (CH, C-3 maj)], 50.1 (CH₂, C-8 min), 49.6 (CH₂, C-4 maj), 49.3 (CH₂, C-8 maj), 49.1 (CH₂, C-4 min), [48.6 (CH₂, C-5 min), 48.3 (CH₂, C-5 maj)], [28.5 (CH₃, Boc C(CH₃) min), 28.1 (CH₃, Boc C(CH₃) maj)], [24.91 (CH₂, C-2 min), 24.85 (CH₂, C-2 maj)], [24.0 (CH₂, C-6 min), 23.8 (CH₂, C-6 maj)].

ESI-LRMS (+): m/z 414.2 ([M+H]⁺, 100%).

HRMS: Found [M+H]⁺ 414.2493. C₂₂H₃₂N₅O₃ requires M+H, 414.2500.

tert-butyl 1-benzyl-8-morpholino-1,4,5,7,8,9-hexahydro-6*H*-pyrazolo[4,3-*d*]azocine-6-carboxylate (129)
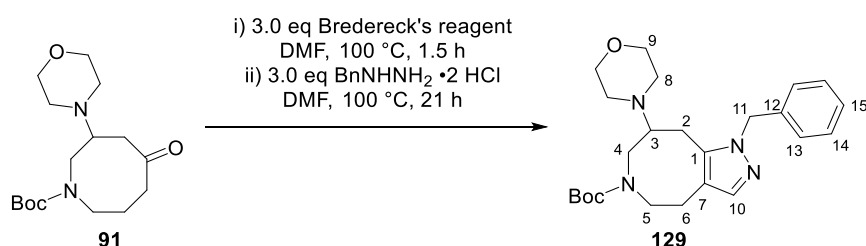
General procedure 6 (page 267) was followed, using ketone **91** (895 mg, 2.86 mmol) and BnNHNH₂ •2 HCl. After removal of volatiles under reduced pressure, NaHCO₃ solution (100 mL) was added and the resulting mixture was extracted with EtOAc (5 × 100 mL). The combined organic extracts were dried over anhydrous Na₂SO₄, filtered and concentrated under reduced pressure. The resulting crude mixture was purified using automatic column chromatography (CH₂Cl₂:7 M NH₃ in MeOH), yielding fused pyrazole **129** as a yellow oil (823 mg, 67%).

R*f* (CH₂Cl₂:7 M NH₃ in MeOH, 9:1): 0.7.

***v*max (neat / cm⁻¹):** 2930 w, 2855 w, 1685 s (C=O), 1409 s, 1163 s, 1111 v s.

¹H-NMR (400 MHz, CDCl₃) (mixture of rotamers, 5:4)[a] δ_H 7.35 − 7.15 (stack, 4H, H-10, H-14, H-15), 7.04 (dd, J = 6.9, 2.2 Hz, 2H, H-13), 5.47 − 5.30 (stack, 2H, [including 5.43 (A of AB, $J_{A–B}$ = 16.0 Hz, 0.4H, H-11 min), 5.35 (B of AB, $J_{B–A}$ = 16.0 Hz, 0.4H, H-11 min), 5.33 (app s, 1.2 H, H-11 maj)], H-11), 4.13 − 4.01 (m, 0.4H, H-4 min or H-5 min), 3.85 − 3.73 (m, 0.6H, H-4 maj or H-5 maj), 3.73 − 3.54 (stack, 5H, H-4 and/or H-5, H-9), 3.07– 2.74 (stack, 2.6H, H-3, H-4, H-5), 2.74 − 2.34 (stack, 8.4H, [including 2.60 − 2.34 (stack, 4H, H-8)], H-2, H-4 min or H-5 min, H-6, H-8), [1.36 (s, 4H, Boc min), 1.31 (s, 5H, Boc maj)].

¹³C-NMR (101 MHz, CDCl₃) (mixture of rotamers) δ_C [155.5 (C, Boc C=O min), 155.4 (Boc, C=O maj)], 138.5 (C, C-1 maj), [138.4 (CH, C-10 min), 138.05 (CH, C-10 maj)], 138.01 (C, C-1 min), [137.7 (C, C-12 min), 137.4 (C, C-12 maj)], 128.8 (CH, C-15), [127.7 (CH, C-14 maj), 127.6 (CH, C-14 min)], [126.8 (CH, C-13 maj), 126.7 (CH, C-13 min)], [117.6 (C, C-7 min), 116.4 (C, C-7 maj)], [79.8 (C, Boc C(CH₃)₃ min), 79.6 (C, Boc C(CH₃)₃ maj)], [67.4 (CH₂, C-9), [62.5 (CH, C-3 min), 60.5 (CH, C-3 maj)], [53.50 (CH₂, C-11 maj), 53.45 (CH₂, C-11 min)], [50.5 (CH₂, C-8 min), 49.7 (CH₂, C-8 maj)], [49.6, 49.5, 49.3, 48.9 (CH₂, C-4, C-5)], [28.5 (CH₃, Boc C(CH₃)₃ min), 28.3 (CH₃, Boc C(CH₃)₃ maj)], [25.6 (CH₂, C-2 min), 25.2 (CH₂, C-2 maj)], [24.5 (CH₂, C-6 min), 24.2 (CH₂, C-6 maj)].

ESI-LRMS (+): m/z 427.2 ([M+H]⁺, 100%).

HRMS: Found [M+H]⁺ 427.2697. C₂₄H₃₅N₄O₃ requires M+H, 427.2704.

tert-butyl 8-morpholino-1-propyl-1,4,5,7,8,9-hexahydro-6*H*-pyrazolo[4,3-*d*]azocine-6-carboxylate (130)
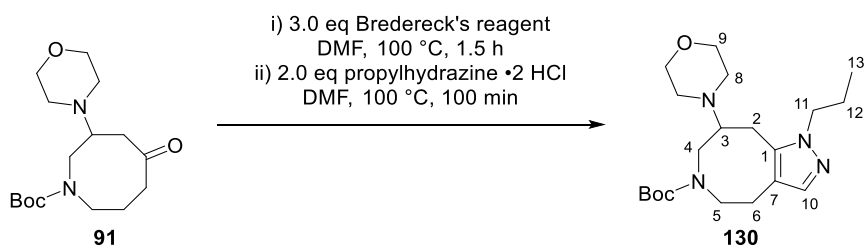
General procedure 6 (page 267) was followed, using ketone **91** (946 mg, 3.03 mmol) and propylhydrazine dihydrochloride (891 mg, 6.06 mmol). After removal of volatiles under reduced pressure, NaHCO₃ solution (30 mL) was added and the resulting mixture was extracted with EtOAc (3 × 30 mL). The combined organic extracts were dried over anhydrous Na₂SO₄,

---

[a] Ratio based on Boc peak integrations in the reported ¹H-NMR spectrum.

filtered and concentrated under reduced pressure. The resulting crude mixture was purified using automatic column chromatography (CH_2Cl_2:7 M NH_3 in MeOH), yielding fused pyrazole **130** as a yellow oil (897 mg, 78%).

v_{max} **(neat / cm^{-1}):** 2967 m, 2933 m, 2874 w, 1677 s (C=O), 1413 s, 1245 s, 1163 s, 1115 s.

^{1}H-NMR (400 MHz, CDCl$_3$) (mixture of rotamers, 5:4)[a] δ_H [7.01 (s, 0.4H, H-10 min), 6.99 (s, 0.6, H-10 maj)], 3.96 – 3.67 (stack, 2.6H, H-5 maj, H-11), 3.59 – 3.41 (stack, 5.4H, H-4, H-5 min, H-9), 3.10 – 2.94 (m, 0.6H, H-3 maj), 2.94 – 2.69 (stack, 1.6H, [including 2.79 – 2.69 (m, 0.6H, H-4 maj)], H-3 min, H-4 maj, H-5 maj), 2.69 – 2.26 (stack, 8.8H, [including 2.69 – 2.55 (stack, 2H, H-2 or H-6), 2.49 – 2.33 (stack, 4H, H-8)], H-2, H-4 min, H-5 min, H-6, H-8), 1.68 – 1.51 (stack, 2H, H-12), [1.19 (s, 4H, Boc min), 1.07 (s, 5H, Boc maj)], 0.69 (app t, J = 7.5 Hz, 3H, H-13).

^{13}C-NMR (101 MHz, CDCl$_3$) (mixture of rotamers) δ_C [154.94 (C, Boc *C*=O maj), 154.88 (C, Boc *C*=O min)], 137.5 (C, C-1 maj), [137.3 (CH, C-10 min), 137.04 (CH, C-10 maj)], 136.97 (C, C-1 min), [116.0 (C, C-7 min), 114.8 (C, C-7 maj)], [79.2 (C, Boc *C*(CH$_3$)$_3$ min), 78.9 (C, Boc *C*(CH$_3$)$_3$ maj)], [66.92 (CH$_2$, C-9 maj), 66.87 (CH$_2$, C-9 min)], [62.1 (CH, C-3 min), 60.1 (CH, C-3 maj)], [50.32 (CH$_2$, C-11 min), 50.29 (CH$_2$, C-11 maj)], [49.9, 49.2, 48.9, 48.7, 48.6, 48.1 (CH$_2$, C-4, C-5, C-8)], [28.0 (C, Boc C(*C*H$_3$)$_3$ min), 27.7 (C, Boc C(*C*H$_3$)$_3$ maj)], 25.0 (CH$_2$, C-2 min or C-6 min), 24.6 (CH$_2$, C-2 maj or C-6 maj), 23.9 (CH$_2$, C-2 min or C-6 min), 23.6 (CH$_2$, C-2 maj or C-6 maj), 23.5 (CH$_2$, C-12), 10.9 (CH$_3$, C-13).

ESI-LRMS (+): m/z 379.2 ([M+H]$^+$, 100%).

HRMS: Found [M+H]$^+$ 379.2698. $C_{20}H_{35}N_4O_3$ requires M+H, 379.2704.

---

[a] Ratio based on Boc peak integrations in the reported ^{1}H-NMR spectrum.

tert-butyl 8-morpholino-1,4,5,7,8,9-hexahydro-6*H*-pyrazolo[4,3-*d*]azocine-6-carboxylate (122)
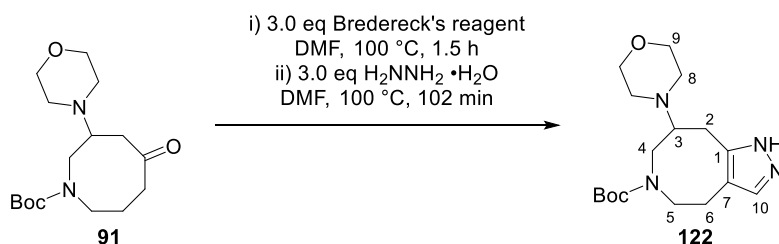
General procedure 6 (page 267) was followed, using ketone **91** (567 mg, 1.82 mmol) and H₂NNH₂•H₂O. After removal of volatiles under reduced pressure, the resulting crude mixture[a] was purified using automatic reverse phase column chromatography (basic), yielding fused pyrazole **122** as an off-white foam (440 mg, 72%).

R$_f$ (CH$_2$Cl$_2$:MeOH, 4:1): 0.1.

***v*$_{max}$ (neat / cm⁻¹):** 2928 m, 1670 s (C=O), 1413 s, 1364 s, 1249 s, 1156 s, 1111 s.

¹H-NMR (400 MHz, CDCl₃) (mixture of rotamers, 5:4)[b] δ_H [(7.19 (s, 0.4 H, H-10 min), 7.16 (s, 0.6 H, H-10 maj)], 4.09 − 3.96 (m, 0.6H, H-5 maj), 3.83 − 3.62 (stack, 1.4H, H-4, H-5 min), 3.62 − 3.42 (stack, 4H, H-9), [3.20 − 3.08 (m, 0.4H, H-3 min), 3.08 − 2.89 (m, 0.6H, H-3 maj)], 2.89 − 2.39 (stack, 10H, [including 2.89 − 2.70 (stack, 2H, H-2), 2.70 − 2.39 (stack, 4H, H-8), 2.64 − 2.39 (stack, 2H, H-6)], H-2, H-4, H-5, H-6, H-8), [1.30 (s, 5H, Boc maj), 1.25 (s, 4H, Boc min)], NH not observed.

¹³C-NMR (101 MHz, CDCl₃) (mixture of rotamers) δ_C [155.4 (C, Boc *C*=O maj), 155.2 (C, Boc *C*=O min)], [144.6 (C, C-1 maj), 143.1 (C, C-1 min)], [133.3 (CH, C-10 min), 131.3 (CH, C-10 maj)], [116.1 (C, C-7 maj), 115.6 (C, C-7 min)], [79.6 (C, Boc *C*(CH₃)₃ maj), 79.3 (C, Boc *C*(CH₃)₃ min)], 67.1 (CH₂, C-9), [62.4 (CH, C-3 maj), 61.0 (CH, C-3 min)], 50.2 (CH₂, C-4 min), 50.1 (CH₂, C-8), 49.8 (CH₂, C-5 maj), 49.7 (CH₂, C-4 maj), 49.4 (CH₂, C-5 min), [28.3 (CH₃, Boc C(*C*H₃)₃ maj), 28.1 (CH₃, Boc C(*C*H₃)₃ min)], [25.8 (CH₂, C-2 maj), 25.2 (CH₂, C-2 min)], [24.0 (CH₂, C-6 min), 23.7 (CH₂, C-6 maj)].

ESI-LRMS (+): m/z 337.2 ([M+H]⁺, 100%).

HRMS: Found [M+H]⁺ 337.2230. C₁₇H₂₉N₄O₃ requires M+H, 337.2234.

---

[a] No aqueous workup was performed, the crude mixture was loaded straight onto the reverse phase column.
[b] Ratio based on Boc peak integrations in the reported ¹H-NMR spectrum.

tert-butyl 1-methyl-8-morpholino-1,4,5,7,8,9-hexahydro-6*H*-pyrazolo[4,3-*d*]azocine-6-carboxylate (131)

tert-butyl 2-methyl-8-morpholino-2,4,5,7,8,9-hexahydro-6*H*-pyrazolo[4,3-*d*]azocine-6-carboxylate (132)
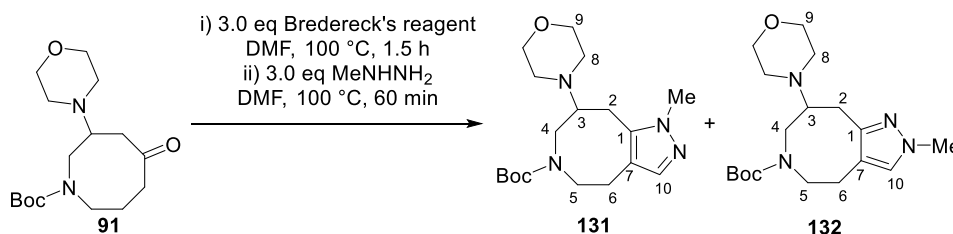
General procedure 6 (page 267) was followed, using ketone **91** (1.40 g, 4.49 mmol) and MeNHNH$_2$. After removal of volatiles under reduced pressure, NaHCO$_3$ solution (10 mL) was added and the resulting mixture was extracted with CH$_2$Cl$_2$ (5 × 15 mL). The combined organic extracts were dried over anhydrous Na$_2$SO$_4$, filtered and concentrated under reduced pressure. The resulting crude mixture was purified using automatic column chromatography (CH$_2$Cl$_2$:7 M NH$_3$ in MeOH), yielding the fused pyrazoles **131** and **132** as a mixture of regioisomers, which were separated *via* SFC (BEH column, CO$_2$:20 mM NH$_3$ in MeOH) to yield, in order of elution, regioisomer **131** as a yellow oil (809 mg, 51%) and then regioisomer **132** as a colourless oil (478 mg, 30%).

(131)

R$_f$ (CH$_2$Cl$_2$:7 M NH$_3$ in MeOH, 9:1): 0.8.

v_{max} (neat / cm^{-1}): 2930 m, 1677 s (C=O), 1409 s, 1249 s, 1159 v s, 1115 v s.

^{1}H-NMR (400 MHz, CDCl$_3$) (mixture of rotamers, 5:4)[a] δ_H [6.99 (s, 0.4 H, H-10 min), 6.96 (s, 0.6 H, H-10 maj)], 3.99 – 3.82 (m, 0.4H, H-5 min), 3.72 – 3.29 (stack, 8.4H, [including [3.63 (s, 1.3H, Me min), 3.58 (s, 1.7H, Me maj)], 3.51 – 3.29 (stack, 4H, H-9)], H-4, H-5, H-9, Me), 3.20 – 3.01 (m, 0.6H, H-3 maj), 2.99 – 2.67 (stack, 2H, H-3 min, H-4, H-5), 2.67 – 2.20 (stack, 8.6H, H-2, H-4 maj or H-5 maj, H-6, H-8), [1.22 (s, 4H, Boc min), 1.11 (s, 5H, Boc maj)].

^{13}C-NMR (101 MHz, CDCl$_3$) (mixture of rotamers) δ_C [155.0 (C, Boc *C*=O maj), 154.8 (C, Boc *C*=O min)], [137.6 (C, C-1 maj), 137.2 (C, C-1 min)], [137.1 (CH, C-10 min), 137.0 (CH, C-10 maj)],

---

[a] Ratio based on Boc peak integrations in the reported ^{1}H-NMR spectrum.

[116.8 (C, C-7 min), 115.5 (C, C-7 maj)], [79.2 (C, Boc C(CH$_3$)$_3$ min), 79.0 (C, Boc C(CH$_3$)$_3$ maj)], [66.9 (CH$_2$, C-9 maj), 66.8 (CH$_2$, C-9 min)], [62.1 (CH, C-3 min), 60.3 (CH, C-3 maj)], 50.3 (CH$_2$, C-8 min), 49.8 (CH$_2$, C-5 min), 49.5 (CH$_2$, C-8 maj), 49.3 (CH$_2$, C-5 maj), [48.6 (CH$_2$, C-4 maj), 48.3 (CH$_2$, C-4 min)], [36.3 (CH$_3$, Me min), 36.1 (CH$_3$, Me maj)], [28.0 (CH$_3$, Boc C(CH$_3$)$_3$ min), 27.7 (CH$_3$, Boc C(CH$_3$)$_3$ maj)], [24.8, 24.5, 24.3, 24.1 (CH$_2$, C-2, C-6)].

ESI-LRMS (+): m/z 351.2 ([M+H]$^+$, 100%), 295.2 (1, [M–C$_4$H$_8$ + H]$^+$).

HRMS: Found [M+H]$^+$ 351.2385. C$_{18}$H$_{31}$N$_4$O$_3$ requires M+H, 351.2391.

SFC t_R (BEH column, CO$_2$:20 mM NH$_3$ in MeOH): 1.76 min

(132)

R$_f$ (CH$_2$Cl$_2$:7 M NH$_3$ in MeOH, 9:1): 0.8.

v_{max} (neat / cm^{-1}): 2930 m, 1685 s (C=O), 1409 s, 1245 s, 1156 v s, 1111 v s.

^{1}H-NMR (400 MHz, CDCl$_3$) (mixture of rotamers, 2:1)[a] δ_H 6.88 (app s, 1H, H-10), 3.95 – 3.82 (m, 0.67H, H-5 min), 3.74 – 3.39 (stack, 8.33H, [including 3.58 (s, 1H, Me min), 3.56 (s, 2H Me maj), 3.54 – 3.39 (stack, 4H, H-9)], H-4 and/or H-5, H-9, Me), [3.05 – 2.92 (m, 0.33H, H-3 min), 2.92 – 2.78 (m, 0.67H, H-3 maj)], 2.78 – 2.29 (stack, 10H, H-2, H-4 and/or H-5, H-6, H-8), [1.20 (s, 6H, Boc maj), 1.16 (s, 3H Boc min)].

^{13}C-NMR (101 MHz, CDCl$_3$) (mixture of rotamers) δ_C [155.2 (C, Boc C=O maj), 154.8 (C, Boc C=O min)], [148.7 (C, C-1 min), 148.5 (C, C-1 maj)], [128.6 (CH, C-10 maj), 128.4 (CH, C-10 min)], [116.6 (C, C-7 min), 116.5 (C, C-7 maj)], [79.2 (C, Boc C(CH$_3$)$_3$ maj), 78.8 (C, Boc C(CH$_3$)$_3$ min)], 67.0 (CH$_2$, C-9), [62.4 (CH, C-3 maj), 61.0 (CH, C-3 min)], [50.3, 49.9, 49.8 (CH$_2$, C-4, C-5, C-8)], 48.8 (CH$_2$, C-5), 38.1 (CH$_3$, Me), [28.04 (CH$_3$, Boc C(CH$_3$)$_3$ maj), 28.00 (CH$_3$, Boc C(CH$_3$)$_3$ min)], [26.3 (CH$_2$, C-2 maj), 25.9 (CH$_2$, C-2 min)], [23.5 (CH$_2$, C-6 min), 23.0 (CH$_2$, C-6 maj)].

ESI-LRMS (+): m/z 351.2 ([M+H]$^+$, 100%), 295.2 (1, [M–C$_4$H$_8$ + H]$^+$).

HRMS: Found [M+H]$^+$ 351.2385. C$_{18}$H$_{31}$N$_4$O$_3$ requires M+H, 351.2391.

SFC t_R (BEH column, CO$_2$:20 mM NH$_3$ in MeOH): 1.89 min

---

[a] Ratio based on Boc peak integrations in the reported ^{1}H-NMR spectrum.

tert-butyl 1-cyclopropyl-8-morpholino-1,4,5,7,8,9-hexahydro-6*H*-pyrazolo[4,3-*d*]azocine-6-carboxylate (133)
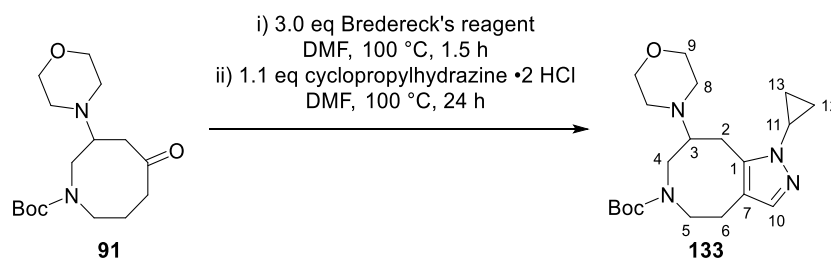
General procedure 6 (page 267) was followed, using ketone **91** (60 mg, 0.19 mmol) and cyclopropylhydrazine •2 HCl. After removal of the volatiles under reduced pressure, NaHCO₃ solution (10 mL) was added and the resulting mixture was extracted with EtOAc (5 × 10 mL). The combined organic extracts were dried over anhydrous Na₂SO₄, filtered and concentrated under reduced pressure. The resulting crude mixture was purified using automatic column chromatography (CH₂Cl₂:7 M NH₃ in MeOH), yielding fused pyrazole **133** as an orange oil (26 mg, 36%).

R*f* (CH₂Cl₂:7 M NH₃ in MeOH, 9:1): 0.9.

νmax (neat / cm⁻¹): 2956 m, 2922 s, 2855 m, 1677 s (C=O), 1413 s, 1364 s, 1245 s, 1159 s, 1111 s.

¹H-NMR (400 MHz, CDCl₃) (mixture of rotamers, 2:1)ᵃ δ_H [7.16 (s, 0.33H, H-10 min), 7.13 (s, 0.67H, H-10 maj)], 4.01 (ddd, *J* = 13.7, 7.0, 4.7 Hz, 0.33H, H-5 min), 3.76 − 3.57 (stack, 5.67H, H-4, H-5 maj, H-9), 3.57 − 3.45 (m, 0.33H, H-11 min), 3.45 − 3.25 (stack, 1.33H, H-3 maj, H-11 maj), 3.16 − 2.43 (stack, 10.33H, H-2, H-3 min, H-4, H-5, H-6, H-8), 1.39 (s, 3H, Boc min), 1.38 − 1.17 (stack, 7H, [including 1.23 (s, 6H, Boc maj)], H-12 and/or H-13, Boc maj), 1.07 − 0.91 (stack, 3H, H-12, H-13).

¹³C-NMR (101 MHz, CDCl₃) (mixture of rotamers) δ_C [155.6 (C, Boc *C*=O maj), 155.5 (C, Boc *C*=O min)], [140.1 (C, C-1 maj), 139.4 (C, C-1 min)], [137.5 (CH, C-10 min), 137.4 (CH, C-10 maj)], [117.0 (C, C-7 min), 115.7 (C, C-7 maj)], [79.8 (C, Boc *C*(CH₃)₃ min), 79.5 (C, Boc *C*(CH₃)₃ maj)], [67.5 (CH₂, C-9 maj), 67.4 (CH₂, C-9 min)], [62.6 (CH, C-3 min), 60.3 (CH, C-3 maj)], 50.5 (CH₂, C-8), [49.7, 49.6, 49.4, 49.3, 48.7 (CH₂, C-4, C-5, C-8)], [30.4 (CH, C-11 min), 30.2 (CH, C-11 maj)], [28.6 (CH₃, Boc C(*CH₃*)₃ min), 28.1 (CH₃, Boc C(*CH₃*)₃ maj)], 24.6 (CH₂, C-2 min or C-6 min), 24.4 (CH₂, C-2 maj or C-6 maj), 24.2 (CH₂, C-2 min or C-6 min), 24.0 (CH₂, C-2 maj or C-6 maj), 7.5

ᵃ Ratio based on H-10 peak integrations in the reported ¹H-NMR spectrum.

(CH$_2$, C-12 min or C-13 min), [7.3, 6.1 (CH$_2$, C-12 maj, C-13 maj)], 6.0 (CH$_2$, C-12 min or C-13 min).

ESI-LRMS (+): m/z 377.2 ([M+H]$^+$, 100%).

HRMS: Found [M+H]$^+$ 377.2537. C$_{20}$H$_{33}$N$_4$O$_3$ requires M+H, 377.2547.

4-(1-cyclopropyl-4,5,6,7,8,9-hexahydro-1*H*-pyrazolo[4,3-*d*]azocin-8-yl)morpholine bis(2,2,2-trifluoroacetate) (133a •2 TFA)
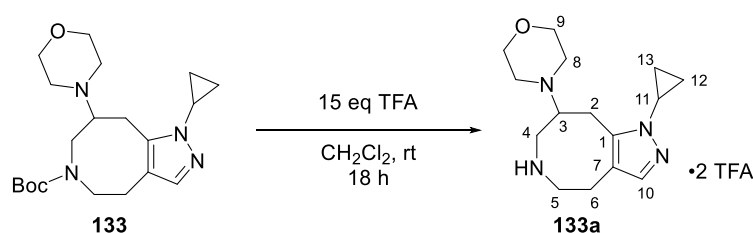
TFA (71 μL, 0.92 mmol) was added to a solution of Boc-amine **133** (23 mg, 0.061 mmol) in CH$_2$Cl$_2$ (122 μL). The resulting mixture was stirred for 18 h at rt, after which time, the volatiles were removed under reduced pressure, yielding amine **133a •2 TFA** as an amber glass (31 mg, quant.).

***ν*$_{max}$ (neat / cm^{-1}):** 1666 s (C=O), 1454 w, 1416 m, 1178 s, 1122 s.

^{1}H-NMR (400 MHz, CDCl$_3$) δ_H 7.37 (s, 1H, H-10), 4.04 − 3.94 (stack, 4H, H-9), 3.84 (dd, *J* = 14.9, 2.7 Hz, 1H, H-2), 3.81 − 3.73 (m, 1H, H-3), 3.73 − 3.69 (stack, 2H, H-4), 3.54 − 3.16 (stack, 8H, H-2, H-5, H-8, H-11), 3.07 − 2.96 (stack, 2H, H-6), 1.18 − 1.10 (stack, 4H, H-12, H-13).

^{13}C-NMR (101 MHz, CDCl$_3$) δ_C 138.9 (CH, C-10), 138.2 (C, C-1), 116.0 (C, C-7), 65.6 (CH$_2$, C-9), 62.0 (CH, C-3), 50.8 (CH$_2$, C-8), 49.3 (CH$_2$, C-4), 45.9 (CH$_2$, C-5), 31.1 (CH, C-11), 24.2 (CH$_2$, C-2), 19.8 (CH$_2$, C-6), [7.3, 7.2 (CH$_2$, C-12, C-13)].

ESI-LRMS (+): m/z 277.1 ([M+H]$^+$, 100%).

HRMS: Found [M+H]$^+$ 277.2017. C$_{15}$H$_{25}$N$_4$O requires M+H, 277.2023.

tert-butyl 1-((2,4-dimethylthiazol-5-yl)methyl)-8-morpholino-1,4,5,7,8,9-hexahydro-6*H*-pyrazolo[4,3-*d*]azocine-6-carboxylate (134)

tert-butyl 2-((2,4-dimethylthiazol-5-yl)methyl)-8-morpholino-2,4,5,7,8,9-hexahydro-6*H*-pyrazolo[4,3-*d*]azocine-6-carboxylate (135)
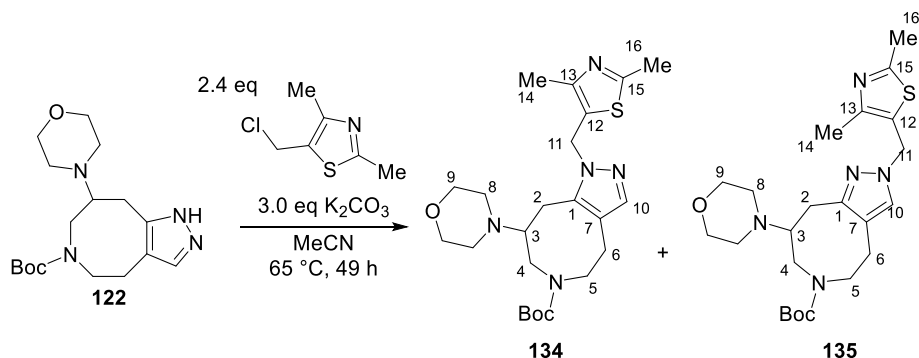
5-(Chloromethyl)-2,4-dimethyl-1,3-thiazole (397 mg, 2.45 mmol) was added to a suspension of fused pyrazole **122** (688 mg, 2.05 mmol) and K_2CO_3 (424 mg, 3.07 mmol) in MeCN (6.8 mL). After stirring for 24 h at 65 °C, another portion of 5-(chloromethyl)-2,4-dimethyl-1,3-thiazole (397 mg, 2.45 mmol) and K_2CO_3 (424 mg, 3.07 mmol) were added. After stirring at 65 °C for a further 25 h, the reaction mixture was poured into $NaHCO_3$ solution (20 mL) and extracted with EtOAc (3 × 20 mL). The organic extracts were dried over anhydrous Na_2SO_4, filtered and concentrated under reduced pressure. The resulting crude mixture was purified *via* automatic flash column chromatography (CH_2Cl_2:7 M NH_3 in MeOH), yielding a mixture of regioisomers (A:B = 1:2)[a] which were separated *via* SFC (BEH column, CO_2:20 mM NH_3 in MeOH), yielding, in order of elution, regioisomer **134** as a yellow oil (132 mg, 14%), and then regioisomer **135** as an amber oil (307 mg, 62wt%[b], 20%).

(134)

R*f* (CH_2Cl_2:7 M NH_3 in MeOH, 9:1): 0.5.

ν*max* (neat / cm⁻¹): 2926 m, 2855 m, 1677 s (C=O), 1409 s, 1364 s, 1245 s, 1159 s, 1115 s.

---

[a] Ratio based on H-10 peak integrations in the crude ¹H-NMR spectrum.
[b] Weight purity determined *via* Q-NMR spectroscopic analysis, using 1,3,5-trimethoxybenzene as an internal standard (single measurement).

¹H-NMR (400 MHz, CDCl₃) (mixture of rotamers, 5:4)[a] δ_H [7.23 (s, 0.4H, H-10 min), 7.20 (s, 0.6H, H-10 maj)], 5.49 − 5.04 (stack, 2H, H-11), 4.08 − 3.96 (m, 0.4H, H-5 min), 3.76 − 3.50 (stack, 5.4H, H-4, H-5, H-9), 3.12 − 2.35 (stack, 17.2H, [including 3.12 − 2.79 (stack, 1H, H-3), 2.81 − 2.69 (stack, 2H, H-2), 2.50 (s, 3H, H-16), 2.39 (s, 3H, H-14)], H-2, H-3, H-4, H-5, H-6, H-8, H-14, H-16), [1.32 (s, 4H, Boc min), 1.23 (s, 5H, Boc maj)].

¹³C-NMR (101 MHz, CDCl₃) (mixture of rotamers) δ_C [164.5 (C, C-15 maj), 164.3 (C, C-15 min)], [155.4 (C, Boc *C*=O maj), 155.3 (C, Boc *C*=O min)], [148.5 (C, C-13 maj), 148.4 (C, C-13 min)], [138.6 (C, C-10 min), 138.3 (C, C-10 maj)], [137.8 (C, C-1 maj), 137.4 (C, C-1 min)], [126.8 (C, C-12 min), 126.6 (C, C-12 maj)], [117.5 (C, C-7 min), 116.4 (C, C-7 maj)], [79.8 (C, Boc *C*(CH₃)₃ min), 79.5 (C, Boc *C*(CH₃)₃ maj)], 67.4 (CH₂, C-9), [62.4 (CH, C-3 min), 60.6 (CH, C-3 maj)], [50.4 (CH₂, C-8 min), 49.7 (CH₂, C-8 maj)], [49.4 (CH₂, C-5 min), 49.2 (CH₂, C-5 maj)], [48.3 (CH₂, C-4 maj), 48.0 (CH₂, C-4 min)], [45.5 (CH₂, C-11 min), 45.4 (CH₂, C-11 maj)], [28.4 (CH₃, Boc C(*C*H₃)₃ min), 28.2 (CH₃, Boc C(*C*H₃)₃ maj)], [26.4 (CH₂, C-2 min), 26.0 (CH₂, C-2 maj)], [24.3 (CH₂, C-6 min), 24.1 (CH₂, C-6 maj)], 19.1 (CH₃, C-16), 15.2 (CH₃, C-14).

ESI-LRMS (+): m/z 462.3 ([M+H]⁺, 100%), 406.2 (5, [M–C₄H₈ + H]⁺).

HRMS: Found [M+H]⁺ 462.2528. C₂₃H₃₆N₅O₃S requires M+H, 462.2533.

SFC *t*R (BEH column, CO₂:20 mM NH₃ in MeOH): 3.81 min

(135)

R*f* (CH₂Cl₂:7 M NH₃ in MeOH, 9:1): 0.5.

***v*max (neat / cm⁻¹):** 2967 m, 2926 m, 2855 w, 1685 s (C=O), 1413 s, 1364 s, 1249 s, 1159 v s, 1115 s.

¹H-NMR (400 MHz, CDCl₃) (mixture of rotamers, 3:2)[b] δ_H [6.92 (s, 0.6H, H-10 maj), 6.91 (s, 0.4H, H-10 min)], 5.12 − 5.01 (stack, 2H, H-11), 3.99 − 3.83 (m, 0.6H, H-5 maj), 3.77 − 3.40 (stack, 5.4H, [including 3.59 − 3.40 (stack, 4H, H-9)], H-4, H-5 min, H-9), [3.13 − 2.98 (m, 0.4H, H-3 min), 2.98 − 2.83 (m, 0.6H, H-3 maj)], 2.83 − 2.30 (stack, 13H, [including 2.83 − 2.59 (stack, 2H, H-2), 2.48 − 2.30 (stack, 2H, H-6), 2.42 (s, 3H, H-16)], H-2, H-4, H-5, H-6, H-8, H-16), [2.23 (s, 1.2H, H-14 min), 2.21 (s, 1.8H, H-14 maj)], [1.23 (s, 5.4H, Boc maj), 1.18 (s, 3.6H, Boc min)].

---

[a] Ratio based on Boc peak integrations in the reported ¹H-NMR spectrum.
[b] Ratio based on Boc peak integrations in the reported ¹H-NMR spectrum.

¹³C-NMR (101 MHz, CDCl₃) (mixture of rotamers) δ_C [164.3 (C, C-15 min), 164.2 (C, C-15 maj)], [155.2 (C, Boc *C*=O maj), 154.9 (C, Boc *C*=O min)], [149.5, 149.4, 149.1 (C, C-1, C-13, resonance overlap)], [127.2 (CH, C-10 maj), 126.9 (CH, C-10 min)], [125.4 (C, C-12 maj), 125.3 (C, C-12 min)], 117.5 (C, C-7), [79.3, (C, Boc *C*(CH₃)₃ maj), 79.0 (C, Boc *C*(CH₃)₃ min)], [67.1 (CH₂, C-9 maj), 67.0 (CH₂, C-9 min)], [62.3 (CH, C-3 maj), 61.1 (CH, C-3 min)], 50.0 (CH₂, C-4 or C-5 or C-8), 49.92 (CH₂, C-8), 49.87 (CH₂, C-4 or C-5 or C-8), 49.6 (CH₂, C-4), 49.0 (CH₂, C-5), [46.61 (CH₂, C-11 maj), 46.56 (CH₂, C-11 min)], [28.14 (CH₃, Boc C(*C*H₃)₃ maj), 28.07 (CH₃, Boc C(*C*H₃)₃ min)], [26.6, (CH₂, C-2 maj), 26.1 (CH₂, C-2 min)], [23.8 (CH₂, C-6 min), 23.4 (CH₂, C-6 maj)], 18.8 (CH₃, C-16), 14.7 (CH₃, C-14).

ESI-LRMS (+): m/z 462.2 ([M+H]⁺, 100%).

HRMS: Found [M+H]⁺ 462.2527. $C_{23}H_{36}N_5O_3S$ requires M+H, 462.2533.

SFC *t*ᵣ (BEH column, CO_2:20 mM NH_3 in MeOH): 4.24 min

tert-butyl 8-morpholino-4,7,8,9-tetrahydroisoxazolo[4,5-*d*]azocine-6(5*H*)-carboxylate (137)
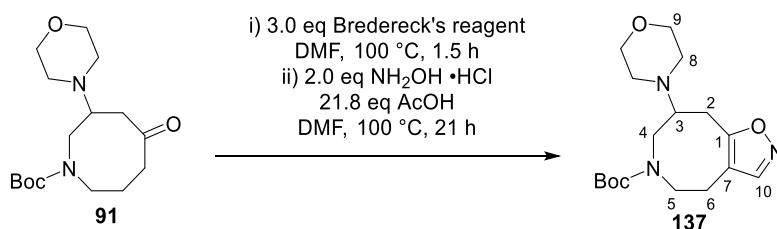
General procedure 6 (page 267) was followed, using ketone **91** (848 mg, 2.71 mmol), NH_2OH •HCl and AcOH (3.4 mL, 59 mmol). After removal of the volatiles under reduced pressure, $NaHCO_3$ solution (50 mL) was added and the resulting mixture was extracted with EtOAc (5 × 50 mL). The combined organic extracts were dried over anhydrous Na_2SO_4, filtered and concentrated under reduced pressure. The resulting crude mixture was purified using basic automatic reverse phase column chromatography, yielding fused isoxazole **137** as a brown oil (635 mg, 69%).

R*f* (CH$_2$Cl$_2$:7 M NH$_3$ in MeOH, 9:1): 0.8.

*v*max (neat / cm⁻¹): 2960 m, 2922 m, 2855 m, 1685 s (C=O), 1413 s, 1364 s, 1249 s, 1159 s, 1115 v s.

¹H-NMR (400 MHz, CDCl₃) (mixture of rotamers, 1:1)ᵃ δ_H [7.98 (s, 0.5H, H-10), 7.96 (s, 0.5H, H-10)], 4.04 (app dd, *J* = 13.7, 4.7 Hz, 0.5H, H-5), 3.80 – 3.55 (stack, 5.5H, H-4, H-5, H-9), [3.37 – 3.24 (m, 0.5H, H-3), 3.21 – 3.09 (m, 0.5H, H-3)], 3.09 – 2.41 (stack, 10H, [including 3.09 – 2.77 (stack, 2H, H-2), 2.77 – 2.57 (stack, 2H, H-6), 2.77 – 2.41 (stack, 4H, H-8)], H-2, H-4, H-5, H-6, H-8), [1.39 (s, 4.5H, Boc), 1.34 (s, 4.5H, Boc)].

¹³C-NMR (101 MHz, CDCl₃) (mixture of rotamers) δ_C [167.4, 166.9 (C, C-1)], [155.5, 155.4 (C, Boc *C*=O)], [151.6, 151.5 (CH, C-10)], [113.1, 112.3 (C, C-7)], [80.3, 80.2 (C, Boc *C*(CH₃)₃)], [67.31, 67.28 (CH₂, C-9)], [62.7, 61.3 (CH, C-3)], [50.33, 50.26 (CH₂, C-4)], [50.1, 49.9 (CH₂, C-8)], [49.5, 49.4 (CH₂, C-5)], [28.5, 28.4 (CH₃, Boc C(*C*H₃)₃], [25.0, 24.7 (CH₂, C-2)], [23.2, 22.9 (CH₂, C-6)].

ESI-LRMS (+): m/z 338.2 ([M+H]⁺, 100%), 282.1 (3, [M–C₄H₈ + H]⁺).

HRMS: Found [M+H]⁺ 338.2068. C₁₇H₂₈N₃O₄ requires M+H, 338.2074.

ᵃ Ratio based on H-3 peak integrations in the reported ¹H-NMR spectrum.

tert-butyl 2-methyl-9-morpholino-5,8,9,10-tetrahydropyrimido[5,4-*d*]azocine-7(6*H*)-carboxylate (150)
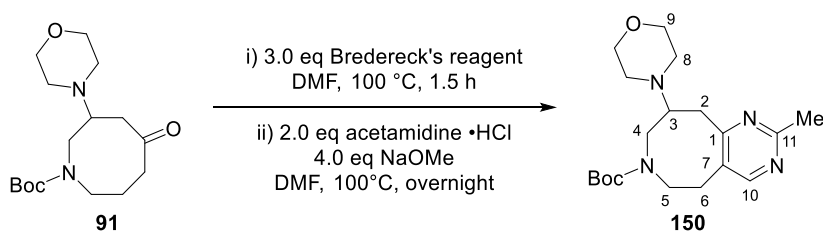
General procedure 6 (page 267) was followed, using ketone **91** (54 mg, 0.17 mmol), acetamidine •HCl and NaOMe (37 mg, 0.69 mmol). After removal of volatiles under reduced pressure, NaHCO$_3$ solution (10 mL) was added and the resulting mixture was extracted with CH$_2$Cl$_2$ (5 × 15 mL). The combined organic extracts were dried over anhydrous Na$_2$SO$_4$, filtered and concentrated under reduced pressure. The resulting crude mixture was purified using automatic column chromatography (CH$_2$Cl$_2$:7 M NH$_3$ in MeOH), yielding fused pyrimidine **150** as a yellow oil (13 mg, 21%).

R$_f$ (CH$_2$Cl$_2$:7 M NH$_3$ in MeOH, 9:1): 0.8.

v_{max} (neat / cm^{-1}): 2967 m, 1685 v s (C=O), 1439 s, 1163 v s, 1115 v s.

^{1}H-NMR (400 MHz, CDCl$_3$) (mixture of rotamers, 11:10)[a] δ_H [8.33 (s, 0.5H, H-10 maj), 8.29 (s, 0.5 H, H-10 min)], 4.15 – 4.03 (m, 0.5H, H-5 maj), 4.03 – 3.95 (m, 0.5H, H-4 min), 3.95 – 3.81 (stack, 1H, H-4 maj, H-5 min), 3.77 – 3.63 (stack, 4H, H-9), [3.30 (app tt, *J* = 11.0, 3.1 Hz, 0.5H, H-3 min), 3.18 (app tt, *J* = 10.6, 3.5 Hz, 0.5H, H-3 maj)], 3.12 – 3.02 (m, 0.5H, H-5 min), 3.02 – 2.85 (stack, 2.5H, H-2, H-5 maj), 2.85 – 2.55 (stack, 10H, [including 2.63 (s, 1.5H, Me min), 2.61 (s, 1.5H, Me maj)], H-4, H-6, H-8, Me), [1.23 (s, 4.7H, Boc maj), 1.14 (s, 4.3H, Boc min)].

^{13}C-NMR (101 MHz, CDCl$_3$) (mixture of rotamers) δ_C [168.3 (C, C-1 min), 167.5 (C, C-1 maj)], [166.4 (C, C-11 min), 166.2 (C, C-11 maj)], [157.0 (CH, C-10 maj), 156.5 (CH, C-10 min)], [154.9 (C, Boc *C*=O maj), 154.4 (C, Boc *C*=O min)], [126.8 (C, C-7 maj), 126.7 (C, C-7 min)], [80.1 (C, Boc *C*(CH$_3$)$_3$ maj), 79.9 (C, Boc *C*(CH$_3$)$_3$ min)], [67.6 (CH$_2$, C-9 min), 67.5 (CH$_2$, C-9 maj)], [63.1 (CH, C-3 maj), 61.4 (CH, C-3 min)], [51.2 (CH$_2$, C-4 min), 50.5 (CH$_2$, C-4 maj)], [49.8 (CH$_2$, C-8 maj), 49.5 (CH$_2$, C-8 min)], [48.0 (CH$_2$, C-5 min), 47.1 (CH$_2$, C-5 maj)], [37.1 (CH$_2$, C-2 min), 37.0 (CH$_2$, C-2 maj)], [28.8 (CH$_2$, C-6 maj), 28.7 (CH$_2$, C-6 min)], [28.2 (CH$_3$, Boc C(*C*H$_3$)$_3$ maj), 28.0 (CH$_3$, Boc C(*C*H$_3$)$_3$ min)], 25.7 (CH$_3$, Me).

---

[a] Ratio based on Boc peak integrations in the reported ^{1}H-NMR spectrum.

ESI-LRMS (+): m/z 363.3 ([M+H]$^+$, 100%), 307.2 (10, [M–C$_4$H$_8$ + H]$^+$).

HRMS: Found [M+H]$^+$ 363.2383. C$_{19}$H$_{31}$N$_4$O$_3$ requires M+H, 363.2391.

tert-butyl 9-morpholino-2-phenyl-5,8,9,10-tetrahydropyrimido[5,4-*d*]azocine-7(6*H*)-carboxylate (153)
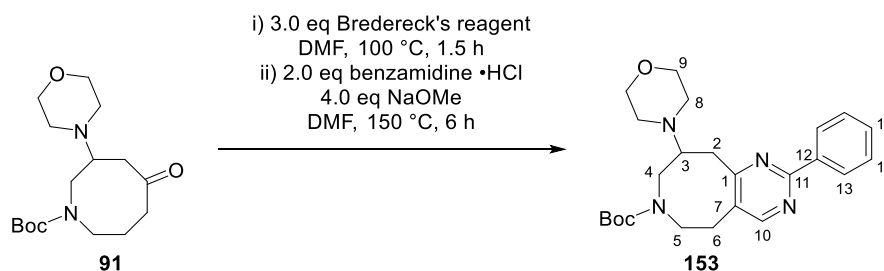
General procedure 6 (page 267) was followed, using ketone **91** (169 mg, 0.541 mmol), benzamidine •HCl (169 mg, 1.08 mmol) and NaOMe (169 mg, 1.08 mmol), whilst performing the second step at 150 °C. After removal of volatiles under reduced pressure, NaHCO$_3$ solution (10 mL) was added and the resulting mixture was extracted with EtOAc (3 × 15 mL). The combined organic extracts were dried over anhydrous Na$_2$SO$_4$, filtered and concentrated under reduced pressure. The resulting crude mixture was purified using automatic column chromatography (CH$_2$Cl$_2$:7 M NH$_3$ in MeOH), yielding fused pyrimidine **153** as an orange oil (111 mg, 48%).

R$_f$ (CH$_2$Cl$_2$:7 M NH$_3$ in MeOH, 9:1): 0.8.

v_{max} (neat / cm^{-1}): 2956 w, 2855 w, 1685 s (C=O), 1543 m, 1420 s, 1163 s, 1115 s.

^{1}H-NMR (400 MHz, CDCl$_3$) (mixture of rotamers, 5:4)[a] δ_H [8.48 (s, 0.6H, H-10 maj), 8.44 (s, 0.4H, H-10 min)], 8.42 − 8.32 (stack, 2H, H-13 or H-14), 7.48 − 7.38 (stack, 3H, H-13 or H-14, H-15), 4.24 − 4.08 (m, 0.4H, H-5 min), 4.07 − 3.83 (stack, 1.6H, H-4, H-5 maj), 3.77 − 3.67 (stack, 4H, H-9), [3.34 (app tt, *J* = 10.7, 3.2 Hz, 0.4H, H-3 min), 3.21 (app tt, *J* = 10.8, 3.3 Hz, 0.6H, H-3 maj)], 3.13 − 2.59 (stack, 10H, [including 3.13 − 2.91 (stack, 2H, H-2), 2.88 − 2.77 (stack, 2H, H-6), 2.88 − 2.59 (stack, 4H, H-8)], H-2, H-4, H-5, H-6, H-8), [1.18 (s, 5H, Boc maj), 1.11 (s, 4H, Boc min)].


[a] Ratio based on Boc peak integrations in the reported ^{1}H-NMR spectrum.

13C-NMR (101 MHz, CDCl₃) (mixture of rotamers) δ_C [168.3 (C, C-1 min), 167.5 (C, C-1 maj)], [163.2 (C, C-11 min), 162.9 (C, C-11 maj)], [157.4 (CH, C-10 maj), 156.8 (CH, C-10 min)], [155.0 (C, Boc *C*=O maj), 154.5 (C, Boc *C*=O min)], [138.0 (C, C-12 maj), 137.9 (C, C-12 min)], [130.3 (CH, Ph min), 130.2 (CH, Ph maj)], [128.5 (CH, Ph min), 128.4 (CH, Ph, maj)], [128.1 (CH, Ph min), 128.02 (CH, Ph maj)], 127.98 (C, C-7), [80.1 (C, Boc *C*(CH₃)₃ maj), 80.0 (C, Boc *C*(CH₃)₃ min)], [67.5 (CH₂, C-9 min), 67.4 (CH₂, C-9 maj)], [63.5 (CH, C-3 maj), 61.7 (CH, C-3 min)], [51.3 (CH₂, C-4 min), 50.7 (CH₂, C-4 maj)], [50.0 (CH₂, C-8 min), 49.6 (CH₂, C-8 maj)], [48.2 (CH₂, C-5 maj), 47.5 (CH₂, C-5 min)], [36.7 (CH₂, C-2 maj), 36.5 (CH₂, C-2 min)], 29.2 (CH₂, C-6), [28.2 (CH₃, Boc C(*CH₃*)₃ maj), 28.0 (CH₃, Boc C(*CH₃*)₃ min)].

ESI-LRMS (+): m/z 425.4 ([M+H]⁺, 100%), 369.3 (1, [M–C₄H₈ + H]⁺).

HRMS: Found [M+H]⁺ 425.2538. C₂₄H₃₃N₄O₃ requires M+H, 425.2547.

tert-butyl 2-amino-9-morpholino-5,8,9,10-tetrahydropyrimido[5,4-*d*]azocine-7(6*H*)-carboxylate (154)
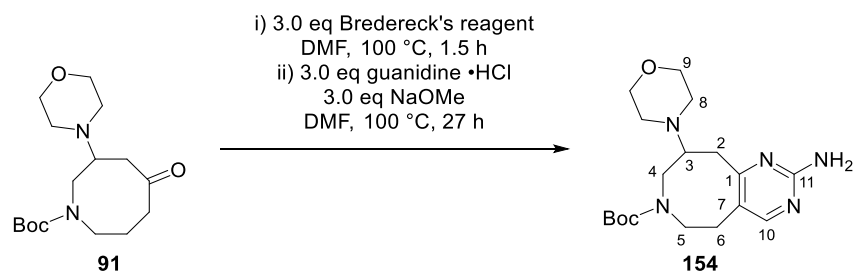
General procedure 6 (page 267) was followed, using ketone **91** (843 mg, 2.70 mmol), guanidine •HCl and NaOMe (437 mg, 8.10 mmol). After removal of volatiles under reduced pressure, the resulting crude mixture was purified using automatic reverse phase column chromatography (basic), yielding fused aminopyrimidine **154** as an off-white solid (550 mg, 56%).

Melting point: 188 − 190 °C dec.

R*f* (CH$_2$Cl$_2$:7 M NH$_3$ in MeOH, 9:1): 0.7.

***v*$_{max}$ (neat / cm^{-1}):** 3329 w (N–H), 2933 w, 2855 w, 1685 m (C=O), 1461 s, 1413 s, 1249 m, 1159 v s, 1111 v s.

^{1}H-NMR (400 MHz, CDCl$_3$) (mixture of rotamers, 1:1)[a] δ_H [8.01 (s, 0.5H, H-10)), 7.97 (s, 0.5H, H-10)], 4.99 (s, 2H, N*H$_2$*), 4.11 − 3.78 (stack, 2H, H-4, H-5), 3.78 − 3.65 (stack, 4H, H-9), [3.36 − 3.26 (m, 0.5H, H-3), 3.20 − 3.11 (m, 0.5H, H-3)], 3.05 − 2.97 (m, 0.5H, H-5), 2.97 − 2.59 (stack, 9.5H, H-2, H-4, H-5, H-6, H-8), [1.29 (s, 4.5H, Boc), 1.21 (s, 4.5H, Boc)].

^{13}C-NMR (101 MHz, CDCl$_3$) (mixture of rotamers) δ_C [168.9, 168.4 (C, C-1)], [162.2, 162.0 (C, C-11)], [158.3, 157.8 (CH, C-10)], [155.1, 154.7 (C, Boc *C*=O)], [119.9, 119.8 (C, C-7)], 80.0 (C, Boc *C*(CH$_3$)$_3$), [67.3, 67.1 (CH$_2$, C-9)], [63.1, 61.6 (CH, C-3)], [50.7, 50.4 (CH$_2$, C-4)], [49.8, 49.6 (CH$_2$, C-8)], [48.4, 47.5 (CH$_2$, C-5)], [36.8, 36.5 (CH$_2$, C-2)], 28.4 (CH$_2$, C-6), [28.3, 28.1 (CH$_3$, Boc C(*CH$_3$*)$_3$)]

ESI-LRMS (+): m/z 364.1 ([M+H]$^+$, 100%).

HRMS: Found [M+H]$^+$ 364.2338. C$_{18}$H$_{30}$N$_5$O$_3$ requires M+H, 364.2343.

---

[a] Ratio based on H-3 peak integrations in the reported ^{1}H-NMR spectrum.

tert-butyl 9-morpholino-2-(phenylamino)-5,8,9,10-tetrahydropyrimido[5,4-*d*]azocine-7(6*H*)-carboxylate (158)
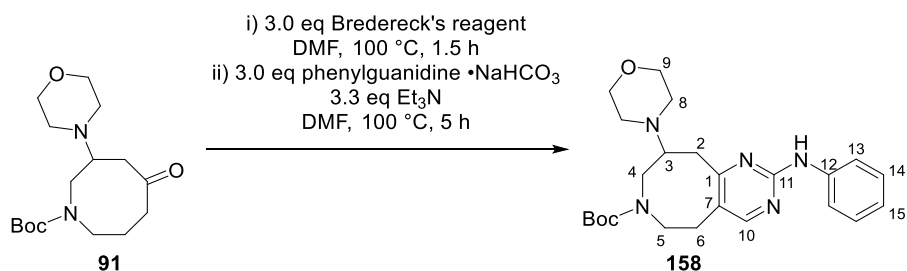
General procedure 6 (page 267) was followed, using ketone **91** (64 mg, 0.21 mmol), phenylguanidine •NaHCO$_3$ and Et$_3$N (94 µL, 0.68 mmol). After removal of volatiles under reduced pressure, NaHCO$_3$ solution (15 mL) was added and the resulting mixture was extracted with EtOAc (3 × 15 mL). The combined organic extracts were dried over anhydrous Na$_2$SO$_4$, filtered and concentrated under reduced pressure. The resulting crude mixture was purified using automatic column chromatography (CH$_2$Cl$_2$:7 M NH$_3$ in MeOH), yielding fused aminopyrimidine **158** as an orange oil (45 mg, 50%).

R$_f$ (CH$_2$Cl$_2$:7 M NH$_3$ in MeOH, 9:1): 0.9.

ν_{max} (neat / cm^{-1}): 3351 m (N–H), 2963 m, 2930 m, 2829 m, 1670 s (C=O), 1588 s, 1528 s, 1435 v s, 1364 s, 1159 s, 1111 s.

^{1}H-NMR (400 MHz, CDCl$_3$) (mixture of rotamers, 5:4)[a] δ_H [8.13 (s, 0.6H, H-10 maj), 8.09 (s, 0.4H, H-10 min)], 7.64 − 7.56 (stack, 2H, H-13), 7.34 − 7.25 (stack, 2H, H-14), 7.14 (app br s, 1H, N*H*), 7.03 − 6.95 (stack, 1H, H-15), 4.18 − 4.04 (m, 0.6H, H-5 maj), 4.01 (dd, *J* = 13.5, 3.5 Hz, 0.4H, H-4 min), 3.95 − 3.80 (stack, 1H, [including 3.90 (dd, *J* = 13.8, 3.8 Hz, 0.6H, H-4 maj)], H-4 maj, H-5 min), 3.79 − 3.60 (stack, 4H, H-9), [3.29 (app tt, *J* = 10.6, 3.5 Hz, 0.4H, H-3 min), 3.24 − 3.09 (m, 0.6H, H-3 maj)], 3.07 − 2.96 (m, 0.6H, H-5 maj), 2.95 − 2.53 (stack, 9.4H [including 2.95 − 2.82 (stack, 2H, H-2), 2.82 − 2.53 (stack, 4H, H-8)], H-2, H-4, H-5 min, H-6, H-8), [1.26 (s, 5H, Boc maj), 1.20 (s, 4H, Boc min)].

---

[a] Ratio based on Boc peak integrations in the reported ^{1}H-NMR spectrum.

13C-NMR (101 MHz, CDCl₃) (mixture of rotamers) δ_C [169.1, 168.3 (C, C-11)], [159.2, 159.1 (C, C-1)], [158.0, 157.3 (CH, C-10)], [155.1, 154.7 (C, Boc *C*=O)], [140.0, 139.9 (C, C-12)], [128.9, 128.9 (CH, C-14)], [122.2, 122.1 (CH, C-15)], 121.0 (C, C-7), [119.0, 118.9 (CH, C-13)], [80.0, 79.9 (C, Boc *C*(CH₃)₃)], [67.5, 67.4 (CH₂, C-9)], [63.4, 61.6 (CH, C-3)], [51.3, 50.8 (CH₂, C-4)], [49.9, 49.5 (CH₂, C-8)], [48.4, 47.7 (CH₂, C-5)], [36.6, 36.5 (CH₂, C-2)], [29.8, 28.6 (CH₂, C-6)], [28.3, 28.1 (CH₃, Boc C(*C*H₃)₃)].

ESI-LRMS (+): m/z 440.2 ([M+H]⁺, 100%).

HRMS: Found [M+H]⁺ 440.2647. $C_{24}H_{34}N_5O_3$ requires M+H, 440.2656.

4-(1-(4-fluorophenyl)-4,5,6,7,8,9-hexahydro-1*H*-pyrazolo[4,3-*d*]azocin-8-yl)morpholine *bis*(2,2,2-trifluoroacetate) (159 •2 TFA)
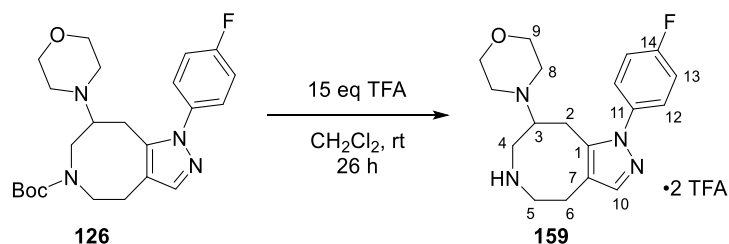
TFA (1.7 mL, 22 mmol) was added to a solution of Boc-amine **126** (620 mg, 1.44 mmol). The resulting mixture was stirred for 26 h at rt, after which time, the volatiles were removed under reduced pressure, yielding deprotected amine **159 •2 TFA** as an off-white solid (804 mg, quant.), which was used as a library precursor without further purification.

v_{max} (neat / cm⁻¹): 1774 w, 1666 br s (C=O), 1513 s, 1423 w, 1129 v s

¹H-NMR (400 MHz, CD₃OD) δ_H 7.62 (s, 1H, H-10), 7.54 − 7.47 (AA' of AA'BB', 2H, H-12 or H-13), 7.37 − 7.27 (BB' of AA'BB', 2H, H-12 or H-13), 3.82 − 3.74 (stack, 4H, H-9), 3.73 − 3.54 (stack, 2H, H-4), 3.48 − 3.36 (stack, 2H, H-3, H-5), 3.28 − 3.14 (stack, 3H, H-2, H-5), 3.14 − 3.05 (stack, 2H, H-6), 3.01 − 2.83 (stack, 4H, H-8), exchangeable protons not observed.

13C-NMR (101 MHz, CD₃OD) δ_C 164.2 (C, d, J_{C-F} = 248.2 Hz, C-14), 161.7 (C, q, J_{C-F} = 35.8 Hz, TFA *C*OOH), 141.0 (CH, C-10), 137.7 (C, C-7), 136.2 (C, d, J_{C-F} = 3.1 Hz, C-11), 129.6 (CH, d, J_{C-F} = 8.9 Hz, C-12), 117.6 (CH, d, J_{C-F} = 23.0 Hz, C-13), 117.3 (C, q, J_{C-F} = 289.2 Hz, TFA *C*F₃), 116.7 (C, C-1), 65.8 (CH₂, C-9), 62.2 (CH, C-3), 50.6 (CH₂, C-8), 45.8 (CH₂, C-4), 24.8 (CH₂, C-2), 19.9 (CH₂, C-6). C-5 peak not observed, but HSQC/HMBC experiments show a potential overlap with the CD₃OD signal.

ESI-LRMS (+): m/z 331.2 ([M+H]$^+$, 100%).

HRMS: Found [M+H]$^+$ 331.1923. $C_{18}H_{24}FN_4O$ requires M+H, 331.1929.

4-(1-benzyl-4,5,6,7,8,9-hexahydro-1*H*-pyrazolo[4,3-*d*]azocin-8-yl)morpholine (161)
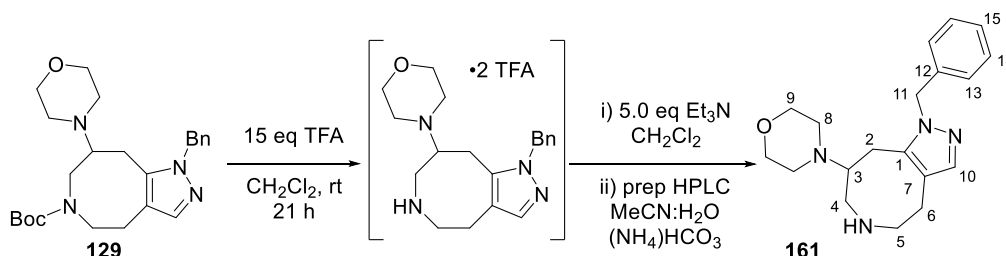
TFA (1.7 mL, 22 mmol) was added to a solution of Boc-amine **129** (632 mg, 1.48 mmol) in CH_2Cl_2 (3 mL). The resulting mixture was stirred at rt for 21 h, after which time, the volatiles were removed under reduced pressure, yielding the crude amine **161 •2 TFA** as an amber oil (990 mg, quant.), which was used as a library precursor without further purification.

An aliquot (0.098 mmol) was dissolved in a solution of Et$_3$N (0.07 mL, 0.5 mmol) and CH_2Cl_2 (0.4 mL). The resulting mixture was stirred overnight in a capped 8 mL vial and then left to evaporate to dryness at rt under atmospheric pressure over 1 h. The resulting mixture was purified *via* preparative basic HPLC, yielding 2° amine **161** as a white powder (16.6 mg, 52%).

***v*$_{max}$ (neat / cm^{-1}):** 3354 br w (N–H), 2915 m, 1810 m, 1454 s, 1405 m, 1111 v s.

^{1}H-NMR (400 MHz, CDCl$_3$) δ_H 7.33 – 7.22 (stack, 4H), 7.12 – 7.07 (m, 2H), 5.39 – 5.24 (m, 2H, H-11), 3.70 – 3.60 (stack, 4H, H-9), 3.11 – 2.88 (stack, 3H), 2.78 (dd, *J* = 14.0, 4.2 Hz, 1H), 2.65 – 2.51 (stack, 3H), 2.51 – 2.41 (stack, 4H, H-8), 2.34 (dd, *J* = 14.7, 3.9 Hz, 1H), 2.03 (dq, *J* = 11.0, 4.1 Hz, 1H), exchangeable protons not observed.

^{13}C-NMR (101 MHz, CDCl$_3$) δ_C 138.8, 138.2, 137.8, 128.9, 127.8, 126.8, 118.8 (C-7), 67.3 (C-9), 65.3 (C-3), [53.6, 51.6, 50.5, 48.9 (C-4, C-5, C-8, C-11)], 27.6 (C-2), 23.7 (C-6).

ESI-LRMS (+): m/z 327.2 ([M+H]$^+$, 100%).

HRMS: Found [M+H]$^+$ 327.2175. $C_{19}H_{27}N_4O$ requires M+H, 327.2179.

4-(1-(pyridin-3-yl)-4,5,6,7,8,9-hexahydro-1*H*-pyrazolo[4,3-*d*]azocin-8-yl)morpholine (160)
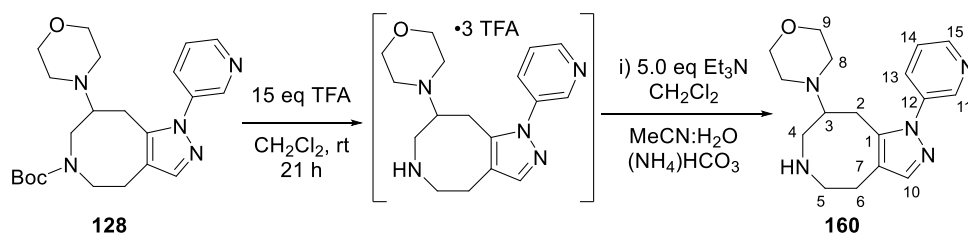
TFA (2.5 mL, 33 mmol) was added to a solution of Boc-amine **128** (671 mg, 1.62 mmol) in CH$_2$Cl$_2$ (3.2 mL). The resulting mixture was stirred at rt for 5 h, after which time, the volatiles were removed under reduced pressure, yielding the crude amine **160** •**3 TFA** as a viscous black oil (1.06 g, quant.), which was used as a library precursor without further purification.

An aliquot (0.110 mmol) was dissolved in a solution of Et$_3$N (0.08 mL, 0.6 mmol) and CH$_2$Cl$_2$ (0.4 mL). The resulting mixture was stirred overnight in a capped 8 mL vial and then left to evaporate to dryness under ambient conditions over 1 h. The resulting mixture was purified *via* preparative basic HPLC, yielding 2° amine **160** as a white powder (18.9 mg, 55%).

v$_{max}$ **(neat / cm^{-1})**: 3347 br w (N–H), 2915 m, 2851 m, 2810 m, 1428 s, 1111 v s.

^{1}H-NMR (400 MHz, CDCl$_3$) δ_H 8.74 (d, *J* = 2.5 Hz, 1H, H-11), 8.64 (dd, *J* = 4.9, 1.5 Hz, 1H, H-15), 7.81 (ddd, *J* = 8.2, 2.5, 1.5 Hz, 1H, H-13), 7.47 (s, 1H, H-10), 7.44 (dd, *J* = 8.2, 4.9 Hz, 1H, H-14), 3.63 − 3.55 (stack, 4H, H-9), 3.15 − 3.03 (stack, 3H), 2.89 (app dd, *J* = 14.3, 3.9 Hz, 1H), 2.76 − 2.55 (stack, 4H), 2.54 − 2.42 (stack, 5H), NH not observed.

^{13}C-NMR (101 MHz, CDCl$_3$) δ_C 149.0 (C-15), 146.2 (C-11), 140.9 (C-10), 139.9 (C-1), 136.9 (C-12), 132.8 (C-13), 123.9 (C-14), 120.0 (C-7), 67.2 (C-9), 66.4 (C-3), 51.0, 50.5, 49.2, 27.1 (C-2), 24.2 (C-6).

ESI-LRMS (+): m/z 314.2 ([M+H]$^+$, 100%).

HRMS: Found [M+H]$^+$ 314.1973. C$_{17}$H$_{24}$N$_5$O requires M+H, 314.1975.

4-(1-propyl-4,5,6,7,8,9-hexahydro-1*H*-pyrazolo[4,3-*d*]azocin-8-yl)morpholine (164)
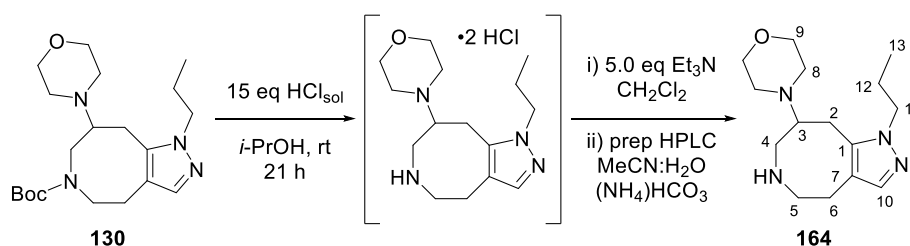
Boc-amine **130** (779 mg, 2.06 mmol) was dissolved in HCl solution (4 M in *i*-PrOH, 7.7 mL, 31 mmol). After stirring at rt for 21 h, the volatiles were removed under reduced pressure, yielding the crude amine **164 •2 HCl** as an off-white solid (723 mg, quant.), which was used as a library precursor without further purification.

An aliquot (0.155 mmol) was dissolved in a solution of Et$_3$N (0.11 mL, 0.79 mmol) and CH$_2$Cl$_2$ (0.4 mL). The resulting mixture was stirred overnight in a capped 8 mL vial and then left to evaporate to dryness under ambient conditions over 1 h. The resulting mixture was purified *via* preparative basic HPLC, yielding amine **164** as a colourless glass (23.7 mg, 55%).

v$_{max}$ (neat / cm^{-1}): 3347 w (N–H), 2922 m, 1454 m, 1409 m, 1286 m, 1115 s.

^{1}H-NMR (400 MHz, CDCl$_3$) δ_H 7.20 (s, 1H, H-10), 4.06 – 3.89 (m, 2H, H-11), 3.80 – 3.62 (stack, 4H, H-9), 3.11 (dd, *J* = 14.7, 4.2 Hz, 1H, H-4), 3.08 – 2.97 (stack, 2H, H-2, H-5), 2.83 (dd, *J* = 14.1, 4.1 Hz, 1H, H-2), 2.70 – 2.43 (stack, 8H, [including 2.52 – 2.43 (m, 1H, H-3)], H-3, H-5, H-6, H-8), 2.39 (dd, *J* = 14.7, 3.9 Hz, 1H, H-4), 1.83 (tq, *J* = 7.3, 7.3 Hz, 2H, H-12), 1.73 (br s, 1H, N*H*), 0.91 (t, *J* = 7.3 Hz, 3H, H-13).

^{13}C-NMR (101 MHz, CDCl$_3$) δ_C 138.3 (C, C-1), 137.8 (CH, C-10), 117.8 (C, C-7), 67.4 (CH$_2$, C-9), 65.9 (CH, C-3), 51.8 (CH$_2$, C-5), 50.7 (CH$_2$, C-11), 50.6 (CH$_2$, C-8), 48.8 (CH$_2$, C-4), 27.6 (CH$_2$, C-6), 24.1 (CH$_2$, C-12), 23.6 (CH$_2$, C-2), 11.4 (CH$_3$, C-13).

ESI-LRMS (+): m/z 279.3 ([M+H]$^+$, 100%).

HRMS: Found [M+H]$^+$ 279.2186. C$_{15}$H$_{27}$N$_4$O requires M+H, 279.2179.

4-(1-methyl-4,5,6,7,8,9-hexahydro-1*H*-pyrazolo[4,3-*d*]azocin-8-yl)morpholine (165)
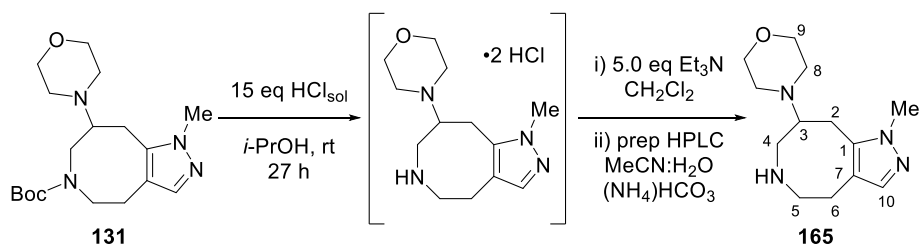
Boc-amine **131** (685 mg, 1.96 mmol) was dissolved in HCl solution (4 M in *i*-PrOH, 7.3 mL, 29 mmol). After stirring at rt for 27 h, the volatiles were removed under reduced pressure, yielding the crude amine **165 •2 HCl** as a beige solid (632 mg, quant.), which was used as a library precursor without further purification.

An aliquot (0.130 mmol) was dissolved in a solution of Et$_3$N (0.10 mL, 0.72 mmol) and CH$_2$Cl$_2$ (0.4 mL). The resulting mixture was stirred overnight in a capped 8 mL vial and then left to evaporate to dryness under ambient conditions over 1 h. The resulting mixture was purified *via* preparative basic HPLC, yielding 2° amine **165** as a white solid (24.9 mg, 77%).

v$_{max}$ **(neat / cm^{-1})**: 3336 w (N–H), 2911 m, 2848 m, 2807 m, 1450 m, 1111 s.

^{1}H-NMR (400 MHz, CDCl$_3$) δ_H 7.17 (s, 1H, H-10), 3.79 (s, 3H, Me), 3.75 − 3.66 (stack, 4H, H-9), 3.13 − 2.98 (stack, 3H), 2.83 (dd, *J* = 13.9, 4.0 Hz, 1H), 2.67 − 2.61 (stack, 4H, H-8), 2.61 − 2.46 (stack, 4H), 2.42 (dd, *J* = 14.7, 4.0 Hz, 1H), NH not observed.

^{13}C-NMR (101 MHz, CDCl$_3$) δ_C 138.7 (C-10), 137.6 (C-1), 118.1 (C-7), 67.4 (C-9), 65.5 (C-3), [51.8, 50.6, 48.9 (C-4, C-5, C-8)], 36.5 (Me), 27.6 (C-2), 23.8 (C-6).

ESI-LRMS (+): m/z 251.1 ([M+H]$^+$, 100%).

HRMS: Found [M+H]$^+$ 251.1863. C$_{13}$H$_{23}$N$_4$O requires M+H, 251.1866.

4-(2-methyl-4,5,6,7,8,9-hexahydro-2*H*-pyrazolo[4,3-d]azocin-8-yl)morpholine (166)
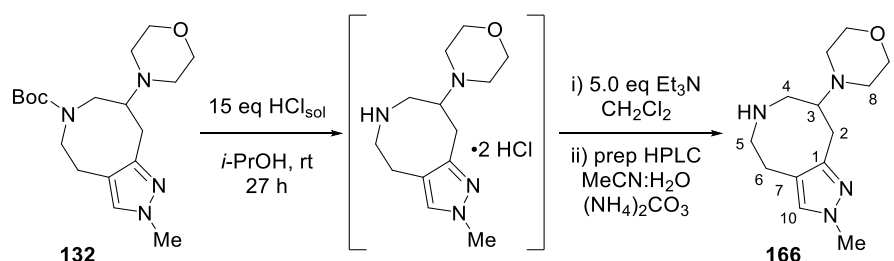
Boc-amine **132** (423 mg, 1.21 mmol) was dissolved in HCl solution (4 M in *i*-PrOH, 4.5 mL, 8 mmol). After stirring at rt for 25 h, the volatiles were removed under reduced pressure, yielding the crude amine **166 •2 HCl** as a beige solid (390 mg, quant.), which was used as a library precursor without further purification.

An aliquot (0.103 mmol) was dissolved in a solution of Et$_3$N (0.06 mL, 0.5 mmol) and CH$_2$Cl$_2$ (0.4 mL). The resulting mixture was stirred overnight in a capped 8 mL vial and then left to evaporate to dryness under ambient conditions over 1 h. The resulting mixture was purified *via* preparative basic HPLC, yielding 2° amine **166** as a colourless glass (16.9 mg, 66%).

v$_{max}$ **(neat / cm^{-1}):** 3332 w (N–H), 2915 m, 2851 m, 2807 m, 1446 m, 1111 s.

^{1}H-NMR (400 MHz, CDCl$_3$) δ_H 7.02 (s, 1H, H-10), 3.79 (s, 3H, Me), 3.74 − 3.64 (stack, 4H, H-9), 3.17 (dd, *J* = 14.5, 4.5 Hz, 1H), 2.99 − 2.89 (stack, 2H), 2.88 − 2.82 (m, 1H), 2.76 − 2.39 (stack, 9H), NH not observed.

^{13}C-NMR (101 MHz, CDCl$_3$) δ_C 150.1 (C-1), 128.7 (C-10), 118.0 (C-7), 67.4 (C-9), 66.1 (C-3), [50.9, 50.7, 48.5 (C-4, C-5, C-8)], 38.6 (Me), 27.0 (C-2), 25.5 (C-6).

ESI-LRMS (+): m/z 251.1 ([M+H]$^+$, 100%).

HRMS: Found [M+H]$^+$ 251.1863. C$_{13}$H$_{23}$N$_4$O requires M+H, 251.1866.

4-(4,5,6,7,8,9-hexahydro-1*H*-pyrazolo[4,3-*d*]azocin-8-yl)morpholine (162)
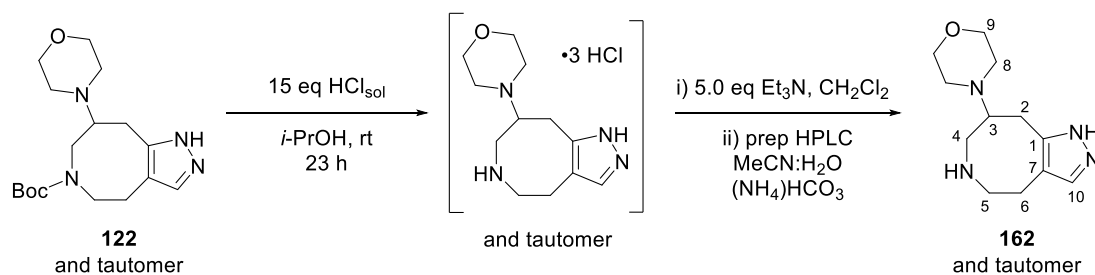
Boc-amine **122** (385 mg, 1.14 mmol) was dissolved in HCl solution (4 M in *i*-PrOH, 4.3 mL, 17 mmol). After stirring at rt for 23 h, the volatiles were removed under reduced pressure, yielding crude amine **162 •3 HCl** as a beige solid (396 mg, quant.), which was used as library precursor without further purification.

An aliquot (0.097 mmol) was dissolved in a solution of Et$_3$N (0.07 mL, 0.5 mmol) and CH$_2$Cl$_2$ (0.4 mL). The resulting mixture was stirred overnight in a capped 8 mL vial and then left to evaporate to dryness under ambient conditions over 1 h. The resulting mixture was purified *via* preparative basic HPLC, yielding 2° amine **162** as an off-white powder (15.7 mg, 68%).

v$_{max}$ (neat / cm^{-1}): 3153 br w (N–H), 2915 m, 2855 m, 2810 m, 1450 m, 1111 s.

^{1}H-NMR (400 MHz, CDCl$_3$) δ_H 7.27 (s, 1H, H-10), 3.75 − 3.61 (stack, 4H, H-9), 3.15 (dd, *J* = 14.5, 4.7 Hz, 1H, H-4), 3.04 (A of ABX, $J_{A–B}$ = 13.9, $J_{A–X}$ = 8.8 Hz, 1H, H-2), 2.96 (ddd, *J* = 13.2, 6.3, 4.2 Hz, 1H, H-5), 2.89 (B of ABX, $J_{B–A}$ = 13.9, $J_{B–X}$ = 4.0 Hz, 1H, H-2), 2.77 − 2.42 (stack, 9H, [including 2.64 − 2.42 (m, 1H, H-3)], H-3, H-4, H-5, H-6, H-8), exchangeable protons not observed.

^{13}C-NMR (101 MHz, CDCl$_3$) δ_C 117.2 (C, C-7), 67.4 (CH$_2$, C-9), 65.9 (CH, C-3), [50.8, 50.7 (CH$_2$, C-5, C-8)], 48.3 (CH$_2$, C-4), 26.5 (CH$_2$, C-2), 25.6 (CH$_2$, C-6). C-1 and C-10 resonances not observed, but an HMBC experiment shows the expected cross peaks at δ_C 146.5 ppm (C-1) and δ_C 130.9 ppm (C-10).

ESI-LRMS (+): m/z 237.3 ([M+H]$^+$, 100%).

HRMS: Found [M+H]$^+$ 237.1707. C$_{12}$H$_{21}$N$_4$O requires M+H, 237.1710.

8-morpholino-4,5,6,7,8,9-hexahydroisoxazolo[4,5-*d*]azocine (163)
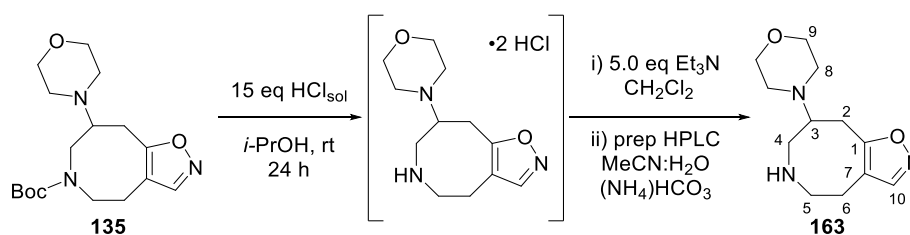
Boc-amine **135** (520 mg, 1.54 mmol) was dissolved in HCl solution (4 M in *i*-PrOH, 5.8 mL, 23 mmol). After stirring at rt for 24 h, the volatiles were removed under reduced pressure, yielding crude amine **163 •2 HCl** as a beige foam, which was used as a library precursor without further purification (478 mg, quant.).

An aliquot (0.105 mmol) was dissolved in a solution of Et$_3$N (0.07 mL, 0.5 mmol) and CH$_2$Cl$_2$ (0.4 mL). The resulting mixture was stirred overnight in a capped 8 mL vial and then left to evaporate to dryness under ambient conditions over 1 h. The resulting mixture was purified *via* preparative basic HPLC, yielding 2° amine **163** as a white powder (14.8 mg, 59%).

v$_{max}$ **(neat / cm⁻¹):** 3358 w (N–H), 2915 m, 2851 m, 2810 m, 1469 s, 1111 v s.

¹H-NMR (400 MHz, CDCl₃) δ_H 7.99 (s, 1H, H-10), 3.75 – 3.61 (stack, 4H, H-9), 3.27 – 3.16 (m, 1H), 3.11 (dd, *J* = 14.6, 5.4 Hz, 1H), 3.01 – 2.86 (stack, 2H), 2.86 – 2.77 (m, 1H), 2.77 – 2.69 (m, 1H), 2.69 – 2.36 (stack, 7H), NH not observed.

¹³C-NMR (101 MHz, CDCl₃) δ_C 168.5 (C, C-1), 151.2 (CH, C-10), 112.8 (C, C-7), 67.3 (CH$_2$, C-9), 65.0 (CH, C-3), 50.4 (CH$_2$, C-8), [49.6, 49.0 (CH$_2$, C-4, C-5)], 25.7 (CH$_2$, C-2), 24.5 (CH$_2$, C-6).

ESI-LRMS (+): m/z 238.1 ([M+H]⁺, 100%).

HRMS: Found [M+H]⁺ 238.1546. C$_{12}$H$_{20}$N$_3$O$_2$ requires M+H, 238.1550.

4-(1-((2,4-dimethylthiazol-5-yl)methyl)-4,5,6,7,8,9-hexahydro-1*H*-pyrazolo[4,3-*d*]azocin-8-yl)morpholine (167)
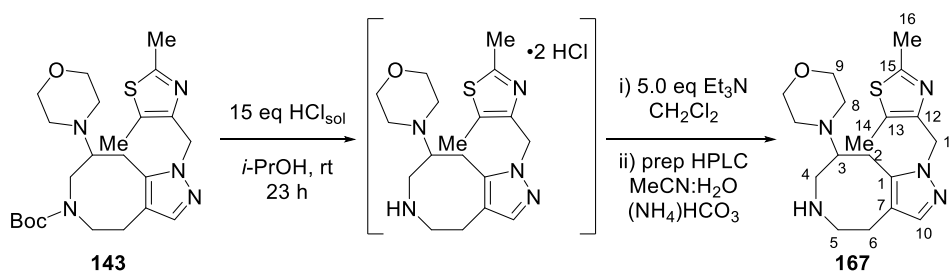
Boc-amine **143** (130 mg, 0.282 mmol) was dissolved in HCl solution (4 M in *i*-PrOH, 1.1 mL, 4.2 mmol). After stirring at rt for 23 h, the volatiles were removed under reduced pressure, yielding crude amine **167 •2 HCl** as a yellow solid (122 mg, quant.), which was used as a library precursor without further purification.

An aliquot (0.059 mmol) was dissolved in a solution of Et$_3$N (0.04 mL, 0.3 mmol) and CH$_2$Cl$_2$ (0.4 mL). The resulting mixture was stirred overnight in a capped 8 mL vial and then left to evaporate to dryness under ambient conditions over 1 h. The resulting mixture was purified *via* preparative basic HPLC, yielding 2° amine **167** as a yellow glass (12.4 mg, 58%).

***v*$_{max}$ (neat / cm^{-1}):** 3340 br w (N–H), 2919 m, 2810 m, 1450 m, 1305 m, 1111 v s.

^{1}H-NMR (400 MHz, CDCl$_3$) δ_H 7.25 (s, 1H, H-10), 5.36 (A of AB, $J_{A–B}$ = 15.9 Hz, 1H, H-11), 5.28 (B of AB, $J_{B–A}$ = 15.9 Hz, 1H, H-11), 3.75 − 3.64 (stack, 4H, H-9), 3.10 − 2.99 (stack, 3H, H-2, H-4, H-5), 2.82 (dd, *J* = 14.1, 4.1 Hz, 1H, H-2), 2.67 − 2.46 (stack, 10H, [including 2.58 (s, 3H, H-16)], H-5, H-6, H-8, H-16), 2.43 (s, 3H, H-14), 2.41 − 2.31 (m, 1H, H-4), 2.29 − 2.21 (m, 1H, H-3).

^{13}C-NMR (101 MHz, CDCl$_3$) δ_C 164.8 (C, C-15), 148.6 (C, C-13), 138.7 (CH, C-10), 138.4 (C, C-1), 127.1 (C, C-12), 118.9 (C, C-7), 67.5 (CH$_2$, C-9), 65.7 (CH, C-3), 51.7 (CH$_2$, C-5), 50.7 (CH$_2$, C-8), 48.7 (CH$_2$, C-4), 45.6 (CH$_2$, C-11), 27.7 (CH$_2$, C-2), 24.2 (CH$_2$, C-6), 19.3 (CH$_3$, C-16), 15.3 (CH$_3$, C-14).

ESI-LRMS (+): m/z 362.1 ([M+H]$^+$, 100%).

HRMS: Found [M+H]$^+$ 362.2018. C$_{18}$H$_{28}$N$_5$OS requires M+H, 362.2009.

4-(2-((2,4-dimethylthiazol-5-yl)methyl)-4,5,6,7,8,9-hexahydro-2*H*-pyrazolo[4,3-*d*]azocin-8-yl)morpholine (168)
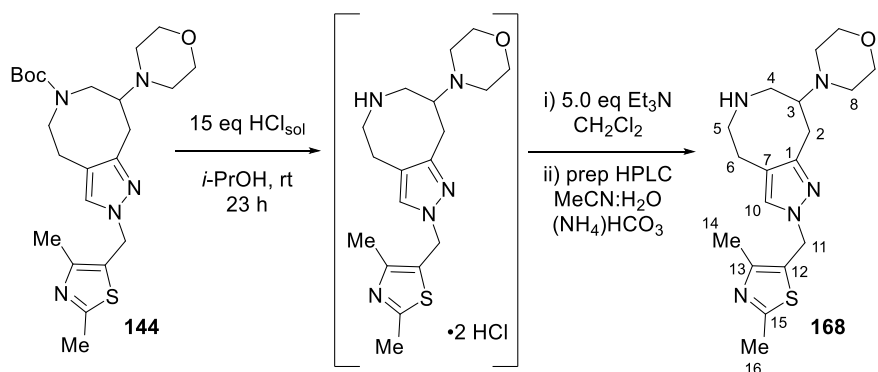
Boc-amine **144** (302 mg, 0.654 mmol) was dissolved in HCl solution (4 M in *i*-PrOH, 2.4 mL, 9.8 mmol). After stirring at rt for 23 h, the volatiles were removed under reduced pressure, yielding crude amine **168 •2 HCl** as an amber powder (282 mg, quant.), which was used as a library precursor without further purification.

An aliquot (0.098 mmol) was dissolved in a solution of Et_3N (0.07 mL, 0.5 mmol) and CH_2Cl_2 (0.4 mL). The resulting mixture was stirred overnight in a capped 8 mL vial and then left to evaporate to dryness under ambient conditions over 1 h. The resulting mixture was purified *via* preparative basic HPLC, yielding 2° amine **168** as a yellow glass (17.4 mg, 49%).

v$_{max}$ (neat / cm^{-1}): 3350 br w (N–H), 2919 m, 2851 m, 2807 m, 1446 s, 1330 m, 1115 v s.

^{1}H-NMR (400 MHz, CDCl$_3$) δ_H 7.01 (s, 1H, H-10), 5.26 (A of AB, $J_{A–B}$ = 15.6 Hz, 1H, H-11), 5.22 (B of AB, $J_{B–A}$ = 15.6 Hz, 1H, H-11), 3.73 − 3.62 (stack, 4H, H-9), 3.18 (dd, J = 14.5, 4.4 Hz, 1H, H-4), 3.02 − 2.88 (stack, 2H, H-2, H-5), 2.84 (B of ABX, $J_{A–B}$ = 13.7, $J_{A–X}$ = 4.0 Hz, 1H, H-2), 2.78 − 2.42 (stack, 12H, H-3, H-4, H-5, H-6, H-8, H-14), 2.38 (s, 3H, H-16), NH not observed.

^{13}C-NMR (101 MHz, CDCl$_3$) δ_C 164.8 (C, C-15), 150.5 (C, C-1), 149.8 (C, C-13), 127.1 (CH, C-10), 125.8 (C, C-12), 118.8 (C, C-7), 67.4 (CH$_2$, C-9), 65.8 (CH, C-3), 50.7 (CH$_2$, C-5, C-8, resonance overlap), 48.3 (CH$_2$, C-4), 47.1 (CH$_2$, C-11), 27.3 (CH$_2$, C-2), 25.5 (CH$_2$, C-6), 19.3 (CH$_3$, C-15), 15.1 (CH$_3$, C-16).

ESI-LRMS (+): m/z 362.1 ([M+H]$^+$, 100%).

HRMS: Found [M+H]$^+$ 362.2016. C$_{18}$H$_{28}$N$_5$OS requires M+H, 362.2009.

9-morpholino-5,6,7,8,9,10-hexahydropyrimido[5,4-*d*]azocin-2-amine (169)
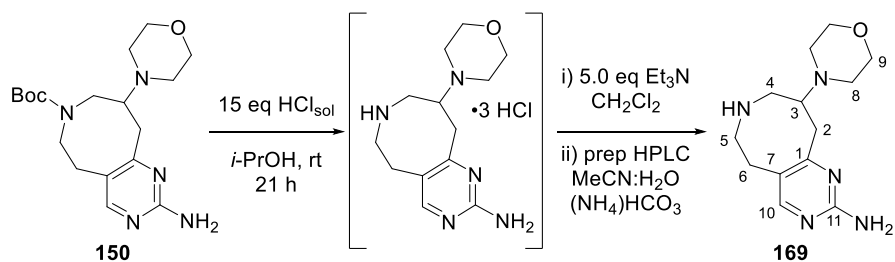
Boc-amine **150** (481 mg, 1.32 mmol) was dissolved in HCl solution (4 M in *i*-PrOH, 5.0 mL, 20 mmol). After stirring at rt for 21 h, the volatiles were removed under reduced pressure, yielding crude amine **169 •3 HCl** as a yellow solid (493 mg, quant.), which was used as a library precursor without further purification.

An aliquot (0.092 mmol) was dissolved in a solution of Et$_3$N (0.06 mL, 0.5 mmol) and CH$_2$Cl$_2$ (0.4 mL). The resulting mixture was stirred overnight in a capped 8 mL vial and then left to evaporate to dryness under ambient conditions over 1 h. The resulting mixture was purified *via* preparative basic HPLC, yielding 2° amine **169** as a yellow glass (3.7 mg, 15%).

ν$_{max}$ **(neat / cm⁻¹):** 3399 m (N–H), 3347 (N–H), 2911 m, 2803 m, 1648 s, 1558 s, 1472 v s, 1103 v s.

¹H-NMR (400 MHz, CDCl₃) δ_H 7.96 (s, 1H, H-10), 4.86 (br s, 2H, N*H*$_2$), 3.76 − 3.65 (stack, 4H, H-9), 3.19 − 3.05 (stack, 3H, H-2, H-4, H-5), 2.82 − 2.53 (stack, 9H, [including 2.82 − 2.68 (stack, 2H, H-2, H-6)], H-2, H-3, H-4, H-6, H-8), 2.54 − 2.43 (m, 1H, H-5), 2° amine proton not observed.

¹³C-NMR (101 MHz, CDCl₃) δ_C 169.6 (C, C-1), 161.9 (C, C-11), 157.9 (CH, C-10), 122.7 (C, C-7), 67.4 (CH$_2$, C-9), 66.9 (CH, C-3), 51.6 (CH$_2$, C-4 or C-5), 50.6 (CH$_2$, C-8), 49.3 (CH$_2$, C-4 or C-5), 35.3 (CH$_2$, C-2), 32.0 (CH$_2$, C-6).

ESI-LRMS (+): m/z 264.1 ([M+H]$^+$, 100%).

HRMS: Found [M+H]$^+$ 264.1824. C$_{13}$H$_{22}$N$_5$O requires M+H, 264.1819.

8. SACE2 Library: selected compound characterisation

8.1. Used building blocks (BB)

159 •2 TFA

161 •2 TFA

160 •3 TFA

162 •3 HCl

163 •2 HCl

165 •2 HCl

166 •2 HCl

169 •3 HCl

164 •2 HCl

167 •2 HCl

168 •2 HCl
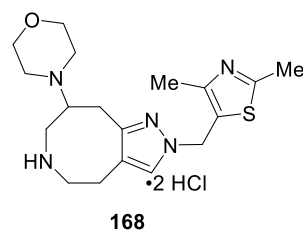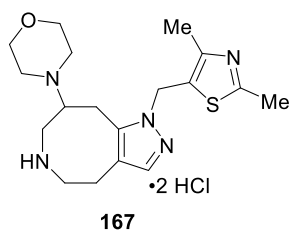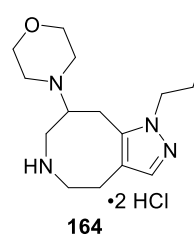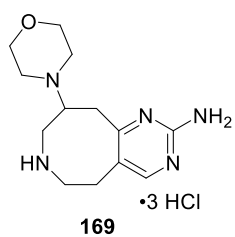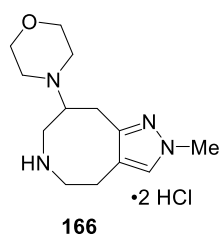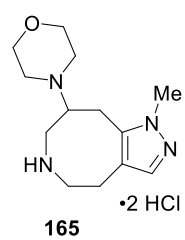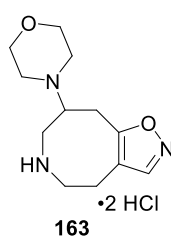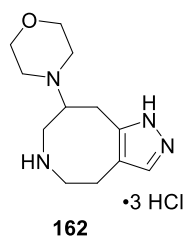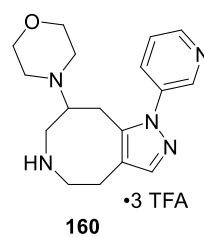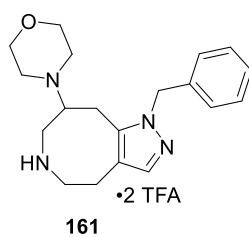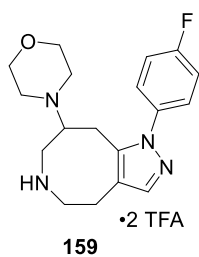
8.2.   GENERAL PROCEDURE 7: sulfonyl chlorides, isocyanates
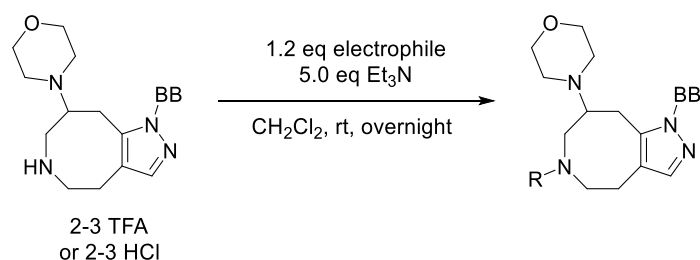
A solution of building block (0.059 – 0.310 mmol) in CH₂Cl₂ᵃ and Et₃N (5.0 eq) were added sequentially to a solution of the electrophile (1.2 eq) in CH₂Cl₂ (0.4 mL) in a capped 8 mL vial. The resulting mixture was stirred overnight and then left to evaporate to dryness at rt under ambient conditions over 1 h. The dry, crude mixture was purified *via* preparative basic HPLC.

8.3.   GENERAL PROCEDURE 8: amide couplings
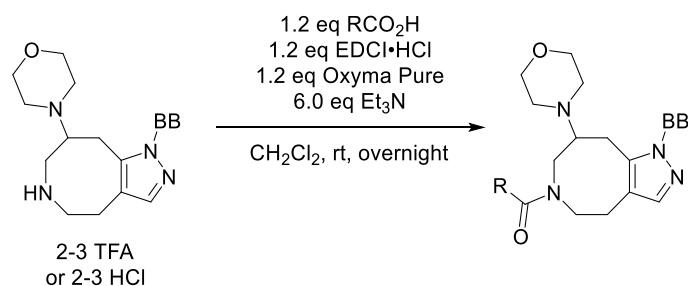
A solution of amine building block (0.059 – 0.160 mmol) in CH₂Cl₂ᵇ and Et₃N (6.0 eq) were added sequentially to a solution of the carboxylic acid (1.2 eq), EDC •HCl (1.2 eq) and Oxyma Pure (1.2 eq) in CH₂Cl₂ (0.4 mL) in a capped 8 mL vial. The resulting mixture was stirred overnight and then left to evaporate to dryness at rt under atmospheric pressure over 1 h. The dry, crude mixture was purified *via* preparative basic HPLC.

---

[a] Volume of CH₂Cl₂ calculated to yield a final reaction concentration of 0.1 M.
[b] Volume of CH₂Cl₂ calculated to yield a final reaction concentration of 0.1 M.

8.4. Compound synthesis and characterisation

4-(6-((2,4-dimethylthiazol-5-yl)sulfonyl)-1-(4-fluorophenyl)-4,5,6,7,8,9-hexahydro-1*H*-pyrazolo[4,3-*d*]azocin-8-yl)morpholine (159a3)
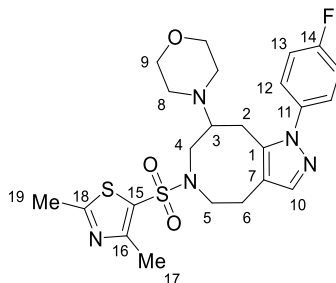
General procedure 7 (page 299) was followed, using building block **159 •2 TFA** (0.090 mmol) as the starting material and **a3** as the electrophile. Sulfonamide **159a3** was obtained as a brown oil (29.8 mg, 66%).

v_{max} **(neat / cm^{-1}):** 2930 w, 2855 w, 2814 w, 1513 v s, 1450 m, 1342 s, 1156 v s, 1115 v s.

^{1}H-NMR (400 MHz, CDCl$_3$) δ_H 7.44 − 7.36 (stack, 3H, H-10, Ar), 7.17 (app t, J = 8.2 Hz, 2H, Ar), 3.67 − 3.43 (stack, 6H), 3.15 − 3.00 (stack, 2H), 3.00 − 2.78 (stack, 4H), 2.78 − 2.66 (m, 1H), 2.65 (s, 3H, Me), 2.62 (s, 3H, Me), 2.47 − 2.39 (stack, 4H).

^{13}C-NMR (101 MHz, CDCl$_3$) δ_C 168.8, 162.1 (d, J_{C-F} = 248.3 Hz, C-14), 156.3, 139.6, 138.8, 136.3 (d, J_{C-F} = 3.1 Hz, C-11), 127.9, 127.5 (d, J_{C-F} = 8.6 Hz, C-12), 116.4, 116.2 (d, J_{C-F} = 22.9 Hz, C-13), 67.2, 63.7, 50.6, 50.1, 49.7, 25.4, 24.2, 19.5, 16.8.

ESI-LRMS (+): m/z 506.2 ([M+H]$^+$, 100%).

HRMS: Found [M+H]$^+$ 506.1686. $C_{23}H_{29}FN_5O_3S_2$ requires M+H, 506.1690.

4-(1-(4-fluorophenyl)-6-(morpholinosulfonyl)-4,5,6,7,8,9-hexahydro-1*H*-pyrazolo[4,3-*d*]azocin-8-yl)morpholine (159a4)
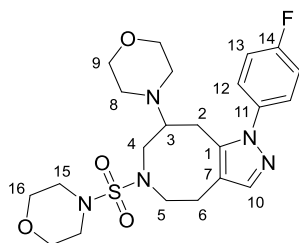
General procedure 7 (page 299) was followed, using building block **159 •2 TFA** (0.090 mmol) as the starting material and **a4** as the electrophile. Sulfonamide **159a4** was obtained as a yellow oil (21.4 mg, 50%).

***v*_{max} (neat / cm⁻¹):** 2922 w, 2822 w, 1513 s, 1320 s, 1223 s, 1144 v s, 1115 v s.

¹H-NMR (400 MHz, CDCl₃) δ_H 7.44 (s, 1H, H-10), 7.37 − 7.31 (m, 2H, Ar), 7.21 − 7.13 (m, 2H, Ar), 3.89 − 3.81 (m, 1H), 3.63 − 3.52 (stack, 8H), 3.44 (ddd, *J* = 12.8, 10.1, 5.3 Hz, 1H), 3.17 (app dt, *J* = 12.7, 4.8 Hz, 1H), 3.11 − 2.83 (stack, 6H), 2.83 − 2.72 (stack, 3H), 2.68 (ddd, *J* = 15.2, 10.1, 5.3 Hz, 1H), 2.55 − 2.44 (stack, 4H).

¹³C-NMR (101 MHz, CDCl₃) δ_C 162.2 (d, J_{C-F} = 248.8 Hz, C-14), [139.4, 139.3 (C-1, C-10)], 136.0 (d, J_{C-F} = 3.0 Hz, C-11), 127.34 (d, J_{C-F} = 8.7 Hz, C-12), 116.5 (C-7), 116.4 (d, J_{C-F} = 22.9 Hz, C-13), 67.2, 66.4, 63.2, 50.4, 50.0, 49.5, 45.9, 25.7, 23.4.

ESI-LRMS (+): m/z 480.2 ([M+H]⁺, 100%).

HRMS: Found [M+H]⁺ 480.2068. C₂₂H₃₁FN₅O₄S requires M+H, 480.2075.

N-ethyl-1-(4-fluorophenyl)-8-morpholino-1,4,5,7,8,9-hexahydro-6*H*-pyrazolo[4,3-*d*]azocine-6-carboxamide (159d1)
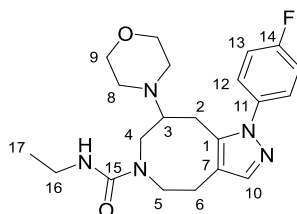
General procedure 7 (page 299) was followed, using building block **159 •2 TFA** (0.090 mmol) as the starting material and **d1** as the electrophile. Urea **159d1** was obtained as a yellow glass (28.9 mg, 80%).

***v*_{max} (neat / cm⁻¹):** 3384 w (N–H), 2963 m, 2930 m, 2855 m, 1629 s (C=O), 1513 v s, 1267 m, 1219 s, 1115 s.

¹H-NMR (400 MHz, CDCl₃) δ_H 7.41 (s, 1H, H-10), 7.40 – 7.32 (m, 2H, Ar), 7.22 – 7.13 (m, 2H, Ar), 4.68 – 4.59 (m, 1H, H-5), 3.74 – 3.55 (stack, 5H, H-4, H-9), 3.33 – 3.11 (m, 2H, H-16), 2.98 – 2.81 (stack, 2H, H-2, H-4), 2.79 – 2.50 (stack, 4H, H-2, H-5, H-6), 2.50 – 2.27 (stack, 5H, H-3, H-8), 1.13 (t, *J* = 7.2 Hz, 3H, H-17), NH not observed.

¹³C-NMR (101 MHz, CDCl₃) δ_C 162.4 (C, d, $J_{C–F}$ = 249.2 Hz, C-14), 159.7 (C, C-15), 140.1 (CH, C-10), 137.8 (C, C-1), 136.0 (C, d, $J_{C–F}$ = 3.2 Hz, C-11), 128.0 (CH, d, $J_{C–F}$ = 8.7 Hz, C-12), 119.9 (C, C-7), 116.3 (CH, d, $J_{C–F}$ = 22.9 Hz, CH, C-13), 67.0 (CH₂, C-9), 65.9 (CH, C-3), [51.9, 51.3 (CH₂, C-4, C-5, C-8, resonance overlap)], 35.4 (CH₂, C-16), 26.4 (CH₂, C-6), 22.7 (CH₂, C-2), 16.5 (CH₃, C-17).

ESI-LRMS (+): m/z 402.3 ([M+H]⁺, 100%).

HRMS: Found [M+H]⁺ 402.2292. C₂₁H₂₉FN₅O₂ requires M+H, 402.2300.

4-(1-benzyl-6-((2,3-dihydrobenzo[*b*][1,4]dioxin-6-yl)sulfonyl)-4,5,6,7,8,9-hexahydro-1*H*-pyrazolo[4,3-*d*]azocin-8-yl)morpholine (161a7)
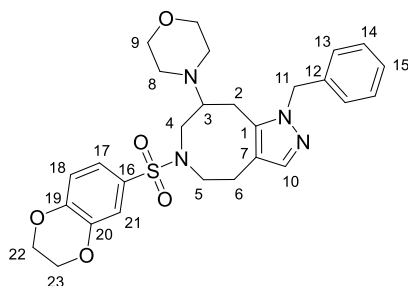
General procedure 7 (page 299) was followed, using building block **161 •2 TFA** (0.098 mmol) as the starting material and **a7** as the electrophile. Sulfonamide **161a7** was obtained as an off-white solid (26.6 mg, 52%).

***v*max (neat / cm⁻¹):** 2937 m, 2855 m, 1580 m, 1491 s, 1282 v s, 1252 v s, 1115 v s.

¹H-NMR (400 MHz, CDCl₃) δ_H 7.35 − 7.22 (stack, 5H), 7.19 (dd, *J* = 8.4, 2.2 Hz, 1H), 7.05 (d, *J* = 7.3 Hz, 2H), 6.93 (d, *J* = 8.5 Hz, 1H), 5.43 (A of AB, J_{A-B} = 16.2 Hz, 1H, H-11), 5.37 (B of AB, J_{B-A} = 16.2 Hz, 1H, H-11), 4.34 − 4.22 (stack, 4H), 3.71 − 3.58 (stack, 4H), 3.58 − 3.48 (m, 1H), 3.43 (dd, *J* = 14.3, 3.9 Hz, 1H), 2.99 − 2.67 (stack, 6H), 2.67 − 2.57 (m, 1H), 2.57 − 2.34 (stack, 4H).

¹³C-NMR (101 MHz, CDCl₃) δ_C 147.5, 143.7, 138.4, 138.2, 137.6, 131.2, 129.0, 127.7, 126.6, 120.9, 117.9, 116.8, 116.4, 67.4, 64.6, 64.3, 63.5, 53.6, 51.4, 50.0, 49.7, 25.4, 24.8.

ESI-LRMS (+): m/z 525.3 ([M+H]⁺, 100%).

HRMS: Found [M+H]⁺ 525.2159. C₂₇H₃₃N₄O₅S requires M+H, 525.2166.

1-benzyl-*N*-(4-(difluoromethoxy)phenyl)-8-morpholino-1,4,5,7,8,9-hexahydro-6*H*-pyrazolo[4,3-*d*]azocine-6-carboxamide (161d3)
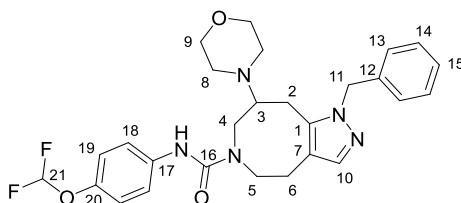
General procedure 7 (page 299) was followed, using building block **161 •2 TFA** (0.196 mmol) as the starting material and **d3** as the electrophile. Urea **161d3** was obtained as a white solid 59.3 mg, 59%).

*v*_{max} (neat / cm⁻¹): 2922 w, 2855 w, 1659 s (C=O), 1506 s, 1200 s, 1118 v s.

¹H-NMR (400 MHz, CDCl₃) δ_H 10.27 (s, 1H, N*H*), 7.35 − 7.23 (stack, 6H, H-10, H-14, H-15, H-18), 7.11 − 7.05 (m, 2H, H-13), 7.05 − 6.99 (m, 2H, H-19), 6.40 (t, J_{H-F} = 73.7 Hz, 1H, H-21), 5.37 (A of AB, J_{A-B} = 16.0 Hz, 1H, H-11), 5.27 (B of AB, J_{B-A} = 16.0 Hz, 1H, H-11), 4.82 − 4.64 (m, 1H, H-5), 3.82 − 3.54 (stack, 5H, H-4, H-9), 2.87 (dd, *J* = 13.6, 3.7 Hz, 1H, H-2), 2.83 − 2.22 (stack, 9H, H-2, H-4, H-5, H-6, H-8), 2.02 − 1.92 (m, 1H, H-3).

¹³C-NMR (101 MHz, CDCl₃) δ_C 157.5 (C, C-16), 146.7 (C, C-20), 138.5 (CH, C-10), [137.5 , 137.3 (C, C-12, C-17)], 136.1 (C, C-1), [129.1, 128.2 (CH, C-14, C-15), 126.8 (CH, C-13), 123.2 (CH, C-18), 120.3 (CH, C-19), 119.9 (C, C-7), 116.2 (CH, t, J_{C-F} = 259.4 Hz, C-21), 66.7 (CH₂, C-9), 65.2 (CH, C-3), 54.0 (CH₂, C-11), 52.5 (CH₂, C-5), [51.5, 51.1 (CH₂, C-4, C-8)], 26.2 (CH₂, C-6), 22.7 (CH₂, C-2).

ESI-LRMS (+): m/z 512.3 ([M+H]⁺, 100%).

HRMS: Found [M+H]⁺ 512.2460. C₂₇H₃₂F₂N₅O₃ requires M+H, 512.2468.

1-(1-benzyl-8-morpholino-1,4,5,7,8,9-hexahydro-6*H*-pyrazolo[4,3-*d*]azocin-6-yl)ethan-1-one (161c2)
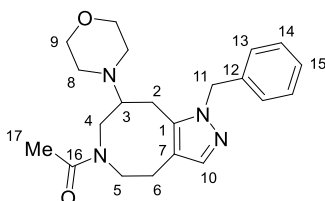
General procedure 8 (page 299) was followed, using building block **161 •2 TFA** (0.098 mmol) as the starting material and **c2** as the carboxylic acid. Amide **161c2** was obtained as a colourless liquid (29.2 mg, 81%).

***v*~max~ (neat / cm⁻¹):** 2933 m, 2855 m, 1621 v s (C=O), 1454 s, 1416 s, 1111 v s.

¹H-NMR (400 MHz, CDCl₃) (mixture of rotamers, 9:1)[a] δ_H 7.36 − 7.18 (stack, 4H, H-10, H-14, H-15), 7.04 − 6.93 (stack, 2H, H-13), 5.47 − 5.25 (stack, 2H, H-11), [4.39 − 4.27 (m, 0.1H, H-4 min), 3.91 − 3.77 (m, 0.9H, H-4 maj)], 3.70 − 3.51 (stack, 5H, H-5, H-9), [3.24 (app dt, *J* = 13.9, 5.6 Hz, 0.9H, H-5 maj), 3.20 − 3.04 (m, 0.1H, H-5 min)], 3.04 − 2.38 (stack, 9.6H, H-2, H-3, H-4, H-6, H-8 maj), 2.37 − 2.25 (stack, 0.4H, H-8 min), [1.87 (s, 0.3H, H-17 min), 1.82 (s, 2.7H, H-17 maj)].

¹³C-NMR (101 MHz, CDCl₃) (mixture of rotamers) δ_C [171.3 (C, C-16 maj), 171.0 (C, C-16 min)], [139.0 (C, C-1 maj), 138.4 (C, C-1 min)], [137.9 (CH, C-10 min), 137.8 (CH, C-10 maj)], [137.34, 137.28 (C, C-12)], [128.9, 128.9, 127.8 (CH, C-14, C-15)], [126.61, 126.58 (CH, C-13)], [117.2 (C, C-7 min), 115.4 (C, C-7 maj)], [67.4 (CH₂, C-9 maj), 67.3 (CH₂, C-9 min)], [63.0 (CH, C-3 min), 59.7 (CH, C-3 maj)], [53.6 (CH₂, C-11 maj), 51.6 (CH₂, C-11 min)], 51.0 (CH₂, C-5 maj), 49.6 (CH₂, C-5 min or C-8 min), 49.5 (CH₂, C-8 maj), [48.5 (CH₂, C-4 maj)], 47.6 (CH₂, C-4 min), [25.4, 24.7, 24.1, 23.2 (CH₂, C-2, C-6)], [22.3 (CH, C-17 maj), 21.7 (CH, C-17 min)]. According to HSQC data, either the C-5 min or C-8 min signal is not observed, or the resonance overlaps with δ_C 49.5 ppm.

ESI-LRMS (+): m/z 369.3 ([M+H]⁺, 100%).

HRMS: Found [M+H]⁺ 369.2279. C₂₁H₂₉N₄O₂ requires M+H, 369.2285.

4-((8-morpholino-1-(pyridin-3-yl)-1,4,5,7,8,9-hexahydro-6*H*-pyrazolo[4,3-*d*]azocin-6-yl)sulfonyl)morpholine (160a4)

---

[a] Ratio based on H-4 peak integrations in the reported ¹H-NMR spectrum at δ_H (CDCl₃) 4.39 − 4.27, 3.91 − 3.77 ppm.
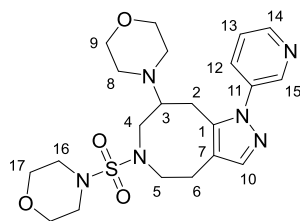
General procedure 7 (page 299) was followed, using building block **160 •3 TFA** (0.220 mmol) as the starting material and **a4** as the electrophile. Sulfonamide **160a4** was obtained as an off-white solid (44.8 mg, 44%).

v_{max} (neat / cm^{-1}): 2956 w, 2855 m, 1454 m, 1320 s, 1148 v s, 1111 v s.

^{1}H-NMR (400 MHz, CDCl$_3$) δ_H 8.68 (d, J = 2.5 Hz, 1H, H-15), 8.65 (dd, J = 4.8, 1.5 Hz, 1H, H-14), 7.76 (ddd, J = 8.2, 2.1, 1.5 Hz, 1H, H-12), 7.50 (s, 1H, H-10), 7.45 (dd, J = 8.2, 4.8 Hz, 1H, H-13), 3.92 – 3.80 (m, 1H, H-4), 3.63 – 3.38 (stack, 9H, H-5, H-9, H-17), 3.16 (app dt, J = 12.8, 4.9 Hz, 1H, H-5), 3.08 – 2.93 (stack, 5H, H-2, H-3, H-4, H-16), 2.94 – 2.74 (stack, 4H, H-2, H-6, H-16), 2.74 – 2.62 (m, 1H, H-6), 2.56 – 2.41 (stack, 4H, H-8).

^{13}C-NMR (101 MHz, CDCl$_3$) δ_C 149.2 (CH, C-14), 146.1 (CH, C-15), 140.4 (CH, C-10), 139.5 (C, C-1), 136.5 (C, C-11), 132.7 (CH, C-12), 124.0 (CH, C-13), 117.3 (C, C-7), [67.1, 66.3 (CH$_2$, C-9, C-17)], 63.3 (CH, C-3), [50.1, 49.5 (CH$_2$, C-4, C-5, C-8, resonance overlap)], 46.0 (CH$_2$, C-16), 25.8 (CH$_2$, C-2), 23.6 (CH$_2$, C-6).

ESI-LRMS (+): m/z 463.2 ([M+H]$^+$, 100%).

HRMS: Found [M+H]$^+$ 463.2114. C$_{21}$H$_{31}$N$_6$O$_4$S requires M+H, 463.2122.

4-(6-methylsulfonyl-1-(pyridin-3-yl)-4,5,6,7,8,9-hexahydro-1*H*-pyrazolo[4,3-*d*]azocin-8-yl)morpholine (160a5)
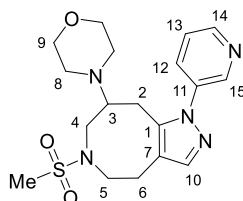
General procedure 7 (page 299) was followed, using building block **160 •3 TFA** (0.110 mmol) as the starting material and **a5** as the electrophile. Sulfonamide **160a5** was obtained as a yellow oil (21.6 mg, 50%).

***v*_{max} (neat / cm⁻¹):** 2930 m, 2855 m, 1431 s, 1320 v s, 1144 v s, 1115 v s.

¹H-NMR (400 MHz, CDCl₃) δ_H 8.75 (d, *J* = 2.6 Hz, 1H), 8.65 (dd, *J* = 4.8, 1.5 Hz, 1H), 7.81 (ddd, *J* = 8.1, 2.5, 1.5 Hz, 1H), 7.51 (s, 1H), 7.45 (dd, *J* = 8.2, 4.7 Hz, 1H), 3.69 – 3.39 (stack, 6H), 3.24 – 3.14 (m, 1H), 3.08 – 2.84 (stack, 5H), 2.78 – 2.65 (stack, 4H, [including 2.70 (s, 3H, Me)]), 2.49 – 2.38 (stack, 4H).

¹³C-NMR (101 MHz, CDCl₃) δ_C 149.1, 146.4, 140.7, 139.2, 136.8, 132.8, 123.9, 117.6, 67.1, 63.9, 50.5, 50.1, 49.9, 37.1, 25.0, 24.6.

ESI-LRMS (+): m/z 392.2 ([M+H]⁺, 100%).

HRMS: Found [M+H]⁺ 392.1743. $C_{18}H_{26}N_5O_3S$ requires M+H, 392.1751.

N-ethyl-8-morpholino-1-(pyridin-3-yl)-1,4,5,7,8,9-hexahydro-6*H*-pyrazolo[4,3-*d*]azocine-6-carboxamide (160d1)
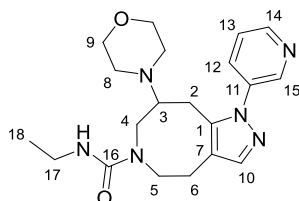
General procedure 7 (page 299) was followed, using building block **160 •3 TFA** (0.110 mmol) as the starting material and **d1** as the electrophile. Urea **160d1** was obtained as a yellow solid (30.1 mg, 71%).

***v*_{max} (neat / cm⁻¹):** v_{max} (neat / cm^{-1}): 3377 w (N–H), 2963 m, 2855 m, 1633 s (C=O), 1431 s, 1267 s, 1115 v s.

¹H-NMR (400 MHz, CDCl₃) δ_H 8.72 (d, J = 2.5 Hz, 1H), 8.68 (dd, J = 4.8, 1.5 Hz, 1H), 7.85 (br s, 1H), 7.78 (app dt, J = 8.2, 1.9 Hz, 1H), 7.50 − 7.42 (stack, 2H), 4.71 − 4.54 (m, 1H), 3.72 − 3.56 (stack, 5H), 3.32 − 3.13 (m, 2H), 3.01 − 2.88 (stack, 2H), 2.85 − 2.75 (m, 1H), 2.75 − 2.54 (stack, 3H), 2.54 − 2.30 (stack, 5H), 1.13 (t, J = 7.2 Hz, 3H, H-18).

¹³C-NMR (101 MHz, CDCl₃) δ_C 159.6, 149.6, 146.6, 141.2, 138.0, 136.5, 133.2, 123.9, 120.7, 66.9, 65.9, 51.7, 51.3, 51.2, 35.4, 26.3, 22.7, 16.5.

ESI-LRMS (+): m/z 385.3 ([M+H]⁺, 100%).

HRMS: Found [M+H]⁺ 385.2339. $C_{20}H_{29}N_6O_2$ requires M+H, 385.2347.

4-(6-((2,4-dimethylthiazol-5-yl)sulfonyl)-4,5,6,7,8,9-hexahydro-1*H*-pyrazolo[4,3-*d*]azocin-8-yl)morpholine (162a3)
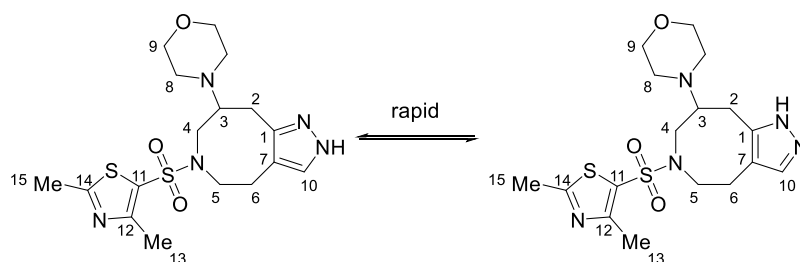
General procedure 7 (page 299) was followed, using building block **162 •3 HCl** (0.097 mmol) as starting material and **a3** as the electrophile. Sulfonamide **162a3** was obtained as a beige powder (27.4 mg, 69%).

***v*~max~ (neat / cm⁻¹):** 3131 w (N–H), 2930 m, 2855 m, 1454 m, 1334 s, 1152 v s, 1111 v s.

¹H-NMR (400 MHz, CDCl₃) δ_H 7.30 (s, 1H, H-10), 3.80 – 3.60 (stack, 6H, H-4, H-5, H-9), 3.18 – 3.07 (stack, 2H, H-3, H-2), 3.02 – 2.94 (m, 1H, H-6), 2.86 – 2.64 (stack, 11H, [including 2.67 (s, 3H, H-15)], H-2, H-4, H-5, H-6, H-8, H-15), 2.63 (s, 3H, H-13), NH not observed.[a]

¹³C-NMR (101 MHz, CDCl₃) δ_C 168.6 (C, C-14), 156.1 (C, C-12), 144.6 (C, C-7), 132.4 (CH, C-10), 127.9 (C, C-11), 115.6 (C, C-1), 67.3 (CH₂, C-9), 64.0 (CH, C-3), [52.0, 50.6 (CH₂, C-4, C-5)], 50.2 (CH₂, C-8), 26.0, (CH₂, C-2), 24.7 (CH₂, C-6), 19.5 (CH₃, C-15), 16.8 (CH₃, C-13).

ESI-LRMS (+): m/z 412.2 ([M+H]⁺, 100%).

HRMS: Found [M+H]⁺ 412.1464. C₁₇H₂₆N₅O₃S₂ requires M+H, 412.1472.

---

[a] Pyrazole presumably exists as a mixture of rapidly interconverting tautomeric forms.

1-(8-morpholino-1,4,5,7,8,9-hexahydro-6*H*-pyrazolo[4,3-*d*]azocin-6-yl)-2-(tetrahydro-2*H*-pyran-4-yl)ethan-1-one (162c1)
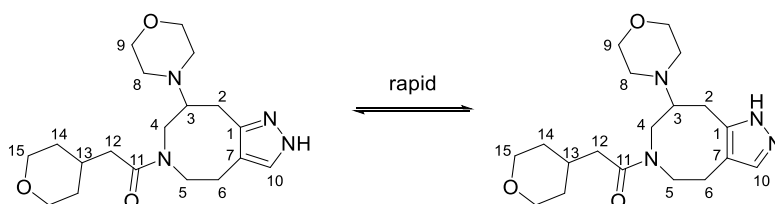
General procedure 8 (page 299) was followed, using building block **162** •**3 HCl** (0.097 mmol) as the starting material and **c1** as the carboxylic acid. Amide **162c1** was obtained as a colourless liquid (20.0 mg, 57%).

v_{max} (neat / cm^{-1}): 3224 w (N–H), 2930 m, 2848 m, 1621 s (C=O), 1420 m, 1115 s.

^{1}H-NMR (400 MHz, CDCl$_3$) (mixture of rotamers, 4:1)[a] δ_H [7.33 (s, 0.8H, H-10 maj), 7.28 (s, 0.2H, H-10 min)], [4.49 − 4.38 (m, 0.2H, H-4 min), 4.06 (dd, *J* = 13.1, 3.9 Hz, 0.8H, H-4 maj)], 3.95 − 3.78 (stack, 2.2H, H-5 min, H-15), 3.78 − 3.61 (stack, 4.8H, H-5 maj, H-9), 3.42 − 3.29 (m, 2H, H-15), 3.29 − 3.03 (stack, 2H, H-3, H-5), 2.91 − 2.77 (stack, 3H, H-2, H-4), 2.77 − 2.57 (stack, 6H, H-6, H-8), 2.17 − 2.03 (stack, 1.2H, H-12, H-13 min), 2.03 − 1.87 (stack, 1.8H, H-12, H-13 maj), 1.65 − 1.40 (stack, 2H, H-14), 1.34 − 1.03 (stack, 2H, H-14), NH not observed.[b]

^{13}C-NMR (101 MHz, CDCl$_3$) (mixture of rotamers) δ_C [172.6 (C, C-11 min), 172.0 (C, C-11 maj)], [116.5 (C, C-7 min), 114.8 (C, C-7 maj)], 68.0 (CH$_2$, C-15), [67.5 (CH$_2$, C-9 maj), 67.4 (CH$_2$, C-9 min)], [64.6 (CH, C-3 min), 60.4 (CH, C-3 maj)], [52.1 (CH$_2$, C-5 min), 50.6 (CH$_2$, C-5 maj)], [50.1 (CH$_2$, C-8 min), 49.9 (CH$_2$, C-8 maj)], [49.4 (CH$_2$, C-4 maj), 49.2 (CH$_2$, C-4 min)], [40.7 (CH$_2$, C-12 maj), 40.2 (CH$_2$, C-12 min)], [33.2, 32.9 (CH$_2$, C-14)], [32.5 (CH, C-13 min), 31.9 (CH, C-13 maj)], [26.5 (CH$_2$, C-2 maj), 25.4 (CH$_2$, C-2 min)], [24.0 (CH$_2$, C-6 maj), 23.0 (CH$_2$, C-6 min)]. C-1, C-10 resonances not observed.

ESI-LRMS (+): m/z 363.3 ([M+H]$^+$, 100%).

HRMS: Found [M+H]$^+$ 363.2383. C$_{19}$H$_{31}$N$_4$O$_3$ requires M+H, 363.2391.

---

[a] Ratio based on H-4 peak integrations in the reported ^{1}H-NMR spectrum at δ_H (CDCl$_3$) 4.49 − 4.38, 4.06 ppm.
[b] Pyrazole presumably exists as a mixture of rapidly interconverting tautomeric forms

N-ethyl-8-morpholino-1,4,5,7,8,9-hexahydro-6*H*-pyrazolo[4,3-*d*]azocine-6-carboxamide (162d1)
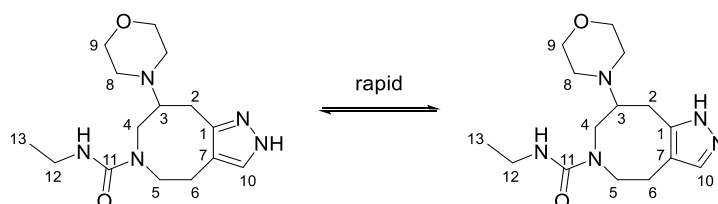
General procedure 7 (page 299) was followed, using building block **162 •3 HCl** (0.097 mmol) as the starting material and **d1** as the electrophile. Urea **162d1** was obtained as a colourless glass (15.1 mg, 51%).

v_{max} **(neat / cm^{-1}):** 3175 w (N–H), 2922 m, 2848 m, 1625 s (C=O), 1584 s, 1267 s, 1118 s.

^{1}H-NMR (400 MHz, CDCl$_3$) δ_H 8.57 (app br s, 1H, EtN*H*CO), 7.29 (s, 1H, H-10), 4.78 – 4.70 (m, 1H, H-5), 3.83 – 3.65 (stack, 5H, H-4, H-9), 3.38 – 3.16 (m, 2H, H-12), 3.05 (dd, J = 11.5, 3.0 Hz, 1H, H-2), 2.89 – 2.69 (stack, 3H, H-4, H-8), 2.69 – 2.55 (stack, 6H, H-2, H-3, H-6, H-8), 2.49 – 2.38 (m, 1H, H-5), 1.17 (t, J = 7.2 Hz, 3H, H-13), pyrazole NH not observed.[a]

^{13}C-NMR (101 MHz, CDCl$_3$) δ_C 160.1 (C, C-11), 118.6 (C, C-7), 67.24 (CH$_2$, C-9), 67.22 (CH, C-3), 52.5 (CH$_2$, C-5), 51.7 (CH$_2$, C-8), 51.4 (CH$_2$, C-4), 35.3 (CH$_2$, C-12), 25.9 (CH$_2$, C-6), 24.6 (CH$_2$, C-2), 16.7 (CH$_3$, C-3). C-1 and C-10 resonances not observed, but HMBC and HSQC cross peaks indicate their presence between δ_C 147 – 145 ppm (C-1) and 130 – 129 ppm (C-10).

ESI-LRMS (+): m/z 308.3 ([M+H]$^+$, 100%).

HRMS: Found [M+H]$^+$ 308.2077. C$_{15}$H$_{26}$N$_5$O$_2$ requires M+H, 308.2081.

---

[a] Pyrazole presumably exists as a mixture of rapidly interconverting tautomeric forms.

8-morpholino-6-(morpholinosulfonyl)-4,5,6,7,8,9-hexahydroisoxazolo[4,5-*d*]azocine (163a4)
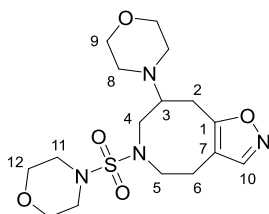
General procedure 7 (page 299) was followed, using building block **163** •**2 HCl** (0.105 mmol) as the starting material and **a4** as the electrophile. Sulfonamide **163a4** was obtained as an off-white solid (24.7 mg, 30%).

v_{max} (neat / cm^{-1}): 2956 w, 2855 m, 1454 m, 1334 m, 1141 s, 1111 s.

^{1}H-NMR (400 MHz, CDCl$_3$) δ_H 8.03 (s, 1H, H-10), 3.76 (dd, *J* = 14.8, 4.4 Hz, 1H, H-4), 3.72 – 3.61 (stack, 9H, H-5, H-9, H-12), 3.24 – 3.13 (stack, 2H, H-2, H-3), 3.12 – 2.98 (stack, 6H, H-2, H-5, H-11), 2.90 (dd, *J* = 14.6, 10.6 Hz, 1H, H-4), 2.80 – 2.71 (m, 1H, H-6), 2.68 – 2.56 (stack, 5H, [including 2.63 – 2.56 (stack, 4H, H-8)], H-6, H-8).

^{13}C-NMR (101 MHz, CDCl$_3$) δ_C 167.6 (C, C-1), 151.3 (CH, C-10), 112.1 (C, C-7), [67.3, 66.3 (CH$_2$, C-9, C-12)], 63.0 (CH, C-3), 51.6 (CH$_2$, C-4), 51.0 (CH$_2$, C-5), 49.8 (CH$_2$, C-8), 46.3 (CH$_2$, C-11), 25.0 (CH$_2$, C-2), 23.5 (CH$_2$, C-6).

ESI-LRMS (+): m/z 387.3 ([M+H]$^+$, 100%).

HRMS: Found [M+H]$^+$ 387.1688. C$_{16}$H$_{27}$N$_4$O$_5$S requires M+H, 387.1697.

N-(4-(difluoromethoxy)phenyl)-8-morpholino-4,7,8,9-tetrahydroisoxazolo[4,5-*d*]azocine-6(5*H*)-carboxamide (163d3)
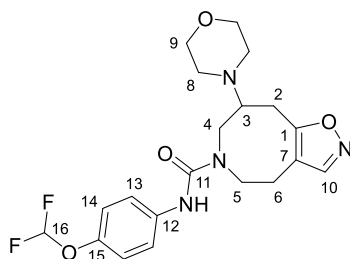
General procedure 7 (page 299) was followed, using building block **163 •2 HCl** (0.105 mmol) as the starting material and **d3** as the electrophile. Urea **163d3** was obtained as a white solid (23.3 mg, 53%).

***v*~max~ (neat / cm⁻¹):** 2952 w, 2848 w, 1659 s (C=O), 1506 s, 1211 s, 1103 s.

¹H-NMR (400 MHz, CDCl₃) δ_H 10.32 (s, 1H, N*H*), 8.06 (s, 1H, H-10), 7.43 – 7.35 (m, 2H, Ar), 7.12 – 7.04 (m, 2H, Ar), 6.46 (t, J_{H-F} = 74.0 Hz, 1H, H-16), 4.83 – 4.71 (m, 1H), 3.99 (d, J = 16.1 Hz, 1H), 3.86 – 3.72 (stack, 4H, H-9), 3.33 – 3.26 (m, 1H), 3.02 – 2.79 (stack, 5H), 2.75 – 2.54 (stack, 5H).

¹³C-NMR (101 MHz, CDCl₃) δ_C 165.8, 157.2, 151.8, 146.9 (t, J_{C-F} = 2.8 Hz), 137.1, 123.1, 120.5, 116.2 (t, J_{C-F} = 259.7 Hz), 115.1, 66.7, 65.7, 52.6, 51.9, 51.7, 24.4, 24.2.

ESI-LRMS (+): m/z 423.3 ([M+H]⁺, 100%).

HRMS: Found [M+H]⁺ 423.1830. $C_{20}H_{25}F_2N_4O_4$ requires M+H, 423.1838.

4-(1-methyl-6-methylsulfonyl-4,5,6,7,8,9-hexahydro-1*H*-pyrazolo[4,3-*d*]azocin-8-yl)morpholine (165a5)
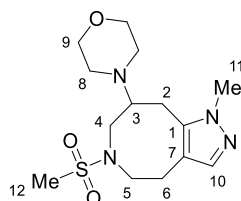
General procedure 7 (page 299) was followed, using building block **165 •2 HCl** (0.130 mmol) as the starting material and **a5** as the electrophile. Sulfonamide **165a5** was obtained as a beige solid (26.7 mg, 31%).

*ν*_max (neat / cm⁻¹)**: 2948 m, 2855 m, 1454 m, 1320 s, 1144 s, 1115 s.

¹H-NMR (400 MHz, CDCl₃) δ_H 7.23 (s, 1H, H-10), 3.85 (s, 3H, H-11), 3.71 − 3.63 (stack, 4H, H-9), 3.59 − 3.50 (stack, 2H, H-4, H-5), 3.11 − 2.97 (stack, 3H, H-2, H-3, H-5), 2.94 − 2.80 (stack, 2H, H-2, H-4), 2.75 (A of ABXY, J_{A-B} = 15.2, J_{A-X} = 8.0, J_{A-Y} = 4.4 Hz, 1H, H-6), 2.71 − 2.60 (stack, 6H, [including 2.68 (s, 3H, H-12)], H-6, H-8, H-12), 2.54 (app dt, J = 11.2, 4.6 Hz, 2H, H-8).

¹³C-NMR (101 MHz, CDCl₃) δ_C 138.2 (C, C-1), 137.6 (CH, C-10), 116.1 (C, C-7), 67.3 (CH₂, C-9), 63.6 (CH, C-3), 51.7 (CH₂, C-5), 50.3 (CH₂, C-8), 49.7 (CH₂, C-4), [37.0, 36.9 (CH₃, C-11, C-12)], [25.4, 25.1 (CH₂, C-2, C-6)].

ESI-LRMS (+): m/z 329.2 ([M+H]⁺, 100%).

HRMS: Found [M+H]⁺ 329.1639. C₁₄H₂₅N₄O₃S requires M+H, 329.1642.

N-(4-(difluoromethoxy)phenyl)-1-methyl-8-morpholino-1,4,5,7,8,9-hexahydro-6*H*-pyrazolo[4,3-*d*]azocine-6-carboxamide (165d3)
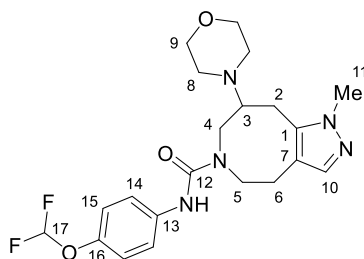
General procedure 7 (page 299) was followed, using building block **165 •2 HCl** (0.260 mmol) as the starting material and **d3** as the electrophile. Urea **165d3** was obtained as a colourless glass (63.0 mg, 56%).

v$_{max}$ (neat / cm^{-1}): 2922 w, 2840 w, 1662 s (C=O), 1506 m, 1211 m, 1111 v s.

^{1}H-NMR (400 MHz, CDCl$_3$) δ_H 10.31 (br s, 1H, N*H*) 7.39 – 7.34 (AA' of AA'BB', 2H, H-14), 7.24 (s, 1H, H-10), 7.10 – 7.04 (BB' of AA'BB', 2H, H-16), 6.45 (t, $J_{H–F}$ = 73.6 Hz, 1H, H-17), 4.88 – 4.70 (m, 1H, H-5), 4.04 – 3.91 (m, 1H, H-4), 3.89 – 3.71 (stack, 7H, [including 3.83 (s, 3H, H-11)], H-9, H-11), 3.06 – 2.90 (stack, 2H, H-2, H-4), 2.90 – 2.76 (stack, 3H, H-2, H-8), 2.76 – 2.60 (stack, 4H, H-6, H-8), 2.60 – 2.41 (stack, 2H, H-3, H-5).

^{13}C-NMR (101 MHz, CDCl$_3$) δ_C 157.5 (C, C-12), 146.8 (C, t, $J_{C–F}$ = 3.0 Hz, C-16), 138.1 (CH, C-10), 137.3 (C, C-13), 136.1 (C, C-1), 123.1 (CH, C-14), 120.4 (CH, C-15), 119.1 (C, C-7), 116.3 (CH, t, $J_{C–F}$ = 259.4 Hz, C-17), 66.7 (CH$_2$, C-9), 66.0 (CH, C-3), 52.8 (CH$_2$, C-5), 52.0 (CH$_2$, C-8), 51.1 (CH$_2$, C-4), 36.5 (CH$_3$, C-11), 26.1 (CH$_2$, C-6), 22.7 (CH$_2$, C-2).

ESI-LRMS (+): m/z 436.3 ([M+H]$^+$, 100%).

HRMS: Found [M+H]$^+$ 436.2146. C$_{21}$H$_{28}$F$_2$N$_5$O$_3$ requires M+H, 436.2155.

4-(6-((2,3-dihydrobenzo[*b*][1,4]dioxin-6-yl)sulfonyl)-2-methyl-4,5,6,7,8,9-hexahydro-2*H*-pyrazolo[4,3-*d*]azocin-8-yl)morpholine (166a7)
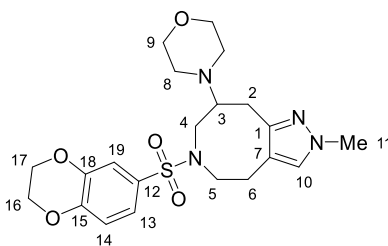
General procedure 7 (page 299) was followed, using building block **166 •2 HCl** (0.103 mmol) as starting material and **a7** as the electrophile. Sulfonamide **166a7** was obtained as a white powder (30.9 mg, 67%).

***v*~max~ (neat / cm⁻¹):** 2937 m, 2855 m, 1495 s, 1286 v s, 1152 s, 1118 s.

¹H-NMR (400 MHz, CDCl₃) δ_H 7.29 − 7.20 (stack, 2H, Ar), 7.04 (s, 1H, H-10), 6.94 (d, *J* = 8.4 Hz, 1H, Ar), 4.35 − 4.26 (stack, 4H, H-16, H-17), 3.80 (s, 3H, H-11), 3.76 − 3.57 (stack, 6H, H-4, H-5, H-9), 3.11 − 3.03 (stack, 2H, H-2, H-3), 2.92 − 2.84 (m, 1H, H-2), 2.80 − 2.58 (stack, 8H, H-4, H-5, H-6, H-8).

¹³C-NMR (101 MHz, CDCl₃) δ_C 149.1 (C, C-1), [147.3, 143.6 (C, C-15, C-18)], 131.3 (C, C-12), 129.0 (CH, C-10), [121.0, 117.8, 116.9 (CH, C-13, C-14, C-19)], 116.4 (C, C-7), 67.5 (CH₂, C-9), 64.6 (CH₂, C-16 or C-17), 64.4 (CH, C-3), 64.3 (CH₂, C-16 or C-17), [51.6, 50.7 (CH₂, C-4, C-5)], 50.1 (CH₂, C-8), 38.7 (CH₃, C-11), 27.1 (CH₂, C-2), 24.3 (CH₂, C-6).

ESI-LRMS (+): m/z 449.2 ([M+H]⁺, 100%).

HRMS: Found [M+H]⁺ 449.1844. C₂₁H₂₉N₄O₅S requires M+H, 449.1853.

N-ethyl-2-methyl-8-morpholino-2,4,5,7,8,9-hexahydro-6*H*-pyrazolo[4,3-*d*]azocine-6-carboxamide (166d1)
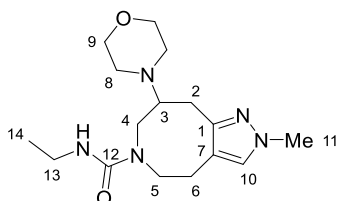
General procedure 7 (page 299) was followed, using building block **166 •2 HCl** (0.103 mmol) as the starting material and **d1** as the electrophile. Urea **166d1** was obtained as a white solid (23.5 mg, 71%).

v$_{max}$ (neat / cm^{-1}): 3355 w (N–H), 2922 m, 2848 m, 1633 s (C=O), 1264 s, 1115 s.

^{1}H-NMR (400 MHz, CDCl$_3$) δ_H 8.66 (br s, 1H, N*H*), 7.03 (s, 1H, H-10), 4.76 (app dt, *J* = 13.8, 3.4 Hz, 1H, H-5), 3.81 – 3.64 (stack, 8H, [including 3.78 (s, 3H, H-11)], H-4, H-9, H-11), 3.35 – 3.13 (m, 2H, H-13), 3.03 – 2.90 (m, 1H, H-2), 2.84 – 2.69 (stack, 3H, H-4, H-8), 2.66 – 2.49 (stack, 6H, H-2, H-3, H-6, H-8), 2.41 – 2.29 (m, 1H, H-5), 1.15 (t, *J* = 7.2 Hz, 3H, H-14).

^{13}C-NMR (101 MHz, CDCl$_3$) δ_C 160.1 (C, C-12), 148.1 (C, C-1), 129.1 (CH, C-10), 119.3 (C, C-7), 67.5 (CH, C-3), 67.2 (CH$_2$, C-9), 52.5 (CH$_2$, C-5), 51.7 (CH$_2$, C-4), 51.4 (CH$_2$, C-8), 38.6 (CH$_3$, C-11), 35.2 (CH$_2$, C-13), 25.9 (CH$_2$, C-6), 25.0 (CH$_2$, C-2), 16.7 (CH$_3$, C-14).

ESI-LRMS (+): m/z 322.3 ([M+H]$^+$, 100%).

HRMS: Found [M+H]$^+$ 322.2236. C$_{16}$H$_{28}$N$_5$O$_2$ requires M+H, 322.2238.

1-(2-methyl-8-morpholino-2,4,5,7,8,9-hexahydro-6*H*-pyrazolo[4,3-*d*]azocin-6-yl)-2-(tetrahydro-2*H*-pyran-4-yl)ethan-1-one (166c2)
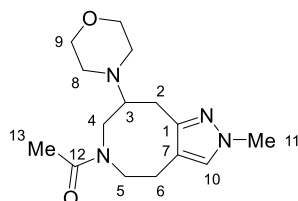
General procedure 8 (page 299) was followed, using building block **166 •2 HCl** (0.103 mmol) as the starting material and **c2** as the carboxylic acid. Amide **166c2** was obtained as an off-white solid (14.6 mg, 48%).

***v*~max~ (neat / cm⁻¹):** 2948 m, 2844 m, 1621 s (C=O), 1415 s, 1249 s, 1111 s.

¹H-NMR (400 MHz, CDCl₃) (mixture of rotamers, 2:1)[a] δ_H 7.09 − 7.04 (stack, 1H, H-10), 4.42 − 4.33 (m, 0.33H, H-5 min), 4.08 (dd, *J* = 13.1, 3.7 Hz, 0.67H, H-4 maj), 3.83 − 3.58 (stack, 8H, [including 3.78 (s, 2H, H-11 maj), 3.76 (s, 1H, H-11 min)], H-4 min, H-5 maj, H-9, H-11), 3.22 − 3.09 (stack, 1.33H, H-3 maj, H-5 maj), 3.00 − 2.89 (m, 0.33H, H-2 min), 2.88 − 2.56 (stack, 9.33H, H-2 maj, H-2 min, H-3 min, H-4 maj, H-4 min, H-5 min, H-6, H-8), [2.06 (s, 1H, H-13 min), 1.91 (s, 2H, H-13 maj)].

¹³C-NMR (101 MHz, CDCl₃) (mixture of rotamers) δ_C [171.7 (C, C-12 min), 170.8 (C, C-12 maj)], [149.5 (C, C-1 maj), 148.5 (C, C-1 min)], [129.4 (CH, C-10 min), 128.6 (CH, C-10 maj)], [116.8 (C, C-7 min), 115.9 (C, C-7 maj)], [67.6 (CH₂, C-9 maj), 67.4 (CH₂, C-9 min)], [64.6 (CH, C-3 min), 60.6 (CH, C-3 maj)], 53.0 (CH₂, C-4 min), 51.8 (CH₂, C-5 maj), 50.3 (CH₂, C-4 maj), [50.1 (CH₂, C-8 min), 50.0 (CH₂, C-8 maj)], 48.4 (CH₂, C-5 min), 38.7 (CH₃, C-11), [26.9 (CH₂, C-2 maj), 26.0 (CH₂, C-2 min)], [24.0 (CH₂, C-6 maj), 22.8 (CH₂, C-6 min)], [22.5 CH₃, C-13 maj), 21.8 (CH₃, C-13 min)].

ESI-LRMS (+): m/z 293.3 ([M+H]⁺, 100%).

HRMS: Found [M+H]⁺ 293.1966. C₁₅H₂₅N₄O₂ requires M+H, 293.1972.

---

[a] Ratio based on H-5 and H-4 peak integrations in the reported ¹H-NMR spectrum at δ_H (CDCl₃) 4.42 − 4.33 and 4.08 ppm, respectively.

7-((2,3-dihydrobenzo[*b*][1,4]dioxin-6-yl)sulfonyl)-9-morpholino-5,6,7,8,9,10-hexahydropyrimido[5,4-*d*]azocin-2-amine (169a7)
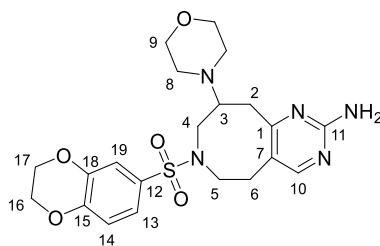
General procedure 7 (page 299) was followed, using building block **169 •3 HCl** (0.092 mmol) as the starting material and **a7** as the electrophile. Sulfonamide **169a7** was obtained as an off-white solid (7.6 mg, 9%).

v_{max} (neat / cm^{-1}): 3462 w (N–H), 3179 w, 1640 m, 1495 s, 1286 v s, 1148 s.

^{1}H-NMR (400 MHz, CDCl$_3$) δ_H 7.88 (s, 1H, H-10), 7.20 (d, *J* = 2.2 Hz, 1H, H-19), 7.11 (dd, *J* = 8.5, 2.2 Hz, 1H, H-13), 6.91 (d, *J* = 8.5 Hz, 1H, H-14), 4.90 (s, 2H, N*H*$_2$), 4.35 − 4.26 (stack, 4H, H-16, H-17), 3.83 − 3.66 (stack, 5H, H-4, H-9), 3.50 (app dt, *J* = 12.7, 8.4 Hz, 1H, H-5), 3.03 (app tt, *J* = 10.1, 3.4 Hz, 1H, H-3), 2.98 − 2.81 (stack, 3H, H-2, H-5), 2.78 − 2.63 (stack, 7H, H-4, H-6, H-8).

^{13}C-NMR (101 MHz, CDCl$_3$) δ_C 168.8 (C, C-1), 162.2 (C, C-11), 157.6 (CH, C-10), 147.5 (C, C-15), 143.6 (C, C-18), 131.1 (C, C-12), 120.9 (CH, C-13), 119.9 (C, C-7), 118.0 (CH, C-14), 116.9 (CH, C-19), 67.5 (CH$_2$, C-9), 64.7 (CH$_2$, C-16 or C-17), 64.5 (CH, C-3), 64.3 (CH$_2$, C-16 or C-17), 50.8 (CH$_2$, C-4), 50.5 (CH$_2$, C-5), 49.6 (CH$_2$, C-8), 37.2 (CH$_2$, C-2), 28.5 (CH$_2$, C-6).

ESI-LRMS (+): m/z 462.2 ([M+H]$^+$, 100%).

HRMS: Found [M+H]$^+$ 462.1798. C$_{21}$H$_{28}$N$_5$O$_5$S requires M+H, 462.1806.

2-amino-*N*-ethyl-9-morpholino-5,8,9,10-tetrahydropyrimido[5,4-*d*]azocine-7(6*H*)-carboxamide (169d1)
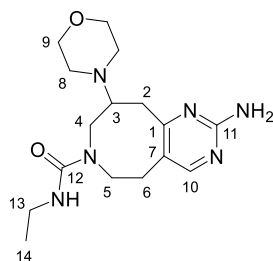
General procedure 7 (page 299) was followed, using building block **169** •**3 HCl** (0.092 mmol) as the starting material and **d1** as the electrophile. Urea **169d1** was obtained as an off-white powder (21.5 mg, 70%).

***v*~max~ (neat / cm⁻¹):** 3411 w (N–H), 3176 w, 2960 w, 2844 w, 1640 s (C=O), 1558 s, 1469 s, 1111 s.

¹H-NMR (400 MHz, CDCl₃) δ_H 8.25 (app s, 1H, EtN*H*CO), 8.00 (s, 1H, H-10), 5.02 (s, 2H, N*H*₂), 4.95 – 4.75 (m, 1H, H-5), 3.83 – 3.64 (stack, 5H, H-4, H-9), 3.35 – 3.08 (m, 2H, H-13), 2.97 – 2.85 (m, 1H, H-2), 2.85 – 2.52 (stack, 9H, H-2, H-3, H-4, H-6, H-8), 2.49 – 2.33 (m, 1H, H-5), 1.15 (t, *J* = 7.2 Hz, 3H, H-14).

¹³C-NMR (101 MHz, CDCl₃) δ_C 167.9 (C, C-11), 162.1 (C, C-1), 160.1 (C, C-12), 158.9 (CH, C-10), 123.0 (C, C-7), 67.3 (CH₂, C-9), 67.1 (CH, C-3), [51.3, 50.9 (CH₂, C-4, C-5, C-8, resonance overlap)], 35.3 (CH₂, C-13), 33.9 (CH₂, C-2), 32.1 (CH₂, C-6), 16.6 (CH₃, C-14).

ESI-LRMS (+): m/z 335.3 ([M+H]⁺, 100%).

HRMS: Found [M+H]⁺ 335.2184. C₁₆H₂₇N₆O₂ requires M+H, 335.2190.

2-amino-*N*-(4-(difluoromethoxy)phenyl)-9-morpholino-5,8,9,10-tetrahydropyrimido[5,4-*d*]azocine-7(6*H*)-carboxamide (169d3)
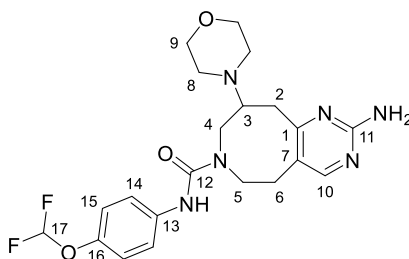
General procedure 7 (page 299) was followed, using building block **169 •3 HCl** (0.092 mmol) as the starting material and **d3** as the electrophile. Urea **169d3** was obtained as a yellow glass (17.8 mg, 43%).

***v*~max~ (neat / cm⁻¹):** 3399 w (N–H), 3176 w, 2945 w, 1633 s (C=O), 1554 s, 1469 s, 1111 v s.

¹H-NMR (400 MHz, DMSO-*d₆*) δ_H 7.98 (s, 1H, H-10), 7.24 − 7.16 (AA' of AA'BB', 2H, H-14), 7.08 (t, $J_{H–F}$ = 74.2 Hz, 1H, H-17), 7.04 − 6.98 (BB' of AA'BB', 2H, H-15), 6.28 (s, 2H, N*H₂*), 3.84 − 3.39 (stack, 7H, H-4, H-5, H-9), 3.39 − 3.18 (m, 1H, H-4), 2.96 − 2.87 (m, 1H, H-3), 2.87 − 2.73 (stack, 2H, H-2, H-6), 2.71 − 2.52 (stack, 6H, H-2, H-6, H-8), urea NH not observed.

¹³C-NMR (101 MHz, DMSO-*d₆*) δ_C 167.9 (C, C-11), 162.5 (C, C-1), 158.1 (CH, C-10), 155.2 (C, C-12), 145.5 (C, C-16), 137.5 (C, C-13), 121.9 (CH, C-14), 119.1 (CH, C-15), 116.6 (CH, t, $J_{C–F}$ = 256.6 Hz, C-17), 66.5 (CH_2, C-9), 63.4 (CH, C-3), 50.7 (CH_2, C-4), 49.6 (CH_2, C-8), 48.1 (CH_2, C-5), 34.6 (CH_2, C-2), 28.2 (CH_2, C-6). C-7 resonance not observed, but HMBC data indicate it may overlap with the resonance at δ_C 119.1 ppm.

ESI-LRMS (+): m/z 449.3 ([M+H]⁺, 100%).

HRMS: Found [M+H]⁺ 449.2101. $C_{21}H_{27}F_2N_6O_3$ requires M+H, 449.2107.

1-(2-amino-9-morpholino-5,8,9,10-tetrahydropyrimido[5,4-*d*]azocin-7(6*H*)-yl)-2-(tetrahydro-2*H*-pyran-4-yl)ethan-1-one (169c1)
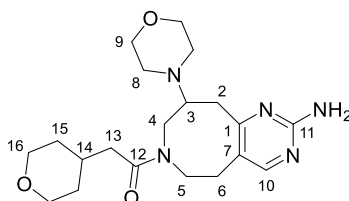
General procedure 8 (page 299) was followed, using building block **169 •3 HCl** (0.092 mmol) as the starting material and **c1** as the carboxylic acid. Amide **169c1** was obtained as a yellow solid (13.3 mg, 37%).

***v*~max~ (neat / cm⁻¹):** 3418 w (N–H), 3302 w, 3198 w, 2922 w, 1625 v s (C=O), 1457 s, 1107 s.

¹H-NMR (400 MHz, CDCl₃) (mixture of rotamers, 3:1)ᵃ δ_H [8.00 (s, 0.75H, H-10 maj), 7.99 (s, 0.25H, H-10 min)], [4.97 (s, 1.5H, N*H₂* maj), 4.91 (s, 0.5H, N*H₂* min)], 4.55 − 4.43 (m, 0.25H, H-5 min), 4.32 − 4.22 (m, 0.75H, H-4 maj), 3.92 − 3.79 (stack, 2.25H, H-4 min, H-16), 3.79 − 3.65 (stack, 4H, H-9), 3.60 (ddd, *J* = 14.0, 11.7, 5.6 Hz, 0.75H, H-5 maj), 3.39 − 3.22 (stack, 2.75H, H-5 maj, H-16), 3.19 − 3.06 (stack, 1H, H-3 maj, H-4 min), 2.95 − 2.57 (stack, 9.25H, H-2, H-3 min, H-4 maj, H-5 min, H-6, H-8), 2.22 − 2.13 (m, 0.25H, H-13 min), 2.05 − 1.88 (stack, 1.25H, H-13, H-14 min), 1.88 − 1.72 (m, 0.75H, H-14 maj), 1.64 (B of ABX, *J*~B–A~ = 15.2, *J*~B–X~ = 7.0 Hz, 0.75H, H-13 maj), 1.58 − 1.40 (stack, 1H, H-15), 1.35 − 0.85 (stack, 3H, H-15).

¹³C-NMR (101 MHz, CDCl₃) (mixture of rotamers) δ_C [172.1 (C, C-12 min), 171.5 (C, C-12 maj)], [169.6 (C, C-11 maj), 168.1 (C, C-11 min)], [162.3 (C, C-1 maj), 162.2 (C, C-1 min)], [158.5 (CH, C-10 min), 157.3 (CH, C-10 maj)], [119.7 (C, C-7 min), 119.2 (C, C-7 maj)], [68.0, 67.93, 67.88, 67.5, 67.3 (CH₂, C-9, C-16)], [64.8 (CH, C-3 min), 60.7 (CH, C-3 maj)], [52.6 (CH₂, C-4 min), 50.3 (CH₂, C-4 maj)], [49.6, 49.5, 49.3 (CH₂, C-5 maj, C-8)], 46.6, (CH₂, C-5 min), [40.5 (CH₂, C-13 maj), 39.7 (CH₂, C-13 min)], [38.1 (CH₂, C-2 maj), 35.2 (CH₂, C-2 min)], [33.04 (CH₂, C-15 min), 33.02 (CH₂, C-15 maj), 32.8 (CH₂, C-15 maj), 32.6 (CH₂, C-15 min)], [32.3 (CH, C-14 min), 31.7 (CH, C-14 maj)], [28.4 (CH₂, C-6 maj), 27.5 (CH₂, C-6 min)].

ESI-LRMS (+): m/z 390.3 ([M+H]⁺, 100%).

HRMS: Found [M+H]⁺ 390.2491. C₂₀H₃₂N₅O₃ requires M+H, 390.2500.

ᵃ Ratio based on N*H₂*, H-5 and H-4 resonance integrations in the reported ¹H-NMR spectrum at δ_H (CDCl₃) [8.00, 7.99], [4.97, 4.91], 4.55 − 4.43 and 4.32 − 4.22 ppm, respectively.

1-(2-amino-9-morpholino-5,8,9,10-tetrahydropyrimido[5,4-*d*]azocin-7(6*H*)-yl)ethan-1-one (169c2)
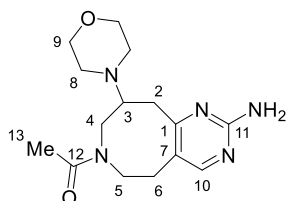
General procedure 8 (page 299) was followed, using building block **169 •3 HCl** (0.092 mmol) as the starting material and **c2** as the carboxylic acid. Amide **169c2** was obtained as a yellow solid (19.7 mg, 70%).

v_{max} (neat / cm^{-1}): 3321 m (NH$_2$), 3183 m, 1633 v s (C=O), 1461 s, 1416 s, 1111 m.

^{1}H-NMR (400 MHz, CDCl$_3$) (mixture of rotamers, 3:1)[a] δ_H [8.01 (s, 0.25H, H-10 min), 7.99 (s, 0.75H, H-10 maj)], [5.02 (s, 1.5H, N*H*$_2$ maj), 4.98 (s, 0.5H, N*H*$_2$ min)], 4.48 − 4.37 (m, 0.25H, H-5 min), 4.30 − 4.18 (m, 0.75H, H-4 maj), 3.91 − 3.79 (m, 0.25H, H-4 min), 3.79 − 3.64 (stack, 4H, H-9), [3.55 (ddd, *J* = 14.0, 11.4, 5.6 Hz, 0.75H, H-5 maj), 3.32 (ddd, *J* = 14.0, 6.1, 2.2 Hz, 0.75H, H-5 maj)], 3.23 − 3.10 (stack, 1H, H-3 maj, H-4 min), 2.92 − 2.58 (stack, 9.25H, H-2, H-3 min, H-4 maj, H-5 min, H-6, H-8), [1.98 (s, 0.75H, H-13 min), 1.70 (s, 2.25H, H-13 maj)].

^{13}C-NMR (101 MHz, CDCl$_3$) (mixture of rotamers) δ_C [171.3 (C, C-12 min), 170.7 (C, C-12 maj)], [169.7 (C, C-11 maj), 167.9 (C, C-11 min)], [162.4 (C, C-1 maj), 162.2 (C, C-1 min)], [158.5 (CH, C-10 min), 157.2 (CH, C-10 maj)], [120.0 (C, C-7 min), 119.1 (C, C-7 maj)], [67.5 (CH$_2$, C-9 maj), 67.3 (CH$_2$, C-9 min)], [64.6 (CH, C-3 min), 60.5 (CH, C-3 maj)], 52.9 (CH$_2$, C-4 min), [50.6, 50.4 (CH$_2$, C-4 maj, C-5 maj)], [49.7 (CH$_2$, C-8 min), 49.3 (CH$_2$, C-8 maj)], 46.8 (CH$_2$, C-5 min), [37.4 (CH$_2$, C-2 maj), 35.5 (CH$_2$, C-2 min)], [28.4 (CH$_2$, C-6 maj), 27.9 (CH$_2$, C-6 min)], [22.4 (CH$_3$, C-13 maj), 21.3 (CH$_3$, C-13 min)].

ESI-LRMS (+): m/z 306.3 ([M+H]$^+$, 100%).

HRMS: Found [M+H]$^+$ 306.1920. C$_{15}$H$_{24}$N$_5$O$_2$ requires M+H, 306.1925.

---

[a] Ratio based on H-5 and H-4 resonance integrations in the reported ^{1}H-NMR spectrum at δ_H (CDCl$_3$) 4.48 − 4.37, [4.30 − 4.18, 3.91 − 3.79] ppm, respectively.

4-(6-methylsulfonyl-1-propyl-4,5,6,7,8,9-hexahydro-1*H*-pyrazolo[4,3-*d*]azocin-8-yl)morpholine (164a5)
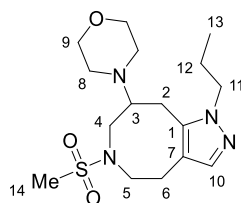
General procedure 7 (page 299) was followed, using building block **164** •**2 HCl** (0.310 mmol) as the starting material and **a5** as the electrophile. Sulfonamide **164a5** was obtained as a colourless oil (77.0 mg, 70%).

*v*_{max} (neat / cm⁻¹): 2941 w, 1454 w, 1409 w, 1320 s, 1137 v s.

¹H-NMR (400 MHz, CDCl₃) δ_H 7.22 (s, 1H, H-10), 4.12 − 3.90 (m, 2H, H-11), 3.70 − 3.60 (stack, 4H, H-9), 3.60 − 3.48 (m, 1H, H-4), 3.44 (ddd, *J* = 13.0, 7.8, 4.5 Hz, 1H, H-5), 3.09 (ddd, *J* = 13.0, 6.9, 4.2 Hz, 1H, H-5), 3.02 − 2.88 (stack, 3H, H-2, H-3, H-4), 2.83 − 2.65 (stack, 2H, H-2, H-6), 2.65 − 2.49 (stack, 8H, [including 2.60 (s, 3H, H-14)], H-6, H-8, H-14), 1.86 − 1.73 (m, 2H, H-12), 0.89 (t, *J* = 7.4 Hz, 3H, H-13).

¹³C-NMR (101 MHz, CDCl₃) δ_C 137.8 (CH, C-10), 137.6 (C, C-1), 115.4 (C, C-7), 67.3 (CH₂, C-9), 63.4 (CH, C-3), 51.01 (CH₂, C-11), 50.96 (CH₂, C-5), 50.0 (CH₂, C-8), 49.4 (CH₂, C-4), 37.3 (CH₃, C-14), 25.0 (CH₂, C-2), 24.8 (CH₂, C-6), 23.9 (CH₂, C-12), 11.3 (CH₃, C-13).

ESI-LRMS (+): m/z 357.3 ([M+H]⁺, 100%).

HRMS: Found [M+H]⁺ 357.1958. C₁₆H₂₉N₄O₃S requires M+H, 357.1955.

N-ethyl-8-morpholino-1-propyl-1,4,5,7,8,9-hexahydro-6*H*-pyrazolo[4,3-*d*]azocine-6-carboxamide (164d1)
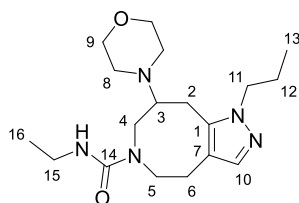
General procedure 7 (page 299) was followed, using building block **164 •2 HCl** (0.310 mmol) as the starting material and **d1** as the electrophile. Urea **164d1** was obtained as a colourless oil (77.5 mg, 72%).

***v*max (neat / cm⁻¹):** 2963 m, 2833 m, 1636 s (C=O), 1457 m, 1264 s, 1118 s.

¹H-NMR (400 MHz, CDCl₃) δ_H 7.93 (br s, 1H, N*H*), 7.17 (s, 1H, H-10), 4.62 − 4.43 (m, 1H, H-5), 4.02 − 3.79 (m, 2H, H-11), 3.79 − 3.55 (stack, 5H, H-4, H-9), 3.29 − 3.08 (m, 2H, H-15), 2.90 − 2.76 (stack, 2H, H-2, H-4), 2.76 − 2.63 (stack, 3H, H-2, H-8), 2.63 − 2.30 (stack, 6H, H-3, H-5, H-6, H-8), 1.90 − 1.72 (m, 2H, H-12), 1.09 (t, *J* = 7.2 Hz, 3H, H-16), 0.88 (t, *J* = 7.4 Hz, 3H, H-13).

¹³C-NMR (101 MHz, CDCl₃) δ_C 159.6 (C, C-14), 138.0 (CH, C-10), 136.1 (C, C-1), 118.4 (C, C-7), 67.0 (CH₂, C-9), 65.6 (CH, C-3), 52.0 (CH₂, C-5), 51.4 (CH₂, C-8), 51.1 (CH₂, C-4), 50.7 (CH₂, C-11), 35.2 (CH₂, C-15), 26.2 (CH₂, C-6), 23.8 (CH₂, C-12), 22.3 (CH₂, C-2), 16.4 (CH₃, C-16), 11.3 (CH₃, C-13).

ESI-LRMS (+): m/z 350.3 ([M+H]⁺, 100%).

HRMS: Found [M+H]⁺ 350.2545. $C_{18}H_{32}N_5O_2$ requires M+H, 350.2551.

4-(2-((2,4-dimethylthiazol-5-yl)methyl)-6-(morpholinosulfonyl)-4,5,6,7,8,9-hexahydro-2*H*-pyrazolo[4,3-*d*]azocin-8-yl)morpholine (168a4)
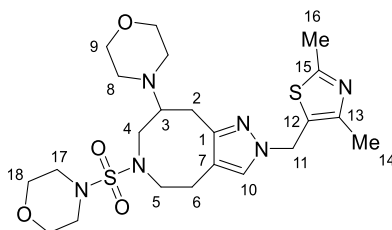
General procedure 7 (page 299) was followed, using building block **168 • 2 HCl** (0.098 mmol) as the starting material and **a4** as the electrophile. Sulfonamide **168a4** was obtained as an off-white solid (28.7 mg, 57%).

*v*_{max} **(neat / cm⁻¹):** 2919 m, 2855 m, 1450 m, 1331 m, 1144 s, 1111 v s.

¹H-NMR (400 MHz, CDCl₃) δ_H 7.07 (s, 1H, H-10), 5.24 (A of AB, J_{A-B} = 15.5 Hz, 1H, H-11), 5.18 (B of AB, J_{B-A} = 15.5 Hz, 1H), 3.86 – 3.78 (m, 1H, H-4), 3.71 – 3.62 (m, 4H, H-18), 3.62 – 3.50 (stack, 4H, H-9), 3.45 (ddd, J = 13.0, 9.5, 4.9 Hz, 1H, H-5), 3.07 – 2.75 (stack, 9H, H-2, H-3, H-4, H-5, H-8), 2.75 – 2.67 (stack, 3H, H-6, H-17), 2.67 – 2.53 (stack, 6H, [including 2.60 (s, 3H, H-16)], H-6, H-17, H-16), 2.39 (s, 3H, H-14).

¹³C-NMR (101 MHz, CDCl₃) δ_C 165.0 (C, C-15), [150.2, 150.1 (C, C-1, C-13)], 127.3 (CH, C-10), 125.3 (C, C-12), 117.1 (C, C-7), 67.5 (CH₂, C-18), 66.3 (CH₂, C-9), 63.3 (CH, C-3), 51.1 (CH₂, C-4, C-5, resonance overlap), 49.9 (CH₂, C-17), 47.1 (CH₂, C-11), 46.1 (CH₂, C-8), 27.5 (CH₂, C-2), 23.6 (CH₂, C-6), 19.3 (CH₃, C-16), 15.1 (CH₃, C-14).

ESI-LRMS (+): m/z 511.3 ([M+H]⁺, 100%).

HRMS: Found [M+H]⁺ 511.2169. C₂₂H₃₅N₆O₄S₂ requires M+H, 511.2156.

4-(6-((2,3-dihydrobenzo[*b*][1,4]dioxin-6-yl)sulfonyl)-2-((2,4-dimethylthiazol-5-yl)methyl)-4,5,6,7,8,9-hexahydro-2*H*-pyrazolo[4,3-*d*]azocin-8-yl)morpholine (168a7)
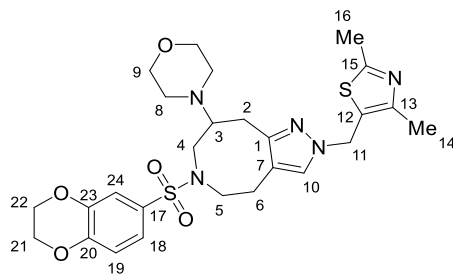
General procedure 7 (page 299) was followed, using building block **168 •2 HCl** (0.098 mmol) as the starting material and **a7** as the electrophile. Sulfonamide **168a7** was obtained as an off-white powder (32.0 mg, 58%).

v$_{max}$ (neat / cm^{-1}): 2922 w, 2851 w, 1491 m, 1334 m, 1282 s, 1148 s, 11145 s.

^{1}H-NMR (400 MHz, CDCl₃) δ_H 7.25 (d, *J* = 2.2 Hz, 1H, H-24), 7.22 (dd, *J* = 8.5, 2.2 Hz, 1H, H-18), 7.01 (s, 1H, H-10), 6.91 (d, *J* = 8.5 Hz, 1H, H-19), 5.25 (A of AB, *J*$_{A–B}$ = 15.5 Hz, 1H, H-11), 5.19 (B of AB, *J*$_{B–A}$ = 15.5 Hz, 1H, H-11), 4.33 – 4.24 (stack, 4H, H-21, H-22), 3.75 – 3.58 (stack, 5H, H-5, H-9), 3.53 (dd, *J* = 14.5, 3.7 Hz, 1H, H-4), 3.14 – 3.01 (stack, 2H, H-3, H-2), 2.92 (dd, *J* = 14.1, 6.1 Hz, 1H, H-2), 2.78 – 2.52 (stack, 11H, [including 2.59 (s, 3H, H-16)], H-4, H-5, H-6, H-8, H-16), 2.37 (s, 3H, H-14).

^{13}C-NMR (101 MHz, CDCl₃) δ_C 164.8 (C, C-15), [149.9, 149.5 (C, C-1, C-13)], [147.4, 143.6 (C, C-20, C-23)], 131.2 (C-17), 127.4 (CH, C-10), 125.7 (C, C-12), 121.0 (CH, C-18), 117.8 (CH, C-19), 117.4 (C, C-7), 116.9 (CH, C-24), 67.5 (CH₂, C-9), [64.6, 64.3 (CH₂, C-21, C-22)], 64.2 (CH, C-3), 51.8 (CH₂, C-5), 50.6 (CH₂, C-4), 50.1 (CH₂, C-8), 47.1 (CH₂, C-11), 26.9 (CH₂, C-2), 24.8 (CH₂, C-6), 19.3 (CH₃, C-16), 15.1 (CH₃, C-14).

ESI-LRMS (+): m/z 560.3 ([M+H]⁺, 100%).

HRMS: Found [M+H]⁺ 560.2012. C₂₆H₃₄N₅O₅S₂ requires M+H, 560.1996.

2-((2,4-dimethylthiazol-5-yl)methyl)-*N*-ethyl-8-morpholino-2,4,5,7,8,9-hexahydro-6*H*-pyrazolo[4,3-*d*]azocine-6-carboxamide (168d1)
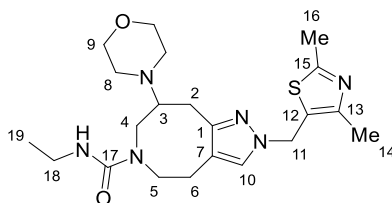
General procedure 7 (page 299) was followed, using building block **168 •2 HCl** (0.098 mmol) as the starting material and **d1** as the electrophile. Urea **168d1** was obtained as a beige powder (27.4 mg, 65%).

v_{max} (neat / cm^{-1}): 3385 w (N–H), 2963 m, 2851 m, 1636 s (C=O), 1450 m, 1264 s, 1115 s.

^{1}H-NMR (400 MHz, CDCl$_3$) δ_H 8.63 (s, 1H, N*H*), 7.01 (s, 1H, H-10), 5.24 (A of AB, $J_{A–B}$ = 15.7 Hz, 1H, H-11), 5.23 (B of AB, $J_{B–A}$ = 15.7 Hz, 1H, H-11), 4.73 (app dt, J = 14.2, 3.7 Hz, 1H, H-5), 3.83 − 3.60 (stack, 5H, H-4, H-9), 3.35 − 3.12 (m, 2H, H-18), 3.04 − 2.93 (m, 1H, H-2), 2.85 − 2.69 (stack, 3H, H-4, H-8), 2.68 − 2.46 (stack, 9H, [including 2.60 (s, 3H, H-16)], H-2, H-3, H-6, H-8, H-16), 2.40 − 2.26 (stack, 4H, [including 2.38 (s, 3H, H-14)], H-5, H-14), 1.15 (t, J = 7.2 Hz, 3H, H-19).

^{13}C-NMR (101 MHz, CDCl$_3$) δ_C 164.9 (C, C-15), 160.1 (C, C-17), 150.1 (C, C-13), 148.7 (C, C-1), 127.6 (CH, C-10), 125.4 (C, C-12), 120.1 (C, C-7), 67.4 (CH, C-3), 67.2 (CH$_2$, C-9), 52.4 (CH$_2$, C-5), [51.7, 51.4 (CH$_2$, C-4, C-8)], 47.2 (CH$_2$, C-11), 35.2 (CH$_2$, C-18), 26.0 (CH$_2$, C-6), 25.0 (CH$_2$, C-2), 19.3 (CH$_3$, C-16), 16.7 (CH$_3$, C-19), 15.1 (CH$_3$, C-14).

ESI-LRMS (+): m/z 433.3 ([M+H]$^+$, 100%).

HRMS: Found [M+H]$^+$ 433.2387. C$_{21}$H$_{33}$N$_6$O$_2$S requires M+H, 433.2380.

1-(2-((2,4-dimethylthiazol-5-yl)methyl)-8-morpholino-2,4,5,7,8,9-hexahydro-6*H*-pyrazolo[4,3-*d*]azocin-6-yl)ethan-1-one (168c2)
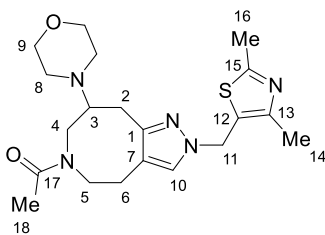
General procedure 8 (page 299) was followed, using building block **168 •2 HCl** (0.098 mmol) as the starting material and **c2** as the carboxylic acid. Amide **168c2** was obtained as a yellow oil (22.1 mg, 56%).

v$_{max}$ (neat / cm^{-1}): 2930 m, 2855 m, 1629 s (C=O), 1416 s, 1252 m, 1115 s.

^{1}H-NMR (400 MHz, CDCl$_3$) (mixture of rotamers, 2:1)[a] δ_H [7.05 (s, 0.33H, H-10 min), 7.04 (s, 0.67H, H-10 maj)], 5.26 – 5.15 (stack, 2H, H-11), 4.42 – 4.33 (m, 0.33H, H-5 min), 4.07 (dd, *J* = 13.1, 3.7 Hz, 0.67H, H-4 maj), 3.78 (dd, *J* = 14.3, 3.3 Hz, 0.33H, H-4 min), 3.74 – 3.59 (stack, 4.67H, H-5 maj, H-9), 3.29 – 3.14 (m, 0.67H, H-3 maj), 3.14 – 3.05 (stack, 1H, H-4 min, H-5 maj), 2.95 – 2.52 (stack, 12.33H, [including 2.60 (s, 2H, H-16 maj), 2.59 (s, 1H, H-16 min)], H-2, H-3 min, H-4 maj, H-5 min, H-6, H-8, H-16), [2.37 (s, 2H, H-14 maj), 2.37 (s, 1H, H-14 min)], [2.05 (s, 1H, H-18 min), 1.87 (s, 2H, H-18 maj)].

^{13}C-NMR (101 MHz, CDCl$_3$) (mixture of rotamers) δ_C [171.5 (C, C-17 min), 170.8 (C, C-17 maj)], [164.9 (C, C-15 maj), 164.8 (C, C-15 min)], [150.0, 149.9, 148.9 (C, C-1, C-13)], [127.8 (CH, C-10 min), 127.0 (CH, C-10 maj)], [125.6 (C, C-12 min), 125.6 (C, C-12 maj)], [117.8 (C, C-7 min), 116.8 (C, C-7 maj)], [67.6 (CH$_2$, C-9 maj), 67.4 (CH$_2$, C-9 min)], [64.3 (CH, C-3 min), 60.3 (CH, C-3 maj)], 52.7 (CH$_2$, C-4 min), 51.7 (CH$_2$, C-5 maj), [50.11, 50.08 (CH$_2$, C-4 maj, C-8 min)], 49.9 (CH$_2$, C-8 maj), 48.7 (CH$_2$, C-5 min), [47.14 (CH$_2$, C-11 min), 47.11 (CH$_2$, C-11 maj)], [27.0 (CH$_2$, C-2 maj), 25.9 (CH$_2$, C-2 min)], [24.0 (CH$_2$, C-6 maj), 23.1 (CH$_2$, C-6 min)], [22.4 (CH$_3$, C-18 maj), 21.7 (CH$_3$, C-18 min)], 19.3 (CH$_3$, C-16), [15.1 (CH$_3$, C-14 maj), 14.9 (CH$_2$, C-14 min)].

ESI-LRMS (+): m/z 404.3 ([M+H]$^+$, 100%).

HRMS: Found [M+H]$^+$ 404.2124. C$_{20}$H$_{30}$N$_5$O$_2$S requires M+H, 404.2115.

---

[a] Ratio based on H-10 and H-18 peak integrations in the reported ^{1}H-NMR spectrum.

(2-((2,4-dimethylthiazol-5-yl)methyl)-8-morpholino-2,4,5,7,8,9-hexahydro-6*H*-pyrazolo[4,3-*d*]azocin-6-yl)(2-methylpyridin-3-yl)methanone (168c5)
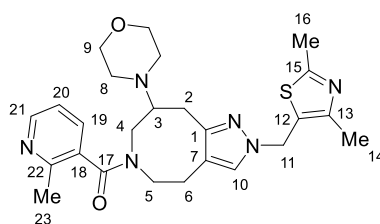
General procedure 8 (page 299) was followed, using building block **168 •2 HCl** (0.098 mmol) as the starting material and **c5** as the carboxylic acid. Amide **168c5** was obtained as a yellow oil (28.6 mg, 61%).

v~max~ (neat / cm⁻¹): 2945 w, 2855 w, 1625 s (C=O), 1416 s, 1133 m, 1150 s.

¹H-NMR (400 MHz, CDCl₃) (mixture of rotamers, 4:1)[a] δ_H [8.48 (dd, *J* = 4.8, 1.8 Hz, 0.2H, H-21 min), 8.41 (dd, *J* = 4.7, 1.9 Hz, 0.8H, H-21 maj)], 7.22 − 6.56 (stack, 2.2H, [including 7.15 (s, 0.2H, H-10 min), 6.94 (s, 0.8H, H-10 maj), 6.89 − 6.56 (m, 0.8H, H-20 maj)], H-10, H-19 min, H-20), 6.56 − 6.26 (m, 0.8H, H-19 maj), 5.42 − 5.16 (stack, 2H, H-11), 4.55 (ddd, *J* = 13.5, 8.3, 5.5 Hz, 0.2H, H-5 min), 4.41 − 4.00 (m, 0.8H, H-4 maj), [3.78 − 3.64 (stack, 3.2H, H-9 maj), 3.50 − 3.42 (stack, 0.8H, H-9 min)], 3.35 − 2.86 (stack, 4.8H, H-2, H-3 maj, H-4, H-5), 2.86 − 2.67 (stack, 4.2H, H-2, H-8 maj), 2.67 − 2.48 (stack, 5H, [including 2.61 (s, 2.4H, H-16 maj), 2.59 (s, 0.6H, H-16 min)], H-6, H-16), 2.48 − 2.11 (stack, 7H, [including 2.42 (s, 3H, H-14), 2.40 (s, 2.4H, H-23 maj)], H-3 min, H-8 min, H-14, H-23).

¹³C-NMR (101 MHz, CDCl₃) (mixture of rotamers) δ_C 170.3 (C, C-17), [165.2, 164.9 (C, C-15)], 154.5 (C, C-22), [150.4, 150.2 (C, C-1, C-13), [149.5, 149.3 (CH, C-21)], 133.5 (CH, C-19), 132.1 (C, C-18), [128.1, 127.2 (CH, C-10)], 125.4 (C, C-12), 120.5 (CH, C-20), [116.8, 115.9 (C, C-7)], [67.6, 67.3 (CH₂, C-9)], 60.53 (CH, C-3), [51.1, 49.5, 49.2, 47.1, 47.1 (CH₂, C-4, C-5, C-8, C-11)], 28.1 (CH₂, C-2), [22.9, 22.4 (CH₂, C-6)], 22.1 (CH₃, C-23), [19.32, 19.28 (CH₃, C-16), 15.1 (CH₃, C-14).

ESI-LRMS (+): m/z 481.3 ([M+H]⁺, 100%).

HRMS: Found [M+H]⁺ 481.2376. C₂₅H₃₃N₆O₂S requires M+H, 481.2380.

---

[a] Ratio based on H-5 and H-4 peak integrations in the reported ¹H-NMR spectrum at δ_H (CDCl₃) 4.55 and 4.41 − 4.00 ppm, respectively.

4-(1-((2,4-dimethylthiazol-5-yl)methyl)-6-((2,4-dimethylthiazol-5-yl)sulfonyl)-4,5,6,7,8,9-hexahydro-1*H*-pyrazolo[4,3-*d*]azocin-8-yl)morpholine (167a3)
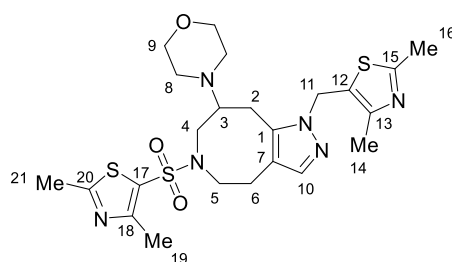
General procedure 7 (page 299) was followed, using building block **167 •2 HCl** (0.059 mmol) as the starting material and **a3** as the electrophile. Sulfonamide **167a3** was obtained as a brown oil (19.1 mg, 60%).

***v*$_{max}$ (neat / cm^{-1}):** 2952 m, 2855 m, 1450 m, 1342 s, 1156 s, 1115 s.

^{1}H-NMR (400 MHz, CDCl$_3$) δ_H 7.27 (s, 1H, H-10), 5.46 (A of AB, J_{A-B} = 15.7 Hz, 1H, H-11), 5.34 (B of AB, J_{B-A} = 15.7 Hz, 1H, H-11), 3.73 – 3.64 (stack, 4H, H-9), 3.64 – 3.47 (stack, 2H, H-4, H-5), 3.03 – 2.34 (stack, 23H, [including 3.03 – 2.93 (m, 1H, H-2), 2.93 – 2.82 (stack, 3H, H-2, H-3, H-5), 2.67 (s, 3H, H-21), 2.61 (s, 3H, H-19), 2.57 (s, 3H, H-16), 2.45 (s, 3H, H-14)], H-2, H-3, H-4, H-5, H-6, H-8, H-14, H-16, H-19, H-21).

^{13}C-NMR (101 MHz, CDCl$_3$) δ_C 168.6 (C, C-20), 165.1 (C, C-15), 156.1 (C, C-18), 148.5 (C, C-13), 138.5 (CH, C-10), 137.8 (C, C-1), 127.8 (C, C-17), 126.9 (C, C-12), 116.3 (C, C-7), 67.5 (CH$_2$, C-9), 63.4 (CH, C-3), 51.4 (CH$_2$, C-5), 50.0 (CH$_2$, C-8), 49.0 (CH$_2$, C-4), 46.0 (CH$_2$, C-11), 26.6 (CH$_2$, C-2), 24.5 (CH$_2$, C-6), [19.5, 19.3 (CH$_3$, C-16, C-21)], 16.9 (CH$_3$, C-19), 15.3 (CH$_3$, C-14).

ESI-LRMS (+): m/z 537.2 ([M+H]$^+$, 100%)..

HRMS: Found [M+H]$^+$ 537.1768. C$_{23}$H$_{33}$N$_6$O$_3$S$_3$ requires M+H, 537.1771.

1-((2,4-dimethylthiazol-5-yl)methyl)-*N*-ethyl-8-morpholino-1,4,5,7,8,9-hexahydro-6*H*-pyrazolo[4,3-*d*]azocine-6-carboxamide (167d1)
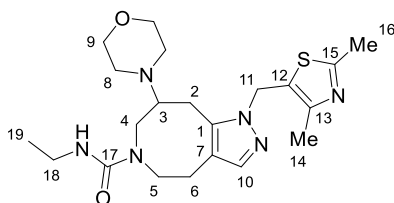
General procedure 7 (page 299) was followed, using building block **167 •2 HCl** (0.059 mmol) as the starting material and **d1** as the electrophile. Urea **167d1** was obtained as an off-white solid (15.3 mg, 60%).

***v*max (neat / cm⁻¹):** 3228 w (N–H), 2922 m, 2837 m, 1633 s (C=O), 1271 s, 1115 s.

¹H-NMR (400 MHz, CDCl₃) δ_H 8.04 (br s, 1H, N*H*), 7.28 (s, 1H, H-10), 5.35 (A of AB, $J_{A–B}$ = 16.0 Hz, 1H, H-11), 5.27 (B of AB, $J_{B–A}$ = 16.0 Hz, 1H, H-11), 4.71 − 4.53 (m, 1H, H-5), 3.84 − 3.57 (stack, 5H, H-4, H-9), 3.35 − 3.12 (m, 2H, H-18), 2.91 − 2.25 (stack, 17H, [including 2.58 (s, 3H, H-16), 2.43 (s, 3H, H-14), 2.36 − 2.25 (m, 1H, H-3)], H-2, H-3, H-4, H-5, H-6, H-8, H-14, H-16), 1.14 (t, *J* = 7.2 Hz, 3H, H-19).

¹³C-NMR (101 MHz, CDCl₃) δ_C 164.9 (C, C-15), 159.8 (C, C-17), 148.5 (C, C-13), 139.0 (CH, C-10), 136.2 (C, C-1), 126.7 (C, C-12), 119.9 (C, C-7), 67.1 (CH₂, C-9), 65.4 (CH, C-3), [52.0, 51.4 (CH₂, C-4, C-5, C-8, resonance overlap)], 45.8 (CH₂, C-11), 35.3 (CH₂, C-18), 26.5 (CH₂, C-2), 22.8 (CH₂, C-6), 19.3 (CH₃, C-16), 16.6 (CH₃, C-19), 15.6 (CH₃, C-14).

ESI-LRMS (+): m/z 433.3 ([M+H]⁺, 100%).

HRMS: Found [M+H]⁺ 433.2374. C₂₁H₃₃N₆O₂S requires M+H, 433.2382.

1-(1-((2,4-dimethylthiazol-5-yl)methyl)-8-morpholino-1,4,5,7,8,9-hexahydro-6*H*-pyrazolo[4,3-*d*]azocin-6-yl)-2-(tetrahydro-2*H*-pyran-4-yl)ethan-1-one (167c1)
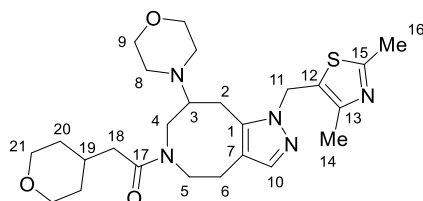
General procedure 8 (page 299) was followed, using building block **167 •2 HCl** (0.059 mmol) as the starting material and **c1** as the carboxylic acid. Amide **167c1** was obtained as a yellow oil (19.4 mg, 67%).

v_{max} (neat / cm^{-1}): 2926 m, 2848 m, 1629 s (C=O), 1450 s, 1420 s, 1133 m.

^{1}H-NMR (400 MHz, CDCl$_3$) δ_H 7.28 (s, 1H, H-10), 5.36 (A of AB, J_{A-B} = 15.8 Hz, 1H, H-11), 5.27 (B of AB, J_{B-A} = 15.8 Hz, 1H, H-11), 3.96 − 3.80 (stack, 3H, H-4, H-21), 3.74 − 3.55 (stack, 5H, H-5, H-9), 3.42 − 3.27 (m, 2H, H-21), 3.26 − 3.14 (m, 1H, H-5), 3.09 − 2.93 (stack, 2H, H-3, H-4), 2.89 − 2.51 (stack, 11H, [including 2.58 (s, 3H, H-16), 2.70 − 2.54 (stack, 4H, H-8)], H-2, H-6, H-8, H-16), 2.44 (s, 3H, H-14), 2.03 − 1.78 (stack, 3H, H-18, H-19), 1.54 − 1.39 (m, 2H, H-20), 1.22 − 1.06 (m, 2H, H-20).

^{13}C-NMR (101 MHz, CDCl$_3$) δ_C 172.0 (C, C-15), 164.9 (C, C-17), 148.8 (C, C-13), 138.4 (C, C-1), 138.2 (CH, C-10), 126.5 (C, C-12), 115.3 (C, C-7), [68.0, 67.6 (CH$_2$, C-9, C-21)], 60.0 (CH, C-3), [49.8, 49.6 (CH$_2$, C-5, C-8)], 47.8 (CH$_2$, C-4), 45.7 (CH$_2$, C-11), 40.6 (CH$_2$, C-18), [33.2, 33.1 (CH$_2$, C-20)], 31.8 (CH, C-19), 26.7 (CH$_2$, C-2), 24.1 (CH$_2$, C-6), 19.3 (CH$_3$, C-16), 15.3 (CH$_3$, C-14).

ESI-LRMS (+): m/z 488.3 ([M+H]$^+$, 100%).

HRMS: Found [M+H]$^+$ 488.2684. C$_{25}$H$_{38}$N$_5$O$_3$S requires M+H, 488.2690.

9. SACE2 Library summary

Table 22: SACE2 library compounds.

Product	Method	MW (Da)	Amount SM (mmol)[a]	Yield (mg)	Yield (%)	t_R (min)[b]	Purity (%)[b]
159	-	330.4	0.179	36.3	61	0.79	100
159a3	7	505.6	0.090	29.8	66	1.04	100
159a4	7	479.6	0.090	21.4	50	0.93	100
159a5	7	408.5	0.090	2.6	7	0.87	96
159a7	7	528.6	0.090	15.7	33	1.10	51
159c1	8	456.6	0.090	30.8	75	0.82	100
159c2	8	372.4	0.090	17.3	52	0.78	99
159c3	8	467.5	0.090	18.0	43	0.75	97
159c5	8	449.5	0.090	17.6	44	0.82	99
159d1	7	401.5	0.090	28.9	80	0.84	100
159d3	7	515.5	0.090	24.1	52	1.11	100
160	-	313.4	0.110	18.9	55	0.63	99
160a3	7	488.6	0.110	13.0	24	0.84	94
160a4	7	462.6	0.220	44.8	44	0.74	100
160a5	7	391.5	0.110	21.6	50	0.67	95
160a7	7	511.6	0.110	28.6	51	0.90	98
160c1	8	439.6	0.110	21.2	44	0.68	98
160c2	8	355.4	0.110	14.2	36	0.63	90
160c3	8	450.5	0.110	19.2	39	0.62	96
160c5	8	432.5	0.220	36.2	38	0.67	92
160d1	7	384.5	0.110	30.1	71	0.67	97
160d3	7	498.5	0.110	22.0	40	0.93	100
161	-	326.4	0.098	16.6	52	0.80	99
161a3	7	501.7	0.098	18.3	37	1.02	88
161a4	7	475.6	0.098	17.0	36	0.92	91
161a5	7	404.5	0.098	1.2	3	0.86	87
161a7	7	524.6	0.098	26.6	52	1.09	98
161c1	8	452.6	0.098	20.4	46	0.83	99
161c2	8	368.5	0.098	29.2	81	0.78	99
161c3	8	463.6	0.098	14.4	32	0.74	86
161c5	8	445.6	0.098	13.9	32	0.81	99
161d1	7	397.5	0.098	25.7	66	0.87	100
161d3	7	511.6	0.196	59.3	59	1.11	100
162	-	236.3	0.097	15.7	68	0.64	95
162a3	7	411.5	0.097	27.4	69	0.95	99
162a4	7	385.5	0.097	9.3	25	0.81	95
162a5	7	314.4	0.097	10.8	35	0.70	90
162a7	7	434.5	0.097	22.7	54	1.05	98
162c1	8	362.5	0.097	20.0	57	0.76	92
162c2	8	278.4	0.097	12.5	46	0.66	79
162c3	8	373.5	0.097	8.2	23	0.65	100
162c5	8	355.4	0.097	15.8	46	0.74	99
162d1	7	307.4	0.097	15.1	51	0.73	98
162d3	7	421.4	0.097	28.8	70	1.12	100
163	-	237.3	0.105	14.8	59	0.49	99
163a3	7	412.5	0.105	14.8	34	1.11	100
163a4	7	386.5	0.210	24.7	30	0.92	99
163a5	7	315.4	0.105	9.7	29	0.80	95
163a7	7	435.5	0.105	31.3	68	1.21	100

Product	Method	MW (Da)	Amount SM (mmol)[a]	Yield (mg)	Yield (%)	t_R (min)[b]	Purity (%)[b]
163c1	8	363.5	0.105	23.5	62	0.81	99
163c2	8	279.3	0.105	14.4	49	0.70	99
163c3	8	374.4	0.105	14.3	36	0.70	98
163c5	8	356.4	0.210	25.2	34	0.79	99
163d1	7	308.4	0.105	21.3	66	0.80	99
163d3	7	422.4	0.105	23.3	53	1.25	99
164	-	278.4	0.155	23.7	55	0.86	99
164a3	7	453.6	0.155	45.3	64	1.19	100
164a4	7	427.6	0.155	40.8	62	1.02	100
164a5	7	356.5	0.310	77.0	70	0.93	100
164a7	7	476.6	0.155	49.9	68	1.30	100
164c1	8	404.6	0.155	45.2	72	0.91	99
164c2	8	320.4	0.155	34.5	69	0.84	99
164c3	8	415.5	0.155	24.3	38	0.81	97
164c5	8	397.5	0.155	42.5	69	0.90	99
164d1	8	349.5	0.310	77.5	72	0.94	100
164d3	8	463.5	0.155	46.1	64	1.36	100
165	-	250.3	0.130	24.9	77	0.69	97
165a3	7	425.6	0.130	29.3	53	1.00	100
165a4	7	399.5	0.130	36.5	70	0.85	99
165a5	7	328.4	0.260	26.7	31	0.76	99
165a7	7	448.5	0.130	43.4	74	1.11	100
165c1	8	376.5	0.130	21.8	45	0.79	97
165c2	8	292.4	0.130	23.5	62	0.70	100
165c3	8	387.5	0.260	38.4	38	0.68	98
165c5	8	369.5	0.130	26.2	55	0.77	99
165d1	7	321.4	0.130	29.7	71	0.79	99
165d3	7	435.5	0.260	63.0	56	1.18	99
166	-	250.3	0.103	16.9	66	0.71	98
166a3	7	425.6	0.103	24.1	55	0.99	99
166a4	7	399.5	0.103	27.5	67	0.85	99
166a5	7	328.4	0.103	10.5	31	0.75	96
166a7	7	448.5	0.103	30.9	67	1.10	100
166c1	8	376.5	0.103	15.3	39	0.80	93
166c2	8	292.4	0.103	14.6	48	0.71	79
166c3	8	387.5	0.103	14.1	35	0.69	97
166c5	8	369.5	0.103	18.9	50	0.77	99
166d1	7	321.4	0.103	23.5	71	0.78	99
166d3	7	435.5	0.103	29.0	65	1.18	99
167	-	361.5	0.059	12.4	58	0.87	100
167a3	7	536.7	0.059	19.1	60	1.15	100
167c1	8	487.7	0.059	19.4	67	0.93	100
167d1	7	432.6	0.059	15.3	60	0.93	100
168	-	361.5	0.098	17.4	49	0.89	100
168a4	7	510.7	0.098	28.7	57	1.02	100
168a7	7	559.7	0.098	32.0	58	1.26	99
168c2	8	403.6	0.098	22.1	56	0.87	85
168c5	8	480.6	0.098	28.6	61	0.91	90
168d1	7	432.6	0.098	27.4	65	0.94	100
169	-	263.3	0.092	3.7	15	0.66	100
169a3	7	438.6	0.092	4.9	12	0.90	98
169a4	7	412.5	0.092	8.7	23	0.79	100
169a5	7	341.4	0.092	6.3	20	0.69	62

Product	Method	MW (Da)	Amount SM (mmol)[a]	Yield (mg)	Yield (%)	t_R (min)[b]	Purity (%)[b]
169a7	7	461.5	0.183	7.6	9	1.00	100
169c1	8	389.5	0.092	13.3	37	0.73	100
169c2	8	305.4	0.092	19.7	70	0.66	99
169c3	8	400.5	0.092	8.6	23	0.64	86
169c5	8	382.5	0.092	13.6	39	0.72	87
169d1	7	334.4	0.092	21.5	70	0.70	99
169d3	7	448.5	0.092	17.8	43	1.06	82

[a]SM: starting material. [b]Retention time (t_R) and purity measured using UPLC. Purity calculated as product peak AUC fraction in the total absorbance chromatogram (210 – 320 nm).

10. SACE3 library precursors

tert-butyl (3a*R**,9a*S**)-2-benzyl-9-oxodecahydro-5*H*-pyrrolo[3,4-*c*]azocine-5-carboxylate (*cis*-181)

tert-butyl (3a*R**,9a*R**)-2-benzyl-9-oxodecahydro-5*H*-pyrrolo[3,4-*c*]azocine-5-carboxylate (*trans*-181)
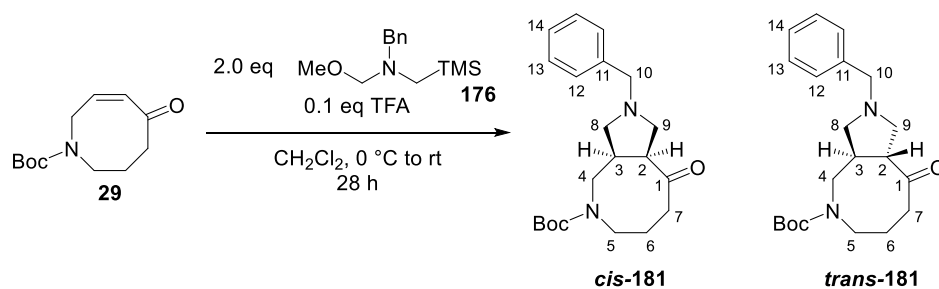
TFA (28.2 µL, 0.366 mmol) was added to an ice-cooled solution of enone **29** (825 mg, 3.66 mmol) and *N*-methoxymethyl-*N*-(trimethylsilylmethyl)benzylamine **176** (1.4 mL, 5.5 mmol) in CH$_2$Cl$_2$ (7.3 mL). The ice bath was left to warm to rt over 2 h. After 24 h at rt, an extra portion of *N*-methoxymethyl-*N*-(trimethylsilylmethyl)benzylamine **176** (0.47 mL, 1.8 mmol) was added. After stirring for a further 2 h at rt, the reaction mixture was poured into NaHCO$_3$ solution (20 mL) and the aqueous phase was extracted with CH$_2$Cl$_2$ (3 × 20 mL). The combined organic extracts were dried over anhydrous Na$_2$SO$_4$, filtered and concentrated under reduced pressure. The resulting crude mixture was purified using automatic column chromatography (heptane:EtOAc) yielding fused pyrrolidine **181** as a yellow oil (1.077 g, 82%, mixture of *cis*:*trans* diastereomers between 5:1 and 4:1 based on ^{1}H-NMR spectroscopic analysis).[a]

325 mg of the mixture of diastereomers was submitted for separation *via* SFC (BEH column, CO$_2$:20 mM NH$_3$ in MeOH) yielding the separated diastereomers (***cis*-181**: 214 mg, ***trans*-181***: 45 mg) as yellow oils.

---

[a] Ratio based on H-4 min peak integration and stacked Boc-peak integration at δ_H (CDCl$_3$) 3.35 and 1.45 ppm, respectively.

(*cis*-181)

cis-181
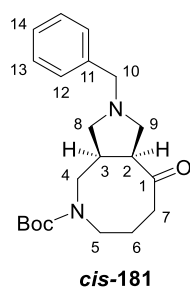
R*f* (heptane:EtOAc, 3:2): 0.4.

*v*max (neat / cm⁻¹): 2971 m, 2926 m, 2796 w, 1689 v s (C=O), 1409 s, 1364 s, 1162 v s.

¹H-NMR (400 MHz, CDCl₃) (mixture of rotamers, 1:1)[a] δ_H 7.35 − 7.17 (stack, 5H, Ph), 3.71 − 3.56 (stack, 2H, H-10), 3.56 − 3.40 (stack, 1.5H, H-4 rot A, H-5), 3.40 − 3.29 (m, 0.5H, H-4 rot B), 3.29 − 3.14 (stack, 1.5H, H-2, H-3 rot A), 3.14 − 2.98 (stack, 1.5H, H-3 rot B, H-4 rot B, H-5 rot B), 2.98 − 2.78 (stack, 3H, H-4 rot A, H-5 rot A, H-8, H-9), [2.73 (dd, *J* = 9.9, 7.8 Hz, 0.5H, H-8 rot B), 2.69 − 2.61 (m, 0.5H, H-8 rot A)], 2.61 − 2.44 (stack, 1H, H-7), 2.37 − 2.25 (stack, 1H, [including 2.33 (app t, *J* = 5.5 Hz, 0.5H, H-7 rot B), 2.29 (app t, *J* = 5.4 Hz, 0.5H, H-7 rot A)], H-7), 2.24 − 2.15 (stack, 1H, H-9), 2.15 − 1.95 (stack, 2H, H-6), 1.45 (app s, 9H, Boc).

¹³C-NMR (101 MHz, CDCl₃) (mixture of rotamers) δ_C [213.5 (C, C-1 maj), 213.2 (C, C-1 min)], [155.2 (C, Boc *C*=O maj), 155.0 (C, Boc *C*=O min)], 138.9 (C, C-11), [128.6 (CH, C-12 min or C-13 min), 128.5 (CH, C-12 maj or C-13 maj)], [128.2 (CH, C-12 min or C-13 min), 128.2 (CH, C-12 maj or C-13 maj)], [127.0 (CH, C-14 min), 126.9 (CH, C-14 maj)], [79.8 (C, Boc *C*(CH₃)₃ min), 79.7 (C, Boc *C*(CH₃)₃ maj)], [60.3 (CH₂, C-10 min), 60.2 (CH₂, C-10 maj)], [58.3 (CH₂, C-9 maj), 58.1 (CH₂, C-9 min)], [54.0 (CH, C-2 maj), 53.2 (CH, C-2 min)], [53.0 (CH₂, C-8 min), 52.7 (CH₂, C-8 maj], [51.9 (CH₂, C-4 maj), 50.9 (CH₂, C-4 min)], [48.5 (CH₂, C-5 maj), 48.1 (CH₂, C-5 min)], [43.2 (CH, C-3 min), 42.1 (CH, C-3 maj)], [39.7 (CH₂, C-7 min), 38.6 (CH₂, C-7 maj)], 28.4 (C, Boc C(*C*H₃)₃), [25.8 (CH₂, C-6 maj), 25.1 (CH₂, C-6 min)].

ESI-LRMS (+): m/z 359.1 ([M+H]⁺, 100%).

HRMS: Found [M+H]⁺ 359.2324. C₂₁H₃₁N₂O₃ requires M+H, 359.2329.

---

[a] Ratio based on H-4 peak integrations in the reported ¹H-NMR spectrum at δ_H (CDCl₃) 3.56 − 3.40, 3.35, 3.29 − 3.14, 3.14 − 2.98 and 2.98 − 2.78 ppm.

(*trans*-181)

trans-181
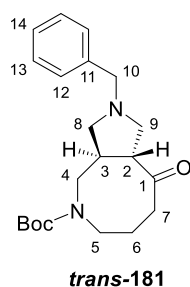
R*f* (heptane:EtOAc, 3:2): 0.4.

ν$_{max}$ (neat / cm^{-1}): 2971 m, 2926 m, 2799 w, 1685 v s (C=O), 1409 s, 1364 s, 1148 s.

^{1}H-NMR (400 MHz, CDCl$_3$) (mixture of rotamers, 5:4)[a] *δ*$_H$ 7.37 − 7.15 (stack, 5H, [including 7.27 − 7.15 (m, 1H, H-14)], Ph), 3.82 − 3.58 (stack, 3.4H, [including 3.82 − 3.72 (m, 0.4H, H-5 min), 3.65 − 3.63 (m, 0.4H, H-4 min), 3.63 − 3.58 (m, 0.6H, H-4 maj)], H-4, H-5 min, H-10), 3.53 (ddd, *J* = 14.2, 9.3, 4.5 Hz, 0.6H, H-5 maj), 3.21 (app dt, *J* = 14.7, 4.9 Hz, 0.6H, H-5 maj), 3.17 − 2.58 (stack, 6.4H, [including 3.17 − 2.97 (stack, 2.4H, H-2, H-4, H-5 min), 2.97 − 2.74 (stack, 3H, H-8, H-9), 2.78 − 2.58 (stack, 1H, H-3)], H-2, H-3, H-4, H-5 min, H-8, H-9), 2.57 − 2.35 (stack, 3H, [including 2.57 − 2.44 (stack, 1H, H-8)], H-7, H-8), 2.22 − 1.90 (stack, 2H, H-6), [1.43 (s, 5H, Boc maj), 1.42 (s, 4H, Boc min)].

^{13}C-NMR (101 MHz, CDCl$_3$) (mixture of rotamers) *δ*$_C$ [212.8 (C, C-1 maj), 212.7 (C, C-1 min)], [155.3 (C, Boc *C*=O maj), 155.2 (C, Boc *C*=O min)], [138.9 (C, C-11 maj), 138.7 (C, C-11 min)], [128.9, 128.8, 128.4 (CH, C-12, C-13, resonance overlap)], 127.2 (CH, C-14), [80.23 (C, Boc *C*(CH$_3$)$_3$ maj), 80.16 (C, Boc *C*(CH$_3$)$_3$ min)], [60.8 (CH$_2$, C-10 min), 60.6 (CH$_2$, C-10 maj)], 56.3 (CH$_2$, C-8), [55.9 (CH$_2$, C-9 min), 55.8 (CH$_2$, C-9 maj)], [54.5 (CH, C-2 maj), 54.0 (CH, C-2 min)], [50.9 (CH$_2$, C-4 min), 50.4 (CH$_2$, C-4 maj)], [47.5 (CH$_2$, C-5 maj), 47.3 (CH$_2$, C-5 min)], [47.1 (CH, C-3 min), 45.3 (CH, C-3 maj)], [41.3 (CH$_2$, C-7 min), 40.8 (CH$_2$, C-7 maj)], [28.52 (CH$_3$, Boc C(*C*H$_3$)$_3$ maj), 28.50 (CH$_3$, Boc C(*C*H$_3$)$_3$ min)], [26.7 (CH$_2$, C-6 maj), 25.6 (CH$_2$, C-6 min)].

ESI-LRMS (+): m/z 359.1 ([M+H]$^{+}$, 100%).

HRMS: Found [M+H]$^{+}$ 359.2325. C$_{21}$H$_{31}$N$_2$O$_3$ requires M+H, 359.2329.

---

[a] Ratio based on Boc peak integrations in the reported ^{1}H-NMR spectrum.

tert-butyl (3aR*,9S*,9aS*)-2-benzyl-9-hydroxydecahydro-5*H*-pyrrolo[3,4-*c*]azocine-5-carboxylate (*cis*-209)
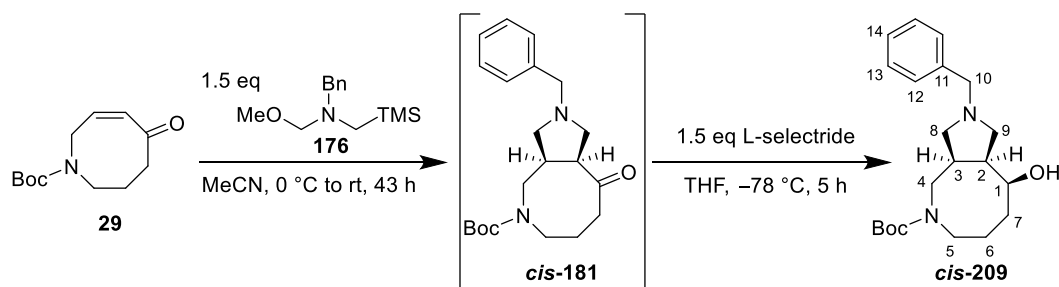
N-Methoxymethyl-*N*-(trimethylsilylmethyl)benzylamine **176** (1.7 mL, 6.7 mmol) was added to an ice-cooled solution of enone **29** (1.04 g, 4.49 mmol) in MeCN (9.0 mL). The ice bath was removed and the reaction mixture was allowed to warm to rt. After stirring for 43 h at rt, the reaction mixture was poured into NaHCO$_3$ solution (20 mL) and the aqueous phase was extracted with CH$_2$Cl$_2$ (3 × 20 mL). The combined organic extracts were dried over anhydrous Na$_2$SO$_4$, filtered and concentrated under reduced pressure. The resulting crude fused pyrrolidine *cis*-**181** was dissolved in THF (11.2 mL) and the solution was cooled to −78 °C. L-Selectride (1.0 M in THF, 6.7 mL, 6.7 mmol) was added in one portion and the resulting solution was stirred at −78 °C. After 5 h, NH$_4$Cl solution (100 mL) was added and the resulting mixture was extracted with CHCl$_3$:*i*-PrOH 3:1 solution (3 × 100 mL). The combined organic extracts were dried over anhydrous Na$_2$SO$_4$, filtered and concentrated under reduced pressure. Purification of the crude product *via* automatic column chromatography (CH$_2$Cl$_2$:7 M NH$_3$ in MeOH) yielded alcohol *cis*-**209** as a yellow oil (1.15 g, 71%).

R$_f$ (CH$_2$Cl$_2$:7 M NH$_3$ in MeOH, 9:1): 0.7.

v$_{max}$ (neat / cm^{-1}): 3436 br w (O–H), 2971 m, 2922 m, 1674 s (C=O), 1409 s, 1364 s, 1159 v s.

^{1}H-NMR (400 MHz, CDCl$_3$) δ_H 7.40 − 7.14 (stack, 5H, Ph), 5.42 (br s, 1H, O*H*), 4.16 − 4.05 (m, 1H, H-1), 3.82 − 3.30 (stack, 4H, [including 3.53 − 3.30 (m, 1H, H-4)], H-4, H-5, H-10), 3.28 − 2.75 (stack, 4H, [including 3.28 − 3.09 (m, 1H, H-4), 3.07 (app dt, *J* = 13.4, 4.2 Hz, 1H, H-5), 2.91 (dd, *J* = 9.1, 9.1 Hz, 1H, H-8)], H-3, H-4, H-5, H-8), 2.75 − 2.35 (stack, 3H, [including 2.75 − 2.59 (m, 1H, H-9)], H-8, H-9), 2.22 − 1.97 (stack, 3H, H-2, H-6, H-7), 1.43 (stack, 11H, [including 1.43 (s, 9H, Boc)], H-6, H-7, Boc).

13C-NMR (101 MHz, CDCl₃) (mixture of rotamers) δ_C 156.2 (C, Boc *C*=O), 138.4 (C, C-11), [128.61, 128.58, 127.3 (CH, Ph)], 79.3 (C, Boc *C*(CH₃)₃), 74.9 (CH, C-1), 62.4 (CH₂, C-9), 60.0 (CH₂, C-10), [55.9, 55.8 (CH₂, C-8)], [47.6, 47.0 (CH₂, C-5)], 45.0 (CH₂, C-4), [44.8, 44.7 (CH, C-2)], [39.1, 37.8 (CH, C-3)], 33.7 (CH₂, C-7), 28.6 (CH₃, Boc C(*C*H₃)₃), [20.3, 20.1 (CH₂, C-6)].

ESI-LRMS (+): m/z 361.1 ([M+H]⁺, 100%).

HRMS: Found [M+H]⁺ 361.2480. C₂₁H₃₃N₂O₃ requires M+H, 361.2486.

(3a*R**,8b*S**)-2-benzyl-2,3,3a,4,6,7,8,8b-octahydro-1*H*-pyrrolo[3,4-*a*]pyrrolizin-5-ium chloride (*cis*-192)

cis-181 → **cis-192**

10 eq HCl (4 M in 1,4-dioxane)

MeOH, rt, 6 days
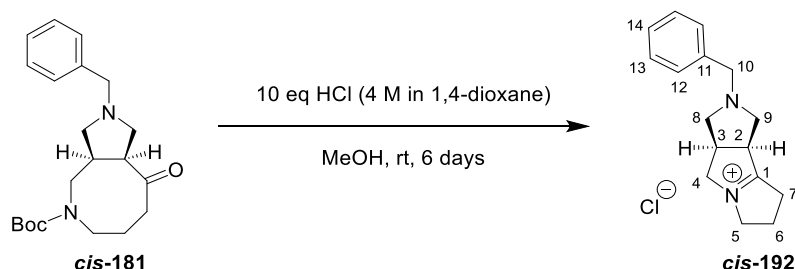
HCl solution (4.0 M in 1,4-dioxane, 711 µL, 2.85 mmol) was added to a stirred solution of ketone *cis*-181 (102 mg, 0.285 mmol) in MeOH (8.6 mL). After 6 days at rt, the volatiles were removed under reduced pressure, yielding iminium chloride *cis*-192 as an off-white foam (78 mg, quant., hygroscopic), which was used in the next step without further purification.

v_{max} (neat / cm⁻¹): 2952 m, 2482 s, 1692 m (C=N), 1454 s, 1398 s, 1119 m.

1H-NMR (400 MHz, CDCl₃) δ_H 7.69 – 7.56 (stack, 2H, H-12 or H-13), 7.49 – 7.36 (stack, 3H, H-12 or H-13, H-14), 4.61 – 4.13 (stack, 4H, [including (4.52 – 4.33 (m, 2H, H-10), 4.27 – 4.13 (m, 1H, H-4 or H-8)], H-2, H-4 or H-8, H-10), 4.13 – 3.74 (stack, 5H, H-4 and/or H-8, H-5, H-3), 3.74 – 3.44 (stack, 3H, H-4 or H-8, H-9), 3.26 – 2.90 (stack, 2H, H-7), 2.78 – 2.50 (stack, 2H, H-6).

13C-NMR (101 MHz, CDCl₃) δ_C 196.8 (C, C-1), [132.2, 131.1, 130.2 (CH, C-12, C-13, C-14)], 59.6 (CH₂, C-4, C-8, resonance overlap), 58.8 (CH₂, C-10), 54.4 (CH₂, C-5, C-9, resonance overlap), 48.9 (CH, C-2), 43.0 (CH, C-3), 32.1 (CH₂, C-7), 25.3 (CH₂, C-6), C-11 resonance not observed.

ESI-LRMS (+): m/z 241.1 ([M]⁺, 100%).

HRMS: Found [M]⁺ 241.1698. C₁₆H₂₁N₂ requires M, 241.1699.

((3a*R**,8a*S**,8b*S**)-2-benzyldecahydropyrrolo[3,4-*a*]pyrrolizine (*cis*-197)

(3a*R**,8a*R**,8b*S**)-2-benzyldecahydropyrrolo[3,4-*a*]pyrrolizine (*trans*-197)
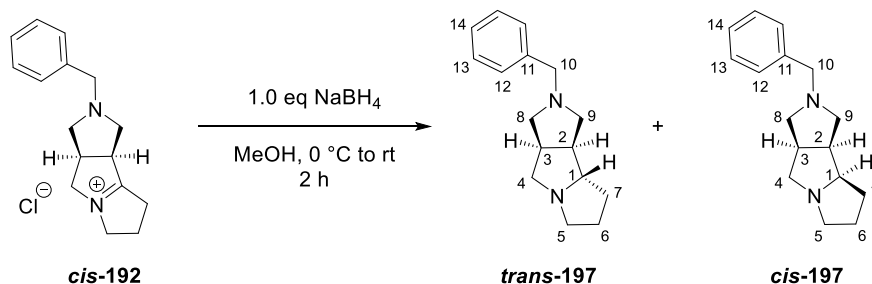
NaBH$_4$ (11 mg, 0.29 mmol) was added to a solution of iminium chloride **cis-192** (79 mg, 0.29 mmol) in MeOH (5.7 mL) at 0 °C. The ice bath was removed and after stirring for 2 h at rt, the reaction mixture was poured into NaHCO$_3$ solution (10 mL), evaporated under reduced pressure to dryness and the residue was redissolved in CH$_2$Cl$_2$ (10 mL).[a] The resulting solution was dried over anhydrous Na$_2$SO$_4$, filtered and concentrated under reduced pressure, yielding the crude 3° amine **197** as a mixture of diastereoisomers (*trans*:*cis* 2:3).[b] The two diastereoisomers were separated using automatic column chromatography (CH$_2$Cl$_2$:7 M NH$_3$ in MeOH), yielding two colourless oils. Mass recovery: 24 mg **trans-197**, 25 mg **cis-197**).[c]

(*trans*-197)

R$_f$ (CH$_2$Cl$_2$:7 M NH$_3$ in MeOH, 9:1): 0.7.

v$_{max}$ (neat / cm^{-1}): 2948 m, 2788 m, 1655 m (C=C), 1454 m, 1271 m, 1133 m.

^{1}H-NMR (400 MHz, CDCl$_3$) δ_H 7.34 − 7.27 (stack, 4H, H-12, H-13), 7.25 − 7.17 (m, 1H, H-14), 3.59 (A of AB, J_{A-B} = 12.9 Hz, 1H, H-10), 3.54 (B of AB, J_{B-A} = 12.9 Hz, 1H, H-10), 3.14 (app td, J = 6.6, 3.6 Hz, 1H, H-1), 3.01 − 2.75 (stack, 3H, [including 3.01 − 2.88 (m, 1H, H-5), 2.89 − 2.80 (m, 1H, H-3), 2.89 − 2.75 (m, 1H, H-4)], H-3, H-4, H-5), 2.66 − 2.51 (stack, 3H, H-5, H-8, H-9), 2.50 − 2.35 (stack, 3H, H-2, H-8, H-9), 2.35 − 2.25 (m, 1H, H-4), 1.99 − 1.84 (stack, 2H, H-6, H-7), 1.79 − 1.65 (m, 1H, H-6), 1.55 − 1.46 (m, 1H, H-7).

---

[a] The product was soluble in both the aqueous and organic phases.
[b] Ratio based on relative integration values for H-1 in the ^{1}H-NMR spectrum.
[c] The author acknowledges that the recovered product fractions were not analytically pure, but 2D-NMR spectroscopic analysis of the major ^{1}H/^{13}C-NMR resonances allowed for tentative assignment of the observed resonances, by analogy with literature compounds (see Appendix 4.1).[19,20]

13C-NMR (101 MHz, CDCl₃) δ_C 139.4 (C, C-11), [128.8, 128.3 (CH, C-12, C-13)], 126.9 (CH, C-14), 72.2 (CH, C-1), [60.1, 59.90, 59.87 (CH₂, C-8, C-9, C-10)], 58.8 (CH₂, C-4), 52.8 (CH₂, C-5), 49.2 (CH, C-2), 43.1 (CH, C-3), 30.5 (CH₂, C-7), 24.5 (CH₂, C-6).

ESI-LRMS (+): m/z 243.3 ([M+H]⁺, 100%)

HRMS: Found [M+H]⁺ 243.1853. $C_{16}H_{23}N_2$ requires M+H, 243.1856.

(*cis*-197)
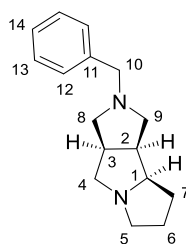
***cis*-197**

R$_f$ (CH₂Cl₂:7 M NH₃ in MeOH 9:1): 0.5.

v_{max} (neat / cm⁻¹): 2948 m, 2788 m, 1655 w (C=C), 1454 m, 1301 m, 1118 m.

1H-NMR (400 MHz, CDCl₃) δ_H 7.36 − 7.24 (stack, 4H, H-12, H-13), 7.27 − 7.16 (m, 1H, H-14), 3.59 (A of AB, J_{A-B} = 13.1 Hz, 1H, H-10), 3.54 (B of AB, J_{B-A} = 13.1 Hz, 1H, H-10), 3.38 (app dt, J = 9.2, 7.3 Hz, 1H, H-1), 3.05 − 2.96 (m, 1H, H-4), 2.94 − 2.80 (stack, 4H, H-2, H-3, H-5), 2.67 (dd, J = 9.5, 2.0 Hz, 1H, H-9), 2.63 − 2.56 (m, 1H, H-8), 2.34 − 2.26 (m, 1H, H-4), 2.19 − 2.11 (stack, 2H, H-8, H-9), 2.10 − 1.98 (m, 1H, H-6), 2.03 − 1.87 (m, 1H, H-7), 1.79 − 1.64 (m, 1H, H-6), 1.57 − 1.44 (m, 1H, H-7).

13C-NMR (101 MHz, CDCl₃) δ_C 139.8 (C, C-11), [128.5, 128.3 (CH, C-12, C-13)], 126.8 (CH, C-14), 69.3 (CH, C-1), 60.0 (CH₂, C-10), 58.9 (CH₂, C-4), 57.9 (CH₂, C-8), 56.6 (CH₂, C-9), 51.7 (CH₂, C-5), 45.0 (CH, C-2), 43.3 (CH, C-3), [24.7, 24.6 (CH₂, C-6, C-7)].

ESI-LRMS (+): m/z 243.3 ([M+H]⁺, 100%).

HRMS: Found [M+H]⁺ 243.1853. $C_{16}H_{23}N_2$ requires M+H, 243.1856.

(3a*S*,9*S*,9a*S*)-2-benzyldecahydro-1*H*-pyrrolo[3,4-*c*]azocin-9-ol (224)
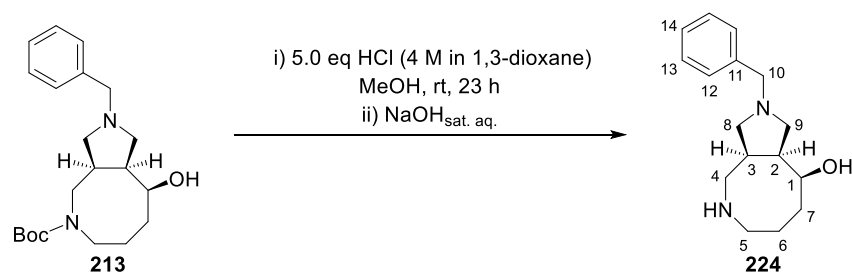
HCl solution (4 M in 1,4-dioxane, 4.5 mL, 18 mmol) was added to a solution of Boc-amine **213** (1.29 g, 3.58 mmol) in MeOH (18 mL). After stirring for 23 h at rt, the volatiles were removed under reduced pressure. NaOH solution (1 M, 50 mL) was added and the resulting mixture was extracted with CHCl$_3$:*i*-PrOH 3:1 solution (3 × 50 mL). The combined organic extracts were dried over anhydrous Na$_2$SO$_4$, filtered and concentrated under reduced pressure, yielding 2° amine **224** as an orange oil (806 mg, 86%).

v$_{max}$ **(neat / cm^{-1}):** 3280 br w (O–H, N–H), 2904 s, 2788 s, 1674 s (C=C), 1454 s, 1126 s.

^{1}H-NMR (400 MHz, CDCl$_3$) δ_H 7.36 – 7.26 (stack, 4H, H-12, H-13), 7.26 – 7.15 (m, 1H, H-14), 3.91 – 3.85 (m, 1H, H-1), 3.68 (A of AB, $J_{A–B}$ = 13.0 Hz, 1H, H-10), 3.64 (B of AB, $J_{B–A}$ = 13.0 Hz, 1H, H-10), 2.95 – 2.73 (stack, 6H, H-4, H-5, H-8, H-9), 2.69 – 2.61 (m, 1H, H-5), 2.61 – 2.48 (m, 1H, H-3), 2.34 (dd, J = 9.1, 5.1 Hz, 1H, H-8), 2.24 (dddd, J = 8.0, 8.0, 8.0, 2.8 Hz, 1H, H-2), 1.96 – 1.84 (m, 1H, H-7), 1.84 – 1.62 (stack, 3H, H-6, H-7), exchangeable protons not observed.

^{13}C-NMR (101 MHz, CDCl$_3$) δ_C 139.6 (C, C-11), [128.8, 128.3 (CH, C-12, C-13)], 126.9 (CH, C-14), 68.8 (CH, C-1), 61.0 (CH$_2$, C-10), 59.7 (CH$_2$, C-8), 57.4 (CH$_2$, C-9), 47.7 (CH$_2$, C-4), 46.2 (CH, C-2), 45.4 (CH$_2$, C-5), 39.3 (CH, C-3), 34.3 (CH$_2$, C-7), 25.3 (CH$_2$, C-6).

ESI-LRMS (+): m/z 261.3 ([M+H]$^+$, 100%).

HRMS: Found [M+H]$^+$ 261.1960. C$_{16}$H$_{25}$N$_2$O requires M+H, 261.1961.

tert-butyl (3a*R**,9*S**,9a*S**)-9-hydroxydecahydro-5*H*-pyrrolo[3,4-*c*]azocine-5-carboxylate (225)
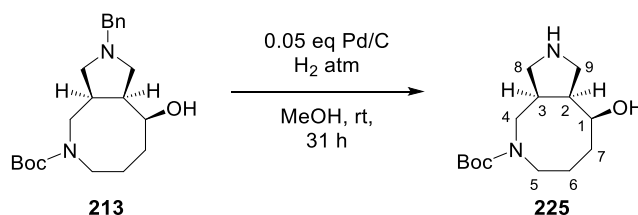
Under a N_2 atmosphere, Pd/C (0.191 g, 10 wt%, 0.179 mmol) was added to a solution of benzylamine **213** (1.29 g, 3.58 mmol) in MeOH (27 mL). The reaction mixture was purged with H_2 gas and stirred under a H_2 atmosphere at rt. After 31 h, the reaction mixture was purged with N_2 gas, filtered over SiO_2 and washed with CH_2Cl_2:7 M NH_3 in MeOH, 9:1 solution. The desired 2° amine product eluted with 7 M NH_3 in MeOH and the filtrate was concentrated under reduced pressure, yielding 2° amine **225** as a white foam (887 mg, 92%), which was used without further purification.

v_{max} **(neat / cm^{-1}):** 3340 br w (N–H, O–H), 2971 m, 2926 m, 1685 s (C=O), 1413 s, 1371 s, 1163 s.

^{1}H-NMR (400 MHz, CDCl$_3$) δ_H 6.57 (s, 1H, OH or N*H*), 4.10 − 4.05 (m, 1H, H-1), 3.72 − 3.37 (stack, 2H, H-4, H-5), 3.36 − 3.22 (stack, 2H, H-9), 3.24 − 3.19 (m, 1H, H-8), 3.09 (dd, *J* = 14.0, 11.5 Hz, 1H, H-4), 3.03 − 2.62 (stack, 3H, [including 3.03 − 2.89 (m, 1H, H-5)], H-3, H-5, H-8), 2.25 − 2.18 (m, 1H, H-2), 2.00 − 1.84 (stack, 2H, H-6, H-7), 1.64 − 1.43 (stack, 2H, H-6, H-7), 1.36 (s, 9H, Boc), NH or OH not observed.

^{13}C-NMR (101 MHz, CDCl$_3$) (mixture of rotamers) δ_C 155.8 (C, Boc *C*=O), 79.7 (C, Boc *C*(CH$_3$)$_3$), 72.6 (CH, C-1), 51.4 (CH$_2$, C-9), 48.5 (CH$_2$, C-8), [48.1, 47.4 (CH$_2$, C-5)], 45.0 (CH, C-2), 44.0 (CH$_2$, C-4), [40.5, 39.3 (CH, C-3)], 34.2 (CH$_2$, C-7), 28.4 (CH$_3$, Boc C(*C*H$_3$)$_3$), [21.7, 21.2 (CH$_2$, C-6)].

ESI-LRMS (+): m/z 271.2 ([M+H]$^+$, 100%), 215.1 (1, [M–C$_4$H$_8$ + H]$^+$).

HRMS: Found [M+H]$^+$ 271.2014. C$_{14}$H$_{27}$N$_2$O$_3$ requires M+H, 271.2016.

(3a*R**,9*S**,9a*S**)-2-benzyl-5-((4-nitrophenyl)sulfonyl)decahydro-1*H*-pyrrolo[3,4-*c*]azocin-9-ol (229)
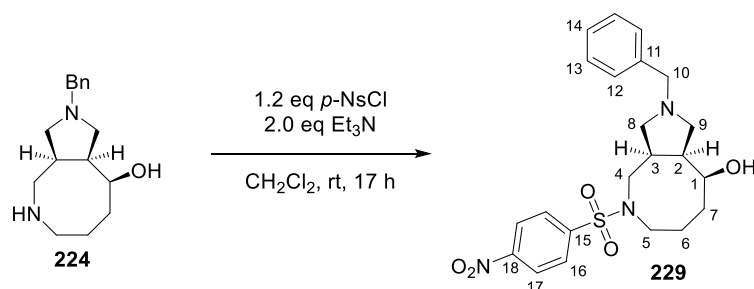
p-NsCl (99 mg, 0.45 mmol) was added to a solution of 2° amine **224** (97 mg, 0.37 mmol) and Et$_3$N (104 µL, 0.745 mmol) in CH$_2$Cl$_2$ (1.9 mL). After stirring for 17 h at rt, the reaction mixture was poured into NaHCO$_3$ solution (5 mL) and extracted with CH$_2$Cl$_2$ (3 × 5 mL). The combined organic extracts were dried over anhydrous Na$_2$SO$_4$, filtered and concentrated under reduced pressure. The resulting crude mixture was purified using automatic column chromatography (CH$_2$Cl$_2$:MeOH), yielding sulfonamide **229** as a yellow oil (65 mg, 39%).

R$_f$ (CH$_2$Cl$_2$:MeOH, 9:1): 0.5.

v_{max} (neat / cm^{-1}): 3198 br w (O–H), 2919 w, 2878 w, 1595 m, 1528 s, 1346 v s, 1159 s.

^{1}H-NMR (400 MHz, CDCl$_3$) δ_H 8.41 − 8.31 (AA' of AA'BB', 2H, H-17), 8.00 − 7.90 (BB' of AA'BB', 2H, H-16), 7.34 − 7.19 (stack, 5H, H-12, H-13, H-14), 4.20 − 4.16 (m, 1H, H-1), 3.72 (A of AB, $J_{A–B}$ = 12.7 Hz, 1H, H-10), 3.62 − 3.46 (stack, 2H, [including 3.56 (B of AB, $J_{B–A}$ = 12.7 Hz, 1H, H-10)], H-5, H-10), 3.20 − 2.98 (stack, 3H, [including 3.07 − 2.98 (m, 1H, H-3)], H-3, H-4), 2.98 − 2.90 (m, 1H, H-9), 2.81 − 2.64 (stack, 2H, H-5, H-9), 2.55 − 2.44 (stack, 2H, H-8), 2.34 − 2.27 (m, 1H, H-2), 2.18 − 2.04 (stack, 2H, H-6, H-7), 1.66 − 1.54 (stack, 2H, H-6, H-7), OH not observed.

^{13}C-NMR (101 MHz, CDCl$_3$) δ_C 150.2 (C, C-18), 143.0 (C, C-15), 138.2 (C, C-11), [128.8, 128.7, 127.5 (CH, C-12, C-13, C-14, C-16, resonance overlap)], 124.5 (CH, C-17), 74.7 (CH, C-1), 62.7 (CH$_2$, C-9), 59.9 (CH$_2$, C-10), 55.4 (CH$_2$, C-8), 48.8 (CH$_2$, C-5), 46.2 (CH$_2$, C-4), 45.1 (CH, C-2), 40.8 (CH, C-3), 32.0 (CH$_2$, C-7), 18.9 (CH$_2$, C-6).

ESI-LRMS (+): m/z 446.1 ([M+H]$^+$, 100%).

HRMS: Found [M+H]$^+$ 446.1730. C$_{22}$H$_{28}$N$_3$O$_5$S requires M+H, 446.1744.

tert-butyl (3a*S**,9*S**,9a*S**)-9-hydroxy-2-((4-nitrophenyl)sulfonyl)decahydro-5*H*-pyrrolo[3,4-*c*]azocine-5-carboxylate (230)
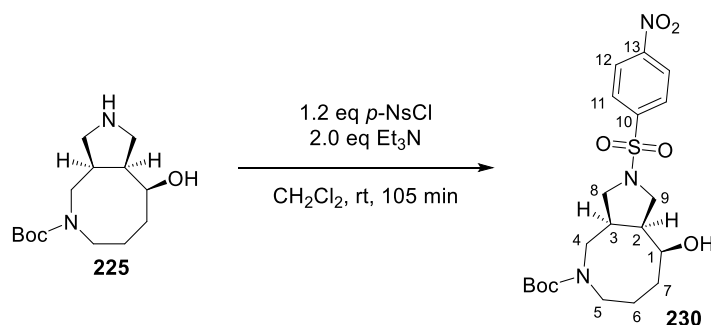
p-NsCl (81 mg, 0.36 mmol) was added to a solution of 2° amine **225** (82 mg, 0.30 mmol) and Et₃N (85 μL, 0.61 mmol) in CH₂Cl₂ (1.5 mL). After stirring for 105 min at rt, the reaction mixture was poured into NaHCO₃ solution (5 mL) and extracted with CH₂Cl₂ (3 × 5 mL). The combined organic extracts were dried over anhydrous Na₂SO₄, filtered and concentrated under reduced pressure. The resulting crude mixture was purified using automatic column chromatography (CH₂Cl₂:MeOH), yielding sulfonamide **230** as a white foam (96 mg, 69%).

R$_f$ (CH₂Cl₂:MeOH, 9:1): 0.7.

ν_{max} **(neat / cm⁻¹):** 3444 br w (O–H), 2974 m, 2930 m, 1670 s (C=O), 1528 s (NO₂), 1349 s, 1156 v s.

¹H-NMR (400 MHz, CDCl₃) δ_H 8.39 − 8.31 (AA' of AA'BB', 2H, H-12), 8.03 − 7.94 (BB' of AA'BB', 2H, H-11), 4.08 − 4.0 (m, 1H, H-1), 3.74 − 3.51 (m, 1H, H-5), 3.53 − 3.30 (stack, 3H, H-4, H-9), 3.30 − 3.10 (stack, 2H, H-8), 2.94 − 2.58 (stack, 3H, H-3, H-4, H-5), 2.32 − 2.21 (m, 1H, H-2), 2.07 (s, 1H, O*H*), 1.92 − 1.73 (stack, 2H, H-6, H-7), 1.73 − 1.47 (stack, 2H, H-6, H-7), 1.38 (s, 9H, Boc).

¹³C-NMR (101 MHz, CDCl₃) δ_C 155.6 (C, Boc *C*=O), 150.1 (C, C-13), 142.5 (C, C-10), 128.7 (CH, C-11), 124.4 (CH, C-12), 80.0 (C, Boc *C*(CH₃)₃), 71.8 (CH, C-1), 52.0 (CH₂, C-8), 49.9 (CH₂, C-9), 48.7 (br, CH₂, C-5), 46.7 (CH, C-2), 46.0 (CH₂, C-4), 39.2 (br, CH, C-3), 33.6 (CH₂, C-7), 28.5 (CH₃, Boc C(*C*H₃)₃), 23.7 (br, CH₂, C-6).

ESI-LRMS (+): m/z 478.0 ([M+Na]⁺, 10%), 400.0 (100, [M−C₄H₈ + H]⁺).

ESI-LRMS (−): m/z 454.1 ([M−H]⁻, 100%).

HRMS: Found [M−C₄H₈ + H]⁺ 400.1163. C₁₆H₂₂N₃O₇S requires M−C₄H₈ + H, 400.1173.

11. SACE3 library

11.1. Used building blocks

224   **225**
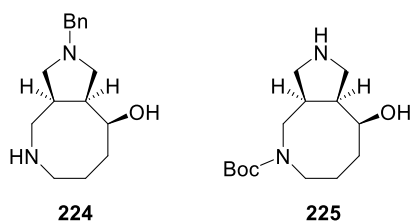
11.2. GENERAL PROCEDURE 9: sulfonyl chlorides, isocyanates

224   **224-R**   **225**   **225-R**
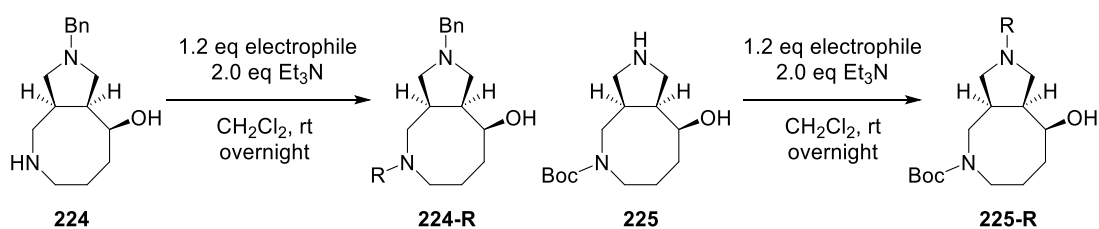
A solution of the amine building block (0.220 or 0.231 mmol) in CH_2Cl_2[a] and Et_3N (2.0 eq) were added sequentially to a solution of the electrophile (1.2 eq) in CH_2Cl_2 (0.4 mL) in a capped 8 mL vial. The resulting mixture was stirred overnight and then left to evaporate to dryness under ambient conditions over 1 h. The dry crude mixture was purified *via* preparative basic HPLC.

11.3. GENERAL PROCEDURE 10: amide couplings

224   **224-R**   **225**   **225-R**

i) 1.2 eq RCO_2H, 1.2 eq EDC •HCl, 1.2 eq Oxyma Pure, 3.0 eq Et_3N, CH_2Cl_2, rt, overnight
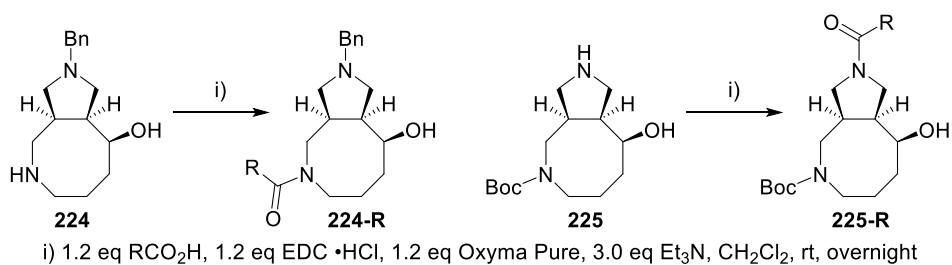
A solution of the building block (0.220 or 0.231 mmol) in CH_2Cl_2[b] and Et_3N (3.0 eq) were added sequentially to a solution of the carboxylic acid (1.2 eq), EDC •HCl (1.2 eq), and Oxyma Pure (1.2 eq) in CH_2Cl_2 (0.4 mL) in a capped 8 mL vial. The resulting mixture was stirred overnight and then left to evaporate to dryness under ambient conditions over 1 h. The dry crude mixture was purified *via* preparative basic HPLC.

---

[a] Volume of CH_2Cl_2 calculated to yield a final reaction concentration of 0.1 M.
[b] Volume of CH_2Cl_2 calculated to yield a final reaction concentration of 0.1 M.

11.4. GENERAL PROCEDURE 11: reductive aminations

i) 1.2 eq R-CHO, 1.2 eq Na(OAc)$_3$BH, CH$_2$Cl$_2$, rt, overnight
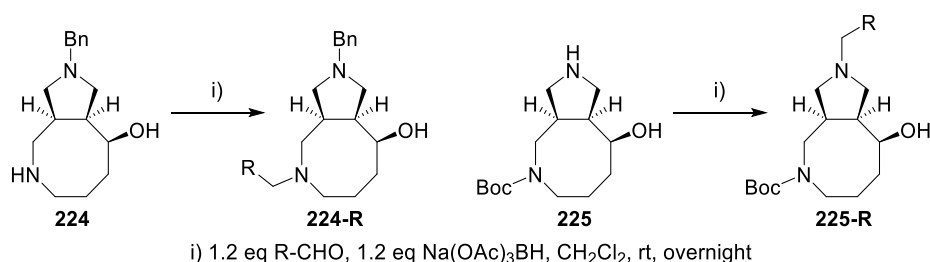
A solution of the building block (0.220 or 0.231 mmol) in CH$_2$Cl$_2$[a] was added to a solution of the aldehyde (1.2 eq) in CH$_2$Cl$_2$ (0.4 mL) in a capped 8 mL vial. NaBH(OAc)$_3$ (1.2 eq) was added at rt.[b] The resulting mixture was stirred overnight and then left to evaporate to dryness under ambient conditions over 1 h. The dry mixture was purified *via* preparative basic HPLC.

11.5. GENERAL PROCEDURE 12: benzyl deprotection
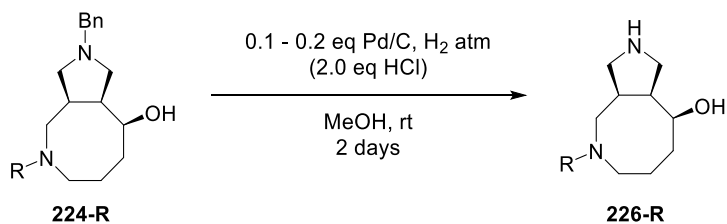
Under a N$_2$ atmosphere, Pd/C (16 mg, 10 wt%, 7.7 µmol) was added to a degassed solution of benzylamine (0.089 − 0.154 mmol) in MeOH (1.5 mL). The resulting mixture was stirred overnight under a H$_2$ atmosphere. The reaction mixture was purged with N$_2$ gas, another portion of Pd/C (16 mg, 10 wt%, 7.7 µmol) was added and the resulting mixture was stirred overnight under a H$_2$ atmosphere. In the case of incomplete hydrogenolysis of the benzyl group after 2 nights, HCl solution (4 M in 1,3-dioxane, 2.0 eq) was added to the reaction mixture, and the reaction mixture was stirred under a H$_2$ atmosphere for another 2 − 19 h. The reaction mixture was purified *via* preparative basic HPLC.

---

[a] Volume of CH$_2$Cl$_2$ calculated to yield a final reaction concentration of 0.1 M.
[b] For aldehyde **e1**, the aldehyde was added after NaBH(OAc)$_3$. Adding **e1** before NaBH(OAc)$_3$ produced a black reaction mixture and reduced product yields. This was not further investigated.

11.6. GENERAL PROCEDURE 13: Boc deprotection
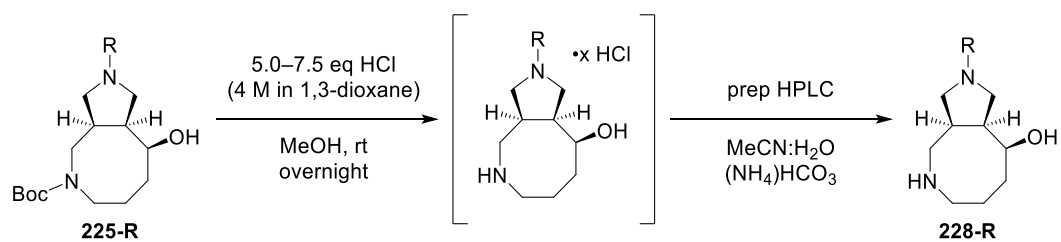
HCl solution (4 M in 1,4-dioxane, 0.194 mL, 0.775 mmol) was added to a solution of Boc-protected amine (0.101 – 0.143 mmol) in MeOH (0.8 mL) in a capped 8 mL vial at rt. After overnight stirring, the reaction mixture was concentrated under reduced pressure, using a Genevac HT-12 centrifugal evaporator. The dry mixture was purified *via* preparative basic HPLC.

11.7. Compound synthesis and characterisation

(3aR*,9S*,9aS*)-2-benzyl-5-((2,4-dimethylthiazol-5-yl)sulfonyl)decahydro-1*H*-pyrrolo[3,4-*c*]azocin-9-ol (224a3)
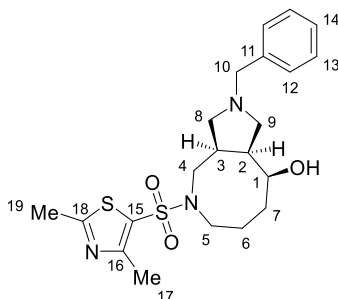
General procedure 9 (page 348) was followed, using building block **224** (0.231 mmol) as the starting material and **a3** as the electrophile. Sulfonamide **224a3** was obtained as a brown powder (46.4 mg, 46%).

v_{max} (neat / cm⁻¹): 3232 w, (O–H), 2915 m, 2818 m, 2781 m, 1342 s, 1290 m, 1152 s.

¹H-NMR (400 MHz, CDCl₃) δ_H 7.36 – 7.18 (stack, 5H, H-12, H-13, H-14), 5.62 (br s, 1H, O*H*), 4.23 – 4.11 (m, 1H, H-1), 3.71 (A of AB, $J_{A–B}$ = 12.8 Hz, 1H, H-10), 3.54 (B of AB, $J_{B–A}$ = 12.8 Hz, 1H, H-10), 3.46 (app td, J = 11.9, 4.9 Hz, 1H, H-5), 3.28 – 3.19 (m, 1H, H-4), 3.19 – 3.07 (m, 1H, H-4), 3.07 – 2.95 (m, 1H, H-3), 2.96 – 2.90 (m, 1H, H-9), 2.88 – 2.80 (m, 1H, H-5), 2.72 – 2.63 (stack, 4H, [including 2.66 (s, 3H, H-19)], H-9, H-19), 2.61 (s, 3H, H-17), 2.57 – 2.42 (stack, 2H, H-8), 2.33 – 2.27 (m, 1H, H-2), 2.22 – 2.05 (stack, 2H, H-6, H-7), 1.67 – 1.53 (stack, 2H, H-6, H-7).

¹³C-NMR (101 MHz, CDCl₃) δ_C 168.5 (C, C-18), 156.2 (C, C-16), 138.3 (C, C-11), [128.6, 127.4 (CH, C-12, C-13, C-14, resonance overlap)], 126.7 (C, C-15), 74.8 (CH, C-1), 62.6 (CH₂, C-9), 59.9 (CH₂, C-10), 55.3 (CH₂, C-8), 48.5 (CH₂, C-5), 46.2 (CH₂, C-4), 45.2 (CH, C-2), 40.7 (CH, C-3), 32.1 (CH₂, C-7), 19.5 (CH₃, C-19), 19.0 (CH₂, C-6), 16.9 (CH₃, C-17).

ESI-LRMS (+): 436.3 ([M+H]⁺, 100%).

HRMS: Found [M+H]⁺ 436.1711. C₂₁H₃₀N₃O₃S₂ requires M+H, 436.1723.

1-((3a*R**,9*S**,9a*S**)-2-benzyl-9-hydroxydecahydro-5*H*-pyrrolo[3,4-*c*]azocin-5-yl)-2-(tetrahydro-2*H*-pyran-4-yl)ethan-1-one (224c1)
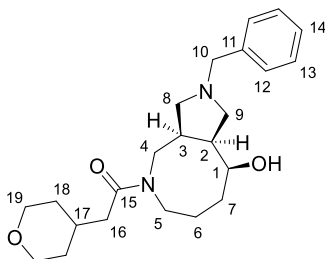
General procedure 10 (page 348) was followed, using building block **224** (0.231 mmol) as the starting material and **c1** as the carboxylic acid. Amide **224c1** was obtained as a yellow oil (58.2 mg, 65%).

v_{max} **(neat / cm^{-1}):** 3403 m (O–H), 2915 s, 2840 m, 1621 s (C=O), 1420 s, 1092 s.

^{1}H-NMR (400 MHz, CDCl$_3$) (mixture of rotamers, 4:1)[a] δ_H 7.33 − 7.19 (stack, 5H, H-12, H-13, H-14), [4.16 − 4.10 (m, 0.2H, H-1 min), 4.10 − 4.05 (m, 0.8H, H-1 maj)], 3.96 − 3.85 (stack, 2H, H-19), 3.81 − 3.50 (stack, 3.2H, [including 3.65 (A of AB, $J_{A–B}$ = 12.9 Hz, 1H, H-10), 3.56 (B of AB, $J_{B–A}$ = 12.9 Hz, 1H, H-10)], H-4 maj, H-4 min and/or H-5 min, H-10), 3.50 − 3.34 (stack, 3H, H-4 min or H-5 min, H-5 maj, H-19), 3.24 (dt, J = 13.1, 4.1 Hz, 0.8H, H-5 maj), 3.19 − 3.00 (stack, 1.8H, H-3 maj, H-4 maj, H-4 min or H-5 min), 2.96 − 2.83 (stack, 1H, H-9), 2.69 (dd, J = 9.0, 5.1 Hz, 0.2H, H-9 min), 2.65 − 2.42 (stack, 3H, H-3 min, H-8, H-9 maj), 2.32 − 1.98 (stack, 5.2H, H-2 min, H-6, H-7, H-16, H-17), 1.98 − 1.90 (m, 0.8H, H-2 maj), 1.71 − 1.50 (stack, 3.2H, H-6, H-7 min, H-18), 1.50 − 1.37 (m, 0.8H, H-7 maj), 1.37 − 1.14 (stack, 2H, H-18), OH not observed.

^{13}C-NMR (101 MHz, CDCl$_3$) (mixture of rotamers) δ_C [172.2, 172.1 (C, C-15)], [138.3, 138.1 (C, C-11)], [128.6, 128.6, 128.5, 127.4, 127.3 (CH, C-12, C-13, C-14)], [75.0, 74.5 (CH, C-1)], 68.0 (CH$_2$, C-19), [62.7, 62.3 (CH$_2$, C-9)], 59.8 (CH$_2$, C-10), [56.2, 55.8 (CH$_2$, C-8)], [48.8, 46.2 (CH$_2$, C-5), [45.5, 45.0 (CH$_2$, C-4)], [44.7, 43.9 (CH, C-2)], 40.8 (CH, C-3 min), [40.7, 40.5 (CH$_2$, C-16)], 36.9 (CH, C-3 maj), [34.8, 33.4, 33.3, 33.23, 33.16 (CH$_2$, C-7, C-18)], [32.3, 32.1 (CH, C-17)], [20.5, 20.3 (CH$_2$, C-6)].

ESI-LRMS (+): 387.4 ([M+H]$^+$, 100%).

HRMS: Found [M+H]$^+$ 387.2631. C$_{23}$H$_{35}$N$_2$O$_3$ requires M+H, 387.2642.

---

[a] Ratio based on H-1 peak integrations in the reported ^{1}H-NMR spectrum.

(3a*R*,9*S*,9a*S*)-2-benzyl-*N*-ethyl-9-hydroxydecahydro-5*H*-pyrrolo[3,4-*c*]azocine-5-carboxamide (224d1)
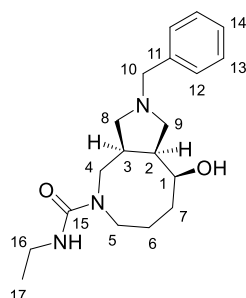
General procedure 9 (page 348) was followed, using building block **224** (0.231 mmol) as the starting material and **d1** as the electrophile. Urea **224d1** was obtained as a colourless oil (43.6 mg, 57%).

v_{max} **(neat / cm^{-1}):** 3347 m (O–H, N–H), 2919 m, 2796 m, 1621 v s (C=O), 1525 v s, 1241 s, 1044 s.

^{1}H-NMR (400 MHz, CDCl$_3$) δ_H 7.33 – 7.17 (stack, 5H, H-12, H-13, H-14), 5.48 (br s, 1H, O*H*), 4.38 (t, *J* = 5.4 Hz, 1H, N*H*), 4.13 – 4.06 (m, 1H, H-1), 3.65 (A of AB, $J_{A–B}$ = 12.8 Hz, 1H, H-10), 3.55 (B of AB, $J_{B–A}$ = 12.8 Hz, 1H, H-10), 3.48 (dd, *J* = 14.2, 5.1 Hz, 1H, H-4), 3.34 – 3.16 (stack, 5H, H-4, H-5, H-16), 2.97 – 2.82 (stack, 2H, H-3, H-9), 2.61 (dd, *J* = 8.8, 5.0 Hz, 1H, H-9), 2.58 – 2.40 (stack, 2H, H-8), 2.26 – 2.03 (stack, 3H, H-2, H-6, H-7), 1.65 – 1.51 (m, 1H, H-6), 1.51 – 1.36 (m, 1H, H-7), 1.11 (t, *J* = 7.2 Hz, 3H, H-17).

^{13}C-NMR (101 MHz, CDCl$_3$) δ_C 158.6 (C, C-15), 138.4 (C, C-11), [128.6, 128.5, 127.3 (CH, C-12, C-13, C-14)], 75.0 (CH, C-1), 62.6 (CH$_2$, C-9), 59.9 (CH$_2$, C-10), 55.8 (CH$_2$, C-8), 47.2 (CH$_2$, C-5), 44.7 (CH, C-2), 44.5 (CH$_2$, C-4), 38.7 (CH, C-3), 35.6 (CH$_2$, C-16), 34.1 (CH$_2$, C-7), 20.4 (CH$_2$, C-6), 15.7 (CH$_3$, C-17).

ESI-LRMS (+): 332.4 ([M+H]$^+$, 100%).

HRMS: Found [M+H]$^+$ 332.2325. C$_{19}$H$_{30}$N$_3$O$_2$ requires M+H, 332.2333.

(3a*S*,9*S*,9a*S*)-2-benzyl-5-ethyldecahydro-1*H*-pyrrolo[3,4-*c*]azocin-9-ol (224e1)
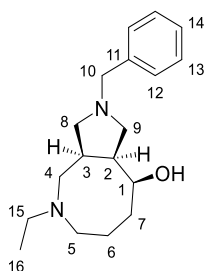
General procedure 11 (page 349) was followed, using building block **224** (0.231 mmol) as the starting material and **e1** as the aldehyde. 3° Amine **224e1** was obtained as a colourless oil (36.9 mg, 55%).

v_{max} **(neat / cm⁻¹):** 2907 s, 2788 s, 1450 s, 1327 m, 1107 s, 1070 s.

¹H-NMR (400 MHz, CDCl₃) δ_H 7.45 – 7.27 (stack, 4H, H-12, H-13), 7.24 – 7.15 (m, 1H, H-14), 3.88 – 3.80 (m, 1H, H-1), 3.68 (A of AB, $J_{A–B}$ = 13.0 Hz, 1H, H-10), 3.64 (B of AB, $J_{B–A}$ = 13.0 Hz, 1H, H-10), 2.94 – 2.66 (stack, 4H, H-4, H-8, H-9), 2.63 – 2.44 (stack, 4H, H-3, H-5, H-15), 2.48 – 2.30 (stack, 3H, H-4, H-5, H-8), 2.28 – 2.16 (m, 1H, H-2), 1.98 – 1.85 (m, 1H, H-7), 1.81 – 1.69 (stack, 2H, H-6), 1.69 – 1.60 (m, 1H, H-7), 1.08 (t, J = 7.2 Hz, 3H, H-16), OH not observed.

¹³C-NMR (101 MHz, CDCl₃) δ_C 139.7 (C, C-11), [128.8, 128.2 (CH, C-12, C-13)], 126.8 (CH, C-14), 68.5 (CH, C-1), 61.0 (CH₂, C-10), 59.9 (CH₂, C-8), 56.9 (CH₂, C-9), 55.2 (CH₂, C-4), 52.6 (CH₂, C-15), 52.0 (CH₂, C-5), 46.5 (CH, C-2), 39.2 (CH, C-3), 34.3 (CH₂, C-7), 25.3 (CH₂, C-6), 12.4 (CH₃, C-16).

ESI-LRMS (+): 289.4 ([M+H]⁺, 100%).

HRMS: Found [M+H]⁺ 289.2265. C₁₈H₂₉N₂O requires M+H, 289.2274.

tert-butyl (3a*S**,9*S**,9a*S**)-2-((2,3-dihydrobenzo[*b*][1,4]dioxin-6-yl)sulfonyl)-9-hydroxydecahydro-5*H*-pyrrolo[3,4-*c*]azocine-5-carboxylate (225a7)
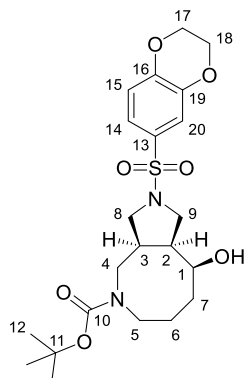
General procedure 9 (page 348) was followed, using building block **225** (0.220 mmol) as the starting material and **a7** as the electrophile. Sulfonamide **225a7** was obtained as a white powder (63.9 mg, 62%).

*v*_{max} **(neat / cm⁻¹):** 3452 w (O–H), 2933 m, 1670 s (C=O), 1491 s, 1282 s, 1152 v s.

¹H-NMR (400 MHz, CDCl₃) δ_H 7.33 (d, *J* = 2.2 Hz, 1H, H-20), 7.29 (dd, *J* = 8.5, 2.2 Hz, 1H, H-14), 6.95 (d, *J* = 8.5 Hz, 1H, H-15), 4.36 − 4.21 (stack, 4H, H-17, H-18), 4.14 − 4.09 (m, 1H, H-1), 3.81 − 3.53 (m, 1H, H-5), 3.49 − 3.22 (stack, 3H, H-4, H-9), 3.20 − 3.06 (stack, 2H, H-8), 2.98 − 2.57 (stack, 3H, H-3, H-4, H-5), 2.43 − 2.21 (m, 1H, H-2), 2.09 − 1.75 (stack, 2H, H-6, H-7), 1.74 − 1.54 (stack, 2H, H-6, H-7), 1.40 (s, 9H, H-12), exchangeable proton not observed.

¹³C-NMR (101 MHz, CDCl₃) δ_C 155.7 (C, C-10), 147.7 (C, C-16), 143.7 (C, C-19), 128.6 (C, C-13), 121.4 (CH, C-14), 117.9 (CH, C-15), 117.3 (CH, C-20), 79.9 (C, C-11), 71.7 (CH, C-1), [64.6, 64.3 (CH₂, C-17, C-18)], 51.8 (CH₂, C-8), 48.5 (CH₂, C-5), 47.0 (CH, C-2), 46.4 (CH₂, C-4), 38.8 (CH, C-3), 33.6 (CH₂, C-7), 28.6 (CH₃, C-12), 23.6 (CH₂, C-6). C-9 resonance not observed, but HSQC cross peaks indicate its presence between δ_C 50 − 48 ppm.

ESI-LRMS (+): 413.3 ([M−C₄H₈ + H]⁺, 100%), 369.3 (40, [M−Boc+H]⁺).

HRMS: Found [M+H]⁺ 469.1990. C₂₂H₃₃N₂O₇S requires M+H, 469.2003.

tert-butyl (3a*R**,9*S**,9a*S**)-2-((4-(difluoromethoxy)phenyl)carbamoyl)-9-hydroxydecahydro-5*H*-pyrrolo[3,4-*c*]azocine-5-carboxylate (225d3)
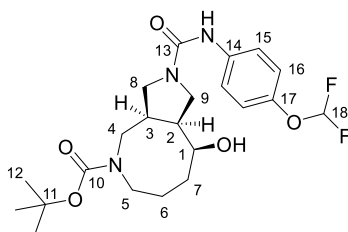
General procedure 9 (page 348) was followed, using building block **225** (0.220 mmol) as the starting material and **d3** as the electrophile. Urea **225d3** was obtained as a colourless glass (50.8 mg, 51%).

v_{max} **(neat / cm^{-1}):** 3329 w (O–H), 2930 w, 1648 s (C=O), 1510 s, 1413 s, 1364 s, 1118 v s.

^{1}H-NMR (400 MHz, CDCl$_3$) δ_H 7.41 – 7.34 (AA' of AA'BB', 2H, H-15 or H-16), 7.04 – 6.97 (BB' of AA'BB', 2H, H-15 or H-16), 6.45 (br s, 1H, OH or N*H*), 6.43 (t, J_{H-F} = 74.4 Hz, 1H, H-18), 4.22 – 4.11 (m, 1H, H-1), 3.80 – 3.60 (stack, 2H, H-5, H-9), 3.60 – 3.52 (m, 1H, H-9), 3.52 – 3.43 (stack, 2H, H-8, OH or N*H*), 3.32 – 3.21 (m, 1H, H-8), 3.06 – 2.82 (stack, 3H, H-3, H-4, H-5), 2.63 – 2.41 (stack, 2H, H-2, H-4), 1.98 – 1.83 (stack, 2H, H-6, H-7), 1.79 – 1.62 (stack, 2H, H-6, H-7), 1.45 (s, 9H, H-12).

^{13}C-NMR (101 MHz, CDCl$_3$) δ_C 155.8 (C, C-10), 154.3 (C, C-13), 146.5 (C, t, J_{C-F} = 2.9 Hz, C-17), 136.8 (C, C-14), [121.0, 120.4 (CH, C-15, C-16)], 116.3 (CH, t, J_{C-F} = 259.4 Hz, C-18), 80.1 (C, C-11), 71.9 (CH, C-1), 50.2 (CH$_2$, C-8), [48.6, 46.8 (CH, C-2, CH$_2$, C-4, C-5, C-9, resonance overlap)], 39.1 (CH, C-3), 33.7 (CH$_2$, C-7), 28.6 (CH$_3$, C-12), 23.8 (CH$_2$, C-6).

ESI-LRMS (+): 456.4 ([M+H]$^+$, 25%), 400.3 (100, [M–C$_4$H$_8$ + H]$^+$), 356.3 (20, [M–Boc+H]$^+$).

HRMS: Found [M+H]$^+$ 456.2292. C$_{22}$H$_{32}$F$_2$N$_3$O$_5$ requires M+H, 456.2305.

tert-butyl (3a*R**,9*S**,9a*S**)-9-hydroxy-2-(2-methylnicotinoyl)decahydro-5*H*-pyrrolo[3,4-*c*]azocine-5-carboxylate (225c5)
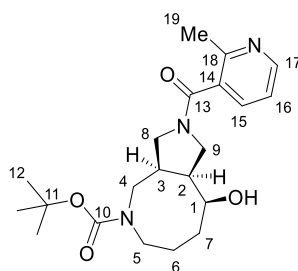
General procedure 10 (page 348) was followed, using building block **225** (0.220 mmol) as the starting material and **c5** as the carboxylic acid. Amide **225c5** was obtained as a yellow glass (43.3 mg, 51%).

v_{max} (neat / cm⁻¹): 3373 w (O–H), 2930 w, 1674 s (C=O), 1618 s, 1409 s, 1364 s, 1163 s.

¹H-NMR (400 MHz, CDCl₃) (mixture of rotamers, 1:1)[a] δ_H 8.52 − 8.43 (stack, 1H, H-17), 7.55 − 7.44 (stack, 1H, H-15), 7.17 − 7.09 (stack, 1H, H-16), [4.18 − 4.11 (m, 0.5H, H-1), 4.07 (app dt, *J* = 8.5, 2.6 Hz, 0.5H, H-1)], 3.83 − 3.78 (m, 1H, H-9), 3.76 − 3.60 (stack, 1.5H, H-4, H-5), 3.60 − 3.45 (stack, 1H, H-4), 3.45 − 3.30 (stack, 1H, H-4, H-9), 3.30 − 3.20 (m, 0.5H, H-9), 3.20 − 3.11 (m, 1H, H-8), 3.07 − 2.77 (stack, 4H, H-3, H-5, H-8, O*H*), [2.52 (s, 1.5H, H-19), 2.50 (s, 1.5H, H-19)], 2.47 − 2.35 (stack, 1H, H-2), 1.98 − 1.53 (stack, 4H, H-6, H-7), [1.44 (s, 4.5H, H-12), 1.40 (s, 4.5H, H-12)].

¹³C-NMR (101 MHz, CDCl₃) (mixture of rotamers) δ_C [168.5, 168.4 (C, C-13)], [155.73, 155.70 (C, C-10)], [154.4, 154.3 (C, C-18)], [149.60, 149.55 (CH, C-17)], 133.9 (CH, C-15), [132.8, 132.6 (C, C-14)], [121.1, 121.0 (CH, C-16)], [80.1, 79.9 (C, C-11)], [72.8, 71.5 (CH, C-1)], 52.4 (CH₂, C-8), 49.9 (CH₂, C-9), [49.5, 48.4, 47.1, 46.6, 45.3 (CH, C-2, CH₂, C-4, C-5, C-8, C-9, resonance overlap)], 44.7 (CH, C-2), [39.9, 38.4 (CH, C-3)], [34.4, 33.7 (CH₂, C-7)], [28.6, 28.5 (CH₃, C-12)], [23.9, 23.0 (CH₂, C-6)], [22.34, 22.28 (CH₃, C-19)].

ESI-LRMS (+): 390.4 ([M+H]⁺, 100%).

HRMS: Found [M+H]⁺ 390.2377. C₂₁H₃₂N₃O₄ requires M+H, 390.2387.

---

[a] Ratio based on observed Me and Boc peak intensities in the reported ¹H-NMR spectrum.

tert-butyl (3a*R**,9*S**,9a*S**)-9-hydroxy-2-(pyridin-2-ylmethyl)decahydro-5*H*-pyrrolo[3,4-*c*]azocine-5-carboxylate (225e2)
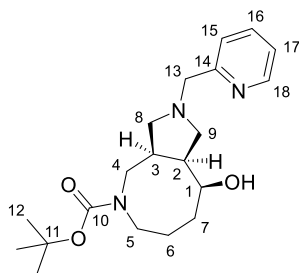
General procedure 11 (page 349) was followed, using building block **225** (0.220 mmol) as the starting material and **e2** as the aldehyde. 3° Amine **225e2** was obtained as a yellow oil (53.8 mg, 68%).

v_{max} (neat / cm^{-1}): 3370 w (O–H), 2919 m, 2803 w, 1685 s (C=O), 1409 s, 1364 s, 1159 s.

^{1}H-NMR (400 MHz, CDCl$_3$) (mixture of rotamers, 1:1)[a] δ_H 8.49 (d, J = 4.3 Hz, 1H, H-18), 7.62 (app dd, J = 7.8, 7.8 Hz, 1H, H-16), 7.29 (d, J = 7.8 Hz, 1H, H-15), 7.18 – 7.08 (stack, 1H, H-17), 4.17 – 4.04 (stack, 1H, H-1), 3.90 – 3.69 (stack, 2H, H-13), 3.69 – 3.31 (stack, 2H, H-4, H-5), 3.23 – 3.08 (m, 1H, H-4), 3.09 – 2.97 (stack, 1.5H, H-3, H-5), 2.97 – 2.70 (stack, 2.5H, H-3, H-9), 2.67 – 2.46 (stack, 2H, H-8), 2.15 – 1.97 (stack, 3H, H-2, H-6, H-7), 1.64 – 1.28 (stack, 11H, [including 1.41 (app s, 9H, H-12)], H-6, H-7, H-12), OH not observed.

^{13}C-NMR (101 MHz, CDCl$_3$) (mixture of rotamers) δ_C 158.4 (C, C-14), 156.2 (C, C-10), 149.2 (CH, C-18), 136.8 (CH, C-16), 122.8 (CH, C-15), 122.3 (CH, C-17), 79.4 (C, C-11), 74.8 (CH, C-1), [62.2, 62.1 (CH$_2$, C-13)], [61.6, 61.5 (CH$_2$, C-9)], [56.1, 56.0 (CH$_2$, C-8)], [47.7, 47.1 (CH$_2$, C-5)], 45.1 (CH$_2$, C-4), [44.9, 44.8 (CH, C-2)], [39.1, 37.9 (CH, C-3)], 33.6 (CH$_2$, C-7), 28.6 (CH$_3$, C-12), [20.6, 20.3 (CH$_2$, C-6)].

ESI-LRMS (+): 362.4 ([M+H]$^+$, 100%).

HRMS: Found [M+H]$^+$ 362.2427. C$_{20}$H$_{32}$N$_3$O$_3$ requires M+H, 362.2438.

---

[a] Ratio based on H-3 peak integrations in the reported ^{1}H-NMR spectrum at δ_H (CDCl$_3$) 3.09 – 2.97 and 2.97 – 2.70 ppm.

(3a*R**,9*S**,9a*S**)-5-((2,4-dimethylthiazol-5-yl)sulfonyl)decahydro-1*H*-pyrrolo[3,4-*c*]azocin-9-ol (226a3)
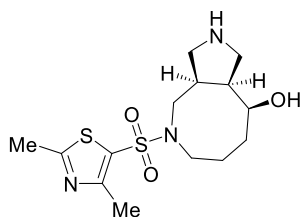
General procedure 12 (page 349) was followed, using benzylamine **224a3** (0.089 mmol) as the starting material. 2° Amine **226a3** was obtained as a brown powder (1.3 mg, 4%).

The amount of material obtained was not found sufficient to provide NMR spectroscopic data with adequate quality. Therefore, selected data are reported.

v$_{max}$ (neat / cm^{-1}): 3243 w (O–H,N–H), 2922 w, 1424 m, 1338 s, 1152 s.

ESI-LRMS (+): 346.2 ([M+H]$^+$, 100%)

HRMS: Found [M+H]$^+$ 346.1245. $C_{14}H_{24}N_3O_3S_2$ requires M+H, 346.1254.

1-((3a*R**,9*S**,9a*S**)-9-hydroxydecahydro-5*H*-pyrrolo[3,4-*c*]azocin-5-yl)-2-(tetrahydro-2*H*-pyran-4-yl)ethan-1-one (226c1)
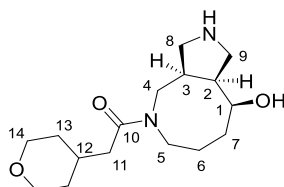
General procedure 12 (page 349) was followed, using benzylamine **224c1** (0.122 mmol) as the starting material. 2° Amine **226c1** was obtained as a yellow glass (29.2 mg, 81%).

*v*_{max} (neat / cm⁻¹): 3377 m (O–H, N–H), 2922 m, 2848 m, 1614 s (C=O), 1416 s, 1088 s.

v_{max} (neat / cm^{-1}): 3377 m (O–H, N–H), 2922 m, 2848 m, 1614 s (C=O), 1416 s, 1088 s.

¹H-NMR (400 MHz, CD₃OD) (mixture of conformational isomers, including hindered rotation around amide bond, 1:1:1:1)[a] δ_H 4.15 – 4.01 (stack, 1H, H-1), 3.98 – 3.86 (stack, 2H, H-14), 3.86 – 3.37 (stack, 5H, H-4, H-8, H-9, H-14), 3.36 – 3.12 (stack, 4H, H-4, H-5, H-8, H-9), 3.06 – 2.89 (stack, 1.5H, H-3, H-8, H-9), 2.89 – 2.78 (m, 0.25H, H-3), 2.69 – 2.59 (m, 0.25H, H-3), 2.56 – 2.45 (m, 0.25H, H-2), 2.45 – 2.23 (stack, 2.75H, H-2, H-11), 2.18 – 1.89 (stack, 3H, H-6, H-7, H-12), 1.89 – 1.59 (stack, 4H, H-6, H-7, H-13), 1.43 – 1.25 (m, 2H, H-13), exchangeable protons not observed.

¹³C-NMR (101 MHz, CD₃OD) (mixture of rotamers) δ_C 174.5 (C, C-10), [73.3, 72.2 (CH, C-1)], [69.0, 68.9 (CH₂, C-14)], [52.0, 51.0, 50.7, 50.3 (CH₂, C-8, C-9)], 46.5 (CH, C-2), 46.1 (CH₂, C-4, C-5, resonance overlap), [41.3, 41.2 (CH₂, C-11)], [39.9, 39.7 (CH, C-3)], [34.6, 34.1 (CH₂, C-7, C-13)], 33.4 (CH, C-12), 24.1 (CH₂, C-6).

ESI-LRMS (+): 297.2 ([M+H]⁺, 100%).

HRMS: Found [M+H]⁺ 297.2167. C₁₆H₂₉N₂O₃ requires M+H, 297.2173.

---

[a] Ratio based on H-3 and H-2 peak integrations in the reported ¹H-NMR spectrum at δ_H (CDCl₃) 2.89 – 2.78, 2.69 – 2.59, 2.56 – 2.45 and 2.45 – 2.23 ppm, respectively.

(3a*R**,9*S**,9a*S**)-*N*-ethyl-9-hydroxydecahydro-5*H*-pyrrolo[3,4-*c*]azocine-5-carboxamide (226d1)
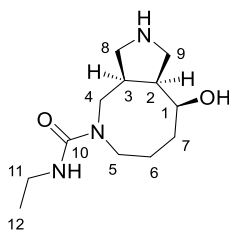
General procedure 12 (page 349) was followed, using benzylamine **224d1** (0.154 mmol) as the starting material. 2° Amine **226d1** was obtained as a colourless glass (18.3 mg, 49%).

N_{max} **(neat / cm^{-1}):** 3317 m (O–H, N–H), 2930 m, 2870 m, 1614 s (C=O), 1525 s, 1402 s, 1208 s.

^{1}H-NMR (400 MHz, D$_2$O) (mixture of rotamers, 1:1)[a] δ_H 4.22 – 4.08 (stack, 1H, H-1), 3.73 – 3.50 (stack, 1.5H, H-4, H-5), 3.49 – 3.28 (stack, 3.5H, H-4, H-8, H-9), 3.22 – 2.85 (stack, 5.5H, H-3, H-4, H-5, H-8, H-11), 2.77 – 2.66 (m, 0.5H, H-3), 2.63 – 2.48 (stack, 1H, H-2), 1.95 – 1.63 (stack, 4H, H-6, H-7), 1.04 (app t, *J* = 7.2 Hz, 3H, H-12), exchangeable protons not observed.

^{13}C-NMR (101 MHz, D$_2$O) (mixture of rotamers) δ_C [163.4, 159.7 (C, C-10)], [71.2, 71.1 (CH, C-1)], 50.2 (CH$_2$, C-8), [48.6, 48.5, 48.4 (CH$_2$, C-5, C-8)], 47.4 (CH, C-2), [47.3, 47.0 (CH$_2$, C-4, C-9)], 45.6 (CH, C-2), 45.5 (CH$_2$, C-4), 44.3 (CH$_2$, C-9), [38.8, 38.5 (CH, C-3)], 35.4 (CH$_2$, C-11), [32.4, 31.9 (CH$_2$, C-7)], [24.9, 23.4 (CH$_2$, C-6)], [15.0, 14.9 (CH$_3$, C-12)].

ESI-LRMS (+): 242.2 ([M+H]$^+$, 100%).

HRMS: Found [M+H]$^+$ 242.1859. C$_{12}$H$_{24}$N$_3$O$_2$ requires M+H, 242.1863.

---

[a] Ratio based on H-3 peak integrations in the reported ^{1}H-NMR spectrum at δ_H (CDCl$_3$) 3.22 – 2.85 and 2.77 – 2.66 ppm.

(3aR*,9S*,9aS*)-5-ethyldecahydro-1H-pyrrolo[3,4-c]azocin-9-ol (226e1)
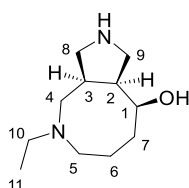
General procedure 12 (page 349) was followed, using benzylamine **224e1** (0.132 mmol) as the starting material. 2° Amine **226e1** was obtained as a white powder (20.4 mg, 78%).

v_{max} (neat / cm^{-1}): 3425 m (O–H, N–H), 2922 m, 2863 m, 1420 v s, 1334 s, 1066 s.

^{1}H-NMR (400 MHz, D$_2$O) (mixture of conformers, 3:2)[a] δ_H 4.13 − 4.02 (stack, 1H, H-1), 3.44 − 3.18 (stack, 3H, H-8, H-9), [3.15 (dd, J = 10.6, 2.2 Hz, 0.4H, H-8 min), 3.07 (dd, J = 11.7, 5.1 Hz, 0.6H, H-8 maj)], 2.89 − 2.75 (m, 0.6H, H-3 maj), 2.75 − 2.48 (stack, 6.4H, H-3 min, H-4, H-5, H-10), 2.48 − 2.32 (stack, 1H, H-2), 2.10 − 1.87 (stack, 1H, H-7), 1.86 − 1.61 (stack, 3H, H-6, H-7), [1.10 (t, J = 7.2 Hz, 1.2H, H-11 min), 1.09 (t, J = 7.3 Hz, 1.8H, H-11 maj)], exchangeable protons not observed.[b]

^{13}C-NMR (101 MHz, D$_2$O) (mixture of conformers) δ_C [68.0 (CH, C-1 maj), 66.7 (CH, C-1 min)], 52.7 (CH$_2$, C-4), [52.1 (CH$_2$, C-10 min), 52.0 (CH$_2$, C-10 maj)], [51.3, 51.0, 50.8, 50.6 (CH$_2$, C-8 min, C-4, C-5)], 49.7 (CH$_2$, C-8 maj), 48.2, 47.0 (CH$_2$, C-9), [46.6 (CH, C-2 min), 45.5 (CH, C-2 maj)], [38.0 (CH, C-3 maj), 37.0 (CH, C-3 min)], [32.7 (CH$_2$, C-7 maj), 31.4 (CH$_2$, C-7 min)], [24.4 (CH$_2$, C-6 min), 23.6 (CH$_2$, C-6 maj)], [11.52 (CH$_3$, C-11 maj), 11.45 (CH$_3$, C-11 min)].

ESI-LRMS (+): 199.3 ([M+H]$^+$, 100%).

HRMS: Found [M+H]$^+$ 199.1802. C$_{11}$H$_{23}$N$_2$O requires M+H, 199.1805.

---

[a] Ratio based on H-8 peak integrations in the reported ^{1}H-NMR spectrum.
[b] ^{1}H-NMR spectroscopic analysis at ∼80 °C shows the H-3, H-7 and H-11 resonances approaching coalescence. Furthermore, LCMS and SFC analysis showed a single compound.

(3a*S**,9*S**,9a*S**)-2-((2,3-dihydrobenzo[*b*][1,4]dioxin-6-yl)sulfonyl)decahydro-1*H*-pyrrolo[3,4-*c*]azocin-9-ol (228a7)
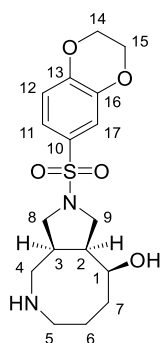
General procedure 13 (page 350) was followed, using Boc-amine **225a7** (0.108 mmol) as the starting material. 2° Amine **228a7** was obtained as an off-white powder (31.2 mg, 78%).

v$_{max}$ (neat / cm^{-1}): 2930 m, 2863 m, 1580 m, 1491 s, 1282 s, 1122 s, 1059 s.

^{1}H-NMR (400 MHz, CD$_3$OD) (mixture of conformers, 4:1)[a] δ_H 7.36 − 7.26 (stack, 2H, H-12, H-17), 7.07 − 7.00 (stack, 1H, H-11), 4.36 − 4.27 (stack, 4H, H-14, H-15), [3.98 − 3.89 (m, 0.8H, H-1 maj), 3.60 − 3.51 (m, 0.2H, H-1 min)], 3.41 − 3.19 (stack, 2.8H, H-4 min, H-8, H-9 maj), 3.16 − 3.02 (stack, 1H, H-8), 2.97 − 2.79 (stack, 1.6H, H-4 min, H-5, H-9 min), 2.78 − 2.69 (m, 0.2H, H-5 min), 2.67 − 2.54 (stack, 1.8H, H-3, H-4 maj), 2.47 (ddd, *J* = 13.8, 10.4, 3.0 Hz, 0.8H, H-5 maj), 2.31 − 2.12 (stack, 1.8H, H-2, H-4 maj), 2.09 − 1.91 (stack, 1H, H-7), 1.91 − 1.68 (stack, 1H, H-6), 1.68 − 1.50 (stack, 2H, H-6, H-7), exchangeable protons not observed.

^{13}C-NMR (101 MHz, CD$_3$OD) (mixture of conformers) δ_C [149.2, 145.2 (C, C-13, C-16)], 130.3 (C, C-10), [122.7, 122.1, 118.9, 118.3, 117.9 (CH, C-11, C-12, C-17)], [69.2 (CH, C-1 min), 67.1 (CH, C-1 maj)], [65.9, 65.6 (CH$_2$, C-14, C-15)], [58.5 (CH$_2$, C-8 min), 53.8 (CH$_2$, C-8 maj)], [53.4, 52.4, 51.0 (CH$_2$, C-4 min, C-5 min, C-9 min)], 49.8 (CH$_2$, C-9 maj), 48.4 (CH, C-2 maj), 46.2 (CH$_2$, C-4 maj), 46.0 (CH, C-2 min), 44.6 (CH, C-3 min), 44.5 (CH$_2$, C-5 maj), 38.4 (CH, C-3 maj), 33.1 (CH$_2$, C-7), [26.4 (CH$_2$, C-6 maj), 26.3 (CH$_2$, C-6 min)].

ESI-LRMS (+): 369.2 ([M+H]$^+$, 100%).

HRMS: Found [M+H]$^+$ 369.1467. C$_{17}$H$_{25}$N$_2$O$_5$S requires M+H, 369.1479.

---

[a] Ratio based on H-1 peak integrations in the reported ^{1}H-NMR spectrum.

(3a*S**,9*S**,9a*S**)-*N*-(4-(difluoromethoxy)phenyl)-9-hydroxydecahydro-2*H*-pyrrolo[3,4-*c*]azocine-2-carboxamide (228d3)
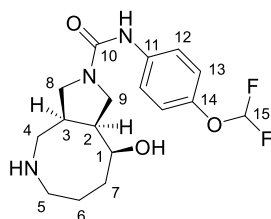
General procedure 13 (page 350) was followed, using Boc-amine **225d3** (0.117 mmol) as the starting material. 2° Amine **228d3** was obtained as a colourless crystalline solid (29.8 mg, 72%).

v_{max} (neat / cm^{-1}): 3295 w (O–H, N–H), 2941 w, 2878 w, 1640 s (C=O), 1513 s, 1416 s, 1375 s, 1103 s, 1029 s.

^{1}H-NMR (400 MHz, CD$_3$OD) (mixture of rotamers, 4:1)[a] δ_H 7.49 − 7.35 (AA' of AA'BB', 2H, H-12 or H-13), 7.12 − 6.97 (BB' of AA'BB', 2H, H-12 or H-13), 6.96 − 6.50 (stack, 1H, [including 6.72 (t, J_{H-F} = 74.3 Hz, 0.8H, H-15 maj)], H-15), [4.09 − 3.99 (m, 0.8H, H-1 maj), 3.79 − 3.69 (m, 0.2H, H-1 min)], 3.68 − 3.40 (stack, 3.2H, H-8, H-9), 3.36 (dd, *J* = 10.3, 2.5 Hz, 0.8H, H-8 maj), 3.25 (dd, *J* = 10.0, 7.6 Hz, 0.2H, H-4 min), 3.13 − 3.02 (m, 0.2H, H-3 min), 3.02 − 2.85 (stack, 1.2H, H-5, H-2 min), 2.83 − 2.64 (stack, 2.6H, H-3 maj, H-4 maj, H-5 min), 2.58 (ddd, *J* = 13.2, 9.7, 2.9 Hz, 0.8H, H-5 maj), 2.48 − 2.34 (stack, 1H, H-2 maj, H-4 min), 2.11 − 1.95 (stack, 1H, H-7), 1.95 − 1.59 (stack, 3H, H-6, H-7), exchangeable protons not observed.

^{1}H-NMR (400 MHz, DMSO-*d$_6$*) (mixture of rotamers, 3:7)[b] δ_H [8.21 (s, 0.3H, CONH *min)*, 8.18 (s, 0.7H, CONH maj)], 7.58 − 7.49 (stack, 2H, H-12 or H-13), 7.17 (app br s, 1H, CH$_2$N*H*CH$_2$ or O*H*), [7.09 (t, J_{H-F} = 74.5 Hz, 0.3H, H-15 min), 7.08 (t, J_{H-F} = 74.5 Hz, 0.7H, H-15 maj)], 7.07 − 7.00 (stack, 2H, H-12 or H-13), 3.87 (m, 0.7H, H-1 maj), 3.59 − 3.19 (stack, 4.3H, H-1 min, H-8, H-9), 3.15 − 3.04 (m, 0.3H, H-4 min), 3.00 − 2.88 (m, 0.3H, H-3 min), 2.86 − 2.68 (stack, 1.3H, H-2 min, H-5), 2.68 − 2.53 (stack, 1.7H, H-3 maj, H-4 maj, H-5 min), 2.48 − 2.36 (stack, 1.4H, H-4 maj, H-5 maj), 2.31 − 2.21 (stack, 1H, H-2 maj, H-4 min), 1.99 − 1.41 (stack, 4H, H-6, H-7), CH$_2$N*H*CH$_2$ or OH not observed.

---

[a] Ratio based on H-1 peak integrations in the reported ^{1}H-NMR spectrum.

[b] Ratio based on H-15 peak integrations in the reported ^{1}H-NMR spectrum. A high-temperature ^{1}H-NMR experiment (∼80 °C) shows rotamer resonances of H-4, H-5 and H-6 migrating towards one another, but no coalescence was observed, nor for the other proton signals. These results combined with consistent signal ratios for both exchangeable and non-exchangeable resonances support the hypothesis of rotamers with a high rotational energy barrier.

¹³C-NMR (101 MHz, CD₃OD) (mixture of rotamers) δ_C [157.2, 157.0 (C, C-10)], 148.2 (C, t, J_{C-F} = 3.0 Hz, C-14), [138.4, 138.2 (C, C-11)], [123.4, 123.3, 120.7 (CH, C-12, C-13)], 118.0 (CH, t, J_{C-F} = 257.6 Hz, C-15), 68.2 (CH, C-1), 58.6 (CH₂, C-4 min), 55.3 (CH₂, C-5 min), 52.0 (CH₂, C-8 maj), [50.1, 49.8 (CH₂, C-8 min, C-9 min)], 48.0 (CH₂, C-9 maj), 46.9 (CH, C-2), 46.4 (CH₂, C-4 maj), 45.8 (CH, C-3), 45.0 (CH₂, C-5 maj), 33.6 (CH₂, C-7), [28.1, 28.0 (CH₂, C-6, C-7)], 26.4 (CH₂, C-6).

ESI-LRMS (+): 378.2 ([M+Na]⁺, 1%), 356.2 (100, [M+H]⁺).

HRMS Found [M+H]⁺ 356.1768. C₁₇H₂₄F₂N₃O₃ requires M+H, 356.1780.

((3a*S**,9*S**,9a*S**)-9-hydroxydecahydro-2*H*-pyrrolo[3,4-*c*]azocin-2-yl)(2-methylpyridin-3-yl)methanone (228c5)
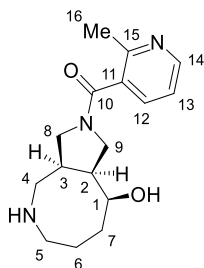
General procedure 13 (page 350) was followed, using Boc-amine **225c5** (0.101 mmol) as the starting material. 2° Amine **228c5** was obtained as a beige powder (9.3 mg, 32%).

v$_{max}$ (neat / cm^{-1}): 3317 m (O–H, N–H), 2930 m, 1607 s (C=O), 1461 s, 1420 s.

^{1}H-NMR (400 MHz, CD$_3$OD) (mixture of rotamers, 1:1)[a] δ_H 8.53 – 8.45 (stack, 1H, H-14), 7.80 – 7.70 (stack, 1H, H-12), 7.40 – 7.31 (stack, 1H, H-13), [4.13 – 4.04 (m, 0.5H, H-1), 3.93 – 3.88 (m, 0.5H, H-1)], 3.87 – 3.64 (stack, 1H, H-9), 3.64 – 3.56 (stack, 1H, H-8), 3.43 – 3.33 (stack, 1H, H-9), 3.10 – 2.95 (stack, 1H, H-8), 2.95 – 2.77 (stack, 2.5H, H-3, H-4, H-5), 2.77 – 2.57 (stack, 2.5H, H-3, H-4, H-5), [2.52 (s, 1.5H, H-16), 2.51 (s, 1.5H, H-16)], 2.49 – 2.34 (stack, 1H, H-2), 2.02 – 1.87 (stack, 1H, H-7), 1.87 – 1.65 (stack, 3H, H-6, H-7), exchangeable protons not observed.

^{13}C-NMR (101 MHz, CD$_3$OD) (mixture of rotamers) δ_C 169.9 (C, C-10), 155.2 (C, C-15), 150.3 (CH, C-14), 136.1 (CH, C-12), 134.2 (C, C-11), 122.9 (CH, C-13), [70.2, 69.0 (CH, C-1)], 54.4 (CH$_2$, C-8), 52.5 (CH$_2$, C-9), 51.8 (CH$_2$, C-8), 50.8 (CH$_2$, C-9), [47.6, 45.9 (CH, C-2)], [45.8, 45.7, 45.3, 45.0 (CH$_2$, C-4, C-5)], [40.1, 38.3 (CH, C-3)], [34.5, 34.0 (CH$_2$, C-7)], [25.6, 25.2 (CH$_2$, C-6)], 21.8 (CH$_3$, C-16).

ESI-LRMS (+): 312.1 ([M+Na]$^+$, 1%), 290.2 (100, [M+H]$^+$).

HRMS: Found [M+H]$^+$ 290.1856. C$_{16}$H$_{24}$N$_3$O$_2$ requires M+H, 290.1863.

---

[a] Ratio based on H-1 peak integrations in the reported ^{1}H-NMR spectrum.

(3a*S**,9*S**,9a*S**)-2-(pyridin-2-ylmethyl)decahydro-1*H*-pyrrolo[3,4-*c*]azocin-9-ol (228e2)
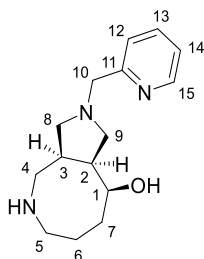
General procedure 13 (page 350) was followed, using Boc-amine **225e2** (0.143 mmol) as the starting material. 2° Amine **228e2** was obtained as an off-white solid (10.4 mg, 28%).

v_{max} **(neat / cm⁻¹):** 3247 m (O–H, N–H), 2915 m, 2814 m, 1532 m, 1476 s, 1279 s.

¹H-NMR (400 MHz, CD₃OD) δ_H 8.48 (dd, *J* = 5.1, 1.8 Hz, 1H, H-15), 7.82 (ddd, *J* = 7.7, 7.7, 1.8 Hz, 1H, H-13), 7.52 (d, *J* = 7.7 Hz, 1H, H-12), 7.32 (dd, *J* = 7.7, 5.1 Hz, 1H, H-14), 3.98 – 3.91 (m, 1H, H-1), 3.86 – 3.77 (m, 2H, H-10), 3.35 – 3.26 (m, 1H, H-4), 3.07 – 2.98 (m, 1H, H-5), 2.98 – 2.87 (stack, 2H, H-8, H-9), 2.87 – 2.72 (stack, 3H, H-4, H-5, H-8 or H-9), 2.65 – 2.52 (m, 1H, H-3), 2.47 – 2.32 (stack, 2H, H-2, H-8 or H-9), 1.99 – 1.88 (m, 1H, H-7), 1.88 – 1.79 (stack, 2H, H-6), 1.79 – 1.66 (m, 1H, H-7), exchangeable protons not observed.

¹³C-NMR (101 MHz, CD₃OD) δ_C 159.7 (C, C-11), 149.6 (CH, C-15), 138.8 (CH, C-13), 125.0 (CH, C-12), 123.9 (CH, C-14), 70.4 (CH, C-1), 62.6 (CH₂, C-10), [60.7, 59.2 (CH₂, C-8, C-9)], 46.2 (CH, C-2), 46.1 (CH₂, C-4), 45.5 (CH₂, C-5), 39.7 (CH, C-3), 35.5 (CH₂, C-7), 23.8 (CH₂, C-6).

ESI-LRMS (+): 284.2 ([M+Na]⁺, 1%), 262.2 (100, [M+H]⁺).

HRMS: Found [M+H]⁺ 262.1907. C₁₅H₂₄N₃O requires M+H, 262.1914.

12. SACE3 Library summary
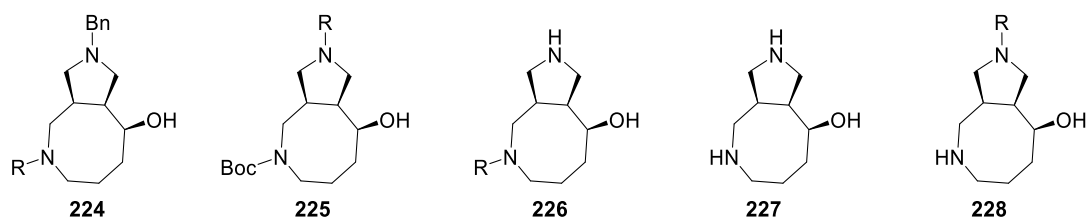
Table 23: SACE3 library compounds.

Product	Method	MW (Da)	Amount SM (mmol)[a]	Yield (mg)	Yield (%)	t_R (min)[b]	Purity (%)[b]	Comment[c]
224	-	260.4	0.231	28.6	48%	1.04	87	-
224a3	9	435.6	0.231	46.4	46%	1.55	96	-
224c1	10	386.5	0.231	58.2	65%	1.16	96	-
224d1	9	331.5	0.231	43.6	57%	1.09	100	-
224e1	11	288.4	0.231	36.9	55%	1.31	96	-
225	-	270.4	0.220	41.3	69%	1.34	72	-
225a7	9	468.6	0.220	63.9	62%	1.43	97	-
225c5	10	389.5	0.220	43.3	51%	1.04	96	-
225d3	9	455.5	0.220	50.8	51%	1.39	98	-
225e2	11	361.5	0.220	53.8	68%	1.20	95	-
226a3	12	345.5	0.089	1.3	4%	1.02	100	-
226c1	12	296.4	0.122	29.2	81%	0.72	100	-
226d1	12	241.3	0.154	18.3	49%	0.59	100	-
226e1	12	198.3	0.132	20.4	78%	n.a.	n.a.	Not UV active
227	12, 13	170.3	0.131	-	-	-	-	Failed purification
228a7	13	368.5	0.108	31.2	78%	1.19	84	Contains $[M-18]^+$ BP
228c5	13	289.4	0.101	9.3	32%	0.77	52	Contains $[M-18]^+$ BP
228d3	13	355.4	0.117	29.8	72%	1.17	89	Contains $[M-18]^+$ BP
228e2	13	261.4	0.143	10.4	28%	0.82	100	-

[a]SM: starting material. [b]Retention time and purity measured using UPLC. Purity calculated as product peak AUC fraction in the total absorbance chromatogram (210 − 320 nm). [c]BP: byproduct, observed *via* LCMS analysis. However, these byproducts were not observed *via* ^{1}H- and ^{13}C-NMR spectroscopic analysis, indicating that the compound may degrade on the LCMS column.

13. Chloride ion content determination

Chloride content was measured experimentally by the Symeres Analytical Facility for a selection of HCl salts, following a chromatographic method:

The sample was prepared twice by accurately weighing 1.0 ± 0.3 mg of compound into a 1 mL flask and dissolving it in H_2O:MeCN 1:1.
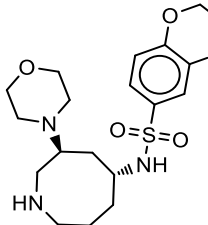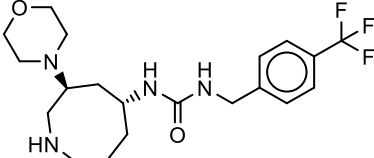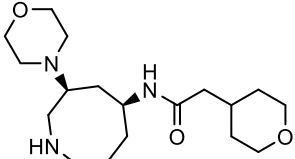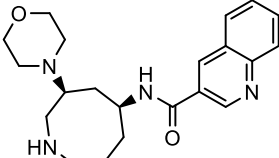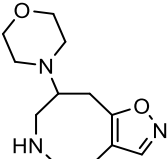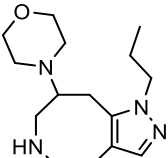
A calibration curve was prepared by weighing 25.00 ± 3.00 mg of NaCl into a 100 mL flask and dissolving it in H_2O. These solutions were measured (method: TrinityP1_iso50_CAD) at injection volumes of 0.2 μL, 0.5 μL, 2 μL, 4μL and 8 μL (*in duplo*). Submitted samples were measured using this method with an injection volume of 2 μL (*in triplo*). The amount of chloride ion present in the sample was calculated *via* the average of CAD responses.

TrinityP1_iso50_CAD Method

Column: Trinity P1 150 × 3.0 mm 3 μ; temperature: 40 °C; flow rate: 0.9 mL min^{-1}; eluent A: 20 mM NH_4OAc in water pH = 5.0; eluent B: MeCN; isocratic: 50% B (for 12 min); detection CAD: neb. gas 40 °C, filter: 3.6 s.

Results

Table 24: Experimentally determined chloride ion content for a selection of HCl salts.

Compound	Base Structure	wt% Cl⁻	#molecule Cl⁻ / salt	n
trans-108a7		16.5	2.3	6
trans-180d4		16.3	2.3	6
cis-108c1		18.7	2.2	3
cis-108c6		21.7	2.9	6
163		21.6	2.1	6
164		24.9	2.6	6

14. Experimental logD measurements

LogD values were measured experimentally by the Symeres Analytical Facility for a selection of library compounds, following the chromatographic method described by Lombardo *et al.*[21]

14.1. Procedure

The sample (18 μL, 10 mM DMSO stock) was diluted with MeOH:H_2O 1:1 solution (80 μL). Sample analysis was achieved using gradient HPLC with three different isocratic mobile phases of 0.25% *n*-octanol in MeOH (60, 65 and 70%) and 20 mM MOPS buffer (pH=7.4) with *n*-decylamine.[a] Sample analysis of compounds with a low ElogD was achieved using gradient HPLC[b] with three different isocratic mobile phases of 0.25% *n*-octanol in MeOH (50, 45 and 40%) and 20 mM MOPS buffer (pH=7.4) with *n*-decylamine. Peaks were detected with a photodiode array at 220 to 320 nm. A calibration curve was produced from a series of reference standards. ElogD(7.4) was then calculated for the sample, based on retention time. Each experiment was performed in triplicate. This method is only for neutral and basic compounds.

Table 25: ElogD values measured for reference standards.

Reference standard	LC-Method	Average ElogD (7.4) (n= 3)	Standard error
estradiol	Normal	4.1	0.02
haloperidol	Normal	2.2	0.05
chlorpromazine	Normal	3.0	0.03
triamterene	Low	1.1	0.11
nifuroxime	Low	1.1	0.01
antipyrine	Low	0.4	0.02

---

[a] The Symeres procedure for MOPS buffer with *n*-decylamine is as follows: 3.240 g MOPS and 5.678 g MOPS sodium salt is dissolved in 200 mL *n*-octanol-saturated water. 3 mL *n*-decylamine is added. Subsequently, 700 mL *n*-octanol-saturated water is added. Hydrochloric acid (1 M) is added until pH = 7.4. The resulting mixture is diluted with *n*-octanol-saturated water to a total volume of 2 L, after which time the solution is filtered over a GHP filter (pore size 0.45 μm). (MOPS: 3-(*N*-morpholino)propanesulfonic acid)

[b] column: Supelcosil LC-ABZ+ (50 × 4.6, 5 μm); flow rate: 2 mL min^{-1}; column temperature: 40 °C

Table 26: ElogD values measured for the selected library compounds.

Compound	LC-Method	Calculated SlogP[a]	Average ElogD (7.4) (n= 3)	Standard error
trans-103a3	Low	0.6	0.8	0.02
trans-104d4	Normal	2.8	3.1	0.04
trans-108d1	Low	0.2	< 0.2[b]	n.a.
cis-103d1	Low	−0.2	< 0.2 [b]	n.a.
cis-104c4	Low	1	0.4	0.02
cis-108c6	Low	1.8	0.7	0.03
159d3	Normal	3.9	3.5	0.03
161a7	Normal	2.2	3.2	0.02
162	Low	−0.2	< 0.2 [b]	n.a.
163a3	Low	1.2	1.3	0.00
164d1	Low	1.1	0.7	0.01
166a4	Low	−0.9	<0.2 [b]	n.a
168c2	Low	1.6	0.5	0.01
169c5	Low	0.7	<0.2 [b]	n.a.
224d1	Low	1.9	< 0.2 [b]	n.a.
224e1	Low	2.2	< 0.2 [b]	n.a.
225a7	Normal	2.1	3.2	0.02
225c5	Low	2.5	1.4	0.07
226c1	Low	0.6	1.3	0.01
228e2	Low	0.9	0.2	0.03

[a] SlogP was calculated using the 'RDKit Descriptor calculation' node in KNIME, using the SlogP calculation reported by Wildman and Crippen.[22, b] Compounds with ElogD <0.2 produced data-points which fell below the range of the calibration curve or co-eluted with the internal standard, preventing accurate measurement of ElogD. n.a.: not applicable.

15. References

1   Bradley G., D. Williams and M. Lawton, *J. Org. Chem.*, 2010, **75**, 8351–8354.

2   H.-S. Lin and L. Paquette, *Synth. Commun.*, 1994, **24**, 2503–2506.

3   Author Guidelines, https://publish.acs.org/publish/author_guidelines?coden=acsccc, (accessed 13 February 2022).

4   N. Nandi, K. Gayen, S. Ghosh, D. Bhunia, S. Kirkham, S. K. Sen, S. Ghosh, I. W. Hamley and A. Banerjee, *Biomacromolecules*, 2017, **18**, 3621–3629.

5   L. Ejim, I. A. Mirza, C. Capone, I. Nazi, S. Jenkins, G.-L. Chee, A. M. Berghuis and G. D. Wright, *Bioorg. Med. Chem.*, 2004, **12**, 3825–3830.

6   M. Morales-Chamorro and A. Vázquez, *Synthesis*, 2019, **51**, 842–847.

7   M. F. El-Mansy, M. Flister, S. Lindeman, K. Kalous, D. S. Sem and W. A. Donaldson, *Chem. Eur. J.*, 2015, **21**, 10886–10895.

8   J. Moran, P. Dornan and A. M. Beauchemin, *Org. Lett.*, 2007, **9**, 3893–3896.

9   N. T. Zaveri, F. Jiang and L. Toll, Nicotinic acetylcholine receptor modulators, WO2011085389A1, 2011.

10   M. A. C. Foley, K. W. Kuntz, L. H. Mitchell, M. J. Munchhof and D. M. Harvey, Substituted pyrrolidine compounds as Antitumor agents, WO2016040504A1, 2016.

11   G. R. Lawton, H. Ji, P. Martásek, L. J. Roman and R. B. Silverman, *Beilstein J. Org. Chem.*, 2009, **5**, 28.

12   L. Lu, S. H. Lahasky, D. Zhang and J. C. Garno, *ACS Appl. Mater. Interfaces*, 2016, **8**, 4014–4022.

13   B. Thiedemann, C. M. L. Schmitz and A. Staubitz, *J. Org. Chem.*, 2014, **79**, 10284–10295.

14   S. H. Park, H. J. Kang, S. Ko, S. Park and S. Chang, *Tetrahedron Asymmetry*, 2001, **12**, 2621–2624.

15   K. Hung, P. W. R. Harris and M. A. Brimble, *Org. Lett.,* 2012, **14**, 5784–5787.

16   M. Gensini and A. de Meijere, *Chem. Eur. J.*, 2004, **10**, 785–790.

17   A. M. Mouna, C. Nguyen, I. Rage, J. Xie, G. Née, J. P. Mazaleyrat and M. Wakselman, *Synth. Commun.*, 1994, **24**, 2429–2435.

18   F. M. Martin, D. J. Mergott and W. M. Owton, Preparation of tetrahydropyrrolothiazinamines as BACE inhibitors, WO2014066132A1, 2014.

19   O. Tsuge, S. Kanemasa, M. Ohe and S. Takenaka, *Bull. Chem. Soc. Jpn.*, 1987, **60**, 4079–4089.

20   W. H. Pearson, P. Stoy and Y. Mi, *J. Org. Chem.*, 2004, **69**, 1919–1939.

21   F. Lombardo, M. Y. Shalaeva, K. A. Tupper and F. Gao, *J. Med. Chem.*, 2001, **44**, 2490–2497.

22   S. A. Wildman and G. M. Crippen, *J. Chem. Inf. Comput. Sci.*, 1999, **39**, 868–873.

APPENDIX

1. Appendices to SACE1 compound library R&D

1.1. Comparison of *o*-Ns 100 and *p*-Ns 102 diastereomers

Cis diastereomer
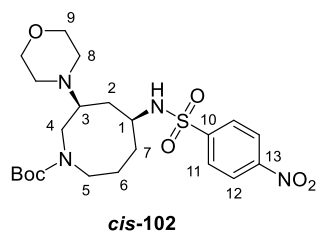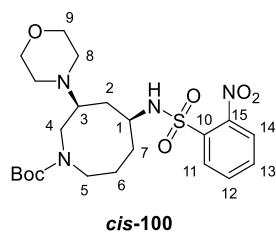
cis-100   *cis*-102

^{1}H-NMR

Assignment *o*-Ns	δ_H *cis*-100 (ppm) (rotamers)	δ_H *cis*-102 (ppm) (rotamers)	Assignment
Boc	1.45, 1.48	1.44, 1.46	Boc
2,6,7, N*H*	1.40 – 2.03	1.33–1.91	2, 6, 7, N*H*
8	2.29–2.69	2.34–2.62	8
3, 4/5	2.73–2.99	2.72–2.93	3, 4/5
1, 4/5, 9	3.57–3.86	3.45–3.92	1, 4/5, 9
12, 13	7.67–7.76	/	
11/14	7.80–7.88	7.99–8.06	11
11/14	8.10–8.16	8.30–8.37	12

^{13}C-NMR

Assignment	δ_C *cis*-100 (ppm) (rotamers)	δ_C *cis*-102 (ppm) (rotamers)	Assignment
6	22.9, 23.2	23.1	6
Boc C(*CH$_3$*)$_3$	28.57, 28.61	28.5	Boc C(*CH$_3$*)$_3$
2, 7	33.3, 33.5	33.9, 34.2	2, 7
4, 5	47.5, 48.44, 48.9	48.8	4/5 (one *CH$_2$* not observed)
8	50.1, 50.6	50.5	8
1	53.6, 53.9	53.0, 53.4	1
3	60.5, 61.6	60.2, 61.6	3
9	67.1	67.2	9
Boc *C*(CH$_3$)$_3$	80.1, 80.2	80.2, 80.3	Boc *C*(CH$_3$)$_3$
11/14	125.36, 125.39, 130.6, 130.8	124.5, 128.1	1, 12
12/13	133.0, 133.3, 133.4	/	/
10	135.7	147.5	10
15	147.9, 148.0	150.0	13
Boc *C*=O	155.4, 155.5	155.5	Boc *C*=O

Trans diastereomer

trans-100
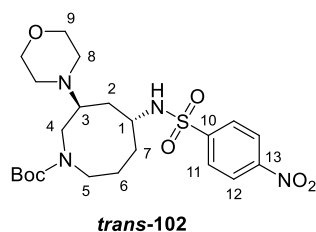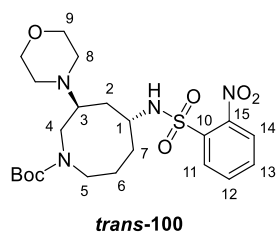
trans-102

¹H-NMR

Assignment	δ_H trans-100 (ppm)	δ_H trans-102 (ppm) (rotamers)	Assignment
Boc	1.44	1.42, 1.47	Boc
2, 6, 7	1.38–1.89	1.35–1.83	2, 6, 7
8	2.31–2.51	2.32–2.57	8
3	2.63–2.81	2.59–2.78	3
4, 5	2.87–3.20	2.80–3.16	4, 5
5	3.33–3.42	3.31–3.45	5
1, 4, 5, 9	3.48–3.79	3.45–3.77	1, 4, 5, 9
NH	5.35	5.65	NH
12,13	7.69–7.78	8.02–8.08	11
11/14	7.83–7.90	8.30–8.36	12
11/14	8.09–8.16	/	/

¹³C-NMR

Assignment	δ_C trans-100 (ppm) (rotamers)	δ_C trans-102 (ppm) (rotamers)	Assignment
6	22.8, 23.9	22.5, 23.7	6
Boc C(CH₃)₃	28.9	28.5	Boc C(CH₃)₃
2, 7	31.3, 31.6	31.3	7
2, 7	33.9, 34.0	33.2, 33.9	2
5	48.2	47.8	5
		48.4	4/5
4, 5, 8	49.7, 50.0, 50.2, 50.3	49.6, 50.2, 50.5	4/5, 8
1	52.3, 52.6	50.8, 51.8	1
3	58.3, 59.1	57.8, 58.9	3
9	67.6	67.2	9
Boc C(CH₃)₃	80.35, 80.44	80.2	Boc C(CH₃)₃
11, 14	125.9, 131.2, 131.3	124.5	12
12, 13	133.3, 134.0	128.3	11
		147.1	13
10,15	135.1, 148.3	150.0	10
Boc C=O	155.6, 155.9	155.3, 155.6	Boc C=O

2. Appendices to SACE1 *in silico* library design R&D

2.1. Selection method comparison

Boxplots and statistical values for the descriptor space coverage of various compound selections, discussed in Section 4.4.1, page 81.
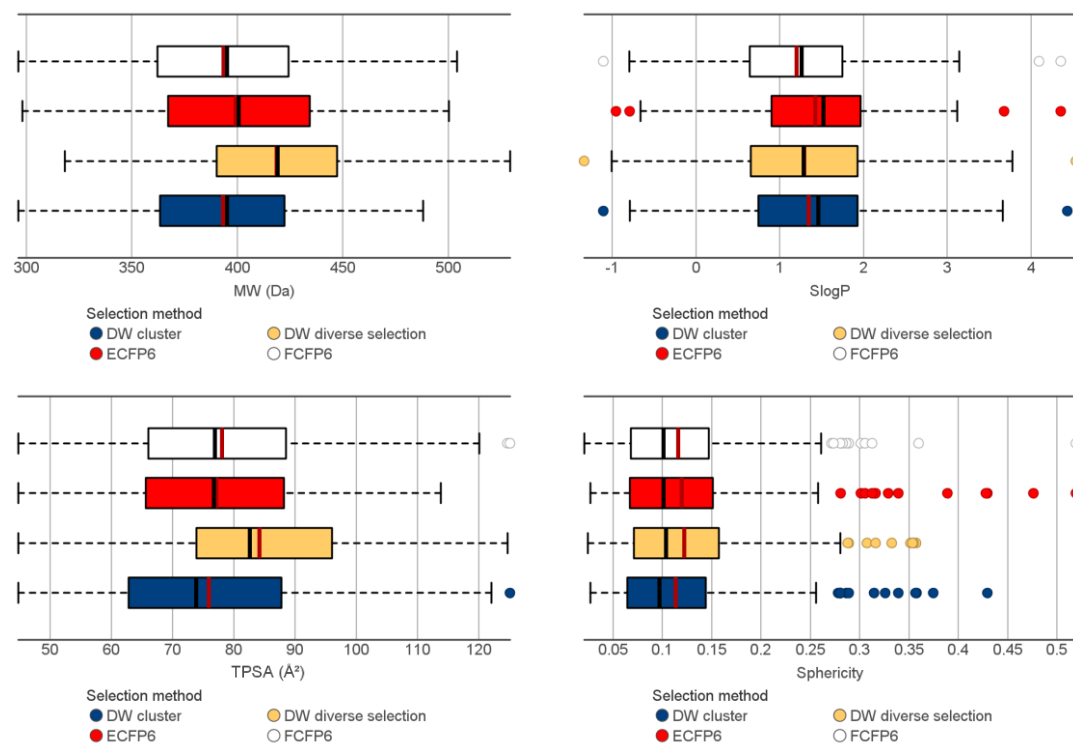
Figure 80: Molecular descriptor ranges covered by compound selections (size: 250 compounds). Mean: red line. Median: black line.

Table 27: Boxplot values for molecular descriptors shown in Figure 80. LAV: lower adjacent value. Q1: 1ˢᵗ quartile. Q3: 3ʳᵈ quartile. UAV: upper adjacent value.

Variable	Fingerprint	Min	LAV	Q1	Mean	Median	Q3	UAV	Max
MW (Da)	DW cluster	296.2	296.2	363.2	393.2	395.2	422.3	488.1	488.1
MW (Da)	DW diverse selection	318.2	318.2	390.2	418.7	419.2	447.1	529.3	529.3
MW (Da)	ECFP6	298.2	298.2	367.2	399.2	400.7	434.3	500.2	500.2
MW (Da)	FCFP6	296.2	296.2	362.2	393.5	395.2	424.2	504.2	504.2
SlogP	DW cluster	−1.10	−0.79	0.74	1.35	1.46	1.93	3.66	4.44
SlogP	DW diverse selection	−1.33	−1.00	0.65	1.29	1.29	1.93	3.78	4.54
SlogP	ECFP6	−0.95	−0.66	0.91	1.43	1.52	1.97	3.12	4.36
SlogP	FCFP6	−1.10	−0.80	0.64	1.20	1.26	1.75	3.15	4.36
TPSA (Å²)	DW cluster	44.8	44.8	62.8	76.0	73.9	87.7	122.1	125.1
TPSA (Å²)	DW diverse selection	44.8	44.8	73.9	84.2	82.7	96.0	124.7	124.7
TPSA (Å²)	ECFP6	44.8	44.8	65.6	77.1	76.8	88.2	113.8	113.8
TPSA (Å²)	FCFP6	44.8	44.8	66.1	78.1	76.9	88.5	120.1	125.1
Sphericity	DW cluster	0.027	0.027	0.065	0.114	0.097	0.144	0.256	0.430
Sphericity	DW diverse selection	0.025	0.025	0.071	0.122	0.104	0.157	0.280	0.358
Sphericity	ECFP6	0.027	0.027	0.067	0.120	0.101	0.151	0.258	0.519
Sphericity	FCFP6	0.021	0.021	0.068	0.116	0.101	0.147	0.261	0.519
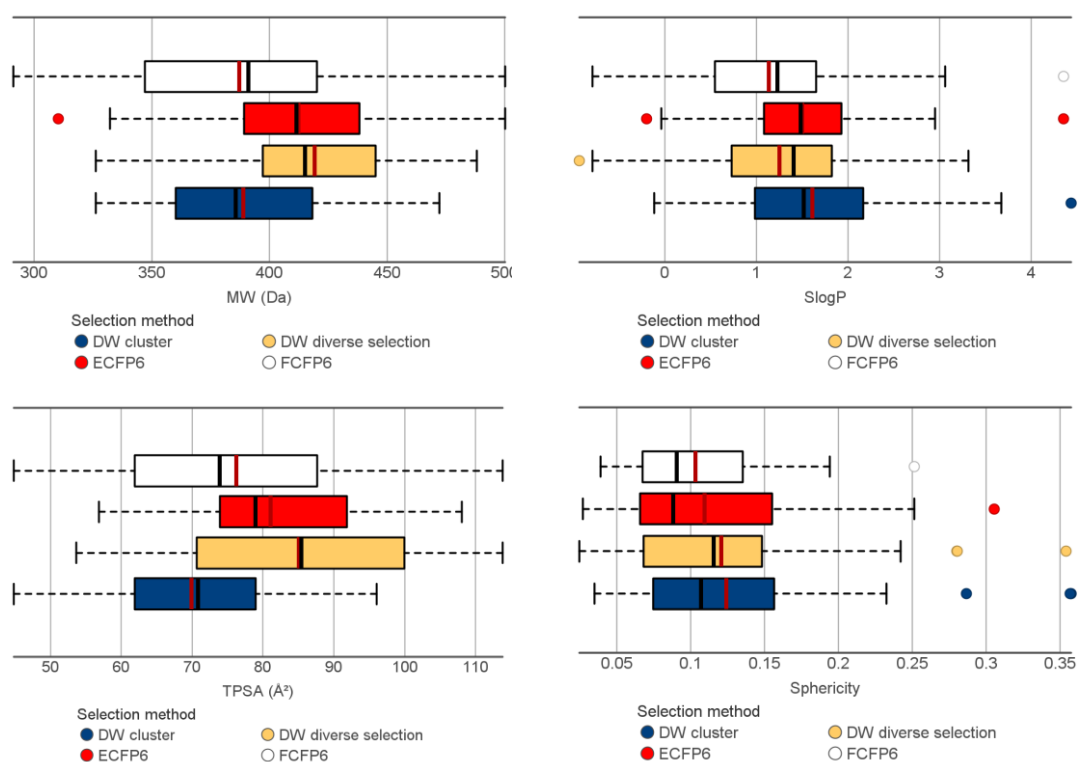
Figure 81: Molecular descriptor ranges covered by compound selections (size: 50 compounds).

Table 28: Boxplot values for molecular descriptors shown in Figure 81. LAV: lower adjacent value. Q1: 1ˢᵗ quartile. Q3: 3ʳᵈ quartile. UAV: upper adjacent value.

Variable	Fingerprint	Min	LAV	Q1	Mean	Median	Q3	UAV	Max
MW (Da)	DW cluster	326.3	326.3	360.3	389.0	385.7	418.2	472.2	472.2
MW (Da)	DW diverse selection	326.3	326.3	397.2	419.3	415.2	445.2	488.2	488.2
MW (Da)	ECFP6	310.2	332.2	389.2	412.6	411.7	438.2	500.2	500.2
MW (Da)	FCFP6	291.2	291.2	347.2	387.3	391.2	420.3	500.2	500.2
SlogP	DW cluster	−0.12	−0.12	0.98	1.62	1.52	2.17	3.68	4.44
SlogP	DW diverse selection	−0.93	−0.79	0.73	1.25	1.41	1.83	3.32	3.32
SlogP	ECFP6	−0.20	−0.04	1.08	1.50	1.49	1.93	2.95	4.36
SlogP	FCFP6	−0.79	−0.79	0.55	1.14	1.23	1.65	3.06	4.36
TPSA (Å^2)	DW cluster	44.8	44.8	61.9	69.9	70.8	79.0	96.0	96.0
TPSA (Å^2)	DW diverse selection	53.6	53.6	70.7	85.1	85.4	99.9	113.8	113.8
TPSA (Å^2)	ECFP6	56.8	56.8	73.9	81.1	79.0	91.8	108.1	108.1
TPSA (Å^2)	FCFP6	44.8	44.8	61.9	76.3	73.9	87.7	113.8	113.8
Sphericity	DW cluster	0.035	0.035	0.074	0.124	0.107	0.157	0.233	0.36
Sphericity	DW diverse selection	0.025	0.025	0.068	0.121	0.116	0.148	0.242	0.35
Sphericity	ECFP6	0.027	0.027	0.066	0.109	0.088	0.155	0.251	0.31
Sphericity	FCFP6	0.039	0.039	0.067	0.103	0.091	0.135	0.194	0.25

2.2.   Library design: reagent pool for enumeration

This is the 50-compound reagent pool, used for library enumeration. The selection of compounds for this pool is described in Section 4.5, page 86.

Sulfonyl chlorides
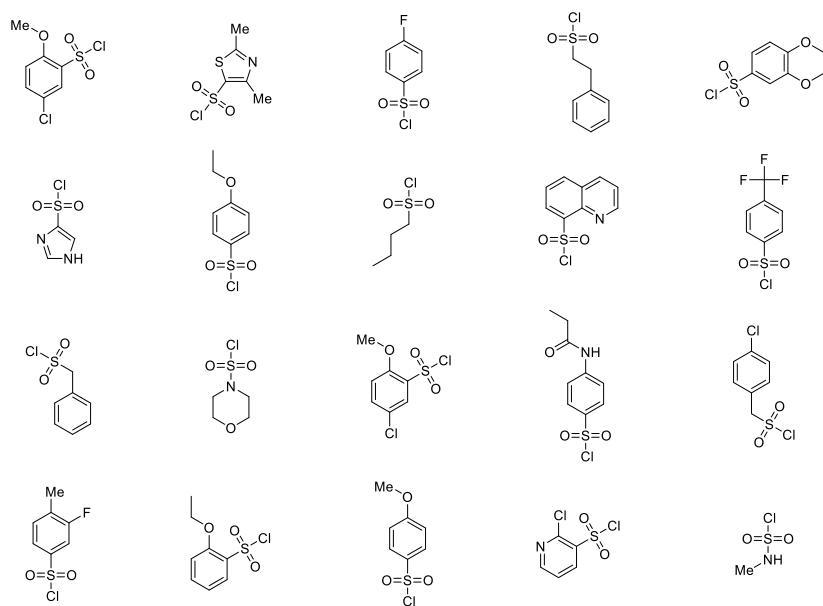
Carboxylic acids
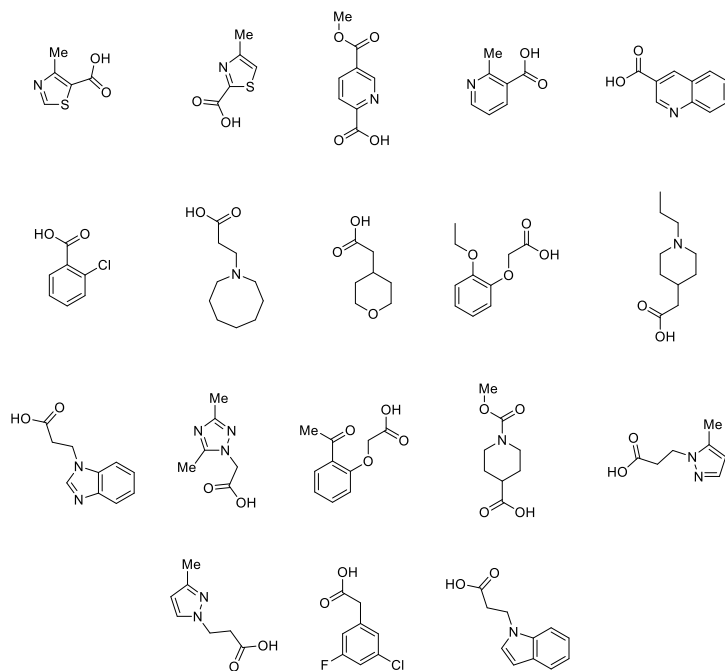
Isocyanates
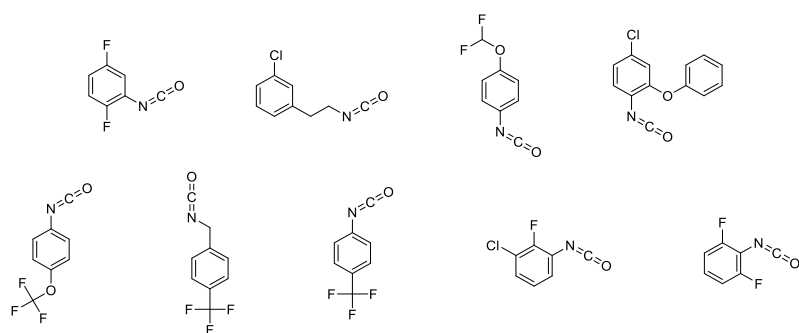
Aryl halides
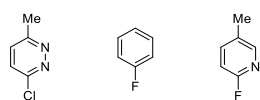
2.3. Most frequently recurring R groups, *cis*-SACE1 diverse selection

These are the most frequently recurring R-groups, obtained in a 200-compound diverse selection of the 51 × 51 combinatorial *cis*-SACE1 enumeration. From this set of R-groups, six R-groups were chosen to yield the 10 × 10 *cis*-SACE1 combinatorial library, discussed in Section 4.6.1, page 89.
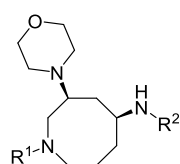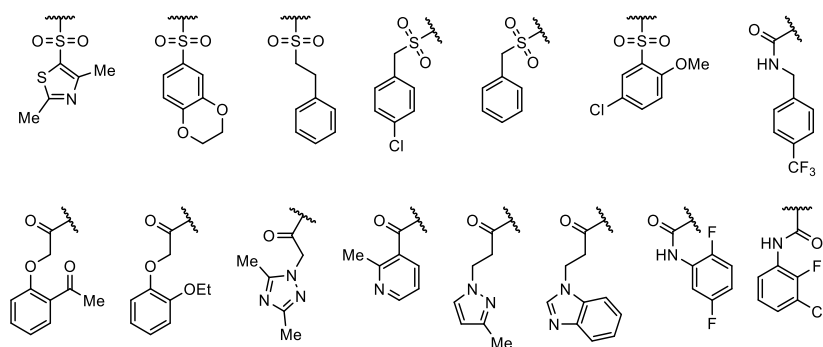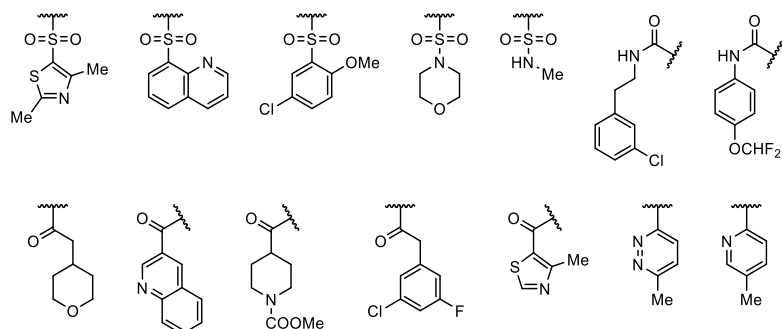
R^1 groups

R² groups

2.4. Most frequently recurring R groups, *trans*-SACE1 diverse selection

These are the most frequently recurring R-groups, obtained in a 200-compound diverse selection of the 51 × 51 combinatorial *trans*-SACE1 enumeration. From this set of R-groups, six R-groups were chosen to yield the 10 × 10 *trans*-SACE1 combinatorial library, discussed in Section 4.6.1, page 89.
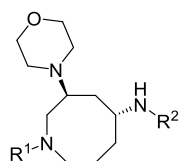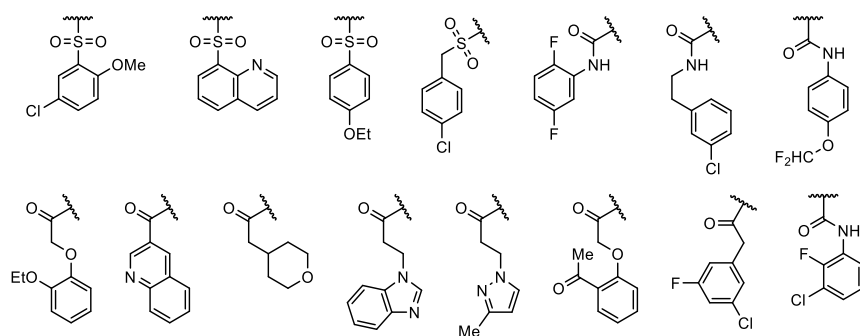
R¹ groups

R² groups
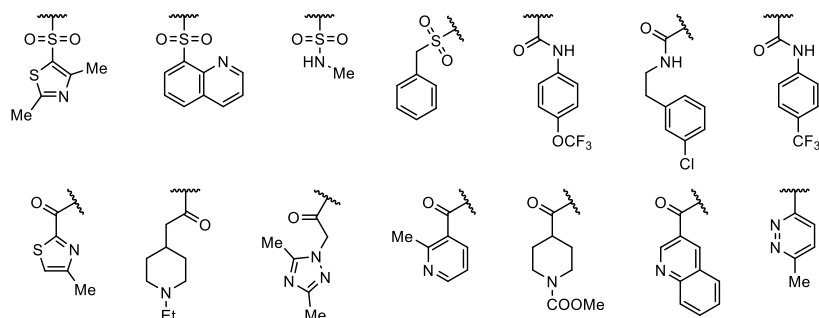
2.5.   SACE1 stereochemistry swap

Boxplots and statistical values for the descriptor space coverage of various compound selections, discussed in Section 4.7, page 97.
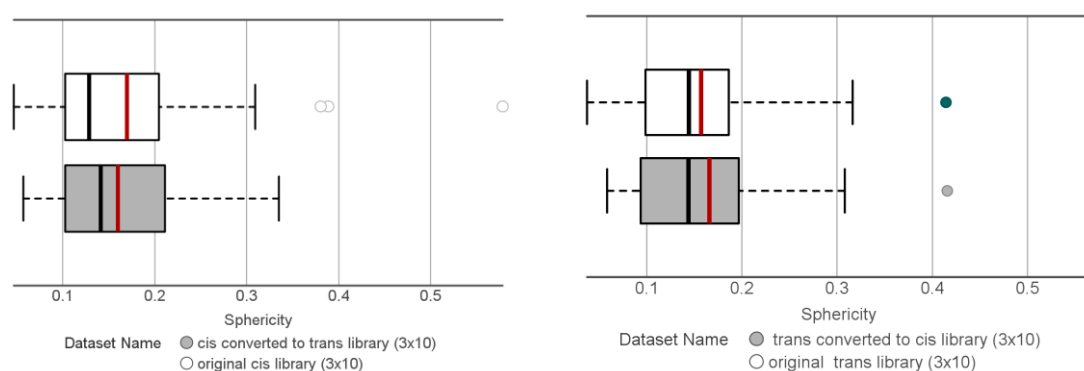
Figure 82: Analysis of the two 3 × 10 libraries with updated stereochemistry. Mean: red line. Median: black line.

Table 29: Boxplot values for sphericity comparison shown in Figure 82. LAV: lower adjacent value. Q1: 1st quartile. Q3: 3rd quartile. UAV: upper adjacent value.

Library	Min	LAV	Q1	Mean	Median	Q3	UAV	Max
cis converted to *trans* library (3 × 10)	0.057	0.057	0.102	0.160	0.141	0.211	0.335	0.335
original *cis* library (3 × 10)	0.047	0.047	0.103	0.170	0.129	0.205	0.309	0.578
trans converted to *cis* library (3 × 10)	0.058	0.058	0.166	0.144	0.094	0.197	0.308	0.566
original *trans* library (3 × 10)	0.037	0.037	0.157	0.144	0.099	0.186	0.316	0.414

3. Appendices to SACE2 *in silico* library design R&D

3.1. SACE2 functionalised pyrazoles: diversity assessment

Two sets of ten representative fused pyrazole analogues were obtained from an enumeration of 104 fused pyrazoles, as discussed in Section 6.1, page 127.

DataWarrior's diverse selection
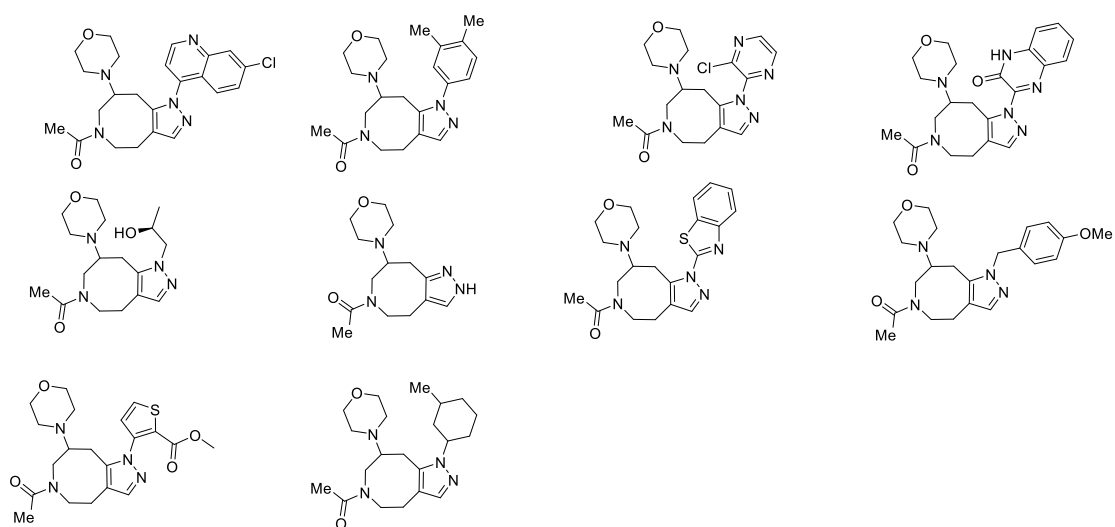
DataWarrior's clustering method: representative compounds
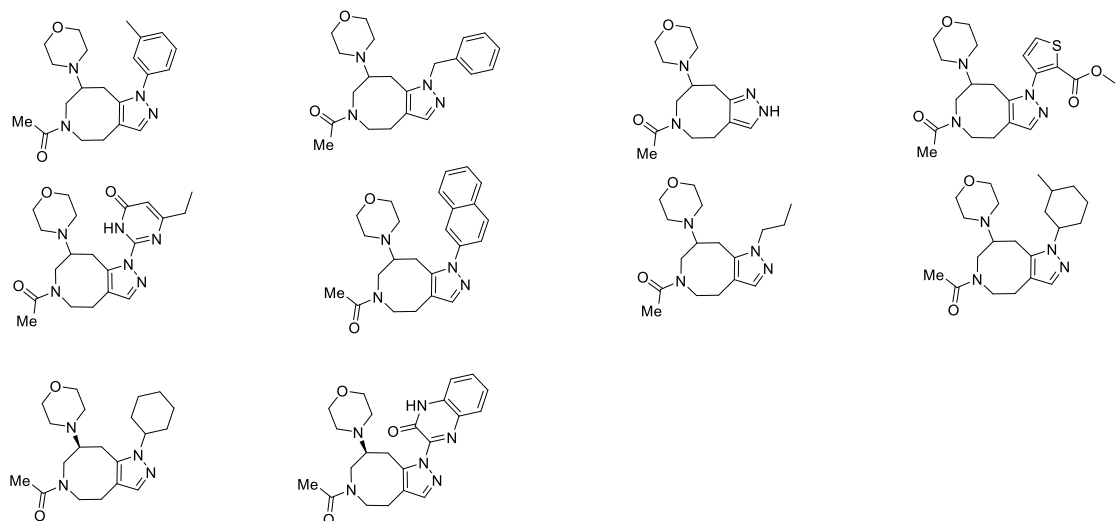
Both selection algorithms yielded heteroaromatic, C-aromatic, aliphatic, benzylic substitutions on the pyrazole, including a non-functionalised pyrazole, justifying the seven chosen building blocks.

3.2. SACE2 diverse selection: most frequently recurring R-groups

These are the most frequently recurring R-groups in the 100-compound diverse selections of the enumerated 7 × 48 (with *N*-Me building blocks) and 5 × 48 (without *N*-Me building blocks) virtual libraries, as discussed in Section 6.2, page 128. From the diverse selection of the 5 × 48 enumeration, six R-groups were chosen.

Diverse selection of 7 × 48 (with *N*-Me building blocks) enumeration
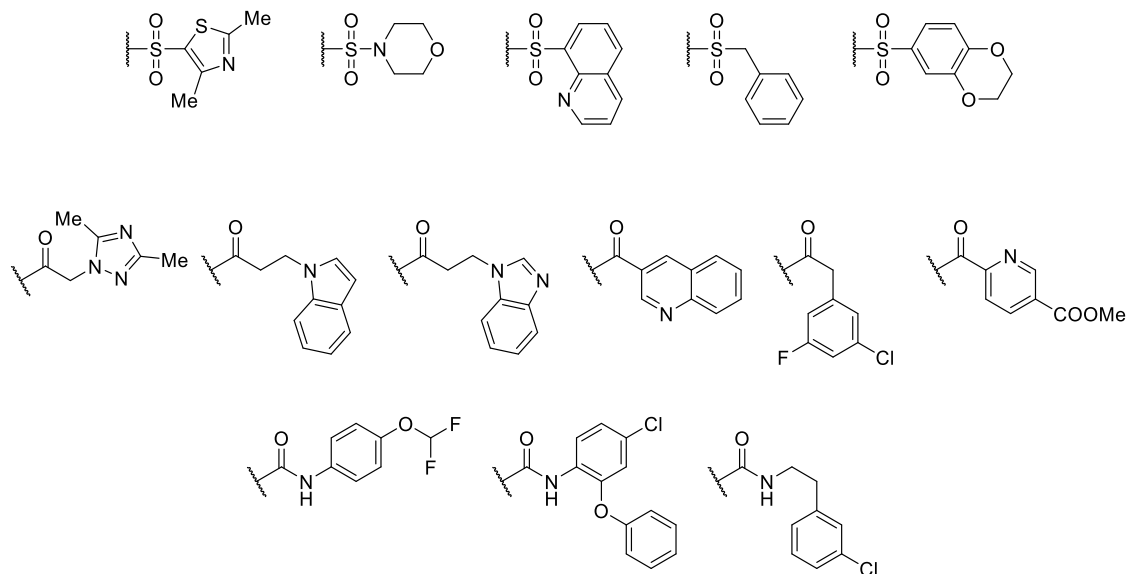
Diverse selection of 5 × 48 (without *N*-Me building blocks) enumeration
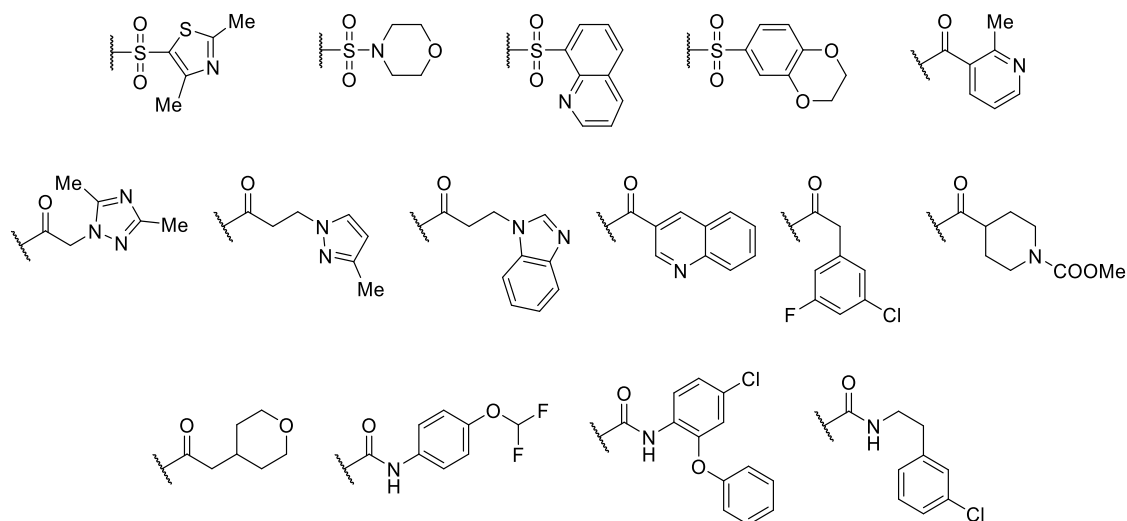
4. SACE3 compound library R&D

4.1. Pyrrolizidine stereochemistry: comparison with literature compounds

197
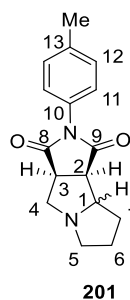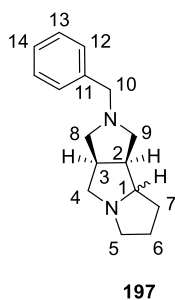
201   Reported by Tsuge *et al.*[a]

Tentative assignment	δ_C *trans*-197 (ppm)	δ_C *cis*-197 (ppm)	Tentative Assignment
C-6	24.5	24.7, 24.6	**C-6, C-7**
C-7	**30.5**		
C-3	43.1	43.3	C-3
C-2	**49.2**	**45.0**	**C-2**
C-5	52.8	51.7	C-5
		56.6	C-9
		57.9	C-8
C-4	58.8	58.9	C-4
C-8, C-9 / C-10	60.1 / 59.90 / 59.87	60.0	C-10
C-1	**72.2**	**69.3**	**C-1**
C-14	126.9	126.8	C-14
C-12, C-13	128.8 / 128.3	128.5 / 128.3	C-12, C-13
C-11	139.4	139.8	C-11

Assignment	δ_C *trans*-201 (ppm)	δ_C *cis*-201 (ppm)	Assignment
Me	21.1	21.1	Me
C-6	23.6	24.8	C-6
C-7	**29.7**	**25.2**	**C-7**
C-3	45.9	48.2	C-3
C-2	**50.1**	**48.4**	**C-2**
C-5	52.0	53.0	C-5
C-4	55.0	54.7	C-4
C-1	**69.1**	**68.4**	**C-1**
Ar CH	126.5	126.0	Ar CH
Ar CH, Ar C	129.8 (resonance overlap)	129.7	Ar CH
Ar C	138.6	129.8	Ar C
C-8, C-9	177.8 / 178.4	179.0 / 177.1	C-8, C-9

[a] O. Tsuge, S. Kanemasa, M. Ohe and S. Takenaka, *Bull. Chem. Soc. Jpn.*, 1987, **60**, 4079–4089.

199   Reported by Pearson *et al.*[a]

Tentative assignment	δ_C *trans*-199 (ppm)	δ_C *cis*-199 (ppm)	Tentative assignment
C-6	23.6	24.9	C-6
C-7	29.7	23.2	C-7
C-3	45.9	48.3	C-3
C-2	50.1	48.5	C-2
C-5	52.0	53.0	C-5
C-4	55.1	54.8	C-4
C-1	69.2	68.6	C-1
Ar CH	126.5	126.0	Ar CH
	128.5	128.6	
Ar C	129.1	129.2	Ar C
	131.9	131.9	
C-8, C-9	177.5	176.9	C-8, C-9
	178.0	178.7	

[a] W. H. Pearson, P. Stoy and Y. Mi, *J. Org. Chem.*, 2004, **69**, 1919–1939.

5. Compound validation R&D

5.1. DrugBank database reference subset

The FDA-approved subset of the DrugBank database, which was compared against the three library designs, discussed in Section 8.2, page 168 was generated as follows: A subset from the DrugBank database v 5.0.10 was downloaded as DataWarrior file *via* the following link: (https://openmolecules.org/DataWarrior/datafiles.html#drugbank). In DataWarrior, the obtained dataset of 9309 compounds was filtered to 190 Da < MW < 560 Da to match the MW range covered by the library designs. FDA-Approved compounds were then separated, by filtering on 'Group' = 'approved'. Subsequently, the following compounds were filtered out of the obtained subset (677 compounds), based on their 'classification class' categories: 'unspecified classification class', 'alkaline earth metal oxoanionic compounds', 'organic carbonic acids and derivatives' ($La_2(CO_3)_3$), 'organic phosphonic acids and derivatives' (included Tc-based contrast reagents), 'organic sulfuric acids and derivatives' (sodium lauryl sulfate), 'organometalloid compounds', 'post-transition metal oxoanionic compounds', 'post-transition metal salts' (TiCl), 'transition metal oxoanionic compounds', 'transition metal salts' (cisplatin). Finally, compounds with 'Classification Kingdom' classifier 'Inorganic compounds' were filtered out, as well as compounds containing Hg. An additional SlogP filter (> −5) removed SlogP outliers (salts). The obtained set was then exported to KNIME as an SDF file, wherein chemical descriptors of choice were calculated. (KNIME failed to read 2 SDF entries, resulting in loss of 2 compounds). The resulting set of 632 compounds was compared to the three library designs. This reference set can be found in the secure RDS folder (see Experimental Section 1.2) and is saved as "211019_Drugbank_510-reference_3D-filt.sdf".
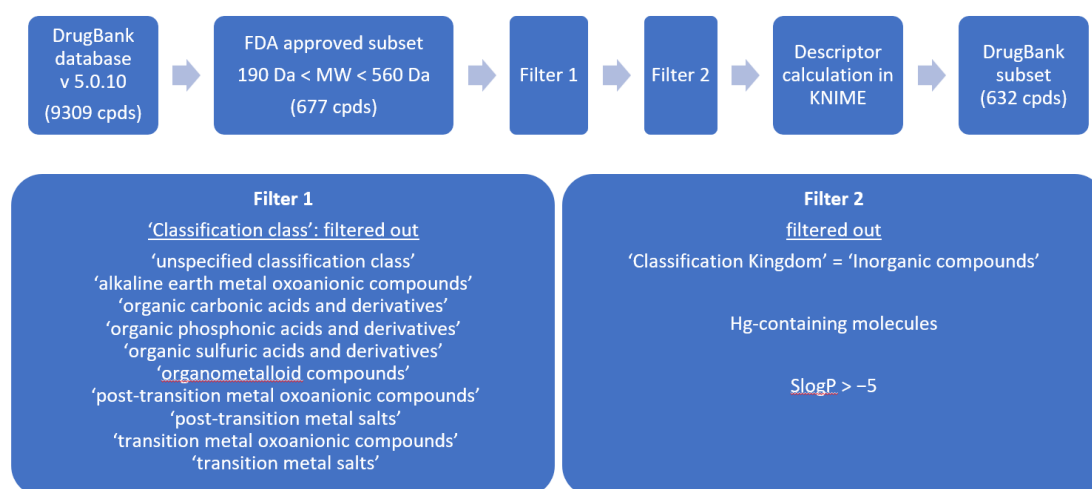
Figure 83: Filtering workflow which yielded the DrugBank subset of 632 compounds.

5.2. Principal Component Analysis: statistical values

Shown below are the statistical values for the PCA performed in Section 8.2.1, page 169.

Table 30: Reported eigenvalues per variable for PCA plots (Figure 69).

Variable Name	pc1	pc2	pc3
TPSA (Å²)	0.5685	−0.0138	0.0200
#H-bond acceptors	0.5371	0.0949	0.2437
#H-bond donors	0.4078	−0.1322	−0.3602
SlogP	−0.3782	−0.3014	0.4499
MW (Da)	0.2565	−0.1236	0.7563
Fsp^3	0.0724	0.1434	−0.0479
npr2	0.0673	−0.6481	−0.1007
npr1	−0.0585	0.6532	0.1534

Table 31: Explained variance (%) per principal component, calculated for PCA plots in Figure 69.

Prinicipal component	Explained variance (%)
pc1	36.1
pc2	23.9
pc3	16.1
pc4	13.7
pc5	5.9
pc6	2.8
pc7	1.1
pc8	0.4

5.3. hERG inhibition assay results

The hERG inhibition assay was run by Dr Michael Morton at ApconiX, following a literature procedure by Bridgland-Taylor *et al*.[a]

Table 32: hERG inhibition assay results.

Compound	*trans*-106d4	*cis*-105	144c5[a]	131	126d3	224e1	226c1
	28	21	20	26	100	72	18
	27	13	17	15	97	79	0
	24	26	51	30	91	74	27
	45	34	18	37	97	74	9
% hERG	32	54	19	30	97	85	6
inhibition	27	25	35	28		90	18
	42		45				15
			12				
			18				
			39				
Average	32	29	27	28	96	79	13

[a] Screening of compound **144c5** was performed twice, resulting in 16 measurements of which six failed.

[a] M. H. Bridgland-Taylor, A. C. Hargreaves, A. Easter, A. Orme, D. C. Henthorn, M. Ding, A. M. Davis, B. G. Small, C. G. Heapy, N. Abi-Gerges, F. Persson, I. Jacobson *et al*., *J Pharmacol Toxicol Methods*, 2006, **54**, 189–199.

6. *In silico* library enumeration and validation: KNIME and DataWarrior

All *in silico* work was performed in KNIME 4.1.3[1] or OSIRIS DataWarrior version 5.2.1[2]. All generated KNIME workflows, DataWarrior files and SDF files are stored on a secure RDS folder (\\its-rds.bham.ac.uk\rdsprojects\c\coxlr-idesign-ceusters), which can be accessed by authorised members of the University of Birmingham.

6.1. KNIME Workflows

KNIME is an open-source platform which allows for modular construction of data-processing workflows. Each module, called a node, performs a clearly defined operation; this might be sorting or filtering data, calculating molecular descriptors or *in silico* chemical reactions. Linking multiple nodes allows for sequential execution of each node, which can be used to establish complex workflows for library enumeration and clustering.[1] The KNIME workflows reported in this thesis were constructed by the author and benefited from review by Symeres' former Principal Computational Scientist, Chimed Janssen.

All work performed in KNIME used nodes by KNIME, RDKit, CDK, Erl Wood, Vernalis and Chemaxon. In the following workflows, all generated data (*e.g.*, fingerprints, physicochemical property descriptors, PMI values) were added to the input dataset as new columns, which were used for subsequent filtering, clustering or data visualisation in DataWarrior.

Workflows generated in KNIME consist of a set of linked nodes, with every node containing at least one input port and one output port (Figure 84). Specific configurations of the used nodes are reported, as well as a short explanation of their function in the workflow. To facilitate visual overview of the workflow, multiple nodes can be organised in a metanode (Figure 84). Besides cleaning up the workflow (by avoiding an excessive number of nodes in the primary workflow), metanodes do not add extra functionality to a workflow. The nodes contained within the metanodes that were used in the generated workflows are also reported in this section.
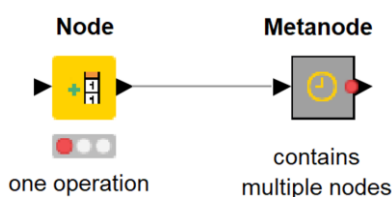
Figure 84: Example of a node and a metanode in KNIME.

6.1.1. Library Enumeration

All library enumerations followed an analogous workflow, generating a dataset which contained the enumerated compounds and appended columns which displayed the used reagent codes, building blocks, and functional group categories for every generated compound. These extra columns facilitated data visualisation and filtering in DataWarrior (Figure 85).
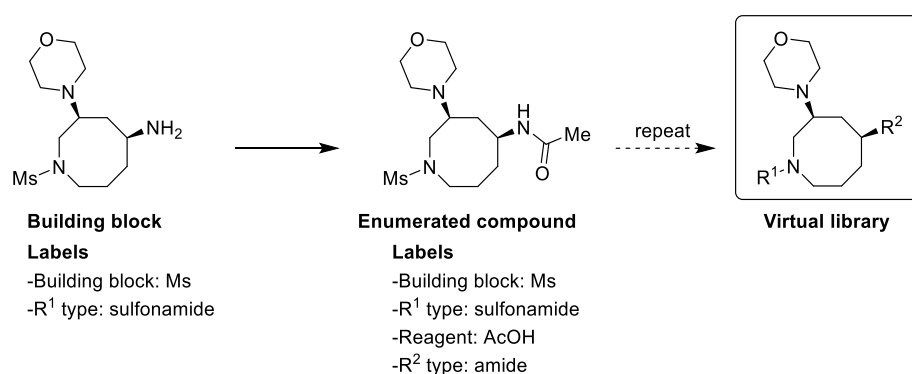
Figure 85: Example of a virtual reaction, adding extra labels to facilitate data processing.

An exemplar workflow is illustrated below (Figure 86). This workflow was used to generate the SACE1 10 × 10 *cis* library described in Section 4.6.1. Similar workflows were used to generate the other libraries.
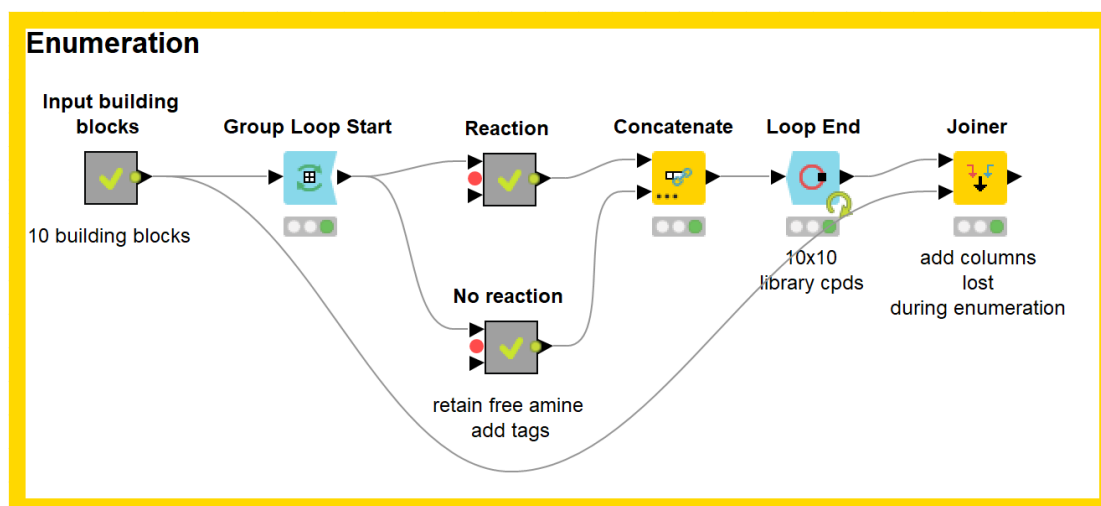
Figure 86: Exemplar enumeration workflow.

Table 33: Nodes used in the exemplar enumeration workflow.

Node name	Description
Input building blocks	Generates building blocks with appended labels (Building block, R^1 type). Metanode, see below
Group Loop Start	Starts an iterative process, running one building block at a time through the enumeration metanodes. Group column = "building block" label.
Reaction	Generates enumerated compounds (with appended labels; Building block, reagent type, R^2 type) by virtual reaction of the building block with a set of nine reagents. Metanode, see below.
No Reaction	Yields the unreacted building block, with appended labels. Metanode, see below.
Concatenate	Adds "no reaction" output row to "reaction" dataset, yielding a set of 10 enumerated compounds, with appended labels.
Loop End	End of the loop, aggregates all data generated during the iterative loop process. Output = 10 × 10 enumerated library, with appended labels.
Joiner	Adds "R^1 type" labels which were lost during the enumeration process back to the enumerated library. Joining column = "building block" label.

6.1.2.   Input building blocks

This metanode was used to generate building blocks with appended labels (Building block, R^1 type). An analogous sequence of nodes was used ten times to generate each building block and its labels, followed by subsequent concatenation of the generated rows (Figure 87).
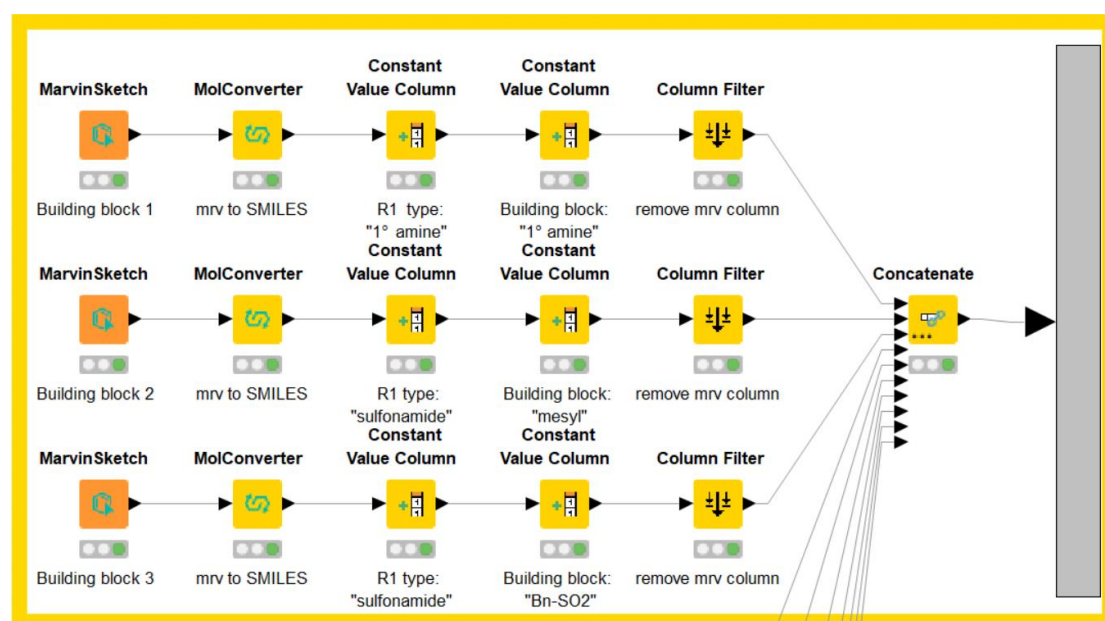
Figure 87: Excerpt of the "Input building blocks" metanode.

393

Table 34: Nodes used in the "input building blocks" metanode.

Node name	Description
MarvinSketch	Building block drawn manually, generates .mrv format
MolConverter	Converts the building block in .mrv format to a SMILES string (in appended column)
Constant Value Column	Append R^1 type label (*e.g.*,"1° amine", "sulfonamide")
Constant Value Column	Append building block label (*e.g.*, "1° amine", "mesyl")
Column Filter	Used to clean up dataset: removes .mrv column (keeps SMILES column)
Concatenate	Links together all of the individually generated rows, creating a table of 10 building blocks.

6.1.3.   Reaction

This metanode was used to generate enumerated compounds (with appended labels; Building block, reagent type, R^2 type) by performing a virtual reaction of the building block with a set of nine reagents (Figure 88).
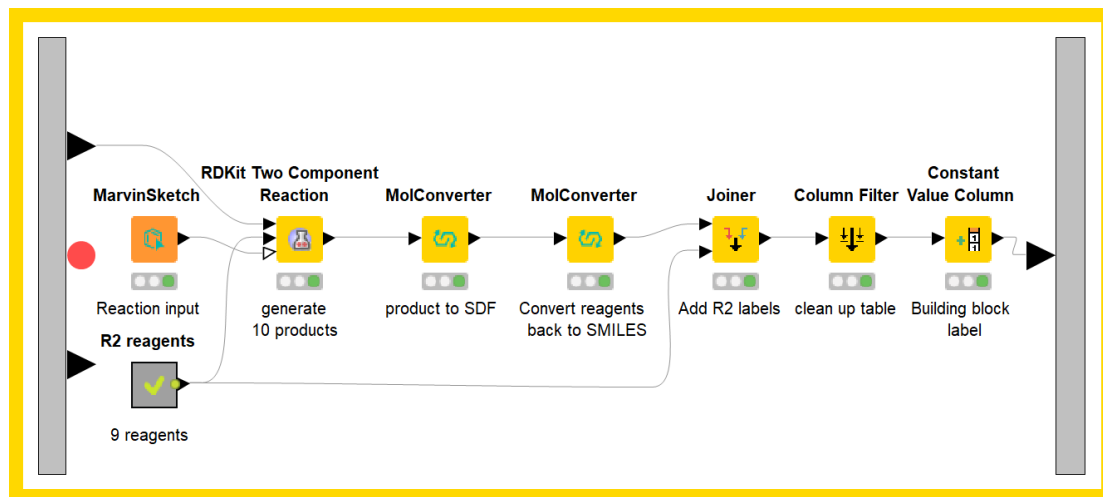
Figure 88:" Reaction" metanode.

Table 35: Nodes used in the "Reaction" metanode.

Node name	Description
MarvinSketch	Provides a manually drawn general reaction scheme
R2 reagents	Provides 9 chosen virtual reagents with appended labels (Reagent, R^2 type). This metanode is built analogously to the "input building blocks" metanode, see above.
RDKit Two Component Reaction	Reacts the input building block with the 9 reagents, following the provided general reaction scheme. Output = 10 reaction products and the used reagents in RDKit Mol format
MolConverter	Converts molecule formats to SDF/SMILES.
Joiner	Append R^2 group labels (Reagent, R^2 type) to the product dataset. Joining column = reagent (SMILES) column
Column Filter	Cleans up dataset to show only the product and R^2 group labels (Reagent, R^2 type).
Constant Value Column	Append "building block" label. Value settings > variable > "building block"

6.1.3.1. MarvinSketch: Reaction input

A general reaction scheme was drawn as the input for the RDKit Two Component reaction. An exemplar reaction scheme is shown below (Scheme 97).
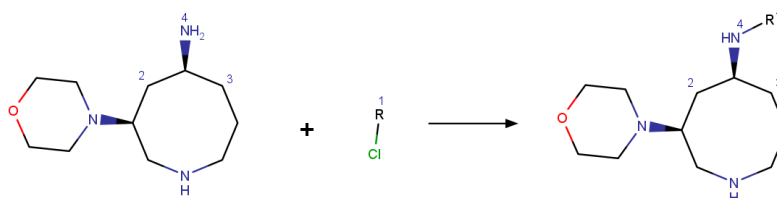
Scheme 97: Exemplar MarvinSketch general reaction scheme.

The input structures of the virtual reagents used for this enumeration are not necessarily the same as the actual reagents that were used in physical synthesis. For example, amides and ureas were generated using the general reaction scheme depicted above, by using R-CO-Cl and R-NHCO-Cl type virtual reagents, respectively. When it came to physical compound synthesis, amides and ureas were synthesised using carboxylic acids and isocyanates, respectively.

6.1.4. No Reaction

This metanode was used to generate the unreacted building block, with appended labels, in the same data format as the virtual reaction product dataset that was generated in the "reaction" metanode (Figure 89).
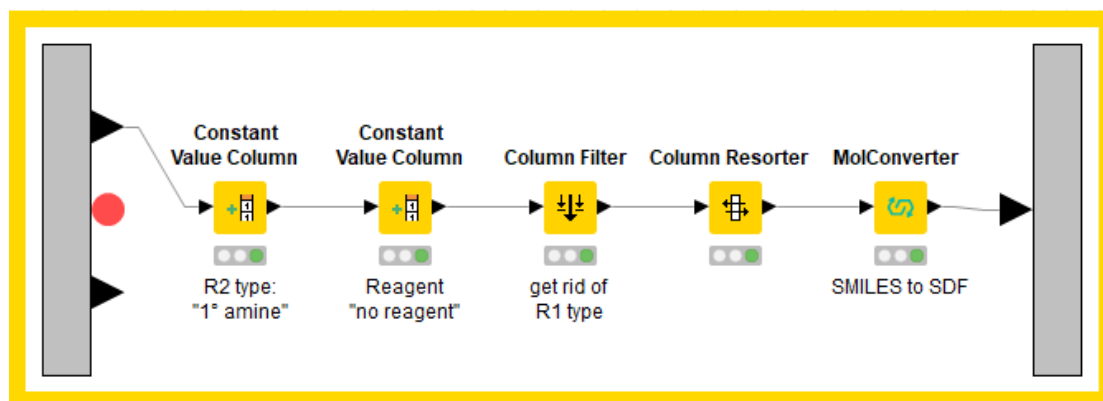
Figure 89: "No reaction" metanode.

Table 36: Nodes usde in the "No reaction" metanode.

Node name	Description
Constant Value Column	Append R2 type and reagent label ("1° amine", "no reagent").
Column Filter	Filters out the "R1 type" column, ensuring the same data content as the virtual reaction product dataset generated in the "reaction" metanode.
Column Resorter	Sorts the data columns in the same order as the virtual reaction product dataset generated in the "reaction" metanode
MolConverter	Converts molecule format to SDF.

6.1.5. Library Clustering

As discussed in Section 4.3, a representative subset of enumerated compounds was chosen from the enumerated libraries for practical synthesis of the physical compound library. The workflow depicted in Figure 90 was used to cluster a set of enumerated compounds from the initially formed enumerated library, based on ECFP6/FCFP6 fingerprints, and then to pick a representative compound for each cluster.[a] Eventually, the DataWarrior 'Select Diverse Set' algorithm was used for selecting library compounds for synthesis instead of this workflow, as discussed in Section 4.4.3.

---

[a] Workflow based on the "Hierarchical Clustering" workflow, available in the KNIME open-source community hub.[3]
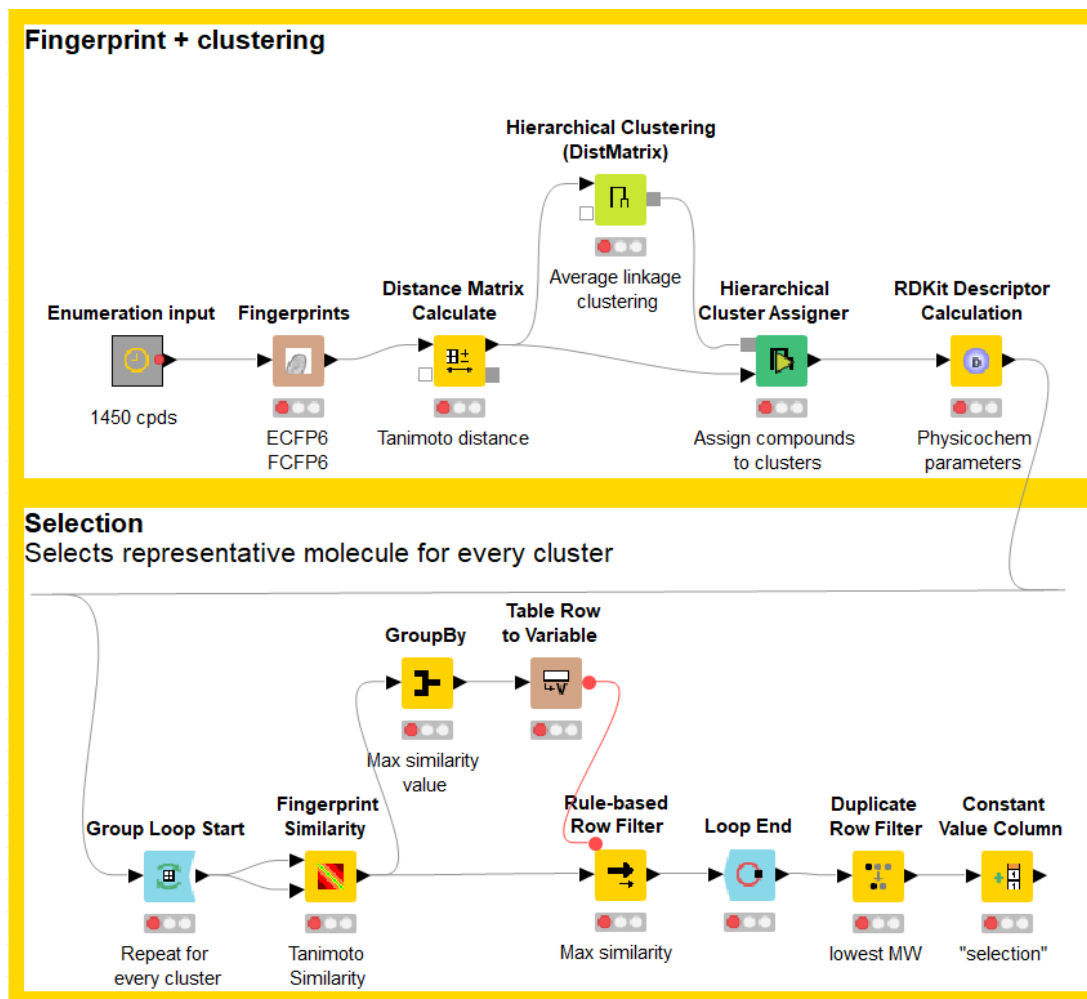
Figure 90: KNIME Library clustering workflow.

Table 37: Nodes used in the library clustering workflow.

Node name	Description
Enumeration input	Dataset of compounds to be clustered, format in RDKit Canon SMILES
Fingerprints	Calculates circular fingerprints, ECFP6/FCFP6
Distance Matrix Calculate	Calculates Tanimoto distances between all molecules in the dataset, based on circular fingerprints. Generates a distance matrix.
Hierarchical Clustering	Clusters the input data hierarchically, based on the input distance matrix. Linkage type = Average Linkage (distance between two clusters (*e.g.,* c1 and c2) is defined as the mean distance between all members in c1 and c2)
Hierarchical Cluster Assigner	Assigns compounds to a cluster, based on the desired cluster count. (50/250 clusters chosen) Generates an extra column to the dataset ("cluster number").

398

RDKit Descriptor Calculation	Calculates physicochemical parameters for dataset molecules (in RDKit Mol format). Selected parameters: SlogP,[a] TPSA, ExactMW, Fsp3, #H-bond donors, #H-bond acceptors, npr1, npr2.
Group Loop Start	Starts an iterative process, by sorting ("grouping") the input based on their cluster number. Once a "group" has passed through all nodes and reaches the "loop end", the next "group" is run through the defined loop. (Applied to in this workflow, a selection is thus made cluster per cluster.)
Fingerprint Similarity	Calculates the average Tanimoto similarity (0 – 1) between every compound in the cluster, for every compound in the cluster, based on its circular fingerprint.
GroupBy	Extracts the maximum Tanimoto similarity value from the input cluster. Group column = "Cluster number", Manual Aggregation based on "Similarity" column, Aggregation = "Maximum"
Table Row to Variable	Turns the extracted maximum Tanimoto similarity value into a Variable, used in the Row Filter node
Rule-based Row Filter	Filters for compounds which display the maximum Tanimoto similarity. Used script: $Similarity$ = $${DMax*(Similarity)}$$ => TRUE
Loop End	End of the loop, aggregates all data generated during the iterative loop process. Output = selection of representative compounds, with maximum mean Tanimoto similarities within their cluster
Duplicate Row Filter	Ensures only one compound passes per cluster: compound with lowest MW passes. Output = selection of 50/250 representative compounds.
Constant Value Column	Adds an extra column to the dataset, constant value = "selection"

6.1.6.   Shape space assessment: PMI data

The following workflow outlined in Figure 91 was used to generate sphericity, npr1 and npr2 values for a given set of molecules, which were used to assess the shape space covered by the given set.[b] This workflow also generated physicochemical property data, providing all calculated data which were used during *in silico* library design. The generated data were subsequently converted to SDF format and evaluated in DataWarrior.

---

[a] SlogP calculation based on method reported by Wildman and Crippen.[4]
[b] Workflow based on the "PMI_v3000" workflow, available in the KNIME open-source community hub.[5]
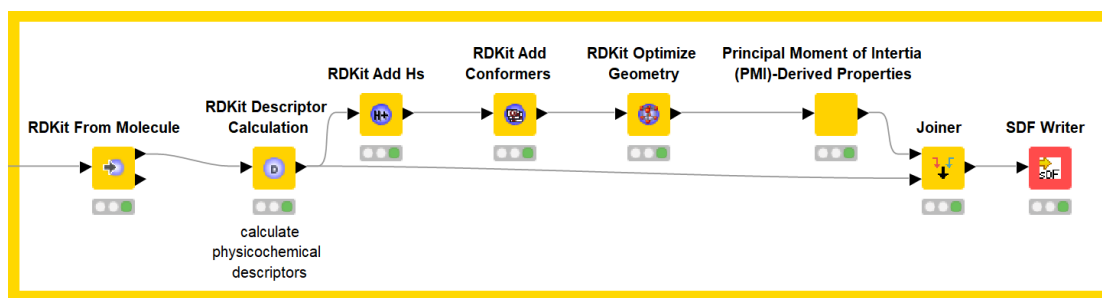
Figure 91: Workflow used to generate PMI data.

Table 38: Nodes used in PMI data workflow.

Node name	Description
RDKit From Molecule	Converts the input molecule format to RDKit Mol format
RDKit Descriptor Calculation	Calculates physicochemical parameters for dataset molecules (in RDKit Mol format). Selected parameters: SlogP,[a] TPSA, ExactMW.
RDKit Add Hs	Adds hydrogens to the RDKit Mol format molecule
RDKit Add Conformers	Used to generate one conformational isomer per molecule (3D coordinates). Preservation of the input chirality was enforced.
RDKit Optimize Geometry	Optimises the geometry for the given input conformer using MMFF94S[5] force fields. (1000000 iterations)
Principal Moment of Intertia (PMI)-Derived Properties (*sic*)	Used to calculate npr1, npr2 and sphericity values
Joiner	Used to add all columns lost during PMI property calculations (including all physicochemical property descriptors and molecule labels). Joining columns = "reference" – "Row ID"
SDF writer	Writes the dataset into an SDF file, saved in a specified directory

---

[a] SlogP calculation based on method reported by Wildman and Crippen.[4]

400

6.1.7. Linear sampling

The workflow shown in Figure 92 was used to produce a linear sample of the diverse selection reported in Section 4.5. Based on the diversity ranking generated by the DataWarrior "Select Diverse Set"algorithm, compounds were systematically selected to provide a selection of the desired size.
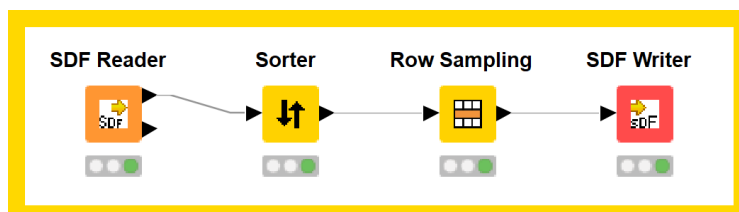
Figure 92: Linear sampling workflow.

Table 39: Nodes used in the linear sampling workflow.

Node name	Description
SDF Reader	Reads SDF file from a specified directory, used to upload the dataset to sample into KNIME
Sorter	Sorts rows by the ¨Diversity Selection Rank¨, ascending.
Row Sampling	Generates a linear sample. Sampling method = Absolute: 50; Linear sampling.
SDF writer	Writes the dataset into an SDF file, saved in a specified directory

6.1.8. Tanimoto similarity

Tanimoto similarities were calculated using ECFP6 fingerprints in the workflow shown in Figure 93.
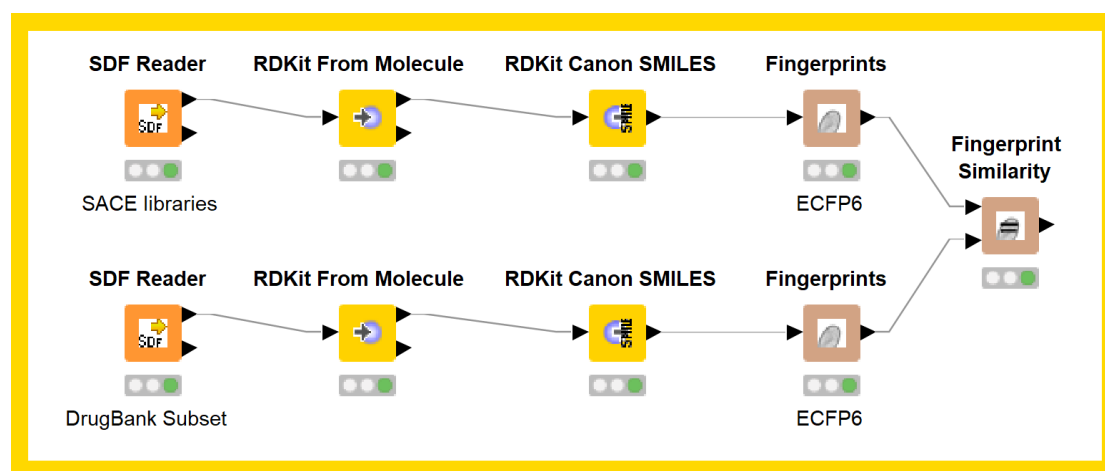
Figure 93: Tanimoto similarity workflow.

Table 40: Nodes used in the Tanimoto similarity workflow.

Node name	Description
SDF Reader	Reads SDF file from a specified directory, used to upload two datasets into KNIME
RDKit From Molecule	Converts the input molecule format to RDKit Mol format
RDKit Canon SMILES	Converts the input molecule format from RDKit Mol format to RDKit Canon SMILES (compatible format for next node)
Fingerprints	Generates ECFP6 fingerprints
Fingerprint Similarity	Generates maximum Tanimoto similarity scores for all compounds in the query dataset (upper input port), which are compared to all compounds in the reference set (lower input port). Aggregation method = maximum

6.2. DataWarrior Workflows

6.2.1. Selection algorithms

DataWarrior uses its own set of fingerprints: the clustering algorithm uses 'SkelSpheres', a non-binary fingerprint,[7] while the 'select diverse set' algorithm uses 'SpheresFp', a circular fingerprint.[8] The dataset to process (SDF format) was opened in DataWarrior and fingerprints were calculated *via* the following path:

Chemistry > From Chemical Structure > Calculate Descriptor > SpheresFp/SkelSpheres.

The desired selection algorithm was applied subsequently.

6.2.2. Clustering

DataWarrior's clustering algorithm was accessed *via* the following path:

Chemistry > Cluster Compounds/Reactions

The pop-up dialogue box was filled in as shown in Figure 94. The desired number of clusters equals the desired number of compounds in the selection.
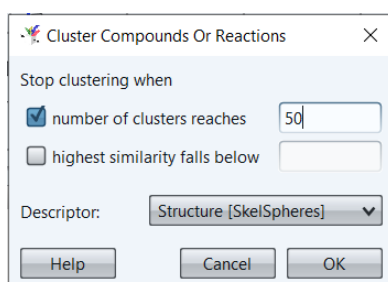
Figure 94: Clustering dialogue box.

Upon clustering, two extra columns are generated: ¨Cluster No¨and ¨Is Representative¨. DataWarrior's built-in filter interface allows for selection of the entries showing "is representative" = "yes", yielding the desired representative selection.

6.2.3. *"Select Diverse Set"*

DataWarrior's "Select Diverse Set" algorithm was accessed *via* the following path:

Chemistry > Select Diverse Set... (*sic*)

The pop-up dialogue box was filled in as shown in Figure 95.
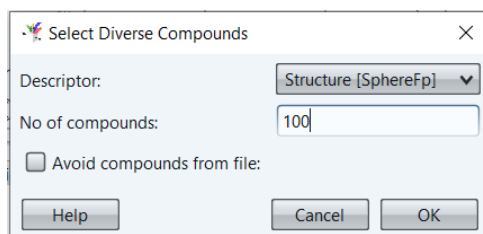
Figure 95: Select Diverse Set dialogue box.

The algorithm generates a new column, called "Diversity Selection Rank". Right-clicking on the column header allows for the inclusion of a "New Slider Filter". Turning on this filter allows for selective visualisation of the diverse selection.

6.2.4. *Principal component analysis*

DataWarrior's principal component analysis was accessed *via* the following path:

Data > Calculate Principal Components

The pop-up dialogue box was filled in as shown in Figure 95. The used parameters were multidimensional MW, SlogP, TPSA, Fsp^3, #H-bond donors, #H-bond acceptors, npr1 and npr2.
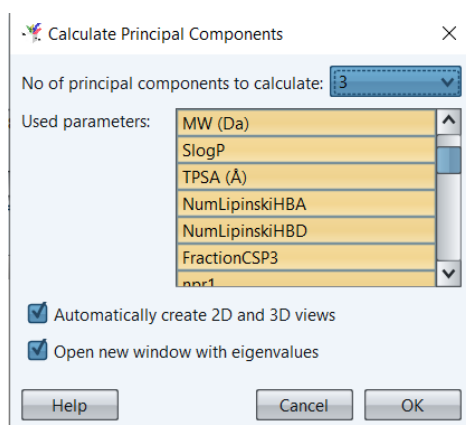
Figure 96: Calculate Principal Components dialogue box.

6.3. References

1   M. R. Berthold, N. Cebron, F. Dill, T. R. Gabriel, T. Kötter, T. Meinl, P. Ohl, C. Sieb, K. Thiel and B. Wiswedel, in *Data Analysis, Machine Learning and Applications*, eds. C. Preisach, H. Burkhardt, L. Schmidt-Thieme and R. Decker, Springer, Berlin, Heidelberg, 2008, pp. 319–326.

2   T. Sander, J. Freyss, M. von Korff and C. Rufener, *J. Chem. Inf. Model.*, 2015, **55**, 460–473.

3   Hierarchical Clustering , https://hub.knime.com/jjmie/spaces/Public/latest/01_HierarchicalClustering~iQXAiw 7eUwoHCZyy, (accessed 1 July 2022).

4   S. A. Wildman and G. M. Crippen, *J. Chem. Inf. Comput. Sci.*, 1999, **39**, 868–873.

5   PMI_v3000, https://hub.knime.com/elsamuel/spaces/Public/latest/PMI%20test/PMI_v3000~5DE7 2TB0cF97WMnP, (accessed 1 July 2022).

6   T. A. Halgren, *J. Comput. Chem.*, 1999, **20**, 720–729.

7   C. Boss, J. Hazemann, T. Kimmerlin, M. von Korff, U. Lüthi, O. Peter, T. Sander and R. Siegrist, *Chim. Int. J. Chem.*, 2017, **71**, 667–677.

8   Molecule or Reaction Similarity and Descriptors, https://openmolecules.org/help/similarity.html, (accessed 2 October 2021).

7. Crystal structure of *cis*-102
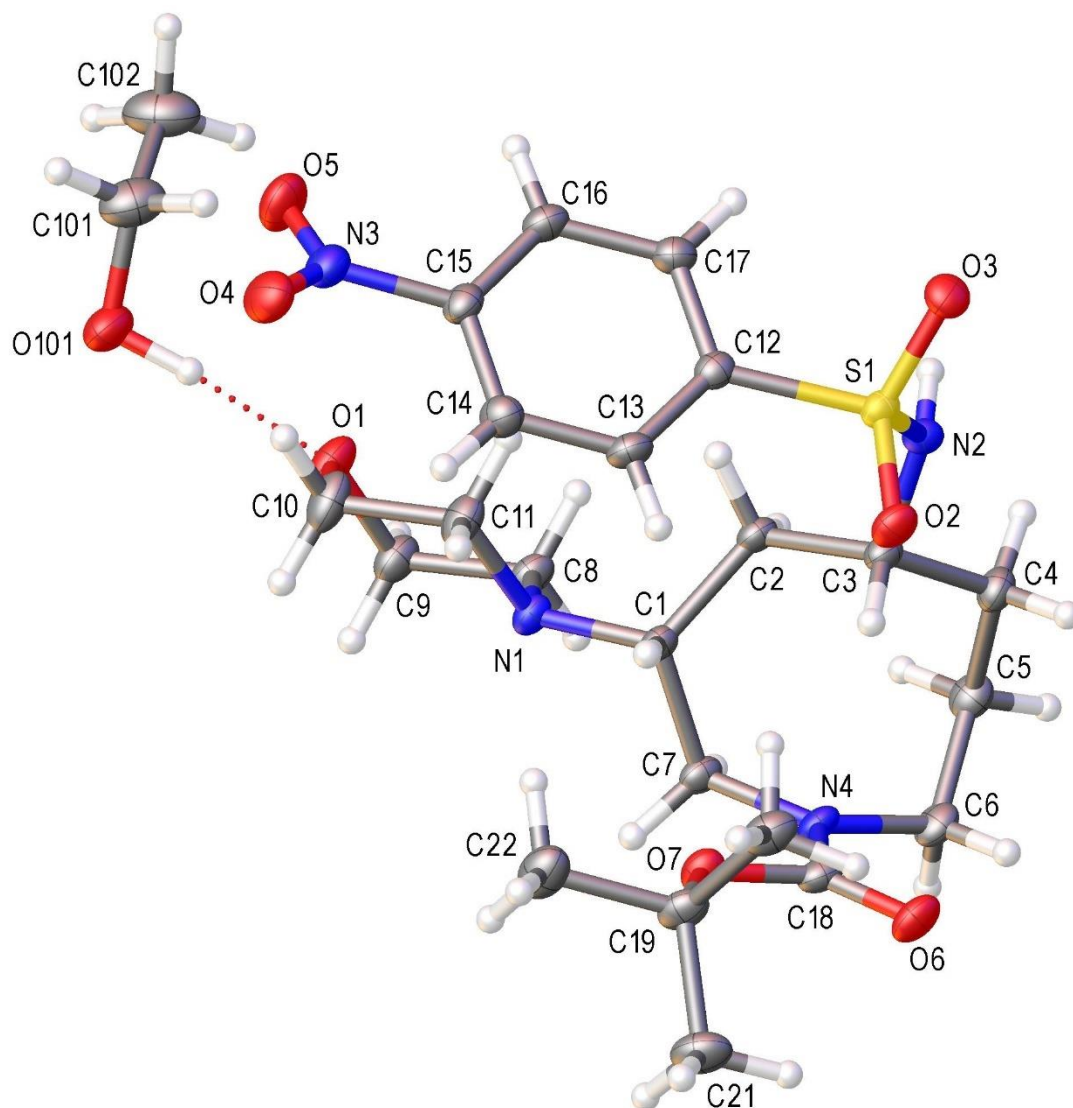
*Figure 97: Crystal structure of **cis-102** (SACE02-061-Fr1) with ellipsoids drawn at the 50 % probability level. The structure contains a molecule of ethanol. Hydrogen bonding is shown using dotted lines.*

The data presented below has been generated, processed and reported by Dr Louise Male at The University of Birmingham.

Table 1 Crystal data and structure refinement for SACE02-061-Fr1.

Identification code	SACE02-061-Fr1
Empirical formula	$C_{24}H_{40}N_4O_8S$
Formula weight	544.66
Temperature/K	100.0(2)
Crystal system	monoclinic
Space group	$P2_1/n$
a/Å	9.6281(2)
b/Å	24.0351(6)
c/Å	12.0478(4)
α/°	90
β/°	103.843(3)
γ/°	90
Volume/Å^3	2707.03(13)
Z	4
ρ_{calc}g/cm^3	1.336
μ/mm^{-1}	1.519
F(000)	1168.0
Crystal size/mm^3	0.161 × 0.114 × 0.051
Radiation	CuKα (λ = 1.54184)
2Θ range for data collection/°	7.356 to 144.246
Index ranges	-11 ≤ h ≤ 11, -29 ≤ k ≤ 29, -14 ≤ l ≤ 13
Reflections collected	45561
Independent reflections	5269 [R_{int} = 0.0605, R_{sigma} = 0.0278]
Data/restraints/parameters	5269/0/346
Goodness-of-fit on F^2	1.137
Final R indexes [I>=2σ (I)]	R_1 = 0.0509, wR_2 = 0.1207
Final R indexes [all data]	R_1 = 0.0543, wR_2 = 0.1230
Largest diff. peak/hole / e Å^{-3}	0.48/-0.36

Table 2 Fractional Atomic Coordinates (×10⁴) and Equivalent Isotropic Displacement Parameters ($Å^2×10^3$) for SACE02-061-Fr1. U_{eq} is defined as 1/3 of of the trace of the orthogonalised U_{IJ} tensor.

Atom	x	y	z	U(eq)
C1	1405(2)	6455.9(8)	2130.9(17)	17.0(4)
C2	1930(2)	7057.5(8)	2403.9(17)	18.1(4)
C3	1825(2)	7432.8(8)	1346.8(18)	18.2(4)
C4	601(2)	7860.6(9)	1193.8(19)	22.6(4)
C5	−855(2)	7636.2(9)	1289.4(19)	23.1(4)
C6	−1499(2)	7199.9(9)	410.9(19)	22.8(4)
C7	−199(2)	6396.0(9)	1554.3(17)	18.9(4)
C8	1250(2)	6278.4(9)	4120.3(17)	20.3(4)
C9	1519(2)	5837.7(10)	5042.1(19)	25.3(5)
C10	3513(3)	5520.4(11)	4437(2)	32.2(5)
C11	3253(2)	5944.9(10)	3480(2)	26.2(5)
C12	5331(2)	6975.8(8)	1755.9(18)	18.3(4)
C13	5294(2)	6440.9(9)	1316.3(18)	21.5(4)
C14	6063(2)	6019.2(9)	1972.7(19)	23.0(4)
C15	6810(2)	6148.6(9)	3076.9(18)	20.7(4)
C16	6848(2)	6675.6(9)	3536.0(18)	21.7(4)
C17	6117(2)	7100.1(9)	2859.8(18)	21.2(4)
C18	−350(2)	6491.1(9)	−510.1(18)	20.1(4)
C19	971(2)	5746.2(9)	−1224.2(18)	23.7(5)
C20	1905(2)	6149.4(10)	−1688(2)	28.1(5)
C21	−249(3)	5516.3(11)	−2150(2)	31.9(5)
C22	1873(3)	5277.9(10)	−564(2)	32.4(5)
N1	1731.9(18)	6080.4(7)	3124.7(14)	18.0(4)
N2	3150.9(18)	7755.9(7)	1404.4(16)	18.3(4)
N3	7628(2)	5705.6(8)	3787.2(17)	26.2(4)
N4	−641.6(18)	6690.7(7)	460.8(14)	18.5(4)
O1	3025.0(17)	5722.4(7)	5394.2(14)	30.3(4)
O2	3813.7(16)	7284.7(6)	−214.1(13)	23.9(3)
O3	5447.2(16)	7969.8(6)	984.3(14)	24.5(3)
O4	8144.5(18)	5340.4(7)	3310.3(16)	34.2(4)
O5	7783(2)	5740.2(8)	4825.4(15)	37.8(4)
O6	−715.2(17)	6722.8(7)	−1441.4(13)	26.2(3)

O7	396.3(16)	6013.7(6)	−314.0(12)	23.0(3)
S1	4431.7(5)	7525.3(2)	882.3(4)	18.13(13)
C101	5928(3)	5493.5(13)	7631(2)	40.3(6)
C102	5938(3)	5874.8(14)	8617(3)	46.2(7)
O101	4648.6(19)	5187.7(8)	7301.5(16)	34.8(4)

Table 3 Anisotropic Displacement Parameters ($\text{Å}^2 \times 10^3$) for SACE02-061-Fr1. The Anisotropic displacement factor exponent takes the form: $-2\pi^2[h^2a^{*2}U_{11}+2hka^*b^*U_{12}+...]$.

Atom	U_{11}	U_{22}	U_{33}	U_{23}	U_{13}	U_{12}
C1	15.1(9)	21.9(10)	13.1(10)	1.9(7)	1.9(7)	0.9(7)
C2	15.4(9)	23.1(10)	14.1(10)	1.0(8)	0.3(8)	0.5(7)
C3	15.5(9)	21.0(10)	16.7(10)	1.7(8)	0.9(8)	−0.6(7)
C4	19.3(10)	23.7(10)	23.6(11)	5.3(8)	2.9(9)	4.2(8)
C5	19.0(10)	27.4(11)	23.4(11)	1.0(9)	5.8(9)	5.1(8)
C6	14.3(9)	30.1(11)	23.3(11)	3.1(9)	3.0(8)	5.0(8)
C7	16.9(10)	25.5(10)	13.6(10)	1.4(8)	2.1(8)	−0.7(8)
C8	18.5(10)	27.5(10)	14.5(10)	0.5(8)	3.1(8)	2.4(8)
C9	22.1(11)	33.1(12)	19.9(11)	5.9(9)	3.6(9)	3.7(9)
C10	28.4(12)	39.8(13)	28.9(13)	12.3(10)	7.7(10)	14.3(10)
C11	20.9(11)	33.0(12)	25.0(12)	7.6(9)	5.7(9)	8.1(9)
C12	14.8(9)	22.3(10)	17.9(10)	1.3(8)	4.1(8)	−0.1(7)
C13	18.1(10)	27.1(11)	17.2(10)	−2.6(8)	0.1(8)	−0.6(8)
C14	22.1(10)	22.4(10)	23.8(11)	−2.8(8)	3.9(9)	1.8(8)
C15	14.9(9)	24.4(10)	21.8(11)	3.2(8)	2.4(8)	1.9(8)
C16	18.5(10)	28.1(11)	16.9(10)	−1.2(8)	1.1(8)	−0.9(8)
C17	19.3(10)	22.8(10)	20.5(11)	−2.5(8)	3.1(8)	−2.2(8)
C18	14.6(9)	27.3(11)	16.8(10)	−0.4(8)	0.6(8)	−1.5(8)
C19	21.8(10)	30.9(11)	17.0(11)	−7.0(8)	2.0(8)	3.1(8)
C20	22.2(11)	39.1(13)	22.1(11)	−2.8(9)	3.5(9)	1.7(9)
C21	27.7(12)	39.8(13)	26.0(13)	−12.2(10)	2.4(10)	−2.3(10)
C22	35.1(13)	34.4(12)	25.7(12)	−4.2(10)	3.0(10)	9.0(10)
N1	16.7(8)	22.9(8)	13.9(8)	2.2(6)	2.7(7)	3.5(6)
N2	17.5(8)	20.0(8)	16.6(9)	−1.6(7)	2.1(7)	−1.1(7)
N3	20.1(9)	28.7(10)	27.2(11)	3.7(8)	0.1(8)	0.6(7)

N4	13.9(8)	26.3(9)	13.5(8)	1.6(7)	−0.4(6)	1.8(7)
O1	25.8(8)	42.3(9)	21.1(8)	9.1(7)	2.2(7)	7.7(7)
O2	25.0(8)	29.7(8)	15.0(7)	0.0(6)	1.1(6)	2.6(6)
O3	21.8(7)	25.0(7)	27.3(8)	3.2(6)	7.2(6)	−3.9(6)
O4	28.2(9)	31.6(9)	39.3(10)	−1.4(7)	1.0(7)	8.3(7)
O5	46.8(11)	38.8(10)	23.1(9)	7.7(7)	−0.9(8)	5.9(8)
O6	24.3(8)	37.2(9)	14.9(8)	3.3(6)	0.5(6)	5.0(6)
O7	26.1(8)	26.1(8)	15.9(7)	−1.0(6)	3.2(6)	4.3(6)
S1	17.3(2)	21.1(2)	15.5(3)	1.89(17)	2.71(19)	−0.10(18)
C101	28.4(13)	54.4(16)	35.9(15)	−4.2(12)	3.8(11)	−4.1(12)
C102	30.3(14)	57.3(18)	50.2(18)	−18.4(14)	8.0(12)	−8.9(12)
O101	29.3(9)	38.3(10)	30.7(10)	7.7(8)	−4.7(7)	−2.7(7)

Table 4 Bond Lengths for SACE02-061-Fr1.

Atom	Atom	Length/Å	Atom	Atom	Length/Å
C1	C2	1.541(3)	C13	C14	1.386(3)
C1	C7	1.541(3)	C14	C15	1.388(3)
C1	N1	1.472(2)	C15	C16	1.379(3)
C2	C3	1.544(3)	C15	N3	1.471(3)
C3	C4	1.542(3)	C16	C17	1.388(3)
C3	N2	1.481(3)	C18	N4	1.355(3)
C4	C5	1.532(3)	C18	O6	1.226(3)
C5	C6	1.513(3)	C18	O7	1.344(3)
C6	N4	1.469(3)	C19	C20	1.517(3)
C7	N4	1.466(3)	C19	C21	1.517(3)
C8	C9	1.512(3)	C19	C22	1.524(3)
C8	N1	1.465(3)	C19	O7	1.487(2)
C9	O1	1.437(3)	N2	S1	1.6109(18)
C10	C11	1.515(3)	N3	O4	1.219(3)
C10	O1	1.430(3)	N3	O5	1.226(3)
C11	N1	1.461(3)	O2	S1	1.4342(16)
C12	C13	1.387(3)	O3	S1	1.4336(15)
C12	C17	1.396(3)	C101	C102	1.499(4)
C12	S1	1.779(2)	C101	O101	1.408(3)

Table 5 Bond Angles for SACE02-061-Fr1.

Atom	Atom	Atom	Angle/°	Atom	Atom	Atom	Angle/°
C2	C1	C7	115.20(16)	O7	C18	N4	111.29(18)
N1	C1	C2	113.97(16)	C20	C19	C22	110.48(19)
N1	C1	C7	107.79(15)	C21	C19	C20	112.6(2)
C1	C2	C3	114.75(16)	C21	C19	C22	111.0(2)
C4	C3	C2	112.67(17)	O7	C19	C20	110.68(18)
N2	C3	C2	112.47(16)	O7	C19	C21	109.92(18)
N2	C3	C4	106.34(16)	O7	C19	C22	101.57(17)
C5	C4	C3	116.32(17)	C8	N1	C1	114.77(16)
C6	C5	C4	114.87(18)	C11	N1	C1	112.29(16)
N4	C6	C5	114.61(17)	C11	N1	C8	108.91(16)
N4	C7	C1	113.84(16)	C3	N2	S1	122.19(14)
N1	C8	C9	109.98(17)	O4	N3	C15	117.98(19)
O1	C9	C8	109.60(17)	O4	N3	O5	124.5(2)
O1	C10	C11	111.02(19)	O5	N3	C15	117.52(19)
N1	C11	C10	110.16(18)	C7	N4	C6	118.60(17)
C13	C12	C17	121.37(19)	C18	N4	C6	119.36(17)
C13	C12	S1	119.83(16)	C18	N4	C7	121.94(17)
C17	C12	S1	118.73(16)	C10	O1	C9	109.29(17)
C14	C13	C12	119.9(2)	C18	O7	C19	121.11(16)
C13	C14	C15	117.8(2)	N2	S1	C12	109.52(9)
C14	C15	N3	118.56(19)	O2	S1	C12	106.34(9)
C16	C15	C14	123.2(2)	O2	S1	N2	108.10(9)
C16	C15	N3	118.20(19)	O3	S1	C12	106.09(9)
C15	C16	C17	118.6(2)	O3	S1	N2	106.27(9)
C16	C17	C12	119.01(19)	O3	S1	O2	120.24(9)
O6	C18	N4	123.8(2)	O101	C101	C102	112.5(2)
O6	C18	O7	124.95(19)				

Table 6 Hydrogen Bonds for SACE02-061-Fr1.

D	H	A	d(D-H)/Å	d(H-A)/Å	d(D-A)/Å	D-H-A/°
N2	H2	O6[1]	0.81(3)	2.06(3)	2.853(2)	168(3)
O101	H101	O1	0.96(4)	1.82(4)	2.767(2)	167(4)

[1]1/2+X,3/2-Y,1/2+Z

Table 7 Torsion Angles for SACE02-061-Fr1.

A	B	C	D	Angle/°	A	B	C	D	Angle/°
C1	C2	C3	C4	106.4(2)	C13	C12	S1	O3	-130.39(17)
C1	C2	C3	N2	-133.41(18)	C13	C14	C15	C16	-1.6(3)
C1	C7	N4	C6	-107.4(2)	C13	C14	C15	N3	179.74(19)
C1	C7	N4	C18	76.3(2)	C14	C15	C16	C17	-0.7(3)
C2	C1	C7	N4	59.2(2)	C14	C15	N3	O4	31.5(3)
C2	C1	N1	C8	53.1(2)	C14	C15	N3	O5	-150.9(2)
C2	C1	N1	C11	-72.0(2)	C15	C16	C17	C12	2.2(3)
C2	C3	C4	C5	-47.6(2)	C16	C15	N3	O4	-147.2(2)
C2	C3	N2	S1	90.9(2)	C16	C15	N3	O5	30.3(3)
C3	C4	C5	C6	-61.2(3)	C17	C12	C13	C14	-0.9(3)
C3	N2	S1	C12	-71.92(18)	C17	C12	S1	N2	-67.58(18)
C3	N2	S1	O2	43.55(18)	C17	C12	S1	O2	175.84(16)
C3	N2	S1	O3	173.89(15)	C17	C12	S1	O3	46.73(18)
C4	C3	N2	S1	-145.32(15)	C20	C19	O7	C18	55.5(2)
C4	C5	C6	N4	61.5(2)	C21	C19	O7	C18	-69.5(2)
C5	C6	N4	C7	53.5(2)	C22	C19	O7	C18	172.82(18)
C5	C6	N4	C18	-130.1(2)	N1	C1	C2	C3	170.31(16)
C7	C1	C2	C3	-64.3(2)	N1	C1	C7	N4	-172.29(16)
C7	C1	N1	C8	-76.1(2)	N1	C8	C9	O1	60.9(2)
C7	C1	N1	C11	158.84(17)	N2	C3	C4	C5	-171.19(18)
C8	C9	O1	C10	-60.8(2)	N3	C15	C16	C17	177.99(18)
C9	C8	N1	C1	174.76(16)	N4	C18	O7	C19	-173.65(17)
C9	C8	N1	C11	-58.4(2)	O1	C10	C11	N1	-58.1(3)
C10	C11	N1	C1	-175.17(18)	O6	C18	N4	C6	2.9(3)
C10	C11	N1	C8	56.6(2)	O6	C18	N4	C7	179.21(19)
C11	C10	O1	C9	59.7(3)	O6	C18	O7	C19	5.8(3)
C12	C13	C14	C15	2.3(3)	O7	C18	N4	C6	-177.67(17)
C13	C12	C17	C16	-1.4(3)	O7	C18	N4	C7	-1.3(3)
C13	C12	S1	N2	115.30(17)	S1	C12	C13	C14	176.18(16)
C13	C12	S1	O2	-1.28(19)	S1	C12	C17	C16	-178.51(16)

Table 8 Hydrogen Atom Coordinates ($Å×10^4$) and Isotropic Displacement Parameters ($Å^2×10^3$) for SACE02-061-Fr1.

Atom	x	y	z	U(eq)
H1	1925.25	6310.85	1586.16	20
H2A	2919.41	7046.51	2834.23	22
H2B	1374.38	7225.11	2889.84	22
H3	1652.31	7195.82	665.49	22
H4A	890.26	8150.29	1762.92	27
H4B	482.65	8032.77	448.79	27
H5A	−751.25	7478.04	2045.58	28
H5B	−1517.92	7945.43	1217.96	28
H6A	−2435.6	7099.96	514.94	27
H6B	−1632.52	7361.55	−345.01	27
H7A	−422.54	6004.15	1427.79	23
H7B	−750.92	6536.36	2070.49	23
H8A	236.86	6364.04	3897.24	24
H8B	1760.69	6615.9	4412.56	24
H9A	1175.7	5966.18	5691.53	30
H9B	1004.34	5500.64	4752.39	30
H10A	3014.59	5178.15	4161.45	39
H10B	4527.42	5438.45	4674.61	39
H11A	3797.49	6279.59	3738.92	31
H11B	3573.63	5796.53	2835.12	31
H13	4753.36	6365.53	582.55	26
H14	6078.67	5661.33	1682.61	28
H16	7352.63	6745	4283.15	26
H17	6149.84	7462.04	3137.84	25
H20A	2485.68	5946.84	−2095.18	42
H20B	2509.74	6348.65	−1065.77	42
H20C	1310.44	6408	−2196.82	42
H21A	−836.76	5817.35	−2519.48	48
H21B	−813.59	5267.93	−1814.05	48
H21C	132.8	5318.27	−2702.58	48
H22A	2317.08	5072.74	−1069.53	49
H22B	1271.87	5033.57	−254.85	49

H22C	2597.04	5432.51	47.39	49
H10C	6057.56	5711.56	6985.84	48
H10D	6726.52	5237.24	7841.02	48
H10E	5230.64	6159.9	8382.27	69
H10F	6865.45	6042.61	8865.87	69
H10G	5724.71	5666	9235.24	69
H2	3440(30)	7948(12)	1960(20)	25(7)
H101	4030(50)	5405(17)	6720(40)	76(12)

Experimental

Single crystals of $C_{24}H_{40}N_4O_8S$ **[SACE02-061-Fr1]** were **[]**. A suitable crystal was selected and **[]** on a **SuperNova, Dual, Cu at home/near, Atlas** diffractometer. The crystal was kept at 100.0(2) K during data collection. Using Olex2 [1], the structure was solved with the ShelXT [2] structure solution program using Intrinsic Phasing and refined with the ShelXL [3] refinement package using Least Squares minimisation.

1. Dolomanov, O.V., Bourhis, L.J., Gildea, R.J, Howard, J.A.K. & Puschmann, H. (2009), J. Appl. Cryst. 42, 339-341.
2. Sheldrick, G.M. (2015). Acta Cryst. A71, 3-8.
3. Sheldrick, G.M. (2015). Acta Cryst. C71, 3-8.

Crystal structure determination of [SACE02-061-Fr1]

Crystal Data for $C_{24}H_{40}N_4O_8S$ (M =544.66 g/mol): monoclinic, space group P2$_1$/n (no. 14), a = 9.6281(2) Å, b = 24.0351(6) Å, c = 12.0478(4) Å, β = 103.843(3)°, V = 2707.03(13) Å^3, Z = 4, T = 100.0(2) K, μ(CuKα) = 1.519 mm^{-1}, $Dcalc$ = 1.336 g/cm^3, 45561 reflections measured (7.356° ≤ 2Θ ≤ 144.246°), 5269 unique (R_{int} = 0.0605, R$_{sigma}$ = 0.0278) which were used in all calculations. The final R_1 was 0.0509 (I > 2σ(I)) and wR_2 was 0.1230 (all data).

Refinement model description

Number of restraints - 0, number of constraints - unknown.
Details:
```
1. Fixed Uiso
 At 1.2 times of:
 All C(H) groups, All C(H,H) groups
 At 1.5 times of:
 All C(H,H,H) groups
2.a Ternary CH refined with riding coordinates:
 C1(H1), C3(H3)
2.b Secondary CH2 refined with riding coordinates:
 C2(H2A,H2B), C4(H4A,H4B), C5(H5A,H5B), C6(H6A,H6B), C7(H7A,H7B),
C8(H8A,H8B),
 C9(H9A,H9B), C10(H10A,H10B), C11(H11A,H11B), C101(H10C,H10D)
2.c Aromatic/amide H refined with riding coordinates:
 C13(H13), C14(H14), C16(H16), C17(H17)
2.d Idealised Me refined as rotating group:
 C20(H20A,H20B,H20C), C21(H21A,H21B,H21C), C22(H22A,H22B,H22C),
C102(H10E,H10F,
 H10G)
```

This report has been created with Olex2, compiled on 2018.05.29 svn.r3508 for OlexSys.

8. Crystal structure of 228d3
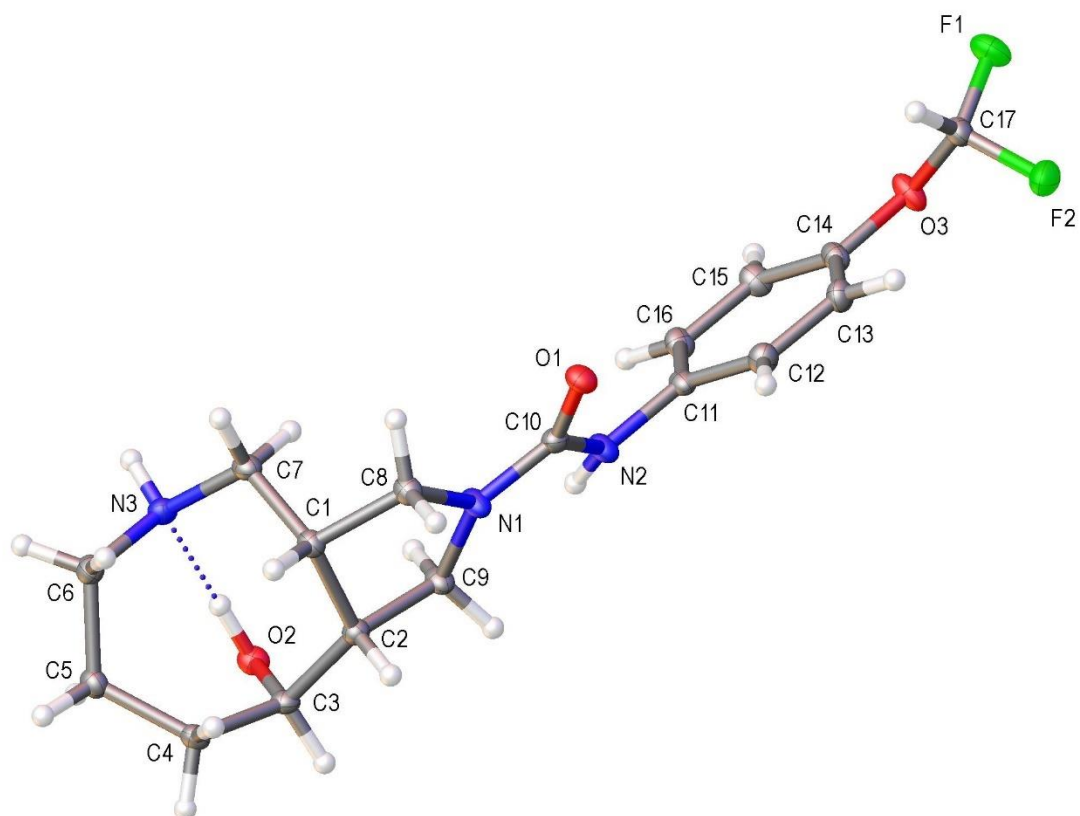
*Figure 98: Crystal structure of **228d3** (SACE3-785) with ellipsoids drawn at the 50 % probability level. Intramolecular hydrogen bonding is shown using a dotted line.*

The data presented below has been generated, processed and reported by Dr Louise Male at The University of Birmingham.

Table 1 Crystal data and structure refinement for SACE3-785.

Identification code	SACE3-785
Empirical formula	$C_{17}H_{23}F_2N_3O_3$
Formula weight	355.38
Temperature/K	100.00(10)
Crystal system	triclinic
Space group	P-1
a/Å	8.5469(2)
b/Å	9.8544(3)
c/Å	10.7470(2)
α/°	80.367(2)
β/°	77.124(2)
γ/°	69.711(2)
Volume/Å^3	823.63(4)
Z	2
ρ_{calc}g/cm^3	1.433
μ/mm^{-1}	0.964
F(000)	376.0
Crystal size/mm^3	0.148 × 0.059 × 0.051
Radiation	Cu Kα (λ = 1.54184)
2Θ range for data collection/°	9.616 to 157.812
Index ranges	-10 ≤ h ≤ 10, -12 ≤ k ≤ 12, -12 ≤ l ≤ 13
Reflections collected	9440
Independent reflections	3285 [R_{int} = 0.0336, R_{sigma} = 0.0357]
Data/restraints/parameters	3285/0/238
Goodness-of-fit on F^2	1.013
Final R indexes [I>=2σ (I)]	R_1 = 0.0352, wR_2 = 0.0889
Final R indexes [all data]	R_1 = 0.0395, wR_2 = 0.0922
Largest diff. peak/hole / e Å^{-3}	0.26/-0.23

Table 2 Fractional Atomic Coordinates (×10^4) and Equivalent Isotropic Displacement Parameters (Å^2×10^3) for SACE3-785. U_{eq} is defined as 1/3 of of the trace of the orthogonalised U_{IJ} tensor.

Atom	x	y	z	U(eq)
C(1)	2473.0(15)	7909.6(13)	−800.7(12)	14.5(3)
C(2)	640.4(15)	7858.2(13)	−437.1(12)	14.3(2)
C(3)	−284.0(15)	7803.3(13)	−1490.3(12)	14.6(2)
C(4)	−93.7(15)	8967.9(13)	−2635.8(12)	15.6(3)
C(5)	1208.5(16)	8395.4(14)	−3824.1(12)	16.7(3)
C(6)	3063.9(16)	7714.8(14)	−3662.9(12)	17.0(3)
C(7)	3785.4(15)	6660.5(14)	−1518.4(12)	16.3(3)
C(8)	2905.5(16)	7792.8(14)	531.2(12)	16.0(3)
C(9)	761.5(16)	6635.9(14)	659.7(12)	16.4(3)
C(10)	2521.9(15)	6056.0(13)	2395.0(12)	14.3(2)
C(11)	2278.4(15)	4020.5(14)	4004.9(12)	15.1(3)
C(12)	2450.3(16)	4488.5(14)	5104.7(12)	17.5(3)
C(13)	2885.6(16)	3494.0(15)	6155.5(12)	17.9(3)
C(14)	3155.6(16)	2039.4(14)	6094.6(12)	16.5(3)
C(15)	2983.8(16)	1555.7(14)	5009.3(13)	18.2(3)
C(16)	2548.5(16)	2551.4(14)	3967.9(12)	17.2(3)
C(17)	4526.8(16)	1208.0(14)	7885.8(12)	17.1(3)
F(1)	5417.3(10)	−115.4(9)	8383.6(8)	25.7(2)
F(2)	3466.7(10)	1885.6(10)	8903.3(8)	26.7(2)
N(1)	2025.6(13)	6802.8(12)	1299.1(10)	16.5(2)
N(2)	1801.1(14)	4992.2(12)	2922.1(11)	16.4(2)
N(3)	3349.7(13)	6430.7(12)	−2697.8(10)	15.5(2)
O(1)	3571.7(11)	6308.2(10)	2877.6(8)	16.9(2)
O(2)	181.6(12)	6380.1(10)	−1886.7(9)	16.5(2)
O(3)	3609.2(13)	968.5(10)	7107.3(9)	21.2(2)

Table 3 Anisotropic Displacement Parameters (Å^2×10^3) for SACE3-785. The Anisotropic displacement factor exponent takes the form: $-2\pi^2[h^2a^{*2}U_{11}+2hka^*b^*U_{12}+...]$.

Atom	U_{11}	U_{22}	U_{33}	U_{23}	U_{13}	U_{12}
C(1)	15.4(6)	14.6(6)	15.2(6)	0.6(5)	−4.1(5)	−7.1(5)
C(2)	13.0(6)	15.2(6)	15.0(6)	−1.0(5)	−2.3(5)	−5.2(4)

Table 3 Anisotropic Displacement Parameters ($\text{Å}^2 \times 10^3$) for SACE3-785. The Anisotropic displacement factor exponent takes the form: $-2\pi^2[h^2a^{*2}U_{11}+2hka^*b^*U_{12}+\ldots]$.

Atom	U_{11}	U_{22}	U_{33}	U_{23}	U_{13}	U_{12}
C(3)	11.9(5)	14.9(6)	17.1(6)	−0.6(5)	−4.0(4)	−4.2(4)
C(4)	14.8(6)	15.2(6)	16.7(6)	0.6(5)	−5.7(5)	−4.0(5)
C(5)	18.0(6)	17.5(6)	15.2(6)	1.5(5)	−4.5(5)	−7.1(5)
C(6)	16.0(6)	19.6(6)	15.7(6)	−0.6(5)	−2.2(5)	−7.0(5)
C(7)	13.2(6)	18.5(6)	17.5(6)	0.9(5)	−4.1(5)	−6.0(5)
C(8)	17.2(6)	16.7(6)	16.4(6)	1.3(5)	−4.4(5)	−8.8(5)
C(9)	14.7(6)	20.9(6)	16.5(6)	1.3(5)	−5.6(5)	−8.8(5)
C(10)	12.6(6)	14.9(6)	15.0(6)	−1.8(5)	−2.7(4)	−3.8(5)
C(11)	11.8(5)	18.7(6)	15.1(6)	1.6(5)	−2.9(4)	−6.3(5)
C(12)	19.5(6)	15.1(6)	17.9(6)	−1.6(5)	−2.2(5)	−6.2(5)
C(13)	20.4(6)	20.5(6)	14.1(6)	−2.9(5)	−2.7(5)	−8.0(5)
C(14)	16.5(6)	20.0(6)	15.2(6)	3.3(5)	−5.3(5)	−9.3(5)
C(15)	21.1(6)	17.3(6)	20.7(7)	0.3(5)	−7.3(5)	−10.5(5)
C(16)	18.9(6)	20.1(6)	16.6(6)	−1.4(5)	−6.0(5)	−9.7(5)
C(17)	17.3(6)	19.6(6)	15.5(6)	0.5(5)	−5.2(5)	−6.8(5)
F(1)	27.1(4)	21.2(4)	29.3(4)	4.9(3)	−14.4(3)	−5.9(3)
F(2)	22.7(4)	36.6(5)	19.0(4)	−6.7(4)	−1.4(3)	−7.0(4)
N(1)	16.9(5)	19.8(5)	17.0(5)	3.7(4)	−7.0(4)	−11.2(4)
N(2)	18.0(5)	17.7(5)	16.6(5)	2.7(4)	−7.7(4)	−9.0(4)
N(3)	14.5(5)	14.2(5)	17.2(5)	−1.9(4)	−3.1(4)	−3.6(4)
O(1)	17.3(4)	18.1(4)	18.5(5)	0.1(4)	−7.5(3)	−7.7(4)
O(2)	16.8(5)	15.5(4)	20.0(5)	−0.5(3)	−5.2(4)	−8.0(4)
O(3)	31.2(5)	20.4(5)	19.4(5)	6.8(4)	−13.9(4)	−15.7(4)

Table 4 Bond Lengths for SACE3-785.

Atom	Atom	Length/Å	Atom	Atom	Length/Å
C(1)	C(2)	1.5440(16)	C(10)	N(2)	1.3758(16)
C(1)	C(7)	1.5306(18)	C(10)	O(1)	1.2414(15)
C(1)	C(8)	1.5330(17)	C(11)	C(12)	1.3922(18)
C(2)	C(3)	1.5353(16)	C(11)	C(16)	1.3908(18)
C(2)	C(9)	1.5309(17)	C(11)	N(2)	1.4161(16)

Table 4 Bond Lengths for SACE3-785.

Atom	Atom	Length/Å	Atom	Atom	Length/Å
C(3)	C(4)	1.5577(17)	C(12)	C(13)	1.3922(18)
C(3)	O(2)	1.4297(15)	C(13)	C(14)	1.3811(19)
C(4)	C(5)	1.5363(17)	C(14)	C(15)	1.3857(18)
C(5)	C(6)	1.5299(17)	C(14)	O(3)	1.4030(15)
C(6)	N(3)	1.4818(16)	C(15)	C(16)	1.3852(18)
C(7)	N(3)	1.4702(16)	C(17)	F(1)	1.3512(15)
C(8)	N(1)	1.4702(16)	C(17)	F(2)	1.3586(15)
C(9)	N(1)	1.4692(15)	C(17)	O(3)	1.3630(15)
C(10)	N(1)	1.3508(16)			

Table 5 Bond Angles for SACE3-785.

Atom	Atom	Atom	Angle/°	Atom	Atom	Atom	Angle/°
C(7)	C(1)	C(2)	116.50(10)	C(16)	C(11)	C(12)	119.30(12)
C(7)	C(1)	C(8)	108.28(10)	C(16)	C(11)	N(2)	118.29(11)
C(8)	C(1)	C(2)	100.83(10)	C(11)	C(12)	C(13)	120.21(12)
C(3)	C(2)	C(1)	119.67(10)	C(14)	C(13)	C(12)	119.47(12)
C(9)	C(2)	C(1)	102.73(9)	C(13)	C(14)	C(15)	121.07(12)
C(9)	C(2)	C(3)	116.22(10)	C(13)	C(14)	O(3)	122.98(11)
C(2)	C(3)	C(4)	110.94(10)	C(15)	C(14)	O(3)	115.95(11)
O(2)	C(3)	C(2)	113.20(10)	C(16)	C(15)	C(14)	119.15(12)
O(2)	C(3)	C(4)	112.68(10)	C(15)	C(16)	C(11)	120.79(12)
C(5)	C(4)	C(3)	115.66(10)	F(1)	C(17)	F(2)	105.51(10)
C(6)	C(5)	C(4)	117.13(10)	F(1)	C(17)	O(3)	106.34(10)
N(3)	C(6)	C(5)	113.00(10)	F(2)	C(17)	O(3)	109.83(10)
N(3)	C(7)	C(1)	114.89(10)	C(9)	N(1)	C(8)	112.31(10)
N(1)	C(8)	C(1)	102.79(9)	C(10)	N(1)	C(8)	120.44(10)
N(1)	C(9)	C(2)	102.11(9)	C(10)	N(1)	C(9)	126.89(10)
N(1)	C(10)	N(2)	115.35(11)	C(10)	N(2)	C(11)	123.13(11)
O(1)	C(10)	N(1)	121.88(11)	C(7)	N(3)	C(6)	114.42(10)
O(1)	C(10)	N(2)	122.76(11)	C(17)	O(3)	C(14)	116.99(10)
C(12)	C(11)	N(2)	122.40(12)				

Table 6 Hydrogen Bonds for SACE3-785.

D	H	A	d(D-H)/Å	d(H-A)/Å	d(D-A)/Å	D-H-A/°
N(2)	H(2A)	O(2)[1]	0.860(18)	2.151(18)	2.9786(14)	161.1(15)
N(3)	H(3A)	O(1)[2]	0.892(17)	2.222(17)	3.0444(14)	153.2(13)
O(2)	H(2B)	N(3)	0.88(2)	1.83(2)	2.6686(14)	158(2)

[1]-X,1-Y,-Z; [2]1-X,1-Y,-Z

Table 7 Torsion Angles for SACE3-785.

A	B	C	D	Angle/°	A	B	C	D	Angle/°
C(1)	C(2)	C(3)	C(4)	−47.59(14)	C(11)	C(12)	C(13)	C(14)	0.40(19)
C(1)	C(2)	C(3)	O(2)	80.22(14)	C(12)	C(11)	C(16)	C(15)	0.02(19)
C(1)	C(2)	C(9)	N(1)	34.37(12)	C(12)	C(11)	N(2)	C(10)	46.96(18)
C(1)	C(7)	N(3)	C(6)	57.86(14)	C(12)	C(13)	C(14)	C(15)	−0.6(2)
C(1)	C(8)	N(1)	C(9)	−15.40(13)	C(12)	C(13)	C(14)	O(3)	179.54(11)
C(1)	C(8)	N(1)	C(10)	158.25(11)	C(13)	C(14)	C(15)	C(16)	0.6(2)
C(2)	C(1)	C(7)	N(3)	54.85(15)	C(13)	C(14)	O(3)	C(17)	−29.91(17)
C(2)	C(1)	C(8)	N(1)	35.82(12)	C(14)	C(15)	C(16)	C(11)	−0.26(19)
C(2)	C(3)	C(4)	C(5)	102.44(12)	C(15)	C(14)	O(3)	C(17)	150.27(12)
C(2)	C(9)	N(1)	C(8)	−12.00(13)	C(16)	C(11)	C(12)	C(13)	−0.09(19)
C(2)	C(9)	N(1)	C(10)	174.85(12)	C(16)	C(11)	N(2)	C(10)	−134.39(13)
C(3)	C(2)	C(9)	N(1)	166.98(10)	F(1)	C(17)	O(3)	C(14)	−153.96(11)
C(3)	C(4)	C(5)	C(6)	−63.28(14)	F(2)	C(17)	O(3)	C(14)	92.34(13)
C(4)	C(5)	C(6)	N(3)	60.43(15)	N(1)	C(10)	N(2)	C(11)	174.41(11)
C(5)	C(6)	N(3)	C(7)	−110.48(12)	N(2)	C(10)	N(1)	C(8)	−169.81(11)
C(7)	C(1)	C(2)	C(3)	−57.51(15)	N(2)	C(10)	N(1)	C(9)	2.84(18)
C(7)	C(1)	C(2)	C(9)	73.04(13)	N(2)	C(11)	C(12)	C(13)	178.55(11)
C(7)	C(1)	C(8)	N(1)	−86.97(11)	N(2)	C(11)	C(16)	C(15)	−178.68(11)
C(8)	C(1)	C(2)	C(3)	−174.40(11)	O(1)	C(10)	N(1)	C(8)	9.37(18)
C(8)	C(1)	C(2)	C(9)	−43.85(11)	O(1)	C(10)	N(1)	C(9)	−177.98(12)
C(8)	C(1)	C(7)	N(3)	167.55(10)	O(1)	C(10)	N(2)	C(11)	−4.76(19)
C(9)	C(2)	C(3)	C(4)	−171.88(10)	O(2)	C(3)	C(4)	C(5)	−25.65(14)
C(9)	C(2)	C(3)	O(2)	−44.06(14)	O(3)	C(14)	C(15)	C(16)	−179.60(11)

Table 8 Hydrogen Atom Coordinates ($Å×10^4$) and Isotropic Displacement Parameters ($Å^2×10^3$) for SACE3-785.

Atom	x	y	z	U(eq)
H(1)	2487.87	8846.65	−1274.97	17
H(2)	−34.02	8757.13	−41.43	17
H(3)	−1492.89	8074.25	−1115.18	17
H(4A)	−1190.57	9445.24	−2890.94	19
H(4B)	221.09	9698.25	−2339.56	19
H(5A)	879.66	7674.86	−4122.66	20
H(5B)	1134.65	9195.48	−4494.9	20
H(6A)	3754.72	7426.66	−4482.59	20
H(6B)	3429.64	8439.67	−3408.59	20
H(7A)	4860.96	6847.53	−1736.35	20
H(7B)	3939.16	5770.69	−945.38	20
H(8A)	4119.16	7390.08	509.51	19
H(8B)	2485.61	8733.98	865.09	19
H(9A)	−319.34	6765.72	1233.89	20
H(9B)	1144	5690.95	336.67	20
H(12)	2273.69	5468.69	5137.59	21
H(13)	2993.76	3806.63	6892.49	21
H(15)	3158.5	575.1	4980.5	22
H(16)	2435.48	2233.65	3235.14	21
H(17)	5273.18	1758.17	7416.03	21
H(2A)	1240(20)	4747(18)	2472(16)	20(4)
H(3A)	4200(20)	5686(18)	−3023(14)	13(4)
H(2B)	1280(30)	6170(20)	−2199(19)	39(5)

Experimental

Single crystals of $C_{17}H_{23}F_2N_3O_3$ **[SACE3-785]** were **[]**. A suitable crystal was selected and **[]** on a **XtaLAB Synergy, Dualflex, HyPix** diffractometer. The crystal was kept at 100.00(10) K during data collection. Using Olex2 [1], the structure was solved with the SHELXT [2] structure solution program using Intrinsic Phasing and refined with the SHELXL [3] refinement package using Least Squares minimisation.

1. Dolomanov, O.V., Bourhis, L.J., Gildea, R.J, Howard, J.A.K. & Puschmann, H. (2009), J. Appl. Cryst. 42, 339-341.
2. Sheldrick, G.M. (2015). Acta Cryst. A71, 3-8.
3. Sheldrick, G.M. (2015). Acta Cryst. C71, 3-8.

Crystal structure determination of [SACE3-785]

Crystal Data for $C_{17}H_{23}F_2N_3O_3$ (M =355.38 g/mol): triclinic, space group P-1 (no. 2), a = 8.5469(2) Å, b = 9.8544(3) Å, c = 10.7470(2) Å, α = 80.367(2)°, β = 77.124(2)°, γ = 69.711(2)°, V = 823.63(4) Å^3, Z = 2, T = 100.00(10) K, μ(Cu Kα) = 0.964 mm^{-1}, $Dcalc$ = 1.433 g/cm^3, 9440 reflections measured (9.616° ≤ 2Θ ≤ 157.812°), 3285 unique (R_{int} = 0.0336, R_{sigma} = 0.0357) which were used in all calculations. The final R_1 was 0.0352 (I > 2σ(I)) and wR_2 was 0.0922 (all data).

Refinement model description

Number of restraints - 0, number of constraints - unknown.

Details:
```
1. Fixed Uiso
 At 1.2 times of:
 All C(H) groups, All C(H,H) groups
2.a Ternary CH refined with riding coordinates:
 C1(H1), C2(H2), C3(H3), C17(H17)
2.b Secondary CH2 refined with riding coordinates:
 C4(H4A,H4B), C5(H5A,H5B), C6(H6A,H6B), C7(H7A,H7B), C8(H8A,H8B),
C9(H9A,H9B)
2.c Aromatic/amide H refined with riding coordinates:
 C12(H12), C13(H13), C15(H15), C16(H16)
```

This report has been created with Olex2, compiled on 2020.11.12 svn.r5f609507 for OlexSys.

9. ¹H-NMR spectrum of a mixture of RCM product 29 & dimer 43

The ¹H-NMR spectra below show co-eluted RCM product **29** and dimer **43**, which have been discussed in Section 2.2.2.